DISSERTATION

IDENTIFICATION OF THE TPC2 INTERACTOME REVEALS TSPAN10 AND OCA7 AS KEY PLAYERS IN THE BIOGENESIS OF MELANOSOMES

Submitted by

Wyatt Beyers

Department of Biochemistry and Molecular Biology

In partial fulfillment of the requirements

For the Degree of Doctor of Philosophy

Colorado State University

Fort Collins, Colorado

Summer 2023

Doctoral Committee:

Advisor: Santiago Di Pietro

Gregory Amberg
Thomas Santangelo
Tingting Yao

ABSTRACT

IDENTIFICATION OF THE TPC2 INTERACTOME REVEALS TSPAN10 AND OCA7 AS KEY PLAYERS IN THE BIOGENESIS OF MELANOSOMES

Many specialized cell types gain their function through the generation of specialized organelles that make or store cell-specific biomolecules. A group of specialized organelles are called Lysosome Related Organelles (LROs) because they are derived from Golgi and endo-lysosomal compartments and their biogenesis depends on trafficking pathways and machinery shared with lysosomes, many have protein contents partially overlapping with lysosomes, and typically have low pH during stages of their maturation. One well-studied model LRO is the melanosome, the organelle in melanocytes and retinal pigment epithelial cells responsible for melanin pigment production in the eyes, hair, and skin, and defects in melanosome function lead to pigmentation diseases such as oculocutaneous albinism.

Melanosome biogenesis is a complex process requiring ubiquitous membrane trafficking machinery to be repurposed for the differentiation of melanosomes from other endosomal compartments and specific delivery of melanosome synthesizing enzymes, Tyrosinase and Tyrosinase Related Proteins 1 and 2. Furthermore, correct melanosome maturation requires remodeling of the melanosome membrane, recycling of membrane trafficking machinery, generation of intraluminal amyloid fibrils with the correct structure for melanin packaging, tight pH control, as well as coordinated influx of copper, zinc, tyrosine, and cysteine for melanin synthesis. These processes require the temporospatial coordination of at least 100 known proteins, and probably dozens more remain undiscovered.

In this dissertation, I present the discovery of new proteins involved in the biogenesis of melanosomes. Proximity biotinylation by promiscuous biotin ligase enzymes followed by biotin pulldown and mass spectrometry has emerged as a powerful technique for the identification of

protein-protein interactions, protein complex determination, and identification of organelle membrane proteomes. I utilized the melanosome localized cation channel, TPC2, genetically fused with the BioID2 biotin ligase, to identify proteins in proximity to TPC2 at the cytosolic surface of melanosome membranes of MNT1 melanoma cells. Through mass spectrometry analysis of biotinylated proteins enriched through Streptactin pulldown, a TPC2 proximity interactome was identified comprising over 200 proteins. Subsequent fluorescence confocal microscopy analysis confirmed several proteins, including PLD1, SV2A, TSPAN10, and OCA7/C10orf11/LRMDA all colocalize highly with TPC2-EGFP, confirming they are new melanosome proteins.

In follow-up functional studies, TSPAN10 and OCA7 were confirmed to be involved in pigmentation, with severe melanin depletion in TSPAN10 or OCA7 knockout MNT1 cells. TSPAN10 and OCA7 both influence the processing of the PMEL protein, which is required for correct melanosome ultrastructure and for melanin packaging. Further investigation of TSPAN10 revealed it functions with the pigmentation associated metalloproteinase, ADAM10, and is required for ADAM10 expression and localization to endosomal compartments. On the other hand, OCA7 was found to work with the melanosome localized Rab proteins, Rab32 and Rab38, and regulates the pH of melanosomes. Thus, the newly defined TPC2 interactome in melanocytes was proven as a valuable dataset that robustly identifies new melanosome proteins.

Chapter 1 of this dissertation provides a broad overview of membrane trafficking pathways, as well as a synopsis of the specific proteins and pathways involved in melanosome biogenesis and homeostasis. Chapter 2 investigates the TPC2 interactome in MNT1 cells, and it characterizes TSPAN10 as a new player in melanosome biogenesis. Finally, Chapter 3 provides a characterization of the OCA7 protein associated with oculocutaneous albinism type 7 and investigates OCA7 function using a newly generated OCA7 knockout cell model.

ACKNOWLEDGEMENTS

My dissertation is the culmination of many years of work in the Biochemistry and Molecular Biology Department at CSU and wouldn't have been possible without the help and contributions of many colleagues and friends.

First and foremost, I would like to thank my faculty mentor, Dr. Santiago Di Pietro. Despite my limited experience in cell biology, he admitted me into his lab and saw promise in me. I am grateful that I got to start off with an exciting and exploratory project, and I have always been granted creative freedom in choosing a direction for my project. One of Santiago's best traits as a mentor is his contagious enthusiasm when he sees that an exploratory experiment worked or when a project is heading in an exciting direction. When things aren't going as well, Santiago always has great suggestions that have helped keep me productive. He encourages me and other students in the lab to think independently and to analyze our experimental results critically. Finally, Santiago's and Andrea's celebratory barbeques are perhaps the best reward for hard work; we never go feeling unappreciated in the Di Pietro Lab.

I thank Andrea Ambrosio, who provided training and many of the protocols I use every day, as well as countless hours of advice and constructive feedback. I strive to be a scientist as focused and efficient as Andrea.

Anna Detry, Lucas Pacheco, and Hania Nini are or were undergraduate students working directly with me on my project. I thank Anna for all of her enthusiastic hard work over the years, contributing many results shown in this dissertation. I am very proud of the scientist she has become. I thank Lucas Pacheco for his work on my project and our many interesting discussions about new ideas and the latest technology. I admire Lucas's curiosity in understanding the rationale and implications for each experiment we did, and how he always analyzed results with attention to statistical robustness. I thank Hania Nini for her hard work imaging and analyzing microscopy images with me since recently joining the lab. I would not have finished everything in

time to complete my dissertation without her help. I also look forward to working with a fellow graduate student Troy Placid, who has stepped up to continue the projects started in this Dissertation.

I also acknowledge other current and former members of the lab. I thank Andrew Lamb for providing advice, experimental feedback, and friendship since I joined the lab. I thank Hallie Febvre for bringing positive energy to the lab daily, for the many fun conversations, for experimental discussion, and for keeping the lab running smoothly over the years. I thank Naser Eadaim for the great conversations and advice about my career and life. I also thank Naser for graciously sharing delicious meals and coffee.

I would like to thank my committee, Greg Amberg, Tom Santangelo, and Tingting Yao, for always encouraging my critical thinking and for helping make graduate school go smoothly. I also appreciate our discussions of potential career paths and encouraging me to be proactive in searching for a postdoc. Besides my committee, I would like to thank faculty members Chaoping Chen, Jennifer DeLuca, Erin Nishimura, Marc Nishimura, Soham Chanda, and Jim Bamburg who all helped with various aspects of my academic growth. I also thank O'Neil Wiggan, Laurie Minamide, Alisa Shaw, and Lubna Tahtamouni who all helped with technical aspects of my project at some point, as well as Laurie Stargell, Kristen Cantonwine, Timothy David, and Emma Reust for their immense administrative support.

Importantly, I need to thank all the friends I made during graduate school who have helped to make graduate school a positive experience. I thank my good friends Lindsay Winkenbach and Dylan Parker who have brought me on many mountain or old town adventures. I thank Scott Burlingham who has pushed me to socialize on many days when I would otherwise be sitting inside working or watching television, and for introducing me to many board games and Pickleball. I am also grateful for my friendships with Ryan Czarny, Craig Marshall, Travis Sanders, Ryan Jeep, Andrew Dillon, and Nally Torres who are all great friends and are responsible for many memorable times throughout graduate school. I also acknowledge everyone else in my

graduate cohort: Zack Hazlett, Zihao Zhao, Matt O' Malley, and Amr Elhamamsy, for your friendship and for going through key years of graduate school with me.

I am extremely grateful for Julie Sun, my best friend and partner, who has spent the last few years, and hopefully many more with me. We had countless adventures throughout graduate school and I appreciate your support and scientific discussion. I look forward to many more years growing with Julie, and I am excited to see where our careers in biology take us.

Finally, I need to acknowledge my family members, who are responsible for my success. I thank Evan Beyers for inspiring me to apply to graduate school at CSU and for many hours of creative discussion and scientific ideas. I thank my father Dan Beyers, for instilling a scientific mind within me and convincing me that a career in biology would be a worthwhile pursuit. I thank my mother Julie Beyers, and my sister Mallory Beyers for your continuous support in my endeavors, and for putting up with many hours of "science talk" during the holiday breaks over the years.

DEDICATION

I dedicate this thesis to my father, Dan Beyers, who inspired my pursuit of a career in Biology and encouraged me to never stop asking questions.

TABLE OF CONTENTS

LIST OF TABLES

LIST OF FIGURES

CHAPTER 1

INTRODUCTION

Summary

This dissertation describes the discovery of new machinery involved in the biogenesis of melanocyte-specific lysosome related organelles called melanosomes. To understand pathways involved in melanosome biogenesis, it is important to first understand basic pathways in membrane trafficking, and how they are adapted to generate cell-specific organelles. Therefore, this introductory chapter first covers canonical membrane trafficking pathways that occur in all Mammalian cells. Then, it describes how ubiquitous membrane pathways are repurposed using cell type-specific machinery to generate specialized organelles, and how membrane trafficking pathways are affected in pigmentation disorders. Finally, it discusses specific pathways in the biogenesis of melanosomes, key enzymes in melanin synthesis, and a host of proteins that maintain the solute gradients within the melanosome lumen to regulate the efficiency of melanogenesis in melanocytes.

Ubiquitous Membrane Trafficking Pathways

Early Secretory Pathway

Membrane trafficking is the process of transporting cellular membranes and their associated proteins, the *cargo*, from one specific cellular compartment or location to another through the generation and transport of membrane-bound vesicles, utilizing a set of membrane trafficking proteins, the *machinery.* Several ubiquitous membrane trafficking pathways are depicted in (**Figure 1.1**).

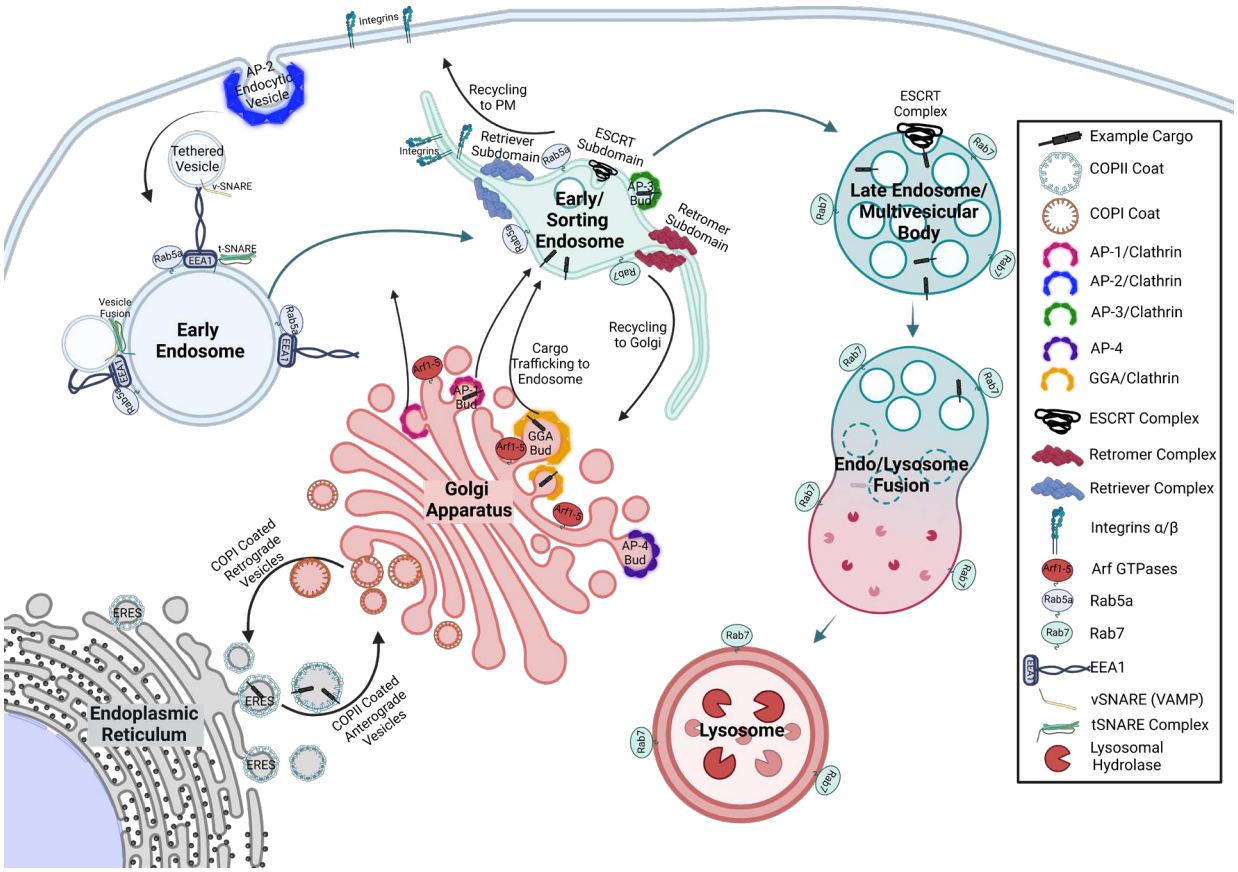

Figure 1.1. Membrane trafficking pathways and endosomal maturation. Integral membrane proteins and soluble secretory proteins, the *cargo*, are co-translationally translocated into the endoplasmic reticulum (ER). Cargos are concentrated into ER exit sites and sent to the Golgi apparatus via COPII-coated vesicles. ER machinery is recycled back to the ER via COPI-coated vesicles. After traversing the Golgi apparatus, cargo concentrates into specific subdomains by interaction with Adaptor Protein (AP) complexes, which concentrate cargos and recruit Clathrin which deforms the membrane, forming buds and subsequently Clathrin-coated vesicles. Cargo is delivered to either the plasma membrane or the endosomal network. From the plasma membrane, cargo is internalized by Clathrin-mediated endocytosis. Endocytic vesicles are captured by extended tethering proteins, such as EEA1, which hold vesicles in proximity to early endosomes containing the surface protein Rab5a. Vesicles contain vesicle-SNARE proteins, which interact with a target-SNARE complex on their target endosomes, and SNARE interactions eventually drive membrane fusion. At early/sorting endosomes, cargos have several possible fates. Plasma membrane proteins, such as Integrins, at endosomes are recognized by the Retriever complex and shunted back to the plasma membrane via recycling tubules. Whereas Golgi apparatus destined cargo recycling is mediated by the Retromer complex. Some proteins are sorted into AP subdomains which form vesicles destined for other organelles. Finally, unneeded cargo is captured by the ESCRT machinery, concentrated on intraluminal vesicles, and eventually degraded by lysosomal hydrolases as the endosome matures into a lysosome. In the cartoon, blue arrows represent endosomal maturation, and black arrows represent membrane trafficking events.

Membrane proteins and secreted proteins, encompassing almost 40% of all expressed proteins in the human proteome, are synthesized and transported following the secretory pathway (1). During the synthesis of secretory proteins, ribosomes are targeted to the Endoplasmic Reticulum (ER) surface by the N terminal signal peptide or hydrophobic helix of the nascent protein, and newly synthesized proteins are translocated into the ER lumen, usually in a co-translational fashion. To achieve ER targeting, Signal Recognition Particles (SRP) in the cytosol recognize exposed signal peptides of nascent polypeptides, stalling further synthesis until the SRP docks on ER-localized SRP receptor and protein translocation via the Sec61 Translocon occurs (2, 3). Upon entry into the lumen, secreted, soluble, or type 1 transmembrane cargoes undergo processing by a signal peptidase to remove their signal peptides. For secreted and soluble cargoes, signal peptide excision releases them from the membrane into the lumen (4). Co-translationally in the ER, glycans are ligated to asparagine (N) residues of secretory proteins by Oligosaccharyltransferase, and N-linked glycosylations aid in folding, sorting, and stability (5).

Although ER forms close contacts with almost every organelle in the cell, ER contact sites are not sites of protein cargo delivery (6). Instead, cargoes are canonically concentrated at ER exit site (ERES) subdomains, before being sent to the ER/Golgi intermediate compartments via COPII coated vesicles, which eventually mature into cis, medial, and trans Golgi apparatus compartments (7, 8). Although, recent high resolution ultrastructural data obtained by focused ion beam milling coupled with scanning electron microscopy (FIB-SEM) has suggested cargo at ERESs are concentrated into a tubular meshwork and delivered to Golgi via tubule structures in addition to vesicles (9).

Within the Golgi apparatus cargoes can be extensively glycosylated by many glycosidases and glycosyltransferases, and some proteins are glycosylated at serine and threonine residues (O-linked glycosylation) in addition to their N-linked glycosylations, that are important for stability and function (10). At the trans-Golgi network, mature cargoes are sorted and sent to their next

destination, such as the plasma membrane, sorting endosomes, or another organelle. To be sorted to the correct cellular destination, transmembrane cargos have cytosol exposed sorting signals that specify interaction with the correct Clathrin adapter protein (AP) complex. For instance, lysosome targeted membrane proteins usually contain one or more canonical sorting signals with the sequence YXXØ or [DE]XXXL[LI], where Ø is a bulky hydrophobic residue, required for their correct association with sorting to lysosomes (11-13). These signals interact with the AP complexes to direct cargo trafficking to and within the endo-lysosomal network or to promote Clathrin mediated internalization of plasma membrane localized cargoes back into the endosomal network.

Adapter Protein Complexes in Cargo Sorting

Clathrin AP complexes are heterotetramers containing core σ and μ subunits that bind cargo sorting motifs, and larger β and γ subunits that interact with Clathrin and accessory proteins to organize a cargo enriched Clathrin coated vesicle (13, 14). For the cell to achieve specific sorting, five different forms of AP complexes are expressed, some with multiple subunit isoforms allowing for a variety of cell type specific AP complexes having many possible combinations (14). AP-1 is localized at the trans Golgi network and endosomes, where it coordinates cargo sorting to endosomes or the plasma membrane. AP-2 is the major endocytic AP complex coordinating Clathrin mediated endocytosis and cargo delivery to early and recycling endosomes. AP-3 is present on early endosomes and directs cargo to late endosomes, lysosomes, or lysosome related organelles. Although AP-1 and AP-3 can both be found on endosomes, they constitute unique subdomains and have unique endosomal sorting functions (15, 16). AP-4 localizes to the trans Golgi network but recognizes sorting signals in addition to YXXØ, YX[FYL][FL]E, FXF, FGSV, and FR, and may form Clathrin independent vesicles as it does not have an obvious Clathrin binding motif (14, 17, 18). AP-4 was found to be required for ATG9A sorting to pre-

autophagosomes (19). AP-5 is the most recently discovered AP complex, localizing to late endosomes, and appears to be Clathrin independent (20).

In addition to the tetrameric AP complexes, there are several monomeric Clathrin adaptors, for example, the Golgi-localized, γ-ear containing, Arf-binding (GGA) family of proteins (21, 22). GGAs are recruited to the Golgi or endosomes through interaction with Arf small GTPases via their GAT domain, select for cargo specifically containing DXXLL sorting motif via their VHS domain, and organize a Clathrin coat via their hinge regions. Interestingly, GGAs themselves contain a DXXLL sorting motif that is suggested to play a GGA phosphorylation dependent auto-inhibitory role by occluding cargo binding (23, 24). GGAs also interact directly with the AP-1 complex, suggesting they may play a cooperative role in cargo sorting (25). Finally, although this section focuses on Clathrin APs in Golgi and endosomal trafficking, it is important to note that multiple non-Clathrin coat protein complexes exist, including coatomer proteins (COP), COPII and COPI, involved in ER to Golgi anterograde and Golgi to ER retrograde vesicle trafficking, respectively, as well as Retromer involved in endosome to Golgi retrograde membrane trafficking (26, 27). Together, a variety of APs and coat proteins having diverse subcellular localizations and recognizing multiple sorting signals enables context dependent control of specific cargo budding.

Receptor Mediated Trafficking of Soluble Cargo

Many of the cargoes following the secretory or endocytic pathways are not transmembrane and therefore lack cytosolic sorting signals to associate with specific adapter proteins. To achieve specific sorting of soluble cargoes, cells utilize transmembrane cargo receptors that bind the cargo in the lumen or extracellular space and bind APs via sorting signals in their cytosolic domain. One important example is the Mannose-6-Phosphate Receptor (MPR) which binds Mannose-6-Phosphate moieties present on soluble lysosomal hydrolases in the Golgi

lumen and has a DXXLL lysosome sorting signal in the cytosol for engagement with Clathrin adaptors including GGAs (13). Although the lysosomal hydrolases alone are unable to sort to lysosomes, interaction with MPR facilitates their correct sorting into lysosome destined vesicles (13). Upon vesicle fusion with endosomes and endosomal maturation, lower endosomal pH induces the dissociation of soluble hydrolases from MPR, allowing for their function in the fluid phase of lysosomes, whereas MPR recycles back to the Golgi for subsequent rounds of trafficking (28). In addition to MPR trafficking of soluble lysosomal hydrolases, other notable examples of receptor mediated sorting strategies include endocytosis of soluble cargoes Transferrin/iron, LDL, and EGF.

Vesicle Fusion with Target Organelles

After vesicles containing cargo are released from a donor compartment, they must locate and fuse with the correct acceptor compartment. At a minimum this involves a vesicle-SNARE (V-SNARE, also called R-SNARE) localized on the vesicle and target-SNAREs (T-SNARE, also called Q-SNARE) on the acceptor organelle. SNARE proteins can be thought of as “molecular zippers,” forming a 4-helix coiled bundle of cis and trans SNAREs and bringing each membrane close enough to drive fusion. Each SNARE protein can only or preferentially function with specific SNARE partners, and with at least 36 different SNARE proteins in the human proteome many dozens of functional combinations can occur in cells (29).

Although SNAREs are the final machinery catalyzing membrane fusions, vesicles have the immense challenge of locating the target membrane in a vast cytoplasm containing a diversity of membranes. To achieve vesicle capture, vesicles, and organelles utilize tethering proteins and tethering complexes. Tethering proteins are linked to the surface of one compartment via interaction with specific surface proteins (often small GTPases) and/or phosphoinositides, and reach out far into the cytosol to bind and tether incoming vesicles with compatible tethering sites (30). Tethering proteins tend to be long coiled coil proteins, and some could potentially extend

hundreds of nanometers, drastically increasing surveillance for incoming cargo. Once incoming vesicles are tethered, they are kept in high local concentration near the target membrane. Finally, Sec1/Munc18 (SM) proteins facilitate the correct formation of a 4-helix SNARE bundle, and the vesicles are fused (31).

Small GTPases in Membrane Trafficking

Small GTPase proteins of the Ras superfamily, especially Arf and Rab proteins, are perhaps the master regulators of membrane trafficking and organelle identity (32-34). Humans express 60 Rab proteins and 6 Arf proteins, affording precise control of membrane trafficking events at each organelle membrane. Most organelles are associated with one or more surface localized Rab or Arf small GTPase proteins. For a few examples, Rab5a localizes to Early Endosomes, Rab7 localizes to late endosomes and lysosomes, Rab11 localizes to recycling endosomes, Arf1-5 localizes to the Golgi, and Arf6 localizes to the plasma membrane (32, 33). Small GTPases are so called “molecular switches,” because, in their GTP bound state, they are in their “on” conformation and actively recruit effector proteins, such as tethering proteins or AP complexes, to the membrane in which they are localized to, whereas upon GTP hydrolysis to the GDP bound state, they are switched to an “off” conformation and cease effector recruitment. While small GTPases are responsible for recruiting effectors, guanine exchange factors (GEFs) and GTPase activating proteins (GAPs) tightly regulate their activity. GEFs turn small GTPases “on” by inducing their exchange of GDP for GTP, promoting effector recruitment, while GAPs turn them “off” by accelerating GTP hydrolysis (33). Small GTPases can be kept in their inactive, GDP bound off state by GDP dissociation Inhibitors (GDIs) and which prevent guanine exchange and extract Rabs from membranes by masking their C terminal Prenylations (34, 35). Thereby, at least some Rabs require their GEF to be recruited from the cytosol and inserted into a specific membrane, as GEF activity promotes simultaneous unmasking of prenylation moieties along with GDP/GTP exchange (34, 36). Another recently described mechanism of Rab regulation is

through an ATP-independent chaperone RabIF, which is required to prevent proteasome mediated decay of multiple Rabs (37).

Recycling or Degradation of Trafficking Machinery and Mislocalized Cargoes

After vesicles fuse with their target organelles, cargo receptors are either degraded or recycled for additional rounds of cargo trafficking. In the absence of recycling, cargo is ubiquitinated, captured by the ESCRT complex in endosomal subdomains, and incorporated into intralumenal vesicles that bud away from the cytosol into the endosome lumen (38). Eventually, multivesicular endosomes containing cargo destined for degradation in their intraluminal vesicles fuse with lysosomes, where the luminal proteins are degraded by lysosomal hydrolases.

Most membrane trafficking machinery components, such as adapter and coat proteins, are cytosolic and associate peripherally with membrane bound compartments. Therefore, recycling of cytosolic machinery is achieved by dissociation from the membrane and diffusion. Some machinery, such as most SNARE proteins, are transmembrane proteins and are typically used many times rather than degraded. Consequently, cells have evolved multiple mechanisms of membrane protein recycling from endosomes back to the trans Golgi network or to the plasma membrane. One route of recycling is sequence independent, constitutive, so called “bulk flow recycling” between early endosomes and the plasma membrane (39). Bulk flow is thought to be the case for the Transferrin Receptor, which allows for rapid cycling of transferrin endocytosis and iron uptake, where individual Transferrin receptors are recycled several times per hour.

Although bulk flow is utilized for some receptors, its lack of specificity is problematic when many different proteins require sorting. Sorting endosomes have the challenge of separating “unwanted” cargo into degradative ESCRT subdomains for internalization and eventual degradation and corralling away recyclable cargo and machinery into retrieval subdomains for retrograde or surface recycling. One major endosomal recycling pathway is sequence dependent

recycling of cargo receptors from endosomes back to the Golgi or to the cell surface, which is facilitated largely by the Retromer complex (40). Retromer is a cytosolic heterocomplex of VPS35, VPS29, VPS26 subunits and one or more Sorting Nexin (SNX) proteins, especially SNX3 or SNX27. SNX27 has a PDZ domain allowing Retromer to recognize PDZ binding motifs of recycled cargoes, while SNX3 recognizes ØX (L/M/V) motifs (41, 42). While the SNX subunits recognize motifs on the recyclable cargo receptors and generate membrane curvature, the VPS35 subunit contributes to the recruitment of WASH, a complex that activates the nucleation of a branched actin network (43). It is suggested that the branched actin network corrals and stabilizes recycling proteins in retrieval microdomains during Retromer mediated recycling (39). Finally, SNX induction of membrane curvature and actin mediated stabilization lead to the generation of membrane tubule carriers concentrated with recycling cargos and machinery. Recycling tubule scission from endosomes occurs in a mechanism involving Myosin VI constriction of the actin cytoskeleton and dynamin mediated membrane pinching (44, 45).

In addition to the Retromer Complex, complexes containing SNX1/2 with SNX5/6, SNX4 and SNX8 are involved in generation of distinct retrograde recycling tubules for several additional cargoes including MPR and ATG9 (46, 47). Finally, a recently described complex called Retriever, together with the CCC complex and SNX17, is responsible for recycling Integrins and other endocytosed proteins containing an NPX(Y/F) motif back to the cell surface (48).

Lysosome Related Organelles

Specialized cell types gain their specialized function through expression of a large suite of cell specific proteins, and in many cases, generation of cell specific organelles (49, 50). To name a few examples, epithelial Lamellar bodies are made in lung alveolar type II epithelial cells and epidermal keratinocytes and function in the synthesis and secretion of surfactants to regulate lung surface tension and to generate a hydrophobic epithelial barrier, respectively (51, 52). α and δ granules are made in megakaryocytes and platelets and function in the storage and exocytosis

of blood clotting factors (53). Lytic granules are formed in cytotoxic T cells and natural killer cells and are used to kill cancer cells and virally infected cells (54). Finally, melanosomes, the primary subject of this dissertation, are made in melanocytes and retinal pigment epithelial cells to synthesize UV protective melanin pigment (55). Despite having a wide array of morphologies and unique functions, each organelle listed above are classified as lysosome related organelles (LROs) because they are Golgi and endosome derived, often share trafficking machinery, share some common cargoes, and have an acidic pH (50). Additional LROs are listed in **Table 1.1**. Despite some similarities to lysosomes, LROs are not simply lysosomes containing additional cargoes. Rather, they take on dramatically different cellular functions, are not hubs of protein degradation, and LROs typically co-exist with lysosomes in the same cell (56).

Table 1.1. Examples of Lysosome Related Organelles and their functions

Organelle	**Cell Type**	**Function**
Melanosome	Melanocytes and Retinal Pigment Epithelial Cells	Synthesize melanin pigment in the eyes, hair and skin for protection from UVR
Dense Granule	Megakaryocytes and Platelets	Storage and release of blood clotting factors including ADP, Ca^{2+} and Serotonin
Alpha Granule	Megakaryocytes and Platelets	Storage and release of blood clotting factors including von Willebrand factor, fibrinogen, and Platelet Factor 4
Weibel Palade Bodies	Endothelial Cells	Storage and secretion of angiogenic and blood clotting factors for angiogenesis and platelet recruitment
Epithelial Lamellar Bodies	Keratinocytes and Type 2 Lung Alveolar Epithelial Cells	Secretion of lipids and surfactant to form an impermeable epithelial barrier, microbe protection, and regulation of alveolar surface tension
Cytotoxic granules	T cells and Natural Killer Cells	Storage and secretion of perforin and granzyme to induce apoptosis of virus infected or cancerous cells
Phagosome	Macrophages, Dendritic Cells	Degradation of internalized bacteria or cell debris
Acrosome	Sperm Cells	Storage and factors for the recognition and penetration of egg cells
Gut Granules	*C. elegans* intestine cells	Nutrient storage and homeostasis

Hermansky Pudlak Syndrome and Griscelli Syndrome associated mutations revealed clues about LRO biogenesis and transport.

Hermansky Pudlak Syndrome (HPS) is a rare syndrome presenting with severe functional defects in multiple cell types due to the impaired ability to generate LROs (49, 57). So far, there are at least 11 forms of HPS, caused by mutations in 11 genes. All HPS patients and HPS mice show varying degrees of oculocutaneous albinism (OCA) and bleeding disorder, while some forms of HPS exhibit additional manifestations such as immunological deficiency, neurological deficiency, and lung diseases (49). Whereas Griscelli Syndrome (GS) manifests with OCA due to insufficient melanin transfer, severe neurological disorder due to impaired exocytosis, and severe immunological disorder due to impaired immunological synapse and exocytosis of lytic granules. While HPS involves the inability to correctly generate LROs, GS involves the inability to correctly transport LROs (49). Both HPS and GS are autosomal recessive disorders. Accordingly, classical genetic studies investigating individuals and their families affected with HPS and GS, as well as inbred mice that spontaneously acquired HPS mutations, were instrumental in the discovery of key machinery in the biogenesis and trafficking of LROs and suggest LROs are closely related despite their distinct functions.

Since the discovery of each HPS mutant, it was found that many of the HPS proteins are part of membrane trafficking complexes that are needed for various membrane trafficking steps during the sorting of cell specific cargoes to LROs. HPS7-9 and HPS11 were all found to be subunits of a large complex called Biogenesis of Lysosome related Organelle Complex (BLOC)-1, which is required for correct trafficking of the melanogenic enzyme, TYRP1 to melanosomes (58-61). It was eventually discovered that BLOC-1 is required for formation of the cargo containing tubules emanating from recycling endosomes required for endosomal cargo recycling (62). In the presence of BLOC-1, the kinesin KIF13A pulls endosomal tubules long distances driving cargo transport. Whereas when BLOC-1 is disrupted, KIF13A is lost from cargo tubules

and accumulates on the vacuolar endosome with unsorted cargo. HSP3, HSP5, and HSP6 are components of BLOC-2, which is required for cargo containing endosomal tubules to be directed towards melanosomes (63, 64). HSP1 and HSP4 form a complex, BLOC-3 which functions as a GEF required to recruit and activate the LRO localized GTPases Rab32 and Rab38 (65). HSP2 (AP3B1) and HSP10 (AP3D1) are components of the AP-3 complex described above, which localizes ubiquitously to endosomes.

Additionally, BLOC-1, BLOC-2 and AP-3 can physically interact and are required for sorting of the melanin synthesizing enzyme TYRP1 and the Tetraspanin CD63 to melanosomes, indicating their collective importance for LRO biogenesis (58). In pigment cells, BLOC-2 and AP-3 work with melanosome localized Rabs, Rab32 and Rab38, to mediate specific sorting of melanogenic enzymes to melanosomes (66). Finally, VAMP7 was found to be the V SNARE necessary for fusion of BLOC-1 tubules containing cargo to melanosomes, and BLOC-3 activation of Rab32 and Rab38 was found to be important for the recycling of VAMP7 (and probably other machinery) back to sorting endosomes (67). Although individual disruption of Rab32 or Rab38 only has mild pigmentation phenotypes in mice, combined Rab32/Rab38 deficiency resulted in obvious HPS clinical signs (68).

Griscelli Syndrome Type 1, Type 2, and Type 3 are associated with mutations in the genes encoding Myosin Va, Rab27a, and Melanophilin, respectively (69-71), and present with varying degrees of severity. For instance, GS Type 2 is the most severe and often lethal, with severe immunological and neurological defects in addition to pigmentation defects, while GS Type 3 phenotypes are more restricted to pigmentation, likely because Melanophilin expression is more specific for pigment cells. After the discovery of the Rab27a link to GS Type 2, it was subsequently shown to be involved in cytotoxic granule exocytosis in immune cells and to regulate melanosome distribution to the cell cortex in human melanocytes (70, 72). Similarly, mutations to Myosin Va or Melanophilin were shown to disrupt melanosome distribution, with melanosomes

accumulating in the perinuclear region rather than the cell cortex or dendritic tips of melanocytes (71, 73). Finally, it was discovered that in melanocytes, Rab27a, Melanophilin, and Myosin Va form a complex required for melanosome capture and short-range motility at the cortical actin cytoskeleton (74). Rab27a recruits its effector Melanophilin, which acts as an adapter for the processive Myosin Va motor, and together, the complex offloads melanosomes from microtubules onto actin filaments, where they await subsequent transfer to neighboring keratinocytes (75). In immune cells, Rab27a likely works with another myosin, MYH9, during the secretion of cytotoxic granules (76).

Together, these findings relating to HPS and GS identified many of the key membrane trafficking machineries involved in cargo trafficking to LROs, machinery recycling from LROs, and LRO transport. However one puzzling aspect is that many of the HPS associated membrane trafficking complexes described above are ubiquitously expressed in most cell types; yet their disruption appears to disproportionately affect cells containing LROs (77). A key ongoing question, then, is how are LROs differentiated from lysosomes if they are made using much of the same ubiquitous membrane trafficking machinery? The answer is that specialized cells must express additional cell type specific machinery and cargoes that repurpose ubiquitous membrane trafficking machinery for the generation of LROs. One example is the LRO localized Rab38, which is very similar in sequence to ubiquitously expressed Rab32 but has heightened expression in LRO producing cells. Identification of additional LRO specific machineries and cargoes is imperative for a complete understanding of LRO biogenesis. The remainder of this chapter will focus on melanosome biogenesis specifically as a model for how unique LROs are made.

Melanosome Biogenesis, Transfer, and Physiological Importance

Melanosomes are the pigment synthesizing LROs of melanocytes and retinal pigment epithelial cells responsible for pigmentation of the eyes, hair, and skin (55). In mammalian skin, melanin is made in melanocytes, but melanocytes only constitute about 5 percent of the cells in

the epidermis. Therefore melanin must be efficiently transferred to neighboring epidermal keratinocytes, and it is thought that a single melanocyte delivers its melanin to approximately 40 neighboring keratinocytes (78). Upon entering keratinocytes, densely packed melanocores are transported by the minus end directed microtubule motor dynein, where many melanocores form a supranuclear melanin cap (79). Ultimately, the melanin cap in epidermal keratinocytes functions to protect nuclei from ultra violet radiation (UVR) induced DNA damage (78). Importance of epidermal melanin synthesis and transfer is evidenced by heightened rates of UVR induced skin cancers in people with hypopigmentation disorders, and an approximately 70 fold higher incidence of skin cancer reported in Caucasian people compared to Black people (80, 81). Additionally, melanin in the eye is required for filtering light and proper eye development, and individuals with the hypopigmentation disorder OCA have ocular defects including poor visual acuity, nystagmus, strabismus, and photophobia (82, 83).

Mutations and normal gene variants affecting animal coat color and pigmentation in humans are prevalent and have easily identifiable phenotypes, which has led to the rapid development of powerful animal and cell models to study melanosome biogenesis. Thus, melanocytes are a popular model cell type for the pursuit of understanding LRO biogenesis. Most proteins discovered to be involved in melanosome biogenesis or function fall into one of the following functional categories: melanin synthesizing enzymes directly involved in making melanin, amyloidogenic proteins responsible for organizing melanin and melanosome ultrastructure, solute transporters that regulate the small molecule contents of melanosomes, ion channels that regulate melanosome pH, membrane trafficking machinery, and signaling proteins that drive the context dependent expression of melanosome cargo. The following sections review many of the known key players specific for melanosome biogenesis and function. Several important proteins regulating melanosome function are depicted in **Figure 1.2**.

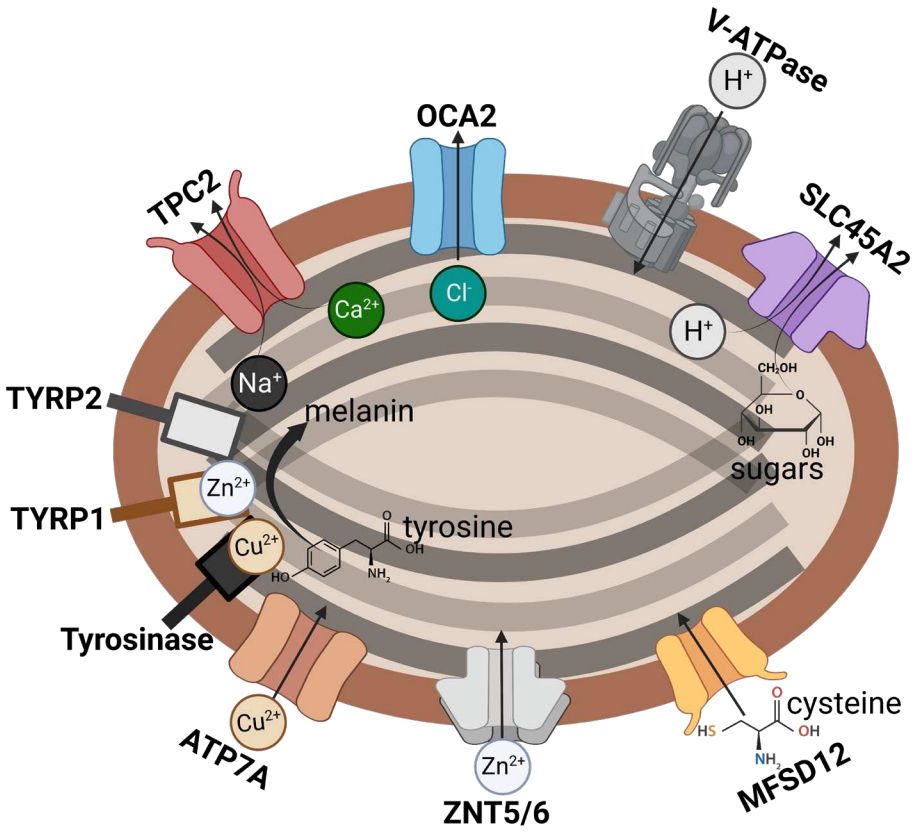

Figure 1.2. Major melanosome proteins and their functions. Tyrosinase catalyzes the rate-limiting reaction in melanin synthesis, conversion of tyrosine and L-DOPA to DOPA-Quinone, which subsequently polymerizes into melanin. TYRP1 and TRYP2 also contribute to melanin synthesis intermediate reactions. Melanin is depicted as grey and brown fibrils. TPC2, OCA2, SLC45A2, and V-ATPase are responsible for balancing melanosome pH, which regulates Tyrosinase enzymatic efficiency. ATP7A is required for copper transport, and copper is required for Tyrosinase enzymatic function. ZNT5/6 is required for zinc transport, which is important for TYRP1 stability. MFSD12 transports cysteine into melanosomes, which enables the synthesis of pheomelanin in addition to eumelanin.

Unsurprisingly, mutations in many of the proteins discussed below are associated with the hypopigmentation disorder, albinism. Unlike HPS or GS proteins, most proteins associated with albinism are only expressed in pigment cells and therefore specifically regulate melanosome function and do not affect function of other LROs. A summary of the albinism associated genes is listed in **Table 1.2**.

Table 1.2. Proteins associated with non-syndromic Ocular Albinism (OA), Oculocutaneous Albinism (OCA), and Cutaneous Albinism (CA).

Protein	Type of Albinism	Protein Function
GPR143	OA1	Regulates size of early-stage melanosomes. Perhaps drives the segregation of melanosome and lysosome biogenesis pathways.
Tyrosinase (TYR)	OCA1	Conversion of Tyrosine to DOPA-Q. Rate limiting enzyme in melanin synthesis.
P Protein/OCA2	OCA2	Melanosome localized Cl^- channel. Regulates melanin synthesis by melanosome neutralization.
Tyrosinase Related Protein 1 (TYRP1)	OCA3	Similar structure and localization to TYR and TYRP2 but melanogenic function is unclear. Potentially regulates TYR activity.
SLC45A2	OCA4	Melanosome localized H^+/sugar symporter. Regulates melanin synthesis through melanosome neutralization.
Unknown	OCA5	Unknown
SLC24A5	OCA6	Na^+/Ca^{2+} antiporter localizing to the trans Golgi and Mitochondria, possibly regulating cargo sorting or Ca^{2+} homeostasis.
LRMDA/C10orf11/ OCA7	OCA7	Peripherally localized to melanosomes via interaction with Rab32/Rab38. Regulates pH through an unknown mechanism. Regulates Integrin trafficking via interaction with the Retriever Complex.
Tyrosinase Related Protein 2 (TYRP2)	OCA8	Tautomerization of the melanin intermediate Dopachrome during melanin synthesis.
Two Pore Channel Two (TPC2)	CA	Melanosome localized Na^+/Ca^{2+} channel. Regulates melanin synthesis by melanosome acidification.

Melanin Synthesizing Enzymes

Melanin is an insoluble polymer responsible for pigmentation of eyes, hair, and skin. In animals, two classes of melanin are made: brown/black eumelanin and yellow/red pheomelanin (84). To synthesize melanin, melanosomes first oxidize the amino acid tyrosine and L-DOPA to DOPA-Quinone via the rate limiting enzyme, Tyrosinase (85-87). Tyrosinase has two copper binding sites that are required for its oxidative activity (88, 89). Notably, Tyrosinase mutations are associated with OCA1, which is the most severe type of albinism due to complete loss of melanin

synthesis (83). In the presence of high levels of the amino acid cysteine, DOPA-Quinone can convert to cysteinylDOPAs which are subsequently oxidized and form the yellow/red pheomelanins (90). After DOPA-Quinone is generated by Tyrosinase in melanosomes, it is subsequently spontaneously reacted to form melanin intermediates including CycloDOPA, Dopachrome, and DHI. Dopachrome is the substrate for Tyrosinase Related Protein 2 (TYRP2, aka dopachrome tautomerase and OCA8), which generates the melanin intermediate DHICA (91). Finally, DHI and DHICA are further oxidized and spontaneously polymerized into eumelanins. Tyrosinase Related Protein 1 (TYRP1) is structurally similar to Tyrosinase and TYRP2, and it is associated with OCA3. However, its specific role in melanin synthesis is disputed, as it is unclear whether TYRP1 directly catalyzes late steps of melanin synthesis, or if it regulates melanin synthesis through modulation of Tyrosinase. TYRP1 has zinc binding sites, and it was recently found that zinc is required for TYRP1 stability and TYRP1 dependent melanogenesis (92).

Interestingly, heterologous expression of Tyrosinase in non-pigment cells results in the synthesis of a dark melanin-like pigment in endo-lysosomes, suggesting Tyrosinase expression alone is sufficient for major steps of melanin production (93, 94). Albeit, the heterologously generated melanin is expected to lack chemical complexity compared to melanocyte melanin, nor can it take on the correct ultrastructure without the presence of the PMEL protein scaffold. Another important observation is that Tyrosinase activity is highly influenced by pH, and melanin synthesis is optimal at a pH of 6.8 (95). Given that efficient Tyrosinase/TYRP mediated melanin synthesis is highly pH sensitive and dependent on the availability of tyrosine, cysteine, Cu^{2+} and Zn^{2+}, there are many possible routes of indirectly regulating melanin synthesis via control of luminal concentration of these amino acids, ions, and pH.

PMEL Protein and its Enzymatic Processing

PMEL is a single pass transmembrane protein that forms amyloid fibrils within melanosomes after multiple proteolytic processing events. Unlike pathological amyloids, PMEL fibrils are functional, providing an ordered network on which melanin pigment is deposited and tightly packaged (96). PMEL fibrils define the ultrastructure of melanosomes, giving melanosomes their distinctive ellipsoid shape with many clearly defined striations. Besides providing an ordered scaffold for melanin deposition, PMEL is proposed to play a protective function by sequestering and accelerating the polymerization of highly reactive oxidative melanin intermediates generated during melanin synthesis (97, 98). Melanosomes are characterized into four stages that are morphologically and biochemically unique (99). Stage I melanosomes are multivesicular endosomes containing a Clathrin coat and small number of intraluminal vesicles containing immature PMEL. Stage II melanosomes contain mature PMEL fibrils but have not synthesized appreciable melanin pigment. Stage III melanosomes contain active melanogenic enzymes and appear densely packed with melanin. Finally, Stage IV melanosomes contain PMEL fibrils that are saturated with melanin. Examples of each melanosome stage as visualized by transmission electron microscopy are shown in **Figure 1.3**.

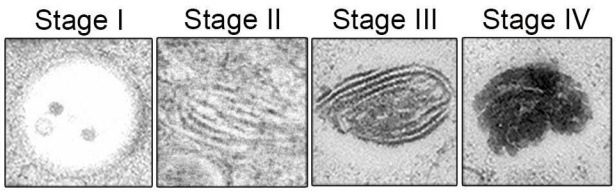

Figure 1.3. **Melanosome stages observed by transmission electron microscopy**. Stage I melanosomes resemble multivesicular endosomes. Stage II melanosomes have PMEL fibrils but lack melanin. Stage III melanosomes have fibrils with visible melanin. Stage IV melanosomes have densely packed melanin.

During the generation of PMEL fibrils, PMEL is sequentially processed by proteases. The first PMEL proteolytic event generating N terminal luminal Mα and transmembrane Mβ fragments occurs by a Proprotein Convertase in early steps of secretion, likely in the trans Golgi network,

priming PMEL for subsequent cleavage reactions (100, 101). However, Mα and Mβ remain disulfide linked, which keeps Mα tethered to the membrane until it localizes to Stage I melanosomes. There, luminal amyloidogenic domains are freed from the limiting membrane by a juxtamembrane shedding reaction catalyzed by BACE2 which cuts a site within Mβ, generating a small transmembrane C terminal fragment which eventually gets degraded by the γ-secretase PSEN2 in lysosomes (102-105). After release from the limiting melanosome membrane, Mα associates with intraluminal vesicles and is subsequently processed during the nucleation of fibrils. It has been suggested that final PMEL proteolytic events before fibrillation are the work of lysosomal proteases that are delivered to melanosomes via transient kiss-and-run fusion events, and lysosomal protease inhibition corresponds to reduced Mα processing (106-109).

pH Independent Solute Transport Regulation of Melanogenesis

Tyrosinase is a copper containing enzyme requiring copper for its activity. Therefore, copper transport in the secretory pathway could be an important form of regulation for melanogenesis. ATP7A and ATP7B were potential candidates for copper transport in melanocytes because of their key roles in copper transport as evidenced by their links to the copper imbalance syndromes, Menkes and Wilson's disease (110, 111). Indeed, it was discovered early on that the pigmentation phenotypes in the "dappled" and "blotchy" spontaneous mouse mutants were caused by mutations in the ATP7A gene, suggesting a function in pigmentation (112). Subsequent investigation using melanocyte models confirmed that ATP7A, but not ATP7B, is expressed in melanocytes and localizes to melanosomes following a BLOC-1 dependent pathway (113). Furthermore, ATP7A depletion resulted in hypopigmented melanocytes, and ATP7A sorting and copper transport to melanosomes is required for Tyrosinase enzymatic activity (113). In non-melanocytes, it was found that ATP7A recycling from endosomal compartments to the trans Golgi or to the plasma membrane relies on the CCC and Retromer complexes and is dependent on cellular copper load (114). Together, these findings suggest

forward and retrograde trafficking and activity of the ATP7A copper transporter controls Tyrosinase function in pigmentation.

While Tyrosinase is a copper containing enzyme, the structurally related TYRP1 is a zinc containing protein functioning in steps of melanogenesis (92, 115). Therefore, a reasonable prediction is that the melanosome biogenesis pathway should contain zinc transporters for TYRP1 to function. In a recent discovery, it was found that zinc transporters including the stable complex ZNT5-6 and ZNT7 function in melanosome biogenesis. ZNT5/ZNT7 double knockout in melanocytes abolished stability of TYRP1 protein, but not Tyrosinase or TYRP2, and phenocopied TYRP1 knockout. Furthermore, lysosomal inhibition rescued TYRP1 protein expression, suggested that in the absence of zinc binding, TYRP1 is mistrafficked and degraded in lysosomes (92).

Another solute important for melanogenesis is the amino acid cysteine. In the presence of high levels of cysteine, melanosomes preferentially synthesize the yellow/red pheomelanins over the brown/black eumelanins (84). MFSD12 was associated with pheomelanin synthesis in a genome wide association study (GWAS) examining pigment dilution in a comparison of white coat and non-white reddish brown coat dog breeds (116). Examining the primary structure of MFSD12 predicts that it is a 12-pass transmembrane protein and suspected small molecule transporter. To test MFSD12 function in melanocytes, Adelmann et al developed a technique to immunoprecipitate intact melanosomes, called MelanoIP, and profile their small molecule luminal contents using LC-MS. Using MelanoIP, it was revealed that cysteine is severely depleted in melanosomes purified from MFSD12 knockout cells, confirming MFSD12 role as the major cysteine transporter in melanocytes and is required for pheomelanin synthesis. Together, these findings indicate solute content in the melanosome lumen is a tightly regulated process coordinated by multiple transporters, and presence of copper, zinc, and the amino acids tyrosine and cysteine are essential for efficient melanin synthesis.

Regulators of Melanosomal pH

Melanosome pH is one major factor contributing to skin color by controlling activity of the rate limiting enzyme Tyrosinase (95, 117). Treatment of melanocytes isolated from Caucasian skin with Bafilomycin A1, which inhibits endo-lysosomal/melanosomal V-ATPase proton pump thus alkalinizing the melanosome lumen, increased Tyrosinase activity 10 fold without influencing Tyrosinase expression. Whereas Bafilomycin A1 treatment of melanocytes from Black skin had no additional effect to already high Tyrosinase activity, suggesting melanosomes from Black skin have a near neutral pH (117). In the past 10 years, several proteins have been identified as regulators of melanosome pH, including two ion channels that are posited to directly influence pH.

The first melanosome ion channel characterized was P protein, aka OCA2, and is associated with the most common form of OCA, and OCA2 SNPs are a major determinant of human eye color (83, 118, 119). OCA2 was discovered to be a chloride channel through patch clamping of whole enlarged endo-lysosomes heterologously expressing GFP-OCA2. Subsequently, OCA2 was found to localize to melanosomes in melanocytes and OCA2 expression raises melanosome pH in a mechanism requiring its functional chloride conducting capacity (118). It is suggested that Cl^- efflux via OCA2 influences membrane potential, thus influencing H^+ influx.

A second pigmentation associated ion channel, Two Pore Channel Two (TPC2), was discovered through a GWAS identifying polymorphisms in TPC2 that are strongly associated with hair color, with two polymorphisms, M484L and G734E that are highly associated with the shift from brown to blonde hair (120). Our lab and others reported TPC2 localizes predominantly to melanosomes in melanocytes and is involved in regulating their melanin synthesis via control of melanosomal pH (121, 122). Additionally, TPC2 was found to negatively regulate melanosome size and Tyrosinase expression (121, 123). Using a whole melanosome patch clamp method as

with OCA2, Bellono et al identified TPC2 conducts sodium efflux from melanosomes, and TPC2 conductance can be activated by the lipid $PI(3,5)P_2$ (122). It was posited that TPC2 Na^+ conductance directly antagonizes the OCA2 chloride channel, allowing for melanosome membrane potential to be tightly regulated. In agreement with this, the M484L polymorphism associated with reduced pigmentation was shown to enhance TPC2 sensitivity to $PI(3,5)P_2$ induced Na^+ conductance (124). However, multiple studies have shown that TPC2 can also conduct Ca^{2+}, especially upon nicotinic acid adenine dinucleotide phosphate (NAADP) activation, which is also suggested to be important for pigmentation (121, 125, 126). Interestingly, an R194C mutation in TPC2 was recently associated with nonsyndromic cutaneous albinism, and the mutation was found to constitutively activate TPC2 via heightened affinity to $PI(3,5)P_2$, influencing both sodium and calcium permeability (127). Of note, TPC2 R194C is the only gain of function mutation associated with nonsyndromic albinism. Finally, TPC2 has putative interactions with membrane trafficking machinery including Rab proteins, SNAREs, the Rab kinase LRRK2, and mTOR, making it likely that TPC2 has membrane trafficking functions at melanosomes in addition to pH regulation (124, 128-133). Together, these results indicate TPC2 is a major regulator of melanosome pH and function. Chapter 2 of the current dissertation identifies a melanocyte specific TPC2 proximity interactome with the goal of identifying new players in melanosome biogenesis.

Based on primary structure, SLC45A2 and SLC24A5, associated with OCA4 and OCA6 respectively, resemble solute transporters making them attractive candidates as regulators of melanosome pH (134, 135). Indeed, SLC45A2 is thought to be a proton/sugar symporter when heterologously expressed in *S. cerevisiae* (136). In a recent study, SLC45A2 was found to localize to pigmented melanosomes in melanocytes, and indeed, it functions to regulate the luminal pH in a mechanism similar to OCA2, drastically influencing pigment synthesis (137). Although it was noted that SLC45A2 and OCA2 occupy slightly different cohorts of melanosomes and may regulate pH at different melanosome stages. Regarding SLC24A5, one group confirmed its

predicted solute transport function, suggesting it is a potassium dependent sodium-calcium exchanger (138). SLC24A5 siRNA mediated knockdown diminishes pigment synthesis, influencing PMEL, Tyrosinase and TYRP1 expression. Despite an initial postulation that SLC24A5 regulates pH at melanosomes, SLC24A5 was instead shown to localize primarily to the trans Golgi in MNT1 and HEK293 cells, and a role for cargo sorting was proposed (138-140). SLC24A5 was also found to localize to mitochondria in mouse melanocytes, providing the first evidence that mitochondrial function can potentially regulate pigmentation in melanosomes via calcium signaling (141).

In Chapter 3 of the current dissertation, OCA7/C10orf11/LRMDA, associated with oculocutaneous albinism type 7, was found to also regulate melanosome pH, although the mechanism of pH control is indirect and not entirely clear (142). Intriguingly, OCA7 is not an ion channel or solute transporter, and we discovered OCA7 is in fact a peripheral membrane protein, localized to melanosomes via a direct interaction with Rab32 and Rab38. Using electron microscopy, we found heightened numbers of Stage I melanosomes in C10orf11 knockout MNT1 cells, and fewer Stage II or Stage III melanosomes, suggesting a melanosome maturation defect. Additionally, immunoblotting discovered defects in the processing of the PMEL protein indicating improper PMEL processing. In recent unpublished observations by a collaborator, it was discovered that the OCA7 C terminus (IRDDQL) closely resembles the SNX17 C terminus (IGDEDL), which engages directly with the Retriever complex required for endosomal recycling of Integrins and many other cargoes (48). Therefore, we hypothesize OCA7 may also function physically and functionally with Retriever. Consistent with this hypothesis, a recent report found OCA7 regulates tension of the plasma membrane which is mediated by Integrins (143). Mass spectrometry analysis of the surface proteome in Retriever depleted cells suggests Retriever controls the recycling of many solute carrier proteins (48). Thus, OCA7 regulation of melanosomal

pH may be due to mistrafficking of one or more solute carrier proteins, such as SLC45A2 (OCA4) or OCA2.

Together, these recent discoveries of proteins regulating melanosome pH have led to a paradigm where tightly regulated control of pH during melanosome maturation is imperative for proper regulation of melanin synthesis, and dysregulation of melanosome pH causes OCA. This chapter outlined many of the membrane trafficking pathways and proteins key to the biogenesis of lysosome related organelles, especially melanosomes. While it covered several of the central players regulating melanin synthesis, solute transport, pH control, and cargo sorting of melanosome proteins, melanosome biogenesis is expected to involve the coordination of many dozens of proteins, and a comprehensive list of all the proteins involved has not yet been established. Therefore, Chapter 2 of this dissertation focuses on a screen to identify new cargo and machinery functioning at the melanosome membrane, and it explores the function one newly discovered melanosome protein, TSPAN10, in melanocytes.

REFERENCES

1. Uhlen, M., Fagerberg, L., Hallstrom, B. M., Lindskog, C., Oksvold, P., Mardinoglu, A. *et al.* (2015) Proteomics. Tissue-based map of the human proteome Science **347**, 1260419 10.1126/science.1260419

2. Gilmore, R., Walter, P., and Blobel, G. (1982) Protein translocation across the endoplasmic reticulum. II. Isolation and characterization of the signal recognition particle receptor Journal of Cell Biology **95**, 470-477 10.1083/jcb.95.2.470

3. Walter, P., Gilmore, R., Muller, M., Blobel, G., and Campbell, P. N. (1982) The protein translocation machinery of the endoplasmic reticulum Philosophical Transactions of the Royal Society of London B, Biological Sciences **300**, 225-228 10.1098/rstb.1982.0168

4. Blobel, G., and Dobberstein, B. (1975) Transfer of proteins across membranes. I. Presence of proteolytically processed and unprocessed nascent immunoglobulin light chains on membrane-bound ribosomes of murine myeloma Journal of Cell Biology **67**, 835-851 10.1083/jcb.67.3.835

5. Helenius, A., and Aebi, M. (2001) Intracellular functions of N-linked glycans Science **291**, 2364-2369 10.1126/science.291.5512.2364

6. Wu, H., Carvalho, P., and Voeltz, G. K. (2018) Here, there, and everywhere: The importance of ER membrane contact sites Science **361**, eaan5835 10.1126/science.aan5835

7. Barlowe, C., Orci, L., Yeung, T., Hosobuchi, M., Hamamoto, S., Salama, N. *et al.* (1994) COPII: a membrane coat formed by Sec proteins that drive vesicle budding from the endoplasmic reticulum Cell **77**, 895-907 10.1016/0092-8674(94)90138-4

8. Viotti, C. (2016) ER to Golgi-Dependent Protein Secretion: The Conventional Pathway Springer New York, 3-29

9. Weigel, A. V., Chang, C.-L., Shtengel, G., Xu, C. S., Hoffman, D. P., Freeman, M. *et al.* (2021) ER-to-Golgi protein delivery through an interwoven, tubular network extending from ER Cell **184**, 2412-2429.e2416 10.1016/j.cell.2021.03.035

10. Frappaolo, A., Karimpour-Ghahnavieh, A., Sechi, S., and Giansanti, M. G. (2020) The Close Relationship between the Golgi Trafficking Machinery and Protein Glycosylation Cells **9**, 2652 10.3390/cells9122652

11. Janvier, K., Kato, Y., Boehm, M., Rose, J. R., Martina, J. A., Kim, B. Y. *et al.* (2003) Recognition of dileucine-based sorting signals from HIV-1 Nef and LIMP-II by the AP-1 gamma-sigma1 and AP-3 delta-sigma3 hemicomplexes J Cell Biol **163**, 1281-1290 10.1083/jcb.200307157

12. Ohno, H., Stewart, J., Fournier, M. C., Bosshart, H., Rhee, I., Miyatake, S. *et al.* (1995) Interaction of tyrosine-based sorting signals with clathrin-associated proteins Science **269**, 1872-1875 10.1126/science.7569928

13. Braulke, T., and Bonifacino, J. S. (2009) Sorting of lysosomal proteins Biochim Biophys Acta **1793**, 605-614 10.1016/j.bbamcr.2008.10.016

14. Park, S. Y., and Guo, X. (2014) Adaptor protein complexes and intracellular transport. In Bioscience reports, Portland Press Ltd,

15. Theos, A. C., Tenza, D., Martina, J. A., Hurbain, I., Peden, A. A., Sviderskaya, E. V. *et al.* (2005) Functions of Adaptor Protein (AP)-3 and AP-1 in Tyrosinase Sorting from Endosomes to Melanosomes Molecular Biology of the Cell **16**, 5356-5372 10.1091/mbc.e05-07-0626

16. Peden, A. A., Oorschot, V., Hesser, B. A., Austin, C. D., Scheller, R. H., and Klumperman, J. (2004) Localization of the AP-3 adaptor complex defines a novel endosomal exit site for lysosomal membrane proteins Journal of Cell Biology **164**, 1065-1076 10.1083/jcb.200311064

17. Dell'Angelica, E. C., Mullins, C., and Bonifacino, J. S. (1999) AP-4, a Novel Protein Complex Related to Clathrin Adaptors Journal of Biological Chemistry **274**, 7278-7285 10.1074/jbc.274.11.7278

18. Yap, C. C., Murate, M., Kishigami, S., Muto, Y., Kishida, H., Hashikawa, T. *et al.* (2003) Adaptor protein complex-4 (AP-4) is expressed in the central nervous system neurons and interacts with glutamate receptor delta2 Mol Cell Neurosci **24**, 283-295 10.1016/s1044-7431(03)00164-7

19. Mattera, R., Park, S. Y., De Pace, R., Guardia, C. M., and Bonifacino, J. S. (2017) AP-4 mediates export of ATG9A from the trans -Golgi network to promote autophagosome formation Proceedings of the National Academy of Sciences **114**, E10697-E10706 10.1073/pnas.1717327114

20. Hirst, J., D. Barlow, L., Francisco, G. C., Sahlender, D. A., Seaman, M. N. J., Dacks, J. B. *et al.* (2011) The Fifth Adaptor Protein Complex PLoS Biology **9**, e1001170 10.1371/journal.pbio.1001170

21. Bonifacino, J. S. (2004) The GGA proteins: adaptors on the move Nature Reviews Molecular Cell Biology **5**, 23-32 10.1038/nrm1279

22. Dell'Angelica, E. C., Puertollano, R., Mullins, C., Aguilar, R. C., Vargas, J. D., Hartnell, L. M. *et al.* (2000) GGAs: A Family of ADP Ribosylation Factor-binding Proteins Relatedto Adaptors and Associated with the Golgi Complex Journal of Cell Biology **149**, 81-94 10.1083/jcb.149.1.81

23. Doray, B., Bruns, K., Ghosh, P., and Kornfeld, S. A. (2002) Autoinhibition of the ligand-binding site of GGA1/3 VHS domains by an internal acidic cluster-dileucine motif Proceedings of the National Academy of Sciences **99**, 8072-8077 10.1073/pnas.082235699

24. Ghosh, P., and Kornfeld, S. (2003) Phosphorylation-induced Conformational Changes Regulate GGAs 1 and 3 Function at the Trans-Golgi Network Journal of Biological Chemistry **278**, 14543-14549 10.1074/jbc.m212543200

25. Doray, B., Ghosh, P., Griffith, J., Geuze, H. J., and Kornfeld, S. (2002) Cooperation of GGAs and AP-1 in packaging MPRs at the trans-Golgi network Science **297**, 1700-1703 10.1126/science.1075327

26. Raote, I., Saxena, S., and Malhotra, V. (2023) Sorting and Export of Proteins at the Endoplasmic Reticulum Cold Spring Harbor Perspectives in Biology **15**, a041258 10.1101/cshperspect.a041258

27. Kovtun, O., Leneva, N., Bykov, Y. S., Ariotti, N., Teasdale, R. D., Schaffer, M. *et al.* (2018) Structure of the membrane-assembled retromer coat determined by cryo-electron tomography Nature **561**, 561-564 10.1038/s41586-018-0526-z

28. Seaman, M. N. J. (2004) Cargo-selective endosomal sorting for retrieval to the Golgi requires retromer Journal of Cell Biology **165**, 111-122 10.1083/jcb.200312034

29. Hong, W. (2005) SNAREs and traffic Biochim Biophys Acta **1744**, 493-517, https://www.ncbi.nlm.nih.gov/pubmed/16038056

30. Brown, F. C., and Pfeffer, S. R. (2010) An update on transport vesicle tethering Molecular Membrane Biology **27**, 457-461 10.3109/09687688.2010.501765

31. SüDhof, T. C., and Rothman, J. E. (2009) Membrane Fusion: Grappling with SNARE and SM Proteins Science **323**, 474-477 10.1126/science.1161748

32. Kjos, I., Vestre, K., Guadagno, N. A., Borg Distefano, M., and Progida, C. (2018) Rab and Arf proteins at the crossroad between membrane transport and cytoskeleton dynamics In Biochimica et Biophysica Acta (BBA) - Molecular Cell Research, Elsevier, 1397-1409

33. Stenmark, H. (2009) Rab GTPases as coordinators of vesicle traffic In Nature Reviews Molecular Cell Biology, Nature Publishing Group, 513-525

34. Homma, Y., Hiragi, S., and Fukuda, M. (2021) Rab family of small GTPases: an updated view on their regulation and functions The FEBS Journal **288**, 36-55 10.1111/febs.15453

35. Matsui, Y., Kikuchi, A., Araki, S., Hata, Y., Kondo, J., Teranishi, Y. *et al.* (1990) Molecular cloning and characterization of a novel type of regulatory protein (GDI) for smg p25A, a ras p21-like GTP-binding protein Mol Cell Biol **10**, 4116-4122 10.1128/mcb.10.8.4116-4122.1990

36. Gerondopoulos, A., Langemeyer, L., Liang, J.-R., Linford, A., and Barr, F. A. (2012) BLOC-3 mutated in Hermansky-Pudlak syndrome is a Rab32/38 guanine nucleotide exchange factor. In Current biology : CB, Elsevier, 2135-2139

37. Gulbranson, D. R., Davis, E. M., Demmitt, B. A., Ouyang, Y., Ye, Y., Yu, H. *et al.* (2017) RABIF/MSS4 is a Rab-stabilizing holdase chaperone required for GLUT4 exocytosis. In Proceedings of the National Academy of Sciences of the United States of America, National Academy of Sciences, E8224-E8233

38. McCullough, J., Frost, A., and Sundquist, W. I. (2018) Structures, Functions, and Dynamics of ESCRT-III/Vps4 Membrane Remodeling and Fission Complexes Annual

Review of Cell and Developmental Biology **34**, 85-109 10.1146/annurev-cellbio-100616-060600

39. Simonetti, B., and Cullen, P. J. (2019) Actin-dependent endosomal receptor recycling In Current Opinion in Cell Biology, Elsevier Current Trends, 22-33

40. Seaman, M. N. J., Michael Mccaffery, J., and Emr, S. D. (1998) A Membrane Coat Complex Essential for Endosome-to-Golgi Retrograde Transport in Yeast Journal of Cell Biology **142**, 665-681 10.1083/jcb.142.3.665

41. Strochlic, T. I., Setty, T. G., Sitaram, A., and Burd, C. G. (2007) Grd19/Snx3p functions as a cargo-specific adapter for retromer-dependent endocytic recycling Journal of Cell Biology **177**, 115-125 10.1083/jcb.200609161

42. Gallon, M., Clairfeuille, T., Steinberg, F., Mas, C., Ghai, R., Sessions, R. B. *et al.* (2014) A unique PDZ domain and arrestin-like fold interaction reveals mechanistic details of endocytic recycling by SNX27-retromer Proceedings of the National Academy of Sciences **111**, E3604-E3613 10.1073/pnas.1410552111

43. Jia, D., Gomez, T. S., Billadeau, D. D., and Rosen, M. K. (2012) Multiple repeat elements within the FAM21 tail link the WASH actin regulatory complex to the retromer Molecular Biology of the Cell **23**, 2352-2361 10.1091/mbc.e11-12-1059

44. Suzuki, S. W., Oishi, A., Nikulin, N., Jorgensen, J. R., Baile, M. G., and Emr, S. D. (2021) A PX-BAR protein Mvp1/SNX8 and a dynamin-like GTPase Vps1 drive endosomal recycling In eLife,

45. Ripoll, L., Heiligenstein, X., Hurbain, I., Domingues, L., Figon, F., Petersen, K. J. *et al.* (2018) Myosin VI and branched actin filaments mediate membrane constriction and fission of melanosomal tubule carriers In The Journal of Cell Biology, jcb.201709055

46. Simonetti, B., Danson, C. M., Heesom, K. J., and Cullen, P. J. (2017) Sequence-dependent cargo recognition by SNX-BARs mediates retromer-independent transport of CI-MPR Journal of Cell Biology **216**, 3695-3712 10.1083/jcb.201703015

47. Ma, M., Burd, C. G., and Chi, R. J. (2017) Distinct complexes of yeast Snx4 family SNX-BARs mediate retrograde trafficking of Snc1 and Atg27 Traffic **18**, 134-144 10.1111/tra.12462

48. McNally, K. E., Faulkner, R., Steinberg, F., Gallon, M., Ghai, R., Pim, D. *et al.* (2017) Retriever is a multiprotein complex for retromer-independent endosomal cargo recycling Nature Cell Biology **19**, 1214-1225 10.1038/ncb3610

49. Banushi, B., and Simpson, F. (2022) Overlapping Machinery in Lysosome-Related Organelle Trafficking: A Lesson from Rare Multisystem Disorders In Cells, Cells,

50. Delevoye, C., Marks, M. S., and Raposo, G. (2019) Lysosome-related organelles as functional adaptations of the endolysosomal system In Current Opinion in Cell Biology, Elsevier Current Trends, 147-158

51. Guillot, L., Nathan, N., Tabary, O., Thouvenin, G., Le Rouzic, P., Corvol, H. *et al.* (2013) Alveolar epithelial cells: master regulators of lung homeostasis Int J Biochem Cell Biol **45**, 2568-2573 10.1016/j.biocel.2013.08.009

52. Mahanty, S., and Setty, S. R. G. (2021) Epidermal Lamellar Body Biogenesis: Insight Into the Roles of Golgi and Lysosomes Front Cell Dev Biol **9**, 701950 10.3389/fcell.2021.701950

53. Sharda, A., and Flaumenhaft, R. (2018) The life cycle of platelet granules F1000Research **7**, 236 10.12688/f1000research.13283.1

54. Ham, H., Medlyn, M., and Billadeau, D. D. (2022) Locked and Loaded: Mechanisms Regulating Natural Killer Cell Lytic Granule Biogenesis and Release Front Immunol **13**, 871106 10.3389/fimmu.2022.871106

55. Le, L., Sirés-Campos, J., Raposo, G., Delevoye, C., and Marks, M. S. (2021) Melanosome Biogenesis in the Pigmentation of Mammalian Skin In Integrative and Comparative Biology, Oxford University Press (OUP),

56. Raposo, G., Tenza, D., Murphy, D. M., Berson, J. F., and Marks, M. S. (2001) Distinct protein sorting and localization to premelanosomes, melanosomes, and lysosomes in pigmented melanocytic cells. In The Journal of cell biology, The Rockefeller University Press, 809-824

57. Hermansky, F., and Pudlak, P. (1959) Albinism associated with hemorrhagic diathesis and unusual pigmented reticular cells in the bone marrow: report of two cases with histochemical studies Blood **14**, 162-169, https://www.ncbi.nlm.nih.gov/pubmed/13618373

58. Di Pietro, S. M., Falcón-Pérez, J. M., Tenza, D., Setty, S. R. G., Marks, M. S., Raposo, G. *et al.* (2006) BLOC-1 Interacts with BLOC-2 and the AP-3 Complex to Facilitate Protein Trafficking on Endosomes Molecular Biology of the Cell **17**, 4027-4038 10.1091/mbc.e06-05-0379

59. Setty, S. R. G., Tenza, D., Truschel, S. T., Chou, E., Sviderskaya, E. V., Theos, A. C. *et al.* (2007) BLOC-1 Is Required for Cargo-specific Sorting from Vacuolar Early Endosomes toward Lysosome-related Organelles Molecular Biology of the Cell **18**, 768-780 10.1091/mbc.e06-12-1066

60. Falcón-Pérez, J. M., Starcevic, M., Gautam, R., and Dell'Angelica, E. C. (2002) BLOC-1, a Novel Complex Containing the Pallidin and Muted Proteins Involved in the Biogenesis of Melanosomes and Platelet-dense Granules Journal of Biological Chemistry **277**, 28191-28199 10.1074/jbc.m204011200

61. Pennamen, P., Le, L., Tingaud-Sequeira, A., Fiore, M., Bauters, A., Van Duong Béatrice, N. *et al.* (2020) BLOC1S5 pathogenic variants cause a new type of Hermansky–Pudlak syndrome Genetics in Medicine **22**, 1613-1622 10.1038/s41436-020-0867-5

62. Delevoye, C., Heiligenstein, X., Ripoll, L., Gilles-Marsens, F., Megan, Ricardo *et al.* (2016) BLOC-1 Brings Together the Actin and Microtubule Cytoskeletons to Generate Recycling Endosomes Current Biology **26**, 1-13 10.1016/j.cub.2015.11.020

63. Di Pietro, S. M., Falcón-Pérez, J. M., and Dell'Angelica, E. C. (2004) Characterization of BLOC-2, a Complex Containing the Hermansky-Pudlak Syndrome Proteins HPS3, HPS5 and HPS6 Traffic **5**, 276-283 10.1111/j.1600-0854.2004.0171.x

64. Dennis, M. K., Mantegazza, A. R., Snir, O. L., Tenza, D., Acosta-Ruiz, A., Delevoye, C. *et al.* (2015) BLOC-2 targets recycling endosomal tubules to melanosomes for cargo delivery Journal of Cell Biology **209**, 563-577 10.1083/jcb.201410026

65. Gerondopoulos, A., Langemeyer, L., Liang, J. R., Linford, A., and Barr, F. A. (2012) BLOC-3 mutated in Hermansky-Pudlak syndrome is a Rab32/38 guanine nucleotide exchange factor In Current Biology, Elsevier Ltd, 2135-2139

66. Bultema, J. J., Ambrosio, A. L., Burek, C. L., and Di Pietro, S. M. (2012) BLOC-2, AP-3, and AP-1 proteins function in concert with Rab38 and Rab32 proteins to mediate protein trafficking to lysosome-related organelles In Journal of Biological Chemistry, 19550-19563

67. Dennis, M. K., Delevoye, C., Acosta-Ruiz, A., Hurbain, I., Romao, M., Hesketh, G. G. *et al.* (2016) BLOC-1 and BLOC-3 regulate VAMP7 cycling to and from melanosomes via distinct tubular transport carriers Journal of Cell Biology **214**, 293-308 10.1083/jcb.201605090

68. Aguilar, A., Weber, J., Boscher, J., Freund, M., Ziessel, C., Eckly, A. *et al.* (2019) Combined deficiency of RAB32 and RAB38 in the mouse mimics Hermansky-Pudlak syndrome and critically impairs thrombosis In Blood Advances, American Society of Hematology, 2368-2380

69. Pastural, E., Barrat, F. J., Dufourcq-Lagelouse, R., Certain, S., Sanal, O., Jabado, N. *et al.* (1997) Griscelli disease maps to chromosome 15q21 and is associated with mutations in the Myosin-Va gene Nature Genetics **16**, 289-292 10.1038/ng0797-289

70. Ménasché, G., Pastural, E., Feldmann, J., Certain, S., Ersoy, F., Dupuis, S. *et al.* (2000) Mutations in RAB27A cause Griscelli syndrome associated with haemophagocytic syndrome Nature Genetics **25**, 173-176 10.1038/76024

71. Ménasché, G., Ho, C. H., Sanal, O., Feldmann, J., Tezcan, I., Ersoy, F. *et al.* (2003) Griscelli syndrome restricted to hypopigmentation results from a melanophilin defect (GS3) or a MYO5A F-exon deletion (GS1) **112**, 450-456 10.1172/jci18264

72. Bahadoran, P., Aberdam, E., Mantoux, F., Buscà, R., Bille, K., Yalman, N. *et al.* (2001) Rab27a: A Key to Melanosome Transport in Human Melanocytes Journal of Cell Biology **152**, 843-850 10.1083/jcb.152.4.843

73. Wu, X., Bowers, B., Rao, K., Wei, Q., and Hammer, J. A. (1998) Visualization of Melanosome Dynamics within Wild-Type and Dilute Melanocytes Suggests a Paradigm for Myosin V Function In Vivo Journal of Cell Biology **143**, 1899-1918 10.1083/jcb.143.7.1899

74. Nagashima, K., Torii, S., Yi, Z., Igarashi, M., Okamoto, K., Takeuchi, T. *et al.* (2002) Melanophilin directly links Rab27a and myosin Va through its distinct coiled-coil regions FEBS Lett **517**, 233-238 10.1016/s0014-5793(02)02634-0

75. Oberhofer, A., Spieler, P., Rosenfeld, Y., Stepp, W. L., Cleetus, A., Hume, A. N. *et al.* (2017) Myosin Va's adaptor protein melanophilin enforces track selection on the microtubule and actin networks in vitro. In Proceedings of the National Academy of Sciences of the United States of America, National Academy of Sciences, E4714-E4723

76. Sanborn, K. B., Rak, G. D., Maru, S. Y., Demers, K., Difeo, A., Martignetti, J. A. *et al.* (2009) Myosin IIA associates with NK cell lytic granules to enable their interaction with F-actin and function at the immunological synapse J Immunol **182**, 6969-6984 10.4049/jimmunol.0804337

77. Bultema, J. J., and Pietro, S. M. D. (2013) Cell type-specific Rab32 and Rab38 cooperate with the ubiquitous lysosome biogenesis machinery to synthesize specialized lysosome-related organelles 16-21

78. Moreiras, H., Seabra, M. C., and Barral, D. C. (2021) Melanin Transfer in the Epidermis: The Pursuit of Skin Pigmentation Control Mechanisms Int J Mol Sci **22**, 10.3390/ijms22094466

79. Byers, H. R., Maheshwary, S., Amodeo, D. M., and Dykstra, S. G. (2003) Role of cytoplasmic dynein in perinuclear aggregation of phagocytosed melanosomes and supranuclear melanin cap formation in human keratinocytes J Invest Dermatol **121**, 813-820 10.1046/j.1523-1747.2003.12481.x

80. Kiprono, S. K., Chaula, B. M., and Beltraminelli, H. (2014) Histological review of skin cancers in African Albinos: a 10-year retrospective review BMC Cancer **14**, 157 10.1186/1471-2407-14-157

81. Gloster, H. M., Jr., and Neal, K. (2006) Skin cancer in skin of color J Am Acad Dermatol **55**, 741-760; quiz 761-744 10.1016/j.jaad.2005.08.063

82. Reissmann, M., and Ludwig, A. (2013) Pleiotropic effects of coat colour-associated mutations in humans, mice and other mammals Semin Cell Dev Biol **24**, 576-586 10.1016/j.semcdb.2013.03.014

83. Grønskov, K., Ek, J., and Brondum-Nielsen, K. (2007) Oculocutaneous albinism In Orphanet Journal of Rare Diseases, BioMed Central, 43

84. D'Alba, L., and Shawkey, M. D. (2019) Melanosomes: Biogenesis, Properties, and Evolution of an Ancient Organelle In Physiological Reviews, American Physiological Society Bethesda, MD 1-19

85. Raper, H. S., and Wormall, A. (1923) The Tyrosinase-Tyrosine Reaction Biochem J **17**, 454-469 10.1042/bj0170454

86. Raper, H. S. (1926) The Tyrosinase-Tyrosine Reaction: Production of l-3.4-Dihydroxyphenylalanine from Tyrosine Biochem J **20**, 735-742 10.1042/bj0200735

87. Raper, H. S. (1927) The Tyrosinase-tyrosine Reaction: Production from Tyrosine of 5: 6-Dihydroxyindole and 5: 6-Dihydroxyindole-2-carboxylic Acid-the Precursors of Melanin Biochem J **21**, 89-96 10.1042/bj0210089

88. Spritz, R. A., Ho, L., Furumura, M., and Hearing, V. J., Jr. (1997) Mutational analysis of copper binding by human tyrosinase J Invest Dermatol **109**, 207-212 10.1111/1523-1747.ep12319351

89. Petris, M. J., Strausak, D., and Mercer, J. F. (2000) The Menkes copper transporter is required for the activation of tyrosinase Hum Mol Genet **9**, 2845-2851 10.1093/hmg/9.19.2845

90. Simon, J. D., andPeles, D. N. (2010) The Red and the Black Accounts of Chemical Research **43**, 1452-1460 10.1021/ar100079y

91. Pennamen, P., Tingaud-Sequeira, A., Gazova, I., Keighren, M., McKie, L., Marlin, S. *et al.* (2020) Dopachrome tautomerase variants in patients with oculocutaneous albinism In bioRxiv, Cold Spring Harbor Laboratory, 2020.2006.2026.171223

92. Wagatsuma, T., Suzuki, E., Shiotsu, M., Sogo, A., Nishito, Y., Ando, H. *et al.* (2023) Pigmentation and TYRP1 expression are mediated by zinc through the early secretory pathway-resident ZNT proteins Communications Biology **6**, 10.1038/s42003-023-04640-5

93. Sirés-Campos, J., Lambertos, A., Cédric Delevoye, Raposo, G., Bennett, D. C., Sviderskaya, E. *et al.* (2021) Mahogunin Ring Finger 1 regulates pigmentation by controlling the pH of melanosomes in melanocytes and melanoma cells In Cellular and Molecular Life Sciences 2021 79:1, Springer, 1-21

94. Borovanský, J., Mommaas, A. M., Smit, N. P. M., Eygendaal, D., Winder, A. J., Vermeer, B. J. *et al.* (1997) Melanogenesis in transfected fibroblasts induces lysosomal activation Archives of Dermatological Research **289**, 145-150 10.1007/s004030050170

95. Ancans, J., Tobin, D. J., Hoogduijn, M. J., Smit, N. P., Wakamatsu, K., and Thody, A. J. (2001) Melanosomal pH controls rate of melanogenesis, eumelanin/phaeomelanin ratio and melanosome maturation in melanocytes and melanoma cells Exp Cell Res **268**, 26-35 10.1006/excr.2001.5251

96. Berson, J. F., Harper, D. C., Tenza, D., Raposo, G., and Marks, M. S. (2001) Pmel17 initiates premelanosome morphogenesis within multivesicular bodies In Molecular Biology of the Cell, 3451-3464

97. Fowler, D. M., Koulov, A. V., Alory-Jost, C., Marks, M. S., Balch, W. E., and Kelly, J. W. (2005) Functional Amyloid Formation within Mammalian Tissue PLoS Biology **4**, e6 10.1371/journal.pbio.0040006

98. Watt, B., van Niel, G., Raposo, G., and Marks, M. S. (2013) PMEL: a pigment cell-specific model for functional amyloid formation In Pigment Cell & Melanoma Research, John Wiley & Sons, Ltd, 300-315

99. Raposo, G., and Marks, M. S. (2007) Melanosomes--dark organelles enlighten endosomal membrane transport. In Nature reviews. Molecular cell biology, NIH Public Access, 786-797

100. Leonhardt, R. M., Vigneron, N., Rahner, C., and Cresswell, P. (2011) Proprotein convertases process Pmel17 during secretion In The Journal of biological chemistry, J Biol Chem, 9321-9337

101. Berson, J. F., Theos, A. C., Harper, D. C., Tenza, D., Raposo, G., and Marks, M. S. (2003) Proprotein convertase cleavage liberates a fibrillogenic fragment of a resident glycoprotein to initiate melanosome biogenesis In Journal of Cell Biology, The Rockefeller University Press, 521-533

102. Kummer, M. P., Maruyama, H., Huelsmann, C., Baches, S., Weggen, S., and Koo, E. H. (2009) Formation of Pmel17 Amyloid Is Regulated by Juxtamembrane Metalloproteinase Cleavage, and the Resulting C-terminal Fragment Is a Substrate for γ-Secretase In Journal of Biological Chemistry, Elsevier, 2296-2306

103. Rochin, L., Hurbain, I., Serneels, L., Fort, C., Watt, B., Leblanc, P. *et al.* (2013) BACE2 processes PMEL to form the melanosome amyloid matrix in pigment cells In Proceedings of the National Academy of Sciences of the United States of America, National Academy of Sciences, 10658-10663

104. van Niel, G., Charrin, S., Simoes, S., Romao, M., Rochin, L., Saftig, P. *et al.* (2011) The Tetraspanin CD63 Regulates ESCRT-Independent and -Dependent Endosomal Sorting during Melanogenesis In Developmental Cell, Cell Press, 708-721

105. Sannerud, R., Esselens, C., Ejsmont, P., Mattera, R., Rochin, L., Arun *et al.* (2016) Restricted Location of PSEN2/γ-Secretase Determines Substrate Specificity and Generates an Intracellular Aβ Pool Cell **166**, 193-208 10.1016/j.cell.2016.05.020

106. Bissig, C., Croisé, P., Heiligenstein, X., Hurbain, I., Lenk, G. M., Kaufman, E. *et al.* (2019) The PIKfyve complex regulates the early melanosome homeostasis required for physiological amyloid formation. In Journal of cell science, The Company of Biologists Ltd, jcs229500

107. Ho, T., Watt, B., Spruce, L. A., Seeholzer, S. H., and Marks, M. S. (2016) The Kringle-like Domain Facilitates Post-endoplasmic Reticulum Changes to Premelanosome Protein (PMEL) Oligomerization and Disulfide Bond Configuration and Promotes Amyloid Formation In The Journal of biological chemistry, J Biol Chem, 3595-3612

108. Leonhardt, R. M., Vigneron, N., Hee, J. S., Graham, M., and Cresswell, P. (2013) Critical residues in the PMEL/Pmel17 N-terminus direct the hierarchical assembly of melanosomal fibrils In Molecular Biology of the Cell, The American Society for Cell Biology 964-981

109. Kawaguchi, M., Hozumi, Y., and Suzuki, T. (2015) ADAM protease inhibitors reduce melanogenesis by regulating PMEL17 processing in human melanocytes In Journal of Dermatological Science, Elsevier Ireland Ltd, 133-142

110. Llanos, R. M., and Mercer, J. F. (2002) The molecular basis of copper homeostasis copper-related disorders DNA Cell Biol **21**, 259-270 10.1089/104454902753759681

111. Maung, M. T., Carlson, A., Olea-Flores, M., Elkhadragy, L., Schachtschneider, K. M., Navarro-Tito, N. *et al.* (2021) The molecular and cellular basis of copper dysregulation

and its relationship with human pathologies FASEB J **35**, e21810 10.1096/fj.202100273RR

112. Mercer, J. F. B., Grimes, A., Ambrosini, L., Lockhart, P., Paynter, J. A., Dierick, H. *et al.* (1994) Mutations in the murine homologue of the Menkes gene in dappled and blotchy mice Nature Genetics **6**, 374-378 10.1038/ng0494-374

113. Setty, S. R. G., Tenza, D., Sviderskaya, E. V., Bennett, D. C., Raposo, G., and Marks, M. S. (2008) Cell-specific ATP7A transport sustains copper-dependent tyrosinase activity in melanosomes. In Nature, NIH Public Access, 1142-1146

114. Phillips-Krawczak, C. A., Singla, A., Starokadomskyy, P., Deng, Z., Osborne, D. G., Li, H. *et al.* (2015) COMMD1 is linked to the WASH complex and regulates endosomal trafficking of the copper transporter ATP7A In Molecular Biology of the Cell, American Society for Cell Biology, 91-103

115. Lai, X., Wichers, H. J., Soler-Lopez, M., and Dijkstra, B. W. (2017) Structure of Human Tyrosinase Related Protein 1 Reveals a Binuclear Zinc Active Site Important for Melanogenesis Angewandte Chemie International Edition **56**, 9812-9815 10.1002/anie.201704616

116. Hédan, B., Cadieu, E., Botherel, N., Dufaure De Citres, C., Letko, A., Rimbault, M. *et al.* (2019) Identification of a Missense Variant in MFSD12 Involved in Dilution of Phaeomelanin Leading to White or Cream Coat Color in Dogs Genes **10**, 386 10.3390/genes10050386

117. Fuller, B. B., Spaulding, D. T., and Smith, D. R. (2001) Regulation of the catalytic activity of preexisting tyrosinase in black and Caucasian human melanocyte cell cultures Exp Cell Res **262**, 197-208 10.1006/excr.2000.5092

118. Bellono, N. W., Escobar, I. E., Lefkovith, A. J., Marks, M. S., and Oancea, E. (2014) An intracellular anion channel critical for pigmentation In eLife, e04543

119. Sturm, R. A., Duffy, D. L., Zhao, Z. Z., Leite, F. P. N., Stark, M. S., Nicholas *et al.* (2008) A Single SNP in an Evolutionary Conserved Region within Intron 86 of the HERC2 Gene Determines Human Blue-Brown Eye Color The American Journal of Human Genetics **82**, 424-431 10.1016/j.ajhg.2007.11.005

120. Sulem, P., Gudbjartsson, D. F., Stacey, S. N., Helgason, A., Rafnar, T., Jakobsdottir, M. *et al.* (2008) Two newly identified genetic determinants of pigmentation in Europeans In Nature Genetics, 835-837

121. Ambrosio, A. L., Boyle, J. A., Aradi, A. E., Christian, K. A., and Di Pietro, S. M. (2016) TPC2 controls pigmentation by regulating melanosome pH and size In Proceedings of the National Academy of Sciences, 5622-5627

122. Bellono, N. W., Escobar, I. E., and Oancea, E. (2016) A melanosomal two-pore sodium channel regulates pigmentation In Scientific Reports, Nature Publishing Group, 1-11

123. Netcharoensirisuk, P., Abrahamian, C., Tang, R., Chen, C.-C., Rosato, A. S., Beyers, W. *et al.* (2021) Flavonoids increase melanin production and reduce proliferation, migration

and invasion of melanoma cells by blocking endolysosomal/melanosomal TPC2 In Scientific Reports, Sci Rep, 8515

124. Chao, Y.-K., Schludi, V., Chen, C.-C., Butz, E., Nguyen, O. N. P., Müller, M. *et al.* (2017) TPC2 polymorphisms associated with a hair pigmentation phenotype in humans result in gain of channel function by independent mechanisms In Proceedings of the National Academy of Sciences, 201705739

125. Lin-Moshier, Y., Keebler, M. V., Hooper, R., Boulware, M. J., Liu, X., Churamani, D. *et al.* (2014) The Two-pore channel (TPC) interactome unmasks isoform-specific roles for TPCs in endolysosomal morphology and cell pigmentation In Proceedings of the National Academy of Sciences, 13087-13092

126. Zhang, J., Guan, X., Shah, K., and Yan, J. (2021) Lsm12 is an NAADP receptor and a two-pore channel regulatory protein required for calcium mobilization from acidic organelles In Nature Communications 2021 12:1, Nature Publishing Group, 1-13

127. Wang, Q., Wang, Z., Wang, Y., Qi, Z., Bai, D., Wang, C. *et al.* (2023) A gain-of-function TPC2 variant R210C increases affinity to PI(3,5)P2 and causes lysosome acidification and hypopigmentation Nature Communications **14**, 10.1038/s41467-023-35786-9

128. Lin-Moshier, Y., Keebler, M. V., Hooper, R., Boulware, M. J., Liu, X., Churamani, D. *et al.* (2014) The Two-pore channel (TPC) interactome unmasks isoform-specific roles for TPCs in endolysosomal morphology and cell pigmentation Proc Natl Acad Sci U S A **111**, 13087-13092 10.1073/pnas.1407004111

129. Grimm, C., Holdt, L. M., Chen, C.-C., Hassan, S., Müller, C., Jörs, S. *et al.* (2014) High susceptibility to fatty liver disease in two-pore channel 2-deficient mice In Nature Communications, Nature Publishing Group, 4699

130. Hockey, L. N., Kilpatrick, B. S., Eden, E. R., Lin-Moshier, Y., Brailoiu, G. C., Brailoiu, E. *et al.* (2015) Dysregulation of lysosomal morphology by pathogenic LRRK2 is corrected by TPC2 inhibition. In Journal of cell science, The Company of Biologists Ltd, 232-238

131. Cang, C., Zhou, Y., Navarro, B., Seo, Y. J., Aranda, K., Shi, L. *et al.* (2013) mTOR regulates lysosomal ATP-sensitive two-pore Na(+) channels to adapt to metabolic state Cell **152**, 778-790 10.1016/j.cell.2013.01.023

132. Ogunbayo, O. A., Duan, J., Xiong, J., Wang, Q., Feng, X., Ma, J. *et al.* (2018) mTORC1 controls lysosomal Ca2+ release through the two-pore channel TPC2. In Science signaling, NIH Public Access,

133. Gómez-Suaga, P., Luzón-Toro, B., Churamani, D., Zhang, L., Bloor-Young, D., Patel, S. *et al.* (2012) Leucine-rich repeat kinase 2 regulates autophagy through a calcium-dependent pathway involving NAADP. In Human molecular genetics, Oxford University Press, 511-525

134. Wei, A. H., Zang, D. J., Zhang, Z., Liu, X. Z., He, X., Yang, L. *et al.* (2013) Exome sequencing identifies SLC24A5 as a candidate gene for nonsyndromic oculocutaneous albinism In Journal of Investigative Dermatology, Nature Publishing Group, 1834-1840

135. Newton, J. M., Cohen-Barak, O., Hagiwara, N., Gardner, J. M., Davisson, M. T., King, R. A. *et al.* (2001) Mutations in the Human Orthologue of the Mouse underwhite Gene (uw) Underlie a New Form of Oculocutaneous Albinism, OCA4 In The American Journal of Human Genetics, 981-988

136. Bartolke, R., Heinisch, J. J., Wieczorek, H., and Vitavska, O. (2014) Proton-associated sucrose transport of mammalian solute carrier family 45: an analysis in Saccharomyces cerevisiae Biochem J **464**, 193-201 10.1042/BJ20140572

137. Le, L., Escobar, I. E., Ho, T., Lefkovith, A. J., Latteri, E., Haltaufderhyde, K. D. *et al.* (2020) SLC45A2 protein stability and regulation of melanosome pH determine melanocyte pigmentation In Molecular Biology of the Cell, American Society for Cell Biology, 2687-2702

138. Ginger, R. S., Askew, S. E., Ogborne, R. M., Wilson, S., Ferdinando, D., Dadd, T. *et al.* (2008) SLC24A5 encodes a trans-Golgi network protein with potassium-dependent sodium-calcium exchange activity that regulates human epidermal melanogenesis. In The Journal of biological chemistry, American Society for Biochemistry and Molecular Biology, 5486-5495

139. Lamason, R. L., Mohideen, M. A., Mest, J. R., Wong, A. C., Norton, H. L., Aros, M. C. *et al.* (2005) SLC24A5, a putative cation exchanger, affects pigmentation in zebrafish and humans Science **310**, 1782-1786 10.1126/science.1116238

140. Rogasevskaia, T. P., Szerencsei, R. T., Jalloul, A. H., Visser, F., Winkfein, R. J., and Schnetkamp, P. P. M. (2019) Cellular localization of the K(+) -dependent Na(+) -Ca(2+) exchanger NCKX5 and the role of the cytoplasmic loop in its distribution in pigmented cells Pigment Cell Melanoma Res **32**, 55-67 10.1111/pcmr.12723

141. Zhang, Z., Gong, J., Sviderskaya, E. V., Wei, A., and Li, W. (2019) Mitochondrial NCKX5 regulates melanosomal biogenesis and pigment production J Cell Sci **132**, 10.1242/jcs.232009

142. Beyers, W. C., Detry, A. M., and Di Pietro, S. M. (2022) OCA7 is a melanosome membrane protein that defines pigmentation by regulating early stages of melanosome biogenesis J Biol Chem **298**, 102669 10.1016/j.jbc.2022.102669

143. Guo, Y. Y., Gao, Y., Hu, Y. R., Zhao, Y., Jiang, D., Wang, Y. *et al.* (2022) The Transient Receptor Potential Vanilloid 2 (TRPV2) Channel Facilitates Virus Infection Through the Ca2+-LRMDA Axis in Myeloid Cells In Advanced Science, Wiley-Blackwell,

CHAPTER 2

THE TPC2 PROXIMITY INTERACTOME IN MELANOCYTES REVEALS TSPAN10 AS A NOVEL REGULATOR OF MELANOSOME BIOGENESIS

Summary

Multiple polymorphisms in the cation channel, TPC2, are highly associated with hair color in genome-wide association studies (GWAS). Using cell models, our lab and others discovered TPC2 localizes to melanosomes, the melanin-synthesizing organelles within melanocytes, where it influences pigmentation via regulation of melanosomal pH, melanosome size, and tyrosinase expression. Here, we utilize a promiscuous biotin ligase fused to TPC2 to identify the TPC2 proximity interactome in MNT1 cells, discovering novel melanosome associated proteins. Using Airyscan confocal fluorescence imaging, Phospholipase D1 (PLD1), Synaptic Vesicle Glycoprotein 2A (SV2A), and Tetraspanin 10 (TSPAN10) were found to colocalize with TPC2-EGFP at melanosomes. Newly generated TSPAN10 knockout (KO) MNT1 cells exhibit hypopigmentation, consistent with recent bioinformatic studies finding an association between TSPAN10 and pigmentation. Immunoblotting for lysosomal and melanosomal proteins reveals defects in premelanosome protein (PMEL) processing and levels of active Cathepsin D. Thin-section electron microscopy analysis of TSPAN10 KO cells revealed an overabundance of aberrant melanosomes with dense melanin aggregates lacking ordered pre-melanosome protein (PMEL) fibrils required for normal melanin deposition. Interestingly, we found TSPAN10 controls expression and maturation of A Disintegrin And Metalloproteinase domain-containing protein 10 (ADAM10), a protease that regulates pigmentation and contributes to PMEL processing. Together, our dataset provides a fruitful list of novel melanosome membrane proteins and implicates TSPAN10 as a major player of pigmentation via the regulation of melanosomal proteases.

Introduction

Pigmentation, the process of producing dark pigment in eyes, hair, and skin, requires the formation of specialized melanin-synthesizing organelles called melanosomes within melanocytes. In the epidermis, melanin is subsequently transferred to neighboring keratinocytes, forming a supranuclear cap where it serves to protect the nucleus from ultraviolet radiation (1, 2). Pigment production in melanocytes is dependent on a complex interplay of many cellular processes, including the generation of melanosomes, expression, and trafficking of melanogenic enzymes to melanosomes, recycling of membrane trafficking machinery, and tight control of melanosomal ultrastructure, pH, solute transport, and lipid composition (3). While melanin is synthesized by only a small number of rate-limiting enzymes, over 100 genes are associated with various steps of pigmentation, and melanosome biogenesis remains incompletely understood (4, 5).

Multiple single nucleotide polymorphisms (SNPs) in the TPC2 gene are associated with pigmentation, with both M484L and G734E substitutions associated with a shift from brown to blonde hair, and R210C substitution underlying an unusual dominantly inherited albinism (6-8). TPC2 is a cation channel that localizes to the limiting membrane of melanosomes and to a smaller extent endo/lysosomes in melanocytes, where it was found to influence pigmentation by negatively regulating melanosome pH, size, and Tyrosinase activity (9-11). While TPC2 M484L and R210C gain of function substitutions are thought to enhance sensitivity to PI(3,5)P2 mediated channel activation, the cytosol exposed C terminal domain of TPC2 was suggested to regulate TPC2 in a distinct mechanism, perhaps via interaction with protein partners (12). One such example is mTOR, which has been shown to co-immunoprecipitate with TPC2, and mTOR inhibition heightens TPC2 Na^+ conductance in patch-clamped endo-lysosomes, having a greater effect on TPC2 734E over TPC2 734G (12, 13).

Because the TPC2 C terminal domain has access to the cytosol, we hypothesized it may have additional interaction partners that regulate its function in pigmentation. Multiple studies have examined the TPC2 interactome using immunoprecipitation/affinity co-purification with mass spectrometry leading to significant insight about TPC2 function (14-17). For instance, two studies screening for TPC2 interactors identified several membrane trafficking proteins, including Rabs, Syntaxins, and VAMPs as putative interactors supporting a role for TPC2 in membrane fusion events (17, 18). This led to the discovery of a Rab binding domain in the N terminal cytosolic domain of TPC2 functionally important for pigmentation and NAADP evoked calcium signaling in *Xenopus* oocytes (16). Recently a similar affinity co-purification approach discovered Lsm12 as an NAADP receptor required for NAADP evoked calcium release from endo-lysosomes via TPCs (15). Despite these important findings, no study has yet interrogated the TPC2 interactome at the specific context of the melanosome membrane, and none have compared the interactomes of C terminal domain variants. Furthermore, prior mass spectrometry screens relied on affinity purification or co-immunoprecipitation which while insightful, are potentially limited to high affinity interactions, as weak, transient, or context dependent interactions can be lost during wash steps. Therefore, we utilized the proximity biotin ligase labeling system, BioID2, to identify proteins working with or in proximity to TPC2 *in situ* at melanosomes with the goal of identifying new players in melanosome biogenesis and pigmentation (19).

Results

The TPC2 proximity interactome in melanocytes identifies membrane trafficking proteins and actin machinery as novel melanosome associated proteins.

To screen for the TPC2 interactome, TPC2 KO background MNT1 cells were transfected with TPC2-734G-BioID2-HA, associated with brown hair, TPC2-734E-BioID2-HA, associated with blonde hair, or TPC2-ΔCT-BioID2-HA, which lacks the last 25 residues of TPC2 encompassing residue 734, to biotinylate proteins in the TPC2 proximity at melanosome membranes (depicted in **Figure 2.1A**). TPC1 is a member of the TPC family having similar structure to TPC2 but unlike TPC2, does not localize to melanosomes in melanocytes, preferentially localizing to early and recycling endosomes in non-melanocyte cell types (20-22). Thus, to establish specificity, TPC2 KO MNT1 cells expressing TPC1-BioID2-HA, Soluble BioID2-HA, or untransfected cells were used as experimental negative controls in proximity biotinylation experiments. Biotinylated proteins from MNT1 cell RIPA buffer lysates were isolated using Streptactin coated beads to be identified by mass spectrometry or analyzed by immunoblotting. As a proof of concept, probing blots with Steptavidin-HRP indicated many proteins are biotinylated by each expressed form of TPC2-BioID2-HA, having distinct biotinylation patterns compared to extracts from MNT1 cells expressing TPC1-BioID2-HA or from untransfected cells (**Figure 2.1B**).

In total, 836 unique proteins were identified in TPC2-734G-BioID2-HA, TPC2-734E-BioID2-HA, and TPC2-ΔCT-BioID2-HA samples by mass spectrometry, with 651 proteins positively enriched for TPC2 compared to experimental negative controls. To further filter out possible false positives, 30 negative control BioID datasets were obtained from the Resource for Evaluation of Protein Interaction Networks (REPRINT) CRAPome database and included in our mass spectrometry analysis, leaving 326 TPC2 enriched proteins with <1 mean spectral count in 30 CRAPome negative controls (**Figure 2.1C** and **Appendix 1**). Additionally, significance analysis of interactome (SAINT) scores were generated using REPRINT as a measure of

specificity, and each TPC2-BioID2-HA dataset was plotted to visualize highly enriched proteins (**Figure 2.1D**) (23). As expected, TPC2 itself was identified as the most highly enriched protein, and known melanosome associated proteins such as MYO5A were enriched in the TPC2 datasets, confirming successful labeling of proteins on the melanosome limiting membrane. Additionally, LRMDA/OCA7 associated with Oculocutaneous Albinism Type 7 (OCA7) was identified, which we characterized as a peripheral melanosome membrane protein in a related study(24). Several of the most highly enriched proteins, Phospholipase D1 (PLD1), Synaptic Vesicle Glycoprotein 2A (SV2A), Tetraspanin 10 (TSPAN10), and Formin Like 2 (FMNL2) are not known melanosome proteins but have putative membrane trafficking related functions, making them attractive candidates as possible regulators of melanosome biogenesis (**Figure 2.1D**). In validation of the mass spectrometry results, PLD1, SV2A, FMNL2, TSPAN10, and LRMDA were detected by western blot of TPC2-BioID2-HA biotin pulldown samples, but not samples from untransfected cells (**Figure 2.2**).

Next, we compiled the TPC2-734E-BioID2-HA, TPC2-734G-BioID2-HA, and TPC2-ΔCT-BioID2-HA melanosome membrane interactomes and compared them with TPC2 interactomes of former studies that used TPC2 affinity purification or TPC2 immunoprecipitation. Former TPC2 co-purification interactome studies utilized HEK293 cells expressing affinity tag fusion constructs including TPC2-One-StrepTag, GFP-TPC2, or TPC2-EGFP-FLAG (15-17). Although our dataset is largely distinct, TMED9, RCN2, SCAMP3, WDR1, ANXA6, ANXA11, and GDI2 overlapped with TPC2 interactomes determined by others and may be worth investigating in future studies (**Figure 2.1E** and **Appendix 2**). TMED9, RCN2, and SCAMP3 are involved in autophagosome biogenesis, calcineurin signaling, and EGFR recycling, respectively, each of which TPC2 is implicated in (17, 25-29). WDR1 is thought to regulate organization of the Actin cytoskeleton(30). Annexin proteins ANXA6 and ANXA11 are calcium dependent membrane scaffolding proteins(31). In a recent pre-print, ANXA11 was reported to be a calcium dependent tether between lysosomes and

ribonucleoprotein condensates to enable the co-trafficking of lysosomes and RNAs(32). GDI2 is a Rab GDP dissociation inhibitor keeping Rab GTPases in their “off” state(33).

Finally, comparison of TPC2-734E, TPC2-734G, and TPC2-ΔCT interactomes suggests many differential interactors that may contribute to functional differences associated with TPC2 polymorphisms (**Figure 2.1F** and **Appendix 3**). However, for the most highly enriched proteins of interest, we were unable to ascertain a clear preference for one TPC2 variant over the other. Thus, we sought to investigate PLD1, SV2A, TSPAN10, and FMNL2 as potential new melanosome proteins irrespective of their potential interaction with TPC2. Raw data for each TPC2 variant and SAINT Probabilities are listed in **Appendix 4.** Finally, we performed an analysis pooling all TPC2-BioID2-HA datasets to examine the melanosome membrane proteome independent of TPC2 variant expressed (**Appendix 5**).

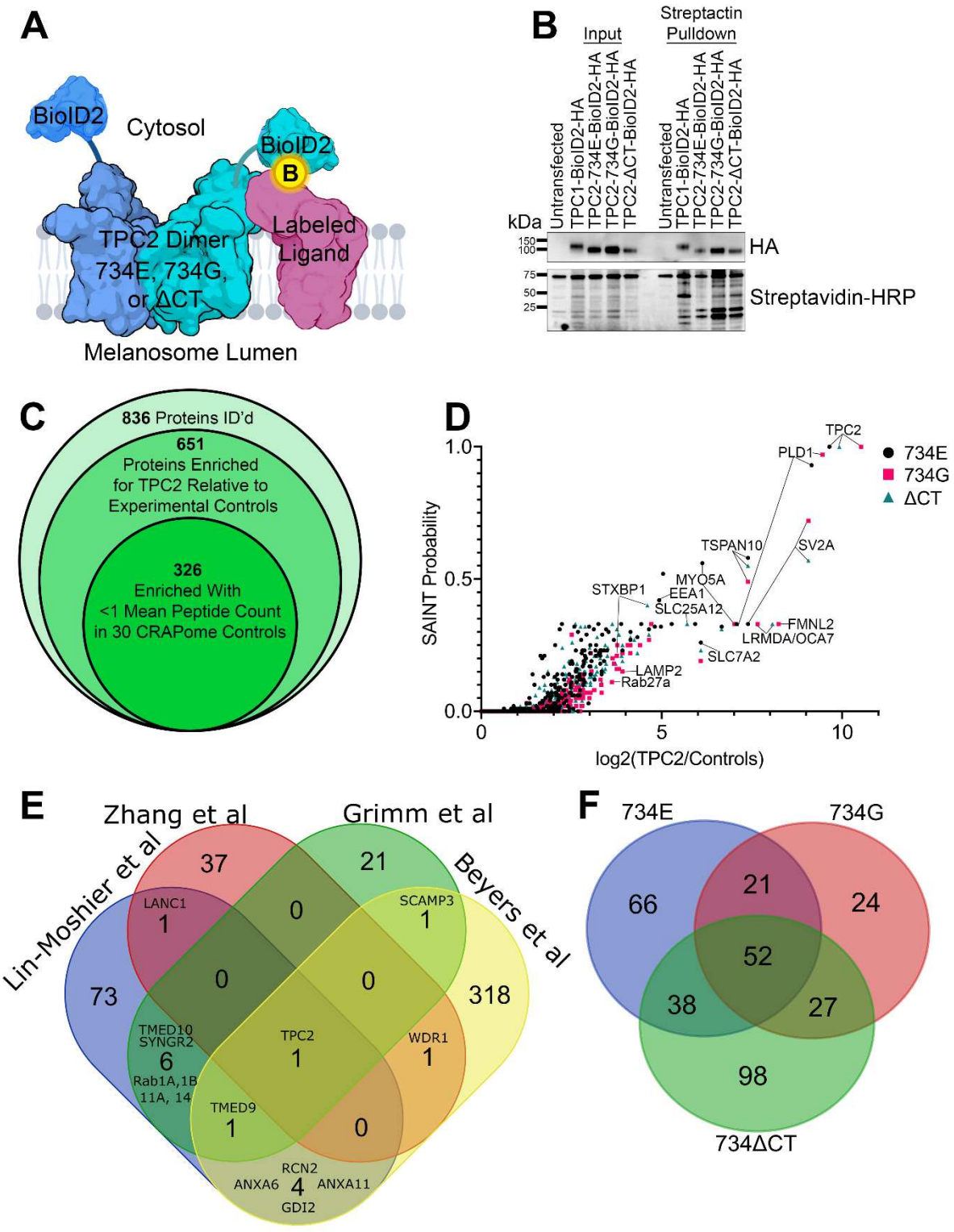

Figure 2.1. The TPC2 proximity interactome in melanocytes identifies membrane trafficking proteins and actin machinery as novel melanosome associated proteins. **(A)** Cartoon depicting TPC2-BioID2 covalently biotinylating an unknown protein in its proximity at the melanosome membrane. BioID2-HA with a flexible linker is fused to the TPC2 C terminus which

is exposed to the cytosol. Three TPC2 variants were used, TPC2-734E-BioID2-HA associated with blonde hair, TPC2-734G-BioID2-HA associated with brown hair, and TPC2-ΔCT-BioID2-HA missing the last 25 residues of the C terminal domain (residues 728-752), and n=3 independent mass spectrometry experiments were performed for each variant. Additional mass spectrometry experiments were performed using negative controls including untransfected cells (n=2), cells expressing soluble BioID2-HA (n=2), and cells expressing TPC1-BioID2-HA (n=1). These 5 negative control interactomes were pooled together for analysis. Experiments were performed in TPC2 KO MNT1 cells to prevent endogenous TPC2 from confounding the analysis. An additional 30 negative control soluble BioID datasets were obtained from the CRAPome database and incorporated into our analysis for a total of n=35 negative experiments. After 24 hours of culture in the presence of Biotin, cells are lysed and biotinylated proteins are pulled down with Streptactin coated beads and identified by mass spectrometry. **(B)** Proof of concept blot indicating TPC1-BioID2-HA, and 734E, 734G, and ΔCT variants of TPC2-BioID2-HA are successfully expressed in MNT1 cells and are pulled down indicating self-biotinylation. Probing with Streptavidin-HRP indicates many proteins are biotinylated and pulled down when BioID2-HA proteins are expressed. **(C)** Venn Diagram depicting filtering of TPC2-BioID2-HA interacting proteins to remove nonspecific false positives. In total 836 unique proteins were identified in Streptactin pulldown mass spectrometry datasets compiled from TPC2-734E-BioID2-HA, TPC2-734G-BioID2-HA and TPC2- ΔCT -BioID2-HA. Of those, 651 were positively enriched for TPC2 relative to 5 experimental negative controls. Of 651 enriched proteins, 326 had less than 1 mean spectral count in 30 CRAPome controls, indicating high specificity. **(D)** Scatter plot of overlayed TPC2-734E, 734G, and ΔCT interactomes. Significance Analysis of INTeractome (SAINT) Probability depicted on the Y axis is a measure of interaction specificity, and log2(TPC2/Controls) depicts TPC2 enrichment. PLD1, TSPAN10, SV2A, and FMNL2 were detected for all three forms of TPC2 analyzed. **(E)** Venn Diagram comparison of the pooled TPC2 interactome determined in the present study with TPC2 interactomes identified in three other studies. SCAMP3, TMED9, WDR1, RCN2, ANXA6, ANXA11, and PDI2 overlapped between our dataset and others. Only positively enriched proteins relative to n=5 experimental negative controls and having <1 mean spectral count in n=30 CRAPome negative control experiments were incorporated into the comparison. For datasets from other papers, all enriched proteins listed were incorporated. **(F)** Venn Diagram comparison of TPC2-734E, TPC2-734G, and TPC2-ΔCT interactomes suggesting each has unique interactions. Only positively enriched proteins relative to n=5 experimental negative controls and having <1 mean spectral count in n=30 CRAPome negative control experiments were incorporated into the comparison.

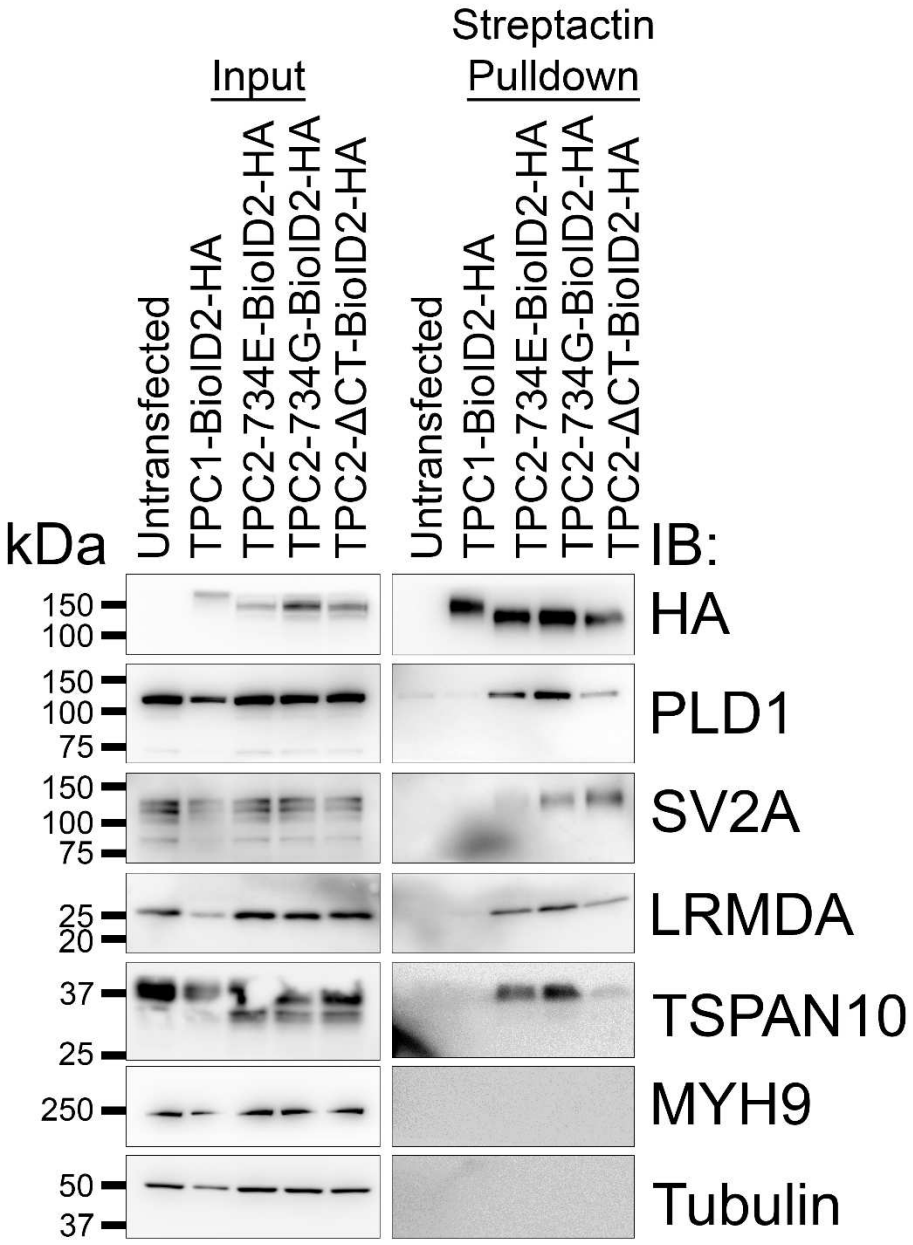

Figure 2.2. PLD1, SV2A, LRMDA, and TSPAN10 are pulled down in TPC2-BioID2-HA Streptactin pulldown assays. Immunoblots of input lysates or Streptactin pulldown samples for untransfected cells, or cells transfected with TPC1-BioID2-HA, or 734E, 734G, or ΔCT Variants of TPC2-BioID2-HA. Immunoblots indicate PLD1, SV2A, LRMDA, and TSPAN10 were enriched in Streptactin pulldowns for TPC2-BioID2-HA expressing cells but not untransfected cells.

PLD1, SV2A and TSPAN10 colocalize with TPC2-EGFP in MNT1 cells

Mass spectrometry data suggested PLD1, SV2A, TSPAN10, and FMNL2 are in proximity to TPC2, but it is important to confirm if they colocalize with TPC2 in cells. TPC2-734G-EGFP or TPC2-734E-EGFP was expressed in a TPC2 KO MNT1 cell background, and cells were fixed and immunostained for endogenous PLD1, SV2A, TSPAN10, as well as actin associated machinery FMNL2, Cortactin (CTTN), Non-Muscle Myosin 2A (MYH9), and Non-Muscle Myosin 2B (MYH10) appearing in our screen. Airyscan super resolution fluorescence microscopy revealed a high degree of colocalization between TPC2-EGFP and PLD1, SV2A, and TSPAN10, and low to moderate colocalization with FMNL2, CTTN, MYH9 and MYH10 as quantified using the Pearson Correlation Coefficient (PCC) (**Figure 2.3A, 2.3B** and **Figure 2.4**). PLD1 and SV2A staining at TPC2 compartments was apparently confined to membrane subdomains, while TSPAN10 appears to be more uniformly distributed on the limiting membrane with TPC2 (**Figure 2.3A, Insets**). Most Cortactin signal was not colocalized with TPC2-EGFP, but some TPC2-EGFP compartments contain a bright spot of Cortactin in agreement with a previous report that suggested Cortactin localizes to recycling subdomains of melanosomes(34). CTTN, MYH9 and MYH10 were chosen because of their high spectral counts in some TPC2-BioID2-HA experiments, but of note, they were also highly detected in negative control experiments from the CRAPome database and may be nonspecific (**Appendix 4**). Therefore, MYH9 and MYH10 low overall colocalization with TPC2-EGFP was unsurprising, and most signal was at structures resembling actin stress fibers at the cell cortex, as expected. Importantly, antibody target specificity was confirmed by siRNA knockdown of each protein that was concomitant with depletion of immunofluorescence and immunoblot signals (**Figure 2.5**). Although our interactome screen was originally intended to identify TPC2 interactors for different TPC2 variants, there were only slight differences in localization of BioID hits in cells expressing 734E versus 734G variants

of TPC2 (**Figure 2.3B**). Thus, we investigated top hits as potential new melanosome proteins regardless of whether they function directly with TPC2.

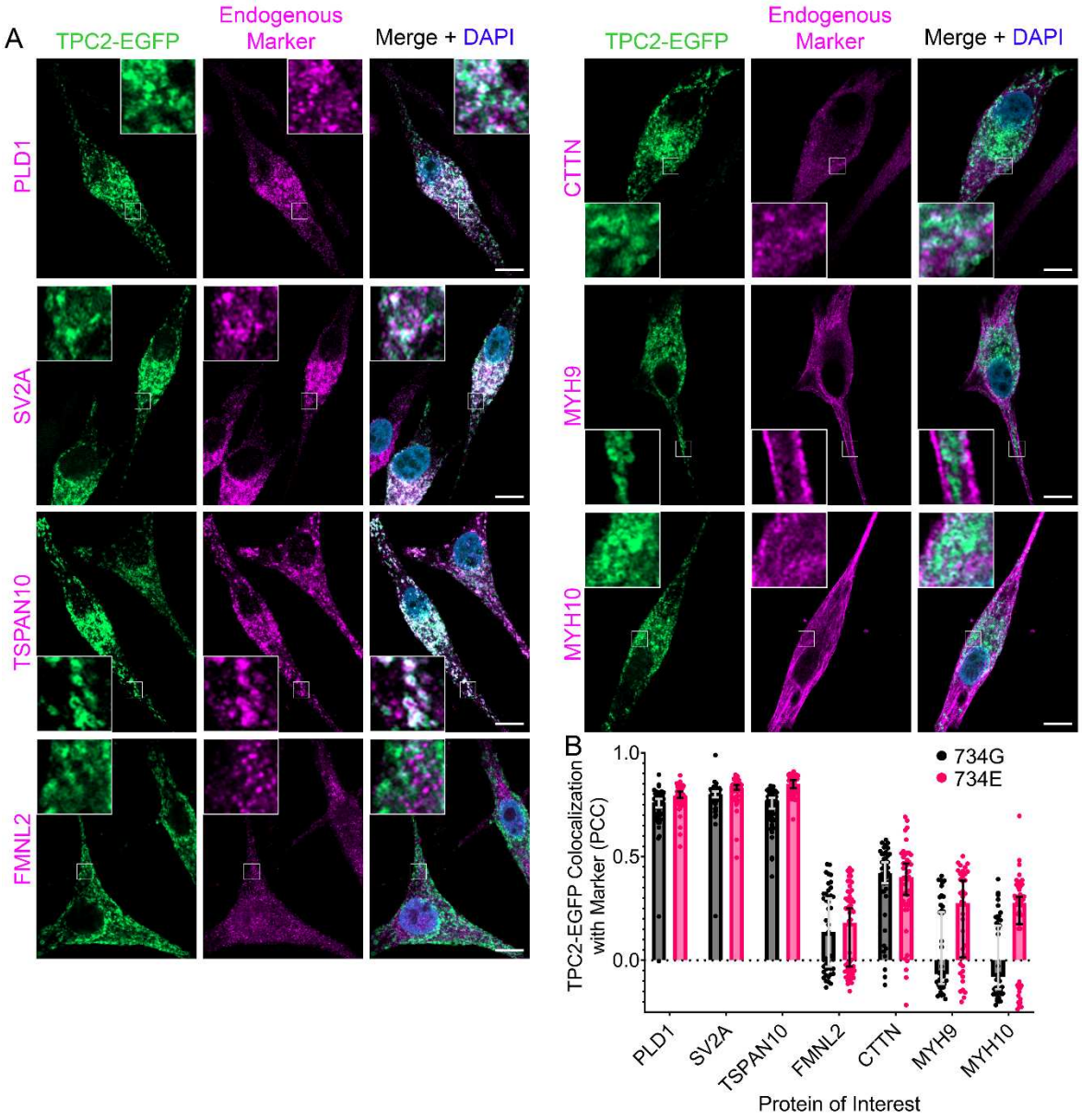

Figure 2.3. PLD1, SV2A and TSPAN10 colocalize with TPC2-EGFP in MNT1 cells.

(A) Representative Airyscan2 super resolution images of MNT1 cells expressing TPC2-734G-EGFP grown for 48 hours in KGM Gold media, fixed with formaldehyde and immunostained for PLD1, SV2A, TSPAN10, FMNL2, CTTN, MYH9 or MYH10. Nuclei were stained with DAPI. High colocalization with TPC2-EGFP was seen for PLD1, SV2A, and TSPAN10. For FMNL2, CTTN, MYH9, and MYH10, some spots of overlap with TPC2-EGFP could be found, but overall, their localizations were largely distinct from TPC2-EGFP. Scale bars indicate 10μm. Zoomed insets are magnified 500%. **(B)** Quantification of immunofluorescence images represented in (A) and

Figure 2.4. The graph indicates the median Pearson Correlation Coefficient (PCC) and error bars represent the 95% confidence interval. For TPC2-734G-EGFP, n=59, n=50, n=51, n=43, n=43, n=40, and n=45 cells were quantified for PLD1, SV2A, TSPAN10, FMNL2, CTTN, MYH9, and MYH10, respectively. For TPC2-734E-EGFP, n=51, n=51, n=50, n=58, n=44, n=39, and n=49 cells were quantified for PLD1, SV2A, TSPAN10, FMNL2, CTTN, MYH9, and MYH10, respectively. Prior to analysis, outliers were removed using the ROUT method for outlier detection in GraphPad Prism.

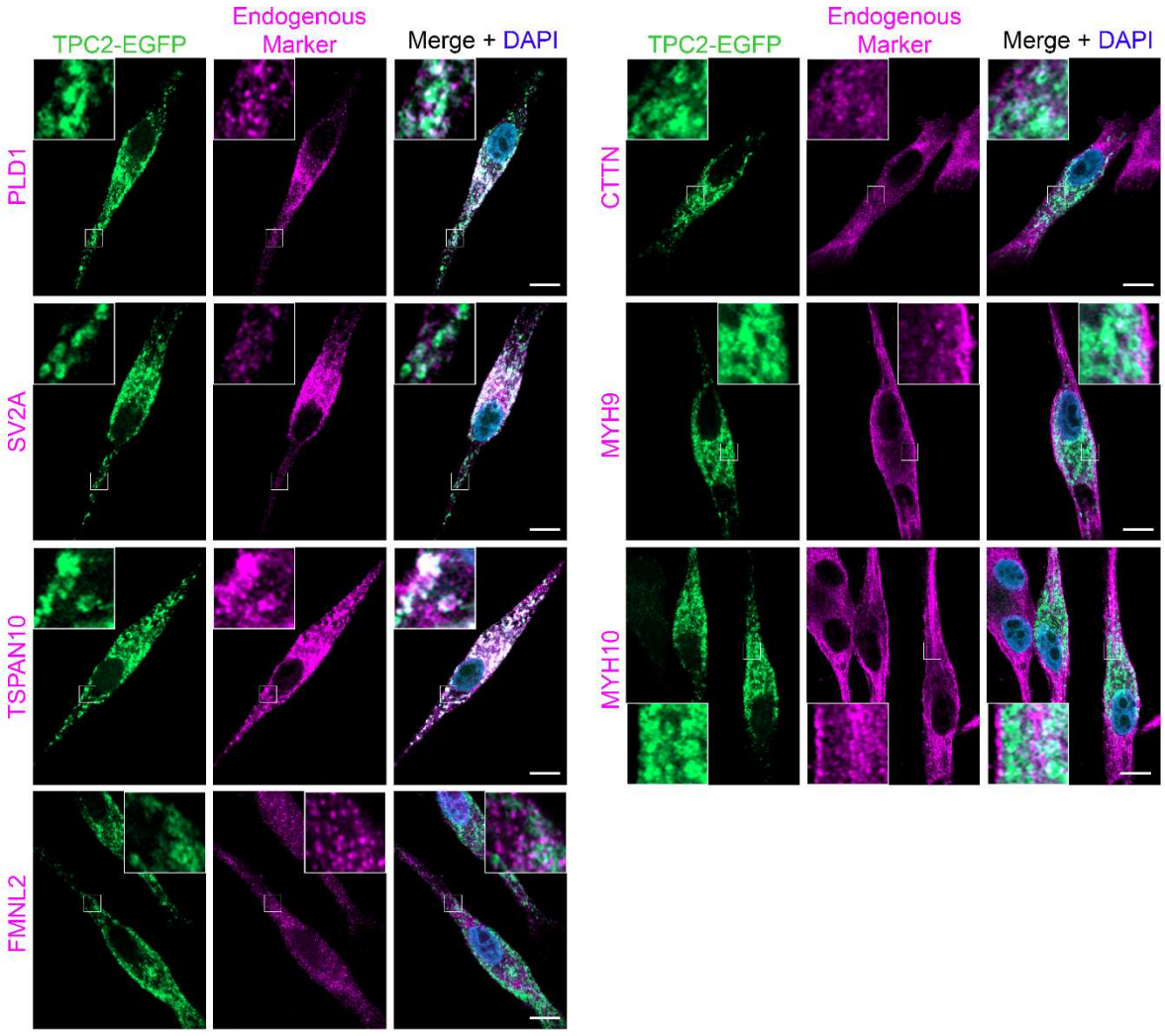

Figure 2.4. PLD1, SV2A and TSPAN10 colocalize with TPC2-734E-EGFP in MNT1 cells.

Representative Airyscan2 super resolution images of MNT1 cells expressing TPC2-734E-EGFP grown for 48 hours in KGM Gold media, fixed with formaldehyde, and immunostained for PLD1, SV2A, TSPAN10, FMNL2, CTTN, MYH9 or MYH10. Nuclei were stained with DAPI. Obvious colocalization was observed between TPC2-734G-EGFP and PLD1, SV2A, and TSPAN10. Quantification is shown in **Figure 2.3B**. Scale bars indicate 10μm. Zoomed insets are magnified 500%.

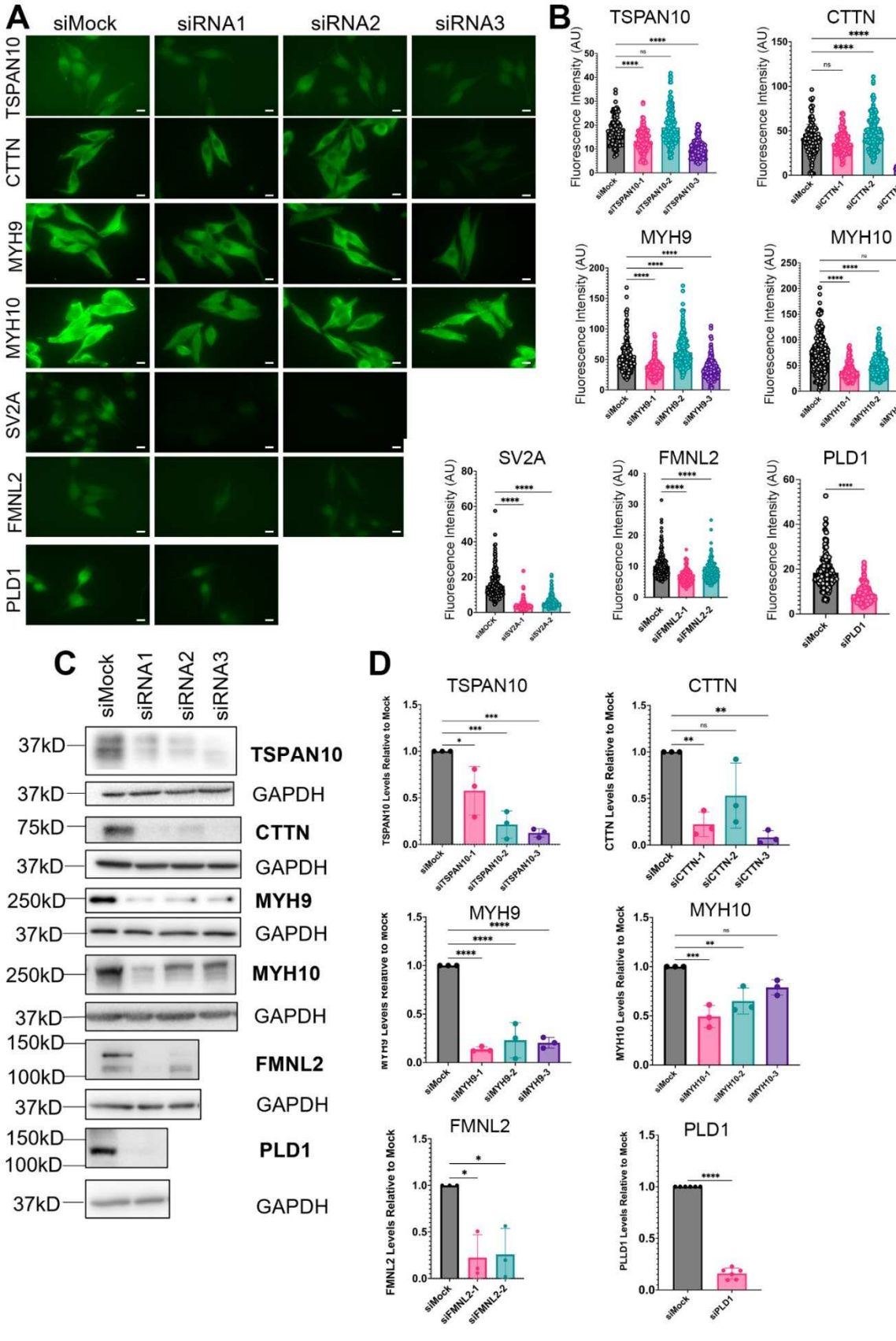
A
siMock
siRNA1
siRNA2
siRNA3
TSPAN10
CTTN
MYH9
MYH10
SV2A
FMNL2
PLD1
B
TSPAN10
CTTN
MYH9
MYH10
SV2A
FMNL2
PLD1
Fluorescence Intensity (AU)
C
siMock
siRNA1
siRNA2
siRNA3
37kD
TSPAN10
GAPDH
75kD
CTTN
250kD
MYH9
MYH10
150kD
100kD
FMNL2
PLD1
D
TSPAN10 Levels Relative to Mock
CTTN Levels Relative to Mock
MYH9 Levels Relative to Mock
MYH10 Levels Relative to Mock
FMNL2 Levels Relative to Mock
PLD1 Levels Relative to Mock

Figure 2.5. Validation of siRNA knockdown efficiency and antibody specificity for immunofluorescence and immunoblotting for various proteins of interest.

(A) Epifluorescence images of MNT1 cells transfected with siRNAs targeting proteins of interest TSPAN10, CTTN, MYH9, MYH10, SV2A, FMNL2, and PLD1 or Mock siRNA for negative controls, and then immunostained with the corresponding antibody. Reduction of fluorescence signal after siRNA knockdown of the corresponding target indicates antibody specificity for immunofluorescence. Scale bars indicate 10μm. **(B)** Quantification of fluorescence intensity for images represented in (A). Graphs indicate the mean ± s.e.m. n=97 cells for siMock, n=88 for siTSPAN10-1, n=131 cells for siTSPAN10-2, and n=141 cells for siTSPAN10-3. n=135 cells for siMock, n=187 cells for siCTTN-1, n=152 cells for siCTTN-2, and n=217 cells for siCTTN-3. n=241 cells for siMock, n=252 cells for siMYH9-1, n=235 cells for siMYH9-2, and n=225 cells for siMYH9-3. n=244 cells for siMock, n=184 cells for siMYH10-1, n=214 cells for siMYH10-2, and n=183 cells for siMYH10-3. n=225 cells for siMock, n=208 cells for siSV2A-1, and n=242 cells for siSV2A-2. n=208 cells for siMock, n=208 cells for siFMNL2-1, and n=268 cells for siFMNL2-2. n=179 for siMock and n=160 for PLD1. **(C)** Immunoblots of cell lysates from cells transfected with siRNAs targeting proteins of interest TSPAN10, CTTN, MYH9, MYH10, FMNL2, and PLD1 or Mock siRNA for negative controls. GAPDH is shown as a loading control. Blots indicate antibody specificity, recognizing targets of the predicted molecular weights by immunoblotting, and siRNAs successfully knockdown proteins of interest. **(D)** Quantification of immunoblots represented in (C). Graphs show the mean ± s.e.m. Statistical significance was tested using One Way ANOVA and post hoc Tukey tests. Lysates from n=6 independent experiments were quantified for PLD1, and n=3 independent experiments were quantified for all other proteins.

Endogenous TSPAN10 localizes to melanosomes and lysosomes in MNT1 cells

TPC2 localizes primarily to melanosomes in melanocytes, but a fraction of TPC2 also localizes to late endosomes and lysosomes(9, 10). We sought to better define the localization of endogenous TSPAN10 by performing immunofluorescence experiments with multiple endogenous markers, including EEA1, PMEL N, MELV, and LAMP2 to mark early endosomes, early-stage melanosomes/pre-melanosome compartments, Stage 3 and Stage 4 melanosomes, and late endosomes/lysosomes respectively. Phalloidin staining, which primarily labels cortical actin stress fibers, was used as a negative control. Endogenous TSPAN10 colocalized highly with LAMP2 and MELV, indicating it localizes to late endosomes/lysosomes in addition to melanosomes in MNT1 cells (**Figure 2.6A and 2.6B**). This result is consistent with another study showing that exogenously expressed TSPAN10 localizes to CD63 labeled late endosomes in HeLa cells(35).

Many lysosome and lysosome related organelle localized membrane proteins contain a cytosol exposed acidic dileucine motif, [DE]XXXL[LI], that promotes interaction with clathrin adapter protein complexes AP-1 and AP-3 to direct their organelle localization(36-39). We noticed a sequence conforming to the acidic dileucine motif in the N terminal cytosolic tail of TSPAN10, sequence **E**RSP**LL**, and sought to test for its importance for melanosome localization. Wild type EGFP-TSPAN10 colocalized highly with TPC2-iRFP in MNT1 cells, whereas EGFP-TSPAN10 LL/AA mutant had striking mislocalization to the plasma membrane, with especially bright labeling at filopodia-like membrane protrusions (**Figure 2.6C**). This result suggests TSPAN10 localizes to melanosomes following a canonical sorting pathway dependent on the AP-1 and/or AP-3 complex(38, 40).

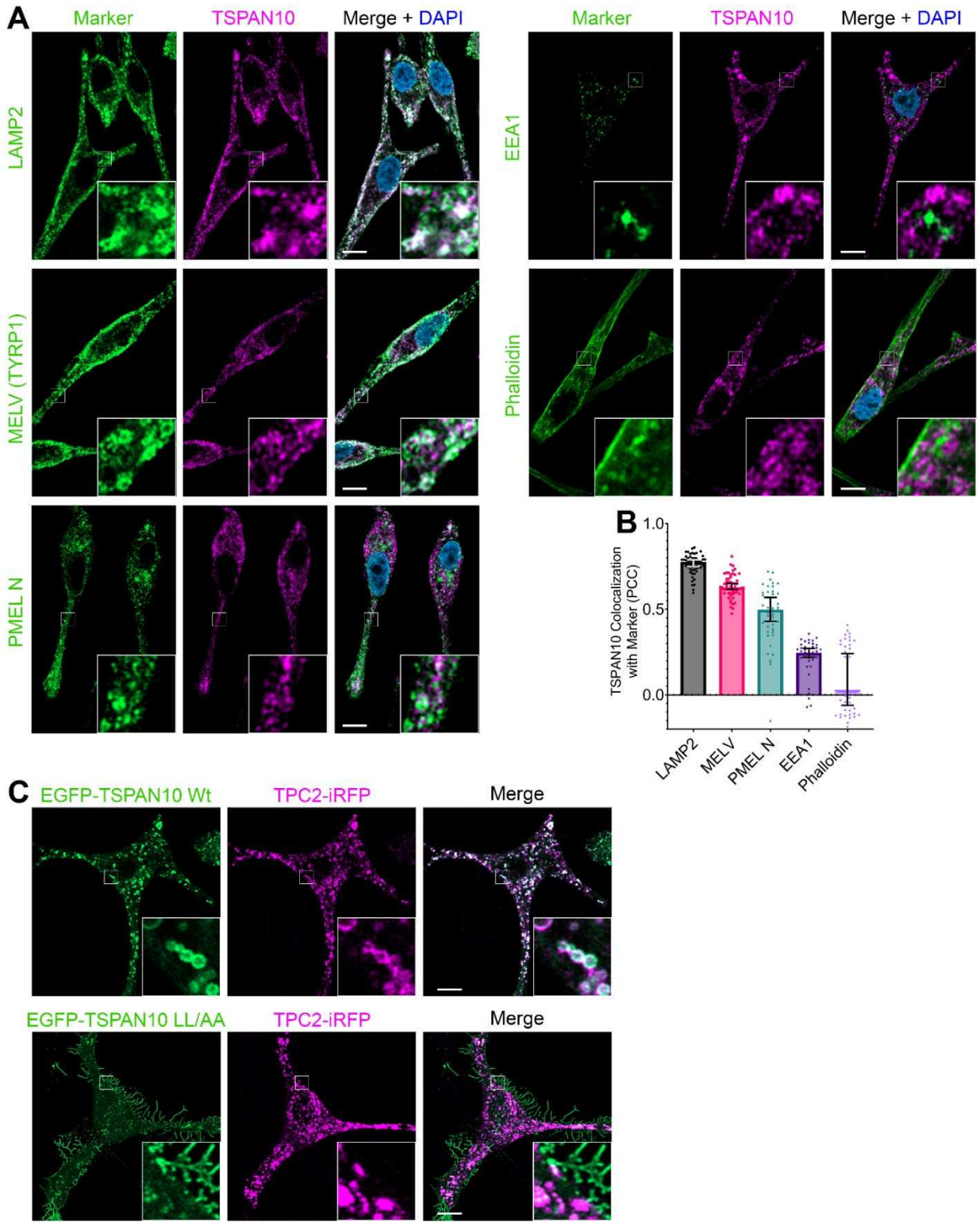

Figure 2.6. Endogenous TSPAN10 localizes to melanosomes and lysosomes in MNT1 cells. **(A)** Airyscan2 super resolution Immunofluorescence images of MNT1 cells stained for endogenous TSPAN10 with LAMP2 (lysosomes), MELV (pigmented melanosomes), PMEL N (early stage melanosomes, and pre-melanosomal compartments), EEA1 (early endosomes and

stage 1 melanosomes), or Phalloidin (F actin). TSPAN10 colocalizes highly with LAMP2 and MELV. Scale bars indicate 10μm and zoomed insets are magnified 600%. **(B)** Quantification of images represented in (A)**.** The Graph depicts the median Pearson Correlation Coefficient with error bars representing the 95% confidence interval. n=55, n=56, n=43, n=41 and n=43 for LAMP2, MELV, PMEL N, EEA1, and Phalloidin, respectively. **(C)** Airyscan2 super resolution live cell images of MNT1 cells exogenously expressing EGFP-TSPAN10 Wild Type or EGFP-TSPAN10 LL/AA dileucine sorting signal mutant with TPC2-iRFP. EGFP-TSPAN10 LL/AA dramatically re-localizes to the plasma membrane, especially filopodia-like membrane protrusions. Scale bars indicate 10μm and zoomed insets are magnified 600%.

TSPAN10 regulates pigmentation in MNT1 cells.

We hypothesized PLD1, SV2A, and TSPAN10 might influence melanosome biogenesis and pigment synthesis in melanocytes considering their newfound localization to TPC2 positive melanosomes. Utilizing CRISPR-Cas9, we generated PLD1 KO, SV2A KO, and TSPAN10 KO MNT1 cells, confirming depletion of each target's expression by western blot (**Figure 2.7A, 2.7B, 2.8A and 2.8B**). MYH10 KO MNT1 cells were also generated and tested because high spectral counts of MYH10 were detected in the initial proximity biotinylation screen. Excitingly, bulk melanin quantification revealed TSPAN10 KO cells are hypopigmented compared to Wild Type MNT1 cells, a phenotype which is plainly apparent by visual inspection of cell pellets (**Figure 2.7C and 2.7D**). In contrast to TSPAN10 KO MNT1 cells, melanin quantification failed to detect significant phenotypes for PLD1 KO, SV2A KO, or MYH10 KO cells (**Figure 2.8C**). Hypopigmentation was also apparent in individual TSPAN10 KO cells by brightfield microscopy (**Figure 2.7E and 2.7F**). Importantly, expression of exogenous EGFP-TSPAN10 rescued pigment levels in TSPAN10 KO cells, suggesting the EGFP-TSPAN10 construct is functional, and hypopigmentation is not an artifact of CRISPR-Cas9 off target effects (**Figure 2.7G and 2.7H**). In fact, rescued cells display more pigmentation than control cells, suggesting that higher levels of TSPAN10 expression can result in heightened pigmentation. Importantly, our results are consistent with a recent GWAS identifying a strong association between TSPAN10 polymorphisms and human eye color, as well as a study finding TSPAN10 expression is

associated with dark pigmentation in ducks (5, 41). Together, our results confirm a TSPAN10 function in pigmentation at the cellular level.

Although a clear phenotype was not confirmed for PLD1, it is worth noting that PLD1 was previously implicated as a negative regulator of pigmentation in mouse melanocytes(42-44). In the former studies, effects of PLD1 perturbation were most pronounced in the context of αMSH stimulated melanogenesis, which was not considered in the present study.

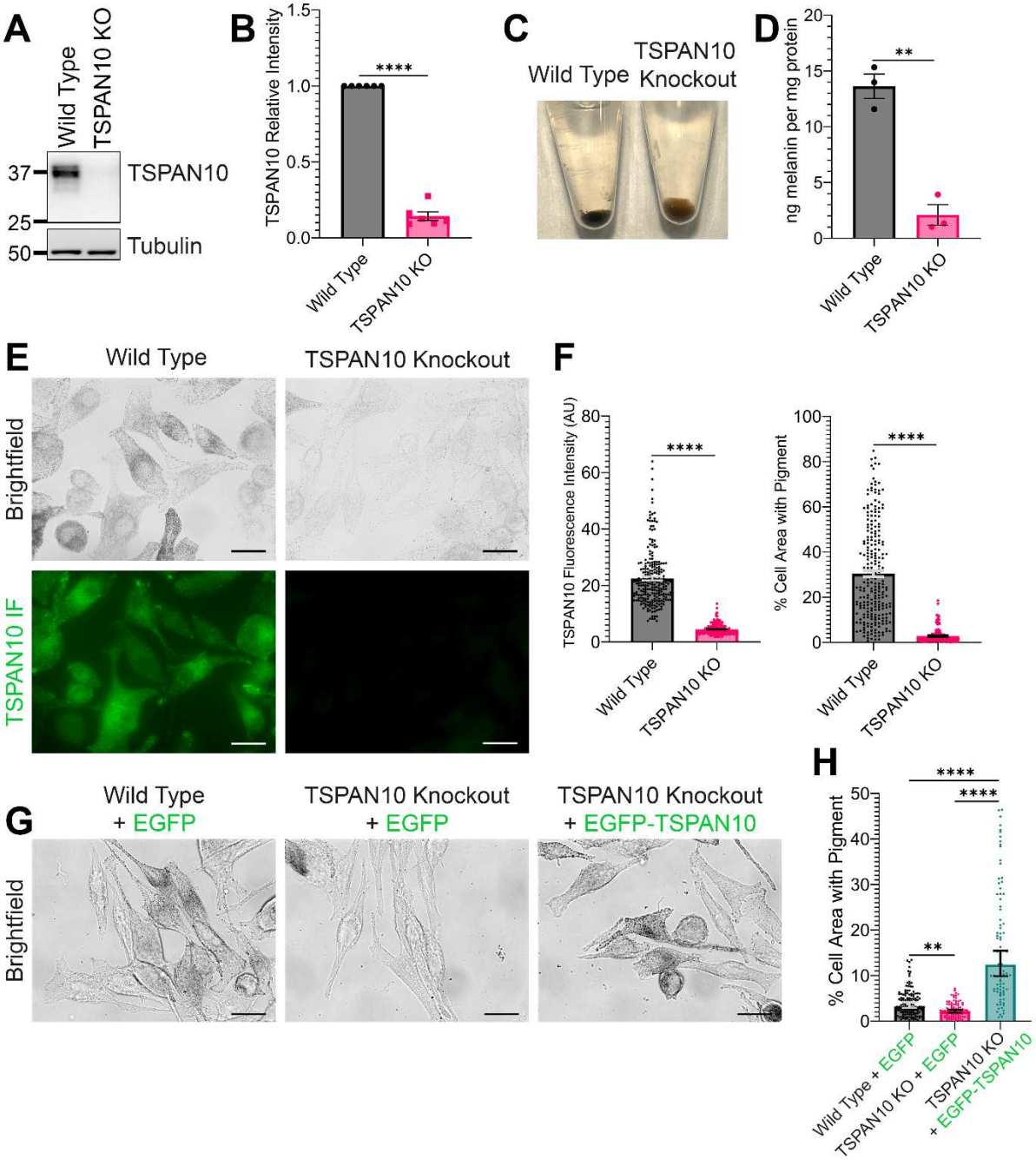

Figure 2.7. TSPAN10 regulates pigmentation in MNT1 cells. (A) Immunoblot of Wild Type and TSPAN10 KO lysates confirming depletion of TSPAN10 in TSPAN10 KO cultures relative to Wild Type (and normalized to Tubulin loading control). **(B)** Quantification of immunoblots represented in (A). The graph shows the mean signal ± s.e.m. for n=6 independent experiments. Significance was tested using Student's T-test. **(C)** Picture showing hypopigmentation in cell pellets of TSPAN10 KO MNT1 cells compared to Wild Type MNT1 cells. 10^6 cells were pelleted in 1.5mL tubes for the picture. **(D)** Melanin quantification assay results comparing pigment in Wild Type and TSPAN10 KO cells**.** The graph shows the mean signal ± s.e.m. for n=3 independent experiments. Significance was tested using the Student's T-test. **(E)** Brightfield and

epifluorescence images of Wild Type and TSPAN10 KO cells immunostained for TSPAN10, showing reduced melanin pigment and confirming TSPAN10 depletion in TSPAN10 KO cells. **(F)** Quantification of endogenous TSPAN10 fluorescence intensity and percent cell area with pigment for images represented in (E). Graphs show the mean ± s.e.m. for n=242 Wild Type cells and n=178 TSPAN10 KO cells. Significance was tested using Student's T-test. **(G)** Brightfield and epifluorescence images of Wild Type and TSPAN10 KO cells transfected with soluble EGFP (Mock) or EGFP-TSPAN10 (Rescue). Images depict a rescue of cellular pigmentation in TSPAN10 KO cells transfected with EGFP-TSPAN10. **(H)** Quantification of images represented in (G). The graph shows median % cell area with pigment with error bars representing the 95% confidence interval. n=137, n=92, and n=93 cells were quantified for Wild Type Mock, TSPAN10 KO Mock, and TSPAN10 KO Rescue, respectively. The Kruskal-Wallis Test was used to test for significance.

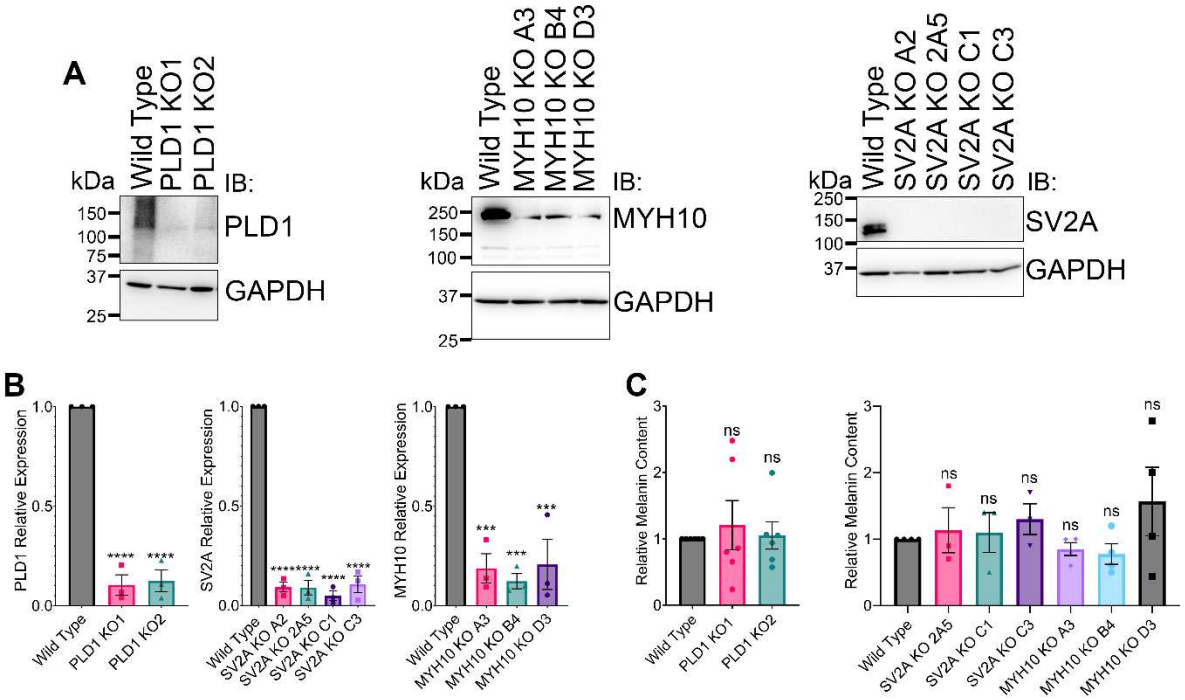

Figure 2.8. PLD1, SV2A, and MYH10 do not regulate basal pigmentation in MNT1 cells.

(A) Immunoblots of RIPA buffer lysates from Wild Type MNT1 cells, or various clonally isolated cultures of PLD1 KO, SV2A KO, or MYH10 KO cells generated by CRISPR-Cas9 mediated knockout indicating successful depletion of each target protein. SV2A immunoblots were performed without boiling samples to prevent SV2A aggregation. **(B)** Quantification of western blots represented in (A). The graphs show the mean ± s.e.m. band intensities relative to Wild Type, normalized to GAPDH loading control. Lysates were analyzed for n=3 independent experiments and statistical significance was tested using one way ANOVA with post hoc Tukey testing. **(C)** Melanin quantification assay results comparing pigment in Wild Type MNT1 cells with various clones of PLD1 KO cells (left graph), or Wild Type with various clones of SV2A KO and MYH10 KO cells (right graph). The graph shows the mean signal ± s.e.m. for n=6 independent lysates for Wild Type and PLD1 (left graph), and n=4 independent lysates for Wild Type, n=3 for SV2A KO lysates, and n=4 for MYH10 KO lysates (right graph). Significance was tested using one way ANOVA with post hoc Tukey tests.

PMEL maturation is altered in TSPAN10 KO cells.

TSPAN10 KO MNT1 cells have a clear hypopigmentation phenotype, and TSPAN10 localizes to melanosomes and lysosomes. Therefore, we sought to better understand how melanin synthesis might be perturbed by immunoblotting for key lysosomal and melanosomal proteins. LAMP2 expression, corresponding to lysosome biogenesis, was not significantly altered in TSPAN10 KO cells (**Figure 2.9A and 2.9B**). Surprisingly, however, we consistently identified heightened processing of the lysosomal hydrolase Cathepsin D into its active form, suggesting aberrant proteolysis activity in lysosomes, or potentially melanosomes, which will be discussed later (**Figure 2.9A and 2.9B**). One major function of some Tetraspanin proteins is to coordinate the trafficking of Integrin proteins and maintain Integrins in Tetraspanin Enriched Microdomains (45). We recently found Integrin Alpha 5 (ITGα5) is expressed in MNT1 cells and partially localizes to lysosomes (unpublished data). Therefore, we tested if ITGα5 expression was affected in TSPAN10 KO cells but were unable to detect a significant phenotype (**Figure 2.9A and 2.9B**). Tyrosinase, the rate limiting enzyme in melanin synthesis had unaltered expression in TSPAN10 KO cells (**Figure 2.9A and 2.9B**). Finally, we investigated the PMEL protein, which is present in all stages of melanosomes and can be an indicator for melanosome biogenesis defects. Strikingly, immunoblotting for the PMEL protein with Wild Type or TSPAN10 KO RIPA lysates showed an obvious defect in PMEL processing. Probing with a PMEL N antibody, which recognizes full length unprocessed PMEL (P1) and the partially processed Mα fragment showed reduced steady state signal in TSPAN10 KO cells. (**Figure 2.9A and 2.9B)**. Probing with HMB45, which recognizes the Mα fragment and the fibril associated processed Rpt domain, showed less Mα fragment and more Rpt domain in TSPAN10 KO cells (**Figure 2.9A and 2.9B**).

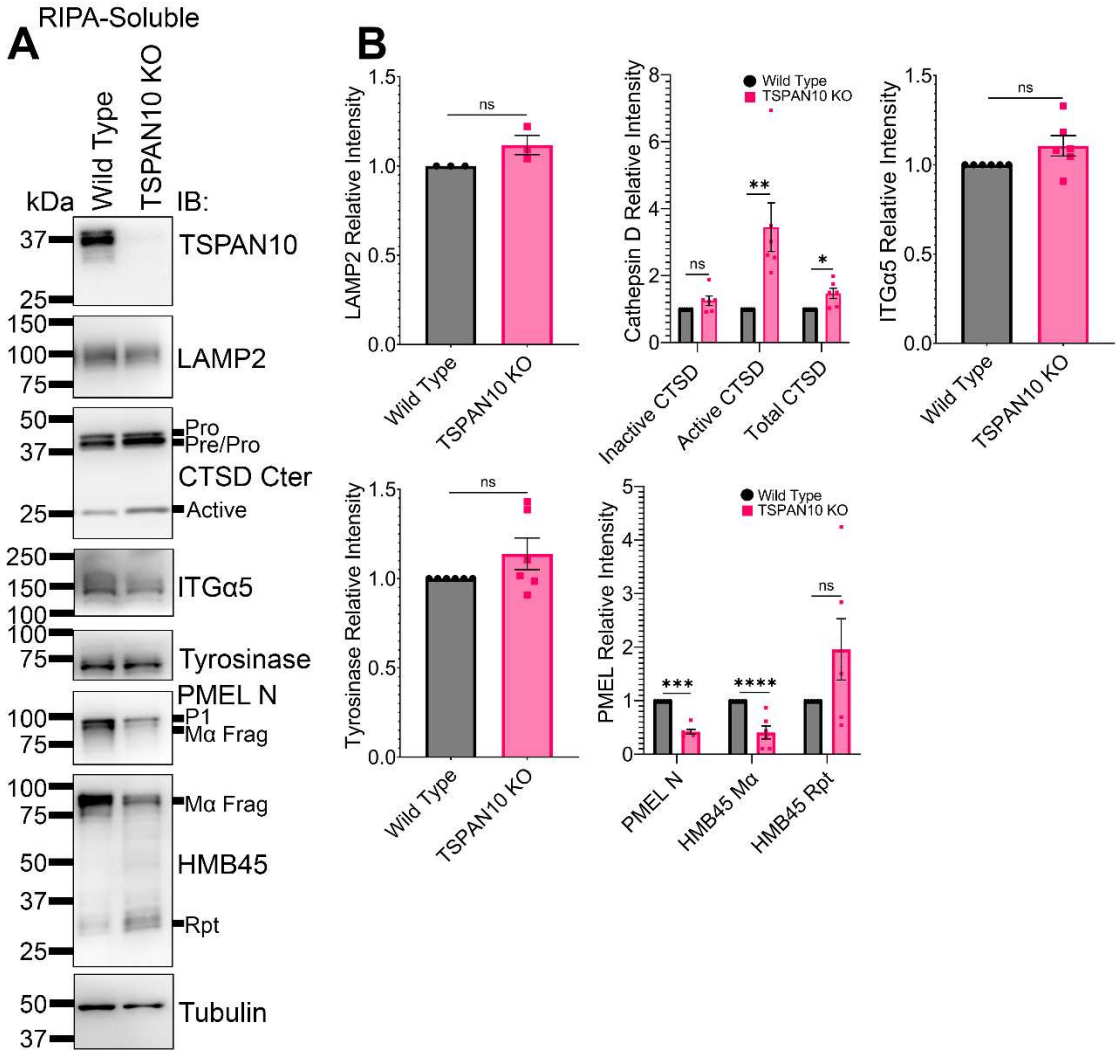

Figure 2.9. PMEL and Cathepsin D maturation are altered in TSPAN10 KO cells.

(A) Immunoblots of RIPA buffer lysates from Wild Type or TSPAN10 KO cells using antibodies for TPAN10, LAMP2, Cathepsin D C terminus, ITGα5, Tyrosinase, PMEL N terminus, PMEL HMB45, and Tubulin. **(B)** Quantification of immunoblots represented in (A). The graphs show the mean ± s.e.m. band intensities relative to Wild Type, normalized to Tubulin loading controls. n=3 independent lysates were analyzed for LAMP2 and n=6 independent lysates were analyzed for every other protein. Statistical significance was tested using the Student's T test.

PMEL protein in melanosomes forms a physiologically functional amyloid fibril that acts as a scaffold for melanin deposition and scavenger of highly toxic melanin intermediates(46-48). To form functional amyloid, the PMEL luminal fibrillogenic Mα fragment is cleaved from the melanosome limiting membrane by BACE2 before it associates with intraluminal vesicles,

undergoes subsequent proteolysis by lysosomal proteases, and finally self-associates into ordered fibrils(49-54).

While the results described above identified a defect in PMEL, they do not tell a complete story as RIPA buffer only partially solubilizes PMEL amyloid fragments, with most amyloid remaining in the insoluble pellet. To better decipher the PMEL defect in TPAN10 KO cells, we performed immunoblots to compare Triton X100 (TX100) soluble and TX100 insoluble PMEL fractions. In pre-melanosome compartments and early-stage melanosomes, full length PMEL and intermediately processed PMEL Mα and Mβ are present and soluble in 1% TX100, while PMEL species in mature fibrils of Stage II-IV melanosomes are mostly insoluble in 1% TX100, requiring SDS and heat to solubilize. First, immunoblotting with a PMEL C terminus antibody recognizing full length soluble PMEL and the mβ fragment showed overall full length PMEL is unaffected, but clearly indicated a reduction in the Mβ fragment, which is thought to be processed by BACE2 (**Figure 2.10A and 2.10B**)(49). Analyzing TX100 soluble and insoluble fractions with HMB45 showed reduced levels of Mα in both fractions and higher levels of the processed repeat domain in the TX100 insoluble fraction (**Figure 2.10A and 2.10B**). Finally, immunoblotting with I51, which recognizes the TX100 insoluble core amyloid fragment of PMEL, showed similar levels between Wild Type and TSPAN10 KO cell lysates (**Figure 2.10A and 2.10B**). Together, these results surprisingly suggest PMEL processing is aberrantly accelerated in TSPAN10 KO cells, as TSPAN10 depletion led to a decrease in Mα and Mβ fragments and accumulation of the processed fibrillar Repeat domain.

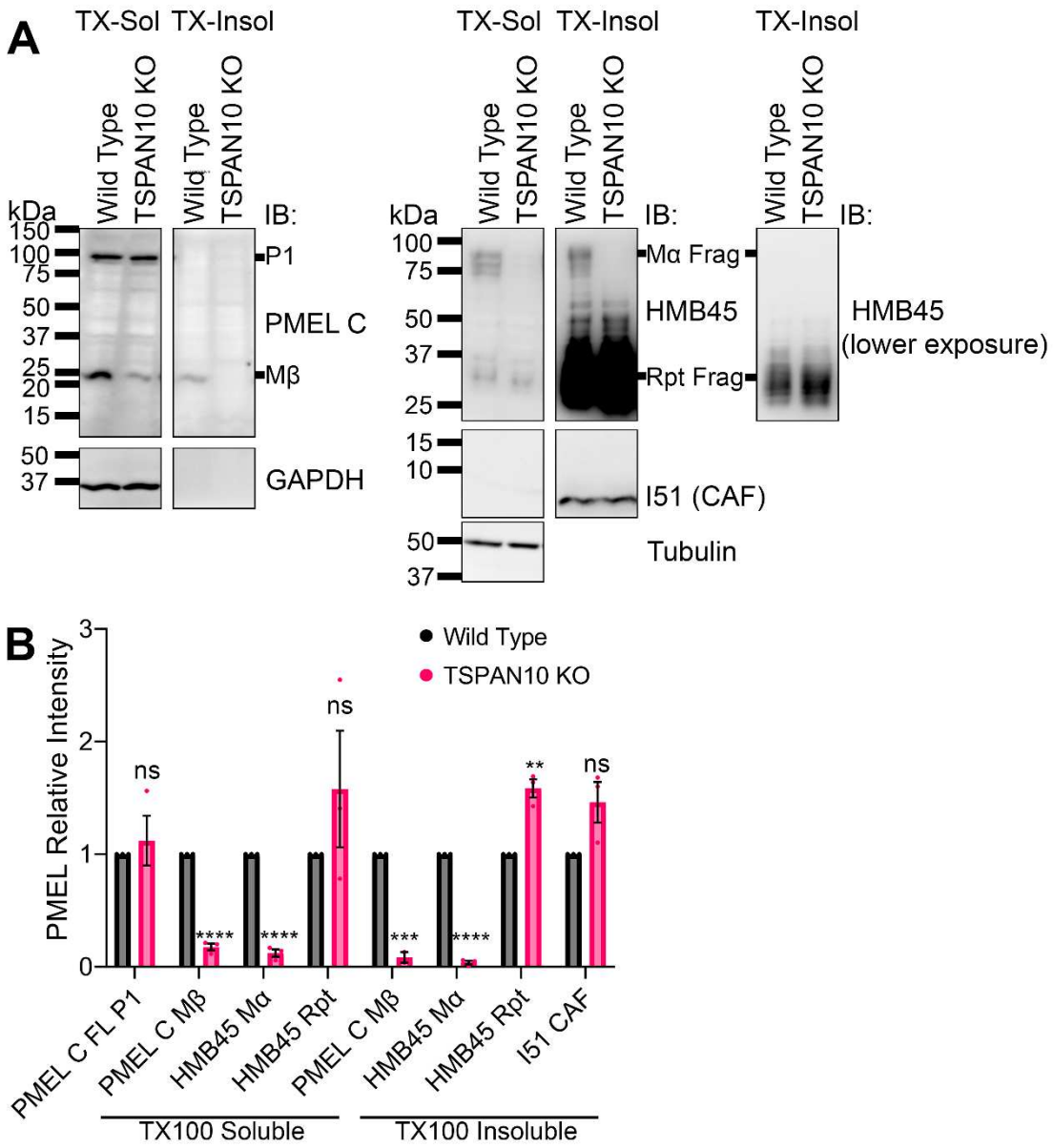

Figure 2.10. TSPAN10 KO MNT1 cells have reduced PMEL Mα and Mβ fragments and heightened insoluble PMEL Rpt domain. **(A)** Immunoblots of TX100 Soluble and TX100 Insoluble lysates from Wild Type or TSPAN10 KO cells, probing with antibodies for PMEL C terminus recognizing P1 and Mβ, GAPDH, PMEL HMB45 recognizing Mα and processed Rpt domain, PMEL I51 recognizing Core Amyloid Fragment, and Tubulin. TX-Soluble and TX-Insoluble images depict the same membrane and same exposures, except the far-right TX-Insoluble HMB45 image which shows a shorter exposure of the same membrane. Therefore, the majority of the PMEL Rpt fragments are TX100-Insoluble. **(B)** Quantification of immunoblots represented in (A). The graphs show the mean ± s.e.m. band intensities relative to Wild Type, normalized to corresponding TX100 soluble GAPDH or Tubulin loading controls. n=3 independent lysates were analyzed for everything except for PMEL C Mβ, which was analyzed for n=2 lysates. Statistical significance was tested using Student's T test.

Interestingly, we observed heightened levels of active Cathepsin D in TSPAN10 KO lysates (**Figure 2.9A and 2.9B)**. It has been shown that inhibition of lysosomal proteases abrogates processing of PMEL Mα fragments, and it was proposed that lysosomes deliver their hydrolases to melanosomes via transient kiss-and-run partial fusion events(51, 54). In one study, impedance of Mα processing associated with reduced Cathepsin D activity, although a clear causative link was not discussed(55). Nonetheless, we hypothesize abnormally accelerated processing of PMEL in TSPAN10 KO cells may be due in part to higher levels of active Cathepsin D.

TSPAN10 KO MNT1 cells have an abundance of aberrant melanosomes lacking ordered PMEL fibrils.

Melanosomes mature through four stages that are visually distinct by electron microscopy (46, 56). Stage I pre-melanosomes resemble multivesicular endosomes with a clathrin coat and are the sites of early proteolytic processing of PMEL (46). Intraluminal domains of PMEL are shed from the limiting melanosome membrane by BACE2 and associate with intraluminal vesicles containing Apolipoprotein E, which act as a seed for PMEL fibrillation(50, 57, 58). Stage II melanosomes have clearly defined mature PMEL fibrils but have not yet synthesized appreciable levels of melanin. Stage III melanosomes contain active melanogenic enzymes and have melanin deposited onto PMEL fibrils. Finally Stage IV melanosomes are mature organelles having very high melanin content that is destined for transfer to neighboring epidermal keratinocytes.

Immunoblots indicated PMEL is aberrantly processed in TSPAN10 KO MNT1 cells. However, retention of high levels of HMB45 staining in TSPAN10 KO made it unclear if altered PMEL processing would manifest in mis-structured melanosomes. To gain more insight into a possible melanosome biogenesis defect, we utilized high pressure freezing and thin section transmission electron microscopy on Wild Type and TSPAN10 KO melanocytes to visualize

melanosome structure in fine detail (**Figure 2.11**). In Wild Type sections, an abundance of Stage I melanosomes resembling multivesicular coated endosomes and Stage II (unpigmented), Stage III (some pigment), and Stage IV (saturated pigment) melanosomes having clearly defined PMEL fibrils are seen in most cells. In contrast, a large fraction of organelles in TSPAN10 KO cells were "aberrant melanosomes," defined here as electron dense compartments, usually with melanin aggregates lacking defined PMEL fibrils. Also apparent in TSPAN10 KO cells was a smaller fraction of Stage I and Stage II melanosomes when compared to Wild Type cells (**Figure 2.11B**). Together, these results suggest TSPAN10 KO MNT1 cells have a broad defect in melanosome biogenesis going beyond regulation of melanin synthesis *per se.*

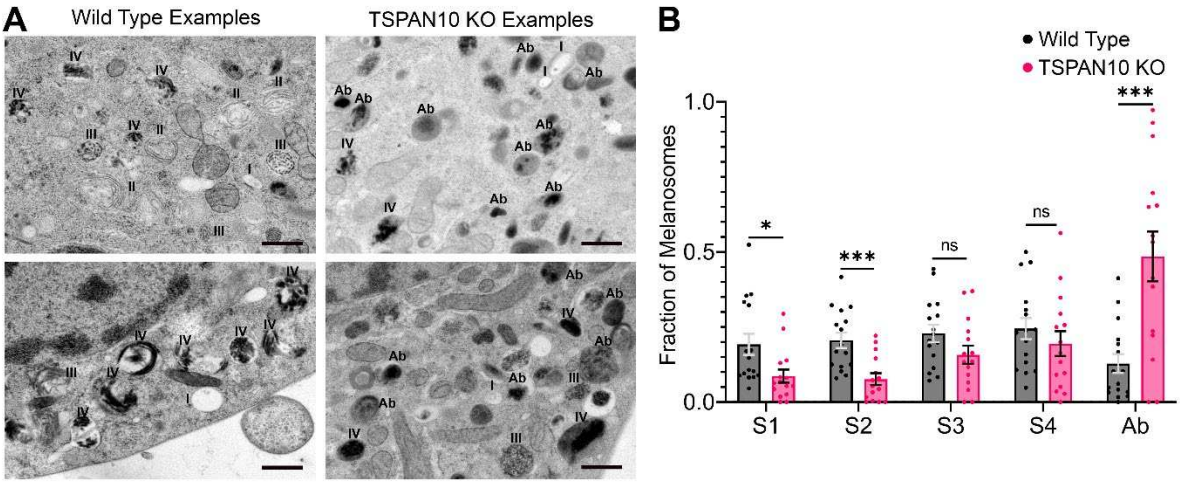

Figure 2.11. TSPAN10 KO MNT1 cells have an abundance of aberrant melanosomes lacking ordered PMEL fibrils. (A) Thin section transmission electron microscopy images of Wild Type or TSPAN10 KO MNT1 cells showing a variety of Stage I (S1), Stage II (S2), Stage III (S3), Stage IV (S4), and aberrant (Ab) melanosomes, captured at 23,000X magnification. Two example frames are shown for each. TSPAN10 KO cells have an abundance of aberrant melanosomes lacking defined PMEL fibrils. Scale bars indicate 500nm. **(B)** Quantification of images represented in (A). Graphs show the mean ± s.e.m. fraction of melanosomes per cell corresponding to the specified stage. n=16 Wild Type cells and n=15 TSPAN10 KO cells were quantified, and statistical significance was tested using the Student's T test.

Intriguingly, another melanosome localized Tetraspanin, CD63, is required for efficient generation of intraluminal vesicles in Stage I melanosomes that are required for proper PMEL fibrillation, and CD63 depletion results in heightened levels of melanosomes containing dense

aggregates similar to TSPAN10 KO cells (58). By immunoblotting, CD63 depletion also reduced levels of the mβ PMEL fragment, similar to what we found in TSPAN10 KO cells(58). Despite these similarities, TSPAN10 KO cells maintained high levels of HMB45 staining by western blot, which was not the case in CD63 depleted cells. Additionally, TSPAN10 depletion has a significant loss of pigmentation not observed in CD63 depleted cells. Therefore, TSPAN10 function at melanosomes is likely independent of CD63.

TSPAN10 controls expression and localization of the protease ADAM10 in MNT1 cells.

TSPAN10 is a member of the TSPANC8 family of Tetraspanin proteins which interact directly with the metalloproteinase ADAM10 and are required for ADAM10 exit from the endoplasmic reticulum (35, 59). Overexpression of TSPANC8 proteins TSPAN5, TSPAN14, and TSPAN15 in HeLa cells directed ADAM10 to the cell surface, whereas expression of TSPAN10 or TSPAN17 directed ADAM10 to late endosomes, leading to a proposed model in which ADAM10 adopts different localizations and therefore acts on unique substrates depending on which TSPANC8 family member is expressed(35). For instance, TSPANC8 protein localization to the cell surface is required for ADAM10 surface localization, and subsequent Notch Receptor signaling(35). Additionally, Evolutionary Rate Conversion (ERC) analysis suggests a robust link in ADAM10 and TSPAN10 covariant evolution, with an ERC score of +0.608 (p=0.0006, top 0.1%)(60). Although TSPAN10 function in melanosome biogenesis has not yet been investigated in cultured melanocytes, ADAM10 is thought to play a role in melanosome biogenesis, as ADAM inhibition led to a reduction in pigmentation, aberrant melanosomes as seen by electron microscopy, and defects in PMEL N terminal processing (52). Therefore, we hypothesized TSPAN10 might function in part to direct ADAM10 to melanosomes and endo-lysosomes in melanocytes, and we sought to re-evaluate ADAM10 localization despite a previous report suggesting ADAM10 has low intracellular colocalization with PMEL in MNT1 cells (61).

Immunofluorescence with an antibody against ADAM10 revealed ADAM10 localizes primarily to intracellular compartments partially colocalizing with TSPAN10 in MNT1 cells, with limited staining at the plasma membrane, with a Pearson Correlation Coefficient (PCC) of 0.54 ± 0.01 (**Figure 2.12A**). Additionally, ADAM10-HA, labeled with an αHA-mCherry ScFv, colocalized with EGFP-TSPAN10 organelles in live cells (**Figure 2.13A**). Strikingly, endogenous ADAM10 fluorescence is partially depleted in TSPAN10 KO cells, with residual ADAM10 localizing to structures resembling endoplasmic reticulum and Golgi, consistent with the model that TSPANC8 family Tetraspanins are required for proper ADAM10 trafficking (**Figure 2.12B and 2.12C**). Immunoblotting of cell extracts with anti ADAM10 antibody confirmed ADAM10 expression and maturation into the active form is impaired in TSPAN10 KO cells (**Figure 2.12D and 2.12E**). Importantly, ADAM10 immunofluorescence signal was rescued in TSPAN10 KO cells with expression of EGFP-TSPAN10 (**Figure 2.13B and 2.13C**).

ADAM10 was predominantly localized to intracellular compartments in our immunofluorescence experiments using permeabilized MNT1 cells. However, ADAM10 is known to have Tetraspanin dependent functions at the cell surface in many cell types (35, 59). Therefore, we sought to test if the surface localized fraction of ADAM10 is affected in TSPAN10 KO MNT1 cells. Surface staining for ADAM10 in the absence of detergent highlighted an appreciable plasma membrane localized pool in both Wild Type and TSPAN10 KO MNT1 cells, however it was significantly reduced in TSPAN10 KO cells, probably due to lower total ADAM10 expression and impaired trafficking (**Figure 2.12F and 2.12G**). Together, these results suggest ADAM10 localizes partially to melanosomes and lysosomes, and to a smaller extent the plasma membrane in MNT1 cells, and that TSPAN10 is a major functional partner of ADAM10 by controlling its expression and localization.

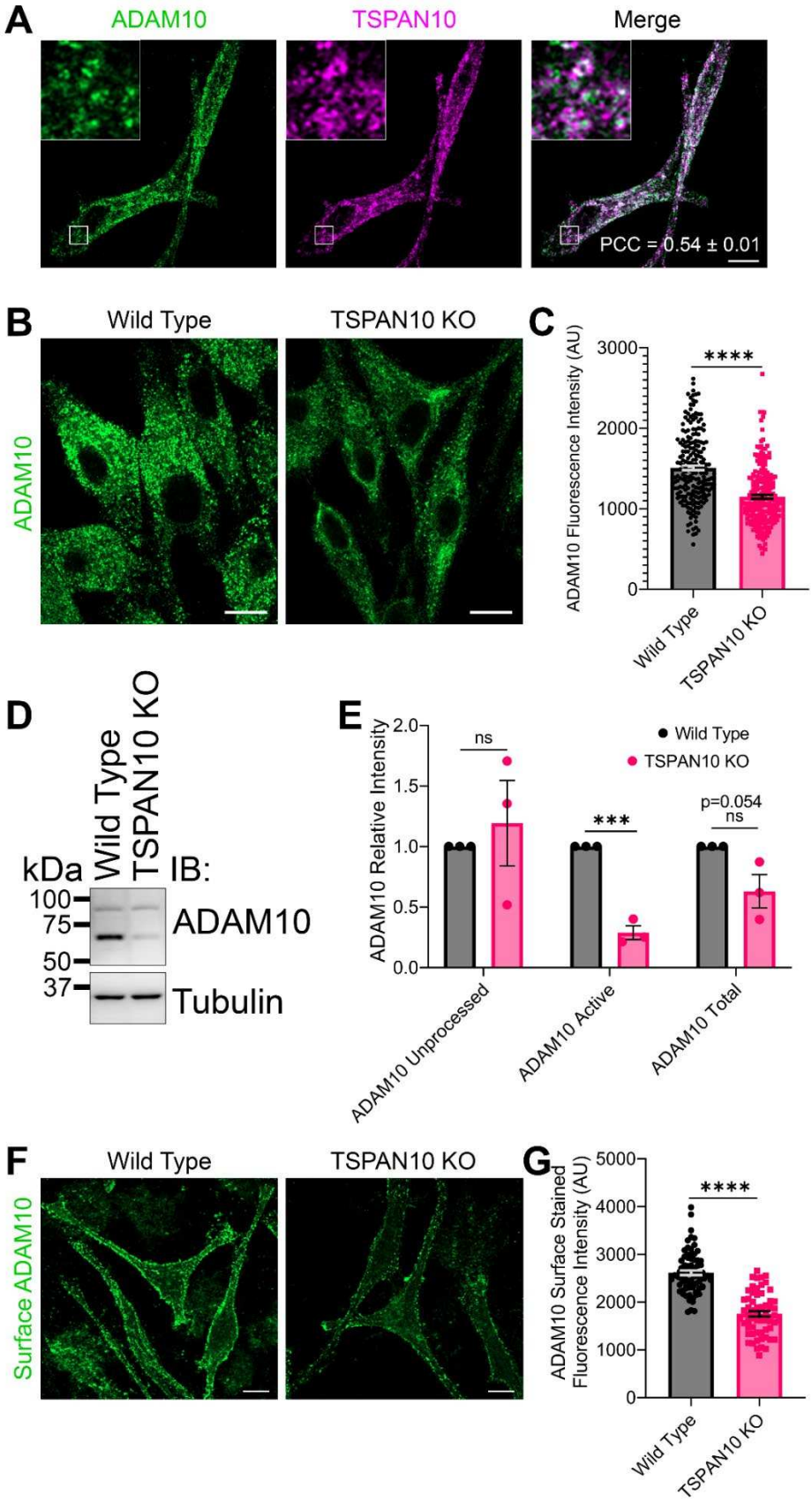
A
ADAM10
TSPAN10
Merge
PCC = 0.54 ± 0.01
B
Wild Type
TSPAN10 KO
ADAM10
C
ADAM10 Fluorescence Intensity (AU)
3000
2000
1000
0
****
Wild Type
TSPAN10 KO
D
Wild Type
TSPAN10 KO
kDa
IB:
100
75
50
37
ADAM10
Tubulin
E
ADAM10 Relative Intensity
2.0
1.5
1.0
0.5
0.0
Wild Type
TSPAN10 KO
ns
***
p=0.054
ns
ADAM10 Unprocessed
ADAM10 Active
ADAM10 Total
F
Wild Type
TSPAN10 KO
Surface ADAM10
G
ADAM10 Surface Stained Fluorescence Intensity (AU)
5000
4000
3000
2000
1000
0
****
Wild Type
TSPAN10 KO

Figure 2.12. TSPAN10 controls expression and localization of the protease ADAM10 in MNT1 cells. (A) Airyscan2 super resolution immunofluorescence images of MNT1 cells stained for ADAM10 and TSPAN10 showing ADAM10 partially localizes to TSPAN10 compartments. Pearson correlation coefficient was determined to be 0.54 ± 0.01 standard deviation for n=3 independent cultures measuring 30-49 cells per culture. Scale bars indicate 10μm and zoomed insets are magnified 600%. **(B)** Airyscan2 super resolution immunofluorescence images of Wild Type or TSPAN10 KO MNT1 cells stained for endogenous ADAM10 showing lower expression in TSPAN10 KO cells. ADAM10 has a punctate distribution resembling endosomal compartments in Wild Type cells but shows a mislocalization to compartments resembling ER or Golgi in TSPAN10 KO cells. Scale bars indicate 10μm. **(C)** Quantification of images represented in (B). The graph shows the mean ± s.e.m. fluorescence intensity of n=213 cells for both Wild Type and TSPAN10 KO cells. Significance was tested using the Student's T test. **(D)** Immunoblots of RIPA lysates from Wild Type or TSPAN10 KO cells indicating less mature active ADAM10 is present in TSPAN10 KO cells. Lysates for ADAM10 immunoblotting were not boiled and were diluted in sample buffer lacking reducing agents to prevent ADAM10 aggregation. **(E)** Quantification of immunoblots represented in (D). The graph shows the mean ± s.e.m. band intensities relative to Wild Type, normalized to Tubulin loading controls. n=3 independent lysates were analyzed, and statistical significance was tested using the Student's T test. **(F)** Airyscan2 super resolution immunofluorescence images of Wild Type or TSPAN10 KO MNT1 cells surface stained for endogenous ADAM10 showing lower surface fluorescence in TSPAN10 KO cells. Surface staining was done by incubating MNT1 cells with anti ADAM10 primary antibody on ice for 30 minutes prior to fixation. Scale bars indicate 10μm. **(G)** Quantification of images represented in (F). The graph indicates the mean ± s.e.m. fluorescence intensity of n=76 cells for Wild Type and n=60 cells for TSPAN10 KO. Significance was tested using the Student's T test.

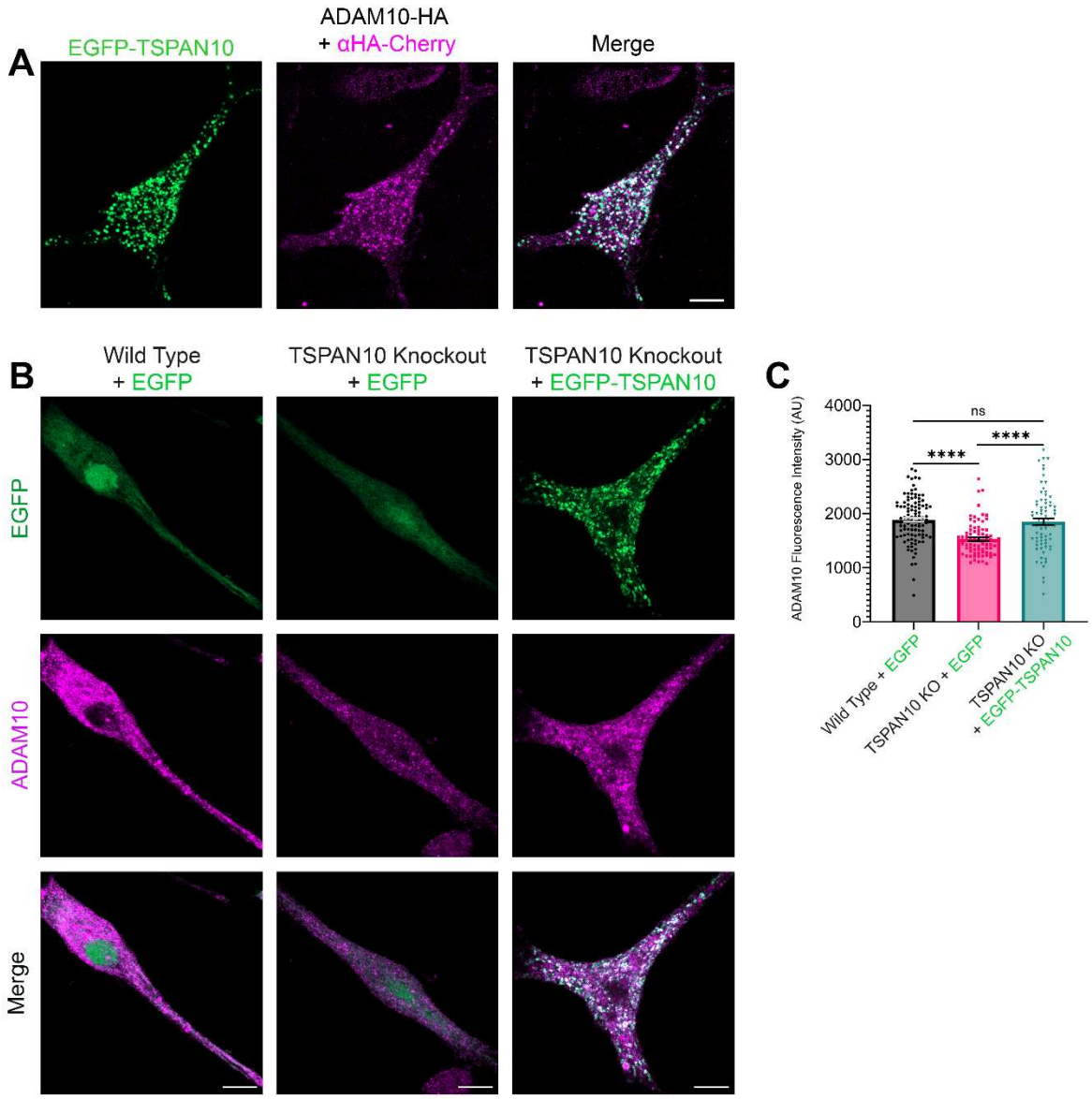

Figure 2.13. ADAM10-HA colocalizes with EGFP-TSPAN10 and ADAM10 expression is rescued in TSPAN10 KO cells transfected with EGFP-TSPAN10. (A) Airyscan2 super resolution live cell fluorescence microscopy of MNT1 cells expressing ADAM10-HA, αHA-mCherry ScFv intrabody, and EGFP-TSPAN10. Images show colocalization between ADAM10-HA and EGFP-TSPAN10. Scale bars indicate 10μm. **(B)** Airyscan2 super resolution fluorescence microscopy of Wild Type MNT1 cells transfected with soluble EGFP and TSPAN10 KO cells transfected with soluble EGFP or EGFP-TSPAN10 and immunostained for endogenous ADAM10. Images indicate ADAM10 fluorescence intensity is recovered when TSPAN10 is re-expressed in TSPAN10 KO cells. Scale bars indicate 10μm. **(C)** Quantification of ADAM10 fluorescence intensity for images represented in (B). The graph shows the mean ± s.e.m. n=109 Wild Type EGFP transfected cells, n=79 TSPAN10 KO EGFP transfected cells, and n=77 TSPAN10 KO EGFP-TSPAN10 transfected cells were analyzed. One way ANOVA with post hoc Tukey test was used to test for significance.

Discussion

Here, we determined the TPC2 proximity interactome in MNT1 melanoma cells, identifying over 200 TPC2 enriched proteins that were nearly absent in negative control experiments. By immunofluorescence microscopy, we demonstrated the utility of this dataset by confirming highly enriched hits PLD1, SV2A, and TSPAN10 are novel melanosome localized proteins. Utilizing newly generated TSPAN10 KO MNT1 cells, we demonstrated TSPAN10 regulates melanosome biogenesis by regulation of melanin synthesis, PMEL amyloidogenesis, and ADAM10 maturation and trafficking. Although TSPAN10 molecular function has not been previously characterized in melanocytes, TSPAN10 was associated with pigmentation in multiple bioinformatic studies. First, a GWAS investigating eye color in 195,000 individuals found the rs6420484 SNP in TSPAN10 to be significantly associated with light vs dark eye color (5). Another study investigated color patterning of Light Brown Mottling Ducks, which contain white ventral body parts and black dorsal body parts. RNA sequencing analysis of dorsal black skin tissue and ventral white skin tissue of embryonic ducks found TSPAN10 is one of several differentially expressed genes that has heightened expression in dorsal skin tissue, implicating it in pigmentation (41). Our results define a melanocyte intrinsic role for TSPAN10, providing important cellular context to the TSPAN10 associations with pigmentation.

Although our data shows TSPAN10 regulates ADAM10 protein expression and maturation, it is not entirely clear how ADAM10 regulates pigmentation. ADAM10 and ADAM17 were initially suggested to be the juxtamembrane sheddases responsible for releasing PMEL Mα ectodomain from the limiting membrane into the lumen using HeLa cells overexpressing PMEL as a model (62). However, it was later found that BACE2 is present at melanosomes in MNT1 cells and is required for efficient sheddase activity, which is necessary for amyloidogenesis in the melanosome lumen(61). In the present study, Mβ fragment levels were reduced in TSPAN10 KO cells, which have reduced ADAM10 expression, further arguing against the idea of ADAM10 being

the juxtamembrane sheddase for PMEL. Another study reinforced a link between ADAM10 and melanosome biogenesis, showing ADAM inhibitors negatively influence pigmentation and lead to fewer mature melanosomes, as well as an accumulation of dense aggregates in melanosomes visible by electron microscopy, presumably due to a PMEL deficiency. Additionally, ADAM10 inhibition only had mild effect on Mβ processing compared to BACE2 depletion, and ADAM10 apparently affected processing of amyloidogenic N terminal fragments of PMEL (52).

We identified significant PMEL abnormalities in TSPAN10 KO MNT1 cells. Heightened signal of TX100 insoluble PMEL Repeat domain and reduced Mα in immunoblots of TSPAN10 KO cell extracts suggests PMEL amyloid is generated in TSPAN10 KO cells and undergoes accelerated processing. However, by thin section electron microscopy, we discovered a melanosome biogenesis defect corresponding to pigmented melanosomes that lack ordered PMEL fibrils in TSPAN10 KO MNT1 cells. Therefore, despite efficient PMEL proteolytic processing, stereotypical fibrils are not generated. Interestingly, we observed heightened levels of active Cathepsin D in TSPAN10 KO cells. We suspect heightened activity of Cathepsin D may be a compensatory effect occurring in the loss of TSPAN10 and ADAM10 at melanosomes, leading to aberrant hyper-processing of PMEL and aberrant PMEL/melanin aggregation. Future studies should further investigate the interplay between TSPAN10 and other melanosomal or lysosomal proteases, to determine if TSPAN10 works specifically with ADAM10, or broadly with multiple proteases. Notably, PMEL mutations alone result in only mild pigmentation phenotypes (63). Therefore, TSPAN10 regulation of melanogenesis likely goes beyond its regulation of PMEL fibrillation. In neurons, ADAM10 has at least 91 unique substrates, including cell signaling proteins such as Notch (64). Thus, we predict TSPAN10 and ADAM10 target a host of substrates in melanocytes, some of which may contribute to efficient melanin synthesis. Also, it is also possible TSPAN10 has ADAM10 independent functions. These possibilities should be explored in future studies.

Given our results and those of others, one might expect ADAM10 mutations to be associated with pigmentation disorders. Surprisingly, ADAM10 mutations are associated with a rare pigmentation disorder, Reticulate Acropigmentation of Kitamura presenting with acral, depressed hyperpigmented spots (65, 66). Histopathological analysis revealed heightened counts of melanocytes in dark spots, and electron microscopy showed large clusters of melanocores within keratinocytes. However, it is unclear if these phenotypes are a result of ADAM10 function in melanosome biogenesis in melanocytes, or broader defects in epidermal structure because of impaired ADAM10 signaling associated functions.

In the present study, we considered TSPAN10 and ADAM10 function in the context of pigmentation. However, it is worth noting that ADAM10 has been implicated in many cellular processes including cell signaling, adhesion, and migration, and ADAM10 is upregulated in melanoma metastasis (67, 68). Likewise, TSPAN10 knockdown, which we expect to reduce ADAM10 expression, led to reduced transwell migration of B16F10 melanoma cells in a screen for genes involved in melanoma migration controlled by the transcription factor Sox10 (69). Therefore, it will be important to investigate the potential role of TSPAN10 regulation of ADAM10 in melanoma metastasis, especially since TSPAN10 expression is limited to a small number of cell types compared to ADAM10, and therefore might have more cell specificity as druggable target (35, 59).

We were unable to detect consistent pigmentation phenotypes in PLD1 KO or SV2A KO MNT1 cells under basal conditions, but we suspect each has functions in MNT1 cells not detected here. In former studies using cultured mouse B16 melanoma cells, PLD1 was shown to be a negative regulator of pigmentation, as PLD1 overexpression led to reduced melanin synthesis, while PLD1 knockdown resulted in heightened melanin synthesis, especially in the context of αMSH induced melanogenesis(42-44). Additionally, PLD1 expression negatively correlated with Tyrosinase and TYRP1 expression, and it was proposed phosphatidic acid (PA), generated by

PLD1, activates mTOR, which in turn suppresses MITF induced melanogenesis(42, 43). Interestingly, TPC2 conductance is negatively influenced by interaction with mTOR(12, 70, 71), and an enticing idea is that PLD1 activity generates PA, which recruits mTOR to melanosome membranes. However paradoxically, mTOR binding and inhibition of TPC2 conductance is expected to alkalinize melanosomes leading to heightened melanin synthesis. Whereas, in B16 cells, rapamycin inhibition of mTOR enhances melanogenesis (42, 72). It will be interesting to test if mTOR is recruited to melanosome membranes in a PLD1 or TPC2 dependent manner, and if PLD1 has a more appreciable pigmentation phenotype in the context of αMSH stimulation of MNT1 cells.

Endogenous SV2A was also found to colocalize with TPC2-EGFP in MNT1 cells, but SV2A KO did not influence basal pigment levels. In neurons, SV2A is localized to synaptic vesicles, where it is thought to prime vesicles for calcium induced exocytosis and is required for correct neurotransmitter release (73, 74). SV2A associates with, and co-traffics with Synaptotagmin, a calcium sensing protein that drives membrane fusion upon calcium excitation (75, 76). Connecting this to melanocyte function, Synaptotagmin-like proteins, notably Slp2-a, are expressed in melanocytes and interact with Rab27a, a Rab protein present on Stage IV terminal melanosomes, and function to coordinate melanosome capture at the cell cortex prior to transfer to keratinocytes (77-79). Therefore, an obvious future direction is to test if SV2A functions with Rab27a and Slp2-a, or other Synaptotagmins, in the exocytosis of melanosomes, especially since SV2A KO cells did not have an obvious melanogenesis defect.

In conclusion, we identified a TPC2 proximity interactome in MNT1 melanoma cells that was fruitful in identifying multiple novel melanosome membrane associated proteins, adding more key players to the continually growing list of pigmentation associated proteins. At least two of the top candidates, TSPAN10 and LRMDA (described previously), were found to have pigmentation phenotypes and regulate steps of melanosome biogenesis(24). We anticipate other hits identified

in our screen will also have functions in melanosome biogenesis, melanosome distribution, transfer to keratinocytes, and melanoma migration.

Materials and Methods

Cell culture and transfection

MNT1 cells were cultured with MNT1 medium containing DMEM (Gibco) with 10% (v/v) FBS (Atlas Biologicals), 10% (v/v) Aim-V media, 1X nonessential amino acids, 1X Penicillin Streptomycin Glutamate (Corning), and 0.25μg/mL Amphotericin B (Gibco) and grown at 37°C with 5% CO2. Cells were passed every 2-4 days depending on confluency.

To transfect cells for microscopy, $3X10^5$ MNT1 cells were pelleted at 200 x g and resuspended in 20μL Lonza SF solution, mixed with 0.4μg of plasmid or 1uL 6μM siRNA (ThermoFisher Silencer Select siRNAs) and nucleofected using 16 well nucleo-cuvette strips and the Lonza 4D nucleofector with program DS-137. siRNAs used in this study are listed in Table 2.1. 10 minutes after nucleofection, cells were transferred to 35mm glass bottom live cell imaging dishes or grown on 12mm cover slips in 35mm dishes containing prewarmed 2mL Keratinocyte Growth Medium Gold (Lonza) media for optimal recovery and imaging. For western blot and mass spectrometry experiments, larger transfections were performed with 1.5X10^6 cells. Cell pellets were resuspended in 100μL SF solution, mixed with 2μg plasmid or 5uL 6μM siRNA, transferred to large nucleocuvettes, and nucleofected with program DS-137 with the Lonza 4D nucleofector. After 10 minutes, cells were resuspended in 37°C MNT1 media and transferred to 10cm or 15cm dishes containing 10mL or 30mL MNT1 media and incubated for 3 days.

Plasmids

Generation of pEGFP-N3-TPC2 (Addgene 80153), pIRFP-N1-TPC2, pmCherry-N3-TPC1 and TPC2-BioID2-HA were described previously(9, 24, 38). pcDNA3-ADAM10-HA (Addgene 65106) was a gift from Axel Ullrich(80). pCMV-15F11-HA-mCherry (Addgene 129591, αHA-ScFv-mCherry) was generously gifted by Tim Stasevich and Ning Zhao(81).

Primers used for cloning and mutagenesis are listed in Table 2.2. TPC2 mutagenesis to mutate residue 734 or delete the last 25 residues was done by inverse PCR with primers having

overlapping 5' ends, digesting with the Infusion enzyme according to the manufacturer's instructions (Takara), and transforming into Stellar E. Coli (Takara). TPC1-BioID2-HA was made by amplifying TPC1 from TPC1-mCherry and Infusion (Takara) mediated insertion into TPC2-BioID2-HA digested with AgeI and HINDIII, replacing TPC2 with TPC1. pEGFP-C2-TSPAN10 was generated by amplifying TSPAN10 from TSPAN10 cDNA (Horizon Discovery MHS6278-202801105) and using Infusion to insert into pEGFP-C2 digested with EcoR1 and Sal1. Subsequent acidic dileucine motif mutagenesis was done by inverse PCR with mutagenic primers having overlapping 15bp 5' overhangs, digestion with Infusion enzyme (Takara) and transforming into Stellar E. coli (Takara). Plasmids were confirmed to have correct inserts by Sanger Sequencing.

Antibodies

Antibodies used in this study are listed in Table 2.3.

CRISPR-Cas9 Mediated Knockout

Generation of TPC2 knockout MNT1 cells was described and validated previously(9). New CRISPR-Cas9 knockout cell lines were generated using the IDT Alt-R CRISPR Cas9 system according to the manual and exactly as described previously(24). crRNAs used to target TSPAN10, PLD1, SV2A, and MYH10 are shown in Table 2.4. Cas9/crRNA/tracrRNA Complexes containing two different crRNAs were combined for each target transfection to increase chances of successful gene disruption. Protein depletion was confirmed by immunoblotting for the target protein.

TPC2 Proximity Biotinylation Experiment

For transfection, TPC2 KO background MNT1 cells were washed, trypsinized, anti-trypsinized and counted. 1.5X10^6 cells were pelleted at 200 X G for 5 minutes, resuspended in 100µL Lonza SF solution, mixed with 2µg plasmid maxiprep at a concentration of 1µg/µL, and nucleofected with program DS-137 in the Lonza 4D nucleofector. 5 transfections were performed for each construct for 7.5X10^6 cells total per dish. Transfected cells were grown in 15cm dishes with MNT1 media containing 250nM avidin for 48 hours in to reduce nonspecific biotin labeling during cell recovery after nucleofection. After 48 hours, avidin containing media was replaced with MNT1 media containing 50µM biotin to promote BioID2 proximity labeling at mature melanosomes for 24 hours. To harvest, 15cm dishes were washed with 10mL PBS and cells were trypsinized, anti trypsinized, and counted. Cells were normalized by cell count and 8.5X10^6 cells were pelleted at 200 X G for 5 minutes at 4°C. Cell pellets were lysed on ice for 10 minutes with 750µL RIPA buffer and briefly vortexed. Lysates were centrifuged for 40 minutes at 16,000 X G at 4°C to pellet insoluble debris. 30µL of the lysates were saved for western blot analysis. Clarified lysates were transferred to epi tubes containing 20µL MagStrep type3 XT magnetic beads (IBA LifeSciences) that had been prewashed with RIPA buffer. Samples were rotated end over end for 30 minutes at 4°C to capture biotinylated proteins. Beads were then harshly washed 4 times with 400µL RIPA buffer by vortexing to remove nonspecific binding. Biotinylated proteins were eluted in 1X SDS Sample Buffer with 0.5X BXT buffer (IBA LifeSciences) containing 25mM biotin to promote efficient elution. Eluted proteins were run in a 4-20% polyacrylamide gel for 15 minutes at 60V to achieve stacking of proteins without separation, and the gel was stained with Lab Safe Gel Blue Dye. Bands containing the stained protein were excised and sent for in gel Trypsin digest and protein identification by mass spectrometry (MS Bioworks Protein ID In-Gel Digest service).

Mass Spectrometry Analysis

In gel trypsin digestion was performed using a ProGest robot. Samples were washed with 25mM ammonium bicarbonate followed by acetonitrile. Then, they were reduced 10mM dithiothreitol at 60°C followed by alkylation with 50mM iodoacetamide at RT. Next, samples were digested with sequencing grade trypsin (Promega) at 37°C for 4h. Finally, samples were quenched with formic acid and the supernatant was analyzed directly without further processing. Half of the digested sample was analyzed by nano LC-MS/MS with a Waters NanoAcquity HPLC system interfaced to a ThermoFisher Q Exactive. Peptides were loaded on a trapping column and eluted over a 75μm analytical column at 350nL/min; both columns were packed with Luna C18 resin (Phenomenex). The mass spectrometer was operated in data-dependent mode, with the Orbitrap operating at 70,000 FWHM and 17,500 FWHM for MS and MS/MS respectively. The fifteen most abundant ions were selected for MS/MS.

Mass spectrometry data were searched using Mascot using the SwissProt Human database, peptide mass tolerance set to 10 ppm, fragment mass tolerance set to 0.02 Da, and max missed cleavages set to 2. Mascot files were first analyzed using Scaffold and subsequently analyzed in excel and GraphPad Prism. The Contaminant Repository for Affinity Purification analysis pipeline was used to generate SAINT scores, and to obtain 30 additional negative control BirA experiments, which are shown in **Appendix 4**. Venn Diagrams were created using http://bioinformatics.psb.ugent.be/webtools/Venn/.

Light Microscopy

Confocal super resolution fluorescence microscopy images were captured with a Zeiss LSM 900 with an Airyscan 2 detector, 405nm, 488nm, 561nm, and 647nm laser lines, and 40X/1.30 NA or 63X/1.40 NA oil immersion objective lenses. During acquisition, the microscope

was set to super resolution mode with frame scanning and default emission filter settings for each corresponding fluorophore to prevent fluorescence bleedthrough. Images were analyzed using FIJI (NIH) and colocalization analyses were done with the EZColocalization plugin(82, 83). Imaged cells were manually segmented, added to the Region Of Interest (ROI) Manager, and mean fluorescence intensity was measured. For colocalization analysis in the EZColocalization plugin, each channel to be analyzed was selected, and the ROI manager was selected as the cell identification input. Pearson Correlation Coefficient with Costes' automatic thresholding was selected as the colocalization method.

Brightfield and epifluorescence images were captured with a Keyence BZX-710 widefield fluorescence microscope with a 100X/1.45NA oil immersion objective lens. Cells were manually segmented in Fiji, added to the ROI manager, and mean fluorescence intensity was measured. To measure cellular pigment in brightfield images, a threshold was manually set to detect pigment, and % percent cell area with detectible pigment was measured.

Electron Microscopy

Electron microscopy was performed exactly as described previously(24).

Immunoblotting

Immunoblots were performed essentially as described previously (24). $1.5X10^6$ cells were seeded into 10cm dishes with 10mL MNT1 media and grown for 3 days before harvesting. To harvest, dishes were washed with 5mL ice cold PBS, then scraped into 5mL fresh ice-cold PBS using a cell lifter and spun down 200 x g for 5 minutes at 4°C. Then cell pellets were resuspended in 250µL RIPA lysis buffer or 1% TX100 in PBS with 1X protease inhibitor cocktail and lysed on ice for 15 minutes with gentle agitation every 5 minutes. Crude lysates were clarified by centrifuging at 16,000 x g for 15 minutes at 4°C. 200µL of the supernatant was mixed with 200µL 2X SDS Sample Buffer and frozen. The remaining supernatant was quantified by Bio Rad

Protein Assay to estimate total protein content according to the manufacturer's instructions. For immunoblots, frozen lysates were thawed and boiled for 5 minutes at 96°C. Approximately 30µg total protein was loaded into 4-20% gradient polyacrylamide gels (Novex wedgewell, Invitrogen) and run for 20 minutes at 80V and 90 minutes at 120V. Then, proteins were transferred to Polyvinylidene Fluoride membranes for 90 minutes at 100V at 4°C. Next, membranes were blocked with 5% milk TBST for 1 hour at RT, probed with primary antibody in 5% milk TBST overnight at 4°C, washed 3X with TBST for 5 minutes each, probed with secondary antibody in 5% milk TBST for 1 hour at RT, washed 3X with TBST for 5 minutes each, and finally developed with ECL Prime (Cytiva) or ECL Select (Cytiva) chemiluminescence reagent with a LAS 500 chemiluminescence CCD imager (GE).

For TPC2-BioID2-HA, ADAM10, and SV2A immunoblots, samples were not boiled as boiling was found to eliminate each protein's signal, presumably due to aggregation. For ADAM10, reducing agent was also removed from sample buffer to improve its electrophoretic behavior. For TX100 insoluble fractions, the insoluble pellet remaining from 1% TX100 lysis was washed for 15 minutes in 1mL 1% TX100 PBS to eliminate residual TX100 soluble protein, vortexing for 10 seconds every 5 minutes. Then, the insoluble material was repelleted 16,000 x g for 15 minutes at 4°C and the supernatant was aspirated. Finally, 250µL Laemmli Sample Buffer containing 4% SDS and DTT was added, and pellets were resuspended. Samples were subsequently boiled for 15 minutes with vortexing every 5 minutes before gel loading.

Immunofluorescence

Cells were grown on top of 12mm diameter coverslips in 35mm dishes with 2mL Keratinocyte Growth Media (Lonza) for 48 hours or MNT1 media for 72 hours (Figure 2.12B). Cultures were fixed using 2.5% methanol free formaldehyde (pierce) for 15 minutes at 37°C. Coverslips were washed for 5 minutes in room temperature PBS, then blocked with 1% BSA,

0.1% saponin in PBS for 30 minutes. Then, coverslips were briefly washed with PBS, moved to a dry surface, and then incubated with 50µL primary antibody diluted in 0.1% BSA, 0.1% saponin in PBS for 1 hour, held to the coverslip by surface tension. Coverslips were then washed briefly in PBS, washed for 5 minutes in PBS, and incubated with 50µL fluorophore conjugated secondary antibody for 1 hour in the dark. Finally, coverslips were stained with 0.4µg/mL DAPI (Invitrogen) PBS for 5 minutes, washed briefly with PBS, washed for 5 minutes with PBS, and mounted onto slides with 10µL ProLong Diamond Antifade mountant (ThermoFisher).

For surface staining of ADAM10, 6 well plates with MNT1 cells growing on coverslips were transferred to ice and media was removed. Then, anti ADAM10 antibody (ab59482), diluted 1:100 in KGM Gold media, was added to coverslips for a 20 minute incubation on ice to prevent internalization. After the incubation, coverslips were washed with ice cold PBS for 20 seconds and then fixed with ice cold 2.5% formaldehyde at 4°C for 20 minutes. After fixation, coverslips were washed twice with PBS, and stained with secondary antibody in PBS with 0.1% Saponin and 0.1% BSA as described above, washed twice with PBS for 5 minutes, and mounted onto slides with 10µL ProLong Diamond Antifade mountant.

Melanin Quantification Assay

1.5X10^6 cells were seeded in 10cm dishes and grown for 72 hours in MNT1 media. Then cells were trypsinized, counted, and 1X10^6 cells were pelleted in 1.5mL screw cap tubes. Cell pellets were homogenized with 0.5mm glass beads in a Beadbug 6 homogenizer, shaking at 2500RPM for 3 cycles of 30 seconds on, 30 seconds off. Tubes were then centrifuged at 16,000 x g for 15 minutes at 4°C, and the supernatant was removed and used to measure total protein content by Bio Rad Protein assay. Then, pellets were washed with 1mL ice cold 100% ethanol and vortexed for 10 seconds. Melanin was repelleted 16,000 x g for 15 minutes at 4°C. Ethanol

was aspirated and then the pellets were dried by evaporating excess moisture by incubating at 37°C for 1 hour. Then, melanin was dissolved by incubating with 10% (v/v) DMSO 1N NaOH for 1 hour at 80°C, vortexing for 10 seconds every 15 minutes. Finally, samples were equilibrated to room temperature for 20 minutes, centrifuged at 16,000 x G for 10 minutes at RT to pellet insoluble material, transferred to 1cm path length cuvettes and absorbance read at 490nm using a Nanodrop One spectrophotometer (Thermo Scientific). Samples were analyzed in technical duplicate and cell pellets from three independent experiments were analyzed. *Sepia officinalis* melanin was used to generate a linear standard curve.

Statistical Analysis

Statistical analysis was performed using Graphpad Prism software. For comparing 2 populations, Student's T test was used. For comparing TPC2 interactomes with negative control interactomes For analyzing 3 or more populations, One Way ANOVA with posthoc Tukey tests were performed. For non-normal distributions with 3 or more populations, Kruskal-Wallis Test was used. Error bars and n values are described in the figure captions. Significance in graphs is depicted as *$p \leq 0.05$; **$p \leq 0.01$; ***$p \leq 0.001$; and ****$p \leq 0.0001$

Table 2.1. List of siRNAs

siRNA Used	siRNA Assay ID	Sequence 5'-3'	Source
siMock - negative control siRNA No. 1	4390843	Proprietary	ThermoFisher
siFMNL2-1	s41619	Proprietary	ThermoFisher
siFMNL2-2	s41620	Proprietary	ThermoFisher
siSV2A-1	s19183	Proprietary	ThermoFisher
siSV2A-2	s19184	Proprietary	ThermoFisher
siCTTN-1	s4665	Proprietary	ThermoFisher
siCTTN-2	n345340	Proprietary	ThermoFisher
siCTTN-3	s4666	Proprietary	ThermoFisher
siMYH9-1	s222	Proprietary	ThermoFisher

siMYH9-2	NA	CCAAAGAGAACGAGAAGAA	Gifted from O'Neil Wiggan(84)
siMYH9-3	s223	Proprietary	ThermoFisher
siMYH10-1	s9169	Proprietary	ThermoFisher
siMYH10-2	s9170	Proprietary	ThermoFisher
siMYH10-3	NA	GGGCCAACATTGAAACATA	Gifted from O'Neil Wiggan(84)
siPLD1	s10637	Proprietary	ThermoFisher
siTSPAN10-1	s38272	Proprietary	ThermoFisher
siTSPAN10-2	s195449	Proprietary	ThermoFisher
siTSPAN10-3	s195448	Proprietary	ThermoFisher

Table 2.2. Primers used for cloning and mutagenesis.

Primer Name	**Sequence (5'-3')**	**Plasmid Generated**
TPC2 Mutagenesis E734G	gggatattctggaggagcccggggaggatgagctcacagaga ggc	pEGFP-N3-TPC2-734G
TPC2 Mutagenesis E734G	gcctctctgtgagctcatcctccccgggctcctccagaatatccc	pEGFP-N3-TPC2-734G
TPC2 Mutagenesis ΔCT	gagctcctgttcaggGTCGACGGTACCGCG	pEGFP-N3-TPC2-ΔCT
TPC2 Mutagenesis ΔCT	cctgaacaggagctccacagtcatctg	pEGFP-N3-TPC2- ΔCT
TPC1 Forward	aggcctgttaaccggtcATGGCTGTGAGTTTGGATG ACG	TPC1-BioID2-HA
TPC1 Reverse	caccgcctccAAGCTTGGTAACGGTCTGGGAGC GCTGG	TPC1-BioID2-HA
TSPAN10 Forward	CTCAAGCTTCGAATTCatggaggaggggagagg	pEGFP-C2-TSPAN10
TSPAN10 Reverse	CCGCGGTACCGTCGACtcagccccgggcg	pEGFP-C2-TSPAN10
TSPAN10 LL/AA Mutagenesis	gcagcgtcccaggaaactgcagg	pEGFP-C2-TSPAN10 LL/AA
TSPAN10 LL/AA Mutagenesis Reverse	ttcctgggacgctgcggggctcctctcccc	pEGFP-C2-TSPAN10 LL/AA

Table 2.3. List of Antibodies

Antibody Name	Source	Catalog Number	Dilution
HA-HorseRadish Peroxidase	Cell Signaling	2999S	1:1000 WB
PLD1	Santa Cruz Biotechnology	sc-28314	1:100 IF, 1:1000 WB
SV2A	Developmental Studies Hybridoma Bank	SV2-Concentrate 0.1 ml	1:100 IF, 1:500 WB

TSPAN10	Proteintech	14430-1-AP	1:100 IF, 1:10,000 WB
FMNL2	Abcam	ab5763	1:100 IF, 1:1000 WB
CTTN	Millipore Sigma	05-180, clone 4F11	1:100 IF, 1:1000 WB
MYH9	Sigma Aldrich	M8064	1:100 IF, 1:1000 WB
MYH10	Sigma Aldrich	M7939	1:100 IF, 1:3000 WB
Tyrosinase	Santa Cruz Biotechnology	sc-20035	1:2000 WB
TYRP1, MELV	Santa Cruz Biotechnology	sc-58438, clone TA99	1:500 IF
PMEL HMB45	Dako	GA052	1:500 IF, 1:3000 WB
PMEL N	Santa Cruz Biotechnology	sc-377325, clone E7	1:1000 WB
PMEL I51	Michael Marks and Ralf Leonhardt	NA	1:1000 WB
PMEL C	LS Bio	C47016	1:500 WB
LAMP2	Santa Cruz Biotechnology	sc18822, clone H4B4	1:500 IF, 1:2000 WB
Cathepsin D C term	Santa Cruz Biotechnology	sc-6486, clone C-20	1:3000 WB
ITGα5	Abcam	ab150361	1:2000 WB
ADAM10	Abcam	ab59482, clone 11G2	1:100 IF, 1:1000 WB
GAPDH	Proteintech	60004-1-Ig	1:1,000,000 WB
Tubulin	Sigma Aldrich	T9026	1:100,000 WB
Anti Mouse IgG HRP Linked	Cytiva	NA931	1:7500 WB
Anti Rabbit IgG HRP Linked	Cytiva	NA934	1:7500 WB
Anti Mouse IgG Alexa fluor 488	Invitrogen	A-11029	1:1000 IF
Anti Rabbit IgG Alexa fluor 488	Invitrogen	A-11034	1:1000 IF
Anti Mouse IgG Alexa fluor 647	Invitrogen	A-21236	1:1000 IF
Anti Rabbit IgG Alexa fluor 647	Invitrogen	A-21245	1:1000 IF
Streptavidin HRP Linked	Pierce	21130	1:3000 Biotin Detection Blot

Table 2.4. IDT Predesigned CRISPR RNA sequences used to knockout genes of interest.

Targeted Gene	**IDT crRNA**	**Targeted Sequence (5'-3')**
TSPAN10	Hs.Cas9.TSPAN10.1.AA	GAGAACACCTGCCTGTTACG
TSPAN10	Hs.Cas9.TSPAN10.1.AC	TTCTGTTCCAGCGTCAAGGA
PLD1	Hs.Cas9.PLD1.1.AA	CACGCGGGAACTCCACTTTG
PLD1	Hs.Cas9.PLD1.1.AC	AGTGCAGAGGTATTTACCCG
SV2A	HS.CAS9.SV2A.1.AA	AAAGCGGGAGTACGATCTTC
SV2A	HS.CAS9.SV2A.1.AB	GTGGCCACACTCCCGTAGGA
MYH10	HS.CAS9.MYH10.1.AB	CTGAAGGATCGCTACTATTC
MYH10	HS.CAS9.MYH10.1.AC	TGGATTCCATCAGAACGCCA

REFERENCES

1. Moreiras, H., Seabra, M. C., and Barral, D. C. (2021) Melanin Transfer in the Epidermis: The Pursuit of Skin Pigmentation Control Mechanisms Int J Mol Sci **22**, 10.3390/ijms22094466

2. Byers, H. R., Maheshwary, S., Amodeo, D. M., and Dykstra, S. G. (2003) Role of cytoplasmic dynein in perinuclear aggregation of phagocytosed melanosomes and supranuclear melanin cap formation in human keratinocytes J Invest Dermatol **121**, 813-820 10.1046/j.1523-1747.2003.12481.x

3. Le, L., Sirés-Campos, J., Raposo, G., Delevoye, C., and Marks, M. S. (2021) Melanosome Biogenesis in the Pigmentation of Mammalian Skin In Integrative and Comparative Biology, Oxford University Press (OUP),

4. Pavan, W. J., and Sturm, R. A. (2019) The Genetics of Human Skin and Hair Pigmentation Annu Rev Genomics Hum Genet **20**, 41-72 10.1146/annurev-genom-083118-015230

5. Simcoe, M., Valdes, A., Liu, F., Furlotte, N. A., Evans, D. M., Hemani, G. *et al.* (2021) Genome-wide association study in almost 195,000 individuals identifies 50 previously unidentified genetic loci for eye color In Science Advances, American Association for the Advancement of Science, 24

6. Sulem, P., Gudbjartsson, D. F., Stacey, S. N., Helgason, A., Rafnar, T., Jakobsdottir, M. *et al.* (2008) Two newly identified genetic determinants of pigmentation in Europeans In Nature Genetics, 835-837

7. Böck, J., Krogsaeter, E., Passon, M., Chao, Y.-K., Sharma, S., Grallert, H. *et al.* (2021) Human genome diversity data reveal that L564P is the predominant TPC2 variant and a prerequisite for the blond hair associated M484L gain-of-function effect In PLOS Genetics, Oancea E, ed. Public Library of Science (PLoS), e1009236

8. Wang, Q., Wang, Z., Wang, Y., Qi, Z., Bai, D., Wang, C. *et al.* (2023) A gain-of-function TPC2 variant R210C increases affinity to PI(3,5)P2 and causes lysosome acidification and hypopigmentation In Nature Communications, Nature Publishing Group,

9. Ambrosio, A. L., Boyle, J. A., Aradi, A. E., Christian, K. A., and Di Pietro, S. M. (2016) TPC2 controls pigmentation by regulating melanosome pH and size In Proceedings of the National Academy of Sciences, 5622-5627

10. Bellono, N. W., Escobar, I. E., and Oancea, E. (2016) A melanosomal two-pore sodium channel regulates pigmentation In Scientific Reports, Nature Publishing Group, 1-11

11. Netcharoensirisuk, P., Abrahamian, C., Tang, R., Chen, C.-C., Rosato, A. S., Beyers, W. *et al.* (2021) Flavonoids increase melanin production and reduce proliferation, migration and invasion of melanoma cells by blocking endolysosomal/melanosomal TPC2 In Scientific Reports, Sci Rep, 8515

12. Chao, Y.-K., Schludi, V., Chen, C.-C., Butz, E., Nguyen, O. N. P., Müller, M. *et al.* (2017) TPC2 polymorphisms associated with a hair pigmentation phenotype in humans result in gain of channel function by independent mechanisms In Proceedings of the National Academy of Sciences, 201705739

13. Cang, C., Zhou, Y., Navarro, B., Seo, Y.-J., Aranda, K., Shi, L. *et al.* (2013) mTOR regulates lysosomal ATP-sensitive two-pore Na(+) channels to adapt to metabolic state. In Cell, NIH Public Access, 778-790

14. Patel, S., Zissimopoulos, S., and Marchant, J. S. (2022) Endo-Lysosomal Two-Pore Channels and Their Protein Partners Springer, Berlin, Heidelberg, 1-16

15. Zhang, J., Guan, X., Shah, K., and Yan, J. (2021) Lsm12 is an NAADP receptor and a two-pore channel regulatory protein required for calcium mobilization from acidic organelles In Nature Communications 2021 12:1, Nature Publishing Group, 1-13

16. Lin-Moshier, Y., Keebler, M. V., Hooper, R., Boulware, M. J., Liu, X., Churamani, D. *et al.* (2014) The Two-pore channel (TPC) interactome unmasks isoform-specific roles for TPCs in endolysosomal morphology and cell pigmentation Proc Natl Acad Sci U S A **111**, 13087-13092 10.1073/pnas.1407004111

17. Grimm, C., Holdt, L. M., Chen, C.-C., Hassan, S., Müller, C., Jörs, S. *et al.* (2014) High susceptibility to fatty liver disease in two-pore channel 2-deficient mice In Nature Communications, Nature Publishing Group, 4699

18. Lin-Moshier, Y., Keebler, M. V., Hooper, R., Boulware, M. J., Liu, X., Churamani, D. *et al.* (2014) The Two-pore channel (TPC) interactome unmasks isoform-specific roles for TPCs in endolysosomal morphology and cell pigmentation In Proceedings of the National Academy of Sciences, 13087-13092

19. Kim, D. I., Jensen, S. C., Noble, K. A., KC, B., Roux, K. H., Motamedchaboki, K. *et al.* (2016) An improved smaller biotin ligase for BioID proximity labeling In Molecular Biology of the Cell, 1188-1196

20. She, J., Guo, J., Chen, Q., Zeng, W., Jiang, Y., and Bai, X.-c. (2018) Structural insights into the voltage and phospholipid activation of the mammalian TPC1 channel In Nature, Nature Publishing Group, 130-134

21. Bellono, N. W., Escobar, I. E., and Oancea, E. (2016) A melanosomal two-pore sodium channel regulates pigmentation Scientific Reports **6**, 26570 10.1038/srep26570

22. Castonguay, J., Orth, J. H. C., Müller, T., Sleman, F., Grimm, C., Wahl-Schott, C. *et al.* (2017) The two-pore channel TPC1 is required for efficient protein processing through early and recycling endosomes Scientific Reports **7**, 10.1038/s41598-017-10607-4

23. Teo, G., Liu, G., Zhang, J., Nesvizhskii, A. I., Gingras, A.-C., and Choi, H. (2014) SAINTexpress: improvements and additional features in Significance Analysis of INTeractome software. In Journal of proteomics, NIH Public Access, 37-43

24. Beyers, W. C., Detry, A. M., and Di Pietro, S. M. (2022) OCA7 is a melanosome membrane protein that defines pigmentation by regulating early stages of melanosome biogenesis J Biol Chem **298**, 102669 10.1016/j.jbc.2022.102669

25. Li, S., Yan, R., Xu, J., Zhao, S., Ma, X., Sun, Q. *et al.* (2022) A new type of ERGIC-ERES membrane contact mediated by TMED9 and SEC12 is required for autophagosome biogenesis Cell Res **32**, 119-138 10.1038/s41422-021-00563-0

26. Mehta, S., Li, H., Hogan, P. G., and Cunningham, K. W. (2009) Domain architecture of the regulators of calcineurin (RCANs) and identification of a divergent RCAN in yeast Mol Cell Biol **29**, 2777-2793 10.1128/MCB.01197-08

27. Aoh, Q. L., Castle, A. M., Hubbard, C. H., Katsumata, O., and Castle, J. D. (2009) SCAMP3 negatively regulates epidermal growth factor receptor degradation and promotes receptor recycling Mol Biol Cell **20**, 1816-1832 10.1091/mbc.e08-09-0894

28. Gómez-Suaga, P., Luzón-Toro, B., Churamani, D., Zhang, L., Bloor-Young, D., Patel, S. *et al.* (2012) Leucine-rich repeat kinase 2 regulates autophagy through a calcium-dependent pathway involving NAADP. In Human molecular genetics, Oxford University Press, 511-525

29. Davis, L. C., Morgan, A. J., and Galione, A. (2020) NAADP-regulated two-pore channels drive phagocytosis through endo-lysosomal Ca(2+) nanodomains, calcineurin and dynamin EMBO J **39**, e104058 10.15252/embj.2019104058

30. Fujibuchi, T., Abe, Y., Takeuchi, T., Imai, Y., Kamei, Y., Murase, R. *et al.* (2005) AIP1/WDR1 supports mitotic cell rounding Biochem Biophys Res Commun **327**, 268-275 10.1016/j.bbrc.2004.11.156

31. de Souza Ferreira, L. P., da Silva, R. A., Gil, C. D., and Geisow, M. J. (2023) Annexin A1, A2, A5, and A6 involvement in human pathologies Proteins 10.1002/prot.26512

32. Nixon-Abell, J., Ruggeri, F. S., Qamar, S., Herling, T. W., Czekalska, M. A., Shen, Y. *et al.* (2023) ANXA11 biomolecular condensates facilitate protein-lipid phase coupling on lysosomal membranes Cold Spring Harbor Laboratory,

33. Yang, C., Slepnev, V. I., and Goud, B. (1994) Rab proteins form in vivo complexes with two isoforms of the GDP-dissociation inhibitor protein (GDI) J Biol Chem **269**, 31891-31899, https://www.ncbi.nlm.nih.gov/pubmed/7989364

34. Ripoll, L., Heiligenstein, X., Hurbain, I., Domingues, L., Figon, F., Petersen, K. J. *et al.* (2018) Myosin VI and branched actin filaments mediate membrane constriction and fission of melanosomal tubule carriers In The Journal of Cell Biology, jcb.201709055

35. Dornier, E., Coumailleau, F., Ottavi, J. F., Moretti, J., Boucheix, C., Mauduit, P. *et al.* (2012) Tspanc8 tetraspanins regulate ADAM10/Kuzbanian trafficking and promote Notch activation in flies and mammals In Journal of Cell Biology, The Rockefeller University Press, 481-496

36. Sitaram, A., Dennis, M. K., Chaudhuri, R., De Jesus-Rojas, W., Tenza, D., Setty, S. R. G. *et al.* (2012) Differential recognition of a dileucine-based sorting signal by AP-1 and AP-3

reveals a requirement for both BLOC-1 and AP-3 in delivery of OCA2 to melanosomes Molecular Biology of the Cell **23**, 3178-3192 10.1091/mbc.e11-06-0509

37. Braulke, T., and Bonifacino, J. S. (2009) Sorting of lysosomal proteins Biochim Biophys Acta **1793**, 605-614 10.1016/j.bbamcr.2008.10.016

38. Ambrosio, A. L., Boyle, J. A., and Di Pietro, S. M. (2015) TPC2 mediates new mechanisms of platelet dense granule membrane dynamics through regulation of Ca2+ release In Molecular Biology of the Cell, American Society for Cell Biology, 3263-3274

39. Park, S. Y., and Guo, X. (2014) Adaptor protein complexes and intracellular transport. In Bioscience reports, Portland Press Ltd,

40. Sitaram, A., Dennis, M. K., Chaudhuri, R., De Jesus-Rojas, W., Tenza, D., Setty, S. R. G. *et al.* (2012) Differential recognition of a dileucine-based sorting signal by AP-1 and AP-3 reveals a requirement for both BLOC-1 and AP-3 in delivery of OCA2 to melanosomes In Molecular Biology of the Cell, 3178-3192

41. Xi, Y., Liu, H., Li, L., Xu, Q., Liu, Y., Wang, L. *et al.* (2020) Transcriptome Reveals Multi Pigmentation Genes Affecting Dorsoventral Pattern in Avian Body In Frontiers in cell and developmental biology, Front Cell Dev Biol,

42. Ohguchi, K., Banno, Y., Nakagawa, Y., Akao, Y., and Nozawa, Y. (2005) Negative regulation of melanogenesis by phospholipase D1 through mTOR/p70 S6 kinase 1 signaling in mouse B16 melanoma cells In Journal of Cellular Physiology, 444-451

43. Ohguchi, K., Banno, Y., Akao, Y., and Nozawa, Y. (2004) Involvement of Phospholipase D1 in Melanogenesis of Mouse B16 Melanoma Cells In Journal of Biological Chemistry, 3408-3412

44. Kageyama, A., Oka, M., Okada, T., Nakamura, S.-i., Ueyama, T., Saito, N. *et al.* (2004) Down-regulation of Melanogenesis by Phospholipase D2 through Ubiquitin Proteasome-mediated Degradation of Tyrosinase In Journal of Biological Chemistry, 27774-27780

45. Bassani, S., andCingolani, L. A. (2012) Tetraspanins: Interactions and interplay with integrins In International Journal of Biochemistry and Cell Biology, Elsevier Ltd, 703-708

46. Raposo, G., Tenza, D., Murphy, D. M., Berson, J. F., and Marks, M. S. (2001) Distinct Protein Sorting and Localization to Premelanosomes, Melanosomes, and Lysosomes in Pigmented Melanocytic Cells✪ In Journal of Cell Biology, The Rockefeller University Press, 809-824

47. Fowler, D. M., Koulov, A. V., Alory-Jost, C., Marks, M. S., Balch, W. E., and Kelly, J. W. (2005) Functional Amyloid Formation within Mammalian Tissue PLoS Biology **4**, e6 10.1371/journal.pbio.0040006

48. Watt, B., van Niel, G., Raposo, G., and Marks, M. S. (2013) PMEL: a pigment cell-specific model for functional amyloid formation In Pigment Cell & Melanoma Research, John Wiley & Sons, Ltd, 300-315

49. Rochin, L., Hurbain, I., Serneels, L., Fort, C., Watt, B., Leblanc, P. *et al.* (2013) BACE2 processes PMEL to form the melanosome amyloid matrix in pigment cells In Proceedings of the National Academy of Sciences of the United States of America, National Academy of Sciences, 10658-10663

50. van Niel, G., Bergam, P., Di Cicco, A., Hurbain, I., Lo Cicero, A., Dingli, F. *et al.* (2015) Apolipoprotein E Regulates Amyloid Formation within Endosomes of Pigment Cells In Cell Reports, Elsevier, 43-51

51. Leonhardt, R. M., Vigneron, N., Hee, J. S., Graham, M., and Cresswell, P. (2013) Critical residues in the PMEL/Pmel17 N-terminus direct the hierarchical assembly of melanosomal fibrils In Molecular Biology of the Cell, The American Society for Cell Biology 964-981

52. Kawaguchi, M., Hozumi, Y., and Suzuki, T. (2015) ADAM protease inhibitors reduce melanogenesis by regulating PMEL17 processing in human melanocytes In Journal of Dermatological Science, Elsevier Ireland Ltd, 133-142

53. Ho, T., Watt, B., Spruce, L. A., Seeholzer, S. H., and Marks, M. S. (2016) The Kringle-like Domain Facilitates Post-endoplasmic Reticulum Changes to Premelanosome Protein (PMEL) Oligomerization and Disulfide Bond Configuration and Promotes Amyloid Formation In The Journal of biological chemistry, J Biol Chem, 3595-3612

54. Bissig, C., Croisé, P., Heiligenstein, X., Hurbain, I., Lenk, G. M., Kaufman, E. *et al.* (2019) The PIKfyve complex regulates the early melanosome homeostasis required for physiological amyloid formation. In Journal of cell science, The Company of Biologists Ltd, jcs229500

55. Liggins, M. C., Flesher, J. L., Jahid, S., Vasudeva, P., Eby, V., Takasuga, S. *et al.* (2018) PIKfyve regulates melanosome biogenesis In PLoS Genetics, Public Library of Science,

56. Seiji, M., Shimao, K., Birbeck, M. S., and Fitzpatrick, T. B. (1963) Subcellular localization of melanin biosynthesis Ann N Y Acad Sci **100**, 497-533, https://www.ncbi.nlm.nih.gov/pubmed/13992624

57. Bissig, C., Rochin, L., and van Niel, G. (2016) PMEL Amyloid Fibril Formation: The Bright Steps of Pigmentation. In International journal of molecular sciences, Multidisciplinary Digital Publishing Institute (MDPI),

58. van Niel, G., Charrin, S., Simoes, S., Romao, M., Rochin, L., Saftig, P. *et al.* (2011) The Tetraspanin CD63 Regulates ESCRT-Independent and -Dependent Endosomal Sorting during Melanogenesis In Developmental Cell, Cell Press, 708-721

59. Haining, E. J., Yang, J., Bailey, R. L., Khan, K., Collier, R., Tsai, S. *et al.* (2012) The TspanC8 subgroup of tetraspanins interacts with A disintegrin and metalloprotease 10 (ADAM10) and regulates its maturation and cell surface expression In The Journal of biological chemistry, J Biol Chem, 39753-39765

60. Clark, N. L., Alani, E., and Aquadro, C. F. (2012) Evolutionary rate covariation reveals shared functionality and coexpression of genes Genome Research **22**, 714-720 10.1101/gr.132647.111

61. Rochin, L., Hurbain, I., Serneels, L., Fort, C., Watt, B., Leblanc, P. *et al.* (2013) BACE2 processes PMEL to form the melanosome amyloid matrix in pigment cells Proc Natl Acad Sci U S A **110**, 10658-10663 10.1073/pnas.1220748110

62. Kummer, M. P., Maruyama, H., Huelsmann, C., Baches, S., Weggen, S., and Koo, E. H. (2009) Formation of Pmel17 amyloid is regulated by juxtamembrane metalloproteinase cleavage, and the resulting C-terminal fragment is a substrate for gamma-secretase In The Journal of biological chemistry, J Biol Chem, 2296-2306

63. Hellström, A. R., Watt, B., Fard, S. S., Tenza, D., Mannström, P., Narfström, K. *et al.* (2011) Inactivation of Pmel Alters Melanosome Shape But Has Only a Subtle Effect on Visible Pigmentation In PLOS Genetics, Public Library of Science, e1002285

64. Kuhn, P.-H., Colombo, A. V., Schusser, B., Dreymueller, D., Wetzel, S., Schepers, U. *et al.* (2016) Systematic substrate identification indicates a central role for the metalloprotease ADAM10 in axon targeting and synapse function eLife **5**, 10.7554/elife.12748

65. Okamura, K., Abe, Y., Araki, Y., Hozumi, Y., Kawaguchi, M., and Suzuki, T. (2016) Behavior of melanocytes and keratinocytes in reticulate acropigmentation of Kitamura Pigment Cell Melanoma Res **29**, 243-246 10.1111/pcmr.12453

66. Kono, M., Sugiura, K., Suganuma, M., Hayashi, M., Takama, H., Suzuki, T. *et al.* (2013) Whole-exome sequencing identifies ADAM10 mutations as a cause of reticulate acropigmentation of Kitamura, a clinical entity distinct from Dowling-Degos disease Hum Mol Genet **22**, 3524-3533 10.1093/hmg/ddt207

67. Lee, S. B., Schramme, A., Doberstein, K., Dummer, R., Abdel-Bakky, M. S., Keller, S. *et al.* (2010) ADAM10 is upregulated in melanoma metastasis compared with primary melanoma In The Journal of investigative dermatology, J Invest Dermatol, 763-773

68. Gangemi, R., Amaro, A., Gino, A., Barisione, G., Fabbi, M., Pfeffer, U. *et al.* (2014) ADAM10 correlates with uveal melanoma metastasis and promotes in vitro invasion In Pigment Cell & Melanoma Research, John Wiley & Sons, Ltd, 1138-1148

69. Seong, I., Min, H. J., Lee, J. H., Yeo, C. Y., Kang, D. M., Oh, E. S. *et al.* (2012) Sox10 controls migration of B16F10 melanoma cells through multiple regulatory target genes In PLoS ONE, PLOS, 31477

70. Cang, C., Zhou, Y., Navarro, B., Seo, Y. J., Aranda, K., Shi, L. *et al.* (2013) mTOR regulates lysosomal ATP-sensitive two-pore Na(+) channels to adapt to metabolic state Cell **152**, 778-790 10.1016/j.cell.2013.01.023

71. Ogunbayo, O. A., Duan, J., Xiong, J., Wang, Q., Feng, X., Ma, J. *et al.* (2018) mTORC1 controls lysosomal Ca2+ release through the two-pore channel TPC2. In Science signaling, NIH Public Access,

72. Busca, R., Bertolotto, C., Ortonne, J. P., and Ballotti, R. (1996) Inhibition of the phosphatidylinositol 3-kinase/p70(S6)-kinase pathway induces B16 melanoma cell differentiation J Biol Chem **271**, 31824-31830 10.1074/jbc.271.50.31824

73. Chang, W.-P., and Südhof, T. C. (2009) SV2 Renders Primed Synaptic Vesicles Competent for Ca²⁺-Induced Exocytosis The Journal of Neuroscience **29**, 883-897 10.1523/jneurosci.4521-08.2009

74. Vogl, C., Tanifuji, S., Danis, B., Daniels, V., Foerch, P., Wolff, C. *et al.* (2015) Synaptic vesicle glycoprotein 2A modulates vesicular release and calcium channel function at peripheral sympathetic synapses European Journal of Neuroscience **41**, 398-409 10.1111/ejn.12799

75. Yao, J., Nowack, A., Kensel-Hammes, P., Gardner, R. G., and Bajjalieh, S. M. (2010) Cotrafficking of SV2 and Synaptotagmin at the Synapse In The Journal of Neuroscience, Society for Neuroscience, 5569

76. Harper, C. B., Small, C., Davenport, E. C., Low, D. W., Smillie, K. J., Martínez-Mármol, R. *et al.* (2020) An epilepsy-associated SV2A mutation disrupts synaptotagmin-1 expression and activity-dependent trafficking In Journal of Neuroscience, Society for Neuroscience, 4586-4595

77. Kuroda, T. S., Fukuda, M., Ariga, H., and Mikoshiba, K. (2002) The Slp Homology Domain of Synaptotagmin-like Proteins 1–4 and Slac2 Functions as a Novel Rab27A Binding Domain Journal of Biological Chemistry **277**, 9212-9218 10.1074/jbc.m112414200

78. Kuroda, T. S., and Fukuda, M. (2004) Rab27A-binding protein Slp2-a is required for peripheral melanosome distribution and elongated cell shape in melanocytes In Nature Cell Biology 2004 6:12, Nature Publishing Group, 1195-1203

79. Fukuda, M. (2006) Rab27 and its effectors in secretory granule exocytosis: a novel docking machinery composed of a Rab27·effector complex In Biochemical Society Transactions, Portland Press, 691-695

80. Gschwind, A. (2003) TACE cleavage of proamphiregulin regulates GPCR-induced proliferation and motility of cancer cells The EMBO Journal **22**, 2411-2421 10.1093/emboj/cdg231

81. Zhao, N., Kamijo, K., Fox, P. D., Oda, H., Morisaki, T., Sato, Y. *et al.* (2019) A genetically encoded probe for imaging nascent and mature HA-tagged proteins in vivo Nature Communications **10**, 10.1038/s41467-019-10846-1

82. Schindelin, J., Arganda-Carreras, I., Frise, E., Kaynig, V., Longair, M., Pietzsch, T. *et al.* (2012) Fiji: an open-source platform for biological-image analysis Nat Methods **9**, 676-682 10.1038/nmeth.2019

83. Stauffer, W., Sheng, H., and Lim, H. N. (2018) EzColocalization: An ImageJ plugin for visualizing and measuring colocalization in cells and organisms Scientific Reports **8**, 10.1038/s41598-018-33592-8

84. Wiggan, O. N., Alisa, Jennifer, and James (2012) ADF/Cofilin Regulates Actomyosin Assembly through Competitive Inhibition of Myosin II Binding to F-Actin Developmental Cell **22**, 530-543 10.1016/j.devcel.2011.12.026

CHAPTER 3

OCA7 IS A MELANOSOME MEMBRANE PROTEIN THAT DEFINES PIGMENTATION BY REGULATING EARLY STAGES OF MELANOSOME BIOGENESIS[*]

Summary

Mutations in C10orf11 (OCA7) cause OculoCutaneous Albinism, a disorder that presents with hypopigmentation in skin, eyes and hair. The OCA7 pathophysiology is unknown and there is virtually no information on the OCA7 protein and its cellular function. Here, we discover that OCA7 localizes to the limiting membrane of melanosomes, the specialized pigment cell organelles where melanin is synthesized. We demonstrate that OCA7 is recruited through interaction with a canonical effector binding surface of melanosome proteins Rab32 and Rab38. Using newly generated OCA7-KO MNT1 cells, we show OCA7 regulates overall melanin levels in a melanocyte autonomous manner by controlling melanosome maturation. Importantly, we found OCA7 regulates premelanosome protein (PMEL) processing, impacting fibrillation and the striations that define transition from melanosome Stage I to Stage II. Furthermore, the melanosome lumen of OCA7-KO cells displays lower pH than control cells. Together, our results reveal OCA7 regulates pigmentation through two well established determinants of melanosome biogenesis and function, PMEL processing and organelle pH.

[*]*The work presented in Chapter 3 was published with the same title in the Journal of Biological Chemistry in November, 2022. Wyatt C Beyers, Anna M. Detry, and Santiago M. Di Pietro. OCA7 is a melanosome membrane protein that defines pigmentation by regulating early stages of melanosome biogenesis. https://doi.org/10.1016/j.jbc.2022.102669.*

Introduction

OculoCutaneous Albinism (OCA) is a disorder displaying loss of melanin pigment in the skin, eyes and hair. OCA patients have heightened susceptibility to skin cancer and poor visual acuity (1-5). Eight forms of OCA exist, and the corresponding genes and protein functions have been elucidated for most of them (4, 6-16). However, while mutations in OCA7 (a.k.a. C10orf11 and LRMDA) were identified in OCA patients and OCA7 SNPs were associated with eyebrow color variations in GWAS analysis, the cellular function of OCA7 and corresponding disease mechanism are unknown (17).

Melanin synthesis occurs in specialized lysosome related organelles called melanosomes, which are classified as Stage I, II, III, or IV largely based on their appearance by electron microscopy. Melanosome biogenesis starts with Stage I melanosomes that resemble multivesicular endosomes, contain the PMEL protein and often present an electron dense coat of clathrin (18). Early stage melanosomes remodel their membranes in a PIKfyve dependent manner and generate intraluminal vesicles in a process involving CD63 (19, 20). An amyloid sequestering protein, Apolipoprotein E (ApoE), is present on the surface of melanosome intraluminal vesicles where it forms a cylindrical structure that functions as a seed for PMEL association and fibrillation (21). PMEL is proteolytically processed, associates with the intraluminal vesicles, and forms functional amyloid fibrils which work to package melanin as it is made (22). Melanosomes containing mature PMEL fibrils show striations by electron microscopy and are classified as Stage II. Subsequent delivery of Tyrosinase family proteins results in melanin synthesis, and pigment begins depositing onto PMEL fibrils thus defining Stage III melanosomes. Additional melanin synthesis and deposition results in more fully pigmented Stage IV melanosomes. Despite this detailed morphological characterization, melanosome biogenesis is not fully understood, particularly with regards to regulation of early stages of maturation.

Here, we reveal OCA7 functions as a melanosome-associated peripheral membrane protein in human melanocytes, likely recruited through interaction with Rab32 and Rab38. OCA7-KO MNT1 melanocytes obtained by CRISPR-Cas9 have reduced melanin content, a defect that was rescued by transient expression of OCA7-EGFP. The PMEL protein is abnormally processed in OCA7-KO cells and forms fewer fibril striations in melanosomes. The melanosome lumen pH, which regulates melanogenic enzyme activity, is lower in OCA7-KO cells. These findings reveal OCA7 regulates melanosome function starting at early stages of the biogenesis process.

Results

OCA7 localizes to melanosome membranes

TPC2 is a melanosome localized cation channel (23, 24). To identify novel proteins on the melanosome membrane, we performed a proximity biotinylation mass spectrometry screen using MNT1 cells expressing TPC2-BioID2. Cells expressing endosome localized TPC1-BioID2 were analyzed in parallel as a control. Details of this screening are reported in Chapter 2 of this dissertation. Surprisingly, we detected endogenous OCA7 specifically in proximity to TPC2-BioID2, providing the first molecular evidence that OCA7 may function at melanosomes. Immunofluorescence experiments with available antibodies for endogenous OCA7 were suspect, resulting in nuclear and random cytoplasmic signal. Therefore, we turned to live cell imaging of exogenously expressed OCA7-EGFP to visualize its localization. Attempts to amplify two potential transcript variants of OCA7 encoding a 226 or 198 amino acid protein from MNT1 cDNA were only successful for the first, suggesting it is the predominant variant. Live cell confocal fluorescence microscopy of OCA7-EGFP expressed in primary human melanocytes showed discrete cytoplasmic puncta that colocalized with melanosome marker mCherry-Rab32 but not peroxisome marker RFP-SKL as quantified by Pearson Correlation Coefficient (PCC) (**Figure 3.1A** and **3.1B**). Consistently, OCA7-EGFP colocalized highly with melanosome markers TPC2-iRFP, mCherry-Rab32, mCherry-Rab38 and mCherry-CD63 in MNT1 cells, a well-validated system to study melanosome biology (representative images shown in **Figure 3.2** and quantification in **Figure 3.1C**). OCA7-EGFP colocalized to a lesser extent with mature melanosome markers, Tyrosinase-mCherry, Tyrp1-mCherry and mCherry-Rab27a (**Figure 3.2** and **Figure 3.1C**). OCA7-EGFP showed low colocalization with endosomal proteins mCherry-Rab7a, mCherry-Rab11a, mCherry-Rab5a and negligible colocalization with ER and peroxisome markers BFP2-KDEL and RFP-SKL (**Figure 3.2** and **Figure 3.1C**). Airyscan super resolution images of OCA7-EGFP overlayed with brightfield images show a small proportion of OCA7-EGFP

decorating pigmented melanosomes (**Figure 3.1D**). The microscopy data confirms OCA7-EGFP localization to melanosomes and suggests an enrichment in less mature melanosomes. During OCA7 localization studies, we observed that fixation of MNT1 cells resulted in loss of OCA7-EGFP puncta, leaving only diffuse OCA7-EGFP signal, likely explaining why immunofluorescence experiments are unreliable. While overexpressed OCA7-EGFP clearly colocalizes with melanosome markers, it is conceivable that endogenously expressed tagless OCA7 may have additional cellular localizations or context dependent localization that we were unable to detect.

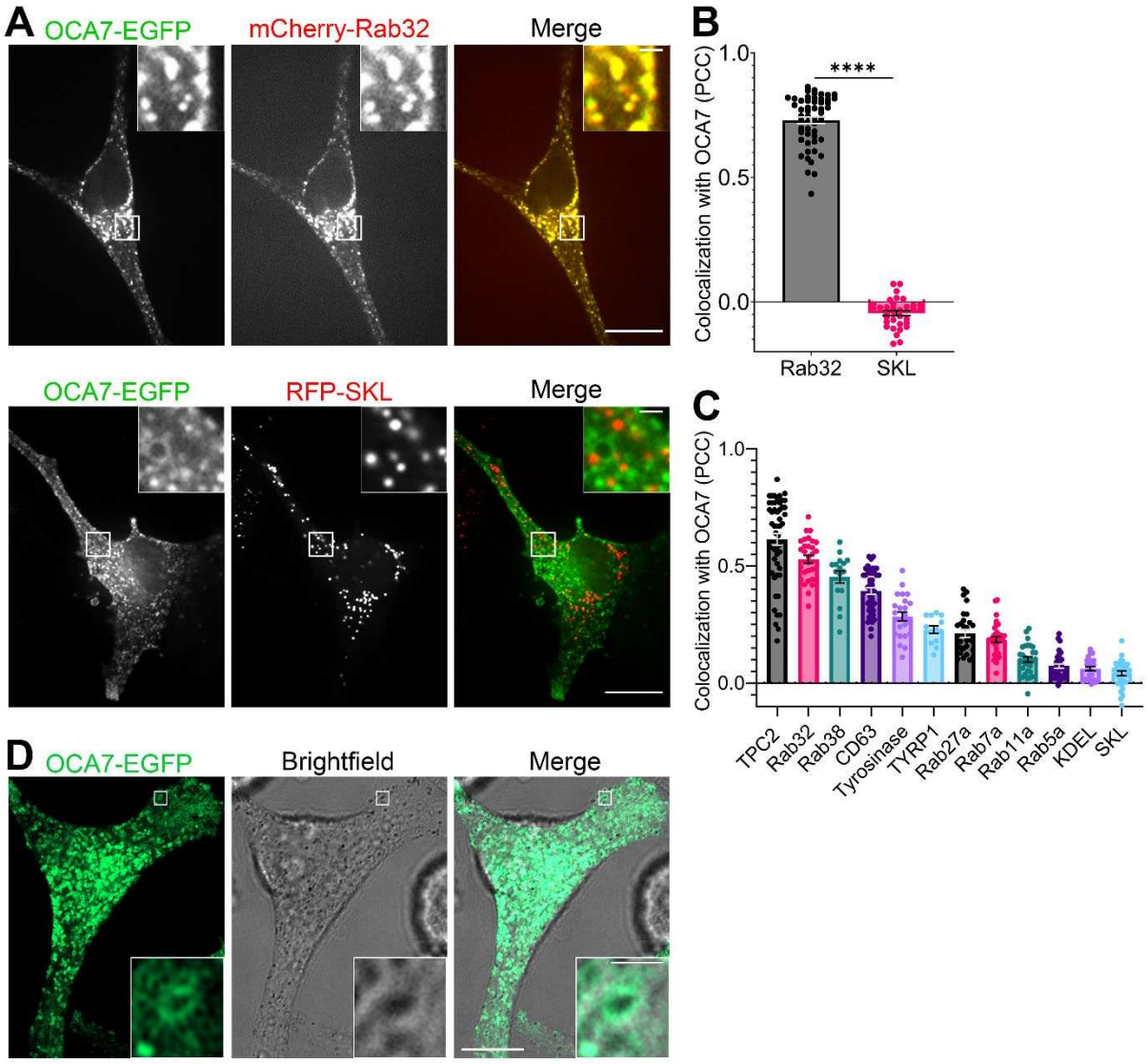

Figure 3.1. OCA7 localizes to melanosomes. **(A)** Spinning disc confocal fluorescence microscopy analysis of live primary human melanocytes co-expressing OCA7-EGFP with mCherry-Rab32 or RFP-SKL. Scale bars indicate 10μm for unmagnified images and 1μm for magnified insets. **(B)** Pearson Correlation Coefficient (PCC) for images from (A). Error bars represent the 95% Confidence Interval (mCherry-Rab32, n=55 cells; RFP-SKL, n=34 cells). **(C)** Colocalization quantification as determined by PCC for images of MNT1 cells expressing OCA7-EGFP with organelle markers from Figure S1, showing median with error bars representing the 95% confidence interval. n=50, n=30, n=16, n=45, n=24, n=13, n=29, n=33, n=31, n=33, n=25, and n=32 cells for TPC2-iRFP, mCherry-Rab32, mCherry-Rab38, mCherry-CD63, Tyrosinase-mCherry, TYRP1-mCherry, mCherry-Rab27a, mCherry-Rab7a, mCherry-Rab11a, mCherry-Rab5a, BFP2-KDEL, and RFP-SKL respectively. **(D)** Live cell Airyscan super resolution and brightfield images of MNT1 melanocytes expressing OCA7-EGFP showing a cohort of OCA7 localizes to membranes surrounding melanin pigment. Scale bars indicate 10μm for unmagnified image and 1μm for magnified inset.

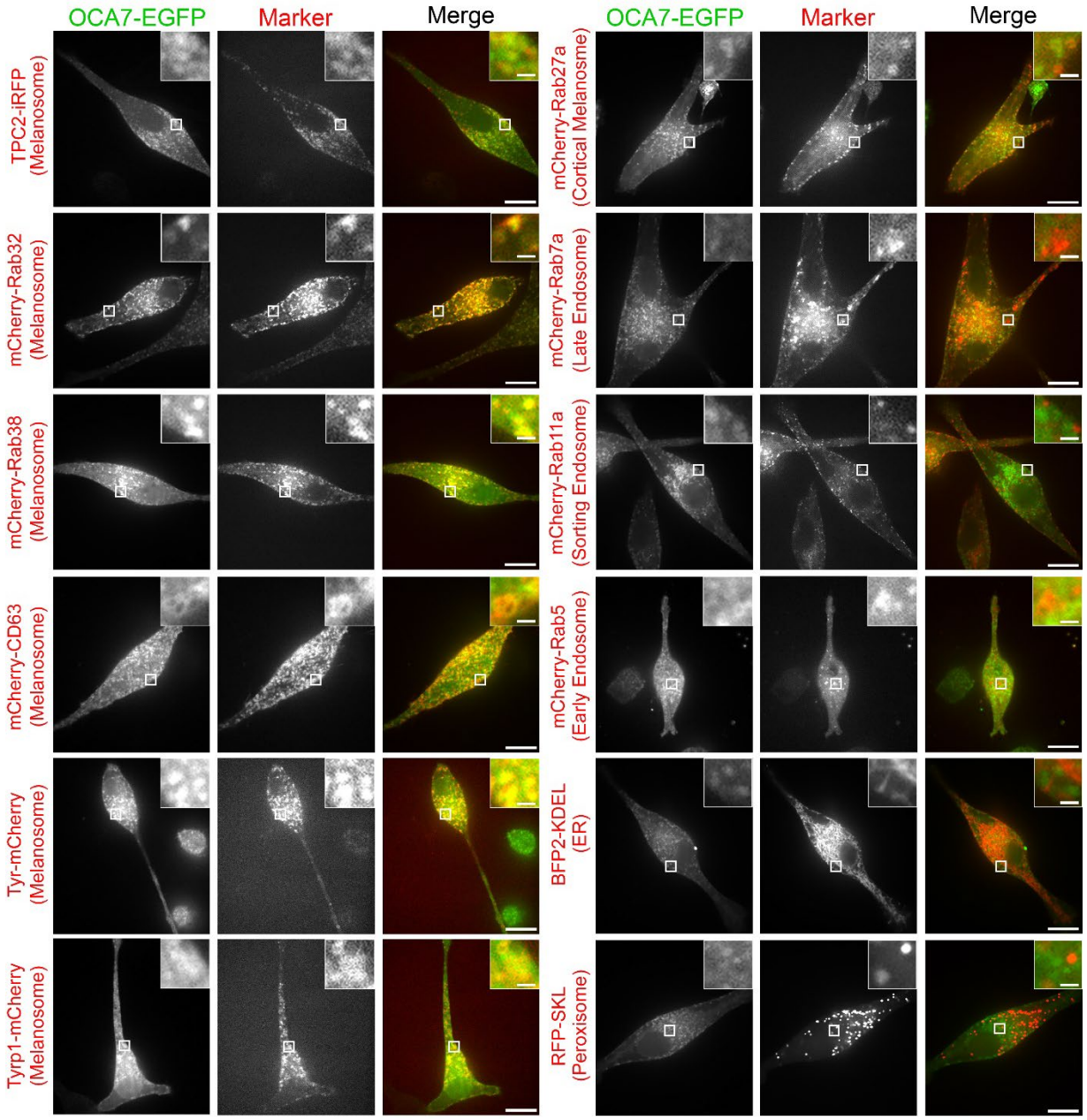

Figure 3.2. OCA7-EGFP colocalizes with melanosome markers. Live cell confocal fluorescence images of MNT1 cells expressing OCA7-EGFP (green) with melanosome markers or various other organelle markers (red). Melanosome markers include TPC2-iRFP, mCherry-Rab32, mCherry-Rab38, mCherry-CD63, Tyr-mCherry, and Tyrp1-mCherry. Other markers include mCherry-Rab27a for stage IV cortical melanosomes, mCherry-Rab7a for late endosomes/lysosomes, mCherry-Rab11a for sorting/recycling endosomes, mCherry-Rab5a for early endosomes, BFP2-KDEL for endoplasmic reticulum and RFP-SKL for peroxisomes. Insets highlight regions where OCA7 is on the same or separate organelles as the marker. Scale bars indicate 10μm.

OCA7 interacts physically with melanosome biogenesis proteins Rab32 and Rab38

The Human Reference Interactome database listed interactions between OCA7 and Rab32, AP1M1, RabIF and EXOSC5 based on unbiased proteome wide yeast two hybrid (Y2H) data (25). We reproduced the positive Y2H result with Rab32 or EXOSC5 but not with AP1M1 or RabIF (**Figure 3.3A**). Rab32 resides on melanosome membranes and is involved in mediating membrane trafficking events during melanosome biogenesis through interaction with various effectors, making it an obvious candidate for a functional interaction with OCA7 (26-28). In contrast, EXOSC5 is a component of a ribonuclease complex in nucleoli, thus it is unlikely to function with OCA7 at melanosomes (29, 30). Rab proteins are thought of as molecular switches because in their GTP bound state, they adopt an “on” conformation and recruit effector proteins to specific organelles. Upon GTP hydrolysis, Rabs switch to the “off” conformation and cease effector recruitment. Mutagenesis of highly conserved residues in Rab GTPases can be exploited to control which nucleotide is bound, a strategy that has been used in previous studies to control whether Rabs, including Rab32 and Rab38, are “on” or “off” (27, 28, 31). We expanded the Y2H analysis to test for interactions between OCA7 and Wild Type (WT) or constitutively active mutants (GTP locked, Q-to-L mutation) of several endosomal or melanosomal Rabs. Dominant negative forms (GDP locked, T-to-N mutation) were also tested for Rab32 and Rab38. Results confirmed OCA7 reactivity toward Rab32, with a preference for the constitutively active mutant Q85L over WT or dominant negative mutant T39N. OCA7 also interacted with Rab38 WT, which is closely related to Rab32, but not with other Rabs tested (**Figure 3.3B**). The data suggests OCA7 interacts specifically with melanosomal Rab proteins involved in melanosome biogenesis. Rab32 has canonical Switch 1 (S1), Interswitch (IS), Switch 2 (S2) regions and a family specific LPNG loop that, based on crystal structure information and the high conservation among Rab proteins, are predicted to form the binding interface for effector protein interactions (**Figure 3.3C**) (31, 32). Additionally, previous studies concerning Rab32 and Rab38 demonstrated that point

mutagenesis of residues in Switch regions can disrupt binding to Varp (VPS9-ankyrin-repeat protein) and Myosin 5C (27, 31, 33). The same point mutant forms of Rab32 were used here to test for their effect on interaction with OCA7 (**Figure 3.3C**). Mutation of S1 (I59A) or the LPNG loop did not impact interaction with OCA7, but mutation of IS (F62A or W80A) or S2 (Y95A) disrupted OCA7 binding, suggesting OCA7 interacts with Rab32 at a canonical Rab effector binding interface involving IS and S2 regions (**Figure 3.3D**).

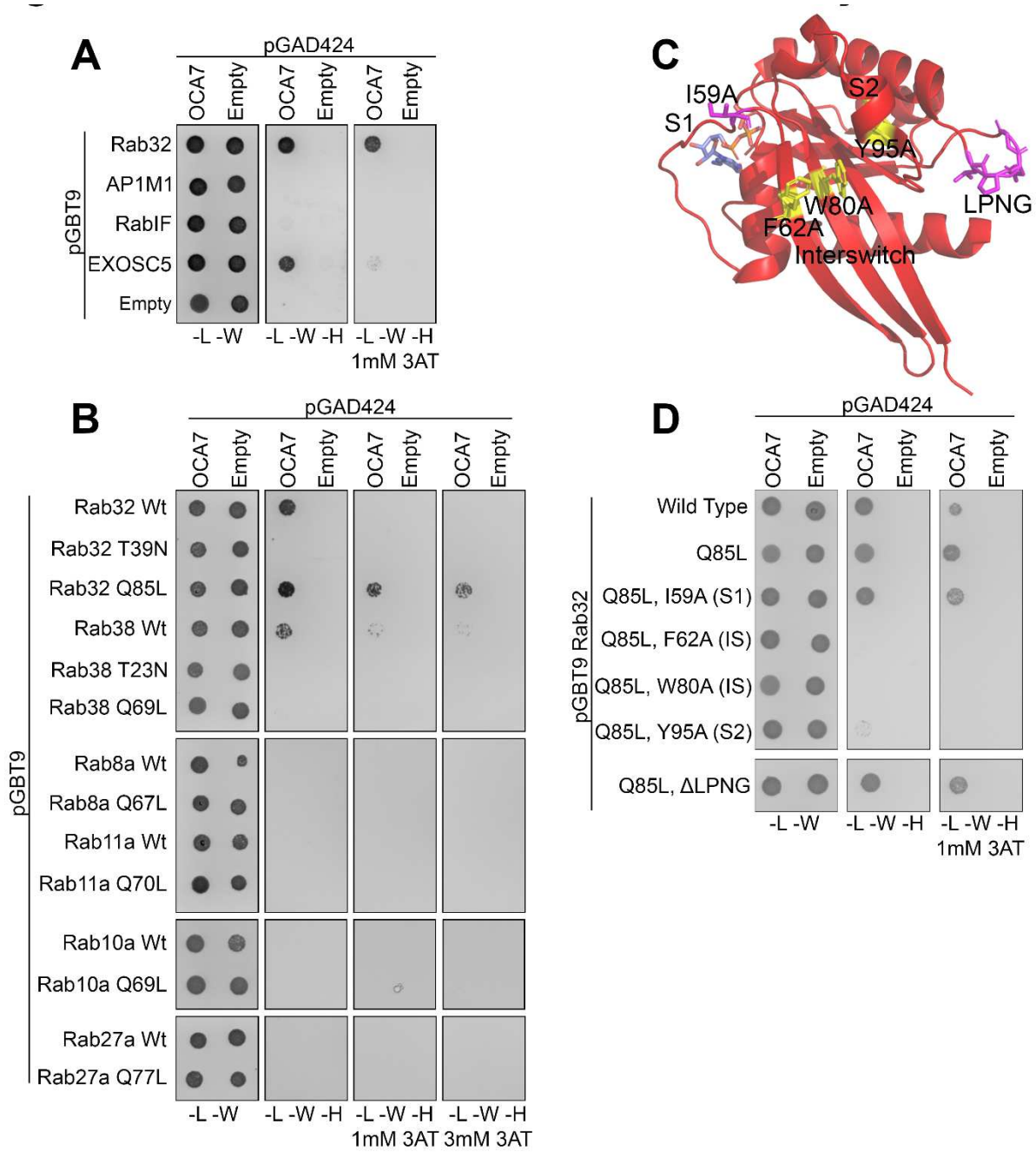

Figure 3.3. OCA7 interacts with Rab32 and Rab38 through the Interswitch and Switch II Regions. (A) Y2H assay showing OCA7 reactivity with Rab32 and EXOSC5 but not AP1M1 or RabIF. Y2H shown is representative of three experiments. **(B)** Y2H assay showing specific interactions between OCA7 and melanosome membrane proteins, Rab32 and Rab38, but not other melanosome or endosome Rabs, Rab8a, Rab10a, Rab11a, or Rab27a or their constitutively active mutants. Y2H shown is representative of two experiments. **(C)** Crystal structure of Rab32 GTP (PDB:6FF8) highlighting the Switch 1 (S1), Interswitch, Switch 2 (S2), and LPNG loop of Rab32 mutated in the Y2H in (D). Residues dispensable for OCA7 reactivity are indicated in magenta and residues that influence reactivity are highlighted in yellow (31). **(D)** Y2H assay to test for Rab32 residues necessary for OCA7 interaction. Rab32 constitutively active mutant

(Q85L) was subsequently mutated in the Switch 1 (I59A), Interswitch (F62A or W80A), Switch 2 (Y95A), or LPNG loop regions to map binding to OCA7. Y2H shown is representative of two experiments. For each yeast two hybrid, growth on +Histidine plates indicates successful co-transformation with pGBT9 and pGAD424 vectors. Growth on –Histidine plates indicates interaction between the bait and prey proteins, and growth on plates containing 3-Amino-1,2,4-triazole (3AT) indicates stronger interactions. The T/N mutation prevents Rabs from exchanging GDP for GTP, keeping it in the "off" conformation. The Q/L mutation prevents Rabs from hydrolyzing GTP, keeping it in the "on" conformation.

OCA7 is peripherally associated with melanosome membranes

OCA7-EGFP localizes to melanosomes but also diffusely in the cytosol, particularly in cells with higher expression levels. Intriguingly, highly expressed OCA7-EGFP displayed a more punctate distribution if mCherry-Rab32 was also overexpressed in the same cell (**Figure 3.4A** and **3.4B**). OCA7 has no predicted transmembrane or membrane-interacting domain, suggesting OCA7 is a peripheral membrane protein recruited through interaction with proteins on the melanosome surface, such as Rab32. Fractionation of MNT1 cell homogenates by ultracentrifugation followed by IB analysis revealed endogenous OCA7 is divided almost evenly between membrane and cytosol fractions, suggesting it is weakly or dynamically associated with membranes (**Figure 3.4C** and **3.4D**). In contrast, integral membrane proteins TYR and CD63, or lipidated membrane proteins Rab32 and Rab38 were highly enriched in the membrane fraction (**Figure 3.4C** and **3.4D**). Fluorescence Recovery After Photobleaching (FRAP) experiments revealed OCA7-EGFP fluorescence at melanosomes recovered in a matter of seconds (T1/2 = 4.6±2.2 s) while mCherry-Rab32 and mCherry-CD63 did not reach half recovery in the timeframe of the assay (**Figure 3.4E, 3.4F** and **3.5**). Together, the data suggest OCA7 is peripherally associated with melanosome membranes where it is dynamically recruited potentially by Rab32/Rab38 and subjected to rapid turnover.

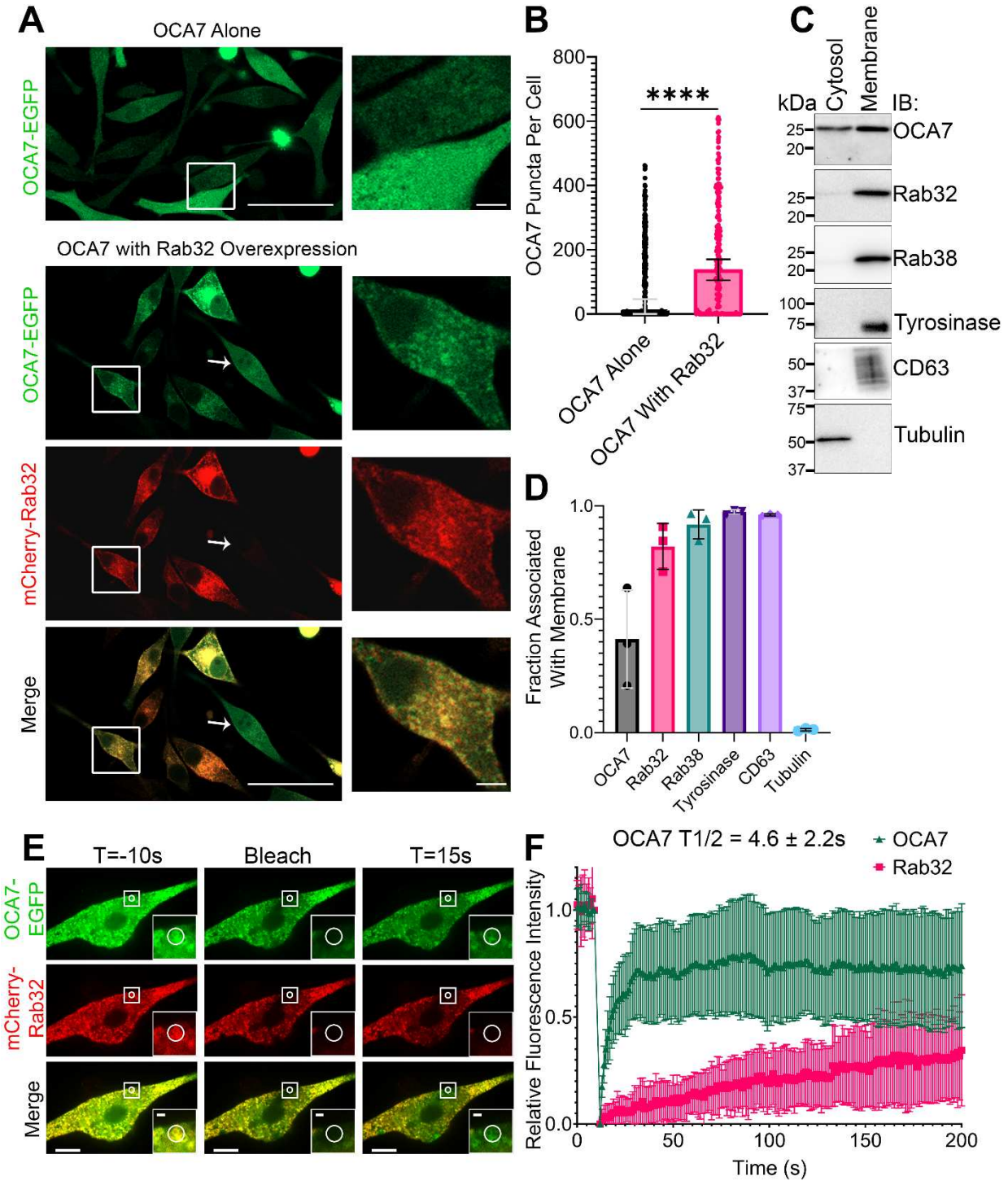

Figure 3.4. OCA7 is peripherally associated with melanosome membranes. (A) Live cell Airyscan SR-4Y confocal fluorescence images of MNT1 melanocytes expressing OCA7-EGFP with or without co-expression of mCherry-Rab32. Magnified insets show areas of cells where OCA7-EGFP has high cytosolic background (OCA7 Alone) or is highly punctate (OCA7 with Rab32 Overexpression). Additionally, the white arrow shows a cell expressing a high level of OCA7-EGFP but not mCherry-Rab32, noting its more diffuse OCA7-GFP distribution compared

to adjacent cells that co-overexpress mCherry-Rab32. Scale bars indicate 50μm for unmagnified image and 5μm for magnified inset. **(B)** Quantification of OCA7-EGFP puncta per cell as determined by single particle analysis using Zeiss Zen Blue software for images depicted in (A). The graph shows the median with error bars representing the 95% confidence interval. Melanosomes were counted in n=370 and n=202 cells for OCA7-EGFP alone or OCA7-EGFP with mCherry-Rab32 respectively. Medians were compared using the Mann-Whitney test. **** corresponds p<0.0001. **(C)** Immunoblotting analysis of membrane and cytosol fractions from MNT1 cell homogenate separated by ultracentrifugation and probed with the indicated antibodies for endogenous proteins. **(D)** Quantification of (C) showing the fraction of each protein in the cytosol and membrane fractions. The graph shows mean ± S.D. Three independent experiments were quantified. **(E)** FRAP experiment with MNT1 cells expressing OCA7-EGFP and mCherry-Rab32. Images are shown for timepoints 10 sec before photobleaching, immediately after, and 15 sec after. Circles in the insets indicate melanosomes analyzed by FRAP. Scale bars indicate 10μm for unmagnified images and 1μm for magnified insets. **(F)** Quantification of FRAP time lapses shown in (E) depicting mean fluorescence signal relative to the timepoint immediately before photobleaching. Error bars represent S.D. (200 timepoints were measured for n=31 melanosomes imaged in 12 cells). OCA7 T1/2 is the mean ± S.D.

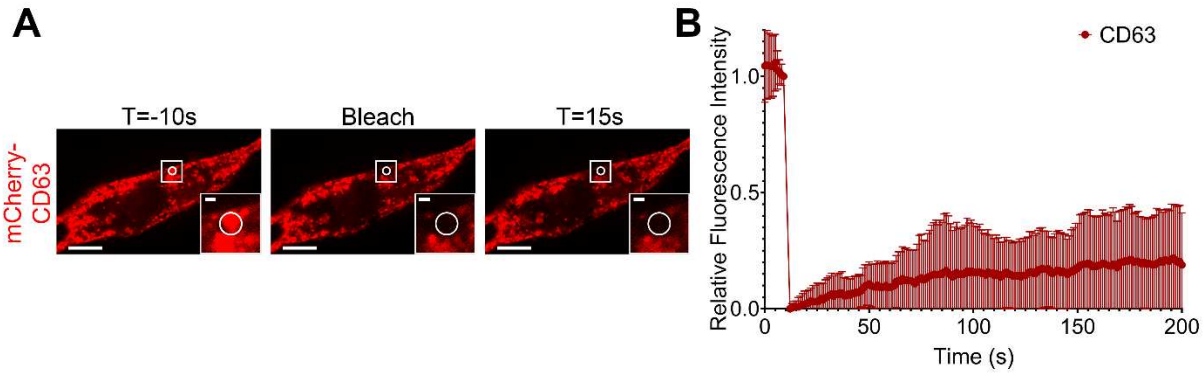

Figure 3.5. mCherry-CD63 recovers slowly after photobleaching. (A) FRAP experiment with MNT1 cells expressing mCherry-CD63, a melanosome localized integral membrane protein, showing slow recovery after photobleaching. Images are shown for timepoints 10 sec before photobleaching, immediately after, and 15 sec after. Circles in the insets indicate melanosomes analyzed by FRAP. Scale bars indicate 10μm. **(B)** Quantification of FRAP time lapses shown in (A) depicting mean fluorescence signal relative to the timepoint immediately before photobleaching. Error bars represent S.D. (200 timepoints were measured for n=31 melanosomes imaged in 12 cells).

Rab32 or Rab38 membrane localization is sufficient for OCA7 recruitment to membranes

We utilized the FRB/FKBP12 heterodimerization system to induce mislocalization of Rab32 or Rab38 and test for OCA7 recruitment (**Figure 3.6A**). We generated plasmids encoding AKAP1-BFP2-FRB, a mitochondria outer membrane marker with a fluorescent protein and

heterodimerization domain, and mCherry-Rab32-CC/AA-FKBP12 containing a complementary heterodimerization domain. The Rab32 C-terminal cysteines were mutated to alanine to prevent geranyl-geranylation and insertion into melanosome membranes. In MNT1 cells expressing AKAP1-BFP2-FRB, mCherry-Rab32-CC/AA-FKBP12 and OCA7-EGFP cultured in the absence of the heterodimerizer (rapalog), mCherry-Rab32-CC/AA-FKBP12 exhibited cytosolic distribution as expected. Upon addition of rapalog, mCherry-Rab32-CC/AA-FKBP12 and OCA7-EGFP were recruited to mitochondria, indicating interaction with Rab32 recruited OCA7 to mitochondria (**Figure 3.6B** and **3.6C**). Demonstrating specificity, while the constitutively active Rab32 mutant (Q85L) showed robust recruitment of OCA7-EGFP to mitochondria, the corresponding dominant negative Rab32 mutant (T39N) displayed reduced recruitment of OCA7-EGFP. Consistently, the constitutively active Switch II mutant form or Rab32 (Q85L, Y95A) showed reduced recruitment of OCA7-EGFP to mitochondria (**Figure 3.6B** and **3.6C**).

Cells showed varying degrees of AKAP1-BFP2-FRB and mCherry-Rab32-CC/AA-FKBP12 heterodimerization after addition of rapalog. Using regression analysis, we found cells having a higher degree of colocalization between AKAP1-BFP2-FRB and mCherry-Rab32-CC/AA-FKBP12 also had higher colocalization between AKAP1-BFP2-FRB and OCA7-EGFP, indicating a positive correlation between dimerization efficiency and OCA7-EGFP recruitment to mitochondria (**Figure 3.6D**, upper panel). In contrast, cells having a high degree of colocalization between AKAP1-BFP2-FRB and dominant negative Rab32 (T39N) did not correlate with higher colocalization between AKAP1-BFP2-FRB and OCA7-EGFP (**Figure 3.6D**, lower panel). Similar to Rab32, mislocalization to mitochondria of WT and constitutively active (Q69L) mCherry-Rab38-CC/AA-FKBP12 was sufficient to mislocalize OCA7-EGFP to mitochondria, while dominant negative (T23N) and Switch II (Y79A) mutants had reduced recruitment capacity (**Figure 3.7**). Together these results indicate Rab32 and Rab38 have the ability to recruit OCA7 to membranes.

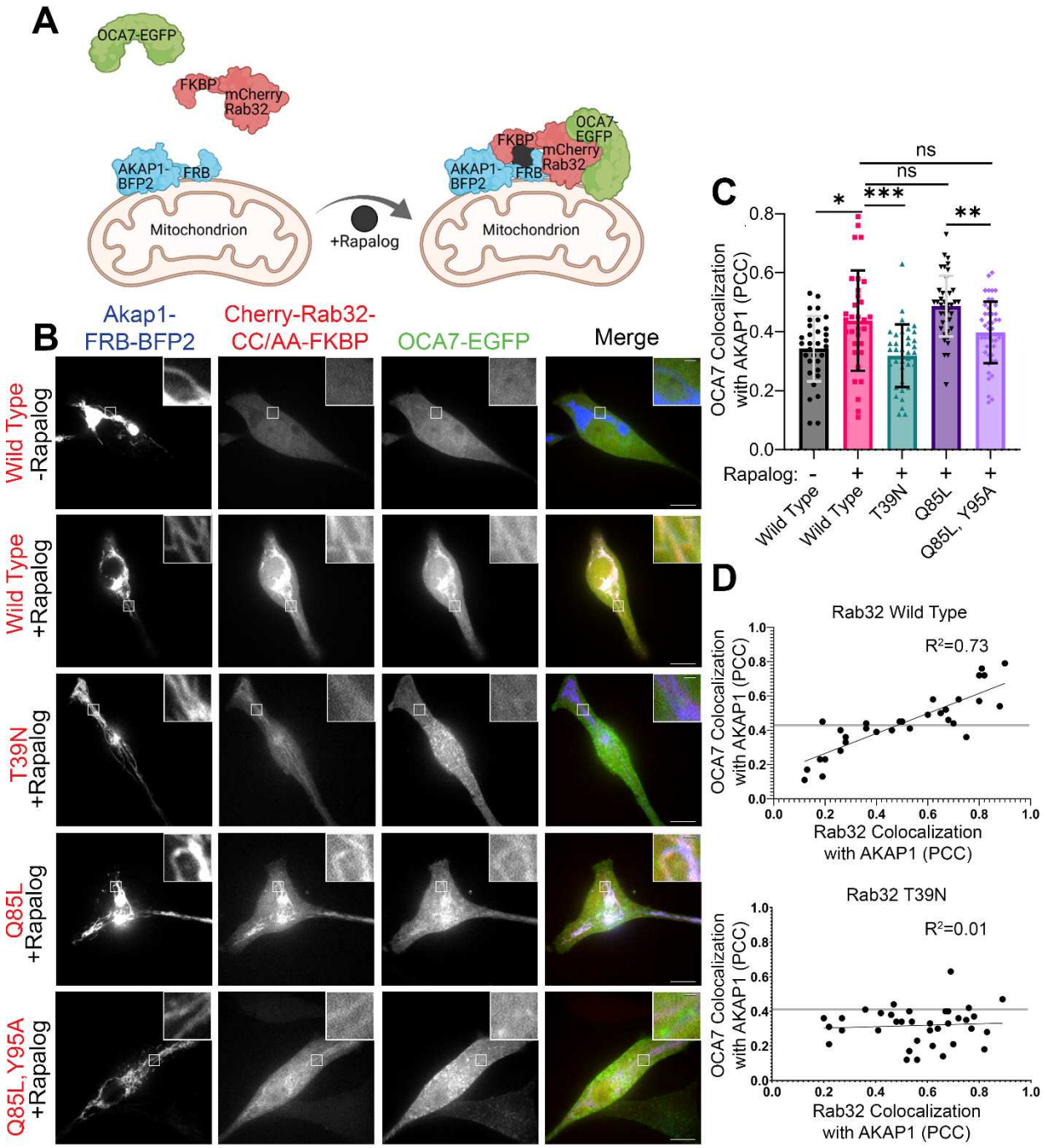

Figure 3.6. Rab32 membrane localization is sufficient for OCA7 recruitment to membranes. **(A)** Cartoon depicting Rab32 mislocalizaton assay. The cartoon was created with Biorender.com. **(B)** Spinning disc confocal fluorescence microscopy images of MNT1 cells expressing OCA7-EGFP, AKAP1-FRB-BFP2, and mCherry-Rab32-CC/AA-FKBP (wild type or various mutants) in the absence or presence of 100nM Rapalog. In the absence of Rapalog, mCherry-Rab32-CC/AA-FKBP has a cytosolic distribution and OCA7-EGFP has a cytosolic or punctate (melanosome) distribution. Upon addition of 100nM Rapalog, mCherry-Rab32-CC/AA-FKBP (wild type and various mutants) relocalize to AKAP1-FRB-BFP2 labeled mitochondria. Concomitantly, OCA7-

EGFP mislocalizes to mitochondria with WT or GTP-locked, constitutively active mutant (Q85L) mCherry-Rab32-CC/AA-FKBP but not the GDP-locked, dominant negative mutant (T39N). Expression of the corresponding Rab32 Q85L,Y95A double mutant (Q85L,Y95A), which is constitutively active but unable to bind OCA7 shows reduced OCA7-EGFP recruitment to mitochondria compared to the Rab32 Q85L constitutively active mutant. Insets show regions where mitochondria are visible (AKAP1-FRB-BFP2 channel). Scale bars indicate 10μm for unmagnified images and 1μm for magnified insets. **(C)** Graph of PCC for images in (B) depicting OCA7-EGFP colocalization with AKAP1-FRB-BFP2, indicating mislocalization to mitochondria. The graph shows mean ± S.D. n=32, n=32, n=36, n=40, and n=48 cells were analyzed for WT -Rapalog, WT +Rapalog, T39N +Rapalog, Q85L +Rapalog, and Q85L,Y95A +Rapalog, respectively. Statistical significance was tested by One way ANOVA and post-hoc Tukey tests. For statistical comparisons, ns,*,**, and *** correspond to $p>0.05$, $p<0.05$, $p<0.01$, and $p<0.001$ respectively. **(D)** Regression analysis investigating the correlation between mCherry-Rab32-CC/AA-FKBP / AKAP1-FRB-BFP2 dimerization efficiency (Rab32 colocalization with AKAP1) and OCA7-EGFP recruitment to mitochondria (OCA7 colocalization with AKAP1). For comparison, the horizontal line in both graphs represents the mean PCC for OCA7-EGFP colocalization with AKAP1-FRB-BFP2 for cells expressing WT Rab32.

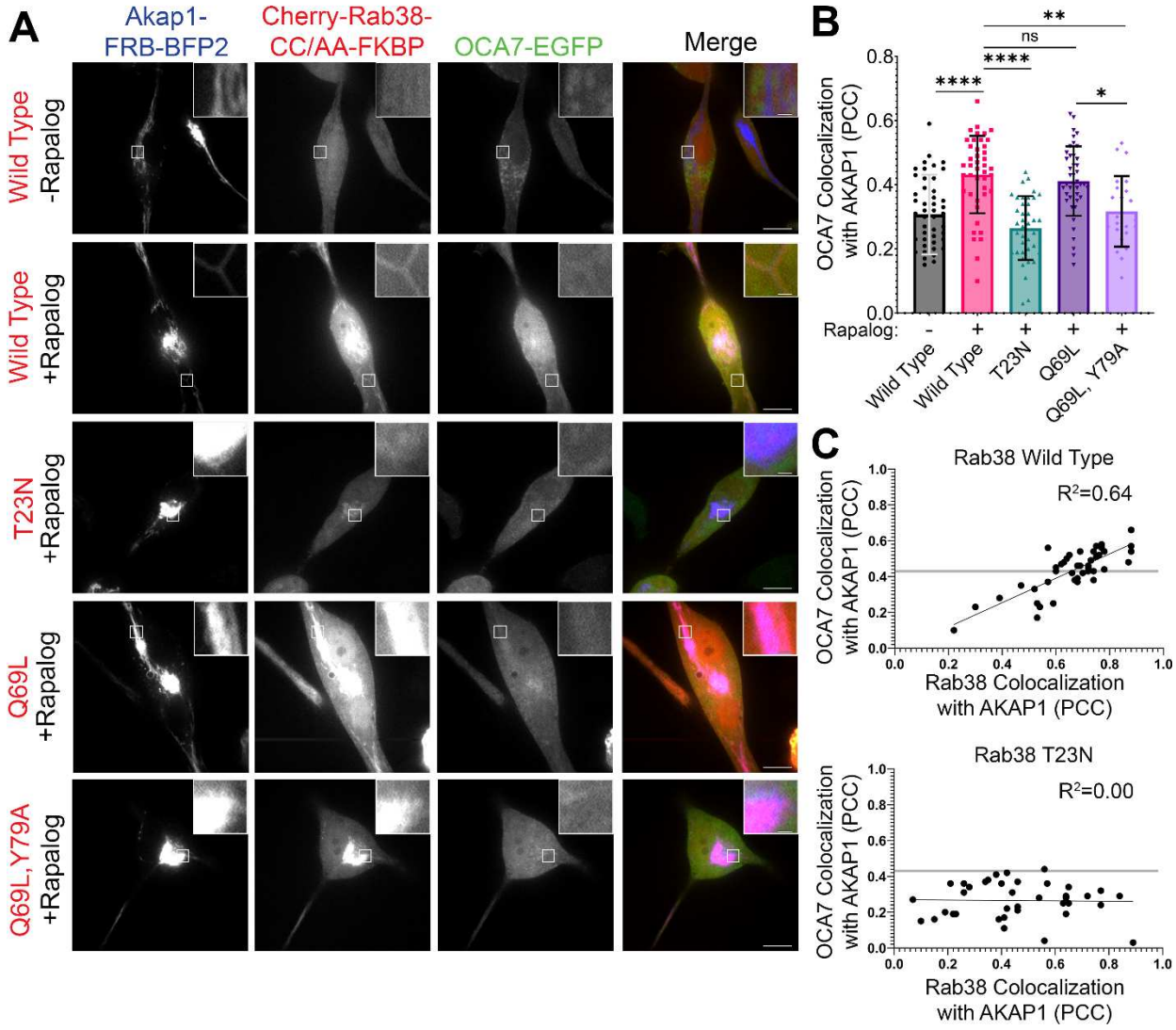

Figure 3.7. Rab38 membrane localization is sufficient for OCA7 recruitment to membranes. **(A)** Spinning disc confocal fluorescence microscopy images of MNT1 cells expressing OCA7-EGFP, Akap1-FRB-BFP2, and mCherry-Rab38-CC/AA-FKBP (wild type or various mutants) in the absence or presence of 100nM Rapalog. In the absence of Rapalog, mCherry-Rab38-CC/AA-FKBP has a cytosolic distribution and OCA7-EGFP has a cytosolic or punctate (melanosome) distribution. Upon addition of 100nM Rapalog, mCherry-Rab38-CC/AA-FKBP (wild type and various mutants) relocalizes to Akap1-FRB-BFP2 labeled mitochondria. Concomitantly, OCA7-EGFP mislocalizes to mitochondria with Wild Type or GTP-locked, constitutively active mutant (Q69L) mCherry-Rab38-CC/AA-FKBP but not the GDP-locked, dominant negative mutant (T23N). Expression of the corresponding Rab38 Q69L, Y79A double mutant (Q69L, Y79A), which is constitutively active but unable to bind OCA7 shows reduced OCA7-EGFP recruitment to mitochondria compared to the Rab38 Q69L constitutively active mutant. Insets show regions where mitochondria are visible (Akap1-FRB-BFP2 channel). Scale bars indicate 10μm. **(B)** Graph of PCC for images in (A) depicting OCA7-EGFP colocalization with Akap1-FRB-BFP2, indicating mislocalization to mitochondria. The graph shows mean ± S.D. n=46, n=43, n=39, n=43, and n=23 cells were analyzed for WT -Rapalog, WT +Rapalog, T23N +Rapalog, Q69L +Rapalog, and Q69L, Y79A +Rapalog, respectively. Statistical significance was tested by One way ANOVA and post-hoc Tukey tests. For statistical comparisons, ns, *,**, and **** correspond to $p>0.05$, $p<0.05$, $p<0.01$, and $p<0.0001$ respectively. **(C)** Regression analysis investigating the correlation between mCherry-Rab38-CC/AA-FKBP / Akap1-FRB-BFP2 dimerization efficiency (Rab38 colocalization with AKAP1, PCC) and OCA7-EGFP recruitment to mitochondria (OCA7 colocalization with AKAP1, PCC). OCA7-EGFP recruitment to mitochondria correlated highly with dimerization efficiency when the Rab38 Wild Type form of mCherry-Rab38-CC/AA-FKBP was expressed but not when the corresponding Rab38 T23N dominant negative mutant was expressed. For comparison, the horizontal line in both graphs represents the mean PCC for OCA7-EGFP colocalization with Akap1-FRB-BFP2 for cells expressing Wild Type Rab38 as a reference.

The OCA7 C-terminus is dispensable for recruitment to melanosomes

Sequence analysis suggests OCA7 consists of an N-terminal Leucine Rich Repeat (LRR) domain and a disordered C-terminal domain (**Figure 3.8A** and **3.8B**). Colocalization analysis of full length or truncations of OCA7-EGFP revealed the C-terminal domain is dispensable for recruitment to melanosomes (**Figure 3.8A-D**). Larger C-terminal truncation including part of the LRR domain or deletion of LRR via N-terminal truncation drastically reduced OCA7-EGFP localization to melanosomes, rendering it cytosolic (**Figure 3.8A-D**). Y2H assays revealed the C-terminal domain of OCA7 is also dispensable for interaction with Rab32 (**Figure 3.8E**). Together, these results suggest the OCA7 LRR domain is necessary and sufficient for interaction with Rab32 and recruitment to melanosomes.

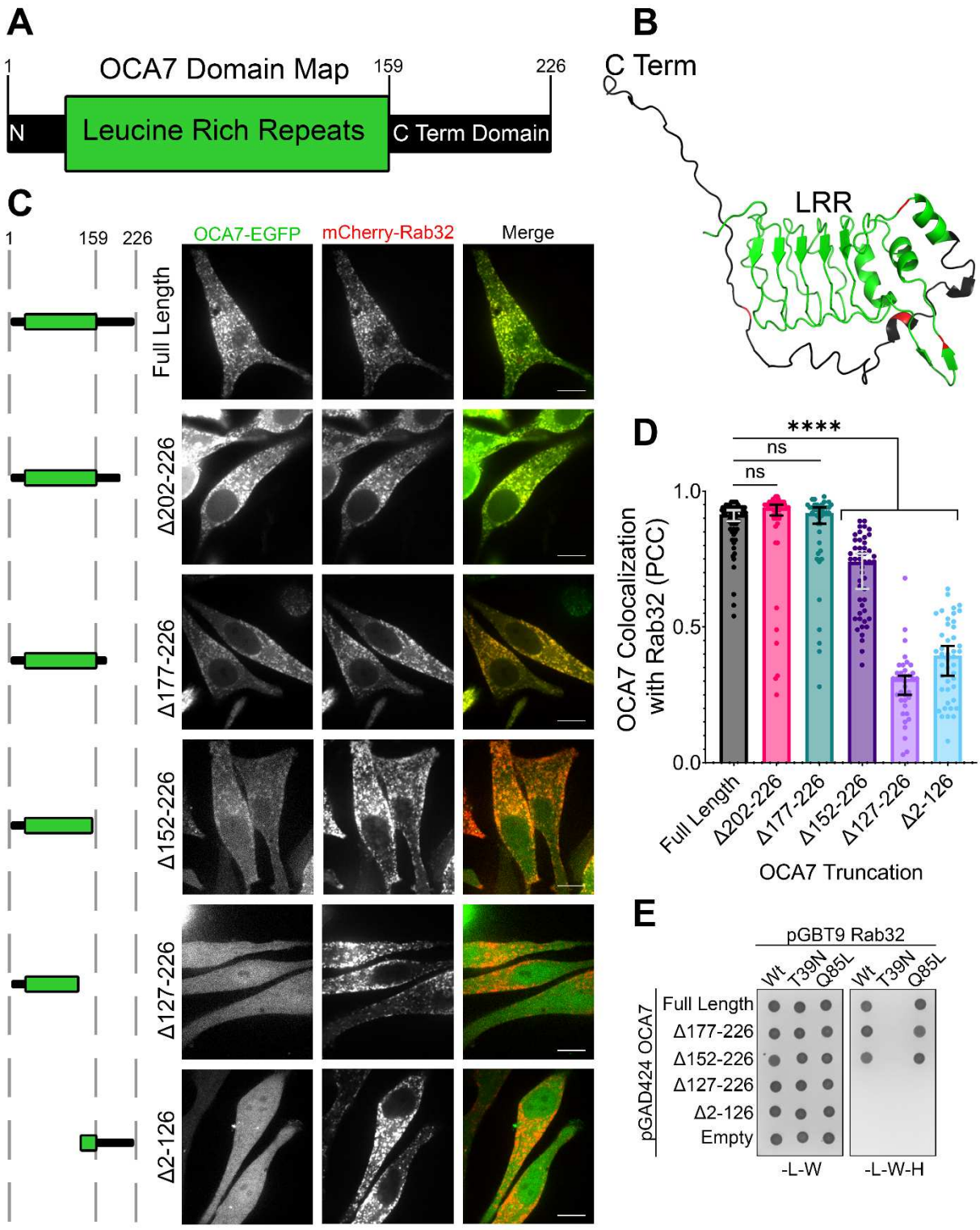

Figure 3.8. The C-terminus of OCA7 is dispensable for interaction with Rab32 and OCA7 recruitment to melanosomes. (A) Domain map depicting OCA7 with a Leucine Rich Repeat domain (LRR) and a disordered domain at the C-terminus. Positions 1, 159, and 226 are marked to show position of residues relative to the LRR domain. **(B)** Predicted molecular structure of

OCA7 generated using the Phyre2 protein fold prediction server showing LRR domain (green) and disordered C-terminal domain (black)(34). Residues highlighted in red indicate locations of each successive 25 amino acid truncation made for the experiment. **(C)** Live cell spinning disc confocal fluorescence microscopy images of MNT1 cells expressing full length or truncated OCA7-EGFP with mCherry-Rab32. Truncation of the disordered C terminus had little or no effect on OCA7-EGFP colocalization with Rab32, but truncation of or into the Leucine Rich Repeat domain disrupted OCA7 punctate distribution. Scale bars indicate 10μm. **(D)** Graph of PCC corresponding to images in (C). The graph shows median with error bars representing the 95% confidence interval. Colocalization was measured for n=66, n=48, n=41, n=48, n=37, and n=44 cells for OCA7 full length, Δ202-226, Δ177-226, Δ152-226, Δ127-226 and Δ2-126 respectively. The Kruskal-Wallis test was used to test significance. For statistical comparisons, ns and **** correspond to $p>0.05$ and $p<0.0001$ respectively. **(E)** Y2H assay showing C-terminally truncated OCA7 maintains interaction with Rab32 but truncation of the LRR domain abolishes interaction. Growth on +Histidine plates indicates successful co-transformation with pGBT9 and pGAD424 vectors, and growth on –Histidine plates indicates interaction between the bait and prey proteins. The T39N mutation prevents Rab32 from exchanging GDP for GTP, keeping it in the “off” conformation. The Q85L mutation prevents Rab32 from hydrolyzing GTP, keeping it in the “on” conformation.

OCA7-KO MNT1 cells are hypopigmented

We employed CRISPR-Cas9 to knock out OCA7 in MNT1 cells to recapitulate OCA Type 7 disease at the cellular level. Genomic DNA sequencing showed the gene was mutated in two clones (KO1 and KO2) (**Figure 3.9A**). IB analysis confirmed absence of the OCA7 protein in corresponding cell lysates (**Figure 3.10A, 3.10B** and **Figure 3.9B**). IP of endogenous OCA7 from MNT1 lysates with an anti-OCA7 antibody and IB with a different anti-OCA7 antibody resulted in strong detection of OCA7 in WT cells and no detection in OCA7-KO cells, confirming the KO cells do not express OCA7 and the ability of the antibodies to react against OCA7 (**Figure 3.9B**). Anti-OCA7 antibodies also recognized recombinant OCA7 (**Figure 3.9C**). Visual inspection of OCA7-KO MNT1 cell pellets containing one million cells revealed a reduction of pigmentation relative to WT cells (**Figure 3.10C**). Melanin quantification of cell homogenates using a spectrophotometric assay confirmed melanin reduction in OCA7-KO cells (**Figure 3.10D**). Additionally, WT and OCA7-KO MNT1 cells were transfected with plasmids encoding EGFP (mock) or OCA7-EGFP (rescue) and imaged by brightfield microscopy confirming hypopigmentation in OCA7-KO cells, and that transient OCA7-EGFP expression rescued pigmentation levels (**Figure 3.10E** and **3.10F**). These data validate the specificity of the OCA7-KO cells and that OCA7-GFP is functional

in pigmentation. Importantly, our findings are consistent with patients diagnosed with OCA Type 7, who have light complexion but retain some skin pigment and tend to have blonde or light brown hair (5, 15, 35).

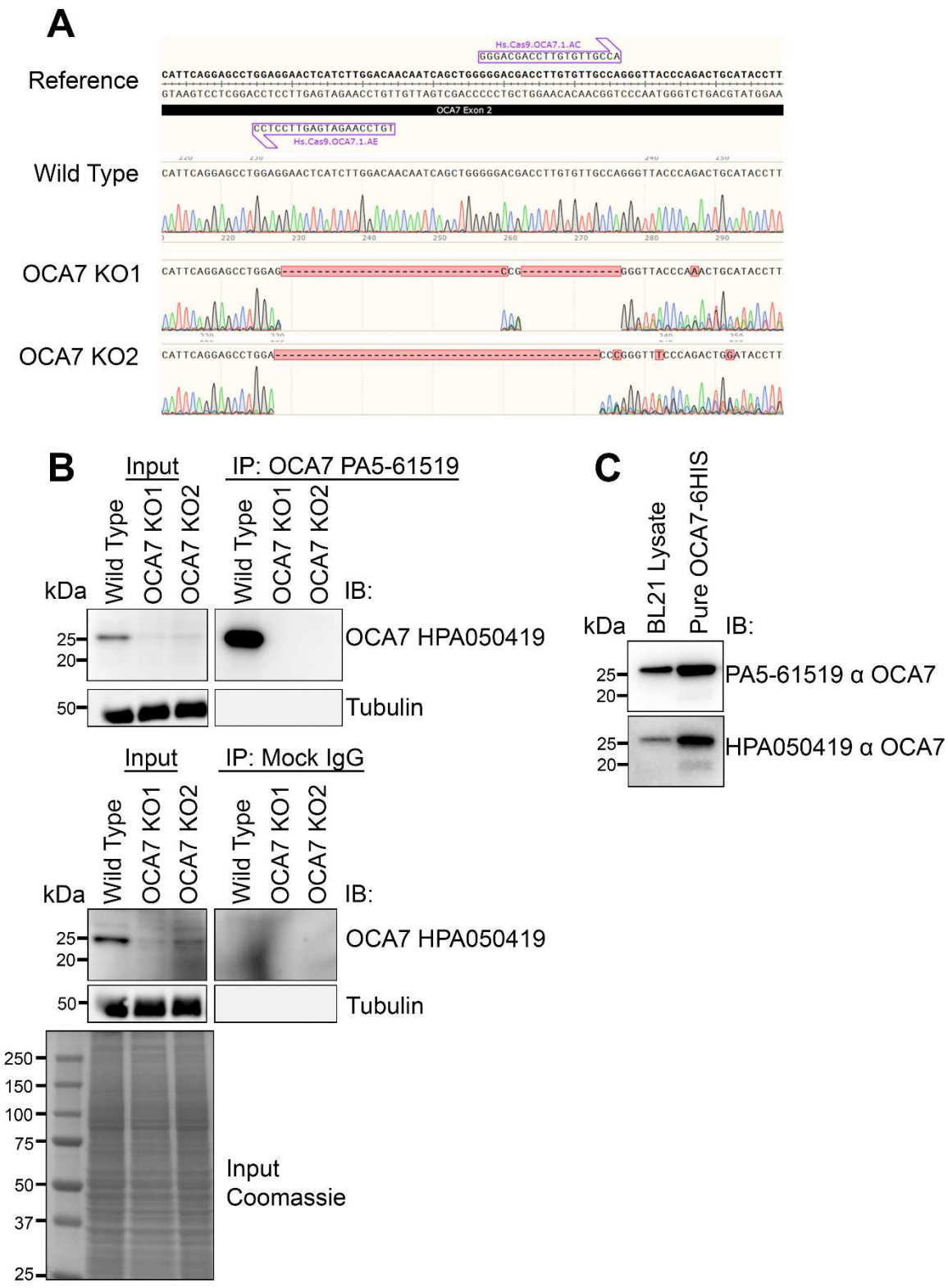

Figure 3.9. Validation of OCA7-KO MNT1 cells and anti-OCA7 antibodies. (A) Sequencing analysis of OCA7 PCR product amplified from genomic DNA obtained from Wild Type or OCA7-

KO MNT1 cell lines. For the OCA7-KO cell lines, red highlighted dashes indicate sequence that was successfully excised via CRISPR-Cas9 and overlapping peaks likely represent indels. **(B)** Immunoblotting (IB) analysis of TX100 cell lysate input and anti-OCA7 or Mock (IgG) immunoprecipitation samples obtained from Wild Type or two different clones of OCA7-KO MNT1 cells used in the study. Samples were immunoprecipitated (IP) with Rabbit anti-OCA7 (PA5-61519) or total rabbit IgG and the immunoblot was probed with a different Rabbit anti-OCA7 (HPA050419) antibody showing specificity for endogenous OCA7. The immunoblots of the IP samples indicate that OCA7 is absent from the OCA7-KO cell lysates and residual signal in the input is likely background. Even gel loading is depicted by immunoblotting for Tubulin and a corresponding Coomassie stained gel. **(C)** Immunoblot of recombinantly expressed OCA7-6His showing both antibodies tested detect OCA7-6His in BL21 bacteria cell lysate or in its pure form.

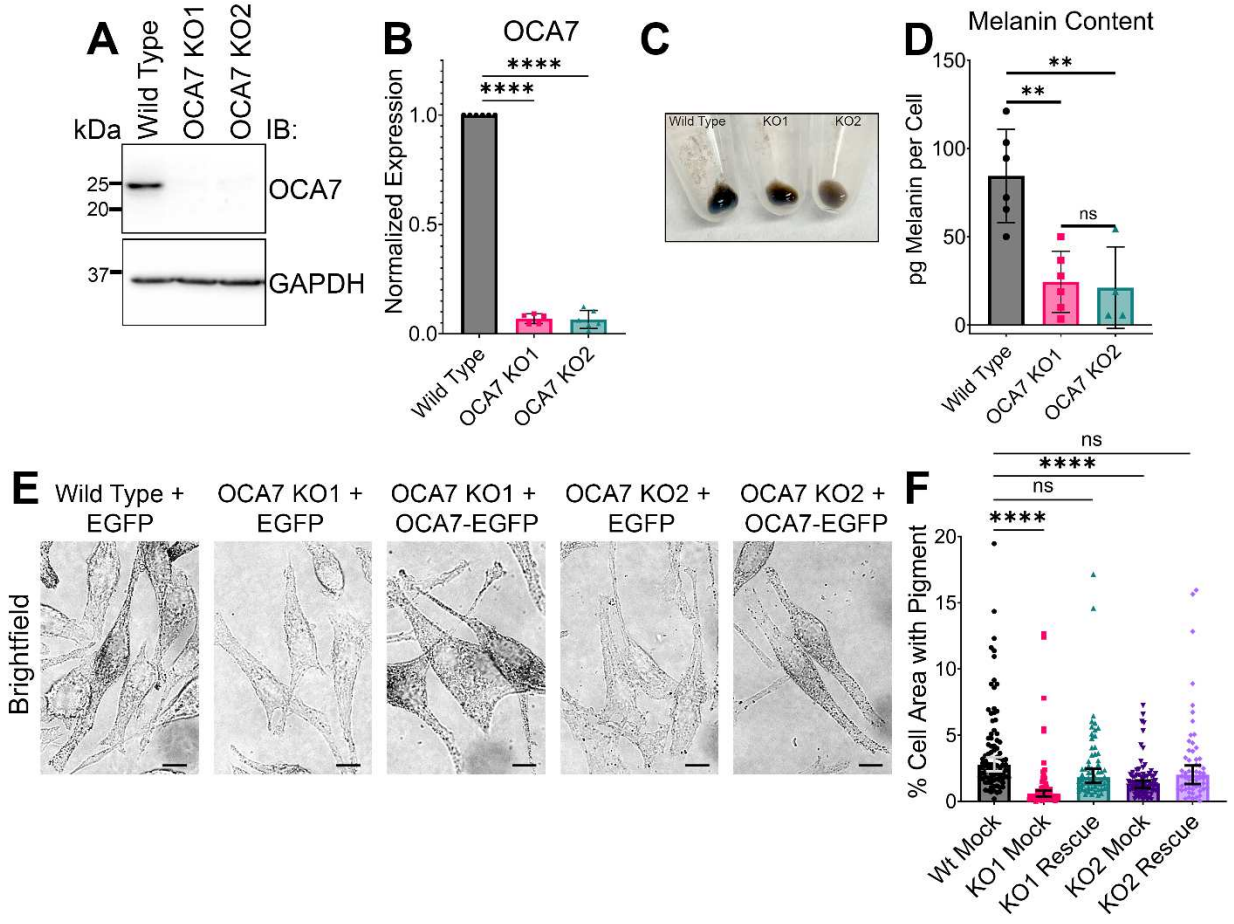

Figure 3.10. OCA7-KO MNT1 cells are hypopigmented. **(A)** IB analysis of total cell extracts from WT or OCA7-KO MNT1 cells showing OCA7 is depleted in both KO clones used in the study. **(B)** Quantification of OCA7 protein levels from immunoblots shown in (A) represented as mean ± S.D normalized to WT (WT, n=6; OCA7-KO1, n=5; OCA7-KO2, n=6). **(C)** Image of one million WT or OCA7-KO cell pellets. **(D)** Quantification of melanin content in WT and OCA7-KO cells determined by bulk melanin quantification assay. Several independent experiments were quantified for WT (n=6), OCA7-KO1 (n=6), and OCA7-KO2 (n=4) and represented as mean ±

S.D. **(E)** Brightfield images of fixed WT or OCA7-KO MNT1 cells transfected with EGFP (Mock) or OCA7-EGFP (Rescue) plasmids. Scale bars indicate 10μm. **(F)** Quantification of pigment in brightfield images depicted in (E) as the percent of the cell area meeting a grey value threshold, corresponding to the percent of the cell containing visible melanin. The graph shows median and error bars represent the 95% confidence interval for WT (n=89 cells), OCA7-KO1 Mock (n=57 cells), OCA7-KO1 Rescue (n=64 cells), OCA7-KO2 Mock (n=76 cells), and OCA7-KO2 Rescue (n=60 cells).

PMEL is aberrantly processed in OCA7-KO MNT1 cells

We sought to understand how pigment is reduced in OCA7-KO cells and reasoned OCA7 might regulate total levels of the enzymes that make melanin or other proteins involved in melanosome biogenesis. IB analysis of total cell extracts generated from WT and OCA7-KO cells with RIPA buffer failed to detect differences in the levels of the melanosome enzymes that synthesize melanin, Tyrosinase, TYRP1 and TYRP2 (**Figure 3.11**). LAMP2, Rab32 and Rab38 also showed unaltered steady state levels in OCA7-KO cells (**Figure 3.11**). PMEL protein is proteolytically processed in melanosomes and forms amyloid fibrils that function as a scaffold for melanin deposition and packing. The HMB45 antibody detects partially processed PMEL Mα fragment and further processed Rpt domain (36, 37). Strikingly, HMB45 IB analysis of total cell extracts generated from OCA7-KO cells with RIPA buffer revealed an accumulation of the partially processed Mα fragment compared to WT cells (**Figure 3.12A** and **3.12B**). Full length PMEL and partially processed intermediates are soluble in TX100 buffers while the highly proteolytically processed PMEL fragments present in fibrils are not, requiring high SDS concentration and high temperature for solubilization. To further test for a PMEL defect, we performed IB analysis with TX100 soluble and TX100 insoluble extracts from WT and OCA7-KO MNT1 cells. Both the PMEL N and HMB45 antibodies showed OCA7-KO cells have an accumulation of TX100 soluble Mα

fragment (**Figure 3.12C** and **3.12D**). The PMEL N antibody also recognizes full length PMEL (P1), which displayed normal steady state levels in OCA7-KO cells (**Figure 3.12C** and **3.12D**). The I51 antibody recognizes the so called “Core Amyloid Fragment” (CAF) of insoluble PMEL fibrils integral to PMEL fibril structure (37-40). IB analysis of TX100 insoluble fractions with I51 found less CAF in OCA7-KO cells compared with WT (**Figure 3.12E** and **3.12F**). These findings suggest PMEL processing is defective in steps after generation of the Mα fragment in OCA7-KO cells.

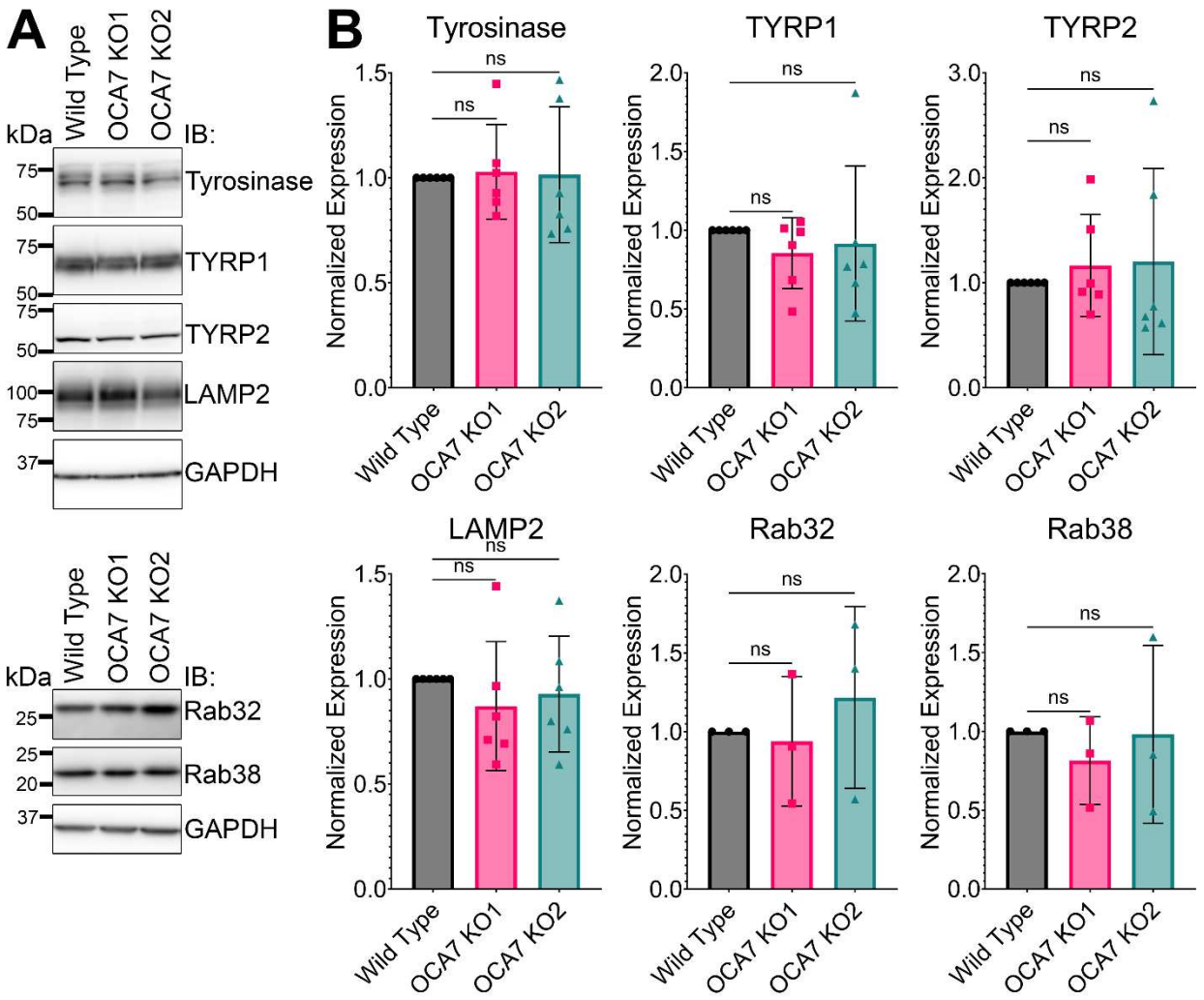

Figure 3.11. The steady state levels of melanogenic enzymes are unaffected in OCA7-KO MNT1 cells.

(A) Immunoblots of RIPA lysates from Wild Type or OCA7-KO MNT1 cells probed with antibodies for Tyrosinase, TYRP1, TYRP2, and other lysosome/late endosome or melanosome proteins LAMP2, Rab32, Rab38, and GAPDH as a loading control. Immunoblots show expression of melanogenic enzymes is unaffected in OCA7-KO cells. **(B)** Quantification of immunoblots shown in (A). The graphs show mean ± S.D and are shown relative to Wild Type. Immunoblots were quantified using RIPA lysates from n=6 independent experiments for Tyrosinase, TYRP1, TYRP2 and LAMP2, and n=3 independent experiments for Rab32 and Rab38. Statistical significance was tested using ordinary one way ANOVA and Tukey post-hoc tests. ns corresponds to p>0.05.

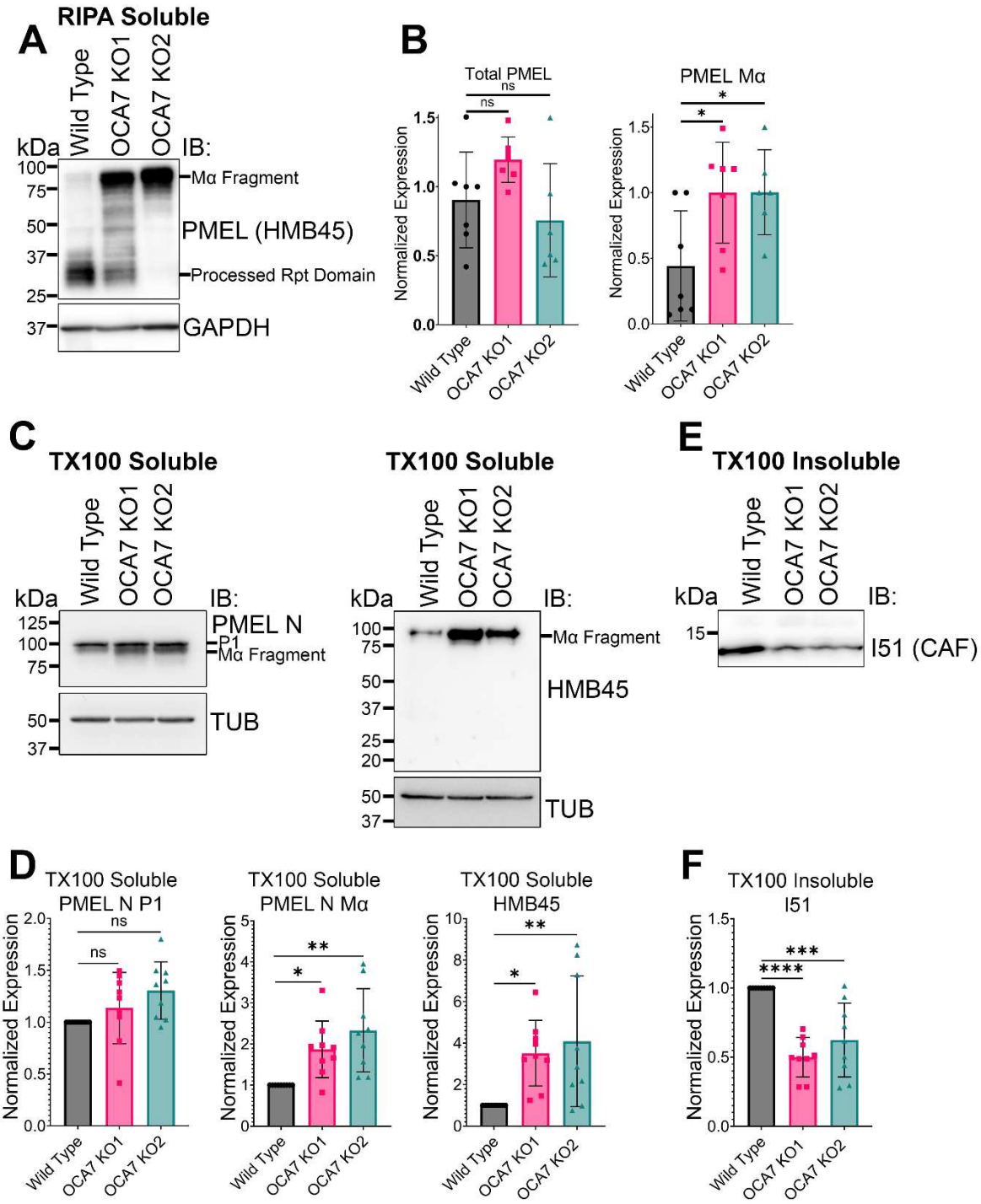

Figure 3.12. PMEL is aberrantly processed in OCA7-KO MNT1 cells. (A) IB analysis of RIPA buffer lysates using antibodies to PMEL (HMB45) show an accumulation of the Mα fragment in OCA7-KO cells. **(B)** Quantification of IBs depicted in (A) showing total HMB45 signal or Mα fragment only (mean ± S.D.; WT, n=7; OCA7-KO1, n=7; OCA7-KO2, n=6). **(C)** Immunoblot of cell lysates prepared with a buffer containing 1% TX100 from WT or OCA7-KO MNT1 cells probed with HMB45, PMEL N or anti-tubulin antibodies. **(D)** Quantification of PMEL full length (P1) and

Mα fragment from immunoblots shown in (C). The graphs show mean ± S.D., n=9 independent experiments were quantified. One way ANOVA and post-hoc Tukey tests were used to test for significance. ns, *, and ** correspond to $p>0.05$, $p<0.05$, and $p<0.01$ respectively. **(E)** Immunoblot of TX100 insoluble cell lysates from WT or OCA7-KO MNT1 cells probed with I51 antibody reactive towards the Core Amyloid Fragment (CAF) of PMEL. **(F)** Quantification for immunoblot shown in (E). The graph shows mean ± S.D for n=9 independent experiments. Immunoblots for TX100 insoluble PMEL were normalized to TX100 soluble Tubulin from the corresponding samples. Statistical significance was tested using one way ANOVA and Tukey post-hoc tests. *** and **** correspond to $p<0.001$ and $p<0.0001$ respectively.

OCA7-KO MNT1 cells have aberrant melanosomes and fewer striated melanosomes

PMEL fragments form electron dense amyloid fibril striations inside melanosomes that get packed with melanin pigment (18). Given a PMEL processing defect was detectable by immunoblotting, we hypothesized a defect in PMEL fibril striation and melanin packing would occur in OCA7-KO cells and be visible by electron microscopy. WT and OCA7-KO MNT1 cells were high pressure frozen and analyzed by thin section transmission electron microscopy. As expected, WT cells had few Stage I melanosomes, an abundance of Stage II and Stage III melanosomes having clear PMEL fibrils, and several Stage IV melanosomes having PMEL fibrils packed with melanin (**Figure 3.13**). In contrast, quantification showed OCA7-KO cells had significantly more Stage I and less Stage II and Stage III melanosomes (**Figure 3.13**). Additionally, OCA7-KO cells had numerous aberrant melanosomes containing a disordered, less electron dense cloud of melanin but lacking stereotypical striations. These results are consistent with a defect in PMEL fibrillation and melanosome biogenesis in OCA7-KO cells.

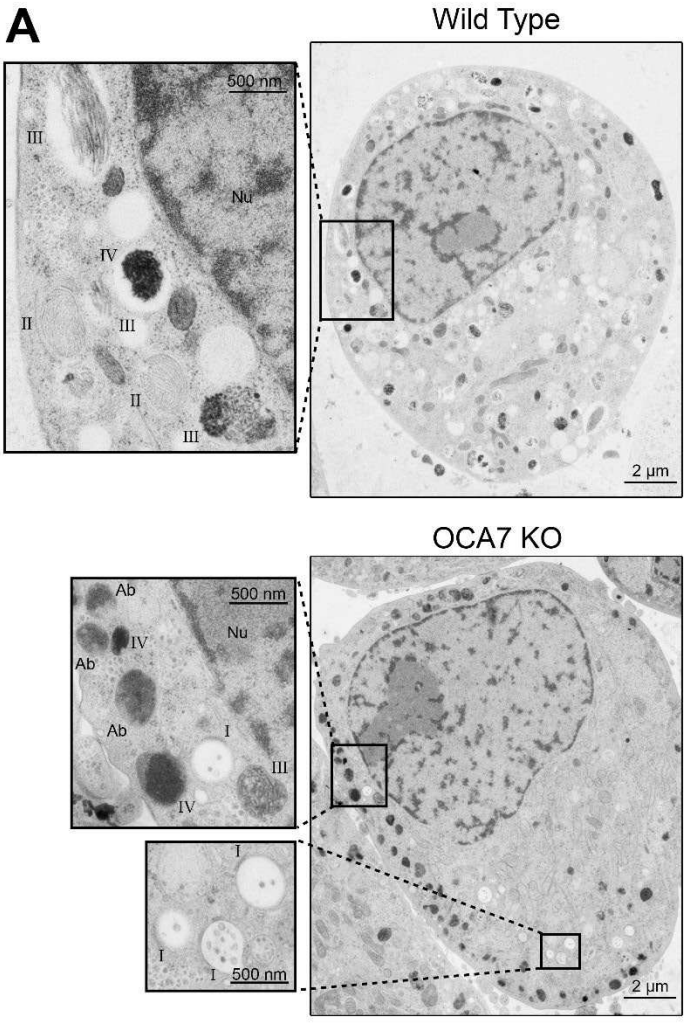
A
Wild Type
500 nm
III
Nu
IV
II
III
II
III
2 µm
OCA7 KO
Ab
500 nm
Nu
IV
Ab
Ab
I
III
IV
I
I
I
500 nm
2 µm

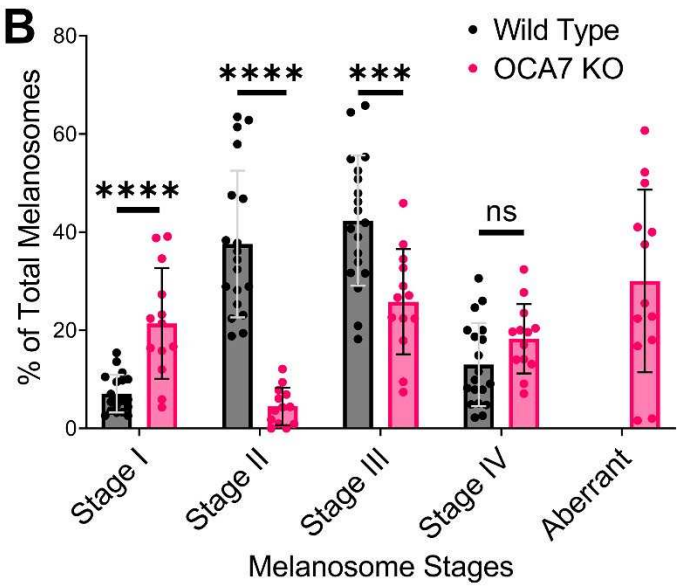
B
Wild Type
OCA7 KO
% of Total Melanosomes
80
60
40
20
0
****
****
***
ns
Stage I
Stage II
Stage III
Stage IV
Aberrant
Melanosome Stages

Figure 3.13. OCA7-KO MNT1 cells have aberrant melanosomes and fewer striated melanosomes. (A) Thin section transmission electron micrographs of WT or OCA7-KO MNT1 cells (6,800x). Magnified insets highlight examples of Stage I, II, III, IV, or aberrant (Ab) melanosomes (30,000x). **(B)** Quantification of the % of melanosomes in each stage per cell in WT and OCA7-KO cells depicted in images from (A) representing the mean ± S.D (WT, n=19 cells; OCA7-KO1, n=13 cells).

Melanosomes are more acidic in OCA7-KO MNT1 cells

The aberrant processing of PMEL likely contributes partially, but not entirely, to the hypopigmentation observed in OCA7-KO MNT1 cells. We reasoned OCA7-KO cells may have a broader defect in melanosome maturation. To test for a melanosome pH defect in OCA7-KO MNT1 cells we used a MElanosome LOcalized pH Sensor (MELOPS) we previously developed. MELOPS is based on the OCA2 protein and contains a pH sensitive fluorophore exposed to the melanosome lumen. Live cell imaging of OCA7-KO MNT1 cells expressing MELOPS showed a small but significant reduction in sensor fluorescence relative to Wild Type cells, which corresponds to a more acidic pH (**Figure 3.14A** and **3.14B**). The MELOPs range of detection is more suitable to sense pH increases than decreases (23). It is possible that the subtle fluorescence intensity decrease detected in OCA7-KO cells may represent an underestimation of the phenotype. Additionally, due to the natural localization of OCA2, MELOPs is more likely to report on more mature melanosomes while OCA7 is enriched in less mature melanosomes (23). To corroborate these results, we incubated Wild Type and OCA7-KO MNT1 cells with Acridine Orange, a dye that accumulates in organelles with low pH including melanosomes and endolysosomal organelles (41). Live cell imaging analysis showed significantly brighter fluorescence in OCA7-KO cells compared to Wild Type cells, confirming they have more acidic organelles (**Figure 3.14C** and **3.14D**). Abnormal luminal pH is known to negatively influence activity of melanogenic enzymes and likely explains why OCA7-KO cells are hypopigmented (42).

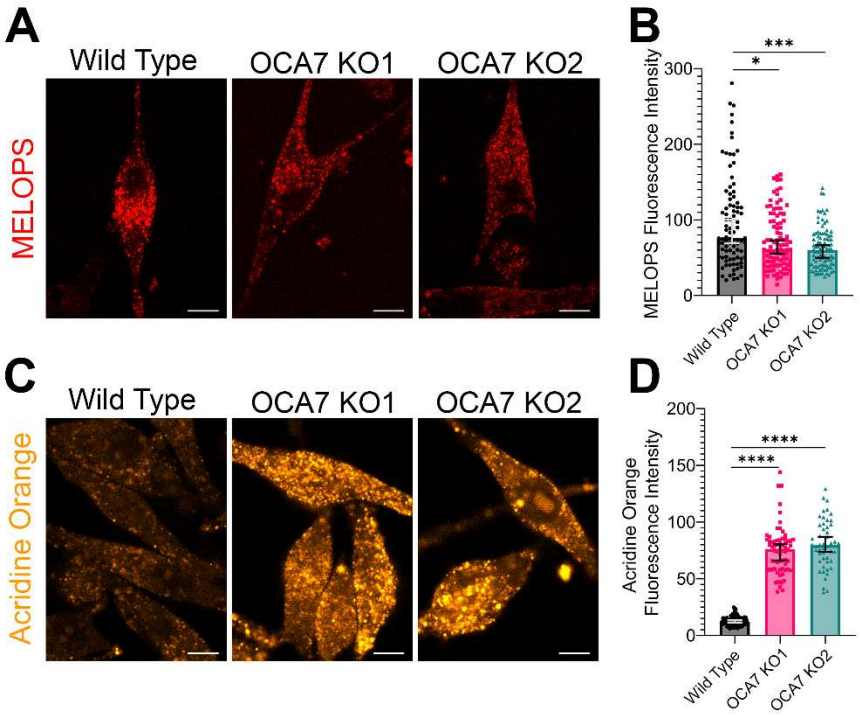

Figure 3.14. OCA7-KO MNT1 cells have melanosomes with lower luminal pH. (A) Laser scanning live cell microscopy images of WT and OCA7-KO MNT1 cells expressing MELOPS. Scale bars indicate 10μm. **(B)** Quantification of images from (A). The graph shows the median MELOPS fluorescence intensity with error bars representing the 95% confidence interval. n=90, n=97 and n=94 cells were analyzed for WT, OCA7-KO1, and OCA7-KO2 respectively. Significance was tested using the Kruskal-Wallis Test. * and **** correspond to $p<0.05$ and $p<0.0001$ respectively. **(C)** Laser scanning live cell confocal microscopy images of WT and OCA7-KO MNT1 cells stained with Acridine Orange. Scale bars indicate 10μm. **(D)** Quantification of images from (C). The graph shows the median fluorescence intensity with error bars representing the 95% confidence interval. n=121, n=65 and n=50 cells were analyzed for Wild Type, OCA7-KO1, and OCA7-KO2 respectively. Significance was tested using the Kruskal-Wallis Test. **** corresponds to $p<0.0001$.

OCA7 functions independently of TPC2

We initially discovered OCA7 at melanosomes through proximity biotinylation by the melanosome localized ion channel TPC2-BioID2-HA. In the present study, we found OCA7 deficiency reduces pigment and pH of melanosomes in MNT1 cells. In a previous study, we established TPC2 depletion increases pigment and pH of melanosomes in MNT1 cells (23). Therefore, an enticing possibility is that OCA7 might work as a negative regulator of TPC2 to

control pH and pigment of melanosomes. We reasoned if OCA7 primary function is to regulate TPC2, then depletion of OCA7 in a TPC2-KO background should not influence pigmentation or pH. Starting with TPC2-KO MNT1 cells used in previous studies, we knocked out OCA7 resulting in TPC2/OCA7 double-KO cells. Immunoblots confirmed efficient depletion of OCA7 in the bulk population of double-KO cells (**Figure 3.15A**). Visualization of cell pellets indicated an obvious reduction in pigmentation in the TPC2/OCA7 double-KO cells compared to parental TPC2-KO cells, suggesting OCA7 does not control pigmentation through TPC2 (**Figure 3.15B**). Furthermore, TPC2/OCA7 double-KO cells had heightened Acridine Orange accumulation relative to TPC2-KO cells, suggesting OCA7 regulates melanosome lumen pH independent of TPC2 (**Figure 3.15C** and **3.15D**). In addition to regulating pH of melanosomes, TPC2 was previously found to regulate basal cytosolic calcium concentration in the vicinity of melanosomes, presumably via calcium release from the melanosome lumen. Here we tested if OCA7 regulates this TPC2 activity (23). TPC2-GCaMP6-mCherry was expressed in WT and OCA7-KO MNT1 cells such that the calcium sensor GCamP6 was localized on the cytosolic side of the melanosome membrane. Determination of the GCaMP6/mCherry fluorescence intensity ratio showed no difference between WT and OCA7-KO cells suggesting calcium regulation by TPC2 is independent of OCA7 (**Figure 3.15E** and **3.15F**). Finally, we tested if OCA7 and TPC2 interact physically using co-immunoprecipitation. Immunoblotting confirmed efficient IP of endogenous OCA7 but failed to detect pulldown of overexpressed TPC2-BioID2-HA (**Figure 3.15G**). Together, we conclude OCA7 and TPC2 probably do not work with each other functionally or physically despite their close proximity at melanosomes.

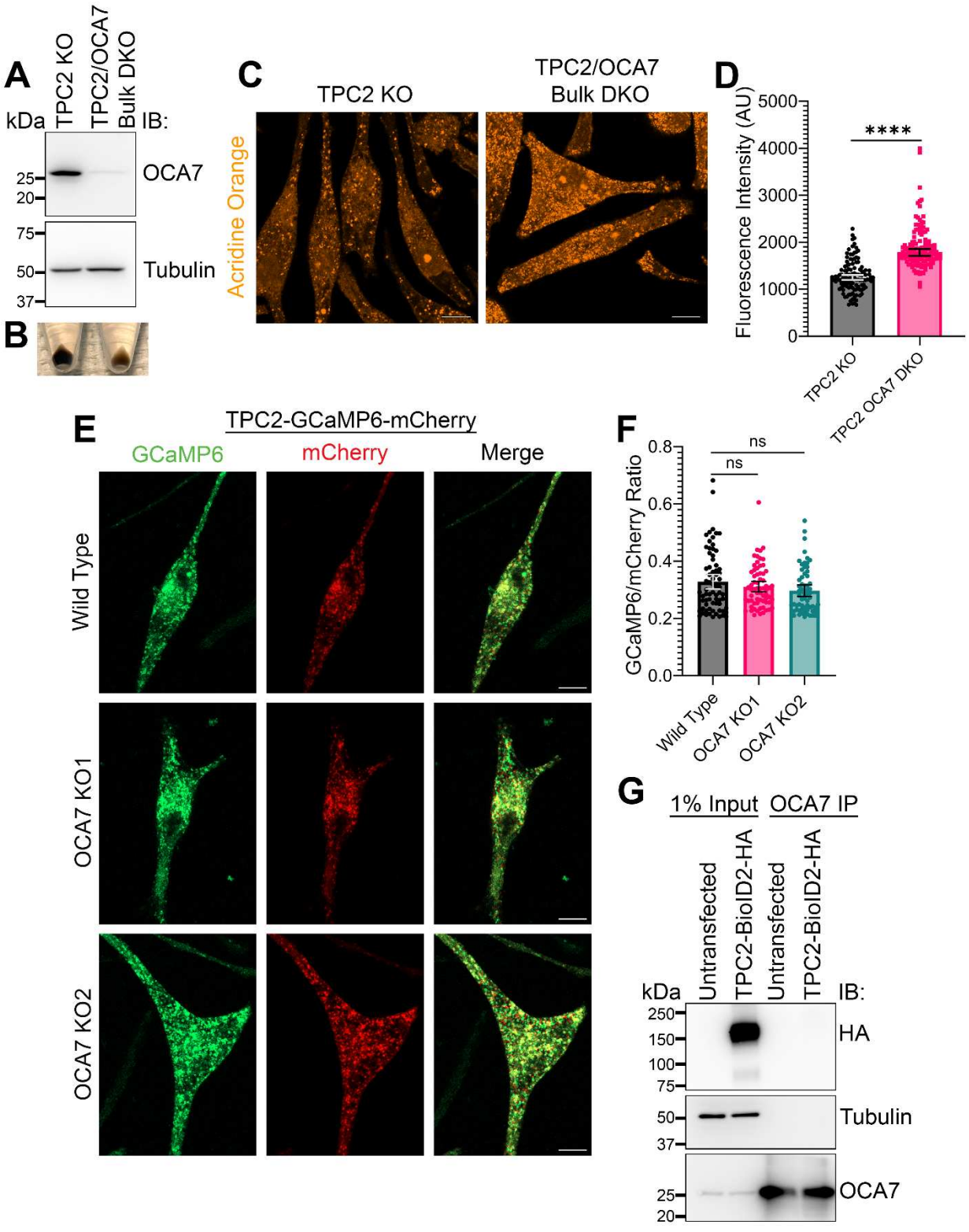

Figure 3.15. OCA7 functions independently of TPC2. (A) Immunoblot of RIPA lysates obtained from parental TPC2 knockout MNT1 cells and bulk TPC2/OCA7 double knockout MNT1 cells indicating efficient reduction of OCA7 protein expression. **(B)** Images of parental TPC2

knockout MNT1 and bulk TPC2/OCA7 double knockout MNT1 cell pellets showing less pigmentation in the double knockout cells. Cell pellets correspond to one 10cm dish approximately 70% confluent. **(C)** Live cell laser scanning Airyscan SR fluorescence microscopy images of TPC2 knockout MNT1 and bulk TPC2/OCA7 double knockout MNT1 cells stained with Acridine Orange for 30 minutes showing heightened Acridine Orange accumulation in the double knockouts. Scale bars indicate 10μm. **(D)** Quantification of Acridine Orange fluorescence intensity for cells from (C). The graph shows median with error bars showing the 95% confidence interval. n=119 and n=128 cells were analyzed for TPC2 KO and TPC2/OCA7 DKO respectively. Significance was tested using the Mann-Whitney test and **** corresponds to $p<0.0001$ **(E)** Live cell laser scanning Airyscan SR fluorescence microscopy images of Wild Type and OCA7 KO MNT1 cells transiently expressing the calcium sensor TPC2-GCaMP6-Cherry. Cells were imaged 24 hours after transfection. Scale bars indicate 10μm. **(F)** Quantification of GCaMP6/mCherry ratio for cells imaged in (E) indicating no difference in basal cytosolic calcium around TPC2. The graph shows the medians with 95% confidence intervals. n=70, n=66, and n=63 cells were analyzed for Wild Type, OCA7 KO1 and OCA7 KO2 respectively. Significance was tested using the Kruskal-Wallis test. n.s corresponds to $p>0.05$ **(G)** Immunoblot analysis of TX100 cell lysate input and anti-OCA7 immunoprecipitation of lysates derived from untransfected MNT1 cells or MNT1 cells overexpressing TPC2-BioID2-HA. The immunoblot indicates endogenous OCA7 does not robustly co-immunoprecipitate with overexpressed TPC2.

Discussion

OCA7 was previously hypothesized to regulate melanocyte differentiation. This idea stemmed from a study finding that depletion of an OCA7 homologue in sea squirt led to embryonic developmental defects resembling β-catenin depletion (43). Another study found OCA7 knockdown appeared to reduce the number of melanocytes in zebrafish as assessed by visualization of pigment at the organismal level (15). However, the same study also found OCA7 mRNA expression occurs downstream of MITF, a transcription factor controlling expression of many melanocyte specific proteins. Therefore, it is unclear if OCA7 is involved in the upstream process of melanocyte differentiation. OCA7 patients retain the capacity to synthesize melanin, suggesting melanocytes are still present, and the idea that OCA7 is involved in melanocyte differentiation has not been supported in humans or mammals. Here we provide evidence for an alternative model in which OCA7 functions at melanosomes where it is needed for normal organelle biogenesis and function (**Figure 3.16**).

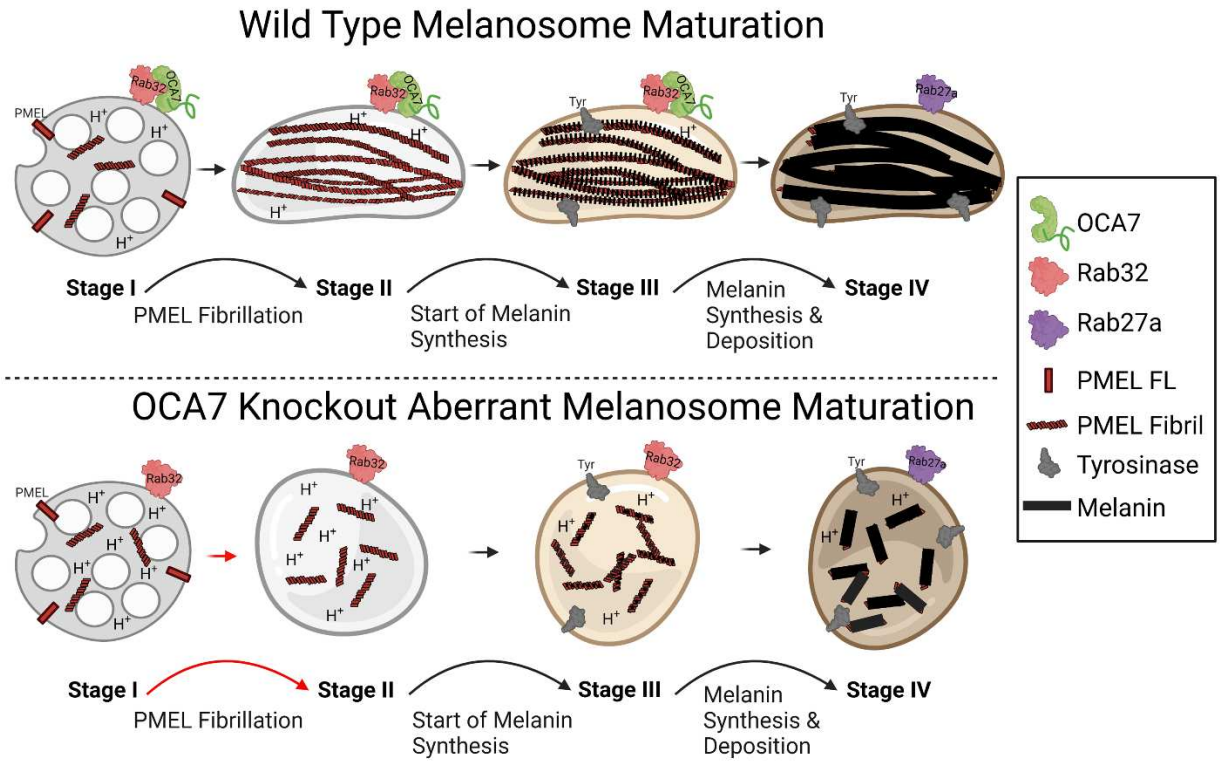

Figure 3.16. Cartoon depiction of melanosome biogenesis defects in OCA7 mutant in melanocytes. In WT melanocytes, OCA7 is present on melanosome membranes through interaction with Rab32 (and Rab38) that requires the OCA7 LRR domain and Rab32 Interswitch and Switch 2 regions. Melanosome biogenesis starts with Stage I melanosomes that resemble multivesicular endosomes defined by the presence of full length and partially processed PMEL protein. As full length PMEL is processed, it forms the Mα fragment that then associates with the intraluminal vesicles, eventually undergoing additional proteolytic processing and self-association into a mature insoluble fibril, and the melanosome is defined as Stage II. Once fibrils are formed, Tyrosinase arrives to the melanosome and begins melanin synthesis, and melanin deposits onto PMEL fibrils, defining Stage III melanosomes. Additional melanin synthesis results on fully pigmented Stage IV melanosomes, which are primarily labelled by Rab27a and not Rab32 and OCA7. In OCA7-KO melanocytes, melanosomes accumulate the PMEL Mα fragment but do not productively form ordered fibrils. Tyrosinase proceeds to make melanin but pigment cannot organize correctly in the absence of normal PMEL fibrils, leading to aberrant Stage IV melanosomes seen by electron microscopy. A lower luminal pH in OCA7 melanosomes results in lower Tyrosinase activity and decreased melanin synthesis, and potentially contributes to PMEL processing defects. The cartoon was created with Biorender.com.

First, several lines of evidence show OCA7 is a melanosome associated peripheral membrane protein enriched in maturing melanosomes: (i) Using an unbiased BioID2 screen, we discovered OCA7 in the proximity of TPC2, a melanosome membrane protein. (ii) Fluorescence microcopy with an array of organelle markers corroborated OCA7 localizes to melanosomes, especially the less mature forms of these organelles. (iii) FRAP and biochemical approaches showed OCA7 is present both in the cytosol and melanosome membranes quickly exchanging between the two pools. (iv) Y2H experiments showed OCA7 interacts with Rab32 and Rab38, two proteins known to function in melanosome biogenesis. This interaction occurs via a Rab canonical effector binding surface and the OCA7 LRR domain and likely mediates OCA7 recruitment to melanosomes.

Second, results indicate OCA7 functions in the biogenesis of melanosomes. OCA7-KO MNT1 cells are hypopigmented but retain expression of melanocyte specific markers Tyr, Tyrp1, and Tyrp2, consistent with the idea that OCA7 regulates pigmentation independent of melanocyte differentiation. Importantly, OCA7-KO MNT1 cells transiently transfected with OCA7-EGFP quickly recover normal pigmentation, thus providing a validated system to study OCA7 at the cellular level. With this cell model we found OCA7 functions at early stages of melanosome biogenesis, specifically in the transition from Stage I to Stage II. This is demonstrated by the

increased numbers of Stage I but reduced numbers of Stage II and Stage III melanosomes in OCA7-KO MNT1 cells determined by electron microscopy. Lack of striations typical of Stage II and Stage III melanosomes is consistent with the PMEL processing defect post generation of the Mα fragment resulting in the accumulation of Mα and reduced CAF observed by IB. Abnormal melanosome luminal pH in OCA7-KO cells may affect the activity of enzymes that cleave PMEL in Stage I melanosomes, proprotein convertase and BACE2, further explaining the maturation defect (44, 45). Aberrant pigmented melanosomes observed by electron microscopy in OCA7-KO MNT1 cells likely reflect the inability of melanin to deposit and concentrate due to reduced PMEL striations. Consistently, similar melanosomes with heterogeneous melanin deposition were observed in PMEL-KO mice and BACE2-KO mice (45, 46). Together, the data shows OCA7 works in early stages of melanosome biogenesis.

OCA7-KO MNT1 cells have a defect in PMEL processing but it is unclear if a PMEL defect alone would lead to OCA. PMEL-KO mice have only a very subtle pigmentation deficiency, and human PMEL variants are associated with pigmentary glaucoma, but not OCA (46, 47). Thus, the PMEL defect alone may not fully explain the OCA7 pigmentation phenotype in patients and MNT1-KO cells. Melanosome lumen pH is known to affect the activity of tyrosinase, the key enzyme in melanin synthesis (41, 42). The lower melanosome luminal pH in OCA7-KO MNT1 cells detected by both MELOPS and Acridine Orange methods is consistent with the reduced melanin levels observed in these cells and in OCA7 patients. Therefore, it is likely that overall OCA7 hypopigmentation is the result of both PMEL processing and fibrillation defect as well as decreased melanin synthesis due to reduced melanosome pH. Future work will investigate how OCA7 regulates melanosome pH. We were unable to confirm a functional or physical interaction between OCA7 and TPC2, but we hypothesize OCA7 may influence pH by working with other ion channels or proton pumps.

In accordance with our findings, it was previously shown that Rab32 deficiency leads to increased PMEL Mα levels (48). Our results suggest OCA7 works with Rab32 to regulate PMEL

fibrillation and melanosome biogenesis. It is worth noting that OCA7 and Rab32 are expressed in several cell types besides melanocytes suggesting OCA7 may also function with other lysosome related organelles (proteinatlas.org/ENSG00000148655-LRMDA, **Figure 3.17A**) (49). For example, Rab32 regulates the maturation of phagosomes in macrophages during pathogen clearance, resides on lysosomes in hepatocytes, and is involved in the biogenesis of platelet dense granules in megakaryocytes (50-54). Interestingly, a recent case report described two OCA7 patients who faced recurring respiratory infections in addition to the expected OCA manifestations suggesting OCA7 may in fact have broader functions (35). Adding to this possibility, recent genome wide association studies listed SNPs in intronic regions of the OCA7 gene to be associated with Covid-19 susceptibility in non-Europeans and with platelet aggregation, suggesting OCA7 may have functions in immune cells and megakaryocytes/platelets, respectively (55, 56). IB analysis of lysates made from imMKCL cells, a well-validated human megakaryocyte cell line, confirmed OCA7 protein expression (**Figure 3.17B**) (57-59). Expression of OCA7-EGFP in differentiated imMKCL cells revealed its localization to membranes of vacuolar compartments that partially overlapped with the platelet dense granule marker VMAT2-mCherry (**Figure 3.17C** and **3.17D**). These results lend credence to the idea that OCA7 may regulate the function of other lysosome related organelles in addition to melanosomes. Such a scenario would suggest the disease caused by OCA7 mutation may impact additional cell types and be better described as a syndrome, such as the Hermansky Pudlak syndrome (60).

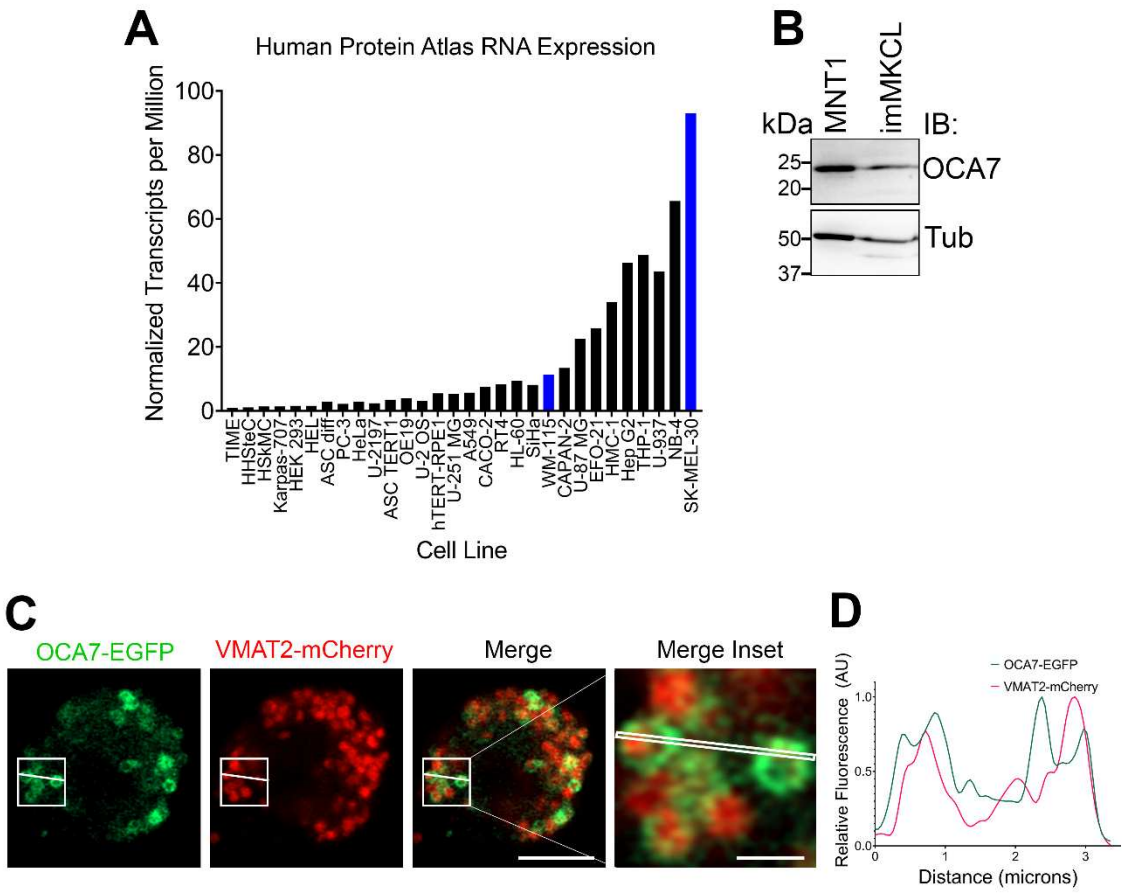

Figure 3.17. OCA7 is expressed in multiple cell types. (A) Graph of OCA7 RNA expression showing the OCA7 gene is expressed in several cell types in addition to melanocytes. The blue bars indicate melanoma cell lines. OCA7 expression data was downloaded from the Human Protein Atlas database and 30 common cell lines are shown. (proteinatlas.org/ENSG00000148655-LRMDA/subcellular). **(B)** Immunoblot of RIPA lysates obtained from MNT1 cells or imMKCL megakaryocytes showing OCA7 is expressed. **(C)** Laser scanning Airyscan SR fluorescence microscopy images of imMKCL cells differentiated for 72 hours expressing OCA7-EGFP and VMAT2-mCherry. OCA7-EGFP is present in some overlapping compartments with VMAT2-mCherry suggesting partial dense granule localization. The scale bar indicates 5μm. **(D)** Line scan analysis of the indicated region in (C) showing an example of OCA7-EGFP colocalized with VMAT2-mCherry

In summary, the present study revealed OCA7 is a melanosome protein that regulates organelle biogenesis and function. The data places OCA7 as one of the few factors known to mediate early stages of melanosome maturation. While important mechanistic clues emerge from our results, more work needs to be done to fully understand OCA7. For example, Rab32 and Rab38 have been implicated both in forward traffic to maturing melanosomes as well as retrieval

from melanosomes to endosomes (26, 48, 61, 62). Future studies should explore if OCA7 function is linked to Rab32/Rab38 forward or retrieval traffic and better define how OCA7 regulates organelle pH. Finally, the possibility that OCA7 regulates other lysosome related organelles in addition to melanosome deserves serious consideration both from basic cell biology and clinical stand points.

Materials and Methods

Cell Culture and Transfection

MNT1 cells were cultured as previously described (26). For microscopy experiments, $0.3X10^6$ cells were resuspended in 20µL Lonza SF solution, mixed with 0.4µg of each plasmid, transferred to 16 well nucleocuvette strips and nucleofected using program DS-137 in a Lonza 4D nucleofector. After 10 minutes, cells were transferred to 35mm glass bottom dishes with 2mL 37°C KGM Gold media and grown 24-72 hours. Nonidentified human neonatal primary epidermal melanocytes (Thermo Fisher Scientific Cat no. C0025C) were cultured in supplemented Medium 254 per manufacturer instructions and nucleofected as described for MNT1 cells. imMKCL cells were cultured as previously described (59, 63) and nucleofected as described for MNT1 cells except program EN-138 was used for nucleofection. 24 hours after transfection, imMKCL cells were transferred to Matrigel coated glass bottom dishes and the media was replaced with fresh media lacking doxycycline to induce differentiation. imMKCL cells were imaged after 72 hours in differentiation media.

Plasmids

Plasmids were generated using Infusion Cloning (Takarabio). Primers were designed to have 15 base pair 5' extensions to overlap with linearized vectors for Infusion cloning. Primer pairs are listed in Table 3.1. OCA7, AP1M1, RabIF, and EXOSC5 were cloned from cDNA originating from MNT1 cells using CloneAmp HiFi PCR Premix (Takarabio) and the Infusion cloning system (Takarabio). To acquire cDNA, total RNA was prepared from MNT1 cells using the RNEasy kit (Qiagen) and converted to cDNA using iScript Reverse Transcriptase Supermix (BioRad). To generate pEGFP-N3-OCA7, OCA7 was amplified from MNT1 cDNA and inserted by Infusion into a linear pEGFP-N3 vector linearized by restriction digestion with HindIII-HF (NEB) and ApaI (NEB). To generate pET30-OCA7-6His for recombinant expression, OCA7 was amplified from pEGFP-N3-OCA7 and inserted by Infusion cloning into pET-30a(+) that was

linearized with NdeI and NotI-HF. To generate pGAD424-OCA7 for Y2H analysis, OCA7 was amplified from pEGFP-N3-OCA7 and inserted by Infusion cloning into pGAD424 linearized with EcoRI-HF and SalI-HF. To generate truncations in pGAD424-OCA7 and pEGFP-N3-OCA7 plasmids, inverse PCR was performed with primers designed to exclude unwanted sequence and add complementary 15 base pair 5' overhangs. After PCR, the linear plasmids were closed by Infusion cloning. pGBT9-AP1M1, pGBT9-RabIF, and pGBT9-EXOSC5 were generated by amplifying each ORF from MNT1 cDNA and inserting by Infusion cloning into pGBT9 linearized by EcoRI-HF and SalI-HF. AKAP1-FRB-BFP2 was generated by digesting AKAP1(31)-FRB-iRFP (gifted by Gerry Hammond, Addgene #139315 (64)) to remove iRFP and using Infusion cloning to insert mBFP2 amplified from pmBFP2-KDEL. To generate pmCherry-Rab32-CC/AA-FKBP and pmCherry-Rab38-CC/AA-FKBP, pmCherry-C2-Rab32 or pmCherry-C2-Rab38 were linearized and mutagenized by inverse PCR to mutate cysteines to alanines. Then FKBP12 was amplified from FKBP12-TOPO-M13-pUC (generously gifted by Soham Chanda) and inserted into the linearized vectors by Infusion cloning. pmCherry-C2-CD63 was subcloned from pEGFP-C2-CD63 (gifted from Paul Luzio, Addgene #62964) by restriction digestion with HindIII-HF and BamHI-HF and T4 Ligation (NEB) into pmCherry-C2 digested with the same enzymes. To generate TPC2-GCaMP6-mCherry, TPC2-GCaMP6 (Addgene #80147) was first mutated to remove the stop codon and add a C terminal AgeI restriction site. Then, pmCherry-N3 was digested with Xma1 and Not1 and the mCherry fragment was ligated into TPC2-GCaMP6 digested with AgeI and Not1, generating TPC2-GCaMP6-mCherry. To generate TPC2-BioID2-HA, TPC2 was amplified from pEGFP-N3-TPC2 (Addgene #80153) and inserted into MCS-Linker-BioID2-HA (gifted from Kyle Roux, Addgene #74224) linearized by inverse PCR. Plasmids were confirmed by Sanger sequencing.

pGBT9-Rab32, pGBT9-Rab38, pGBT9-Rab8, pGBT9-Rab11a, pGBT9-Rab10a, pGBT9-Rab27a, and their mutants for Y2H were generated and validated for a previous study (27). pmCherry-C2-Rab32, pmCherry-C2-Rab38, pmCherry-N3-Tyrosinase, pmCherry-N3-Tyrp1,

pmCherry-C2-Rab27a, pmCherry-C2-Rab7a, pmCherry-C2-Rab11a, pmCherry-C2-Rab5a, pmRFP-N1-SKL, pmBFP2-KDEL, piRFP-N1-TPC2, MELOPS, and VMAT2-mCherry for microscopy experiments were all generated and validated for previous studies (23, 26, 27, 53, 63, 65). pmaxGFP is from Lonza.

Antibodies

Primary antibodies used were C10orf11/LRMDA/OCA7 (PA5-61519, ThermoFisher, 1:1000), C10orf11/LRMDA/OCA7 (HPA050419, Atlas Antibodies, 1:1000), Tubulin (T9026, Sigma, 1:100,000), GAPDH (60004-1-Ig, ProteinTech, 1:500,000), PMEL N (E-7, SC-377325, 1:1000), PMEL Rpt (HMB45, Dako, 1:1000), PMEL CAF (I51,generously provided by Michael Marks and Ralf Leonhardt, 1:1000), CD63 (sc-5275, 1:1000), CD81 (B-11, sc166029, 1:2000), Tyrosinase (T311, sc-20035, 1:1000), TYRP1 (MelV, TA99, sc-58438 ,1:1000), TYRP2 (C-9, sc-74439, 1:1000), LAMP2 (H4B4, sc-18822, 1:1000), HA Tag-HRP (Cell Signaling 2999S, 1:1000,). Rab32 and Rab38 are noncommercial Rabbit polyclonal antibodies previously characterized and used at 1:1000 (26). Secondary antibodies were HRP conjugated Anti Mouse IgG (NA931, Cytiva, 1:7500) and Anti Rabbit IgG (NA934, Cytiva, 1:7500) for immunoblotting.

CRISPR-Cas9 Mediated Knockout

OCA7/LRMDA knockout in MNT1 cells was achieved by nucleofecting Cas9/crRNA/tracrRNA ribonucleoprotein complexes into Wild Type MNT1 cells according to the manufacturer's protocol (IDT Alt-R CRISPR-Cas9 System). Two predesigned crRNAs, Hs.Cas9.LRMDA.1.AC and Hs.Cas9.LRMDA.1.AE were selected from IDT to target *OCA7/LRMDA* exon 2 with high specificity (Table 3.2). To generate each ribonucleoprotein (RNP) complex, 5μL 200μM crRNA and 5μL 200μM tracrRNA were mixed and heated at 95°C for 5 minutes and allowed to cool to room temperature. 2.1μL PBS, 1.2μL crRNA:tracrRNA duplex, and 1.7μL 61μM Cas9 were mixed and incubated at room temperature for 20 minutes. MNT1 cells

(300,000 cells) were resuspended in 20 µL Lonza SF nucleofection solution and mixed with 5µL of each RNP and 1µL of IDT electroporation enhancer for a final volume of 31µL. The mix was transferred to a well of a Lonza 16 well nucleocuvette strip and nucleofected using program DS-137. After nucleofection, 70µL 37°C media was added to the suspension and the suspension was transferred to a 35mm culture dish with 2mL 37°C MNT1 media and incubated for 72 hours. For single clone isolation, the OCA7-KO cells were trypsinized and diluted to 5 cells/mL in MNT1 media, and 200µL was seeded into wells of 96 well plates. The following day, wells containing only a single cell were marked and single cells were grown, replacing the media every 4 days. To genotype colonies, genomic DNA was prepared using the QuickExtract reagent according to the manufacturer's instructions (Biosearch Technologies) and sequence surrounding exon 2 was amplified with primers listed in the Table 3.3. PCR products were run in a 1.5% agarose gel in 1X TAE buffer and bands were excised and purified using a gel purification kit (GE Illustra). DNA was sequenced using Sanger Sequencing, confirming both crRNAs had worked. OCA7 protein deficiency was confirmed by whole lysate immunoblotting and lack of signal after immunoprecipitation.

Light Microscopy

Spinning disk confocal fluorescence images were captured with an Olympus IX81 configured with an Andor iXon Ultra camera and phasor holographic photobleaching system (3i) using a 100X/1.40NA oil immersion objective lens. The microscope was equipped with lasers for 405nm, 488nm, 561nm, and 640nm and emission filter wheels for 521nm, 607nm, and 700nm. Confocal Airyscan SR images were taken with a Zeiss LSM 900 with Airyscan 2 detector using a 63X/1.40NA Oil immersion or 40X/1.30NA oil immersion objective lenses. Live cells were imaged in humidified stage incubators set to 37°C with 5% CO2. Brightfield images for melanin pigment quantification were captured with a Keyence BZ-X710 Wide field fluorescence microscope using a 100X/1.45NA objective lens. Images taken with the Olympus IX81 were analyzed with

Slidebook 6 software (3i). Colocalization analysis was performed by manually segmenting cells and creating corresponding masks for each cell, subtracting background fluorescence, and using the Colocalization module with Costes autothresholding to measure Pearson Correlation Coefficient. In some cases (Figure 1B, Figure 1C and Figure 5D) a 2D Laplacian filter using a 3X3 kernel (-1,-1,-1;-1,8,-1;-1,-1,-1) was applied before colocalization analysis. Image J was used to analyze fluorescence intensity in images taken with the Zeiss LSM 900. Cells were manually segmented in Image J, background was subtracted, and mean fluorescence intensity was measured. Line scan fluorescence intensity analysis was performed in Image J by making a straight line through regions of interest and plotting fluorescence intensity with the Plot Profile tool. Zeiss Zen Blue software was used for semi-automated cell segmentation and counting of single fluorescent melanosome puncta in melanocytes. To do so, binary masks were made using thresholding to segment individual cells and an additional mask was made to highlight individual melanosome puncta. The Analyze Interactively module was used to check the automated cell segmentation and separate cells manually if necessary. Individual melanosomes were counted for each cell. Cell pigment was measured in brightfield images using Image J. Cells in images were manually segmented and a threshold was set to highlight melanosomes inside of cells. Then the area of the entire cell and the area filled by pigmented melanosomes was calculated and the percent of the cell area with pigment was calculated.

Fluorescence Recovery After Photobleaching (FRAP)

For the FRAP experiment, 0.3X10^6 Wild Type MNT1 cells were nucleofected with 400ng of pEGFP-N3-OCA7 and pmCherry-C2-Rab32 or pmCherry-C2-CD63 plasmids in 20μL Lonza SF solution using Nucleofector 4D program DS-137 (Lonza), transferred to glass bottom microscopy dishes and incubated for 72 hours with KGM Gold media. On the day of imaging, the media was replaced with fresh media containing 10μM Nocodazole and incubated for approximately 90 minutes prior to imaging to prevent melanosome movement on microtubules.

During imaging, 2μm diameter circles were made in Slidebook6 to target melanosomes with the Phasor photobleaching device. For each cell, 3 separate melanosomes were photobleached and their fluorescence intensity was recorded during timelapse imaging. Timelapses acquired 10 frames at 1 second intervals before photobleaching, photobleaching ensued for 1 second, and an additional 190 frames were captured to measure recovery. The phasor was set to photobleach each area with the 488nm laser and the 561nm laser for 500ms each. To analyze FRAP curves, fluorescence intensity of photobleached ROIs was plotted using the Slidebook 6 FRAP Analysis module and corrected for imaging induced photobleaching using an unbleached ROI as a reference. Photobleach corrected FRAP curves were compiled in Graphpad Prism and modeled using a one phase decay curve fitting to calculate T1/2 of recovery for OCA7-EGFP.

Rab32/38 Mislocalization Assay

For the induced dimerization experiments, 0.3X10^6 Wild Type MNT1 cells were nucleofected with 200ng of pEGFP-N3-OCA7, 500ng AKAP1-FRB-BFP2, and 400ng pmCherry-C2-Rab32-CC/AA-FKBP or pmCherry-C2-Rab38-CC/AA-FKBP plasmids in 20μL Lonza SF solution using Nucleofector 4D program DS-137 (Lonza), transferred to glass bottom microscopy dishes and incubated for 24 hours with KGM Gold media. Dishes were first imaged in the absence of dimerization reagent. Then, the media was replaced with fresh media containing 100nM Rapalog (Takara A/C heterodimerizer) and cells were incubated for one hour to achieve efficient dimerization. After incubating with Rapalog, dishes of cells were imaged again to test for OCA7-EGFP recruitment to Rab32/38 labeled mitochondria. Colocalization analysis was performed in Slidebook6.

MELOPS Melanosome pH Experiment

For the MELOPS experiment, $0.3X10^6$ Wild Type or OCA7-KO MNT1 cells were nucleofected with 450ng MELOPS plasmid and 200ng pmaxGFP soluble GFP plasmid (Lonza) as described in the Cell Culture and Transfection section. Cells were incubated in KGM Gold

media for 24 hours in 35mm glass bottom dishes before imaging with a Zeiss LSM900 set to Airyscan SR mode with excitation set to 587nm and detection set to 565-700nm. During imaging, transfected cells were located with the green fluorescence channel (488nm excitation, 490-575nm detection) to prevent bias. MELOPS was quantified by measuring red fluorescence intensity of manually drawn ROIs in Image J.

Acridine Orange Staining of Acidic Organelles

For acridine orange experiments, $0.3X10^6$ Wild Type or OCA7-KO MNT1 cells were seeded in 35mm glass bottom dishes with 2mL 37°C KGM Gold media and grown for 24 hours. To stain cells, media was aspirated from the dish and cells were incubated with 2mL Acridine Orange (BioRad**,** ICT937) diluted to 1µM in KGM Gold media for 30 minutes in a humidified cell culture incubator at 37°C and 5% CO2. After the incubation, cells were washed twice for 1 minute with 2mL 37°C PBS. After washing, 2mL fresh KGM Gold media was added to the dish and the cells were placed in the humidified stage incubator of a Zeiss LSM900 microscope and immediately imaged in confocal mode with excitation set to 488nm and detection of 400-700nm. Images were analyzed by measuring fluorescence intensity of manually drawn ROIs in image J.

Electron Microscopy

Pelleted cells were resuspended in growth media supplemented with cryo-protectant (2% sucrose, 150mM D-mannitol) and spun down to a loose pellet. A few microliters of pelleted cells were subjected to high pressure frizzing using a Wohlwend Compact 02 high pressure freezer (Technotrade International, Manchester, NH) as previously described(66). Frozen samples were then freeze-substituted in anhydrous acetone containing 2% osmium tetroxide and 0.2% uranyl acetate and embedded in Epon/Araldite resin. Thin sections (80 nm) were cut using a Leica UCT ultramicrotome, collected on Formvar-coated copper slot grids and post-stained with 2% aqueous uranyl acetate followed by Reynold's lead citrate. The samples were imaged with a Tecnai T12 Spirit Transmission Electron Microscope, operating at 100 kV using an AMT CCD camera. Each

cell analyzed was first imaged at low-magnification (X 6,800) followed by sufficient high-magnification captures (x 18,500-49,000) of different cell regions to cover the entire cell (5-10 high-magnification pictures per cell). For each cell, melanosomes were identified by their typical morphology using the low magnification image and then confirmed with the corresponding high magnification images. Quantification was performed by counting the number of Stage I, Stage II, Stage III, Stage IV and aberrant melanosomes observed for each cell and reporting them as % of total melanosomes per cell.

Immunoblotting

$1.5X10^6$ cells were seeded in 10cm dishes with 10mL MNT1 media and incubated for 72 hours in a humidified 37°C incubator. To harvest cells, dishes were washed with 5mL ice cold PBS, scraped into suspension with 5mL ice cold PBS using cell lifters and pelleted at 200 x g at 4°C for 5 minutes. Cell pellets were resuspended in 250µL RIPA buffer (150mM NaCl, 1% w/v TX100, 0.1% w/v SDS, 1% w/v deoxycholate, 20mM Tris HCL pH 8.0, 1mM EDTA) or 1% TX100 in PBS with 1X protease inhibitor cocktail (0.2mM AEBSF, 0.15µM Aprotinin, 1.5µM E-64, 1µM Leupeptin, 1.5µM Bestatin) and lysed on ice for 15 minutes, gently agitating every 5 minutes. Lysates were centrifuged at 16,000 x g at 4°C for 15 minutes to pellet melanin and insoluble debris. 10µL aliquots of each lysate were taken and diluted 1:10 for total protein quantification using a Bradford Assay (BioRad Protein Assay) for normalized gel loading. 100µL of remaining lysate was mixed with 100µL 2X Laemmli sample buffer (which contains 8% SDS) and incubated for 5 minutes at 96°C. For immunoblots, 30µg of total protein was loaded into precast 4-20% gradient polyacrylamide tris glycine gels (Invitrogen Novex WedgeWell). Protein was transferred to PVDF membranes and membranes were blocked in 5% (w/v) milk TBST at room temperature for 1 hour. Primary antibodies were diluted in 5% (w/v) milk TBST and incubated with blots overnight at 4°C. Membranes were washed 3 times in TBST for 5 minutes, incubated with secondary antibodies diluted in 5% (w/v) milk TBST for 1 hour at room temperature, washed 3

times in TBST for 5 minutes, and developed with ECL Prime chemiluminescence reagent (Cytiva). Blots were quantified in Image J using the gel analyzer tool after background subtraction. Band intensities were normalized to GAPDH or Tubulin loading controls.

For PMEL blots, Triton X-100 insoluble lysates were prepared by resuspending the insoluble pellet from 1% (w/v) TX100 lysates with 1mL 1%(w/v) TX100 and incubating on ice 15 minutes to wash. Suspended insoluble material was pelleted at 16,000 x g at 4°C for 15 minutes. After aspirating the wash, pellets were resuspended in 1X Laemmli sample buffer (which contains 4% SDS), incubated 5 minutes at 96°C in a heat block, vortexed, incubated 5 more minutes at 96°C in a heat block, spun for 10 seconds at 16,000 x g and the supernatant loaded into gels. Immunoblot band intensities for TX100 insoluble lysates were normalized to Tubulin signal from the corresponding TX100 soluble lysate immunoblot.

Membrane and Cytosol Fractionation

MNT1 cells were grown for 3 days to 70-90% confluency in a 10cm culture dish with MNT1 media. To harvest, the dish was washed with ice cold PBS and cells were scraped into suspension in 5mL PBS using a cell lifter. Cells were centrifuged for 5 minutes at 200 x g at 4°C. The pellet was resuspended in 400µL M/C buffer containing 10 mm HEPES, pH 7.5, 250 mm sucrose, 1 mm dithiothreitol, 1 mm EGTA, 0.5 mm MgCl2, 1 mm GTPγS, and 1X protease inhibitor cocktail. Cells were homogenized by passing through a 25 gauge needle, passing up and down 15 times. The resulting homogenate was centrifuged 15 minutes at 1000 x g at 4°C to pellet nuclei and debris. The supernatant containing cytoplasm was transferred to ultracentrifuge tubes and centrifuged for 30 minutes at 60,000 RPM in a TLA 100.3 rotor (Beckman Coulter) at 4°C. The supernatant containing cytosolic proteins was transferred to a separate tube and TX100 was added for 1% (w/v) total, and the pellet containing the membrane fraction was solubilized in an equivalent volume of 1% (w/v) TX100 containing M/C buffer on ice for 15 minutes. Membrane and cytosol fractions were analyzed by immunoblotting.

Immunoprecipitation

For immunoprecipitation for Fig. S4B, 2µg of Rabbit anti-OCA7 (PA5-61519) or Irrelevant Rabbit IgG was prebound to 40µL Protein A Sepharose beads (GE Healthcare), incubating for 30 minutes at room temperature with 1mL IP buffer containing 50mM Hepes pH 7.4, 100mM KCL, 1mM DTT, 1mM EDTA, 1X protease inhibitor cocktail and 1% (w/v) TX100. After binding, beads were centrifuged at 2000 x g for 10 seconds and the supernatant was aspirated before storing on ice. Wild Type or OCA7-KO cells were grown in 15cm culture dishes with 30mL MNT1 media to 80-90% confluency. Dishes were washed with 10mL ice cold PBS and cells were scraped into suspension in 10mL ice cold PBS using cell lifters, pelleted, resuspended in 1mL IP buffer and lysed on ice for 15 minutes with gentle agitation every 3 minutes. Crude lysates were centrifuged at 16,000 x g at 4°C for 15 minutes. Supernatants were incubated with 100µL Protein A Sepharose for 10 minutes on ice to remove proteins that nonspecifically bind to the beads. Samples were then centrifuged at 2000 x g for 10 seconds to pellet the Sepharose. Next, 100µL of the supernatant was taken as input and the remaining supernatant was incubated with the antibody bound Protein A Sepharose for 1 hour at 4°C, rotating end over end. After binding, samples were centrifuged at 2000 x g for 10 seconds and the supernatant was aspirated. Beads were washed 3 times with 1mL IP buffer containing 0.1% (w/v) TX100 and once with IP buffer lacking TX100, centrifuging at 2000 x g for 10 seconds. After the last wash, 40µL Laemmli sample buffer was added to the beads and samples were stored at -20°C before immunoblotting for OCA7 and Tubulin. For the Co-IP experiment in Fig S6G, a slightly modified protocol was used. 3.0X10^6 MNT1 cells were nucleofected with 4µg TPC2-BioID2-HA plasmid and seeded into a 10cm dish with 10mL MNT1 media. Untransfected MNT1 cells were used as a control. Cells were harvested for Co-IP at 72 hours and lysed in 500µL IP buffer consisting of PBS with 1% (w/v) TX100 and 1X protease inhibitor cocktail for 30 minutes on ice. Insoluble material was pelleted at 16,000 x g for 15 minutes at 4°C and the supernatant was incubated with 2µg of Rabbit anti-OCA7

antibody (PA5-61519) for 30 minutes, then incubated with 40µL Protein A Sepharose bead slurry for 90 minutes. Next, the beads were washed three times with 500µL of PBS with 0.1% TX100. Finally, OCA7 and associated protein was eluted with 60µL 1X Laemmli sample buffer.

Recombinant OCA7 Expression

Recombinant OCA7 protein encoded in pET30(+)-OCA7-6his plasmid was expressed in BL21 codon plus *E. coli* and purified using the TALON cobalt affinity resin (Thermo Scientific 89964) as described previously(67).

Yeast Two Hybrid Assay

Competent AH109 strain of yeast were prepared and frozen as described and Y2H analysis was performed essentially as described(68, 69). To transform the AH109 yeast, cells were resuspended in 375µL 40% (w/v) PEG 3350 with 0.1M Lithium Acetate and mixed with 25µL of carrier DNA (Salmon Sperm DNA previously boiled for 5 minutes, cooled on ice) for 0.125mg/mL final concentration. 500ng of each pGBT9-Bait and pGAD424-Prey plasmid was mixed with the suspension and the suspension was briefly vortexed and incubated at 30°C for 30 minutes. Yeast suspensions were briefly vortexed and incubated for 15 minutes at 42°C. After the incubations, yeast were centrifuged for 2 minutes at 1000 x g at 4°C. Pellets were resuspended in 300µL of water and 100µL was plated on Synthetic Dropout media lacking Leucine and Tryptophan (SD -L-W) media to select for yeast cells containing both plasmids and plates were incubated for 72 hours at 30°C. Colonies were isolated and subcultured on new plates for 24 hours at 30°C. Liquid cultures were prepared by placing colonies into culture tubes containing 2mL SD -L-W and grown overnight. Saturated cultures were diluted 1:10 in water, and 3µL spots were made on SD -L-W, SD -L-W-H, SD -L-W-H + 3-Amino-1,2,4-triazole (3AT) plates. Plates were imaged after 72-hour incubation at 30°C. Growth on plates lacking histidine (H)

indicates a positive interaction between the bait and prey proteins, and growth with 3AT indicates stronger interactions.

Melanin Quantification

For pigment determination, cells were grown in T75 flasks with MNT1 media for 72 hours. Cells were washed and trypsinized with 0.05% Trypsin 0.53mM EDTA, anti-trypsinized with MNT1 media and counted with a Neubauer chamber (Hausser Scientific). 10^6 cells were pelleted in 1.7mL screw cap tubes at 200 x g for 5 minutes at 4°C. Pellets were resuspended in 500µL ice cold PBS with 1X protease inhibitor cocktail and 50µL of 0.5mm glass beads (Biospec) were added to each tube. Cells were homogenized using a Beadbug-6 homogenizer set to 2500 RPM with 3 cycles of 30 seconds on and 30 seconds off. Tubes were then centrifuged at 16,000 x g at 4°C for 15 minutes to pellet melanin. Supernatants containing soluble protein were transferred to separate tubes and used for total protein content determination by BioRad Protein Assay. Melanin Pellets were washed by adding 500µL 100% Ethanol and vortexing for 5 seconds. Melanin was pelleted again by centrifuging at 16,000 x g at 4°C for 5 minutes. The ethanol supernatant was aspirated and residual ethanol was evaporated by incubating open tubes at 37°C for 30 minutes. After drying the pellets, 1000µL freshly diluted 10% (v/v) DMSO, 1N NaOH in PBS was added to each pellet and vortexed to resuspend the melanin and incubated for 1 hour at 80°C to solubilize melanin. Tubes were vortexed again 10 minutes into the incubation and again at 60 minutes to keep melanin suspended. Meanwhile, *Sepia officinalis* melanin was suspended in 10% (v/v) DMSO, 1N NaOH in PBS, diluted in series to generate a standard curve, and incubated at 80°C for 1 hour with other melanin samples. After the incubation, tubes were incubated at room temperature for 20 minutes and centrifuged at 16,000 x g for 10 minutes at room temperature to pellet insoluble material. Supernatants were transferred to 1mL cuvettes with 1cm path length and absorbance was measured at 490nm using a NanoDrop One spectrophotometer (Thermo

Scientific). The linear *Sepia officinalis* standard curve was used to calculate melanin concentration in each melanocyte sample.

Statistical Analysis

Statistical analysis was performed in GraphPad Prism. Sample distributions were tested for normality using the Shapiro-Wilk test. For datasets with 2 populations, a Student's T test (Fig. 8B) or Mann-Whitney test (Fig. 1B, 3B) were performed as parametric or nonparametric tests, respectively. For datasets with 3 or more populations, One Way ANOVA with post hoc Tukey test (Fig. 4C, 6B, 6D, 7B, 7D, 7F, 9B, 9D, 9F and 9H) or Kruskal-Wallis test (Fig. 5D, 6F) were used as parametric or nonparametric tests, respectively. N values and error bars are described in each figure caption. Significance is depicted as $*P \leq 0.05$; $**P \leq 0.01$; $***P \leq 0.001$; $****P \leq 0.0001$.

Table 3.1. Primers for Cloning.

Primer Name	Sequence (5'-3')	Plasmid Made
OCA7 Forward	TCTCGAGCTCAAGCTATGGCCGGGCTCGT	pEGFP-N3-OCA7
OCA7 Reverse	TGGCGATGGATCCCGCGAGCTGGTCATCTCGGATAAACCT	pEGFP-N3-OCA7
OCA7 Forward	AAGGAGATATACATATGATGGCCGGGCTCGTGG	pET30(+)-OCA7-6his
OCA7 Reverse	TGCTCGAGTGCGGCCGCGAGCTGGTCATCTCGGA	pET30(+)-OCA7-6his
OCA7 Forward	AAAAGAGATCGAATTGGCCGGGATGGCCGGGCTCGT	pGAD424-OCA7
OCA7 Reverse	ATCTCTGCAGGTCGATCAGAGCTGGTCATCTCGGATAAAC	pGAD424-OCA7
AP1M1 Forward	TGTATCGCCGGAATTCATGTCCGCCAGCGCCGTCTAC	pGBT9-AP1M1
AP1M1 Reverse	TTGGCTGCAGGTCGACTCACTGGGTCCGGAGCTGGTAATCTC	pGBT9-AP1M1

RabIF Forward	TGTATCGCCGGAATTCATGGAACCAGCGGAGCAG	pGBT9-RabIF
RabIF Reverse	TTGGCTGCAGGTCGACTTACTCATGGGAAACTCGTTCCAAGG	pGBT9-RabIF
EXOSC5 Forward	TGTATCGCCGGAATTCATGGAGGAGGAGACGCATACT	pGBT9-EXOSC5
EXOSC5 Reverse	TTGGCTGCAGGTCGACTCAGCTCTTGGAGTAACGCC	pGBT9-EXOSC5
mBFP2 Forward	CAGACTACGCACCGGTTATGGTGTCTAAGGGCGAAGAGC	AKAP1-FRB-BFP2
mBFP2 Reverse	TCTAGAGTCGCGGCCGCTTAATTAAGCTTGTGCCCCAGTTTG	AKAP1-FRB-BFP2
pmCherry-Rab32 CC/AA Mutagenesis Forward	GTCGACGGTACCGCGGGC	pmCherry-C2-Rab32-CC/AA-FKBP
pmCherry-Rab32 CC/AA Mutagenesis Reverse	GGCAGCCTGGGATTTGTTCTCTGCTCTCAAGG	pmCherry-C2-Rab32-CC/AA-FKBP
FKBP12 Forward	AAATCCCAGGCTGCCGGAGTGCAGGTGGAAACCATCTC	pmCherry-C2-Rab32-CC/AA-FKBP
FKBP12 Reverse	CGCGGTACCGTCGACTCATTCCAGTTTTAGAAGCTCCACATCG	pmCherry-C2-Rab32-CC/AA-FKBP
pmCherry-Rab38 CC/AA Mutagenesis Forward	GTCGACGGTACCGCGGGC	pmCherry-C2-Rab38-CC/AA-FKBP
pmCherry-Rab38 CC/AA Mutagenesis Reverse	GGATTTGGCAGCGCCAGAGGCGCTGGCAACCTTG	pmCherry-C2-Rab38-CC/AA-FKBP
FKBP12 Forward	GGCGCTGCCAAATCCGGAGTGCAGGTGGAAACCATCTC	pmCherry-C2-Rab38-CC/AA-FKBP

FKBP12 Reverse	CGCGGTACCGTCGACTCATTCCAGTTTTAGAAGCTCCACATCG	pmCherry-C2-Rab38-CC/AA-FKBP
GCaMP6 C Terminus Forward For addition of restriction site	CGCCACGTGATGACAAACCTTGG	TPC2-GCaMP6-mCherry
GCaMP6 C Terminus Reverse For addition of restriction site	TTTTGCGGCCGCTTTTTACCGGTGATGGCTGATTATGATCTAGA GTCGTGGCCGCTGACTTCGCTGTCATC	TPC2-GCaMP6-mCherry
TPC2 Forward	GCCTGTTAACCGGTCATGGCGGAACCCCAGGC	TPC2-BioID2-HA
TPC2 Reverse	ACTTCCACCGCCTCCAAGCTTCCTGCACAGCCAC	TPC2-BioID2-HA
MCS-13X Linker-BioID2-HA Linearization Forward	GACCGGTTAACAGGCCTTAAGCG	TPC2-BioID2-HA
MCS-13X Linker-BioID2-HA Linearization Reverse	GGAGGCGGTGGAAGTGGAG	TPC2-BioID2-HA

Table 3.2. OCA7 Knockout Predesigned crRNA.

IDT crRNA	Targeted Sequence in OCA7 Gene (5'-3')
Hs.Cas9.OCA7.1.AC	GGGACGACCTTGTGTTGCCA
Hs.Cas9.OCA7.1.AE	TGTCCAAGATGAGTTCCTCC

Table 3.3. OCA7 Knockout Genotyping Primers.

Primer Name	Sequence (5'-3')
Forward	CAATGCGTGAAGGATGCGGT
Reverse	TCTGAAGTGTCCCGAGTGCC

REFERENCES

1. Federico, J. R., and Krishnamurthy, K. (2022) Albinism In StatPearls, StatPearls Publishing. StatPearls Publishing LLC., Treasure Island (FL)

2. Grønskov, K., Ek, J., and Brondum-Nielsen, K. (2007) Oculocutaneous albinism In Orphanet Journal of Rare Diseases, BioMed Central, 43

3. Marti, A., Lasseaux, E., Ezzedine, K., Léauté-Labrèze, C., Boralevi, F., Paya, C. *et al.* (2018) Lessons of a day hospital: Comprehensive assessment of patients with albinism in a European setting In Pigment Cell and Melanoma Research, 318-329

4. Pavan, W. J., and Sturm, R. A. (2019) The Genetics of Human Skin and Hair Pigmentation Annu Rev Genomics Hum Genet **20**, 41-72 10.1146/annurev-genom-083118-015230

5. Montoliu, L., Grønskov, K., Wei, A.-H., Martínez-García, M., Fernández, A., Arveiler, B. *et al.* (2014) Increasing the complexity: new genes and new types of albinism In Pigment Cell & Melanoma Research, John Wiley & Sons, Ltd (10.1111), 11-18

6. Bellono, N. W., Escobar, I. E., Lefkovith, A. J., Marks, M. S., and Oancea, E. (2014) An intracellular anion channel critical for pigmentation In eLife, e04543

7. Garrido, G., Fernández, A., and Montoliu, L. (2021) HPS11 and OCA8: Two new types of albinism associated with mutations in BLOC1S5 and DCT genes In Pigment cell & melanoma research, NLM (Medline), 10-12

8. K, B., and Purohit, R. (2013) Mutational analysis of TYR gene and its structural consequences in OCA1A In Gene, Elsevier, 184-195

9. Kausar, T., Bhatti, M., Ali, M., Shaikh, R., and Ahmed, Z. (2013) OCA5, a novel locus for non-syndromic oculocutaneous albinism, maps to chromosome 4q24 In Clinical Genetics, John Wiley & Sons, Ltd, 91-93

10. Le, L., Escobar, I. E., Ho, T., Lefkovith, A. J., Latteri, E., Haltaufderhyde, K. D. *et al.* (2020) SLC45A2 protein stability and regulation of melanosome pH determine melanocyte pigmentation In Molecular Biology of the Cell, American Society for Cell Biology, 2687-2702

11. Pennamen, P., Tingaud-Sequeira, A., Gazova, I., Keighren, M., McKie, L., Marlin, S. *et al.* (2020) Dopachrome tautomerase variants in patients with oculocutaneous albinism In bioRxiv, Cold Spring Harbor Laboratory, 2020.2006.2026.171223

12. Suzuki, T., and Tomita, Y. (2008) Recent advances in genetic analyses of oculocutaneous albinism types 2 and 4 In Journal of Dermatological Science, Elsevier, 1-9

13. Wei, A. H., Zang, D. J., Zhang, Z., Liu, X. Z., He, X., Yang, L. *et al.* (2013) Exome sequencing identifies SLC24A5 as a candidate gene for nonsyndromic oculocutaneous albinism In Journal of Investigative Dermatology, Nature Publishing Group, 1834-1840

14. Zhang, Z., Gong, J., Sviderskaya, E. V., Wei, A., and Li, W. (2019) Mitochondrial NCKX5 regulates melanosomal biogenesis and pigment production In Journal of Cell Science, Company of Biologists Ltd,

15. Grønskov, K., Dooley, C. M., Østergaard, E., Kelsh, R. N., Hansen, L., Levesque, M. P. *et al.* (2013) Mutations in c10orf11, a melanocyte-differentiation gene, cause autosomal-recessive albinism. In American journal of human genetics, Elsevier, 415-421

16. Kamaraj, B., and Purohit, R. (2014) Mutational analysis of oculocutaneous albinism: a compact review. In BioMed research international, Hindawi Limited, 905472

17. Peng, F., Zhu, G., Hysi, P. G., Eller, R. J., Chen, Y., Li, Y. *et al.* (2019) Genome-Wide Association Studies Identify Multiple Genetic Loci Influencing Eyebrow Color Variation in Europeans J Invest Dermatol **139**, 1601-1605 10.1016/j.jid.2018.12.029

18. Raposo, G., and Marks, M. S. (2007) Melanosomes--dark organelles enlighten endosomal membrane transport. In Nature reviews. Molecular cell biology, NIH Public Access, 786-797

19. van Niel, G., Charrin, S., Simoes, S., Romao, M., Rochin, L., Saftig, P. *et al.* (2011) The Tetraspanin CD63 Regulates ESCRT-Independent and -Dependent Endosomal Sorting during Melanogenesis In Developmental Cell, Cell Press, 708-721

20. Bissig, C., Croisé, P., Heiligenstein, X., Hurbain, I., Lenk, G. M., Kaufman, E. *et al.* (2019) The PIKfyve complex regulates the early melanosome homeostasis required for physiological amyloid formation. In Journal of cell science, The Company of Biologists Ltd, jcs229500

21. van Niel, G., Bergam, P., Di Cicco, A., Hurbain, I., Lo Cicero, A., Dingli, F. *et al.* (2015) Apolipoprotein E Regulates Amyloid Formation within Endosomes of Pigment Cells In Cell Reports, Elsevier, 43-51

22. Berson, J. F., Harper, D. C., Tenza, D., Raposo, G., and Marks, M. S. (2001) Pmel17 initiates premelanosome morphogenesis within multivesicular bodies In Molecular Biology of the Cell, 3451-3464

23. Ambrosio, A. L., Boyle, J. A., Aradi, A. E., Christian, K. A., and Di Pietro, S. M. (2016) TPC2 controls pigmentation by regulating melanosome pH and size In Proceedings of the National Academy of Sciences, 5622-5627

24. Bellono, N. W., Escobar, I. E., and Oancea, E. (2016) A melanosomal two-pore sodium channel regulates pigmentation In Scientific Reports, Nature Publishing Group, 1-11

25. Luck, K., Kim, D. K., Lambourne, L., Spirohn, K., Begg, B. E., Bian, W. *et al.* (2020) A reference map of the human binary protein interactome Nature **580**, 402-408 10.1038/s41586-020-2188-x

26. Bultema, J. J., Ambrosio, A. L., Burek, C. L., and Di Pietro, S. M. (2012) BLOC-2, AP-3, and AP-1 proteins function in concert with Rab38 and Rab32 proteins to mediate protein trafficking to lysosome-related organelles In Journal of Biological Chemistry, 19550-19563

27. Bultema, J. J., Boyle, J. A., Malenke, P. B., Martin, F. E., Dell'Angelica, E. C., Cheney, R. E. *et al.* (2014) Myosin vc interacts with Rab32 and Rab38 proteins and works in the biogenesis and secretion of melanosomes. In The Journal of biological chemistry, American Society for Biochemistry and Molecular Biology, 33513-33528

28. Tamura, K., Ohbayashi, N., Maruta, Y., Kanno, E., Itoh, T., and Fukuda, M. (2009) Varp is a novel Rab32/38-binding protein that regulates Tyrp1 trafficking in melanocytes Mol Biol Cell **20**, 2900-2908 10.1091/mbc.E08-12-1161

29. Mukherjee, D., Gao, M., O'Connor, J. P., Raijmakers, R., Pruijn, G., Lutz, C. S. *et al.* (2002) The mammalian exosome mediates the efficient degradation of mRNAs that contain AU-rich elements In The EMBO Journal, John Wiley & Sons, Ltd, 165-174

30. Okuda, E. K., Gonzales-Zubiate, F. A., Gadal, O., and Oliveira, C. C. (2020) Nucleolar localization of the yeast RNA exosome subunit Rrp44 hints at early pre-rRNA processing as its main function In Journal of Biological Chemistry, American Society for Biochemistry and Molecular Biology Inc., 11195-11213

31. McGrath, E., Waschbüsch, D., Baker, B. M., and Khan, A. R. (2019) LRRK2 binds to the Rab32 subfamily in a GTP-dependent manner via its armadillo domain In Small GTPases, 1-14

32. Pylypenko, O., Hammich, H., Yu, I. M., and Houdusse, A. (2018) Rab GTPases and their interacting protein partners: Structural insights into Rab functional diversity In Small GTPases, Taylor and Francis Inc., 22-48

33. Tamura, K., Ohbayashi, N., Ishibashi, K., and Fukuda, M. (2011) Structure-function analysis of VPS9-ankyrin-repeat protein (Varp) in the trafficking of tyrosinase-related protein 1 in melanocytes J Biol Chem **286**, 7507-7521 10.1074/jbc.M110.191205

34. Kelley, L. A., Mezulis, S., Yates, C. M., Wass, M. N., and Sternberg, M. J. (2015) The Phyre2 web portal for protein modeling, prediction and analysis Nat Protoc **10**, 845-858 10.1038/nprot.2015.053

35. Kiliç, M., Hazar Özcan, M., Taskin, E., Yildirim, H., and Şen, A. (2021) Oculocutaneous Albinism Type 7 with Recurrent Infections: A Case Report In Asthma Allergy Immunol, 50-55

36. Harper, D. C., Theos, A. C., Herman, K. E., Tenza, D., Raposo, G., and Marks, M. S. (2008) Premelanosome amyloid-like fibrils are composed of only Golgi-processed forms of Pmel17 that have been proteolytically processed in endosomes In Journal of Biological Chemistry, 2307-2322

37. Watt, B., van Niel, G., Fowler, D. M., Hurbain, I., Luk, K. C., Stayrook, S. E. *et al.* (2009) N-terminal domains elicit formation of functional Pmel17 amyloid fibrils In Journal of Biological Chemistry, 35543-35555

38. Mitchell, S. M., Graham, M., Liu, X., and Leonhardt, R. M. (2021) Identification of critical amino acid residues in the regulatory N-terminal domain of PMEL In Scientific Reports, Springer Science and Business Media LLC, 7730

39. Hee, J. S., Mitchell, S. M., Liu, X., and Leonhardt, R. M. (2017) Melanosomal formation of PMEL core amyloid is driven by aromatic residues Sci Rep **7**, 44064 10.1038/srep44064

40. Graham, M., Tzika, A. C., Mitchell, S. M., Liu, X., and Leonhardt, R. M. (2019) Repeat domain-associated O-glycans govern PMEL fibrillar sheet architecture Sci Rep **9**, 6101 10.1038/s41598-019-42571-6

41. Sires-Campos, J., Lambertos, A., Delevoye, C., Raposo, G., Bennett, D. C., Sviderskaya, E. *et al.* (2021) Mahogunin Ring Finger 1 regulates pigmentation by controlling the pH of melanosomes in melanocytes and melanoma cells Cell Mol Life Sci **79**, 47 10.1007/s00018-021-04053-9

42. Ancans, J., Tobin, D. J., Hoogduijn, M. J., Smit, N. P., Wakamatsu, K., and Thody, A. J. (2001) Melanosomal pH controls rate of melanogenesis, eumelanin/phaeomelanin ratio and melanosome maturation in melanocytes and melanoma cells Exp Cell Res **268**, 26-35 10.1006/excr.2001.5251

43. Wada, S., Hamada, M., Kobayashi, K., and Satoh, N. (2008) Novel genes involved in canonical Wnt/β-catenin signaling pathway in early Ciona intestinalis embryos In Development, Growth & Differentiation, John Wiley & Sons, Ltd, 215-227

44. Berson, J. F., Theos, A. C., Harper, D. C., Tenza, D., Raposo, G., and Marks, M. S. (2003) Proprotein convertase cleavage liberates a fibrillogenic fragment of a resident glycoprotein to initiate melanosome biogenesis In Journal of Cell Biology, The Rockefeller University Press, 521-533

45. Rochin, L., Hurbain, I., Serneels, L., Fort, C., Watt, B., Leblanc, P. *et al.* (2013) BACE2 processes PMEL to form the melanosome amyloid matrix in pigment cells Proc Natl Acad Sci U S A **110**, 10658-10663 10.1073/pnas.1220748110

46. Hellström, A. R., Watt, B., Fard, S. S., Tenza, D., Mannström, P., Narfström, K. *et al.* (2011) Inactivation of Pmel Alters Melanosome Shape But Has Only a Subtle Effect on Visible Pigmentation In PLOS Genetics, Public Library of Science, e1002285

47. Lahola-Chomiak, A. A., Footz, T., Nguyen-Phuoc, K., Neil, G. J., Fan, B., Allen, K. F. *et al.* (2019) Non-Synonymous variants in premelanosome protein (PMEL) cause ocular pigment dispersion and pigmentary glaucoma Hum Mol Genet **28**, 1298-1311 10.1093/hmg/ddy429

48. Gerondopoulos, A., Langemeyer, L., Liang, J.-R., Linford, A., and Barr, F. A. (2012) BLOC-3 mutated in Hermansky-Pudlak syndrome is a Rab32/38 guanine nucleotide exchange factor. In Current biology : CB, Elsevier, 2135-2139

49. Uhlen, M., Fagerberg, L., Hallstrom, B. M., Lindskog, C., Oksvold, P., Mardinoglu, A. *et al.* (2015) Proteomics. Tissue-based map of the human proteome Science **347**, 1260419 10.1126/science.1260419

50. Hu, Z.-q., Rao, C.-l., Tang, M.-l., zhang, Y., Lu, X.-x., Chen, J.-g. *et al.* (2019) Rab32 GTPase, as a direct target of miR-30b/c, controls the intracellular survival of Burkholderia pseudomallei by regulating phagosome maturation In PLOS Pathogens, Oswald E, ed. Public Library of Science, e1007879

51. Baldassarre, M., Solano-Collado, V., Balci, A., Colamarino, R. A., Dambuza, I. M., Reid, D. M. *et al.* (2021) The Rab32/BLOC-3-dependent pathway mediates host defense against different pathogens in human macrophages In Science Advances, American Association for the Advancement of Science, eabb1795

52. Drizyte-Miller, K., Chen, J., Cao, H., Schott, M. B., and McNiven, M. A. (2020) The small GTPase Rab32 resides on lysosomes to regulate mTORC1 signaling In Journal of Cell Science, Company of Biologists Ltd,

53. Ambrosio, A. L., Boyle, J. A., and Di Pietro, S. M. (2012) Mechanism of platelet dense granule biogenesis: study of cargo transport and function of Rab32 and Rab38 in a model system Blood **120**, 4072-4081 10.1182/blood-2012-04-420745

54. Aguilar, A., Weber, J., Boscher, J., Freund, M., Ziessel, C., Eckly, A. *et al.* (2019) Combined deficiency of RAB32 and RAB38 in the mouse mimics Hermansky-Pudlak syndrome and critically impairs thrombosis In Blood Advances, American Society of Hematology, 2368-2380

55. Thibord, F., Chan, M. V., Chen, M. H., and Johnson, A. D. (2022) A year of Covid-19 GWAS results from the GRASP portal reveals potential genetic risk factors HGG Adv 100095 10.1016/j.xhgg.2022.100095

56. Keramati, A. R., Chen, M. H., Rodriguez, B. A. T., Yanek, L. R., Bhan, A., Gaynor, B. J. *et al.* (2021) Genome sequencing unveils a regulatory landscape of platelet reactivity Nat Commun **12**, 3626 10.1038/s41467-021-23470-9

57. Nakamura, S., Takayama, N., Hirata, S., Seo, H., Endo, H., Ochi, K. *et al.* (2014) Expandable megakaryocyte cell lines enable clinically applicable generation of platelets from human induced pluripotent stem cells Cell Stem Cell **14**, 535-548 10.1016/j.stem.2014.01.011

58. Ito, Y., Nakamura, S., Sugimoto, N., Shigemori, T., Kato, Y., Ohno, M. *et al.* (2018) Turbulence Activates Platelet Biogenesis to Enable Clinical Scale Ex Vivo Production Cell **174**, 636-648 e618 10.1016/j.cell.2018.06.011

59. Ambrosio, A. L., Febvre, H. P., and Di Pietro, S. M. (2022) Syntaxin 12 and COMMD3 are new factors that function with VPS33B in the biogenesis of platelet alpha-granules Blood **139**, 922-935 10.1182/blood.2021012056

60. Huizing, M., Helip-Wooley, A., Westbroek, W., Gunay-Aygun, M., and Gahl, W. A. (2008) Disorders of lysosome-related organelle biogenesis: clinical and molecular genetics. In Annual review of genomics and human genetics, NIH Public Access, 359-386

61. Dennis, M. K., Delevoye, C., Acosta-Ruiz, A., Hurbain, I., Romao, M., Hesketh, G. G. *et al.* (2016) BLOC-1 and BLOC-3 regulate VAMP7 cycling to and from melanosomes via distinct tubular transport carriers In Journal of Cell Biology, Rockefeller University Press, 293-308

62. Marubashi, S., Shimada, H., Fukuda, M., and Ohbayashi, N. (2016) RUTBC1 functions as a GTPase-activating protein for Rab32/38 and regulates melanogenic enzyme trafficking

in melanocytes In Journal of Biological Chemistry, American Society for Biochemistry and Molecular Biology Inc., 1427-1440

63. Ambrosio, A. L., and Di Pietro, S. M. (2019) Mechanism of platelet α-granule biogenesis: study of cargo transport and the VPS33B-VPS16B complex in a model system In Blood Advances, American Society of Hematology, 2617-2626

64. Zewe, J. P., Miller, A. M., Sangappa, S., Wills, R. C., Goulden, B. D., and Hammond, G. R. V. (2020) Probing the subcellular distribution of phosphatidylinositol reveals a surprising lack at the plasma membrane J Cell Biol **219**, 10.1083/jcb.201906127

65. Ambrosio, A. L., Boyle, J. A., and Di Pietro, S. M. (2015) TPC2 mediates new mechanisms of platelet dense granule membrane dynamics through regulation of Ca2+ release In Molecular Biology of the Cell, American Society for Cell Biology, 3263-3274

66. Giddings, T. H., Jr., Morphew, M. K., and McIntosh, J. R. (2017) Preparing Fission Yeast for Electron Microscopy Cold Spring Harb Protoc **2017**, 10.1101/pdb.prot091314

67. Di Pietro, S. M., Cascio, D., Feliciano, D., Bowie, J. U., and Payne, G. S. (2010) Regulation of clathrin adaptor function in endocytosis: novel role for the SAM domain EMBO J **29**, 1033-1044 10.1038/emboj.2010.5

68. Gietz, R. D., and Schiestl, R. H. (2007) Frozen competent yeast cells that can be transformed with high efficiency using the LiAc/SS carrier DNA/PEG method In Nature Protocols 2007 2:1, Nature Publishing Group, 1-4

69. Starcevic, M., and Dell'Angelica, E. C. (2004) Identification of Snapin and Three Novel Proteins (BLOS1, BLOS2, and BLOS3/Reduced Pigmentation) as Subunits of Biogenesis of Lysosome-related Organelles Complex-1 (BLOC-1) * In Journal of Biological Chemistry, Elsevier, 28393-28401

OVERALL SUMMARY AND FUTURE DIRECTIONS

Classical genetics and Genome Wide Association Studies have been instrumental in identifying over 100 genes associated with pigmentation, and follow-up *in vitro* and *in vivo* studies determined functional roles for many of the pigmentation associated proteins in regulating the biogenesis of melanosomes. While these findings have led to a significant understanding of how melanosomes and other Lysosome Related Organelles (LROs) are formed, there is still an incomplete picture and many of the players in LRO biogenesis are still missing. Several key questions remain. What proteins regulate melanosome pH and how do melanocytes coordinate the trafficking and function of solute transporters and ion channels, such as TPC2? How are cargoes specifically directed to melanosomes rather than other endosomal compartments? How are membrane proteins recycled from melanosomes? What enzymes are required to process the PMEL protein into fibrillogenic fragments?

In Chapter 2 of this dissertation, we utilized MNT1 cells expressing TPC2-BioID2-HA to biotinylate, pulldown and identify proteins in the proximity to TPC2 at melanosome membranes, effectively generating a list of the melanosome membrane surface proteome, a powerful new resource to start addressing some of the questions above, identifying hundreds of proteins functioning close to TPC2, many of which have not been identified in melanocytes before. Using super resolution Airyscan confocal fluorescence microscopy, we demonstrated the utility of this newly determined TPC2 melanosome membrane proteome by confirming that several hits including TSPAN10, PLD1, SV2A (Chapter 2), and OCA7 (aka LRMDA and C10orf11) (Chapter 3) are all novel melanosome localized proteins. CRISPR mediated knockout of each gene listed above in MNT1 melanocytes led to the discovery that TSPAN10 and OCA7 are positive regulators of pigmentation.

Following up on TSPAN10 function at melanosomes, we discovered it regulates the processing of PMEL, leading to dense melanin aggregates in melanosomes of TSPAN10 knockout cells. PMEL processing is controlled by sequential proteolytic steps catalyzed by pro protein convertase, BACE2, possibly ADAM10, and additional unknown lysosomal hydrolases (1-4). Excitingly, we discovered TSPAN10 Is required for ADAM10 maturation and trafficking to endosomal compartments such as lysosomes and melanosomes, where it possibly works to process PMEL fibrillogenic fragments that give rise to ordered, melanin packed fibrils. Of note, in most cell types ADAM10 localizes primarily to the cell surface where it works to shed dozens of substrates from the plasma membrane (5-9). This dissertation provides a rare example of a cell type in which ADAM10 primarily localizes to intracellular compartments, and it identified TSPAN10 as new cell type specific machinery working to reroute cargo that is normally targeted to the plasma membrane.

Although PMEL N terminal fragments are putative ADAM10 substrates, we suspect ADAM10 may act on several melanosomal proteins, especially because hypopigmentation in TSPAN10 KO cells cannot be attributed to a defect in PMEL alone, as PMEL deficiency only causes mild hypopigmentation *in vivo* (10). One important future direction will be to identify the ADAM10 substrates in melanocytes. Multiple strategies should be considered. First, known ADAM10 substrates should be carefully surveyed to find proteins with known regulatory roles in melanogenesis. Next, the expression and localization of key melanogenic enzymes should be tested in TSPAN10 KO cells. Total Tyrosinase protein expression was not significantly altered in TSPAN10 KO MNT1 cells, but Tyrosinase related proteins TYRP1 and TYRP2 were not examined. Third, an unbiased quantitative proteomics approach could be used to determine ADAM10 substrates. Wild Type cells with ADAM10 activity should cleave substrates, leading to their eventual degradation in lysosomes or secretion into the extracellular media. Whereas

TSPAN10 KO or ADAM10 inhibited cells would be expected to accumulate integral membrane substrates at melanosomes or other endosomal compartments, and therefore they will not be shed into the media and should not be degraded as rapidly at lysosomes. Thus, proteomics of the secreted proteins in the extracellular media or of whole cell lysates should determine ADAM10 substrates when comparing Wild Type and TSPAN10 KO or ADAM10 inhibited melanocytes. Together, these follow up studies will shed light on melanosome biogenesis as well as melanoma metastasis, as ADAM10 upregulation is correlated to melanoma metastasis, but the mechanisms are not entirely defined (11, 12).

Chapter 3 of this dissertation focused on the first characterization of OCA7 in a pigment cell model, discovering that OCA7 association with albinism is likely melanocyte intrinsic, as its knockout in MNT1 melanoma cells resulted in hypopigmentation. We discovered OCA7 peripherally associates with melanosome membranes through protein/protein interactions with Rab32 and Rab38. Interestingly, OCA7 KO MNT1 cells have multiple defects in melanosome biogenesis and function, with aberrant PMEL fibril maturation affecting melanin organization, and low melanosome pH, impacting the activity of melanogenic enzymes. Although OCA7 was originally discovered through its proximity to TPC2 (Chapter 2) we were unable to detect a physical or functional connection between the two proteins. Thus, the mechanism of OCA7 function at melanosomes is a matter of ongoing investigation.

As discussed in Chapter 1, a recent unpublished observation by collaborators found that the OCA7 C terminus (IRDDQL) resembles the SNX17 C terminus (IGDEDL), which interacts directly with the Retriever complex required for endosomal recycling of many cargoes including Integrin proteins(13). Therefore, we hypothesize OCA7 may also function physically and functionally with Retriever. If this is the case, then OCA7 could be regulating melanosomal pH by controlling the recycling of multiple melanosome localized ion channels and solute transporters, such as the chloride channel OCA2 or the proton transporter SLC45A2, each of which are

associated with oculocutaneous albinism. Therefore, follow up studies should investigate a physical and functional link between OCA7 and Retriever. Do they physically interact directly as predicted? Does OCA7 knockout phenocopy defects observed when Retriever is disrupted, such as mistrafficking of Integrin proteins to lysosomes? Conversely, does disruption of the Retriever complex phenocopy OCA7 albinism phenotypes in MNT1 cells, such as low melanosomal pH? Does OCA7 work with Retriever in all cell types or is OCA7 function restricted to pigment cells? Answering these questions will be key to determining the molecular function of OCA7 and will enlighten how the Retriever complex coordinates recycling of cargo.

Another important future direction for both TSPAN10 and OCA7 is the development and study of animal models to test the extent of their functions. We discovered TSPAN10 and OCA7 regulate pigmentation in melanocytes. Therefore, I expect mutant animals to be hypopigmented. However, according to the human protein atlas, TSPAN10 and OCA7 are expressed in multiple cell types, and in Chapter 3, we provide evidence that OCA7 protein is expressed in a megakaryocyte cell line (14, 15). Therefore, I hypothesize TSPAN10 and OCA7 may influence LRO function in multiple cell types, and their depletion in animals may lead to multisystem syndromes such as Hermansky Pudlak Syndrome, which could manifest with bleeding disorder, immunodeficiency, and/or neurological deficits. One study utilizing morpholinos to deplete OCA7 expression in zebrafish embryos found OCA7 regulates epidermal pigmentation *in vivo*(16). Interestingly, it was noted that many OCA7 depleted embryos exhibited epidermal blistering and folding of the fins in addition to hypopigmentation, thus OCA7 likely has non-melanocyte functions. Furthermore, morphant embryos exhibited developmental arrest at 48-72 hours post fertilization; although it is unclear if developmental arrest was due to OCA7 depletion or nonspecific morpholino induced p53 activation of apoptotic cell death. Therefore, utilization of updated technologies such as CRISPR-Cas9 mediated knockout to abrogate OCA7 expression in mice or zebrafish will be instrumental in fully understanding OCA7 pathophysiology *in vivo.*

In conclusion, this dissertation contributes a substantial advancement to the fields of membrane trafficking and specifically melanosome biogenesis. My findings provide a new melanosome membrane proteome that was successful in identifying several new melanosome proteins, some of which were confirmed to regulate steps of melanosome biogenesis. This work provides the first functional understanding of TSPAN10 and OCA7 in melanocytes and lays the groundwork for future studies that will investigate their mechanistic roles, such as regulation of ADAM10 and the Retriever Complex, respectively.

REFERENCES

1. Kawaguchi, M., Hozumi, Y., and Suzuki, T. (2015) ADAM protease inhibitors reduce melanogenesis by regulating PMEL17 processing in human melanocytes In Journal of Dermatological Science, Elsevier Ireland Ltd, 133-142

2. Rochin, L., Hurbain, I., Serneels, L., Fort, C., Watt, B., Leblanc, P. *et al.* (2013) BACE2 processes PMEL to form the melanosome amyloid matrix in pigment cells Proc Natl Acad Sci U S A **110**, 10658-10663 10.1073/pnas.1220748110

3. Berson, J. F., Theos, A. C., Harper, D. C., Tenza, D., Raposo, G., and Marks, M. S. (2003) Proprotein convertase cleavage liberates a fibrillogenic fragment of a resident glycoprotein to initiate melanosome biogenesis In Journal of Cell Biology, The Rockefeller University Press, 521-533

4. Bissig, C., Rochin, L., and van Niel, G. (2016) PMEL Amyloid Fibril Formation: The Bright Steps of Pigmentation. In International journal of molecular sciences, Multidisciplinary Digital Publishing Institute (MDPI),

5. Kuhn, P.-H., Colombo, A. V., Schusser, B., Dreymueller, D., Wetzel, S., Schepers, U. *et al.* (2016) Systematic substrate identification indicates a central role for the metalloprotease ADAM10 in axon targeting and synapse function eLife **5**, 10.7554/elife.12748

6. Haining, E. J., Yang, J., Bailey, R. L., Khan, K., Collier, R., Tsai, S. *et al.* (2012) The TspanC8 subgroup of tetraspanins interacts with A disintegrin and metalloprotease 10 (ADAM10) and regulates its maturation and cell surface expression In The Journal of biological chemistry, J Biol Chem, 39753-39765

7. Dornier, E., Coumailleau, F., Ottavi, J. F., Moretti, J., Boucheix, C., Mauduit, P. *et al.* (2012) Tspanc8 tetraspanins regulate ADAM10/Kuzbanian trafficking and promote Notch activation in flies and mammals In Journal of Cell Biology, The Rockefeller University Press, 481-496

8. Arduise, C., Abache, T., Li, L., Billard, M., Chabanon, A., Ludwig, A. *et al.* (2008) Tetraspanins regulate ADAM10-mediated cleavage of TNF-alpha and epidermal growth factor J Immunol **181**, 7002-7013 10.4049/jimmunol.181.10.7002

9. Harrison, N., Koo, C. Z., and Tomlinson, M. G. (2021) Regulation of ADAM10 by the TspanC8 Family of Tetraspanins and Their Therapeutic Potential International Journal of Molecular Sciences **22**, 6707 10.3390/ijms22136707

10. Hellström, A. R., Watt, B., Fard, S. S., Tenza, D., Mannström, P., Narfström, K. *et al.* (2011) Inactivation of Pmel Alters Melanosome Shape But Has Only a Subtle Effect on Visible Pigmentation In PLOS Genetics, Public Library of Science, e1002285

11. Gangemi, R., Amaro, A., Gino, A., Barisione, G., Fabbi, M., Pfeffer, U. *et al.* (2014) ADAM10 correlates with uveal melanoma metastasis and promotes in vitro invasion In Pigment Cell & Melanoma Research, John Wiley & Sons, Ltd, 1138-1148

12. Lee, S. B., Schramme, A., Doberstein, K., Dummer, R., Abdel-Bakky, M. S., Keller, S. *et al.* (2010) ADAM10 is upregulated in melanoma metastasis compared with primary melanoma In The Journal of investigative dermatology, J Invest Dermatol, 763-773

13. McNally, K. E., Faulkner, R., Steinberg, F., Gallon, M., Ghai, R., Pim, D. *et al.* (2017) Retriever is a multiprotein complex for retromer-independent endosomal cargo recycling Nature Cell Biology **19**, 1214-1225 10.1038/ncb3610

14. Uhlen, M., Fagerberg, L., Hallstrom, B. M., Lindskog, C., Oksvold, P., Mardinoglu, A. *et al.* (2015) Proteomics. Tissue-based map of the human proteome Science **347**, 1260419 10.1126/science.1260419

15. Thul, P. J., Akesson, L., Wiking, M., Mahdessian, D., Geladaki, A., Ait Blal, H. *et al.* (2017) A subcellular map of the human proteome Science **356**, 10.1126/science.aal3321

16. Grønskov, K., Dooley, C. M., Østergaard, E., Kelsh, R. N., Hansen, L., Levesque, M. P. *et al.* (2013) Mutations in c10orf11, a melanocyte-differentiation gene, cause autosomal-recessive albinism. In American journal of human genetics, Elsevier, 415-421

APPENDIX 1

FILTERING OF TPC2-BIOID2-HA DATA CORRESPONDING TO FIGURE 2.1C

This table depicts the filtering of TPC2-BioID2-HA interacting proteins to remove nonspecific false positives. In total 836 unique proteins were identified in Streptactin pulldown mass spectrometry datasets compiled from TPC2-734E-BioID2-HA, TPC2-734G-BioID2-HA and TPC2- ΔCT -BioID2-HA (first column). Of those, 651 were enriched for TPC2-BioID2-HA streptactin pulldowns relative to 5 experimental negative controls (second column). Of 651 enriched proteins, 326 hits had less than 1 mean spectral count in 30 CRAPome controls, indicating high specificity (third column).

All Identified Proteins (836)	Enriched Proteins (651)	Enriched Proteins Absent in CRAPome Controls (326)
TPCN2	SPTBN1	TPCN2
MYO5A	TPCN2	MYO5A
PLD1	TUBB3	PLD1
SV2A	SPTAN1	SV2A
FMNL2	ACTC1	FMNL2
LRMDA	MYO5A	LRMDA
SLC25A12	SNRNP200	SLC25A12
TSPAN10	PLD1	TSPAN10
PELP1	KRT76	PELP1
MOGS	THRAP3	MOGS
GPR143	SV2A	GPR143
MANF	HIST1H2BJ	MANF
ARFGEF2	MAP4	ARFGEF2
ITGA9	AP1B1	ITGA9
HCN3	NUP205	HCN3
TMEM2	ACTN1	TMEM2
GBA	EIF4G1	GBA
MFN2	TOP2A	MFN2
LNPEP	FMNL2	LNPEP
TWISTNB	PRPF40A	TWISTNB
ZKSCAN7	SMARCA1	ZKSCAN7
SPRR1B	HDLBP	SPRR1B
MRPL43	BAZ1B	MRPL43
DDX11L8	LRMDA	DDX11L8
SEMA4C	NUP155	SEMA4C
MYO18A	TOP2B	MYO18A
TGOLN2	GLG1	TGOLN2
NPC1	PITRM1	NPC1
AGAP2	GCN1	AGAP2
PCDHA6	SLC25A12	PCDHA6
CD276	PLEKHA5	CD276
ZNF800	SYMPK	ZNF800
CALML5	RPL23A	CALML5
SLC4A2	EPS15	SLC4A2
POLR1A	ZFR	POLR1A
SLC7A2	ZC3HAV1	SLC7A2
OSBP	SKIV2L2	OSBP
PRKCI	DDX46	PRKCI
PAFAH1B1	TSPAN10	PAFAH1B1
DENND1A	PELP1	DENND1A

PI4K2A	APEX1	PI4K2A
CYB5R3	ATP2B4	CYB5R3
CELSR2	PHF6	CELSR2
SARS	AP2A1	SARS
TTYH3	HMGN2	TTYH3
TROVE2	FAM120A	TROVE2
MRPL47	FUS	MRPL47
MRPL38	SPAG9	MRPL38
FDPS	U2SURP	FDPS
PRB1	EPB41L2	PRB1
PSAT1	BCLAF1	PSAT1
SPRR2E	MOGS	SPRR2E
TF	GPR143	TF
ANP32B	MANF	ANP32B
FKBP10	ACTR2	FKBP10
BRIP1	LAP3	BRIP1
HARS	MRPL24	HARS
NSUN5	IGF2R	NSUN5
ZFP62	SUPT5H	ZFP62
NAA25	HMGB1	NAA25
GLG1	OSBPL8	UGGT1
APEX1	CNOT1	CLUH
UGGT1	PPP1R12A	NOMO1
CLUH	CYFIP1	EEA1
NOMO1	DDX42	TRPV2
EEA1	EPB41L3	LAMP2
TRPV2	CKAP5	PYGB
KRR1	ADNP	DNAJC9
LAMP2	LIMA1	STXBP1
PYGB	CHD4	DPP4
DNAJC9	ARFGEF2	ATP6V0A1
STXBP1	ITGA9	RCN2
DPP4	HCN3	ATIC
ATP6V0A1	TMEM2	TGM3
ACTR2	GBA	PLCD3
RCN2	MFN2	MYO1D
ATIC	LNPEP	ECM1
RBM12B	TWISTNB	P3H1
FOXK1	ZKSCAN7	GSR
MYO1D	SPRR1B	PRKCE
TGM3	MRPL43	AKR1B1
PLCD3	KRR1	LTA4H
UPF1	UTP20	SOD2
ACTR3	PML	CAPN5

PSMA4	ASAH1	RAB27A
PABPN1	PDCD11	SCARB1
MRPL21	PTCD3	PCYOX1
RFTN1	G6PD	RAD23B
ECM1	FKBP15	PHKA2
P3H1	ILVBL	GPRIN3
HYOU1	PCMT1	ACR
GSR	UBA2	CNDP2
PRKCE	SUPT6H	GOT1
AKR1B1	NKRF	PIP
LAP3	TRIM25	CUL1
AP1B1	H1FX	PGM1
PAK1IP1	HLA-A	APEH
SOD2	CACYBP	SORD
LTA4H	WDR11	CTNNBL1
CAPN5	CHD1	PEBP1
RAB27A	SRSF4	VPS35
ATP2B4	TRIP12	ANXA11
SCARB1	SETSIP	SACM1L
PCYOX1	SMC4	LAMP1
MYH10	MSH6	PSAP
PHF6	RBM14	ABCB6
FKBP3	PCBP3	GNS
ZNF660	COPG1	HSDL1
VPS35	TCERG1	OPA1
CD44	RPL24	PMEL
ATP13A1	SMARCA4	NOM1
DHX57	LARP1	LGALS3
PHKA2	PCCA	NR4A3
GPRIN3	DDX11L8	AHSG
RAD23B	SEMA4C	NANS
UTP20	MYO18A	MDH1
ANXA11	TGOLN2	M6PR
TTN	NPC1	VPS13C
HK2	AGAP2	TYRP1
LAMP1	PCDHA6	CALU
PSAP	CD276	WDR1
SACM1L	ZNF800	S100A9
ACR	CALML5	NELFB
CNDP2	SLC4A2	FLOT2
GOT1	POLR1A	KPRP
FLII	SLC7A2	PRKD2
PIP	OSBP	CD63
CUL1	PRKCI	GSN

PGM1	PAFAH1B1	AP1G1
APEH	DENND1A	CAPG
SORD	PI4K2A	NQO1
CTNNBL1	CYB5R3	GLG1
APMAP	CELSR2	RBM12B
ZNF493	SARS	FOXK1
ARPC1B	TTYH3	UPF1
PEBP1	TROVE2	TTN
RAB32	MRPL47	RAB32
TNPO1	MRPL38	RBM12
IQGAP1	FDPS	ZNF660
KANK1	PRB1	ZNF235
EPB41L5	PSAT1	TOMM70
OPA1	SPRR2E	CLPTM1
ABCB6	TF	ANXA6
LETM1	ANP32B	AGPS
GNS	FKBP10	APEX1
SPTBN1	BRIP1	KRR1
ANXA6	HARS	ACTR3
SEC24C	NSUN5	PSMA4
PMEL	ZFP62	PABPN1
HSDL1	NAA25	MRPL21
MRPL24	RBM12B	RFTN1
ZNF235	FOXK1	TNPO1
MDH1	ACTR3	OPTN
NOM1	PSMA4	LETM1
MCM2	PABPN1	DSC1
NR4A3	MRPL21	ST13
RBM12	RFTN1	CTNNB1
PML	ATP13A1	TXNRD1
ASAH1	DHX57	ATP13A1
TYRP1	FLII	DHX57
HSD17B4	APMAP	HK2
LGALS3	ZNF493	HSD17B4
M6PR	ARPC1B	ACTR2
PITRM1	ATP1B3	FLII
ZBTB11	MLX	APMAP
VPS13C	TMED9	ZNF493
AHSG	PTCD1	ARPC1B
NANS	RNF40	PAK1IP1
DSC1	MARCKSL1	EPB41L5
CALU	VPS26A	MCM2
RECQL	DIS3	TALDO1
IGF2R	EIF2S2	LAP3

WDR1	ACBD3	ATP1B3
DNAJC13	NSF	DHTKD1
PRKD2	CYCS	CD44
CD63	PCNA	CLCN7
GSN	SCAMP3	ZBTB11
AIFM1	STT3A	CAT
TOMM70	POP1	UTP20
AARS	AP3S1	ATP2B4
FLOT2	ABCE1	FKBP3
ATP1B3	YTHDF3	DNM2
S100A9	STAG2	FKBP4
CTNNB1	RABL6	PML
MRPL44	FAM129B	ASAH1
DNM2	SCAF4	TXLNA
NAA15	LEO1	BSG
IMMT	DHX8	MRPL44
POR	PFAS	MLX
KPRP	CUL4A	TMED9
HK1	DOCK7	NAA15
MYO1C	KPNA2	FAU
ITGB1	CTCF	MYO1C
CAPG	DNAJB1	TKT
NELFB	SRP14	PDCD11
OPTN	TPM3	PTCD1
NQO1	FAM91A1	RNF40
AP1G1	HTATSF1	PHF6
DHTKD1	SMCHD1	MRPL24
NCSTN	SLC25A11	PTCD3
PDCD11	EIF2A	MARCKSL1
PRKD1	PDS5A	VPS26A
GPI	GTF3C1	RECQL
FKBP4	UNC45A	SEC24C
FLOT1	CAD	SRSF2
NPEPPS	STAT1	HYOU1
CLTC	HDGFL2	KANK1
TKT	TARDBP	RPS25
RPL32	WASHC2A	LRRC59
AGPS	KLC1	IGF2R
PRKD3	HIST1H1T	DIS3
S100A8	ARF3	CPT1A
PTCD3	USP7	SRRT
VAT1	STRAP	AASS
DCD	THOC2	ERO1A
CPT1A	CDC5L	RPL35

IFI16	NUP153	UFL1
KRT76	TPR	G6PD
GOT2	MYH10	SUPT6H
ACSL1	PRPF8	EIF2S2
P4HB	AP3D1	NOC2L
IARS2	AP3B1	USP5
TMEM263	SMC1A	AIFM1
TXNRD1	IARS	SEC23B
TALDO1	MYH9	API5
PGK1	HYOU1	FKBP15
RPL37A	EZR	ITGB1
ANXA5	PRPF6	AARS
CTSD	EPRS	DCD
TPI1	HCFC1	HK1
SRRT	RRBP1	ACBD3
GSTO1	UGGT1	GARS
AASS	PRKDC	NDUFS2
AP3B1	KTN1	ANP32E
TXLNA	CLUH	NARS2
IGSF8	NOMO1	GDI2
CLPTM1	POR	HM13
RPL35	OGDH	ILVBL
LRRC59	SF3B2	NSF
RPS25	ITGB1	CTR9
NARS2	PDHA1	RPL32
SLC1A4	EEA1	DSG1
ZNF616	TRPV2	IQGAP1
SAMM50	CTTN	TNPO3
CALR	LAMP2	PITRM1
RPS27A	PYGB	CYCS
FARSB	DNAJC9	UBXN4
GDI2	PAK1IP1	AP1B1
ACAA1	FKBP3	SUPT5H
FAU	CTR9	RPL37A
DSG1	RAD50	DLST
VCL	SMARCC2	AP2A1
AHCY	GOLGA2	POR
MLX	EIF3A	PCMT1
TMEM214	RPL37A	UBA2
ST13	LARS	PCNA
TMED9	SAFB	DDX27
TM9SF2	STXBP1	NPEPPS
IDH1	EIF3B	DDX41
DNAJA1	DPP4	AHCY

CAT	UPF1	GNAS
GFPT1	CCAR2	SCAMP3
TARS	KIF5B	HGS
PRKCSH	RECQL	IMMT
AP2A1	SMC3	DNAJA1
MAGED2	ATP6V0A1	SUMO3
CTR9	RCN2	NPLOC4
PPIB	NAA15	PNPT1
CTNNA1	GARS	STT3A
FH	RPL36A	FKBP8
DDX54	SNRNP70	RPL36A
PDIA4	ATP5C1	HMGN2
NOC2L	DCTN1	TARS
MSN	ESYT1	FAM120A
SRSF2	EEF1A2	CTNNA1
G6PD	VARS	POP1
HADHB	DVL3	PLEKHA5
RRBP1	ATIC	AP3S1
LDHB	NUP93	ABCE1
CLCN7	CAPRIN1	SSB
PTCD1	IPO7	YTHDF3
RNF40	TGM3	IARS2
MDH2	PLCD3	AHCYL1
ALDOA	AASS	STAG2
TFRC	DDX27	DNAJC13
COPA	MYO1D	HNRNPUL2
CANX	SEC24C	HMGB1
RBM28	DNAJA1	KARS
YBX1	EIF3CL	TPD52L2
HGS	DBN1	ATP5O
CAP1	MTA2	NKRF
SUPT5H	NUMA1	ACSL4
AGK	SFPQ	COPB2
GARS	G3BP1	RBM28
RPL19	HGS	TRIM25
VCP	ACSL4	PPM1G
FKBP15	ECM1	ADRM1
RPL36	P3H1	RPS27A
DSP	GSR	RABL6
CHCHD3	DHTKD1	H1FX
IST1	TXLNA	FUBP1
MARCKSL1	FAU	HADHB
VPS26A	SRSF2	STIP1
LARS2	UFL1	COPA

USP5	NDUFS2	FAM129B
NOC3L	GNAS	SEC61A1
HNRNPUL2	CLPX	PFKP
OAT	PRDX3	SYMPK
SLC25A13	ARF4	CLIC1
RPL7	GFM1	VCL
RALY	RBM25	ATP6V1B2
DDB1	CTNND1	OSBPL8
SSB	RPL21	SCAF4
ACSL3	SLC7A5	NCKAP1
RPL4	EDC4	USO1
HSP90B1	UBAP2L	IDH3B
DDX27	HNRNPUL2	SLC25A13
HMGN2	TLN1	PDCD6IP
PLEKHA5	CTPS1	LEO1
PNPT1	SMARCA5	P4HB
NPLOC4	RPS8	AP2B1
UFL1	FLNA	NME2
GAPDH	DNAJC13	PSMD1
DIS3	PRKCE	HLA-A
BSG	DHX30	ESYT2
UBA1	AKR1B1	RRP12
GANAB	DCD	
PFKP	DHX15	
CNP	ZNF660	
RPL13A	DNM2	
ATP1A1	AHCYL1	
XPO1	ESYT2	
HM13	NOL6	
FAM120A	CD44	
AP2B1	NOP2	
ILVBL	IQGAP1	
SHMT2	TARS	
TOP1	IPO5	
DLAT	MARCKS	
RAB38	ZNF326	
RPS5	DDX3X	
SURF6	FASN	
TMEM163	CTNNA1	
KARS	MATR3	
PFKM	IARS2	
FUBP1	GTF2I	
DHX30	GNL2	
PDCD6IP	LTA4H	

PDIA3	PNPT1	
UBXN4	SPG20	
STT3B	RPS7	
NDUFS2	ALDH18A1	
NDUFA9	NPEPPS	
SPTAN1	HK2	
STIP1	CLIC1	
BCAP31	NSUN2	
CSE1L	SOD2	
RPL18	CAPN5	
ACLY	XRN2	
PSMD1	SUPT16H	
NUP205	ACTB	
PPIF	SSB	
SUPT6H	DARS	
EIF2S2	TRIM28	
NOP53	RAB27A	
RPL8	PARP1	
DLST	SF3B1	
NME2	HSPH1	
IPO5	MSN	
NNT	EFTUD2	
EPHX1	SRRT	
ANP32E	AARS	
PCMT1	DDX21	
UBA2	CDK2	
SEC23B	KARS	
API5	PSMD3	
MCM5	TNPO1	
HSPA4	COPB1	
RPL36A	TTN	
MCM3	CPT1A	
GNAS	RRP12	
HADHA	DDX1	
SYMPK	RPN2	
CAND1	RAB32	
RPL3	SQSTM1	
LMNA	EIF5B	
IGHA1	ZNF235	
ACBD3	UBXN4	
RPN1	PPM1G	
ACSL4	SEPT7	
MSH2	TMPO	
GTPBP4	SCARB1	

CLIC1	PCYOX1	
LONP1	RAD23B	
HLA-A	RBM12	
COPB2	ANP32E	
CDK2	SEC61A1	
DLD	NCKAP1	
ATP2A2	GMPS	
RPL14	NOLC1	
SND1	ZC3H11A	
LDHA	RUVBL1	
AP3D1	PHKA2	
NSF	GPRIN3	
ERO1A	ACR	
AFG3L2	CNDP2	
RPSA	GOT1	
DARS	PIP	
OGDH	CUL1	
HSP90AA1	PGM1	
CYCS	APEH	
PDIA6	SORD	
RRP12	CTNNBL1	
YWHAB	PEBP1	
SRSF6	OPTN	
HMGB1	CLCN7	
HSPH1	BSG	
TXNDC5	DDX41	
IDH3A	SUMO3	
GORASP2	FKBP8	
AHCYL1	TPD52L2	
GNL3	ATP5O	
PSMD2	ADRM1	
RPL34	USO1	
ACO2	RPL30	
XRCC5	RBM39	
FXR1	SNRPD1	
JUP	ABCF2	
IDH2	ARCN1	
EZR	SURF4	
PCNA	BRIX1	
YWHAE	EIF3D	
EEF2	RPS16	
NUP155	DYNC1H1	
CS	SEPT7	
RPL35A	SUGP2	

SCAMP3	SERBP1	
HSP90AB1	FTSJ3	
ATP6V1A	LONP1	
IPO7	VPS35	
RPL13	ACTN4	
PKM	RPL32	
NAMPT	MYO1C	
PRPF6	ANXA11	
SPG20	MYBBP1A	
STOML2	KANK1	
TNPO3	PDCD6IP	
RSL1D1	SLC25A6	
OSBPL8	LETM1	
PRPF40A	NAMPT	
XRN2	CALD1	
PPM1G	MCM2	
KRT1	MSH2	
MTHFD1	DSP	
LRPPRC	SACM1L	
STT3A	CORO1C	
DDX41	XPO1	
PHB	ANXA2	
VARS	MRPL44	
YWHAZ	CCT5	
MRPS5	CLTC	
NOP2	RPL35A	
FLG2	LAMP1	
MCM6	NPLOC4	
GNB2	EPB41L5	
PSMD12	PTBP1	
YWHAG	GANAB	
SUPT16H	SDHA	
PABPC4	PSMD2	
NKRF	PSAP	
TRIM25	NOC2L	
SUMO3	EIF2S3	
ACADVL	HNRNPU	
SLC25A3	AFG3L2	
ATP5B	TRAP1	
ACADM	DSC1	
PSMD3	USP5	
SDHA	ACADM	
H1FX	HNRNPD	
ACTN1	DHX9	

HNRNPH2	HSPA4	
XRCC6	AIFM1	
PSMC4	ADAR	
VDAC1	DDX54	
FKBP8	ANXA6	
ESYT2	MCM7	
RPL29	RBBP4	
UQCRC2	RAN	
RPL6	NASP	
FTSJ3	LRPPRC	
IARS	COPA	
PARP1	CAP1	
UQCRC1	VCL	
NUP93	HSD17B4	
EEF1G	ABCB6	
RPL28	GNS	
POP1	HSDL1	
HSPD1	KHSRP	
RPL7A	OPA1	
HSPA5	PMEL	
KRT9	NARS2	
EIF3B	DSG1	
LTF	FUBP1	
NSUN2	NME2	
MYH9	HDAC1	
MTA2	CAND1	
CNOT1	IMMT	
NDUFS1	ILF3	
CPT2	MTHFD1	
AP3S1	MCM6	
ABCE1	PHGDH	
PRDX4	ZBTB11	
HRNR	JUP	
SLC3A2	NOM1	
MATR3	PSMD1	
SEC61A1	LGALS3	
PHGDH	FKBP4	
NOL6	NR4A3	
RPS6	AHSG	
EIF3CL	NANS	
YTHDF3	SEC23B	
HNRNPH1	API5	
RPL26	IDH3B	
FARSA	SMC2	

RAB5C	SRSF7	
RPL27	MARS	
ALDH1B1	SLC3A2	
NCKAP1	HIST1H1E	
STAG2	HSPA1A	
ILF3	SLC25A13	
IDH3B	SHMT2	
DDX1	MDH1	
RPS3A	DDX5	
PPP2R1A	PABPC4	
ENO1	RPS3A	
KTN1	M6PR	
PSMC1	HM13	
DHX9	PDIA4	
EIF3A	MCM3	
GLUD1	YBX1	
SMC1A	SRSF6	
DBN1	VPS13C	
COPB1	HNRNPL	
HSD17B12	COPB2	
RPS13	RPL29	
HNRNPU	TYRP1	
RPL5	HK1	
PHB2	NNT	
PABPC1	NPM1	
MARCKS	CALU	
SSRP1	PPP2R1A	
RPL18A	SF3A1	
ANXA2	ATP5A1	
RPL23A	NOP53	
RABL6	NCL	
RPN2	ATP6V1A	
CAPRIN1	WDR1	
SLC25A5	PFKP	
TPD52L2	CANX	
SMC2	XRCC5	
RPS9	VCP	
ATP5O	HADHB	
ATP5A1	OAT	
ATAD3A	TOMM70	
RAD50	SYNCRIP	
ADAR	TALDO1	
PTBP1	RPL26	
ADRM1	PCBP2	

FAM129B	CAT	
CLPX	RPL27	
PPIA	SSRP1	
KPNB1	S100A9	
RPL15	NELFB	
ILF2	CLPTM1	
CFL1	ST13	
SCAF4	ERO1A	
KHSRP	TNPO3	
LEO1	ATP6V1B2	
RPS2	HSPB1	
GTF2I	ENO2	
SMARCC2	BUB3	
MCM7	RPS24	
CACYBP	SLC25A5	
GSTP1	EEF1A1	
ZNF326	GNL3	
DDX5	P4HB	
EPS15	AHCY	
WDR11	RBM28	
EFTUD2	RPN1	
USO1	HIST1H3	
ATP6V1B2	HNRNPK	
PA2G4	EEF2	
ACTN4	GDI2	
SF3B3	CCT3	
CYFIP1	RPL35	
HSPA9	CTNNB1	
CHD1	FLOT2	
ACAA2	ATP2A2	
MCM4	RPS25	
DHX8	TUBA1B	
CTTN	HNRNPH1	
SNRNP70	LDHB	
HIST1H4	TFRC	
NCL	KPRP	
PFAS	RPS27A	
CORO1C	AP2B1	
CUL4A	RPL5	
RBBP4	TUFM	
VIM	HSP90B1	
PDHA1	NAP1L1	
HNRNPL	PDIA3	
SRSF4	LRRC59	

DOCK7	STIP1	
LARS	ATP1A1	
TRIP12	ACO2	
HNRNPM	YWHAE	
FUS	RSL1D1	
SRSF7	HSPA5	
PRDX3	EEF1G	
RPLP0	PRKD2	
HSPB1	CD63	
VAPA	GSN	
ACTG1	LDHA	
RPL30	HNRNPH2	
DDOST	SLC25A3	
SNRNP200	AP1G1	
RPS3	AGPS	
SYNCRIP	TXNRD1	
KPNA2	DLST	
PRPF8	FARSA	
SETSIP	ATP5B	
HDAC1	HSPD1	
RPS11	RPL14	
TUBB3	CAPG	
EIF2S3	UBA1	
CTCF	NQO1	
DNAJB1	PA2G4	
EIF4A1	MCM4	
ATP5C1	HSP90AB1	
RPL10A	NOC3L	
TOP2B	RPL8	
RPS8	EIF4A1	
PPP1R12A	ACLY	
LMNB1	RPS6	
HNRNPAB	VIM	
PRDX6	RPL19	
HSPA8	MCCC1	
HNRNPC	PKM	
TECR	TKT	
RBM39	LMNA	
HIST1H1C	RPL7	
CCAR2		
GMPS		
RAB1A		
EIF5B		
HIST1H2BK		

SMC3		
ARF4		
PGAM1		
VDAC2		
GFM1		
PMPCB		
RPL9		
SMC4		
EIF4A3		
MYBBP1A		
G3BP1		
TRAP1		
GOLGA2		
MSH6		
DYNLL1		
SRP14		
TPM3		
SNRPD1		
RTN4		
RPL12		
HIST1H3		
FAM91A1		
TUBB4B		
CCT3		
RBM14		
PRKDC		
RPL22		
TUBB		
RBM25		
SMARCA1		
PRDX1		
ACTC1		
ETFA		
SET		
CCT4		
SPAG9		
SAFB		
HTATSF1		
TUFM		
TRIM28		
CTNND1		
SMCHD1		
SLC25A11		
EIF2A		

TCP1		
RPS4X		
HNRNPF		
ABCF2		
TLN1		
PCBP3		
NAP1L1		
ARCN1		
RPL21		
PDS5A		
SURF4		
CCT5		
SF3A3		
CCT6A		
GTF3C1		
BRIX1		
ENO2		
COPG1		
HNRNPR		
EIF3D		
GNL2		
SF3A1		
HNRNPD		
DVL3		
DHX15		
RAB7A		
RPS7		
DCTN1		
SLC7A5		
SMARCA5		
MARS		
RACK1		
SQSTM1		
HNRNPA1		
TUBA1B		
RPL10		
SLC25A6		
UNC45A		
HDLBP		
CAD		
CCT7		
ZFR		
THRAP3		
STAT1		

TCERG1		
HSPA1A		
PDHB		
SF3B1		
HDGFL2		
ZC3HAV1		
HIST1H1E		
SFPQ		
HIST1H2BJ		
HNRNPK		
RPL24		
SKIV2L2		
KIF5B		
EPRS		
TARDBP		
WASHC2A		
ESYT1		
RPS16		
DYNC1H1		
EDC4		
FASN		
RAN		
EEF1A1		
HCFC1		
PCBP1		
CTPS1		
SEPT9		
PCBP2		
DDX21		
EEF1D		
BUB3		
RPS24		
ALDH18A1		
TOP2A		
KLC1		
HIST1H2A		
CCT2		
SMARCA4		
RPS14		
SEPT7		
NPM1		
SF3B2		
HIST1H1T		
CCT8		

CALD1		
MCCC2		
DDX42		
ARF3		
NASP		
DDX39A		
ACTB		
USP7		
RPL11		
GCN1		
MCCC1		
NOLC1		
ZC3H11A		
EIF4G1		
PRPF19		
STRAP		
HNRNPA2B1		
MAP4		
DDX3X		
PUF60		
U2SURP		
THOC2		
NONO		
EPB41L3		
NUMA1		
SART3		
CKAP5		
EPB41L2		
BCLAF1		
CDC5L		
BAZ1B		
FLNA		
DDX46		
PC		
UBAP2L		
ADNP		
LIMA1		
SUGP2		
LARP1		
TMPO		
EEF1A2		
RUVBL1		
NUP153		
SERBP1		

ACACB		
CHD4		
TPR		
PCCA		

APPENDIX 2

COMPARISON OF TPC2-BIOID2-HA MELANOSOME MEMBRANE INTERACTOME WITH TPC2 AFFINITY PURIFICATION INTERACTOMES FROM FORMER STUDIES CORRESPONDING TO FIGURE 2.1E

This table compares the pooled TPC2-BioID2-HA interactomes determined in the present study with TPC2 interactomes identified in three former studies. SCAMP3, TMED9, WDR1, RCN2, ANXA6, ANXA11, and PDI2 overlapped between our dataset and others. Only positively enriched proteins relative to n=5 experimental negative controls and having <1 mean spectral count in n=30 CRAPome negative control experiments were incorporated into the comparison. For datasets from other papers, all enriched proteins listed were incorporated.

TPC2 Interactomes From 4 Studies			
Lin-Moshier et al	Zhang et al	Grimm et al	Beyers et al
TPCN2	TPCN2	TPCN2	TPCN2
LANC1	FARP1	SYNGR2	MYO5A
SEPT2	TIM50	BCAP31	PLD1
TES	RT25	ARL8B	SV2A
OST48	RAD50	VAMP2	FMNL2
MARE1	TDRD3	RTN4	LRMDA
GPI8	BMP2K	STX12	SLC25A12
SNP23	C19L1	RPN1	TSPAN10
B2RDY9	OBSCN	VTI1B	PELP1
SCFD1	LIN7A	LMAN1	MOGS
ML12B	ATPO	BAT3/BAG6	GPR143
ATP1A1	C2D1A	TMX1	MANF
TMED1	PEF1	HMGB2	ARFGEF2
PTPLAD1	EPB41	RAB14	ITGA9
SURF4	NOL12	VPS45	HCN3
SLC25A5	CCNL2	RAB1A	TMEM2
PGRMC1	LSM12	TFRC	GBA
SLC3A2	MGME1	STX6	MFN2
ALDOA	ZO2	RAB1B	LNPEP
ANXA1	MIRO2	STX7	TWISTNB
TM9SF1	SH3R1	TMED10	ZKSCAN7
PRDX1	CPNE1	RAB11A	SPRR1B
TMEM33	SUCB2	SYNGR1	MRPL43
GDI2	ZN700	TMED9	DDX11L8
VDAC1	SSH1	ATP6V0D1	SEMA4C
MYH9	PININ	CPD	MYO18A
PHB2	DCAF7	SCAMP3	TGOLN2
TM165	CENPP	VAMP3	NPC1
MRS2	HEXI2	RAB1C	AGAP2
CERS2	FHAD1	RAB11B	PCDHA6
SFXN1	CAND1		CD276
AUP1	LANC1		ZNF800
SLC7A5	WDR1		CALML5
CHP	PUR2		SLC4A2
VIP36	CBX4		POLR1A
LMNA	GTF2I		SLC7A2
RCN2	LLPH		OSBP
PPA1	RM20		PRKCI
HSP90AA1	PRS6A		PAFAH1B1
CAP1	TCEA3		DENND1A
SYNGR2			PI4K2A
CALR			CYB5R3

PNKD			CELSR2
STX16			SARS
BAG2			TTYH3
FITM2			TROVE2
MTOR			MRPL47
ATXN2L			MRPL38
SGMR1			FDPS
HAX1			PRB1
SEPT9			PSAT1
TMED2			SPRR2E
TMED3			TF
TMED4			ANP32B
TMED5			FKBP10
TMED7			FANCJ
TMED9			HARS
TMED10			NSUN5
SLC25A6			ZFP62
ANXA2			NAA25
ANXA3			UGGT1
ANXA4			CLUH
ANXA5			NOMO1
ANXA6			EEA1
ANXA7			TRPV2
ANXA11			LAMP2
TM9SF2			PYGB
TM9SF3			DNAJC9
PRDX4			STXBP1
PRDX6			DPP4
VDAC2			ATP6V0A1
VDAC3			RCN2
SFXN2			ATIC
SFXN4			TGM3
SYNGR3			PLCD3
STX18			MYO1D
RAB8A			ECM1
RAC1			P3H1
RAB10			GSR
RAB1B			PRKCE
RAB21			AKR1B1
RAB14			LTA4H
RAB11A			SOD2
RAB7A			CAPN5
RAB1A			RAB27A
RAB5C			SCARB1

			PCYOX1
			RAD23B
			PHKA2
			GPRIN3
			ACR
			CNDP2
			GOT1
			PIP
			CUL1
			PGM1
			APEH
			SORD
			CTNNBL1
			PEBP1
			VPS35
			ANXA11
			SACM1L
			LAMP1
			PSAP
			ABCB6
			GNS
			HSDL1
			OPA1
			PMEL
			NOM1
			LGALS3
			NR4A3
			AHSG
			NANS
			MDH1
			M6PR
			VPS13C
			TYRP1
			CALU
			WDR1
			S100A9
			NELFB
			FLOT2
			KPRP
			PRKD2
			CD63
			GSN
			AP1G1
			CAPG

			NQO1
			GLG1
			RBM12B
			FOXK1
			UPF1
			TTN
			RAB32
			RBM12
			ZNF660
			ZNF235
			TOMM70
			CLPTM1
			ANXA6
			AGPS
			APEX1
			KRR1
			ACTR3
			PSMA4
			PABPN1
			MRPL21
			RFTN1
			TNPO1
			OPTN
			LETM1
			DSC1
			ST13
			CTNNB1
			TXNRD1
			ATP13A1
			DHX57
			HK2
			HSD17B4
			ACTR2
			FLII
			APMAP
			ZNF493
			ARPC1B
			PAK1IP1
			EPB41L5
			MCM2
			TALDO1
			LAP3
			ATP1B3
			DHTKD1

			CD44
			CLCN7
			ZBTB11
			CAT
			UTP20
			ATP2B4
			FKBP3
			DNM2
			FKBP4
			PML
			ASAH1
			TXLNA
			BSG
			MRPL44
			MLX
			TMED9
			NAA15
			FAU
			MYO1C
			TKT
			PDCD11
			PTCD1
			RNF40
			PHF6
			MRPL24
			PTCD3
			MARCKSL1
			VPS26A
			RECQL
			SEC24C
			SRSF2
			HYOU1
			KANK1
			RPS25
			LRRC59
			IGF2R
			DIS3
			CPT1A
			SRRT
			AASS
			ERO1A
			RPL35
			UFL1
			G6PD

			SUPT6H
			EIF2S2
			NOC2L
			USP5
			AIFM1
			SEC23B
			API5
			FKBP15
			ITGB1
			AARS
			DCD
			HK1
			ACBD3
			GARS
			NDUFS2
			ANP32E
			NARS2
			GDI2
			HM13
			ILVBL
			NSF
			CTR9
			RPL32
			DSG1
			IQGAP1
			TNPO3
			PITRM1
			CYCS
			UBXN4
			AP1B1
			SUPT5H
			RPL37A
			DLST
			AP2A1
			POR
			PCMT1
			UBA2
			PCNA
			DDX27
			NPEPPS
			DDX41
			AHCY
			GNAS
			SCAMP3

			HGS
			IMMT
			DNAJA1
			SUMO3
			NPLOC4
			PNPT1
			STT3A
			FKBP8
			RPL36A
			HMGN2
			TARS
			FAM120A
			CTNNA1
			POP1
			PLEKHA5
			AP3S1
			ABCE1
			SSB
			YTHDF3
			IARS2
			AHCYL1
			STAG2
			DNAJC13
			HNRNPUL2
			HMGB1
			KARS
			TPD52L2
			ATP5O
			NKRF
			ACSL4
			COPB2
			RBM28
			TRIM25
			PPM1G
			ADRM1
			RPS27A
			RABL6
			H1FX
			FUBP1
			HADHB
			STIP1
			COPA
			FAM129B
			SEC61A1

			PFKP
			SYMPK
			CLIC1
			VCL
			ATP6V1B2
			OSBPL8
			SCAF4
			NCKAP1
			USO1
			IDH3B
			SLC25A13
			PDCD6IP
			LEO1
			P4HB
			AP2B1
			NME2
			PSMD1
			HLA-A
			ESYT2
			RRP12

APPENDIX 3

COMPARISON OF TPC2-734E-BIOID2-HA, TPC2-734G-BIOID2-HA, AND TPC2-ΔCT-BIOID2-HA INTERACTOMES CORRESPONDING TO FIGURE 2.1F

This table compares TPC2-734E-BioID2-HA, TPC2-734G-BioID2-HA, AND TPC2-ΔCT-BioID2-HA interactomes in MNT1 cells suggesting each has unique interactions. n=3 independent experiments were performed for each version of TPC2. Only positively enriched proteins relative to n=5 experimental negative controls and having <1 mean spectral count in n=30 CRAPome negative control experiments were incorporated into the comparison.

TPC2-734E-BioID2 Analysis				TPC2-734G-BioID2 Analysis				TPC2-ΔCT-BioID2 Analysis			
Prey Name	Mean spectral count of n=3 TPC2-BioID2-HA PD	Mean spectral count of n=5 Experimental Controls	Mean spectral count of n=30 CRAPome Controls	Prey Name	Mean spectral count of n=3 TPC2-BioID2-HA PD	Mean spectral count of n=5 Experimental Controls	Mean spectral count of n=30 CRAPome Controls	Prey Name	Mean spectral count of n=3 TPC2-BioID2-HA PD	Mean spectral count of n=5 Experimental Controls	Mean spectral count of n=30 CRAPome Controls
TPCN2	8.00	0.00	0.00	TPCN2	14.67	0.00	0.00	TPCN2	9.67	0.00	0.00
PLD1	5.67	0.00	0.00	MYO5A	8.67	0.00	0.00	SV2A	5.33	0.00	0.00
TSPAN10	1.67	0.00	0.00	PLD1	7.00	0.00	0.00	LRMDA	2.67	0.00	0.00
SV2A	1.67	0.00	0.00	SV2A	5.33	0.00	0.00	SLC25A12	2.00	0.00	0.00
PELP1	1.67	0.00	0.00	FMNL2	3.00	0.00	0.00	TSPAN10	1.67	0.00	0.00
MOGS	1.33	0.00	0.00	LRMDA	2.00	0.00	0.00	MANF	1.33	0.00	0.00
GPR143	1.33	0.00	0.00	TSPAN10	1.67	0.00	0.00	PLD1	1.33	0.00	0.00
FMNL2	1.00	0.00	0.00	PRKCI	0.67	0.00	0.00	TWISTNB	1.00	0.00	0.00
ARFGEF2	1.00	0.00	0.00	PAFAH1B1	0.67	0.00	0.00	ZKSCAN7	1.00	0.00	0.00
ITGA9	1.00	0.00	0.00	DENND1A	0.67	0.00	0.00	SPRR1B	1.00	0.00	0.00
HCN3	1.00	0.00	0.00	PCDHA6	0.67	0.00	0.00	GPR143	1.00	0.00	0.00
TMEM2	1.00	0.00	0.00	PI4K2A	0.67	0.00	0.00	MRPL43	1.00	0.00	0.00
GBA	1.00	0.00	0.00	CYB5R3	0.67	0.00	0.00	MOGS	0.67	0.00	0.00
MFN2	1.00	0.00	0.00	CELSR2	0.67	0.00	0.00	DDX11L8	0.67	0.00	0.00
LNPEP	1.00	0.00	0.00	SARS	0.67	0.00	0.00	TROVE2	0.67	0.00	0.00
DDX11L8	0.67	0.00	0.00	SPRR1B	0.67	0.00	0.00	MRPL47	0.67	0.00	0.00
SEMA4C	0.67	0.00	0.00	TTYH3	0.67	0.00	0.00	MRPL38	0.67	0.00	0.00
MYO18A	0.67	0.00	0.00	PYGB	1.67	0.40	0.00	FMNL2	0.67	0.00	0.00
TGOLN2	0.67	0.00	0.00	NOMO1	2.00	0.60	0.00	FDPS	0.67	0.00	0.00
NPC1	0.67	0.00	0.00	MYO1D	8.67	3.20	0.00	REV_P04280	0.67	0.00	0.00
AGAP2	0.67	0.00	0.00	CLUH	2.67	1.00	0.00	PSAT1	0.67	0.00	0.00
PCDHA6	0.67	0.00	0.00	UGGT1	3.00	1.20	0.00	SPRR2E	0.67	0.00	0.00
CD276	0.67	0.00	0.00	LAMP2	1.00	0.40	0.00	TF	0.67	0.00	0.00
ZNF800	0.67	0.00	0.00	DNAJC9	1.00	0.40	0.00	PI4K2A	0.67	0.00	0.00
SPRR1B	0.67	0.00	0.00	PRKCE	4.00	1.80	0.00	CYB5R3	0.67	0.00	0.00
CALML5	0.67	0.00	0.00	TGM3	1.33	0.60	0.00	TMEM2	0.67	0.00	0.00
SLC4A2	0.67	0.00	0.00	ATIC	1.67	0.80	0.00	ANP32B	0.67	0.00	0.00
POLR1A	0.67	0.00	0.00	STXBP1	1.67	0.80	0.00	FKBP10	0.67	0.00	0.00
SLC7A2	0.67	0.00	0.00	CAPN5	2.67	1.40	0.00	REV_Q9BX63	0.67	0.00	0.00
OSBP	0.67	0.00	0.00	EEA1	3.67	2.00	0.00	HARS	0.67	0.00	0.00
MRPL43	0.67	0.00	0.00	RAB27A	4.33	2.40	0.00	NSUN5	0.67	0.00	0.00

LAMP2	1.67	0.40	0.00	ACR	0.67	0.40	0.00	ZFP62	0.67	0.00	0.00
ATP6V0A1	1.33	0.40	0.00	CNDP2	0.67	0.40	0.00	NAA25	0.67	0.00	0.00
ECM1	1.00	0.40	0.00	GOT1	0.67	0.40	0.00	TTYH3	0.67	0.00	0.00
P3H1	1.00	0.40	0.00	ECM1	0.67	0.40	0.00	LAMP2	1.67	0.40	0.00
GSR	0.67	0.40	0.00	PIP	0.67	0.40	0.00	DNAJC9	1.67	0.40	0.00
PHKA2	0.67	0.40	0.00	GPRIN3	0.67	0.40	0.00	STXBP1	3.00	0.80	0.00
GPRIN3	0.67	0.40	0.00	CUL1	0.67	0.40	0.00	RCN2	1.33	0.40	0.00
NOMO1	3.00	0.60	0.00	PGM1	0.67	0.40	0.00	PYGB	1.33	0.40	0.00
TRPV2	2.67	0.60	0.00	HSDL1	1.33	1.00	0.00	ATIC	2.33	0.80	0.00
TGM3	1.67	0.60	0.00	NOM1	14.00	11.20	0.00	GSR	1.00	0.40	0.00
PLCD3	1.67	0.60	0.00	AHSG	1.00	0.80	0.00	AKR1B1	2.67	1.20	0.00
SCARB1	1.00	0.60	0.00	DPP4	1.00	0.80	0.00	LTA4H	2.00	1.00	0.00
PCYOX1	1.00	0.60	0.00	VPS13C	31.00	26.40	0.00	RAB27A	4.00	2.40	0.00
S100A9	0.67	0.60	0.00	RAD23B	0.67	0.60	0.00	PRKCE	3.00	1.80	0.00
DPP4	2.67	0.80	0.00	SCARB1	0.67	0.60	0.00	CLUH	1.67	1.00	0.00
NR4A3	1.00	0.80	0.00	NELFB	0.67	0.60	0.00	RAD23B	1.00	0.60	0.00
CLUH	5.00	1.00	0.00	TRPV2	0.67	0.60	0.00	SCARB1	1.00	0.60	0.00
GNS	1.33	1.00	0.00	PLCD3	0.67	0.60	0.00	NOMO1	1.00	0.60	0.00
UGGT1	7.00	1.20	0.00	S100A9	0.67	0.60	0.00	PLCD3	1.00	0.60	0.00
SOD2	2.67	1.40	0.00	PCYOX1	0.67	0.60	0.00	APEH	0.67	0.40	0.00
CAPN5	2.33	1.40	0.00	FLOT2	8.00	7.40	0.00	SORD	0.67	0.40	0.00
M6PR	1.67	1.40	0.00	MDH1	3.67	3.60	0.00	ACR	0.67	0.40	0.00
LAMP1	2.33	1.60	0.00	OPA1	5.67	5.60	0.00	CTNNBL1	0.67	0.40	0.00
PRKCE	2.67	1.80	0.00	GLG1	1.00	0.00	0.04	ATP6V0A1	0.67	0.40	0.00
EEA1	9.00	2.00	0.00	ACTR3	0.67	0.00	0.04	PIP	0.67	0.40	0.00
ABCB6	2.67	2.00	0.00	TNPO1	2.67	1.60	0.04	PEBP1	0.67	0.40	0.00
PSAP	4.00	2.80	0.00	DSC1	1.67	1.20	0.04	VPS35	5.67	3.60	0.00
MDH1	4.33	3.60	0.00	UPF1	1.00	0.80	0.04	ANXA11	4.33	2.80	0.00
OPA1	7.33	5.60	0.00	TTN	1.67	1.40	0.04	SACM1L	3.00	2.00	0.00
CD63	6.67	6.40	0.00	RAB32	1.33	1.20	0.04	UGGT1	1.67	1.20	0.00
GSN	6.67	6.40	0.00	RBM12	0.67	0.60	0.04	EEA1	2.67	2.00	0.00
PRKD2	8.33	8.00	0.00	FLII	0.67	0.00	0.07	PMEL	3.67	2.80	0.00
TYRP1	14.67	12.60	0.00	EPB41L5	20.33	14.00	0.07	LGALS3	3.00	2.40	0.00
GLG1	2.33	0.00	0.03	HK2	1.67	1.20	0.07	NR4A3	1.00	0.80	0.00
RBM12B	0.67	0.00	0.03	MCM2	5.67	4.40	0.07	AHSG	1.00	0.80	0.00
FOXK1	0.67	0.00	0.03	DHTKD1	0.67	0.40	0.11	NANS	1.00	0.80	0.00
CYB5R3	0.67	0.00	0.03	MLX	0.67	0.00	0.14	DPP4	1.00	0.80	0.00
RBM12	1.00	0.60	0.03	TXLNA	0.67	0.40	0.14	MDH1	4.33	3.60	0.00

ZNF660	1.00	0.60	0.03	MYO1C	3.33	3.00	0.14	SOD2	1.67	1.40	0.00
CLPTM1	0.67	0.60	0.03	PTCD1	0.67	0.00	0.18	CALU	6.00	5.20	0.00
RAD23B	0.67	0.60	0.03	PTCD3	0.67	0.00	0.18	MYO1D	3.67	3.20	0.00
UPF1	2.67	0.80	0.03	SEC24C	2.00	1.00	0.18	WDR1	5.00	4.40	0.00
ZNF235	1.00	0.80	0.03	HYOU1	1.33	0.80	0.18	TRPV2	0.67	0.60	0.00
RAB32	2.00	1.20	0.03	KANK1	20.33	13.20	0.18	S100A9	0.67	0.60	0.00
TTN	2.33	1.40	0.03	RECQL	0.67	0.60	0.18	PCYOX1	0.67	0.60	0.00
AGPS	1.67	1.60	0.03	AASS	0.67	0.60	0.21	KPRP	3.00	2.80	0.00
TOMM70	3.33	3.00	0.03	ERO1A	0.67	0.60	0.21	GSN	6.67	6.40	0.00
ANXA6	7.00	6.60	0.03	UFL1	0.67	0.40	0.25	AP1G1	1.67	1.60	0.00
MYO5A	4.67	0.00	0.07	NOC2L	2.00	1.40	0.25	TYRP1	13.00	12.60	0.00
ATP13A1	0.67	0.00	0.07	USP5	1.67	1.20	0.25	CAPG	9.67	9.40	0.00
DHX57	0.67	0.00	0.07	AIFM1	5.67	5.60	0.25	NQO1	5.33	5.20	0.00
HK2	2.33	1.20	0.07	DCD	2.67	1.20	0.29	APEX1	1.67	0.00	0.04
LETM1	3.67	2.40	0.07	ITGB1	0.67	0.40	0.29	KRR1	1.00	0.00	0.04
HSD17B4	4.00	3.00	0.07	NDUFS2	0.67	0.40	0.29	PSMA4	0.67	0.00	0.04
VPS35	4.33	3.60	0.07	AARS	3.00	2.60	0.29	ACTR3	0.67	0.00	0.04
LAP3	1.00	0.00	0.10	NSF	0.67	0.00	0.32	FOXK1	0.67	0.00	0.04
ATP1B3	0.67	0.00	0.10	CTR9	0.67	0.40	0.32	PABPN1	0.67	0.00	0.04
FLII	0.67	0.00	0.10	DSG1	3.67	2.80	0.32	MRPL21	0.67	0.00	0.04
DHTKD1	1.00	0.40	0.10	IQGAP1	8.00	6.40	0.32	GLG1	0.67	0.00	0.04
CLCN7	0.67	0.40	0.10	SUPT5H	1.33	0.00	0.36	RFTN1	0.67	0.00	0.04
CAT	1.33	1.20	0.10	DLST	1.67	1.60	0.36	ZNF660	1.33	0.60	0.04
CD44	3.00	1.40	0.10	PCMT1	0.67	0.00	0.39	TTN	2.33	1.40	0.04
ZBTB11	6.33	5.00	0.10	DDX27	1.67	0.60	0.39	ZNF235	1.33	0.80	0.04
UTP20	1.00	0.00	0.13	NPEPPS	2.67	2.20	0.39	OPTN	0.67	0.40	0.04
PML	1.00	0.00	0.13	POR	0.67	0.60	0.39	LETM1	3.33	2.40	0.04
ASAH1	1.00	0.00	0.13	DNAJA1	1.67	1.00	0.43	ANXA6	9.00	6.60	0.04
TXLNA	1.00	0.40	0.13	HGS	1.33	0.80	0.43	TNPO1	2.00	1.60	0.04
BSG	0.67	0.40	0.13	SUMO3	0.67	0.40	0.43	UPF1	1.00	0.80	0.04
MRPL44	2.67	1.80	0.13	IMMT	9.00	8.60	0.43	DSC1	1.33	1.20	0.04
ATP2B4	1.67	0.00	0.17	NPLOC4	1.67	1.60	0.43	RBM12	0.67	0.60	0.04
PDCD11	1.00	0.00	0.17	FKBP8	0.67	0.40	0.46	ST13	0.67	0.60	0.04
PTCD1	0.67	0.00	0.17	PNPT1	1.33	1.00	0.46	CTNNB1	16.67	15.40	0.04
RNF40	0.67	0.00	0.17	HMGN2	1.00	0.00	0.50	TXNRD1	1.67	1.60	0.04
IGF2R	1.33	0.00	0.20	RPL36A	1.33	0.40	0.50	ACTR2	1.33	0.00	0.07
DIS3	0.67	0.00	0.20	POP1	0.67	0.00	0.57	APMAP	0.67	0.00	0.07
PTCD3	0.67	0.00	0.20	AP3S1	0.67	0.00	0.61	ZNF493	0.67	0.00	0.07

RECQL	2.00	0.60	0.20	ABCE1	0.67	0.00	0.61	ARPC1B	0.67	0.00	0.07
SEC24C	2.00	1.00	0.20	SSB	1.67	1.60	0.61	PAK1IP1	1.67	0.40	0.07
CPT1A	2.33	1.40	0.20	PLEKHA5	0.67	0.00	0.64	HK2	2.00	1.20	0.07
MYO1D	7.33	3.20	0.20	AHCYL1	1.00	0.60	0.64	MCM2	6.00	4.40	0.07
UFL1	1.00	0.40	0.23	TPD52L2	0.67	0.40	0.71	TALDO1	2.00	1.80	0.07
AASS	1.67	0.60	0.23	KARS	2.33	1.80	0.71	LAP3	1.33	0.00	0.11
FKBP15	1.00	0.00	0.27	DNAJC13	4.33	3.60	0.71	UTP20	1.00	0.00	0.11
ITGB1	2.00	0.40	0.27	PPM1G	1.33	0.80	0.75	ATP2B4	0.67	0.00	0.11
SEC23B	1.00	0.80	0.27	ADRM1	0.67	0.40	0.75	ATP1B3	0.67	0.00	0.11
DCD	1.67	1.20	0.27	RPS27A	13.67	12.80	0.75	FKBP3	1.67	0.40	0.11
AARS	4.33	2.60	0.27	H1FX	0.67	0.00	0.79	DHTKD1	1.00	0.40	0.11
HK1	10.67	9.20	0.27	RABL6	0.67	0.00	0.82	DNM2	1.33	0.60	0.11
USP5	1.33	1.20	0.30	USO1	0.67	0.40	0.89	FKBP4	3.00	2.40	0.11
HM13	1.67	1.40	0.30	IDH3B	1.00	0.80	0.89	TMED9	0.67	0.00	0.14
PITRM1	2.33	0.00	0.33	OSBPL8	0.67	0.00	0.93	ASAH1	0.67	0.00	0.14
CYCS	0.67	0.00	0.33	PSMD1	4.00	3.20	0.93	NAA15	1.33	0.40	0.14
CTR9	1.67	0.40	0.33	AP2B1	5.33	5.00	0.93	FAU	1.00	0.40	0.14
HYOU1	6.00	0.80	0.33					MRPL44	2.67	1.80	0.14
UBXN4	1.33	0.80	0.33					MYO1C	4.00	3.00	0.14
AP2A1	1.00	0.00	0.37					TKT	15.67	15.60	0.14
POR	1.67	0.60	0.37					PHF6	1.67	0.00	0.18
SCAMP3	0.67	0.00	0.40					MRPL24	1.33	0.00	0.18
HGS	2.00	0.80	0.40					PTCD3	1.00	0.00	0.18
IMMT	11.00	8.60	0.40					MARCKSL1	0.67	0.00	0.18
GNAS	1.00	0.40	0.43					VPS26A	0.67	0.00	0.18
SUMO3	0.67	0.40	0.43					RECQL	1.67	0.60	0.18
PNPT1	2.00	1.00	0.43					SEC24C	2.67	1.00	0.18
SUPT6H	1.00	0.00	0.47					SRSF2	1.00	0.40	0.18
RPL36A	1.33	0.40	0.47					HYOU1	1.33	0.80	0.18
NPEPPS	2.33	2.20	0.47					RPS25	3.67	3.40	0.18
SRRT	4.67	2.80	0.47					LRRC59	4.00	3.80	0.18
MYO1C	4.67	3.00	0.47					IGF2R	1.00	0.00	0.21
HMGN2	1.33	0.00	0.50					SRRT	3.33	2.80	0.21
DDX27	1.33	0.60	0.50					RPL35	4.33	4.00	0.21
TARS	2.00	1.60	0.50					G6PD	1.00	0.00	0.25
FAM120A	1.67	0.00	0.53					SUPT6H	0.67	0.00	0.25
POP1	0.67	0.00	0.57					EIF2S2	0.67	0.00	0.25
IQGAP1	13.33	6.40	0.57					AIFM1	7.67	5.60	0.25

PLEKHA5	2.00	0.00	0.60					SEC23B	1.00	0.80	0.25
CTNNA1	3.67	1.80	0.60					API5	1.00	0.80	0.25
UBA2	0.67	0.00	0.63					NOC2L	1.67	1.40	0.25
YTHDF3	0.67	0.00	0.63					USP5	1.33	1.20	0.25
IARS2	5.67	2.80	0.63					ACBD3	0.67	0.00	0.29
STAG2	0.67	0.00	0.67					GARS	1.33	0.40	0.29
DNAJC13	8.00	3.60	0.67					NDUFS2	1.00	0.40	0.29
MCM2	6.67	4.40	0.67					DCD	2.00	1.20	0.29
HNRNPUL2	3.33	1.40	0.70					ANP32E	1.00	0.60	0.29
SUPT5H	1.33	0.00	0.73					ITGB1	0.67	0.40	0.29
NKRF	1.00	0.00	0.73					AARS	4.00	2.60	0.29
ACSL4	2.00	0.80	0.73					NARS2	3.67	2.80	0.29
KARS	2.67	1.80	0.73					GDI2	5.00	4.60	0.29
COPB2	2.33	2.00	0.73					ILVBL	1.00	0.00	0.32
AIFM1	6.00	5.60	0.73					NSF	0.67	0.00	0.32
RBM28	6.33	5.80	0.73					RPL32	4.67	3.00	0.32
RABL6	0.67	0.00	0.77					TNPO3	0.67	0.60	0.32
FUBP1	3.67	2.80	0.80					IQGAP1	6.67	6.40	0.32
COPA	5.67	4.20	0.80					AP1B1	4.00	0.00	0.36
SYMPK	2.00	0.00	0.83					RPL37A	2.33	0.60	0.36
OSBPL8	1.33	0.00	0.87					AP2A1	1.67	0.00	0.39
H1FX	0.67	0.00	0.87					PCMT1	1.00	0.00	0.39
SCAF4	0.67	0.00	0.87					UBA2	1.00	0.00	0.39
LEO1	0.67	0.00	0.90					PCNA	0.67	0.00	0.39
AP2B1	5.33	5.00	0.90					POR	3.00	0.60	0.39
VCL	8.33	7.00	0.90					NPEPPS	4.33	2.20	0.39
P4HB	21.00	19.20	0.90					DDX41	0.67	0.40	0.39
HLA-A	1.00	0.00	0.97					AHCY	6.33	5.80	0.39
USO1	0.67	0.40	0.97					GNAS	1.67	1.60	0.39
ESYT2	1.33	0.60	0.97					DNAJA1	2.67	1.00	0.43
RRP12	2.33	1.40	0.97					HGS	2.00	0.80	0.43
PDCD6IP	4.00	2.60	0.97					SUMO3	0.67	0.40	0.43
								NPLOC4	2.33	1.60	0.43
								STT3A	0.67	0.00	0.46
								PNPT1	1.67	1.00	0.46
								HMGN2	1.67	0.00	0.50
								RPL36A	1.00	0.40	0.50
								TARS	3.33	1.60	0.50

								CTNNA1	2.00	1.80	0.54
								ABCE1	0.67	0.00	0.61
								SSB	3.00	1.60	0.61
								PLEKHA5	0.67	0.00	0.64
								AHCYL1	1.33	0.60	0.64
								IARS2	3.67	2.80	0.64
								HMGB1	1.33	0.00	0.71
								KARS	3.00	1.80	0.71
								ATP5O	0.67	0.40	0.71
								TRIM25	1.00	0.00	0.75
								ADRM1	0.67	0.40	0.75
								PPM1G	1.00	0.80	0.75
								RPS27A	13.00	12.80	0.75
								H1FX	1.00	0.00	0.79
								FUBP1	3.33	2.80	0.79
								HADHB	8.00	7.20	0.79
								STIP1	4.00	3.80	0.79
								FAM129B	0.67	0.00	0.82
								SEC61A1	1.00	0.60	0.82
								PFKP	5.00	4.40	0.82
								SYMPK	1.33	0.00	0.86
								CLIC1	2.33	1.20	0.86
								VCL	9.33	7.00	0.86
								ATP6V1B2	0.67	0.60	0.86
								NCKAP1	1.00	0.60	0.89
								SLC25A13	6.67	5.80	0.89
								PDCD6IP	2.67	2.60	0.89
								OSBPL8	1.00	0.00	0.93
								NME2	3.67	2.80	0.93
								PSMD1	4.00	3.20	0.93
								AP2B1	5.33	5.00	0.93
								HLA-A	0.67	0.00	0.96

APPENDIX 4

LIST OF TPC2-BIOID2-HA RAW DATA

The table shows a list of all proteins identified in TPC2-BioID2-HA experiments and their spectral counts. Spectral counts corresponding to independent experiments are separated by a vertical bar. n=3 experiments are shown for TPC2-734E-BioID2-HA, TPC2-734G-BioID2-HA and TPC2-ΔCT-BioID2-HA experiments. n=5 negative control experiments including untransfected MNT1 cells (n=2), MNT1 cells expressing soluble BioID2-HA (n=2), MNT1 cells expressing TPC1-BioID2-HA (n=1) are shown as experimental negative controls, and n=30 CRAPome BirA Biotin Ligase negative controls are also shown. The table is sorted by SAINT probability, with 1 corresponding to highly specific, and 0 corresponding to no specificity.

bait	prey accession	prey Gene	TPC2-BioID2-HA Spectral Counts	Spectral Counts in Experimental Negative Controls	Spectral Counts in CRAPome Controls	SAINT Prob.
TPCN2_734E	Q8NHX9	TPCN2	6|5|13	0|0|0|0|0	0|0|0|0|0|0|0|0|0|0|0| 0|0|0|0|0|0|0|0|0|0|0| 0|0|0|0|0|0|0|0	1
TPCN2_734G	Q8NHX9	TPCN2	12|13|19	0|0|0|0|0	0|0|0|0|0|0|0|0|0|0|0| 0|0|0|0|0|0|0|0|0|0|0| 0|0|0|0|0|0|0|0	1
TPCN2_DeltaCT	Q8NHX9	TPCN2	10|6|13	0|0|0|0|0	0|0|0|0|0|0|0|0|0|0|0| 0|0|0|0|0|0|0|0|0|0|0| 0|0|0|0|0|0|0|0	1
TPCN2_734G	Q13393	PLD1	3|9|9	0|0|0|0|0	0|0|0|0|0|0|0|0|0|0|0| 0|0|0|0|0|0|0|0|0|0|0| 0|0|0|0|0|0|0|0	0.97
TPCN2_734E	Q13393	PLD1	2|5|10	0|0|0|0|0	0|0|0|0|0|0|0|0|0|0|0| 0|0|0|0|0|0|0|0|0|0|0| 0|0|0|0|0|0|0|0	0.93
TPCN2_734G	Q7L0J3	SV2A	2|2|12	0|0|0|0|0	0|0|0|0|0|0|0|0|0|0|0| 0|0|0|0|0|0|0|0|0|0|0| 0|0|0|0|0|0|0|0	0.72
TPCN2_734E	Q9H1Z9	TSPAN10	3|0|2	0|0|0|0|0	0|0|0|0|0|0|0|0|0|0|0| 0|0|0|0|0|0|0|0|0|0|0| 0|0|0|0|0|0|0|0	0.58
TPCN2_DeltaCT	Q7L0J3	SV2A	0|2|14	0|0|0|0|0	0|0|0|0|0|0|0|0|0|0|0| 0|0|0|0|0|0|0|0|0|0|0| 0|0|0|0|0|0|0|0	0.57
TPCN2_734E	Q9Y4I1	MYO5A	3|0|11	0|0|0|0|0	0|0|0|0|0|0|0|0|0|0|0| 0|0|0|0|0|0|0|0|0|0|0| 0|0|0|0|0|0|2|0	0.56
TPCN2_DeltaCT	Q9H1Z9	TSPAN10	2|0|3	0|0|0|0|0	0|0|0|0|0|0|0|0|0|0|0| 0|0|0|0|0|0|0|0|0|0|0| 0|0|0|0|0|0|0|0	0.55

TPCN2_734E	O75153	CLUH	10|0|5	5|0|0|0|0	0|0|0|0|0|0|0|0|0|0|0|0|0|0|0|0|0|0|0|0|0|0|0|0|0|0|0|0	0.52
TPCN2_734G	Q9H1Z9	TSPAN10	2|0|3	0|0|0|0|0	0|0|0|0|0|0|0|0|0|0|0|0|0|0|0|0|0|0|0|0|0|0|0|0|0|0|0|0	0.49
TPCN2_734E	Q15075	EEA1	23|0|4	0|0|6|0|4	0|0|0|0|0|0|0|0|0|0|0|0|0|0|0|0|0|0|0|0|0|0|0|0|0|0|0|0	0.42
TPCN2_DeltaCT	P61764	STXBP1	6|0|3	2|2|0|0|0	0|0|0|0|0|0|0|0|0|0|0|0|0|0|0|0|0|0|0|0|0|0|0|0|0|0|0|0	0.4
TPCN2_734E	Q13724	MOGS	4|0|0	0|0|0|0|0	0|0|0|0|0|0|0|0|0|0|0|0|0|0|0|0|0|0|0|0|0|0|0|0|0|0|0|0	0.33
TPCN2_734E	P46940	IQGAP1	30|0|10	12|6|9|0|5	0|0|0|0|0|0|1|0|1|0|0|0|0|0|0|0|2|2|1|0|0|1|0|0|0|0|1|4|4	0.33
TPCN2_734E	Q9Y4L1	HYOU1	18|0|0	4|0|0|0|0	0|0|1|0|0|1|0|1|0|0|0|0|1|0|0|0|0|0|0|0|0|0|1|0|0|0|0|0|1|4	0.33
TPCN2_734E	P35221	CTNNA1	11|0|0	7|0|0|0|2	2|2|0|0|0|0|1|0|0|1|0|0|0|0|0|0|0|2|2|2|2|0|1|0|0|0|0|0|0|3	0.33
TPCN2_734E	Q9NYU2	UGGT1	21|0|0	4|0|0|0|2	0|0|0|0|0|0|0|0|0|0|0|0|0|0|0|0|0|0|0|0|0|0|0|0|0|0|0|0	0.33
TPCN2_734E	P27487	DPP4	8|0|0	2|0|0|0|2	0|0|0|0|0|0|0|0|0|0|0|0|0|0|0|0|0|0|0|0|0|0|0|0|0|0|0|0	0.33
TPCN2_734E	Q7L0J3	SV2A	0|0|5	0|0|0|0|0	0|0|0|0|0|0|0|0|0|0|0|0|0|0|0|0|0|0|0|0|0|0|0|0|0|0|0|0	0.33

TPCN2_734E	P51810	GPR143	4|0|0	0|0|0|0|0	0|0|0|0|0|0|0|0|0|0|0|0|0|0|0|0|0|0|0|0|0|0|0|0|0|0|0|0	0.33
TPCN2_734E	Q92896	GLG1	7|0|0	0|0|0|0|0	0|0|0|0|0|0|0|0|0|0|0|0|0|0|0|0|0|0|0|0|0|0|0|1|0|0|0	0.33
TPCN2_734E	Q8IZL8	PELP1	5|0|0	0|0|0|0|0	0|0|0|0|0|0|0|0|0|0|0|0|0|0|0|0|0|0|0|0|0|0|0|0|0|0|0	0.33
TPCN2_734G	Q9H2I8	LRMDA	0|0|6	0|0|0|0|0	0|0|0|0|0|0|0|0|0|0|0|0|0|0|0|0|0|0|0|0|0|0|0|0|0|0|0	0.33
TPCN2_734G	Q96PY5	FMNL2	0|0|9	0|0|0|0|0	0|0|0|0|0|0|0|0|0|0|0|0|0|0|0|0|0|0|0|0|0|0|0|0|0|0|0	0.33
TPCN2_734G	Q92896	GLG1	3|0|0	0|0|0|0|0	0|0|0|0|0|0|0|0|0|0|0|0|0|0|0|0|0|0|0|0|0|0|0|1|0|0|0	0.33
TPCN2_734G	Q9Y4I1	MYO5A	0|0|26	0|0|0|0|0	0|0|0|0|0|0|0|0|0|0|0|0|0|0|0|0|0|0|0|0|0|0|0|0|0|0|0	0.33
TPCN2_DeltaCT	Q9H2I8	LRMDA	0|0|8	0|0|0|0|0	0|0|0|0|0|0|0|0|0|0|0|0|0|0|0|0|0|0|0|0|0|0|0|0|0|0|0	0.33
TPCN2_DeltaCT	P55145	MANF	0|0|4	0|0|0|0|0	0|0|0|0|0|0|0|0|0|0|0|0|0|0|0|0|0|0|0|0|0|0|0|0|0|0|0	0.33
TPCN2_DeltaCT	O75746	SLC25A12	6|0|0	0|0|0|0|0	0|0|0|0|0|0|0|0|0|0|0|0|0|0|0|0|0|0|0|0|0|0|0|1|0	0.33
TPCN2_DeltaCT	Q10567	AP1B1	12|0|0	0|0|0|0|0	0|1|2|0|0|2|0|0|0|0|0|0|0|0|0|0|0|0|0|0|0|0|0|1|0|2|2|0|0|0|0|1	0.33

TPCN2_DeltaCT	Q13393	PLD1	0|0|4	0|0|0|0|0	0|0|0|0|0|0|0|0|0|0|0|0|0|0|0|0|0|0|0|0|0|0|0|0|0|0|0|0	0.33
TPCN2_DeltaCT	Q01546	KRT76	0|0|20	0|0|0|0|0	1|2|0|1|1|0|0|9|5|5|0|0|0|1|0|2|2|0|1|1|1|0|0|0|0|1|1|2|0|2	0.33
TPCN2_734E	Q5JRX3	PITRM1	7|0|0	0|0|0|0|0	0|0|0|0|0|0|0|2|1|1|0|2|3|0|0|0|0|0|0|0|0|0|1|0|0|0|0|0|0|0	0.32
TPCN2_734E	Q96PY5	FMNL2	0|0|3	0|0|0|0|0	0|0|0|0|0|0|0|0|0|0|0|0|0|0|0|0|0|0|0|0|0|0|0|0|0|0|0|0	0.32
TPCN2_734E	Q9Y5S1	TRPV2	8|0|0	0|0|0|0|3	0|0|0|0|0|0|0|0|0|0|0|0|0|0|0|0|0|0|0|0|0|0|0|0|0|0|0|0	0.32
TPCN2_734E	Q9Y6D5	ARFGEF2	3|0|0	0|0|0|0|0	0|0|0|0|0|0|0|0|0|0|0|0|0|0|0|0|0|0|0|0|0|0|0|0|0|0|0|0	0.32
TPCN2_734E	Q13797	ITGA9	3|0|0	0|0|0|0|0	0|0|0|0|0|0|0|0|0|0|0|0|0|0|0|0|0|0|0|0|0|0|0|0|0|0|0|0	0.32
TPCN2_734E	Q9P1Z3	HCN3	3|0|0	0|0|0|0|0	0|0|0|0|0|0|0|0|0|0|0|0|0|0|0|0|0|0|0|0|0|0|0|0|0|0|0|0	0.32
TPCN2_734E	Q9UHN6	TMEM2	3|0|0	0|0|0|0|0	0|0|0|0|0|0|0|0|0|0|0|0|0|0|0|0|0|0|0|0|0|0|0|0|0|0|0|0	0.32
TPCN2_734E	Q9NSE4	IARS2	17|0|0	8|0|0|0|6	0|0|0|0|0|0|0|2|4|1|4|4|3|0|0|0|0|0|0|0|0|0|0|0|0|0|0|0|0|1	0.32
TPCN2_734E	P04062	GBA	3|0|0	0|0|0|0|0	0|0|0|0|0|0|0|0|0|0|0|0|0|0|0|0|0|0|0|0|0|0|0|0|0|0|0|0	0.32

TPCN2_734E	O95140	MFN2	3|0|0	0|0|0|0|0	0|0|0|0|0|0|0|0|0|0|0|0|0|0|0|0|0|0|0|0|0|0|0|0|0|0|0|0|0|0|0	0.32
TPCN2_734E	Q15155	NOMO1	9|0|0	0|0|0|0|3	0|0|0|0|0|0|0|0|0|0|0|0|0|0|0|0|0|0|0|0|0|0|0|0|0|0|0|0|0|0|0	0.32
TPCN2_734E	Q9UIQ6	LNPEP	3|0|0	0|0|0|0|0	0|0|0|0|0|0|0|0|0|0|0|0|0|0|0|0|0|0|0|0|0|0|0|0|0|0|0|0|0|0|0	0.32
TPCN2_DeltaCT	P16435	POR	9|0|0	3|0|0|0|0	0|0|0|0|0|0|0|1|2|2|1|1|1|0|0|0|0|0|2|1|0|0|0|0|0|0|0|0|0|0|0|0|0	0.32
TPCN2_DeltaCT	P62910	RPL32	0|3|11	0|3|5|3|4	0|0|2|0|1|1|0|0|0|0|0|0|0|0|0|0|1|0|0|0|0|0|0|1|2|1|0|0|0|0	0.32
TPCN2_734E	Q01082	SPTBN1	50|0|0	0|0|0|0|0	2|0|0|0|0|0|0|1|0|1|0|0|0|0|0|1|0|8|9|8|5|0|3|0|0|0|2|1|26|0	0.31
TPCN2_734E	P23634	ATP2B4	5|0|0	0|0|0|0|0	0|0|0|1|0|0|0|0|0|0|0|0|0|1|0|0|0|0|0|0|0|0|0|0|0|1|0|0|2|0	0.31
TPCN2_734E	Q9P2E9	RRBP1	51|0|0	5|0|0|5|4	1|1|0|1|1|0|0|1|1|0|1|1|1|2|3|2|4|22|26|13|12|0|1|0|0|0|14|10|0|0	0.31
TPCN2_734E	P13473	LAMP2	5|0|0	2|0|0|0|0	0|0|0|0|0|0|0|0|0|0|0|0|0|0|0|0|0|0|0|0|0|0|0|0|0|0|0|0|0|0|0	0.31
TPCN2_DeltaCT	Q3B726	TWISTNB	0|0|3	0|0|0|0|0	0|0|0|0|0|0|0|0|0|0|0|0|0|0|0|0|0|0|0|0|0|0|0|0|0|0|0|0|0|0|0	0.31
TPCN2_DeltaCT	Q9P0L1	ZKSCAN7	0|0|3	0|0|0|0|0	0|0|0|0|0|0|0|0|0|0|0|0|0|0|0|0|0|0|0|0|0|0|0|0|0|0|0|0|0|0|0	0.31

TPCN2_DeltaCT	Q9NWT1	PAK1IP1	0|0|5	0|0|2|0|0	0|0|0|0|0|0|0|0|0|0|1|1|0|0|0|0|0|0|0|0|0|0|0|0|0|0|0|0|0|0	0.31
TPCN2_DeltaCT	P22528	SPRR1B	0|0|3	0|0|0|0|0	0|0|0|0|0|0|0|0|0|0|0|0|0|0|0|0|0|0|0|0|0|0|0|0|0	0.31
TPCN2_DeltaCT	P51810	GPR143	3|0|0	0|0|0|0|0	0|0|0|0|0|0|0|0|0|0|0|0|0|0|0|0|0|0|0|0|0|0|0|0|0	0.31
TPCN2_DeltaCT	Q8N983	MRPL43	0|3|0	0|0|0|0|0	0|0|0|0|0|0|0|0|0|0|0|0|0|0|0|0|0|0|0|0|0|0|0|0|0	0.31
TPCN2_734E	Q8IXT5	RBM12B	2|0|0	0|0|0|0|0	0|0|0|0|0|0|0|0|0|0|0|0|0|0|0|0|0|0|0|0|0|0|0|1|0	0.3
TPCN2_734E	P85037	FOXK1	2|0|0	0|0|0|0|0	0|0|0|0|0|0|0|0|0|0|0|0|0|0|1|0|0|0|0|0|0|0|0|0|0	0.3
TPCN2_734E	Q00610	CLTC	109|0|26	69|24|28|0|33	2|4|0|1|1|0|1|8|12|10|3|2|4|2|2|0|0|1|2|3|1|3|1|0|3|1|3|1|1|20	0.3
TPCN2_734E	P00387	CYB5R3	0|0|2	0|0|0|0|0	0|0|0|0|0|0|0|0|0|0|0|0|0|0|0|0|0|0|0|0|0|0|0|0|1	0.3
TPCN2_734E	O94832	MYO1D	6|0|16	7|0|3|0|6	0|0|0|0|0|0|0|0|0|0|0|0|0|0|0|0|0|0|0|0|0|0|0|6|0	0.3
TPCN2_734E	Q92900	UPF1	3|2|3	0|2|0|2|0	0|0|0|0|0|1|0|0|0|0|0|0|0|0|0|0|0|0|0|0|0|0|0|0|0	0.3
TPCN2_734E	P16070	CD44	9|0|0	3|0|0|0|4	1|0|0|0|0|0|0|0|0|0|0|0|0|0|0|0|0|2|0|0|0|0|0|0|0	0.29

TPCN2_734E	P46063	RECQL	6|0|0	0|0|0|0|3	0|0|1|0|0|1|1|0|0|0|0|0|1|0|0|0|0|0|0|0|0|0|1|0|0|0|0|0|0|1	0.29
TPCN2_734G	P46940	IQGAP1	24|0|0	12|6|9|0|5	0|0|0|0|0|0|1|0|1|0|0|0|0|0|0|0|2|2|1|0|0|1|0|0|0|0|1|4|4	0.29
TPCN2_Delta CT	P28838	LAP3	4|0|0	0|0|0|0|0	0|0|0|0|0|0|0|0|0|0|1|1|0|0|0|1|0|0|0|0|0|0|0|0|0|0|0|0|0|0|0	0.29
TPCN2_Delta CT	P13473	LAMP2	5|0|0	2|0|0|0|0	0|0|0|0|0|0|0|0|0|0|0|0|0|0|0|0|0|0|0|0|0|0|0|0|0|0|0	0.29
TPCN2_Delta CT	Q8WXX5	DNAJC9	0|0|5	0|2|0|0|0	0|0|0|0|0|0|0|0|0|0|0|0|0|0|0|0|0|0|0|0|0|0|0|0|0|0|0	0.29
TPCN2_734E	Q93050	ATP6V0A1	4|0|0	0|0|0|0|2	0|0|0|0|0|0|0|0|0|0|0|0|0|0|0|0|0|0|0|0|0|0|0|0|0|0|0	0.28
TPCN2_Delta CT	P61158	ACTR3	2|0|0	0|0|0|0|0	0|0|0|0|0|0|0|0|0|0|0|0|0|0|0|0|0|0|0|0|0|0|0|0|0|0|0	0.28
TPCN2_Delta CT	P10155	TROVE2	2|0|0	0|0|0|0|0	0|0|0|0|0|0|0|0|0|0|0|0|0|0|0|0|0|0|0|0|0|0|0|0|0|0|1	0.28
TPCN2_Delta CT	Q9HD33	MRPL47	0|2|0	0|0|0|0|0	0|0|0|0|0|0|0|0|0|0|0|0|0|0|0|0|0|0|0|0|0|0|0|0|0|0|1	0.28
TPCN2_Delta CT	P85037	FOXK1	2|0|0	0|0|0|0|0	0|0|0|0|0|0|0|0|0|0|0|0|0|0|1|0|0|0|0|0|0|0|0|0|0|0|0	0.28
TPCN2_Delta CT	P14324	FDPS	0|0|2	0|0|0|0|0	0|0|0|0|0|0|0|0|0|0|0|0|0|0|0|0|0|0|0|0|0|0|0|0|0|0|1	0.28

TPCN2_DeltaCT	Q7Z2W9	MRPL21	0|2|0	0|0|0|0|0	0|0|0|0|0|0|0|0|0|0|0| 1|0|0|0|0|0|0|0|0|0|0| 0|0|0|0|0|0|0|0	0.28
TPCN2_DeltaCT	P00387	CYB5R3	0|0|2	0|0|0|0|0	0|0|0|0|0|0|0|0|0|0|0| 0|0|0|0|0|0|0|0|0|0|0| 0|0|0|0|0|0|0|1	0.28
TPCN2_DeltaCT	Q92896	GLG1	2|0|0	0|0|0|0|0	0|0|0|0|0|0|0|0|0|0|0| 0|0|0|0|0|0|0|0|0|0|0| 0|0|0|0|1|0|0|0	0.28
TPCN2_DeltaCT	Q00688	FKBP3	0|0|5	0|0|2|0|0	0|0|1|0|0|0|0|0|0|0|0| 0|0|0|0|0|0|0|0|0|0|0| 2|0|0|0|0|0|0|1	0.28
TPCN2_DeltaCT	Q14699	RFTN1	2|0|0	0|0|0|0|0	0|0|0|0|0|0|0|0|0|0|0| 0|0|0|0|0|0|0|0|0|0|0| 1|0|0|0|0|0|0|0	0.28
TPCN2_734E	Q08188	TGM3	0|5|0	0|0|0|3|0	0|0|0|0|0|0|0|0|0|0|0| 0|0|0|0|0|0|0|0|0|0|0| 0|0|0|0|0|0|0|0	0.27
TPCN2_734E	P04179	SOD2	8|0|0	4|0|0|0|3	0|0|0|0|0|0|0|0|0|0|0| 0|0|0|0|0|0|0|0|0|0|0| 0|0|0|0|0|0|0|0	0.27
TPCN2_734E	P05556	ITGB1	6|0|0	0|0|0|0|2	0|0|0|0|0|0|0|0|0|0|0| 0|0|0|0|0|0|1|1|1|2|0| 0|0|0|0|2|1|0|0	0.27
TPCN2_734E	Q8N3E9	PLCD3	0|0|5	0|0|3|0|0	0|0|0|0|0|0|0|0|0|0|0| 0|0|0|0|0|0|0|0|0|0|0| 0|0|0|0|0|0|0|0	0.27
TPCN2_734G	P11216	PYGB	5|0|0	2|0|0|0|0	0|0|0|0|0|0|0|0|0|0|0| 0|0|0|0|0|0|0|0|0|0|0| 0|0|0|0|0|0|0|0	0.27
TPCN2_DeltaCT	P31939	ATIC	4|0|3	4|0|0|0|0	0|0|0|0|0|0|0|0|0|0|0| 0|0|0|0|0|0|0|0|0|0|0| 0|0|0|0|0|0|0|0	0.27

TPCN2_734E	A8MPP1	DDX11L8	2|0|0	0|0|0|0|0	0|0|0|0|0|0|0|0|0|0|0|0|0|0|0|0|0|0|0|0|0|0|0|0|0|0|0|0	0.26
TPCN2_734E	Q9C0C4	SEMA4C	2|0|0	0|0|0|0|0	0|0|0|0|0|0|0|0|0|0|0|0|0|0|0|0|0|0|0|0|0|0|0|0|0|0|0|0	0.26
TPCN2_734E	Q92614	MYO18A	2|0|0	0|0|0|0|0	0|0|0|0|0|0|0|0|0|0|0|0|0|0|0|0|0|0|0|0|0|0|0|0|0|0|0|0	0.26
TPCN2_734E	O43493	TGOLN2	2|0|0	0|0|0|0|0	0|0|0|0|0|0|0|0|0|0|0|0|0|0|0|0|0|0|0|0|0|0|0|0|0|0|0|0	0.26
TPCN2_734E	O15118	NPC1	2|0|0	0|0|0|0|0	0|0|0|0|0|0|0|0|0|0|0|0|0|0|0|0|0|0|0|0|0|0|0|0|0|0|0|0	0.26
TPCN2_734E	Q99490	AGAP2	0|0|2	0|0|0|0|0	0|0|0|0|0|0|0|0|0|0|0|0|0|0|0|0|0|0|0|0|0|0|0|0|0|0|0|0	0.26
TPCN2_734E	Q9UN73	PCDHA6	0|0|2	0|0|0|0|0	0|0|0|0|0|0|0|0|0|0|0|0|0|0|0|0|0|0|0|0|0|0|0|0|0|0|0|0	0.26
TPCN2_734E	Q5ZPR3	CD276	2|0|0	0|0|0|0|0	0|0|0|0|0|0|0|0|0|0|0|0|0|0|0|0|0|0|0|0|0|0|0|0|0|0|0|0	0.26
TPCN2_734E	Q2TB10	ZNF800	0|2|0	0|0|0|0|0	0|0|0|0|0|0|0|0|0|0|0|0|0|0|0|0|0|0|0|0|0|0|0|0|0|0|0|0	0.26
TPCN2_734E	P22528	SPRR1B	0|2|0	0|0|0|0|0	0|0|0|0|0|0|0|0|0|0|0|0|0|0|0|0|0|0|0|0|0|0|0|0|0|0|0|0	0.26
TPCN2_734E	Q9NZT1	CALML5	0|2|0	0|0|0|0|0	0|0|0|0|0|0|0|0|0|0|0|0|0|0|0|0|0|0|0|0|0|0|0|0|0|0|0|0	0.26

TPCN2_734E	P04920	SLC4A2	2|0|0	0|0|0|0|0	0|0|0|0|0|0|0|0|0|0|0|0|0|0|0|0|0|0|0|0|0|0|0|0|0|0|0|0|0|0|0	0.26
TPCN2_734E	O95602	POLR1A	2|0|0	0|0|0|0|0	0|0|0|0|0|0|0|0|0|0|0|0|0|0|0|0|0|0|0|0|0|0|0|0|0|0|0|0|0|0|0	0.26
TPCN2_734E	P52569	SLC7A2	2|0|0	0|0|0|0|0	0|0|0|0|0|0|0|0|0|0|0|0|0|0|0|0|0|0|0|0|0|0|0|0|0|0|0|0|0|0|0	0.26
TPCN2_734E	P22059	OSBP	2|0|0	0|0|0|0|0	0|0|0|0|0|0|0|0|0|0|0|0|0|0|0|0|0|0|0|0|0|0|0|0|0|0|0|0|0|0|0	0.26
TPCN2_734E	Q8N983	MRPL43	0|2|0	0|0|0|0|0	0|0|0|0|0|0|0|0|0|0|0|0|0|0|0|0|0|0|0|0|0|0|0|0|0|0|0|0|0|0|0	0.26
TPCN2_Delta CT	P61513	RPL37A	0|0|7	0|3|0|0|0	1|0|0|0|0|2|0|1|1|1|1|1|1|1|0|0|0|0|0|0|0|0|0|0|0|0|0|0|0|0|1|0	0.26
TPCN2_734E	P17643	TYRP1	38|0|6	25|10|8|0|20	0|0|0|0|0|0|0|0|0|0|0|0|0|0|0|0|0|0|0|0|0|0|0|0|0|0|0|0|0|0|0	0.25
TPCN2_734E	O60313	OPA1	22|0|0	18|0|0|0|10	0|0|0|0|0|0|0|0|0|0|0|0|0|0|0|0|0|0|0|0|0|0|0|0|0|0|0|0|0|0|0	0.25
TPCN2_734E	Q1KMD3	HNRNPUL2	10|0|0	7|0|0|0|0	1|1|0|0|0|0|1|1|2|0|1|1|1|2|2|0|0|0|0|0|1|0|0|0|0|0|2|1|0|4	0.25
TPCN2_734G	P61158	ACTR3	2|0|0	0|0|0|0|0	0|0|0|0|0|0|0|0|0|0|0|0|0|0|0|0|0|0|0|0|0|0|0|0|0|0|0|0|0|0|1|0|0|0|0|0|0|0|0	0.25
TPCN2_734G	Q9NYU2	UGGT1	9|0|0	4|0|0|0|2	0|0|0|0|0|0|0|0|0|0|0|0|0|0|0|0|0|0|0|0|0|0|0|0|0|0|0|0|0|0|0	0.25

TPCN2_734G	P00387	CYB5R3	0|0|2	0|0|0|0|0	0|0|0|0|0|0|0|0|0|0|0|0|0|0|0|0|0|0|0|0|0|0|0|0|0|0|0|0|0|0|0|1	0.25
TPCN2_734G	Q15155	NOMO1	6|0|0	0|0|0|0|3	0|0|0|0|0|0|0|0|0|0|0|0|0|0|0|0|0|0|0|0|0|0|0|0|0|0|0|0|0|0|0	0.25
TPCN2_734G	O94832	MYO1D	6|2|18	7|0|3|0|6	0|0|0|0|0|0|0|0|0|0|0|0|0|0|0|0|0|0|0|0|0|0|0|0|0|0|0|0|0|0|6|0	0.25
TPCN2_DeltaCT	Q13601	KRR1	0|0|3	0|0|0|0|0	0|0|0|1|0|0|0|0|0|0|0|0|0|0|0|0|0|0|0|0|0|0|0|0|0|0|0|0|0|0|1|0	0.25
TPCN2_DeltaCT	P61160	ACTR2	0|0|4	0|0|0|0|0	0|0|0|0|0|0|1|0|0|0|0|0|0|0|0|0|0|0|0|0|0|0|0|0|0|0|0|0|0|0|1|1	0.25
TPCN2_DeltaCT	P46940	IQGAP1	20|0|0	12|6|9|0|5	0|0|0|0|0|0|1|0|1|0|0|0|0|0|0|0|0|2|2|1|0|0|1|0|0|0|0|1|4|4	0.24
TPCN2_DeltaCT	Q8IWS0	PHF6	0|0|5	0|0|0|0|0	1|0|1|0|0|1|1|0|0|0|0|0|0|1|0|0|0|0|0|0|0|0|0|0|0|0|0|0|0|0|2	0.24
TPCN2_DeltaCT	P51159	RAB27A	0|3|9	4|0|2|2|4	0|0|0|0|0|0|0|0|0|0|0|0|0|0|0|0|0|0|0|0|0|0|0|0|0|0|0|0|0|0|0	0.24
TPCN2_734E	Q8WZ42	TTN	7|0|0	3|0|0|0|4	0|0|0|0|0|0|0|0|0|0|0|0|0|0|0|0|0|0|0|0|0|0|0|0|0|0|0|0|0|0|0	0.23
TPCN2_734E	Q9BZL6	PRKD2	0|0|25	0|12|22|0|6	0|0|0|0|0|0|0|0|0|0|0|0|0|0|0|0|0|0|0|0|0|0|0|0|0|0|0|0|0|0|0	0.23
TPCN2_734E	O95202	LETM1	11|0|0	5|0|0|0|7	0|0|0|0|0|0|0|0|0|0|0|0|1|0|0|0|0|0|0|0|0|0|0|0|0|0|0|0|0|0|1	0.23

TPCN2_734E	P28838	LAP3	3|0|0	0|0|0|0|0	0|0|0|0|0|0|0|0|0|0|1|1|0|0|0|1|0|0|0|0|0|0|0|0|0|0|0|0|0	0.23
TPCN2_734E	P50416	CPT1A	7|0|0	2|0|0|0|5	1|0|0|0|0|0|0|0|0|0|0|0|0|1|1|0|0|1|1|0|0|0|0|0|0|1|0|0|0	0.23
TPCN2_734E	Q16610	ECM1	3|0|0	0|0|0|0|2	0|0|0|0|0|0|0|0|0|0|0|0|0|0|0|0|0|0|0|0|0|0|0|0|0	0.23
TPCN2_734E	O15484	CAPN5	0|7|0	0|0|0|7|0	0|0|0|0|0|0|0|0|0|0|0|0|0|0|0|0|0|0|0|0|0|0|0|0|0	0.23
TPCN2_734E	Q16891	IMMT	30|0|3	24|2|0|0|17	0|0|1|1|0|0|0|1|2|2|0|2|1|0|0|0|1|0|0|0|0|0|1|0|0|0|0|0|0|0	0.23
TPCN2_734E	Q32P28	P3H1	3|0|0	0|0|0|0|2	0|0|0|0|0|0|0|0|0|0|0|0|0|0|0|0|0|0|0|0|0|0|0|0|0	0.23
TPCN2_734E	Q02156	PRKCE	0|0|8	0|0|9|0|0	0|0|0|0|0|0|0|0|0|0|0|0|0|0|0|0|0|0|0|0|0|0|0|0|0	0.23
TPCN2_DeltaCT	Q13724	MOGS	2|0|0	0|0|0|0|0	0|0|0|0|0|0|0|0|0|0|0|0|0|0|0|0|0|0|0|0|0|0|0|0|0	0.23
TPCN2_DeltaCT	A8MPP1	DDX11L8	2|0|0	0|0|0|0|0	0|0|0|0|0|0|0|0|0|0|0|0|0|0|0|0|0|0|0|0|0|0|0|0|0	0.23
TPCN2_DeltaCT	Q96DV4	MRPL38	0|2|0	0|0|0|0|0	0|0|0|0|0|0|0|0|0|0|0|0|0|0|0|0|0|0|0|0|0|0|0|0|0	0.23
TPCN2_DeltaCT	Q96PY5	FMNL2	0|0|2	0|0|0|0|0	0|0|0|0|0|0|0|0|0|0|0|0|0|0|0|0|0|0|0|0|0|0|0|0|0	0.23

TPCN2_DeltaCT	REV_P042	REV_P04280	0|2|0	0|0|0|0|0	0|0|0|0|0|0|0|0|0|0|0|0|0|0|0|0|0|0|0|0|0|0|0|0|0|0|0|0	0.23
TPCN2_DeltaCT	Q9Y617	PSAT1	0|0|2	0|0|0|0|0	0|0|0|0|0|0|0|0|0|0|0|0|0|0|0|0|0|0|0|0|0|0|0|0|0|0|0|0	0.23
TPCN2_DeltaCT	P22531	SPRR2E	0|0|2	0|0|0|0|0	0|0|0|0|0|0|0|0|0|0|0|0|0|0|0|0|0|0|0|0|0|0|0|0|0|0|0|0	0.23
TPCN2_DeltaCT	P02787	TF	2|0|0	0|0|0|0|0	0|0|0|0|0|0|0|0|0|0|0|0|0|0|0|0|0|0|0|0|0|0|0|0|0|0|0|0	0.23
TPCN2_DeltaCT	Q9BTU6	PI4K2A	0|0|2	0|0|0|0|0	0|0|0|0|0|0|0|0|0|0|0|0|0|0|0|0|0|0|0|0|0|0|0|0|0|0|0|0	0.23
TPCN2_DeltaCT	Q9UHN6	TMEM2	2|0|0	0|0|0|0|0	0|0|0|0|0|0|0|0|0|0|0|0|0|0|0|0|0|0|0|0|0|0|0|0|0|0|0|0	0.23
TPCN2_DeltaCT	Q96AY3	FKBP10	2|0|0	0|0|0|0|0	0|0|0|0|0|0|0|0|0|0|0|0|0|0|0|0|0|0|0|0|0|0|0|0|0|0|0|0	0.23
TPCN2_DeltaCT	REV_Q9BX	REV_Q9BX63	0|2|0	0|0|0|0|0	0|0|0|0|0|0|0|0|0|0|0|0|0|0|0|0|0|0|0|0|0|0|0|0|0|0|0|0	0.23
TPCN2_DeltaCT	Q96P11	NSUN5	2|0|0	0|0|0|0|0	0|0|0|0|0|0|0|0|0|0|0|0|0|0|0|0|0|0|0|0|0|0|0|0|0|0|0|0	0.23
TPCN2_DeltaCT	Q8NB50	ZFP62	0|0|2	0|0|0|0|0	0|0|0|0|0|0|0|0|0|0|0|0|0|0|0|0|0|0|0|0|0|0|0|0|0|0|0|0	0.23
TPCN2_DeltaCT	Q14CX7	NAA25	2|0|0	0|0|0|0|0	0|0|0|0|0|0|0|0|0|0|0|0|0|0|0|0|0|0|0|0|0|0|0|0|0|0|0|0	0.23

TPCN2_DeltaCT	Q9C0H2	TTYH3	2|0|0	0|0|0|0|0	0|0|0|0|0|0|0|0|0|0|0|0|0|0|0|0|0|0|0|0|0|0|0|0|0|0|0|0|0|0|0	0.23
TPCN2_DeltaCT	Q96QK1	VPS35	14|0|3	8|4|2|0|4	0|0|0|0|0|0|0|0|0|0|0|0|0|0|0|0|0|0|0|0|0|0|0|0|0|0|0|0|0|0|2	0.23
TPCN2_734E	P07602	PSAP	10|0|2	6|0|2|0|6	0|0|0|0|0|0|0|0|0|0|0|0|0|0|0|0|0|0|0|0|0|0|0|0|0|0|0|0|0|0|0	0.22
TPCN2_734E	P51659	HSD17B4	12|0|0	8|0|0|0|7	0|0|0|0|0|0|0|0|0|0|0|0|0|0|0|0|0|0|0|0|0|0|0|0|0|0|0|0|0|0|2	0.22
TPCN2_734E	Q13637	RAB32	0|6|0	0|0|0|2|4	0|0|0|0|0|0|0|0|0|0|0|0|0|0|0|0|1|0|0|0|0|0|0|0|0|0|0|0|0|0|0	0.22
TPCN2_734E	P19367	HK1	29|0|3	19|2|2|0|23	0|0|0|0|0|0|1|0|0|0|0|0|0|0|0|0|0|0|0|0|0|0|0|0|0|0|0|0|0|0|5	0.22
TPCN2_734G	Q709C8	VPS13C	0|0|93	0|52|76|0|4	0|0|0|0|0|0|0|0|0|0|0|0|0|0|0|0|0|0|0|0|0|0|0|0|0|0|0|0|0|0|0	0.22
TPCN2_734G	O75153	CLUH	8|0|0	5|0|0|0|0	0|0|0|0|0|0|0|0|0|0|0|0|0|0|0|0|0|0|0|0|0|0|0|0|0|0|0|0|0|0|0	0.22
TPCN2_734G	Q02156	PRKCE	0|0|12	0|0|9|0|0	0|0|0|0|0|0|0|0|0|0|0|0|0|0|0|0|0|0|0|0|0|0|0|0|0|0|0|0|0|0|0	0.22
TPCN2_DeltaCT	P11216	PYGB	2|0|2	2|0|0|0|0	0|0|0|0|0|0|0|0|0|0|0|0|0|0|0|0|0|0|0|0|0|0|0|0|0|0|0|0|0|0|0	0.22
TPCN2_DeltaCT	P53992	SEC24C	8|0|0	5|0|0|0|0	0|0|0|0|0|0|0|1|1|2|0|0|1|0|0|0|0|0|0|0|0|0|0|0|0|0|0|0|0|0|1	0.22

TPCN2_734E	P52789	HK2	7|0|0	0|0|0|0|6	0|0|0|0|0|0|0|1|0|0|0|0|0|0|0|0|1|0|0|0|0|0|0|0|0|0|0|0|0|0|0	0.21
TPCN2_734E	O75165	DNAJC13	18|6|0	0|0|0|15|3	0|0|0|0|1|0|0|0|0|0|0|0|0|0|0|0|3|5|2|2|0|0|1|1|0|2|3|0|0	0.21
TPCN2_734E	Q9NP58	ABCB6	8|0|0	5|0|0|0|5	0|0|0|0|0|0|0|0|0|0|0|0|0|0|0|0|0|0|0|0|0|0|0|0|0|0|0|0	0.21
TPCN2_734E	Q96AE4	FUBP1	11|0|0	7|0|0|0|7	3|0|2|1|1|2|1|0|0|0|0|0|0|2|2|0|0|0|0|0|1|0|3|0|0|1|1|2|0|2	0.21
TPCN2_734E	Q92621	NUP205	11|0|0	0|0|0|0|0	0|0|8|2|3|1|0|0|1|1|1|1|0|0|0|2|3|1|1|1|1|1|5|3|1|0|1|0|3|0	0.21
TPCN2_734G	P61764	STXBP1	5|0|0	2|2|0|0|0	0|0|0|0|0|0|0|0|0|0|0|0|0|0|0|0|0|0|0|0|0|0|0|0|0|0|0|0	0.21
TPCN2_DeltaCT	P08133	ANXA6	21|0|6	13|6|6|0|8	0|0|0|0|0|1|0|0|0|0|0|0|0|0|0|0|0|0|0|0|0|0|0|0|0|0|0|0	0.21
TPCN2_DeltaCT	Q96A35	MRPL24	0|4|0	0|0|0|0|0	0|0|0|0|0|0|0|1|1|0|1|1|1|0|0|0|0|0|0|0|0|0|0|0|0|0|0|0|0	0.21
TPCN2_DeltaCT	P15121	AKR1B1	4|0|4	4|0|0|0|2	0|0|0|0|0|0|0|0|0|0|0|0|0|0|0|0|0|0|0|0|0|0|0|0|0|0|0|0	0.21
TPCN2_DeltaCT	Q02156	PRKCE	0|0|9	0|0|9|0|0	0|0|0|0|0|0|0|0|0|0|0|0|0|0|0|0|0|0|0|0|0|0|0|0|0|0|0|0	0.21
TPCN2_734E	P11717	IGF2R	4|0|0	0|0|0|0|0	0|1|0|0|0|0|0|0|0|0|0|0|0|0|1|1|0|0|0|1|1|0|0|0|0|0|1|0|0|0	0.2

TPCN2_734E	Q13813	SPTAN1	32|0|0	0|0|0|0|0	7|5|1|0|2|0|1|3|1|3|0|0|0|4|2|1|2|11|14|10|17|0|4|0|1|2|4|5|16|0	0.2
TPCN2_734E	Q96QK1	VPS35	11|0|2	8|4|2|0|4	0|0|0|0|0|0|0|0|0|0|0|0|0|0|0|0|0|0|0|0|0|0|0|0|0|0|0|0|0|2	0.2
TPCN2_734G	Q15075	EEA1	11|0|0	0|0|6|0|4	0|0|0|0|0|0|0|0|0|0|0|0|0|0|0|0|0|0|0|0|0|0|0|0|0|0|0|0|0	0.2
TPCN2_DeltaCT	Q8WZ42	TTN	7|0|0	3|0|0|0|4	0|0|0|0|0|0|0|0|0|0|0|0|0|0|1|0|0|0|0|0|0|0|0|0|0|0|0|0|0|0	0.2
TPCN2_734E	Q8WTV0	SCARB1	3|0|0	3|0|0|0|0	0|0|0|0|0|0|0|0|0|0|0|0|0|0|0|0|0|0|0|0|0|0|0|0|0|0|0|0|0	0.19
TPCN2_734E	P08133	ANXA6	17|0|4	13|6|6|0|8	0|0|0|0|0|1|0|0|0|0|0|0|0|0|0|0|0|0|0|0|0|0|0|0|0|0|0|0|0	0.19
TPCN2_734E	Q9UDR5	AASS	5|0|0	3|0|0|0|0	0|0|0|0|0|1|0|0|0|0|0|0|0|0|0|0|0|1|0|1|0|1|0|1|1|0|0|1|0	0.19
TPCN2_734E	P40925	MDH1	11|0|2	11|2|0|0|5	0|0|0|0|0|0|0|0|0|0|0|0|0|0|0|0|0|0|0|0|0|0|0|0|0|0|0|0|0	0.19
TPCN2_734E	Q9UHG3	PCYOX1	3|0|0	3|0|0|0|0	0|0|0|0|0|0|0|0|0|0|0|0|0|0|0|0|0|0|0|0|0|0|0|0|0|0|0|0|0	0.19
TPCN2_734G	P41743	PRKCI	0|0|2	0|0|0|0|0	0|0|0|0|0|0|0|0|0|0|0|0|0|0|0|0|0|0|0|0|0|0|0|0|0|0|0|0|0	0.19
TPCN2_734G	P43034	PAFAH1B1	2|0|0	0|0|0|0|0	0|0|0|0|0|0|0|0|0|0|0|0|0|0|0|0|0|0|0|0|0|0|0|0|0|0|0|0|0	0.19

TPCN2_734G	Q8TEH3	DENND1A	0|0|2	0|0|0|0|0	0|0|0|0|0|0|0|0|0|0|0|0|0|0|0|0|0|0|0|0|0|0|0|0|0|0|0|0	0.19
TPCN2_734G	Q9UN73	PCDHA6	0|2|0	0|0|0|0|0	0|0|0|0|0|0|0|0|0|0|0|0|0|0|0|0|0|0|0|0|0|0|0|0|0|0|0|0	0.19
TPCN2_734G	Q9BTU6	PI4K2A	0|2|0	0|0|0|0|0	0|0|0|0|0|0|0|0|0|0|0|0|0|0|0|0|0|0|0|0|0|0|0|0|0|0|0|0	0.19
TPCN2_734G	Q9HCU4	CELSR2	2|0|0	0|0|0|0|0	0|0|0|0|0|0|0|0|0|0|0|0|0|0|0|0|0|0|0|0|0|0|0|0|0|0|0|0	0.19
TPCN2_734G	P49591	SARS	2|0|0	0|0|0|0|0	0|0|0|0|0|0|0|0|0|0|0|0|0|0|0|0|0|0|0|0|0|0|0|0|0|0|0|0	0.19
TPCN2_734G	P22528	SPRR1B	0|2|0	0|0|0|0|0	0|0|0|0|0|0|0|0|0|0|0|0|0|0|0|0|0|0|0|0|0|0|0|0|0|0|0|0	0.19
TPCN2_734G	Q9C0H2	TTYH3	2|0|0	0|0|0|0|0	0|0|0|0|0|0|0|0|0|0|0|0|0|0|0|0|0|0|0|0|0|0|0|0|0|0|0|0	0.19
TPCN2_Delta CT	P00390	GSR	3|0|0	2|0|0|0|0	0|0|0|0|0|0|0|0|0|0|0|0|0|0|0|0|0|0|0|0|0|0|0|0|0|0|0|0	0.19
TPCN2_Delta CT	P35222	CTNNB1	41|0|9	38|10|11|0|18	0|0|0|0|0|0|0|0|0|0|0|0|0|0|0|0|0|0|0|0|0|0|0|0|0|0|0|0	0.19
TPCN2_Delta CT	Q01082	SPTBN1	31|0|0	0|0|0|0|0	2|0|0|0|0|0|0|1|0|1|0|0|0|0|0|1|0|8|9|8|5|0|3|0|0|0|2|1|26|0	0.19
TPCN2_Delta CT	P50995	ANXA11	10|0|3	7|0|2|0|5	0|0|0|0|0|0|0|0|0|0|0|0|0|0|0|0|0|0|0|0|0|0|0|0|0|0|0|0	0.19

TPCN2_734E	O94826	TOMM70	10|0|0	6|0|0|0|9	0|0|0|0|0|0|0|0|0|1|0|0|0|0|0|0|0|0|0|0|0|0|0|0|0|0|0|0|0|0	0.18
TPCN2_734E	P49736	MCM2	20|0|0	16|2|0|0|4	0|0|0|0|0|2|0|0|0|0|0|0|0|0|0|0|0|0|0|0|0|0|0|0|0|18	0.18
TPCN2_734E	Q9BXP5	SRRT	14|0|0	11|0|0|0|3	0|0|0|0|0|0|0|0|0|2|0|2|0|0|0|0|0|1|1|0|0|0|0|0|0|0|0|0|0|8	0.18
TPCN2_734E	P11279	LAMP1	5|0|2	3|0|2|0|3	0|0|0|0|0|0|0|0|0|0|0|0|0|0|0|0|0|0|0|0|0|0|0|0|0|0|0|0|0	0.18
TPCN2_734G	O15484	CAPN5	0|8|0	0|0|0|7|0	0|0|0|0|0|0|0|0|0|0|0|0|0|0|0|0|0|0|0|0|0|0|0|0|0|0|0|0|0	0.18
TPCN2_DeltaCT	P09960	LTA4H	4|0|2	3|0|0|0|2	0|0|0|0|0|0|0|0|0|0|0|0|0|0|0|0|0|0|0|0|0|0|0|0|0|0|0|0|0	0.18
TPCN2_DeltaCT	P46063	RECQL	5|0|0	0|0|0|0|3	0|0|1|0|0|1|1|0|0|0|0|0|1|0|0|0|0|0|0|0|0|0|1|0|0|0|0|0|0|1	0.18
TPCN2_DeltaCT	O75153	CLUH	5|0|0	5|0|0|0|0	0|0|0|0|0|0|0|0|0|0|0|0|0|0|0|0|0|0|0|0|0|0|0|0|0|0|0|0|0	0.18
TPCN2_734E	O75691	UTP20	3|0|0	0|0|0|0|0	0|0|0|0|0|0|0|0|0|0|0|0|0|0|0|0|0|1|2|0|0|0|0|0|0|0|1|0	0.17
TPCN2_734E	P29590	PML	3|0|0	0|0|0|0|0	0|0|1|0|0|1|0|0|0|0|0|0|0|0|0|0|0|0|0|0|0|0|0|0|0|0|1|0|0|1|0|0|0|0	0.17
TPCN2_734E	Q13510	ASAH1	3|0|0	0|0|0|0|0	0|0|1|0|2|0|1|0|0|0|0|0|0|0|0|0|0|0|0|0|0|0|0|0|0|0|0|0|0|0	0.17

TPCN2_734E	P20645	M6PR	5|0|0	4|0|0|0|3	0|0|0|0|0|0|0|0|0|0|0|0|0|0|0|0|0|0|0|0|0|0|0|0|0|0|0|0|0|0|0	0.17
TPCN2_734E	Q9H9J2	MRPL44	0|8|0	0|0|0|9|0	0|0|0|0|0|0|0|1|0|1|1|0|1|0|0|0|0|0|0|0|0|0|0|0|0|0|0|0|0|0|0	0.17
TPCN2_DeltaCT	O95202	LETM1	10|0|0	5|0|0|0|7	0|0|0|0|0|0|0|0|0|0|0|1|0|0|0|0|0|0|0|0|0|0|0|0|0|0|0|0|0|1	0.17
TPCN2_DeltaCT	Q15075	EEA1	8|0|0	0|0|6|0|4	0|0|0|0|0|0|0|0|0|0|0|0|0|0|0|0|0|0|0|0|0|0|0|0|0|0|0|0|0|0|0	0.17
TPCN2_DeltaCT	P81605	DCD	0|6|0	0|0|0|4|2	0|0|0|0|0|0|0|2|2|2|1|1|0|0|0|0|0|0|0|0|0|0|0|0|0|0|0|0|0|0|0	0.17
TPCN2_734E	P35222	CTNNB1	33|0|9	38|10|11|0|18	0|0|0|0|0|0|0|0|0|0|0|0|0|0|0|0|0|0|0|0|0|0|0|0|0|0|0|0|0|0|0	0.16
TPCN2_734E	P53992	SEC24C	6|0|0	5|0|0|0|0	0|0|0|0|0|0|0|1|1|2|0|0|1|0|0|0|0|0|0|0|0|0|0|0|0|0|0|0|0|0|1	0.16
TPCN2_734G	Q08188	TGM3	0|4|0	0|0|0|3|0	0|0|0|0|0|0|0|0|0|0|0|0|0|0|0|0|0|0|0|0|0|0|0|0|0|0|0|0|0|0|0	0.16
TPCN2_734G	P31939	ATIC	5|0|0	4|0|0|0|0	0|0|0|0|0|0|0|0|0|0|0|0|0|0|0|0|0|0|0|0|0|0|0|0|0|0|0|0|0|0|0	0.16
TPCN2_DeltaCT	Q9BZL6	PRKD2	0|0|21	0|12|22|0|6	0|0|0|0|0|0|0|0|0|0|0|0|0|0|0|0|0|0|0|0|0|0|0|0|0|0|0|0|0|0|0	0.16
TPCN2_DeltaCT	O60313	OPA1	16|0|0	18|0|0|0|10	0|0|0|0|0|0|0|0|0|0|0|0|0|0|0|0|0|0|0|0|0|0|0|0|0|0|0|0|0|0|0	0.16

TPCN2_DeltaCT	Q9NTJ5	SACM1L	7|0|2	3|0|0|0|7	0|0|0|0|0|0|0|0|0|0|0|0|0|0|0|0|0|0|0|0|0|0|0|0|0|0|0|0|0|0|0	0.16
TPCN2_DeltaCT	P33121	ACSL1	30|0|5	31|4|0|0|29	0|0|0|0|0|0|0|0|0|0|0|0|0|0|0|0|0|0|0|0|0|0|0|0|0|0|0|0|0|0|0	0.16
TPCN2_DeltaCT	Q6AZW8	ZNF660	0|0|4	0|3|0|0|0	0|0|0|0|0|0|0|0|0|0|0|0|0|0|0|0|0|0|0|0|0|0|0|1|0|0|0|0|0|0	0.16
TPCN2_734E	Q9HD20	ATP13A1	2|0|0	0|0|0|0|0	0|1|0|0|0|0|0|0|0|0|0|0|0|0|0|0|0|0|0|0|0|0|0|0|0|0|0|0|0|0|0	0.15
TPCN2_734E	Q6P158	DHX57	2|0|0	0|0|0|0|0	0|0|0|0|0|0|0|0|0|0|0|1|1|0|0|0|0|0|0|0|0|0|0|0|0|0|0|0|0|0|0	0.15
TPCN2_734E	Q16666	IFI16	7|0|0	10|0|0|0|3	0|0|0|0|0|0|0|0|0|0|0|0|0|0|0|0|0|0|0|0|0|0|0|0|0|0|0|0|0|0|0	0.15
TPCN2_734G	P13473	LAMP2	3|0|0	2|0|0|0|0	0|0|0|0|0|0|0|0|0|0|0|0|0|0|0|0|0|0|0|0|0|0|0|0|0|0|0|0|0|0|0	0.15
TPCN2_734G	Q8WXX5	DNAJC9	0|0|3	0|2|0|0|0	0|0|0|0|0|0|0|0|0|0|0|0|0|0|0|0|0|0|0|0|0|0|0|0|0|0|0|0|0|0|0	0.15
TPCN2_734G	Q92973	TNPO1	8|0|0	5|0|0|0|3	0|0|0|0|0|1|0|0|0|0|0|0|0|0|0|0|0|0|0|0|0|0|0|0|0|0|0|0|0|0|2	0.15
TPCN2_DeltaCT	P17931	LGALS3	7|0|2	3|2|3|0|4	0|0|0|0|0|0|0|0|0|0|0|0|0|0|0|0|0|0|0|0|0|0|0|0|0|0|0|0|0|0|2	0.15
TPCN2_DeltaCT	Q8WTV0	SCARB1	3|0|0	3|0|0|0|0	0|0|0|0|0|0|0|0|0|0|0|0|0|0|0|0|0|0|0|0|0|0|0|0|0|0|0|0|0|0|0	0.15

TPCN2_DeltaCT	P17643	TYRP1	29|0|10	25|10|8|0|20	0|0|0|0|0|0|0|0|0|0|0|0|0|0|0|0|0|0|0|0|0|0|0|0|0|0|0|0|0|0|0	0.15
TPCN2_DeltaCT	P00505	GOT2	15|0|0	11|0|2|0|14	0|0|0|0|0|0|0|0|0|0|0|0|0|0|0|0|0|0|0|0|0|0|0|0|0|0|0|0|0|0|0	0.15
TPCN2_DeltaCT	P27695	APEX1	0|0|5	0|0|0|0|0	0|0|0|0|0|0|0|0|0|0|0|0|0|0|0|0|0|0|0|0|0|0|0|0|0|0|0|0|1|4	0.15
TPCN2_DeltaCT	Q9NYU2	UGGT1	5|0|0	4|0|0|0|2	0|0|0|0|0|0|0|0|0|0|0|0|0|0|0|0|0|0|0|0|0|0|0|0|0|0|0|0|0|0|0	0.15
TPCN2_DeltaCT	Q15155	NOMO1	3|0|0	0|0|0|0|3	0|0|0|0|0|0|0|0|0|0|0|0|0|0|0|0|0|0|0|0|0|0|0|0|0|0|0|0|0|0|0	0.15
TPCN2_DeltaCT	Q8N3E9	PLCD3	0|0|3	0|0|3|0|0	0|0|0|0|0|0|0|0|0|0|0|0|0|0|0|0|0|0|0|0|0|0|0|0|0|0|0|0|0|0|0	0.15
TPCN2_DeltaCT	P05455	SSB	9|0|0	3|0|0|0|5	0|2|3|2|0|4|0|0|0|0|0|0|0|0|2|0|0|1|0|1|1|0|1|0|0|0|0|0|1|3	0.15
TPCN2_734E	Q6PD62	CTR9	5|0|0	2|0|0|0|0	1|0|2|0|0|0|0|0|0|0|0|0|0|0|0|1|1|1|0|2|0|1|0|0|0|0|0|0|1|0	0.14
TPCN2_734E	Q92570	NR4A3	3|0|0	2|0|0|0|2	0|0|0|0|0|0|0|0|0|0|0|0|0|0|0|0|0|0|0|0|0|0|0|0|0|0|0|0|0|0|0	0.14
TPCN2_734E	Q9NTZ6	RBM12	3|0|0	3|0|0|0|0	0|0|0|0|0|1|0|0|0|0|0|0|0|0|0|0|0|0|0|0|0|0|0|0|0|0|0|0|0|0|0	0.14
TPCN2_734E	O60488	ACSL4	6|0|0	4|0|0|0|0	1|1|0|0|0|1|2|1|1|2|1|0|0|0|0|0|1|1|2|1|1|1|1|0|0|1|1|1|1|0	0.14

TPCN2_734E	P00390	GSR	2|0|0	2|0|0|0|0	0|0|0|0|0|0|0|0|0|0|0|0|0|0|0|0|0|0|0|0|0|0|0|0|0|0|0|0	0.14
TPCN2_734E	P06396	GSN	13|0|7	17|2|8|0|5	0|0|0|0|0|0|0|0|0|0|0|0|0|0|0|0|0|0|0|0|0|0|0|0|0|0|0|0	0.14
TPCN2_734E	P46019	PHKA2	2|0|0	0|0|0|0|2	0|0|0|0|0|0|0|0|0|0|0|0|0|0|0|0|0|0|0|0|0|0|0|0|0|0|0|0	0.14
TPCN2_734E	Q96HY7	DHTKD1	3|0|0	0|0|0|0|2	0|0|0|0|0|0|0|0|0|0|1|1|1|0|0|0|0|0|0|0|0|0|0|0|0|0|0|0	0.14
TPCN2_734E	Q9NZB2	FAM120A	5|0|0	0|0|0|0|0	1|0|1|1|0|0|0|0|0|0|0|1|0|1|2|0|0|1|1|1|1|0|1|0|0|1|1|2|0|0	0.14
TPCN2_734E	Q6ZVF9	GPRIN3	0|0|2	0|0|2|0|0	0|0|0|0|0|0|0|0|0|0|0|0|0|0|0|0|0|0|0|0|0|0|0|0|0|0|0|0	0.14
TPCN2_734E	Q6AZW8	ZNF660	0|0|3	0|3|0|0|0	0|0|0|0|0|0|0|0|0|0|0|0|0|0|0|0|0|0|0|0|0|0|1|0|0|0|0|0	0.14
TPCN2_734E	O14964	HGS	6|0|0	4|0|0|0|0	0|0|2|0|0|1|1|0|0|0|0|0|0|0|0|0|0|0|0|0|0|3|1|2|1|1|0|0|0|0	0.14
TPCN2_734E	Q14690	PDCD11	3|0|0	0|0|0|0|0	0|0|0|0|0|0|0|0|0|0|0|0|0|0|0|1|1|0|0|0|2|0|0|0|0|0|1|0	0.14
TPCN2_734E	P43007	SLC1A4	8|0|0	11|0|0|0|6	0|0|0|0|0|0|0|0|0|0|0|0|0|0|0|0|0|0|0|0|0|0|0|0|0|0|0|0	0.14
TPCN2_734G	Q9BZL6	PRKD2	0|0|24	0|12|22|0|6	0|0|0|0|0|0|0|0|0|0|0|0|0|0|0|0|0|0|0|0|0|0|0|0|0|0|0|0	0.14

TPCN2_DeltaCT	P52789	HK2	6|0|0	0|0|0|0|6	0|0|0|0|0|0|0|1|0|0|0|0|0|0|0|0|1|0|0|0|0|0|0|0|0|0|0|0|0|0|0	0.14
TPCN2_DeltaCT	P40967	PMEL	8|0|3	7|0|2|0|5	0|0|0|0|0|0|0|0|0|0|0|0|0|0|0|0|0|0|0|0|0|0|0|0|0|0|0	0.14
TPCN2_DeltaCT	Q9H9J2	MRPL44	0|8|0	0|0|0|9|0	0|0|0|0|0|0|0|1|0|1|1|0|1|0|0|0|0|0|0|0|0|0|0|0|0|0|0|0	0.14
TPCN2_DeltaCT	Q16891	IMMT	24|0|0	24|2|0|0|17	0|0|1|1|0|0|0|1|2|2|0|2|1|0|0|0|1|0|0|0|0|0|1|0|0|0|0|0|0|0	0.14
TPCN2_734E	P04181	OAT	24|0|0	18|2|2|0|14	0|0|0|0|0|0|0|3|2|4|4|6|6|0|0|0|0|0|0|0|0|0|1|0|0|0|0|0|0|6	0.13
TPCN2_734E	Q7L2E3	DHX30	12|0|0	5|0|0|0|4	0|0|2|0|0|0|0|2|3|6|7|4|4|0|0|0|0|0|0|0|0|0|1|0|0|1|0|0|3|0	0.13
TPCN2_734E	O00116	AGPS	5|0|0	3|0|0|0|5	0|0|0|0|0|0|0|1|0|0|0|0|0|0|0|0|0|0|0|0|0|0|0|0|0|0|0	0.13
TPCN2_734E	P40967	PMEL	7|0|0	7|0|2|0|5	0|0|0|0|0|0|0|0|0|0|0|0|0|0|0|0|0|0|0|0|0|0|0|0|0|0|0	0.13
TPCN2_734E	Q92542	NCSTN	3|0|0	5|0|0|0|0	0|0|0|0|0|0|0|0|0|0|0|0|0|0|0|0|0|0|0|0|0|0|0|0|0|0|0	0.13
TPCN2_734G	O60313	OPA1	17|0|0	18|0|0|0|10	0|0|0|0|0|0|0|0|0|0|0|0|0|0|0|0|0|0|0|0|0|0|0|0|0|0|0	0.13
TPCN2_734G	P81605	DCD	2|6|0	0|0|0|4|2	0|0|0|0|0|0|0|2|2|2|1|1|0|0|0|0|0|0|0|0|0|0|0|0|0|0|0|0	0.13

TPCN2_734G	Q16891	IMMT	27|0|0	24|2|0|0|17	0|0|1|1|0|0|0|1|2|2|0|2|1|0|0|0|1|0|0|0|0|0|1|0|0|0|0|0|0|0	0.13
TPCN2_Delta CT	P04179	SOD2	5|0|0	4|0|0|0|3	0|0|0|0|0|0|0|0|0|0|0|0|0|0|0|0|0|0|0|0|0|0|0|0|0|0|0	0.13
TPCN2_Delta CT	O75691	UTP20	3|0|0	0|0|0|0|0	0|0|0|0|0|0|0|0|0|0|0|0|0|0|1|2|0|0|0|0|0|0|0|0|1|0	0.13
TPCN2_Delta CT	O95782	AP2A1	5|0|0	0|0|0|0|0	0|0|3|0|0|2|0|0|0|0|0|0|0|0|0|0|0|0|0|0|0|1|2|0|1|1|0|1|0|0	0.13
TPCN2_Delta CT	P40925	MDH1	9|0|4	11|2|0|0|5	0|0|0|0|0|0|0|0|0|0|0|0|0|0|0|0|0|0|0|0|0|0|0|0|0|0|0	0.13
TPCN2_Delta CT	Q8TAT6	NPLOC4	7|0|0	4|0|0|0|4	0|0|2|1|0|3|3|0|0|0|0|0|0|0|0|0|0|0|1|0|0|0|0|0|2|0|0|0|0	0.13
TPCN2_Delta CT	Q14590	ZNF235	0|0|4	0|4|0|0|0	0|0|0|0|0|0|0|0|0|0|0|0|0|0|0|0|0|0|0|0|0|0|0|0|1|0|0|0|0|0|0	0.13
TPCN2_734E	Q9HCM4	EPB41L5	6|8|28	6|11|17|12|24	0|0|0|0|0|0|1|0|0|0|0|0|0|0|0|0|0|0|0|0|1|0|0|0|0|0|0|0	0.12
TPCN2_734E	P49588	AARS	8|0|5	11|0|2|0|0	0|0|0|1|0|1|5|0|0|0|0|0|0|0|0|0|0|0|0|0|0|0|1|0|0|0|0|0|0	0.12
TPCN2_734E	Q9NW13	RBM28	17|0|2	16|0|0|2|11	0|0|1|1|1|0|4|0|0|1|0|0|0|0|2|3|1|0|0|0|1|0|1|0|0|1|1|2|2|0	0.12
TPCN2_734E	P15586	GNS	2|0|2	2|0|0|0|3	0|0|0|0|0|0|0|0|0|0|0|0|0|0|0|0|0|0|0|0|0|0|0|0|0|0|0	0.12

TPCN2_734E	P06702	S100A9	0|2|0	0|0|0|3|0	0|0|0|0|0|0|0|0|0|0|0|0|0|0|0|0|0|0|0|0|0|0|0|0|0|0|0|0	0.12
TPCN2_734E	Q14590	ZNF235	0|0|3	0|4|0|0|0	0|0|0|0|0|0|0|0|0|0|0|0|0|0|0|0|0|0|0|0|0|1|0|0|0|0|0|0	0.12
TPCN2_734E	Q5T749	KPRP	0|6|0	0|0|9|5|0	0|0|0|0|0|0|0|0|0|0|0|0|0|0|0|0|0|0|0|0|0|0|0|0|0|0|0|0	0.12
TPCN2_734G	Q9HCM4	EPB41L5	15|14|32	6|11|17|12|24	0|0|0|0|0|0|1|0|0|0|0|0|0|0|0|0|0|0|0|0|0|1|0|0|0|0|0|0	0.12
TPCN2_734G	P33121	ACSL1	30|0|0	31|4|0|0|29	0|0|0|0|0|0|0|0|0|0|0|0|0|0|0|0|0|0|0|0|0|0|0|0|0|0|0|0	0.12
TPCN2_DeltaCT	Q96AG4	LRRC59	0|0|12	2|7|10|0|0	1|0|1|0|0|0|0|0|0|0|0|0|0|0|0|0|0|0|1|1|0|1|0|0|0|0|0|0|4	0.12
TPCN2_DeltaCT	P07602	PSAP	8|0|0	6|0|2|0|6	0|0|0|0|0|0|0|0|0|0|0|0|0|0|0|0|0|0|0|0|0|0|0|0|0|0|0|0	0.12
TPCN2_DeltaCT	P51659	HSD17B4	9|0|0	8|0|0|0|7	0|0|0|0|0|0|0|0|0|0|0|0|0|0|0|0|0|0|0|0|0|0|0|0|0|0|0|2	0.12
TPCN2_734E	P08962	CD63	12|0|8	11|7|6|0|8	0|0|0|0|0|0|0|0|0|0|0|0|0|0|0|0|0|0|0|0|0|0|0|0|0|0|0|0	0.11
TPCN2_734E	O43747	AP1G1	4|0|0	4|0|0|0|4	0|0|0|0|0|0|0|0|0|0|0|0|0|0|0|0|0|0|0|0|0|0|0|0|0|0|0|0	0.11
TPCN2_734E	Q99536	VAT1	20|0|8	22|6|6|0|18	0|0|0|0|0|0|0|0|0|0|0|0|0|0|0|0|0|0|0|0|0|0|0|0|0|0|0|0	0.11

TPCN2_734G	P51159	RAB27A	2|5|6	4|0|2|2|4	0|0|0|0|0|0|0|0|0|0|0|0|0|0|0|0|0|0|0|0|0|0|0|0|0|0|0|0	0.11
TPCN2_734G	P40925	MDH1	11|0|0	11|2|0|0|5	0|0|0|0|0|0|0|0|0|0|0|0|0|0|0|0|0|0|0|0|0|0|0|0|0|0|0|0	0.11
TPCN2_734G	P19367	HK1	25|0|0	19|2|2|0|23	0|0|0|0|0|0|1|0|0|0|0|0|0|0|0|0|0|0|0|0|0|0|0|0|0|0|0|5	0.11
TPCN2_DeltaCT	P37837	TALDO1	6|0|0	6|0|0|0|3	0|0|0|0|0|1|0|0|0|0|0|0|0|0|0|0|0|0|0|0|0|0|0|0|0|0|0|0	0.11
TPCN2_DeltaCT	P13798	APEH	2|0|0	2|0|0|0|0	0|0|0|0|0|0|0|0|0|0|0|0|0|0|0|0|0|0|0|0|0|0|0|0|0|0|0|0	0.11
TPCN2_DeltaCT	Q00796	SORD	2|0|0	2|0|0|0|0	0|0|0|0|0|0|0|0|0|0|0|0|0|0|0|0|0|0|0|0|0|0|0|0|0|0|0|0	0.11
TPCN2_DeltaCT	P10323	ACR	2|0|0	2|0|0|0|0	0|0|0|0|0|0|0|0|0|0|0|0|0|0|0|0|0|0|0|0|0|0|0|0|0|0|0|0	0.11
TPCN2_DeltaCT	Q9NR45	NANS	3|0|0	4|0|0|0|0	0|0|0|0|0|0|0|0|0|0|0|0|0|0|0|0|0|0|0|0|0|0|0|0|0|0|0|0	0.11
TPCN2_DeltaCT	Q8WYA6	CTNNBL1	2|0|0	2|0|0|0|0	0|0|0|0|0|0|0|0|0|0|0|0|0|0|0|0|0|0|0|0|0|0|0|0|0|0|0|0	0.11
TPCN2_DeltaCT	Q9HDC9	APMAP	2|0|0	0|0|0|0|0	0|0|0|0|0|0|0|1|0|0|0|0|0|0|0|0|0|0|0|0|0|0|0|0|0|1|0|0	0.11
TPCN2_DeltaCT	Q6ZR52	ZNF493	0|0|2	0|0|0|0|0	0|1|0|0|0|0|0|0|0|0|0|0|0|0|0|0|0|0|0|0|0|0|0|0|0|0|0|0|0	0.11

TPCN2_DeltaCT	O75083	WDR1	10|0|5	12|3|3|0|4	0|0|0|0|0|0|0|0|0|0|0|0|0|0|0|0|0|0|0|0|0|0|0|0|0|0|0|0|0|0|1|0	0.11
TPCN2_DeltaCT	O15143	ARPC1B	2|0|0	0|0|0|0|0	0|0|0|0|0|0|0|0|1|0|1|0|0|0|0|0|0|0|0|0|0|0|0|0|0|0|0|0|0|0|0	0.11
TPCN2_DeltaCT	P06396	GSN	14|0|6	17|2|8|0|5	0|0|0|0|0|0|0|0|0|0|0|0|0|0|0|0|0|0|0|0|0|0|0|0|0|0|0|0|0|0|0	0.11
TPCN2_DeltaCT	O43747	AP1G1	5|0|0	4|0|0|0|4	0|0|0|0|0|0|0|0|0|0|0|0|0|0|0|0|0|0|0|0|0|0|0|0|0|0|0|0|0|0|0	0.11
TPCN2_DeltaCT	Q93050	ATP6V0A1	2|0|0	0|0|0|0|2	0|0|0|0|0|0|0|0|0|0|0|0|0|0|0|0|0|0|0|0|0|0|0|0|0|0|0|0|0|0|0	0.11
TPCN2_DeltaCT	Q9BXJ9	NAA15	4|0|0	2|0|0|0|0	0|0|0|1|0|3|0|0|0|0|0|0|0|0|0|0|0|0|0|0|0|0|0|0|0|0|0|0|0|0|0	0.11
TPCN2_DeltaCT	P42766	RPL35	0|2|11	7|6|7|0|0	0|0|1|0|0|0|0|0|0|0|0|0|0|0|0|0|0|0|0|0|0|0|0|0|0|0|0|0|0|0|0	0.11
TPCN2_DeltaCT	P12273	PIP	0|2|0	0|0|0|2|0	0|0|0|0|0|0|0|0|0|0|0|0|0|0|0|0|0|0|0|0|0|0|0|0|0|0|0|0|0|0|0	0.11
TPCN2_DeltaCT	O14964	HGS	6|0|0	4|0|0|0|0	0|0|2|0|0|1|1|0|0|0|0|0|0|0|0|0|0|0|0|0|0|3|1|2|1|1|0|0|0|0	0.11
TPCN2_DeltaCT	P30086	PEBP1	0|0|2	2|0|0|0|0	0|0|0|0|0|0|0|0|0|0|0|0|0|0|0|0|0|0|0|0|0|0|0|0|0|0|0|0|0|0|0	0.11
TPCN2_DeltaCT	Q92973	TNPO1	6|0|0	5|0|0|0|3	0|0|0|0|0|1|0|0|0|0|0|0|0|0|0|0|0|0|0|0|0|0|0|0|0|0|0|0|0|0|2	0.11

TPCN2_734E	P40222	TXLNA	3|0|0	2|0|0|0|0	0|0|0|1|1|0|0|0|0|0|0|0|0|0|0|0|0|0|0|0|0|0|1|0|0|1|0|0|0|0	0.1
TPCN2_734E	Q9HAU0	PLEKHA5	6|0|0	0|0|0|0|0	4|4|1|0|0|1|2|0|0|0|0|0|0|0|2|0|0|0|0|2|1|0|1|0|0|0|0|0|0|0	0.1
TPCN2_734E	P16435	POR	5|0|0	3|0|0|0|0	0|0|0|0|0|0|0|1|2|2|1|1|1|0|0|0|0|0|2|1|0|0|0|0|0|0|0|0|0|0	0.1
TPCN2_734E	P04040	CAT	4|0|0	3|0|0|0|3	0|0|0|0|0|0|0|1|1|1|0|0|0|0|0|0|0|0|0|0|0|0|0|0|0|0|0|0	0.1
TPCN2_734E	Q92797	SYMPK	6|0|0	0|0|0|0|0	1|2|1|1|0|0|1|0|0|0|0|0|0|0|1|0|0|2|1|3|2|1|3|1|1|2|0|1|1|0	0.1
TPCN2_734E	P54709	ATP1B3	2|0|0	0|0|0|0|0	0|0|1|2|0|0|0|0|0|0|0|0|0|0|0|0|0|0|0|0|0|0|0|0|0|0|0|0|0	0.1
TPCN2_734E	Q13045	FLII	2|0|0	0|0|0|0|0	0|0|1|0|0|0|0|0|0|0|0|0|0|0|0|0|0|0|0|0|0|0|0|1|0|0|0|0|1	0.1
TPCN2_734G	Q14678	KANK1	14|16|31	0|14|33|5|14	1|0|1|0|0|0|0|0|0|0|0|0|0|0|0|0|0|0|0|0|0|0|3|0|0|0|0|0|0|0	0.1
TPCN2_734G	P06396	GSN	16|0|0	17|2|8|0|5	0|0|0|0|0|0|0|0|0|0|0|0|0|0|0|0|0|0|0|0|0|0|0|0|0|0|0|0|0	0.1
TPCN2_DeltaCT	Q92570	NR4A3	3|0|0	2|0|0|0|2	0|0|0|0|0|0|0|0|0|0|0|0|0|0|0|0|0|0|0|0|0|0|0|0|0|0|0|0|0	0.1
TPCN2_DeltaCT	P15559	NQO1	11|0|5	10|6|3|0|7	0|0|0|0|0|0|0|0|0|0|0|0|0|0|0|0|0|0|0|0|0|0|0|0|0|0|0|0|0	0.1

TPCN2_DeltaCT	P02765	AHSG	3|0|0	0|0|0|2|2	0|0|0|0|0|0|0|0|0|0|0|0|0|0|0|0|0|0|0|0|0|0|0|0|0|0|0|0|0|0|0	0.1
TPCN2_DeltaCT	P54727	RAD23B	3|0|0	3|0|0|0|0	0|0|0|0|0|0|0|0|0|0|0|0|0|0|0|0|0|0|0|0|0|0|0|0|0|0|0|0|0|0|1	0.1
TPCN2_DeltaCT	P29401	TKT	34|0|13	31|14|10|0|23	1|0|0|0|0|0|0|0|0|0|0|0|0|0|0|0|1|0|0|0|0|0|1|0|0|1|0|0|0|0|2	0.1
TPCN2_DeltaCT	O14980	XPO1	12|0|4	9|2|3|0|5	0|0|1|0|0|4|3|3|1|3|1|1|1|0|0|1|1|0|0|0|0|2|1|4|2|1|0|0|4|2	0.1
TPCN2_DeltaCT	P40121	CAPG	19|0|10	19|8|7|0|13	0|0|0|0|0|0|0|0|0|0|0|0|0|0|0|0|0|0|0|0|0|0|0|0|0|0|0|0|0|0|0	0.1
TPCN2_DeltaCT	P27487	DPP4	3|0|0	2|0|0|0|2	0|0|0|0|0|0|0|0|0|0|0|0|0|0|0|0|0|0|0|0|0|0|0|0|0|0|0|0|0|0|0	0.1
TPCN2_DeltaCT	Q16881	TXNRD1	5|0|0	6|0|0|0|2	0|0|0|0|0|0|0|0|0|0|0|0|0|0|0|0|0|0|0|0|0|0|0|0|0|0|0|0|1|0|0|0	0.1
TPCN2_DeltaCT	Q96HY7	DHTKD1	3|0|0	0|0|0|0|2	0|0|0|0|0|0|0|0|0|0|1|1|1|0|0|0|0|0|0|0|0|0|0|0|0|0|0|0|0|0|0	0.1
TPCN2_DeltaCT	Q99536	VAT1	21|0|8	22|6|6|0|18	0|0|0|0|0|0|0|0|0|0|0|0|0|0|0|0|0|0|0|0|0|0|0|0|0|0|0|0|0|0|0	0.1
TPCN2_DeltaCT	Q92542	NCSTN	3|0|0	5|0|0|0|0	0|0|0|0|0|0|0|0|0|0|0|0|0|0|0|0|0|0|0|0|0|0|0|0|0|0|0|0|0|0|0	0.1
TPCN2_DeltaCT	Q5T749	KPRP	0|3|6	0|0|9|5|0	0|0|0|0|0|0|0|0|0|0|0|0|0|0|0|0|0|0|0|0|0|0|0|0|0|0|0|0|0|0|0	0.1

TPCN2_734E	Q969P0	IGSF8	3|0|0	4|0|0|0|2	0|0|0|0|0|0|0|0|0|0|0|0|0|0|0|0|0|0|0|0|0|0|0|0|0|0|0|0|0|0|0	0.09
TPCN2_734E	Q15031	LARS2	9|0|0	7|0|0|0|8	0|0|0|0|0|0|0|2|0|0|1|2|5|0|0|0|0|0|0|0|0|0|0|0|0|0|0|0|0|0|0	0.09
TPCN2_734E	Q3SXM5	HSDL1	0|2|0	0|0|0|0|5	0|0|0|0|0|0|0|0|0|0|0|0|0|0|0|0|0|0|0|0|0|0|0|0|0|0|0|0|0|0|0	0.09
TPCN2_734E	Q9NTJ5	SACM1L	4|0|0	3|0|0|0|7	0|0|0|0|0|0|0|0|0|0|0|0|0|0|0|0|0|0|0|0|0|0|0|0|0|0|0|0|0|0|0	0.09
TPCN2_734G	Q5T749	KPRP	0|8|0	0|0|9|5|0	0|0|0|0|0|0|0|0|0|0|0|0|0|0|0|0|0|0|0|0|0|0|0|0|0|0|0|0|0|0|0	0.09
TPCN2_734G	P53992	SEC24C	6|0|0	5|0|0|0|0	0|0|0|0|0|0|0|1|1|2|0|0|1|0|0|0|0|0|0|0|0|0|0|0|0|0|0|0|0|0|1	0.09
TPCN2_DeltaCT	Q9Y5S1	TRPV2	2|0|0	0|0|0|0|3	0|0|0|0|0|0|0|0|0|0|0|0|0|0|0|0|0|0|0|0|0|0|0|0|0|0|0|0|0|0|0	0.09
TPCN2_DeltaCT	P49588	AARS	9|0|3	11|0|2|0|0	0|0|0|1|0|1|5|0|0|0|0|0|0|0|0|0|0|0|0|0|0|0|0|0|0|0|0|0|0|0|0	0.09
TPCN2_DeltaCT	P20645	M6PR	4|0|0	4|0|0|0|3	0|0|0|0|0|0|0|0|0|0|0|0|0|0|0|0|0|0|0|0|0|0|0|0|0|0|0|0|0|0|0	0.09
TPCN2_DeltaCT	Q96AE4	FUBP1	10|0|0	7|0|0|0|7	3|0|2|1|1|2|1|0|0|0|0|0|0|2|2|0|0|0|0|0|1|0|3|0|0|1|1|2|0|2	0.09
TPCN2_DeltaCT	P06702	S100A9	0|2|0	0|0|0|3|0	0|0|0|0|0|0|0|0|0|0|0|0|0|0|0|0|0|0|0|0|0|0|0|0|0|0|0|0|0|0|0	0.09

TPCN2_DeltaCT	Q9UHG3	PCYOX1	2|0|0	3|0|0|0|0	0|0|0|0|0|0|0|0|0|0|0|0|0|0|0|0|0|0|0|0|0|0|0|0|0|0|0|0	0.09
TPCN2_DeltaCT	Q96I59	NARS2	9|2|0	6|0|0|0|8	0|0|0|0|0|0|0|1|1|1|4|0|1|0|0|0|0|0|0|0|0|0|0|0|0|0|0|0|0	0.09
TPCN2_DeltaCT	Q08554	DSC1	0|4|0	0|0|2|4|0	0|0|0|0|0|0|0|1|0|0|0|0|0|0|0|0|0|0|0|0|0|0|0|0|0|0|0	0.09
TPCN2_DeltaCT	Q92900	UPF1	3|0|0	0|2|0|2|0	0|0|0|0|0|1|0|0|0|0|0|0|0|0|0|0|0|0|0|0|0|0|0|0|0|0|0	0.09
TPCN2_734E	P51159	RAB27A	0|4|3	4|0|2|2|4	0|0|0|0|0|0|0|0|0|0|0|0|0|0|0|0|0|0|0|0|0|0|0|0|0|0|0|0	0.08
TPCN2_734E	Q8WUH6	TMEM263	0|0|5	0|4|5|0|0	0|0|0|0|0|0|0|0|0|0|0|0|0|0|0|0|0|0|0|0|0|0|0|0|3|1	0.08
TPCN2_734E	P33121	ACSL1	23|0|4	31|4|0|0|29	0|0|0|0|0|0|0|0|0|0|0|0|0|0|0|0|0|0|0|0|0|0|0|0|0|0|0|0	0.08
TPCN2_734E	Q08554	DSC1	0|3|0	0|0|2|4|0	0|0|0|0|0|0|0|1|0|0|0|0|0|0|0|0|0|0|0|0|0|0|0|0|0|0|0	0.08
TPCN2_734G	Q8WZ42	TTN	5|0|0	3|0|0|0|4	0|0|0|0|0|0|0|0|0|0|0|0|0|1|0|0|0|0|0|0|0|0|0|0|0|0|0|0	0.08
TPCN2_734G	P52789	HK2	5|0|0	0|0|0|0|6	0|0|0|0|0|0|0|1|0|0|0|0|0|1|0|0|0|0|0|0|0|0|0|0|0|0|0|0	0.08
TPCN2_734G	P08133	ANXA6	15|0|0	13|6|6|0|8	0|0|0|0|0|1|0|0|0|0|0|0|0|0|0|0|0|0|0|0|0|0|0|0|0|0|0|0	0.08

TPCN2_734G	P51659	HSD17B4	9|0|0	8|0|0|0|7	0|0|0|0|0|0|0|0|0|0|0|0|0|0|0|0|0|0|0|0|0|0|0|0|0|0|0|0|0|2	0.08
TPCN2_734G	Q3SXM5	HSDL1	2|2|0	0|0|0|0|5	0|0|0|0|0|0|0|0|0|0|0|0|0|0|0|0|0|0|0|0|0|0|0|0|0|0|0|0|0|0	0.08
TPCN2_734G	Q5C9Z4	NOM1	12|23|7	11|6|6|22|11	0|0|0|0|0|0|0|0|0|0|0|0|0|0|0|0|0|0|0|0|0|0|0|0|0|0|0|0|0|0	0.08
TPCN2_DeltaCT	P05109	S100A8	0|0|3	0|0|2|3|0	0|0|0|0|0|0|0|0|0|0|0|0|0|0|0|0|0|0|0|0|0|0|0|0|0|0|0|0|0|0	0.08
TPCN2_DeltaCT	P49736	MCM2	16|0|2	16|2|0|0|4	0|0|0|0|0|2|0|0|0|0|0|0|0|0|0|0|0|0|0|0|0|0|0|0|0|0|0|0|0|18	0.08
TPCN2_DeltaCT	Q15046	KARS	9|0|0	7|0|0|0|2	0|0|1|1|2|0|0|0|0|0|0|0|0|0|0|2|3|0|0|0|0|4|1|0|3|3|0|0|0|2	0.08
TPCN2_DeltaCT	P55786	NPEPPS	9|0|4	9|0|0|0|2	0|0|1|0|1|2|2|0|0|0|0|0|0|0|0|0|0|0|0|0|0|0|3|0|1|1|0|0|2|1	0.08
TPCN2_DeltaCT	Q00610	CLTC	85|0|17	69|24|28|0|33	2|4|0|1|1|0|1|8|12|10|3|2|4|2|2|0|0|1|2|3|1|3|1|0|3|1|3|1|1|20	0.08
TPCN2_DeltaCT	P07339	CTSD	13|0|5	12|4|5|2|11	0|0|0|0|0|0|0|0|0|0|0|0|0|0|0|0|0|0|0|0|0|0|0|0|0|0|0|0|0|0	0.08
TPCN2_DeltaCT	Q9NSE4	IARS2	11|0|0	8|0|0|0|6	0|0|0|0|0|0|0|2|4|1|4|4|3|0|0|0|0|0|0|0|0|0|0|0|0|0|0|0|0|1	0.08
TPCN2_DeltaCT	P60174	TPI1	13|0|5	16|5|4|0|9	0|0|0|0|0|0|0|0|0|0|0|0|0|0|0|0|0|0|0|0|0|0|0|0|0|0|0|0|0|0	0.08

TPCN2_DeltaCT	O15484	CAPN5	0|3|0	0|0|0|7|0	0|0|0|0|0|0|0|0|0|0|0|0|0|0|0|0|0|0|0|0|0|0|0|0|0|0|0|0|0|0|0	0.08
TPCN2_DeltaCT	Q9Y512	SAMM50	4|0|0	4|0|0|0|4	0|0|0|0|0|0|0|0|0|0|0|0|0|0|0|0|0|0|0|0|0|0|0|0|0|0|0|0|0|0|0	0.08
TPCN2_734E	O96005	CLPTM1	2|0|0	0|0|0|0|3	0|0|0|0|0|0|0|0|0|0|0|0|0|1|0|0|0|0|0|0|0|0|0|0|0|0|0|0|0|0|0	0.07
TPCN2_734E	P02765	AHSG	2|0|0	0|0|0|2|2	0|0|0|0|0|0|0|0|0|0|0|0|0|0|0|0|0|0|0|0|0|0|0|0|0|0|0|0|0|0|0	0.07
TPCN2_734E	P54727	RAD23B	2|0|0	3|0|0|0|0	0|0|0|0|0|0|0|0|0|0|0|0|0|0|0|0|0|0|0|0|0|0|0|0|0|0|0|0|0|0|1	0.07
TPCN2_734E	P00505	GOT2	9|0|0	11|0|2|0|14	0|0|0|0|0|0|0|0|0|0|0|0|0|0|0|0|0|0|0|0|0|0|0|0|0|0|0|0|0|0|0	0.07
TPCN2_734E	O00159	MYO1C	10|0|4	8|2|0|0|5	1|0|0|0|0|0|0|0|0|0|0|0|0|0|1|1|0|0|0|0|0|1|0|0|0|0|0|10|0	0.07
TPCN2_734E	P63010	AP2B1	16|0|0	16|0|0|0|9	1|1|6|0|0|2|0|3|0|1|0|0|0|0|0|0|0|0|0|2|1|4|2|2|0|0|1|0|1	0.07
TPCN2_734E	Q9Y512	SAMM50	3|0|0	4|0|0|0|4	0|0|0|0|0|0|0|0|0|0|0|0|0|0|0|0|0|0|0|0|0|0|0|0|0|0|0|0|0|0|0	0.07
TPCN2_734E	Q92973	TNPO1	4|0|0	5|0|0|0|3	0|0|0|0|0|1|0|0|0|0|0|0|0|0|0|0|0|0|0|0|0|0|0|0|0|0|0|0|0|0|2	0.07
TPCN2_734G	P02765	AHSG	3|0|0	0|0|0|2|2	0|0|0|0|0|0|0|0|0|0|0|0|0|0|0|0|0|0|0|0|0|0|0|0|0|0|0|0|0|0|0	0.07

TPCN2_734G	P49736	MCM2	17|0|0	16|2|0|0|4	0|0|0|0|0|2|0|0|0|0|0|0|0|0|0|0|0|0|0|0|0|0|0|0|0|0|0|0|0|0|0|18	0.07
TPCN2_734G	P10323	ACR	2|0|0	2|0|0|0|0	0|0|0|0|0|0|0|0|0|0|0|0|0|0|0|0|0|0|0|0|0|0|0|0|0|0|0|0|0|0|0	0.07
TPCN2_734G	Q96KP4	CNDP2	2|0|0	2|0|0|0|0	0|0|0|0|0|0|0|0|0|0|0|0|0|0|0|0|0|0|0|0|0|0|0|0|0|0|0|0|0|0|0	0.07
TPCN2_734G	Q14254	FLOT2	0|15|9	0|3|17|6|11	0|0|0|0|0|0|0|0|0|0|0|0|0|0|0|0|0|0|0|0|0|0|0|0|0|0|0|0|0|0|0	0.07
TPCN2_734G	P27487	DPP4	3|0|0	2|0|0|0|2	0|0|0|0|0|0|0|0|0|0|0|0|0|0|0|0|0|0|0|0|0|0|0|0|0|0|0|0|0|0|0	0.07
TPCN2_734G	P17174	GOT1	2|0|0	2|0|0|0|0	0|0|0|0|0|0|0|0|0|0|0|0|0|0|0|0|0|0|0|0|0|0|0|0|0|0|0|0|0|0|0	0.07
TPCN2_734G	Q16610	ECM1	2|0|0	0|0|0|0|2	0|0|0|0|0|0|0|0|0|0|0|0|0|0|0|0|0|0|0|0|0|0|0|0|0|0|0|0|0|0|0	0.07
TPCN2_734G	Q92542	NCSTN	3|0|0	5|0|0|0|0	0|0|0|0|0|0|0|0|0|0|0|0|0|0|0|0|0|0|0|0|0|0|0|0|0|0|0|0|0|0|0	0.07
TPCN2_734G	P12273	PIP	0|2|0	0|0|0|2|0	0|0|0|0|0|0|0|0|0|0|0|0|0|0|0|0|0|0|0|0|0|0|0|0|0|0|0|0|0|0|0	0.07
TPCN2_734G	Q6ZVF9	GPRIN3	0|0|2	0|0|2|0|0	0|0|0|0|0|0|0|0|0|0|0|0|0|0|0|0|0|0|0|0|0|0|0|0|0|0|0|0|0|0|0	0.07
TPCN2_734G	P36871	PGM1	2|0|0	2|0|0|0|0	0|0|0|0|0|0|0|0|0|0|0|0|0|0|0|0|0|0|0|0|0|0|0|0|0|0|0|0|0|0|0	0.07

TPCN2_734G	P43007	SLC1A4	8|0|0	11|0|0|0|6	0|0|0|0|0|0|0|0|0|0|0|0|0|0|0|0|0|0|0|0|0|0|0|0|0|0|0|0	0.07
TPCN2_DeltaCT	O94826	TOMM70	6|0|0	6|0|0|0|9	0|0|0|0|0|0|0|0|0|1|0|0|0|0|0|0|0|0|0|0|0|0|0|0|0|0|0|0	0.07
TPCN2_DeltaCT	P50570	DNM2	4|0|0	3|0|0|0|0	0|0|0|1|0|0|1|0|0|0|0|0|0|0|0|0|0|0|0|0|0|0|1|0|0|0|0|0|3	0.07
TPCN2_DeltaCT	P08962	CD63	12|0|7	11|7|6|0|8	0|0|0|0|0|0|0|0|0|0|0|0|0|0|0|0|0|0|0|0|0|0|0|0|0|0|0|0	0.07
TPCN2_DeltaCT	Q969P0	IGSF8	3|0|0	4|0|0|0|2	0|0|0|0|0|0|0|0|0|0|0|0|0|0|0|0|0|0|0|0|0|0|0|0|0|0|0|0	0.07
TPCN2_DeltaCT	Q96EY7	PTCD3	3|0|0	0|0|0|0|0	0|0|0|0|0|0|0|1|0|1|1|1|1|0|0|0|0|0|0|0|0|0|0|0|0|0|0|1|0	0.07
TPCN2_DeltaCT	P11717	IGF2R	3|0|0	0|0|0|0|0	0|1|0|0|0|0|0|0|0|0|0|0|0|0|1|1|0|0|0|1|1|0|0|0|0|1|0|0|0	0.07
TPCN2_DeltaCT	Q96CV9	OPTN	2|0|0	2|0|0|0|0	0|0|1|0|0|0|0|0|0|0|0|0|0|0|0|0|0|0|0|0|0|0|0|0|0|0|0|0	0.07
TPCN2_DeltaCT	Q9NW13	RBM28	16|0|0	16|0|0|2|11	0|0|1|1|1|0|4|0|0|1|0|0|0|0|2|3|1|0|0|0|1|0|1|0|0|1|1|2|2|0	0.07
TPCN2_DeltaCT	P54709	ATP1B3	2|0|0	0|0|0|0|0	0|0|1|2|0|0|0|0|0|0|0|0|0|0|0|0|0|0|0|0|0|0|0|0|0|0|0|0|0	0.07
TPCN2_DeltaCT	P12081	HARS	0|0|2	0|0|0|0|0	0|0|0|0|0|0|0|0|0|0|0|0|0|0|0|0|0|0|0|0|0|0|0|0|0|0|0|4	0.07

TPCN2_DeltaCT	P07954	FH	13|0|2	12|0|3|0|10	0|0|0|0|0|0|0|2|2|2|2|1|1|0|0|0|0|0|0|0|0|0|0|0|0|0|0|0|0|0	0.07
TPCN2_734E	O00203	AP3B1	9|0|4	3|0|0|0|0	0|2|6|2|1|2|3|0|0|0|0|0|0|0|0|0|1|0|0|0|2|6|1|2|2|0|0|2|4	0.06
TPCN2_734E	P05109	S100A8	0|0|2	0|0|2|3|0	0|0|0|0|0|0|0|0|0|0|0|0|0|0|0|0|0|0|0|0|0|0|0|0|0|0|0|0	0.06
TPCN2_734E	P29401	TKT	30|0|16	31|14|10|0|23	1|0|0|0|0|0|0|0|0|0|0|0|0|0|0|1|0|0|0|0|0|1|0|0|1|0|0|0|0|2	0.06
TPCN2_734E	Q8TCS8	PNPT1	6|0|0	3|0|0|0|2	0|0|0|0|0|0|0|1|1|0|6|1|4|0|0|0|0|0|0|0|0|0|0|0|0|0|0|0|0|0	0.06
TPCN2_734E	Q8TCT9	HM13	5|0|0	3|0|0|0|4	0|0|1|0|0|0|1|0|1|1|2|1|2|0|0|0|0|0|0|0|0|0|0|0|0|0|0|0|0|0	0.06
TPCN2_734E	Q14254	FLOT2	2|12|2	0|3|17|6|11	0|0|0|0|0|0|0|0|0|0|0|0|0|0|0|0|0|0|0|0|0|0|0|0|0|0|0|0|0	0.06
TPCN2_734E	P50995	ANXA11	4|0|3	7|0|2|0|5	0|0|0|0|0|0|0|0|0|0|0|0|0|0|0|0|0|0|0|0|0|0|0|0|0|0|0|0|0	0.06
TPCN2_734E	Q5C9Z4	NOM1	3|19|10	11|6|6|22|11	0|0|0|0|0|0|0|0|0|0|0|0|0|0|0|0|0|0|0|0|0|0|0|0|0|0|0|0|0	0.06
TPCN2_734E	P07237	P4HB	44|0|19	35|17|14|0|30	0|0|0|0|0|0|0|5|1|3|0|1|1|0|0|0|0|0|0|0|0|0|0|2|0|0|0|0|1|0|13	0.06
TPCN2_734E	Q5T1M5	FKBP15	3|0|0	0|0|0|0|0	1|1|0|1|0|0|0|0|0|0|0|0|0|1|0|0|0|0|1|2|0|0|0|0|0|1|0|0	0.06

TPCN2_734E	P15121	AKR1B1	0|0|2	4|0|0|0|2	0|0|0|0|0|0|0|0|0|0|0|0|0|0|0|0|0|0|0|0|0|0|0|0|0|0|0|0|0|0|0	0.06
TPCN2_734G	P29401	TKT	33|0|7	31|14|10|0|23	1|0|0|0|0|0|0|0|0|0|0|0|0|0|0|0|1|0|0|0|0|0|1|0|0|1|0|0|0|0|2	0.06
TPCN2_734G	Q8WTV0	SCARB1	2|0|0	3|0|0|0|0	0|0|0|0|0|0|0|0|0|0|0|0|0|0|0|0|0|0|0|0|0|0|0|0|0|0|0|0|0|0|0	0.06
TPCN2_734G	P00505	GOT2	11|0|0	11|0|2|0|14	0|0|0|0|0|0|0|0|0|0|0|0|0|0|0|0|0|0|0|0|0|0|0|0|0|0|0|0|0|0|0	0.06
TPCN2_734G	Q9Y5S1	TRPV2	2|0|0	0|0|0|0|3	0|0|0|0|0|0|0|0|0|0|0|0|0|0|0|0|0|0|0|0|0|0|0|0|0|0|0|0|0|0|0	0.06
TPCN2_734G	P35222	CTNNB1	31|0|6	38|10|11|0|18	0|0|0|0|0|0|0|0|0|0|0|0|0|0|0|0|0|0|0|0|0|0|0|0|0|0|0|0|0|0|0	0.06
TPCN2_734G	P49588	AARS	9|0|0	11|0|2|0|0	0|0|0|1|0|1|5|0|0|0|0|0|0|0|0|0|0|0|0|0|0|0|0|0|0|0|0|0|0|0|0	0.06
TPCN2_734G	P20645	M6PR	4|0|0	4|0|0|0|3	0|0|0|0|0|0|0|0|0|0|0|0|0|0|0|0|0|0|0|0|0|0|0|0|0|0|0|0|0|0|0	0.06
TPCN2_734G	Q13637	RAB32	0|4|0	0|0|0|2|4	0|0|0|0|0|0|0|0|0|0|0|0|0|0|0|0|1|0|0|0|0|0|0|0|0|0|0|0|0|0|0	0.06
TPCN2_734G	Q8N3E9	PLCD3	0|0|2	0|0|3|0|0	0|0|0|0|0|0|0|0|0|0|0|0|0|0|0|0|0|0|0|0|0|0|0|0|0|0|0|0|0|0|0	0.06
TPCN2_734G	P06702	S100A9	0|2|0	0|0|0|3|0	0|0|0|0|0|0|0|0|0|0|0|0|0|0|0|0|0|0|0|0|0|0|0|0|0|0|0|0|0|0|0	0.06

TPCN2_734G	Q9UHG3	PCYOX1	2|0|0	3|0|0|0|0	0|0|0|0|0|0|0|0|0|0|0|0|0|0|0|0|0|0|0|0|0|0|0|0|0|0|0|0|0|0	0.06
TPCN2_734G	Q92900	UPF1	0|3|0	0|2|0|2|0	0|0|0|0|0|1|0|0|0|0|0|0|0|0|0|0|0|0|0|0|0|0|0|0|0|0|0|0|0|0|0	0.06
TPCN2_734G	Q16666	IFI16	6|0|0	10|0|0|0|3	0|0|0|0|0|0|0|0|0|0|0|0|0|0|0|0|0|0|0|0|0|0|0|0|0|0|0|0|0|0	0.06
TPCN2_DeltaCT	Q53H12	AGK	0|4|0	0|2|3|0|3	0|0|0|0|0|0|1|0|0|0|0|0|0|0|0|0|0|0|0|0|0|0|0|0|0|0|0|0|0|0	0.06
TPCN2_DeltaCT	Q9BXP5	SRRT	10|0|0	11|0|0|0|3	0|0|0|0|0|0|0|0|0|2|0|2|0|0|0|0|0|1|1|0|0|0|0|0|0|0|0|0|0|0|8	0.06
TPCN2_DeltaCT	Q9NP58	ABCB6	4|0|0	5|0|0|0|5	0|0|0|0|0|0|0|0|0|0|0|0|0|0|0|0|0|0|0|0|0|0|0|0|0|0|0|0|0|0	0.06
TPCN2_DeltaCT	P55084	HADHB	21|0|3	21|0|0|0|15	0|0|0|0|0|0|0|1|3|4|5|5|4|0|0|0|0|0|0|0|0|0|0|0|0|0|0|0|0|0|0	0.06
TPCN2_DeltaCT	P16070	CD44	4|0|0	3|0|0|0|4	1|0|0|0|0|0|0|0|0|0|0|0|0|0|0|0|0|2|0|0|0|0|0|0|0|0|0|0|0|0	0.06
TPCN2_DeltaCT	P11413	G6PD	0|0|3	0|0|0|0|0	0|2|0|0|0|0|0|0|0|1|0|0|0|0|0|0|0|0|1|1|1|0|0|0|1|0|0|0|0|0	0.06
TPCN2_DeltaCT	P09110	ACAA1	3|0|0	3|0|0|0|3	0|0|0|0|0|0|0|0|0|0|0|0|0|0|0|0|0|0|0|0|0|0|0|0|0|0|0|0|0|0	0.06
TPCN2_DeltaCT	O00410	IPO5	10|0|0	8|0|0|0|0	0|0|0|0|0|2|0|3|0|3|2|1|1|0|0|0|0|1|4|0|1|2|4|1|1|0|1|2|0|4	0.06

TPCN2_DeltaCT	O94832	MYO1D	3|0|8	7|0|3|0|6	0|0|0|0|0|0|0|0|0|0|0|0|0|0|0|0|0|0|0|0|0|0|0|0|0|0|0|0|6|0	0.06
TPCN2_DeltaCT	P43007	SLC1A4	6|0|0	11|0|0|0|6	0|0|0|0|0|0|0|0|0|0|0|0|0|0|0|0|0|0|0|0|0|0|0|0|0|0|0|0	0.06
TPCN2_734E	Q8TC26	TMEM163	3|0|0	6|0|0|0|4	0|0|0|0|0|0|0|0|0|0|0|0|0|0|0|0|0|0|0|0|0|0|0|0|0|0|0|0	0.05
TPCN2_734E	P51798	CLCN7	2|0|0	0|0|0|0|2	0|0|1|0|0|0|0|0|0|0|0|0|0|2|0|0|0|0|0|0|0|0|0|0|0|0|0|0|0	0.05
TPCN2_734E	O75127	PTCD1	0|2|0	0|0|0|0|0	0|0|0|0|0|0|0|0|0|0|0|1|2|2|0|0|0|0|0|0|0|0|0|0|0|0|0|0|0	0.05
TPCN2_734E	P18206	VCL	18|0|7	15|9|11|0|0	0|3|2|0|0|5|4|0|0|0|0|0|0|0|1|0|0|0|2|0|1|2|3|0|1|0|0|0|0|3	0.05
TPCN2_734E	Q9NZM5	NOP53	0|16|0	10|0|0|13|6	3|1|2|2|3|0|2|0|0|0|0|0|0|3|1|2|1|3|5|1|3|3|2|0|0|1|3|2|2|0	0.05
TPCN2_734E	O94874	UFL1	3|0|0	0|0|0|0|2	2|0|0|0|0|0|0|0|0|0|0|0|0|0|0|0|0|0|0|1|2|0|1|0|1|0|0|0|0|0	0.05
TPCN2_734E	P02786	TFRC	27|0|9	19|9|11|0|17	2|1|0|0|0|0|0|8|4|4|3|4|3|0|1|3|0|1|2|2|1|0|0|0|0|0|0|0|0|0	0.05
TPCN2_734E	O75150	RNF40	2|0|0	0|0|0|0|0	0|0|0|1|2|0|0|0|0|0|0|0|0|0|0|0|0|0|0|0|0|0|1|1|0|0|0|0|0|0	0.05
TPCN2_734G	P05109	S100A8	0|3|0	0|0|2|3|0	0|0|0|0|0|0|0|0|0|0|0|0|0|0|0|0|0|0|0|0|0|0|0|0|0|0|0|0	0.05

TPCN2_734G	P09960	LTA4H	3|0|0	3|0|0|0|2	0|0|0|0|0|0|0|0|0|0|0|0|0|0|0|0|0|0|0|0|0|0|0|0|0|0|0|0|0|0|0	0.05
TPCN2_734G	P08962	CD63	12|0|5	11|7|6|0|8	0|0|0|0|0|0|0|0|0|0|0|0|0|0|0|0|0|0|0|0|0|0|0|0|0|0|0|0|0|0|0	0.05
TPCN2_734G	O75083	WDR1	9|0|0	12|3|3|0|4	0|0|0|0|0|0|0|0|0|0|0|0|0|0|0|0|0|0|0|0|0|0|0|0|0|0|0|0|1|0	0.05
TPCN2_734G	P50995	ANXA11	6|0|0	7|0|2|0|5	0|0|0|0|0|0|0|0|0|0|0|0|0|0|0|0|0|0|0|0|0|0|0|0|0|0|0|0|0|0|0	0.05
TPCN2_734G	P07602	PSAP	6|0|0	6|0|2|0|6	0|0|0|0|0|0|0|0|0|0|0|0|0|0|0|0|0|0|0|0|0|0|0|0|0|0|0|0|0|0|0	0.05
TPCN2_734G	Q16881	TXNRD1	4|0|0	6|0|0|0|2	0|0|0|0|0|0|0|0|0|0|0|0|0|0|0|0|0|0|0|0|0|0|0|0|0|0|0|0|1|0|0|0	0.05
TPCN2_734G	P40967	PMEL	6|0|0	7|0|2|0|5	0|0|0|0|0|0|0|0|0|0|0|0|0|0|0|0|0|0|0|0|0|0|0|0|0|0|0|0|0|0|0	0.05
TPCN2_734G	Q13045	FLII	2|0|0	0|0|0|0|0	0|0|1|0|0|0|0|0|0|0|0|0|0|0|0|0|0|0|0|0|0|0|0|0|0|0|0|0|0|0|1	0.05
TPCN2_734G	Q13616	CUL1	2|0|0	2|0|0|0|0	0|0|0|0|0|0|0|0|0|0|0|0|0|0|0|0|0|0|0|0|0|0|0|0|0|0|0|0|0|0|1	0.05
TPCN2_734G	Q08554	DSC1	0|3|2	0|0|2|4|0	0|0|0|0|0|0|0|1|0|0|0|0|0|0|0|0|0|0|0|0|0|0|0|0|0|0|0|0|0|0|0	0.05
TPCN2_734G	P35580	MYH10	15|0|111	0|9|0|0|0	0|1|12|8|11|0|0|0|1|1|0|1|0|0|0|0|1|4|9|1|2|11|19|11|9|15|4|3|131|41	0.05

TPCN2_DeltaCT	Q9NTZ6	RBM12	2|0|0	3|0|0|0|0	0|0|0|0|0|1|0|0|0|0|0|0|0|0|0|0|0|0|0|0|0|0|0|0|0|0|0|0|0|0|0	0.05
TPCN2_DeltaCT	P18206	VCL	19|0|9	15|9|11|0|0	0|3|2|0|0|5|4|0|0|0|0|0|0|0|1|0|0|0|2|0|1|2|3|0|1|0|0|0|0|3	0.05
TPCN2_DeltaCT	P41250	GARS	4|0|0	2|0|0|0|0	0|0|0|0|0|0|0|1|0|2|2|1|1|0|0|0|0|0|0|1|0|0|0|0|0|0|0|0|0|0|1	0.05
TPCN2_DeltaCT	Q9Y3T9	NOC2L	5|0|0	3|0|0|2|2	0|0|1|0|4|0|0|0|0|0|0|0|0|0|0|0|0|0|0|0|0|0|0|0|0|1|1|0|0|2|0	0.05
TPCN2_DeltaCT	P63010	AP2B1	16|0|0	16|0|0|0|9	1|1|6|0|0|2|0|3|0|1|0|0|0|0|0|0|0|0|0|2|1|4|2|2|0|0|1|0|1	0.05
TPCN2_DeltaCT	Q99805	TM9SF2	2|0|0	2|0|0|0|2	0|0|0|0|0|0|0|0|0|0|0|0|0|0|0|0|0|0|0|0|0|0|0|0|0|0|0|0|0|0|0	0.05
TPCN2_734E	Q92575	UBXN4	4|0|0	2|0|0|0|2	0|0|1|1|0|3|1|0|0|0|0|0|0|0|0|0|0|0|0|1|0|0|1|0|1|1|0|0|0|0	0.04
TPCN2_734E	Q9Y2L1	DIS3	2|0|0	0|0|0|0|0	0|0|0|1|0|2|1|0|0|0|0|0|0|0|0|0|0|0|0|0|0|0|0|0|0|1|0|0|1|0	0.04
TPCN2_734E	Q96EY7	PTCD3	2|0|0	0|0|0|0|0	0|0|0|0|0|0|0|1|0|1|1|1|1|0|0|0|0|0|0|0|0|0|0|0|0|0|0|0|0|1|0	0.04
TPCN2_734E	Q15139	PRKD1	0|10|38	18|34|35|10|12	0|0|0|0|0|0|0|0|0|0|0|0|0|0|0|0|0|0|0|0|0|0|0|0|0|0|0|0|0|0|0	0.04
TPCN2_734E	P55786	NPEPPS	7|0|0	9|0|0|0|2	0|0|1|0|1|2|2|0|0|0|0|0|0|0|0|0|0|0|0|0|0|0|0|0|0|0|0|0|0|0|0|3|0|1|1|0|0|2|1	0.04

TPCN2_734E	P35613	BSG	2|0|0	0|0|0|0|2	0|0|0|0|0|0|0|0|0|0|0|0|0|0|0|0|0|0|0|0|0|0|1|0|0|0|0|0|0|3	0.04
TPCN2_734E	Q8TCJ2	STT3B	4|0|0	5|0|0|0|7	1|0|0|0|0|1|0|0|0|0|0|0|0|0|0|0|0|0|0|0|0|0|0|0|0|0|0|0|0	0.04
TPCN2_734E	P53621	COPA	14|0|3	9|0|3|4|5	1|0|0|0|0|0|1|0|0|0|0|0|0|0|1|0|0|0|1|1|0|0|1|0|0|0|0|0|0|18	0.04
TPCN2_734G	P04179	SOD2	3|0|0	4|0|0|0|3	0|0|0|0|0|0|0|0|0|0|0|0|0|0|0|0|0|0|0|0|0|0|0|0|0|0|0|0|0	0.04
TPCN2_734G	P17643	TYRP1	23|0|4	25|10|8|0|20	0|0|0|0|0|0|0|0|0|0|0|0|0|0|0|0|0|0|0|0|0|0|0|0|0|0|0|0|0	0.04
TPCN2_734G	Q9NR45	NANS	2|0|0	4|0|0|0|0	0|0|0|0|0|0|0|0|0|0|0|0|0|0|0|0|0|0|0|0|0|0|0|0|0|0|0|0|0	0.04
TPCN2_734G	Q8WUH6	TMEM263	0|0|5	0|4|5|0|0	0|0|0|0|0|0|0|0|0|0|0|0|0|0|0|0|0|0|0|0|0|0|0|0|0|0|3|1	0.04
TPCN2_734G	Q9NW13	RBM28	16|0|0	16|0|0|2|11	0|0|1|1|1|0|4|0|0|1|0|0|0|0|2|3|1|0|0|0|1|0|1|0|0|1|1|2|2|0	0.04
TPCN2_734G	Q9UH92	MLX	2|0|0	0|0|0|0|0	0|0|0|0|0|4|0|0|0|0|0|0|0|0|0|0|0|0|0|0|0|0|0|0|0|0|0|0|0	0.04
TPCN2_734G	Q9H9J2	MRPL44	0|5|0	0|0|0|9|0	0|0|0|0|0|0|0|1|0|1|1|0|1|0|0|0|0|0|0|0|0|0|0|0|0|0|0|0|0	0.04
TPCN2_734G	P15121	AKR1B1	3|0|0	4|0|0|0|2	0|0|0|0|0|0|0|0|0|0|0|0|0|0|0|0|0|0|0|0|0|0|0|0|0|0|0|0|0	0.04

TPCN2_DeltaCT	Q8TC26	TMEM163	3|0|0	6|0|0|0|4	0|0|0|0|0|0|0|0|0|0|0|0|0|0|0|0|0|0|0|0|0|0|0|0|0|0|0|0|0|0|0	0.04
TPCN2_DeltaCT	P49006	MARCKSL1	2|0|0	0|0|0|0|0	0|0|3|0|1|0|0|0|0|0|0|0|0|0|0|0|0|0|0|0|0|0|0|0|0|0|0|0|0|0|0	0.04
TPCN2_DeltaCT	P25789	PSMA4	0|0|2	0|0|0|0|0	0|0|1|0|0|0|0|0|0|0|0|0|0|0|0|0|0|0|0|0|0|0|0|0|0|0|0|0|0|0|5	0.04
TPCN2_DeltaCT	P06744	GPI	17|0|14	18|11|13|0|10	0|0|0|0|0|0|0|0|0|0|0|0|0|0|0|0|0|0|0|0|0|0|0|0|0|0|0|0|0|0|0	0.04
TPCN2_DeltaCT	P78417	GSTO1	4|0|4	6|2|3|0|3	0|0|0|0|0|0|0|0|0|0|0|0|0|0|0|0|0|0|0|0|0|0|0|0|0|0|0|0|0|0|0	0.04
TPCN2_DeltaCT	Q15031	LARS2	8|0|0	7|0|0|0|8	0|0|0|0|0|0|0|2|0|0|1|2|5|0|0|0|0|0|0|0|0|0|0|0|0|0|0|0|0|0|0	0.04
TPCN2_DeltaCT	Q9HCM4	EPB41L5	7|0|25	6|11|17|12|24	0|0|0|0|0|0|1|0|0|0|0|0|0|0|0|0|0|0|0|1|0|0|0|0|0|0|0|0|0|0|0	0.04
TPCN2_DeltaCT	P09543	CNP	9|0|0	12|0|0|0|8	0|0|0|0|0|0|0|2|0|2|1|1|1|0|0|0|0|0|0|0|0|0|0|0|0|0|0|0|0|0|0	0.04
TPCN2_DeltaCT	O95831	AIFM1	17|0|6	13|0|2|0|13	0|0|1|1|2|1|0|0|0|0|0|0|0|0|0|0|0|0|0|0|0|0|0|0|0|0|0|0|0|0|0	0.04
TPCN2_DeltaCT	O00116	AGPS	3|0|0	3|0|0|0|5	0|0|0|0|0|0|0|1|0|0|0|0|0|0|0|0|0|0|0|0|0|0|0|0|0|0|0|0|0|0|0	0.04
TPCN2_DeltaCT	Q9BVK6	TMED9	2|0|0	0|0|0|0|0	0|0|0|0|0|0|0|0|0|0|1|1|0|2|0|0|0|0|0|0|0|0|0|0|0|0|0|0|0|0|0	0.04

TPCN2_DeltaCT	P05204	HMGN2	0|0|5	0|0|0|0|0	0|0|0|1|3|0|0|0|0|0|0|0|0|0|0|0|0|0|0|0|0|0|4|0|0|6|0|0|0|1	0.04
TPCN2_DeltaCT	Q13510	ASAH1	2|0|0	0|0|0|0|0	0|0|1|0|2|0|1|0|0|0|0|0|0|0|0|0|0|0|0|0|0|0|0|0|0|0|0|0	0.04
TPCN2_DeltaCT	P11279	LAMP1	3|0|0	3|0|2|0|3	0|0|0|0|0|0|0|0|0|0|0|0|0|0|0|0|0|0|0|0|0|0|0|0|0|0|0|0	0.04
TPCN2_DeltaCT	P57729	RAB38	2|0|0	2|0|0|0|4	0|0|0|0|0|0|0|0|0|0|0|0|0|0|0|0|0|0|0|0|0|0|0|0|0|0|0|0	0.04
TPCN2_DeltaCT	P08758	ANXA5	10|0|7	11|7|4|0|10	0|0|0|0|0|0|0|0|0|0|0|0|0|0|0|0|0|0|0|0|0|0|0|0|0|0|0|0	0.04
TPCN2_DeltaCT	P19367	HK1	18|0|0	19|2|2|0|23	0|0|0|0|0|0|1|0|0|0|0|0|0|0|0|0|0|0|0|0|0|0|0|0|0|0|0|5	0.04
TPCN2_734E	P13667	PDIA4	20|0|2	19|0|0|0|12	0|0|0|0|0|0|0|1|0|3|2|0|1|0|0|0|0|0|0|0|0|0|0|2|0|0|0|0|0|0|23	0.03
TPCN2_734E	Q16795	NDUFA9	0|2|0	0|0|0|2|2	0|0|0|0|0|0|0|0|0|0|0|0|0|0|2|1|0|0|0|0|0|0|0|0|0|0|0|0	0.03
TPCN2_734E	O95625	ZBTB11	7|6|6	0|0|4|10|11	2|0|0|0|0|0|0|0|0|0|0|0|0|0|0|0|0|0|0|0|0|0|0|0|0|0|0|0	0.03
TPCN2_734E	Q8TDD1	DDX54	4|35|4	18|2|0|28|13	0|0|7|1|5|1|2|0|0|0|0|0|0|0|0|4|4|0|0|0|0|2|12|3|6|9|1|0|6|0	0.03
TPCN2_734E	P05204	HMGN2	0|0|4	0|0|0|0|0	0|0|0|1|3|0|0|0|0|0|0|0|0|0|0|0|0|0|0|0|0|0|0|0|4|0|0|6|0|0|0|1	0.03

TPCN2_734E	P14314	PRKCSH	22|0|7	22|11|6|0|15	0|0|0|0|0|0|0|0|1|1|0|1|0|0|0|0|0|0|0|0|0|0|2|0|0|0|0|0|0|10	0.03
TPCN2_734E	Q16881	TXNRD1	2|0|0	6|0|0|0|2	0|0|0|0|0|0|0|0|0|0|0|0|0|0|0|0|0|0|0|0|0|0|0|1|0|0|0	0.03
TPCN2_734E	Q8WTT2	NOC3L	5|27|5	10|4|8|26|14	0|1|6|3|3|0|1|0|0|0|0|0|0|0|0|1|0|2|2|2|1|4|5|2|1|4|0|1|3|0	0.03
TPCN2_734E	O14617	AP3D1	4|0|20	0|0|4|0|0	2|5|16|5|3|3|5|1|0|1|0|1|0|4|4|2|2|2|8|6|7|2|10|2|2|5|2|6|1|6	0.03
TPCN2_734E	O95782	AP2A1	3|0|0	0|0|0|0|0	0|0|3|0|0|2|0|0|0|0|0|0|0|0|0|0|0|0|0|0|0|1|2|0|1|1|0|1|0|0	0.03
TPCN2_734E	O00410	IPO5	9|0|0	8|0|0|0|0	0|0|0|0|0|2|0|3|0|3|2|1|1|0|0|0|0|1|4|0|1|2|4|1|1|0|1|2|0|4	0.03
TPCN2_734E	P45974	USP5	4|0|0	6|0|0|0|0	0|0|0|0|0|0|0|0|0|0|0|0|0|0|0|0|0|0|0|0|0|0|1|4|1|0|1|0|0|0|2	0.03
TPCN2_734G	Q92570	NR4A3	2|0|0	2|0|0|0|2	0|0|0|0|0|0|0|0|0|0|0|0|0|0|0|0|0|0|0|0|0|0|0|0|0|0|0	0.03
TPCN2_734G	O94826	TOMM70	5|0|0	6|0|0|0|9	0|0|0|0|0|0|0|0|0|1|0|0|0|0|0|0|0|0|0|0|0|0|0|0|0|0|0	0.03
TPCN2_734G	P54727	RAD23B	2|0|0	3|0|0|0|0	0|0|0|0|0|0|0|0|0|0|0|0|0|0|0|0|0|0|0|0|0|0|0|0|0|0|1	0.03
TPCN2_734G	Q9NTZ6	RBM12	2|0|0	3|0|0|0|0	0|0|0|0|0|1|0|0|0|0|0|0|0|0|0|0|0|0|0|0|0|0|0|0|0|0|0	0.03

TPCN2_734G	O95202	LETM1	5|0|0	5|0|0|0|7	0|0|0|0|0|0|0|0|0|0|0|1|0|0|0|0|0|0|0|0|0|0|0|0|0|0|0|0|0|1	0.03
TPCN2_734G	Q8WX92	NELFB	2|0|0	0|0|0|0|3	0|0|0|0|0|0|0|0|0|0|0|0|0|0|0|0|0|0|0|0|0|0|0|0|0|0|0|0|0|1	0.03
TPCN2_734G	P55786	NPEPPS	8|0|0	9|0|0|0|2	0|0|1|0|1|2|2|0|0|0|0|0|0|0|0|0|0|0|0|0|0|0|0|0|0|0|3|0|1|1|0|0|2|1	0.03
TPCN2_734G	O95831	AIFM1	17|0|0	13|0|2|0|13	0|0|1|1|2|1|0|0|0|0|0|0|0|0|0|0|0|0|0|0|0|0|0|0|0|0|2|0|0|0|0|0|1|14	0.03
TPCN2_734G	Q9NX63	CHCHD3	2|0|0	0|0|0|0|4	0|0|0|0|0|0|0|0|0|0|0|0|0|0|0|0|0|0|0|0|0|0|0|0|0|0|0|0|0|0	0.03
TPCN2_734G	O43747	AP1G1	3|0|0	4|0|0|0|4	0|0|0|0|0|0|0|0|0|0|0|0|0|0|0|0|0|0|0|0|0|0|0|0|0|0|0|0|0|0	0.03
TPCN2_734G	O14617	AP3D1	3|0|21	0|0|4|0|0	2|5|16|5|3|3|5|1|0|1|0|1|0|4|4|2|2|2|8|6|7|2|10|2|2|5|2|6|1|6	0.03
TPCN2_734G	Q6NUQ4	TMEM214	2|0|0	2|0|0|0|2	0|0|0|0|0|0|0|0|0|0|0|0|0|0|0|0|0|0|0|0|0|0|0|0|0|0|0|0|0|0	0.03
TPCN2_734G	P63010	AP2B1	16|0|0	16|0|0|0|9	1|1|6|0|0|2|0|3|0|1|0|0|0|0|0|0|0|0|0|0|2|1|4|2|2|0|0|1|0|1	0.03
TPCN2_734G	P11279	LAMP1	3|0|0	3|0|2|0|3	0|0|0|0|0|0|0|0|0|0|0|0|0|0|0|0|0|0|0|0|0|0|0|0|0|0|0|0|0|0	0.03
TPCN2_734G	P08758	ANXA5	11|0|2	11|7|4|0|10	0|0|0|0|0|0|0|0|0|0|0|0|0|0|0|0|0|0|0|0|0|0|0|0|0|0|0|0|0|0	0.03

TPCN2_734G	P53990	IST1	2|0|0	4|0|0|0|0	0|0|0|0|0|0|0|0|0|0|0|0|0|0|0|0|0|1|0|0|0|0|0|0|0|0|0|0|0|0|0|0	0.03
TPCN2_734G	Q96QK1	VPS35	7|0|0	8|4|2|0|4	0|0|0|0|0|0|0|0|0|0|0|0|0|0|0|0|0|0|0|0|0|0|0|0|0|0|0|0|0|0|2	0.03
TPCN2_DeltaCT	O75436	VPS26A	2|0|0	0|0|0|0|0	0|0|0|0|0|0|0|1|0|1|1|0|2|0|0|0|0|0|0|0|0|0|0|0|0|0|0|0|0|0|1	0.03
TPCN2_DeltaCT	P04040	CAT	3|0|0	3|0|0|0|3	0|0|0|0|0|0|0|1|1|1|0|0|0|0|0|0|0|0|0|0|0|0|0|0|0|0|0|0|0|0	0.03
TPCN2_DeltaCT	Q86U42	PABPN1	2|0|0	0|0|0|0|0	0|0|0|0|0|0|0|0|0|0|0|0|0|0|0|0|0|0|0|0|0|0|0|0|0|0|0|0|0|2|3	0.03
TPCN2_DeltaCT	P50416	CPT1A	4|0|0	2|0|0|0|5	1|0|0|0|0|0|0|0|0|0|0|0|0|1|1|0|0|1|1|0|0|0|0|0|0|0|1|0|0|0	0.03
TPCN2_DeltaCT	P23634	ATP2B4	2|0|0	0|0|0|0|0	0|0|0|1|0|0|0|0|0|0|0|0|0|1|0|0|0|0|0|0|0|0|0|0|0|0|1|0|0|2|0	0.03
TPCN2_DeltaCT	P51572	BCAP31	5|0|0	8|0|0|0|6	0|1|0|0|0|0|0|0|0|0|0|0|0|1|0|0|0|0|0|0|0|0|0|0|0|0|0|0|0|0|0	0.03
TPCN2_DeltaCT	Q8TCJ2	STT3B	4|0|0	5|0|0|0|7	1|0|0|0|0|1|0|0|0|0|0|0|0|0|0|0|0|0|0|0|0|0|0|0|0|0|0|0|0|0|0	0.03
TPCN2_DeltaCT	P62861	FAU	0|0|3	0|0|2|0|0	0|0|1|0|0|0|0|0|0|0|0|0|0|0|0|0|0|0|0|0|0|0|0|0|0|0|0|0|0|0|3	0.03
TPCN2_DeltaCT	Q13637	RAB32	0|2|0	0|0|0|2|4	0|0|0|0|0|0|0|0|0|0|0|0|0|0|0|0|0|1|0|0|0|0|0|0|0|0|0|0|0|0|0	0.03

TPCN2_DeltaCT	Q06210	GFPT1	3|0|3	7|0|0|0|4	0|0|0|0|0|0|0|0|0|0|0|0|0|0|0|0|0|0|0|0|0|1|0|0|1|0|0|0|0|0	0.03
TPCN2_DeltaCT	A1L0T0	ILVBL	3|0|0	0|0|0|0|0	0|0|2|0|0|1|2|0|0|0|0|0|0|0|0|0|0|0|0|0|0|0|2|0|0|2|0|0|0|0	0.03
TPCN2_734E	O14980	XPO1	10|0|7	9|2|3|0|5	0|0|1|0|0|4|3|3|1|3|1|1|1|0|0|1|1|0|0|0|0|2|1|4|2|1|0|0|4|2	0.02
TPCN2_734E	O95831	AIFM1	15|0|3	13|0|2|0|13	0|0|1|1|2|1|0|0|0|0|0|0|0|0|0|0|0|0|0|0|0|0|0|0|0|0|2|0|0|0|0|0|1|14	0.02
TPCN2_734E	O75955	FLOT1	2|7|0	0|2|11|5|9	0|0|0|0|0|0|0|0|0|0|0|0|0|0|0|0|0|0|0|0|0|0|0|0|0|0|0|0|0|0	0.02
TPCN2_734E	O75083	WDR1	4|0|5	12|3|3|0|4	0|0|0|0|0|0|0|0|0|0|0|0|0|0|0|0|0|0|0|0|0|0|0|0|0|0|0|0|0|1|0	0.02
TPCN2_734E	O43852	CALU	12|0|3	9|4|2|0|11	0|0|0|0|0|0|0|0|0|0|0|0|0|0|0|0|0|0|0|0|0|0|0|0|0|0|0|0|0|18	0.02
TPCN2_734E	Q06210	GFPT1	2|0|2	7|0|0|0|4	0|0|0|0|0|0|0|0|0|0|0|0|0|0|0|0|0|0|0|0|0|0|0|0|0|0|0|0|0|1|0|0|1|0|0|0|0|0	0.02
TPCN2_734E	P83881	RPL36A	0|0|4	0|0|2|0|0	1|0|1|1|1|4|2|0|0|0|0|0|0|0|0|2|0|0|0|0|0|0|1|0|0|1|0|0|0|0	0.02
TPCN2_734E	Q15437	SEC23B	3|0|0	4|0|0|0|0	0|0|0|0|0|1|2|1|0|0|0|0|0|0|0|0|0|0|0|0|0|0|1|1|0|1|0|0|0|0|1	0.02
TPCN2_734E	Q9NSD9	FARSB	5|0|6	9|3|2|0|5	0|0|0|1|0|2|1|0|0|0|0|0|0|0|0|0|0|0|0|0|0|0|0|0|0|0|0|0|0|1	0.02

TPCN2_734E	O94906	PRPF6	8|0|0	2|0|0|0|0	0|0|6|2|2|2|0|1|0|2|1|1|1|0|2|3|2|0|2|1|5|2|5|0|1|2|1|0|1|3	0.02
TPCN2_734G	Q8TC26	TMEM163	3|0|0	6|0|0|0|4	0|0|0|0|0|0|0|0|0|0|0|0|0|0|0|0|0|0|0|0|0|0|0|0|0|0|0|0	0.02
TPCN2_734G	P40222	TXLNA	2|0|0	2|0|0|0|0	0|0|0|1|1|0|0|0|0|0|0|0|0|0|0|0|0|0|0|0|0|0|1|0|0|1|0|0|0|0	0.02
TPCN2_734G	O00203	AP3B1	6|2|9	3|0|0|0|0	0|2|6|2|1|2|3|0|0|0|0|0|0|0|0|0|0|1|0|0|0|2|6|1|2|2|0|0|2|4	0.02
TPCN2_734G	P37837	TALDO1	3|0|0	6|0|0|0|3	0|0|0|0|0|1|0|0|0|0|0|0|0|0|0|0|0|0|0|0|0|0|1|0|0|0|0|0|0|0	0.02
TPCN2_734G	O75127	PTCD1	0|2|0	0|0|0|0|0	0|0|0|0|0|0|0|0|0|0|1|2|2|0|0|0|0|0|0|0|0|0|0|0|0|0|0|0|0|0	0.02
TPCN2_734G	Q53H12	AGK	0|0|3	0|2|3|0|3	0|0|0|0|0|0|1|0|0|0|0|0|0|0|0|0|0|0|0|0|0|0|1|0|0|0|0|0|0|0	0.02
TPCN2_734G	P04040	CAT	3|0|0	3|0|0|0|3	0|0|0|0|0|0|0|1|1|1|0|0|0|0|0|0|0|0|0|0|0|0|0|0|0|0|0|0|0	0.02
TPCN2_734G	Q969P0	IGSF8	2|0|0	4|0|0|0|2	0|0|0|0|0|0|0|0|0|0|0|0|0|0|0|0|0|0|0|0|0|0|0|0|0|0|0|0|0	0.02
TPCN2_734G	Q96EY7	PTCD3	2|0|0	0|0|0|0|0	0|0|0|0|0|0|0|1|0|1|1|1|1|0|0|0|0|0|0|0|0|0|0|0|0|0|0|0|1|0	0.02
TPCN2_734G	Q15139	PRKD1	11|15|39	18|34|35|10|12	0|0|0|0|0|0|0|0|0|0|0|0|0|0|0|0|0|0|0|0|0|0|0|0|0|0|0|0|0	0.02

TPCN2_734G	Q15031	LARS2	8|0|0	7|0|0|0|8	0|0|0|0|0|0|0|2|0|0|1|2|5|0|0|0|0|0|0|0|0|0|0|0|0|0|0|0|0|0|0	0.02
TPCN2_734G	P07099	EPHX1	3|0|0	3|0|0|0|8	0|0|0|0|0|0|0|0|0|0|0|0|0|0|0|0|0|0|0|0|0|0|0|0|0|0|0	0.02
TPCN2_734G	O95625	ZBTB11	4|9|2	0|0|4|10|11	2|0|0|0|0|0|0|0|0|0|0|0|0|0|0|0|0|0|0|0|0|0|0|0|0|0|0	0.02
TPCN2_734G	P40121	CAPG	15|0|7	19|8|7|0|13	0|0|0|0|0|0|0|0|0|0|0|0|0|0|0|0|0|0|0|0|0|0|0|0|0|0|0	0.02
TPCN2_734G	Q00610	CLTC	80|0|7	69|24|28|0|33	2|4|0|1|1|0|1|8|12|10|3|2|4|2|2|0|0|1|2|3|1|3|1|0|3|1|3|1|1|20	0.02
TPCN2_734G	O75955	FLOT1	3|8|5	0|2|11|5|9	0|0|0|0|0|0|0|0|0|0|0|0|0|0|0|0|0|0|0|0|0|0|0|0|0|0|0	0.02
TPCN2_734G	Q9NP58	ABCB6	3|0|0	5|0|0|0|5	0|0|0|0|0|0|0|0|0|0|0|0|0|0|0|0|0|0|0|0|0|0|0|0|0|0|0	0.02
TPCN2_734G	Q9NTJ5	SACM1L	3|0|0	3|0|0|0|7	0|0|0|0|0|0|0|0|0|0|0|0|0|0|0|0|0|0|0|0|0|0|0|0|0|0|0	0.02
TPCN2_734G	P51572	BCAP31	5|0|0	8|0|0|0|6	0|1|0|0|0|0|0|0|0|0|0|0|0|1|0|0|0|0|0|0|0|0|0|0|0|0|0|0	0.02
TPCN2_734G	P16070	CD44	3|0|0	3|0|0|0|4	1|0|0|0|0|0|0|0|0|0|0|0|0|0|0|0|2|0|0|0|0|0|0|0|0|0|0	0.02
TPCN2_734G	P10515	DLAT	2|0|0	2|0|0|0|2	0|0|0|0|0|0|0|0|0|0|0|1|1|0|0|0|0|0|0|0|0|0|0|0|0|0|0	0.02

TPCN2_734G	Q8TCJ2	STT3B	4|0|0	5|0|0|0|7	1|0|0|0|0|1|0|0|0|0|0|0|0|0|0|0|0|0|0|0|0|0|0|0|0|0|0|0|0|0|0	0.02
TPCN2_734G	Q96HY7	DHTKD1	2|0|0	0|0|0|0|2	0|0|0|0|0|0|0|0|0|0|1|1|1|0|0|0|0|0|0|0|0|0|0|0|0|0|0|0|0|0|0	0.02
TPCN2_734G	Q99536	VAT1	17|0|2	22|6|6|0|18	0|0|0|0|0|0|0|0|0|0|0|0|0|0|0|0|0|0|0|0|0|0|0|0|0|0|0|0|0|0|0	0.02
TPCN2_734G	P45974	USP5	5|0|0	6|0|0|0|0	0|0|0|0|0|0|0|0|0|0|0|0|0|0|0|0|0|0|0|0|0|0|0|0|0|0|0|0|0|1|4|1|0|1|0|0|0|2	0.02
TPCN2_734G	Q06210	GFPT1	4|0|0	7|0|0|0|4	0|0|0|0|0|0|0|0|0|0|0|0|0|0|0|0|0|0|0|0|0|0|0|0|0|0|0|0|0|1|0|0|1|0|0|0|0|0	0.02
TPCN2_734G	Q02413	DSG1	0|7|4	0|0|6|8|0	0|0|0|0|0|0|0|3|4|2|0|0|0|0|0|0|0|0|0|0|0|0|0|0|0|0|0|0|0|0|0	0.02
TPCN2_734G	P07954	FH	11|0|0	12|0|3|0|10	0|0|0|0|0|0|0|2|2|2|2|1|1|0|0|0|0|0|0|0|0|0|0|0|0|0|0|0|0|0|0	0.02
TPCN2_DeltaCT	Q9Y3U8	RPL36	0|2|5	2|4|4|4|2	0|0|1|0|1|0|0|0|0|0|0|0|0|0|0|0|0|0|0|0|0|0|0|0|0|0|0|0|0|1|0	0.02
TPCN2_DeltaCT	Q8TCS8	PNPT1	5|0|0	3|0|0|0|2	0|0|0|0|0|0|0|1|1|0|6|1|4|0|0|0|0|0|0|0|0|0|0|0|0|0|0|0|0|0|0	0.02
TPCN2_DeltaCT	P01876	IGHA1	0|2|0	0|5|0|3|0	0|0|0|0|0|0|0|0|0|0|0|0|0|0|0|0|0|0|0|0|0|0|0|0|0|0|0|0|0|0|0	0.02
TPCN2_DeltaCT	P50395	GDI2	10|0|5	11|4|3|0|5	3|2|0|0|0|0|0|0|0|0|0|0|0|0|0|0|0|0|0|0|1|0|0|0|1|0|0|0|0|1|0|4	0.02

TPCN2_DeltaCT	Q9Y4L1	HYOU1	4|0|0	4|0|0|0|0	0|0|1|0|0|1|0|1|0|0|0|0|1|0|0|0|0|0|0|0|0|0|1|0|0|0|0|0|1|4	0.02
TPCN2_DeltaCT	O00159	MYO1C	8|0|4	8|2|0|0|5	1|0|0|0|0|0|0|0|0|0|0|0|0|0|0|1|1|0|0|0|0|0|1|0|0|0|0|0|10|0	0.02
TPCN2_DeltaCT	Q9NZM5	NOP53	0|15|0	10|0|0|13|6	3|1|2|2|3|0|2|0|0|0|0|0|0|3|1|2|1|3|5|1|3|3|2|0|0|1|3|2|2|0	0.02
TPCN2_DeltaCT	Q14257	RCN2	4|0|0	0|0|0|0|2	0|0|0|0|0|0|0|0|0|0|0|0|0|0|0|0|0|0|0|0|0|0|0|0|0|0|0|0|0|15	0.02
TPCN2_DeltaCT	P22061	PCMT1	0|0|3	0|0|0|0|0	1|0|0|0|0|0|1|1|1|2|0|0|1|1|1|0|0|0|1|0|1|0|0|0|0|0|0|0|0|0	0.02
TPCN2_DeltaCT	P62851	RPS25	0|3|8	2|4|5|4|2	0|0|0|0|0|0|0|1|0|0|0|0|1|0|0|0|0|0|0|0|0|0|2|1|0|0|0|0|0|8	0.02
TPCN2_DeltaCT	P63092	GNAS	0|0|5	0|2|3|0|3	0|0|0|0|0|1|1|2|2|1|1|0|1|0|0|1|0|0|0|0|0|0|1|0|0|0|0|0|0|2	0.02
TPCN2_DeltaCT	O14617	AP3D1	4|0|20	0|0|4|0|0	2|5|16|5|3|3|5|1|0|1|0|1|0|4|4|2|2|2|8|6|7|2|10|2|2|5|2|6|1|6	0.02
TPCN2_DeltaCT	O43852	CALU	13|0|5	9|4|2|0|11	0|0|0|0|0|0|0|0|0|0|0|0|0|0|0|0|0|0|0|0|0|0|0|0|0|0|0|0|0|18	0.02
TPCN2_DeltaCT	P45974	USP5	4|0|0	6|0|0|0|0	0|0|0|0|0|0|0|0|0|0|0|0|0|0|0|0|0|0|0|0|0|0|0|0|0|0|0|0|0|1|4|1|0|1|0|0|0|2	0.02
TPCN2_DeltaCT	P26639	TARS	6|0|4	4|2|0|0|2	0|0|2|1|0|0|3|0|0|0|0|0|0|0|0|0|0|0|0|0|1|0|1|5|0|1|0|0|0|0|1	0.02

TPCN2_DeltaCT	Q01518	CAP1	23|0|6	20|4|4|0|8	2|3|5|0|1|4|1|0|0|0|0|0|0|0|0|0|0|0|0|0|0|1|8|5|0|7|0|1|0|0|10	0.02
TPCN2_DeltaCT	Q13247	SRSF6	12|0|0	7|0|0|0|10	4|1|2|1|5|2|0|1|1|0|1|1|1|2|2|2|3|1|1|1|1|0|5|0|0|3|1|1|1|5	0.02
TPCN2_DeltaCT	Q16666	IFI16	3|0|0	10|0|0|0|3	0|0|0|0|0|0|0|0|0|0|0|0|0|0|0|0|0|0|0|0|0|0|0|0|0|0|0|0|0	0.02
TPCN2_734E	P99999	CYCS	2|0|0	0|0|0|0|0	1|2|0|0|0|0|0|0|0|0|0|1|0|1|0|0|0|1|0|3|1|0|0|0|0|0|0|0|0|0	0.01
TPCN2_734E	P78417	GSTO1	0|0|3	6|2|3|0|3	0|0|0|0|0|0|0|0|0|0|0|0|0|0|0|0|0|0|0|0|0|0|0|0|0|0|0|0|0	0.01
TPCN2_734E	Q7KZ85	SUPT6H	3|0|0	0|0|0|0|0	1|0|0|1|0|0|1|0|0|0|0|0|0|0|0|0|1|0|1|0|0|1|0|1|0|0|1|6	0.01
TPCN2_734E	O14828	SCAMP3	2|0|0	0|0|0|0|0	1|1|0|0|0|3|1|1|0|1|2|0|0|0|0|0|0|1|0|0|0|0|0|0|0|0|1|0|0	0.01
TPCN2_734E	Q13423	NNT	16|0|0	9|0|3|0|11	0|0|0|0|0|0|0|8|7|8|5|8|4|0|0|0|0|0|0|0|0|0|0|0|0|0|0|0|0|0|0	0.01
TPCN2_734E	O75694	NUP155	8|0|0	0|0|0|0|0	0|1|0|0|0|3|3|4|2|4|4|0|3|0|0|4|2|2|1|3|4|0|4|0|0|0|0|1|1|2	0.01
TPCN2_734E	Q5JWF2	GNAS	0|3|0	0|0|0|2|0	0|0|0|0|0|1|1|2|2|1|1|0|1|0|0|1|0|0|0|0|0|0|1|0|0|0|0|0|0|2	0.01
TPCN2_734E	Q96GQ7	DDX27	4|0|0	3|0|0|0|0	1|0|0|0|0|0|0|1|2|1|0|2|0|0|1|0|1|0|0|0|0|0|2|0|0|0|0|0|4|0	0.01

TPCN2_734E	P40121	CAPG	11|0|11	19|8|7|0|13	0|0|0|0|0|0|0|0|0|0|0|0|0|0|0|0|0|0|0|0|0|0|0|0|0|0|0|0|0|0|0	0.01
TPCN2_734E	Q5JTH9	RRP12	7|0|0	0|0|0|2|5	0|0|3|0|1|0|0|0|0|0|0|0|0|0|0|2|2|5|2|2|0|0|4|0|1|4|1|2|0|0	0.01
TPCN2_734E	P36957	DLST	4|0|0	5|0|0|0|3	0|0|0|0|0|0|0|1|2|2|1|2|2|0|0|0|0|0|0|0|0|0|0|0|0|0|0|0|0|0|0	0.01
TPCN2_734E	P81605	DCD	2|3|0	0|0|0|4|2	0|0|0|0|0|0|0|2|2|2|1|1|0|0|0|0|0|0|0|0|0|0|0|0|0|0|0|0|0|0	0.01
TPCN2_734E	Q8NBS9	TXNDC5	3|0|0	4|0|0|0|3	0|0|0|0|0|0|0|2|0|1|1|2|2|0|0|0|0|0|0|0|0|0|0|0|0|0|0|0|0|0|1	0.01
TPCN2_734E	P55084	HADHB	16|0|3	21|0|0|0|15	0|0|0|0|0|0|0|1|3|4|5|5|4|0|0|0|0|0|0|0|0|0|0|0|0|0|0|0|0|0|0	0.01
TPCN2_734E	O94806	PRKD3	15|13|54	31|46|46|14|26	0|0|0|0|0|0|0|0|0|0|0|0|0|0|0|0|0|0|0|0|0|0|0|0|0|0|0|0|0|0	0.01
TPCN2_734E	O00267	SUPT5H	4|0|0	0|0|0|0|0	1|0|0|1|0|1|0|1|0|0|0|0|0|2|1|1|0|0|0|0|0|0|0|0|0|1|1|0|0|12	0.01
TPCN2_734E	Q8WUM4	PDCD6IP	4|0|8	6|0|7|0|0	0|0|1|1|1|3|5|1|0|1|0|0|0|0|0|0|0|0|0|0|0|2|3|2|2|2|0|1|4|0	0.01
TPCN2_734E	P55854	SUMO3	2|0|0	0|0|0|0|2	1|1|0|1|0|0|1|0|0|0|0|0|0|1|1|0|0|0|1|0|1|0|1|0|0|1|1|1|1|0	0.01
TPCN2_734E	P60174	TPI1	8|0|4	16|5|4|0|9	0|0|0|0|0|0|0|0|0|0|0|0|0|0|0|0|0|0|0|0|0|0|0|0|0|0|0|0|0|0	0.01

TPCN2_734E	Q9BZE4	GTPBP4	2|9|0	9|0|0|7|6	3|1|2|3|2|0|0|0|0|0|0|0|1|1|1|1|2|2|1|0|3|1|0|1|0|1|1|0	0.01
TPCN2_734E	Q9H8Y8	GORASP2	2|0|0	2|0|0|0|2	1|0|0|0|0|2|0|0|0|0|0|0|2|0|0|0|0|1|0|1|0|0|0|0|0|0|0|0	0.01
TPCN2_734E	P42766	RPL35	0|4|6	7|6|7|0|0	0|0|1|0|0|0|0|0|0|0|0|0|0|0|0|0|0|0|0|0|1|3|0|1|0|0|0|0	0.01
TPCN2_734E	P40926	MDH2	14|0|4	18|6|5|0|13	0|0|0|0|0|0|0|0|0|0|0|0|0|0|0|0|0|0|0|0|0|5|0|0|0|0|0|0|5	0.01
TPCN2_734E	P49207	RPL34	0|3|0	0|0|0|2|3	0|1|2|0|1|0|0|0|0|0|0|0|0|1|0|1|1|0|0|0|0|1|1|1|1|1|0|0|0|0	0.01
TPCN2_734E	P07954	FH	8|0|3	12|0|3|0|10	0|0|0|0|0|0|0|2|2|2|2|1|1|0|0|0|0|0|0|0|0|0|0|0|0|0|0|0|0	0.01
TPCN2_734E	Q14697	GANAB	23|0|3	19|4|2|0|5	0|0|0|0|0|0|0|7|5|5|3|5|1|0|0|0|0|0|0|1|0|0|3|0|0|0|0|0|0|23	0.01
TPCN2_734E	P08758	ANXA5	0|0|7	11|7|4|0|10	0|0|0|0|0|0|0|0|0|0|0|0|0|0|0|0|0|0|0|0|0|0|0|0|0|0|0|0	0.01
TPCN2_734E	O75400	PRPF40A	9|0|0	0|0|0|0|0	1|2|3|5|5|2|3|0|0|0|0|0|0|1|0|1|1|1|3|3|2|2|6|2|3|5|2|2|4|0	0.01
TPCN2_734G	Q16795	NDUFA9	0|2|0	0|0|0|2|2	0|0|0|0|0|0|0|0|0|0|0|0|0|0|0|2|1|0|0|0|0|0|0|0|0|0|0|0|0	0.01
TPCN2_734G	P06744	GPI	16|0|2	18|11|13|0|10	0|0|0|0|0|0|0|0|0|0|0|0|0|0|0|0|0|0|0|0|0|0|0|0|0|0|0|0	0.01

TPCN2_734G	O75165	DNAJC13	10|3|0	0|0|0|15|3	0|0|0|0|1|0|0|0|0|0|0|0|0|0|0|0|0|3|5|2|2|0|0|1|1|0|2|3|0|0	0.01
TPCN2_734G	Q15046	KARS	7|0|0	7|0|0|0|2	0|0|1|1|2|0|0|0|0|0|0|0|0|0|0|2|3|0|0|0|0|4|1|0|3|3|0|0|0|2	0.01
TPCN2_734G	Q8TCT9	HM13	4|0|0	3|0|0|0|4	0|0|1|0|0|0|1|0|1|1|2|1|2|0|0|0|0|0|0|0|0|0|0|0|0|0|0|0|0|0	0.01
TPCN2_734G	P78417	GSTO1	4|0|0	6|2|3|0|3	0|0|0|0|0|0|0|0|0|0|0|0|0|0|0|0|0|0|0|0|0|0|0|0|0|0|0	0.01
TPCN2_734G	P46459	NSF	2|0|0	0|0|0|0|0	0|0|1|0|0|1|1|0|0|0|0|0|0|0|0|0|0|0|0|0|1|1|1|1|2|0|0|0|0	0.01
TPCN2_734G	P18206	VCL	17|0|0	15|9|11|0|0	0|3|2|0|0|5|4|0|0|0|0|0|0|0|1|0|0|0|2|0|1|2|3|0|1|0|0|0|0|3	0.01
TPCN2_734G	P01876	IGHA1	0|2|0	0|5|0|3|0	0|0|0|0|0|0|0|0|0|0|0|0|0|0|0|0|0|0|0|0|0|0|0|0|0|0|0	0.01
TPCN2_734G	Q9Y4L1	HYOU1	4|0|0	4|0|0|0|0	0|0|1|0|0|1|0|1|0|0|0|0|1|0|0|0|0|0|0|0|0|0|1|0|0|0|0|0|1|4	0.01
TPCN2_734G	O94874	UFL1	2|0|0	0|0|0|0|2	2|0|0|0|0|0|0|0|0|0|0|0|0|0|0|0|0|0|1|2|0|1|0|1|0|0|0|0|0	0.01
TPCN2_734G	Q96GQ7	DDX27	5|0|0	3|0|0|0|0	1|0|0|0|0|0|0|1|2|1|0|2|0|0|1|0|1|0|0|0|0|0|2|0|0|0|0|0|4|0	0.01
TPCN2_734G	P36957	DLST	5|0|0	5|0|0|0|3	0|0|0|0|0|0|0|1|2|2|1|2|2|0|0|0|0|0|0|0|0|0|0|0|0|0|0|0|0	0.01

TPCN2_734G	Q9BXP5	SRRT	8|0|0	11|0|0|0|3	0|0|0|0|0|0|0|0|0|2|0|2|0|0|0|0|0|1|1|0|0|0|0|0|0|0|0|0|0|8	0.01
TPCN2_734G	O00116	AGPS	2|0|0	3|0|0|0|5	0|0|0|0|0|0|0|1|0|0|0|0|0|0|0|0|0|0|0|0|0|0|0|0|0|0|0	0.01
TPCN2_734G	P60174	TPI1	10|0|2	16|5|4|0|9	0|0|0|0|0|0|0|0|0|0|0|0|0|0|0|0|0|0|0|0|0|0|0|0|0|0|0	0.01
TPCN2_734G	P46063	RECQL	2|0|0	0|0|0|0|3	0|0|1|0|0|1|1|0|0|0|0|0|1|0|0|0|0|0|0|0|0|0|1|0|0|0|0|0|0|1	0.01
TPCN2_734G	P30405	PPIF	4|0|0	5|0|0|0|2	0|0|0|0|0|0|0|1|1|1|1|1|1|0|0|0|0|0|0|0|0|0|1|0|0|0|0|0|0|0	0.01
TPCN2_734G	Q9Y3T9	NOC2L	4|2|0	3|0|0|2|2	0|0|1|0|4|0|0|0|0|0|0|0|0|0|0|0|0|0|0|0|0|0|0|1|1|0|0|2|0	0.01
TPCN2_734G	Q9Y512	SAMM50	2|0|0	4|0|0|0|4	0|0|0|0|0|0|0|0|0|0|0|0|0|0|0|0|0|0|0|0|0|0|0|0|0|0|0	0.01
TPCN2_734G	Q01518	CAP1	22|0|0	20|4|4|0|8	2|3|5|0|1|4|1|0|0|0|0|0|0|0|0|0|0|0|0|0|1|8|5|0|7|0|1|0|0|10	0.01
TPCN2_734G	Q8TAT6	NPLOC4	5|0|0	4|0|0|0|4	0|0|2|1|0|3|3|0|0|0|0|0|0|0|0|0|0|0|0|1|0|0|0|0|0|2|0|0|0	0.01
TPCN2_734G	P83881	RPL36A	0|0|4	0|0|2|0|0	1|0|1|1|1|4|2|0|0|0|0|0|0|0|2|0|0|0|0|0|0|1|0|0|1|0|0|0|0	0.01
TPCN2_734G	O14964	HGS	4|0|0	4|0|0|0|0	0|0|2|0|0|1|1|0|0|0|0|0|0|0|0|0|0|0|0|0|0|3|1|2|1|1|0|0|0|0	0.01

TPCN2_734G	Q96HE7	ERO1A	2|0|0	0|0|0|0|3	0|0|0|0|0|0|0|1|1|1|1|1|1|0|0|0|0|0|0|0|0|0|0|0|0|0|0|0|0|0|0	0.01
TPCN2_DeltaCT	O00203	AP3B1	8|0|4	3|0|0|0|0	0|2|6|2|1|2|3|0|0|0|0|0|0|0|0|0|1|0|0|0|2|6|1|2|2|0|0|2|4	0.01
TPCN2_DeltaCT	Q08AN1	ZNF616	5|0|12	5|3|16|9|9	0|0|0|0|0|0|0|0|0|0|0|0|0|0|0|0|0|0|0|0|0|0|0|0|0|1|0|0|0|0|0|0	0.01
TPCN2_DeltaCT	Q8TCT9	HM13	4|0|0	3|0|0|0|4	0|0|1|0|0|0|1|0|1|1|2|1|2|0|0|0|0|0|0|0|0|0|0|0|0|0|0|0|0|0	0.01
TPCN2_DeltaCT	P46459	NSF	2|0|0	0|0|0|0|0	0|0|1|0|0|1|1|0|0|0|0|0|0|0|0|0|0|0|0|1|1|1|2|0|0|0|0	0.01
TPCN2_DeltaCT	Q15139	PRKD1	0|0|36	18|34|35|10|12	0|0|0|0|0|0|0|0|0|0|0|0|0|0|0|0|0|0|0|0|0|0|0|0|0|0|0|0|0|0	0.01
TPCN2_DeltaCT	P07099	EPHX1	2|0|0	3|0|0|0|8	0|0|0|0|0|0|0|0|0|0|0|0|0|0|0|0|0|0|0|0|0|0|0|0|0|0|0|0|0|0	0.01
TPCN2_DeltaCT	Q14254	FLOT2	2|0|10	0|3|17|6|11	0|0|0|0|0|0|0|0|0|0|0|0|0|0|0|0|0|0|0|0|0|0|0|0|0|0|0|0|0|0	0.01
TPCN2_DeltaCT	P36957	DLST	4|0|0	5|0|0|0|3	0|0|0|0|0|0|0|1|2|2|1|2|2|0|0|0|0|0|0|0|0|0|0|0|0|0|0|0|0|0	0.01
TPCN2_DeltaCT	Q9UKM9	RALY	3|0|0	5|0|0|0|0	1|0|0|0|0|0|0|0|1|0|0|0|1|0|0|0|0|0|0|0|0|0|0|0|0|0|0|0|0|9	0.01
TPCN2_DeltaCT	P35221	CTNNA1	6|0|0	7|0|0|0|2	2|2|0|0|0|0|1|0|0|1|0|0|0|0|0|0|0|2|2|2|2|0|1|0|0|0|0|0|0|3	0.01

TPCN2_DeltaCT	Q92797	SYMPK	4|0|0	0|0|0|0|0	1|2|1|1|0|0|1|0|0|0|0|0|0|0|1|0|0|2|1|3|2|1|3|1|1|2|0|1|1|0	0.01
TPCN2_DeltaCT	P05556	ITGB1	2|0|0	0|0|0|0|2	0|0|0|0|0|0|0|0|0|0|0|0|0|0|0|0|0|1|1|1|2|0|0|0|0|0|2|1|0|0	0.01
TPCN2_DeltaCT	Q13813	SPTAN1	26|0|0	0|0|0|0|0	7|5|1|0|2|0|1|3|1|3|0|0|0|4|2|1|2|11|14|10|17|0|4|0|1|2|4|5|16|0	0.01
TPCN2_DeltaCT	P30447	HLA-A	10|0|0	8|0|0|0|8	0|0|0|0|0|0|0|4|3|5|2|2|5|0|0|0|0|1|1|0|0|0|1|0|0|0|2|1|0|2	0.01
TPCN2_DeltaCT	Q8WUH6	TMEM263	0|0|3	0|4|5|0|0	0|0|0|0|0|0|0|0|0|0|0|0|0|0|0|0|0|0|0|0|0|0|0|0|3|1	0.01
TPCN2_DeltaCT	P11387	TOP1	0|0|21	5|11|22|0|0	4|3|1|0|0|4|2|0|0|0|0|0|0|0|1|2|1|2|2|0|1|2|1|0|0|0|0|1|1|16	0.01
TPCN2_DeltaCT	P26038	MSN	26|0|25	22|7|9|0|12	11|6|6|0|0|9|4|6|1|2|3|3|1|4|5|0|0|0|1|2|2|2|0|1|1|0|2|1|0|2	0.01
TPCN2_DeltaCT	P40926	MDH2	15|0|4	18|6|5|0|13	0|0|0|0|0|0|0|0|0|0|0|0|0|0|0|0|0|0|0|0|0|0|0|0|0|5|0|0|0|0|0|0|5	0.01
TPCN2_DeltaCT	P20042	EIF2S2	2|0|0	0|0|0|0|0	3|0|1|0|0|1|1|0|0|0|0|0|0|0|0|0|0|0|0|0|0|0|0|0|1|0|0|0|0|4	0.01
TPCN2_DeltaCT	P00558	PGK1	29|0|15	36|11|10|0|20	0|0|0|0|0|0|0|1|0|1|1|0|1|0|0|0|0|0|0|0|0|0|0|2|0|0|0|0|0|0|8	0.01
TPCN2_DeltaCT	Q15437	SEC23B	3|0|0	4|0|0|0|0	0|0|0|0|0|1|2|1|0|0|0|0|0|0|0|0|0|0|0|0|0|1|1|0|1|0|0|0|0|1	0.01

TPCN2_DeltaCT	O75306	NDUFS2	3|0|0	0|0|0|0|2	0|0|0|0|0|0|0|0|0|2|2|3|1|0|0|0|0|0|0|0|0|0|0|0|0|0|0|0|0|2	0.01
TPCN2_DeltaCT	Q9NSD9	FARSB	6|0|2	9|3|2|0|5	0|0|0|1|0|2|1|0|0|0|0|0|0|0|0|0|0|0|0|0|0|0|0|0|0|0|0|1	0.01
TPCN2_DeltaCT	P23526	AHCY	12|0|7	11|6|8|0|4	0|0|0|0|0|0|1|2|0|2|0|0|2|0|0|0|0|0|0|0|0|0|3|0|0|0|0|1|0|7	0.01
TPCN2_DeltaCT	Q9BZZ5	API5	3|0|0	2|0|0|0|2	0|1|1|0|1|0|1|0|0|0|0|0|0|0|0|0|0|0|0|0|0|1|1|0|1|0|0|0|0|3	0.01
TPCN2_DeltaCT	Q9H3P7	ACBD3	2|0|0	0|0|0|0|0	1|0|1|0|0|2|2|0|0|0|0|0|0|0|0|0|0|0|0|0|0|0|2|0|0|0|0|0|0|0	0.01
TPCN2_DeltaCT	O75874	IDH1	23|0|12	29|14|9|0|15	0|1|0|0|0|4|0|0|0|0|0|0|0|0|0|0|0|0|0|2|1|0|0|0|0|0|0|0|0	0.01
TPCN2_734E	P68363	TUBA1B	21|7|14	30|18|19|7|16	50|62|131|117|90|134|224|24|23|22|21|17|21|43|49|45|51|27|53|35|46|135|116|152|136|132|3	0
TPCN2_734E	Q9Y3U8	RPL36	0|3|2	2|4|4|4|2	0|0|1|0|1|0|0|0|0|0|0|0|0|0|0|0|0|0|0|0|0|0|0|0|0|1|0	0
TPCN2_734E	Q96N67	DOCK7	2|0|0	0|0|0|0|0	0|0|7|4|3|0|2|0|0|0|0|0|0|0|0|0|0|0|0|0|0|7|5|1|2|3|0|0|0|1	0
TPCN2_734E	P40227	CCT6A	11|0|5	21|5|5|2|14	3|3|91|55|52|32|12|2|0|2|1|0|0|2|0|11|29|1|3|3|2|77|42|145|126|78|0|1|12|56	0
TPCN2_734E	P05534	HLA-A	0|0|3	0|0|0|0|0	0|0|0|0|0|0|0|4|3|5|2|2|5|0|0|0|0|1|1|0|0|0|1|0|0|0|2|1|0|2	0

TPCN2_734E	O00148	DDX39A	0|0|2	4|0|0|0|3	11|7|10|17|13|7|9|5|6|5|4|1|3|7|6|14|5|3|4|5|2|6|20|8|13|7|4|5|9|7	0
TPCN2_734E	Q92572	AP3S1	0|0|0	0|0|0|0|0	0|1|1|1|1|2|3|0|0|0|0|0|0|0|1|0|0|0|1|0|1|2|0|0|1|2|0|1|3	0
TPCN2_734E	Q08AN1	ZNF616	3|8|9	5|3|16|9|9	0|0|0|0|0|0|0|0|0|0|0|0|0|0|0|0|0|0|0|0|0|0|0|0|0|0|0|0|1|0|0|0|0|0|0	0
TPCN2_734E	P35527	KRT9	9|44|48	37|44|47|57|42	9|11|15|19|4|1|9|109|96|123|40|36|51|6|8|35|10|8|7|18|6|1|11|2|2|18|32|52|1|15	0
TPCN2_734E	P62753	RPS6	0|19|5	10|8|5|14|4	4|4|15|13|14|9|14|5|3|4|3|3|3|4|3|10|9|0|1|1|0|10|10|9|10|9|7|2|7|6	0
TPCN2_734E	P62750	RPL23A	0|0|0	0|0|0|0|0	0|1|8|4|4|9|9|0|0|0|0|0|0|0|0|3|7|0|0|0|0|3|7|3|1|5|1|0|3|2	0
TPCN2_734E	P22392	NME2	3|0|4	5|3|3|0|3	0|0|7|0|0|11|3|1|0|0|1|2|1|0|0|0|0|0|0|0|0|0|0|0|0|0|0|0|0|0|0|11	0
TPCN2_734E	P04075	ALDOA	20|0|14	30|13|12|2|20	0|2|0|0|0|0|0|1|1|2|1|1|2|1|2|0|0|1|1|1|1|0|7|0|0|0|1|0|0|16	0
TPCN2_734E	P61978	HNRNPK	12|0|5	11|3|2|0|10	29|32|22|39|26|34|30|16|13|15|14|12|12|33|32|26|16|19|25|26|30|29|38|25|23|27|25|24|27|8	0
TPCN2_734E	P28370	SMARCA1	0|0|0	0|0|0|0|0	9|7|10|11|13|4|2|0|0|0|0|0|0|9|7|45|26|3|8|6|9|3|16|6|5|9|8|10|5|0	0
TPCN2_734E	P15559	NQO1	4|0|0	10|6|3|0|7	0|0|0|0|0|0|0|0|0|0|0|0|0|0|0|0|0|0|0|0|0|0|0|0|0|0|0|0|0|0|0	0

TPCN2_734E	P46977	STT3A	0|0|0	0|0|0|0|0	2|1|0|0|0|0|2|0|1|1|1|1|1|2|1|0|0|0|0|0|0|0|0|0|0|0|0|0|1|0	0
TPCN2_734E	Q14247	CTTN	18|10|15	17|0|6|2|3	45|42|44|50|41|81|84|2|1|0|0|0|0|61|67|59|38|31|39|40|60|22|29|21|27|40|47|41|0|7	0
TPCN2_734E	P49790	NUP153	2|0|0	0|0|0|0|0	39|40|25|37|30|21|28|5|5|3|2|6|3|51|43|53|38|38|56|57|68|18|23|14|8|31|45|46|13|0	0
TPCN2_734E	Q3YEC7	RABL6	0|0|2	0|0|0|0|0	0|0|1|4|1|2|3|0|0|0|0|0|0|0|0|0|0|0|0|0|0|0|3|1|1|2|5|0|0|0|0	0
TPCN2_734E	Q04637	EIF4G1	11|0|0	0|0|0|0|0	46|43|78|71|36|47|49|0|0|0|0|0|0|57|52|25|24|26|44|43|52|38|57|27|25|49|31|31|1|13	0
TPCN2_734E	Q3B726	TWISTNB	0|0|0	0|0|0|0|0	0|0|0|0|0|0|0|0|0|0|0|0|0|0|0|0|0|0|0|0|0|0|0|0|0|0|0|0|0|0|0	0
TPCN2_734E	P30048	PRDX3	0|0|0	2|0|0|0|0	1|2|0|1|0|1|0|3|6|4|2|3|3|1|1|2|0|1|2|1|1|0|9|0|1|1|2|1|0|4	0
TPCN2_734E	Q13200	PSMD2	15|0|4	11|2|3|0|6	1|0|13|5|3|7|4|1|0|0|0|0|0|0|0|1|2|0|0|0|0|6|9|3|3|0|0|0|3|30	0
TPCN2_734E	P18077	RPL35A	0|0|3	3|3|3|4|3	1|0|6|3|22|1|3|2|1|1|1|1|1|0|0|6|5|0|0|0|0|0|3|0|1|6|0|0|1|0	0
TPCN2_734E	P0C0S8	HIST1H2A	0|0|3	4|4|3|0|2	10|7|16|23|16|15|23|2|3|3|2|2|1|9|11|17|28|7|12|9|10|21|33|36|23|24|8|7|14|16	0
TPCN2_734E	P30041	PRDX6	0|0|3	3|5|3|0|0	5|9|2|3|2|9|7|3|2|2|1|2|1|4|3|2|1|1|0|3|4|4|6|2|5|1|2|1|4|12	0

TPCN2_734E	P07910	HNRNPC	2|3|0	10|0|0|3|6	6|8|2|11|16|2|4|12|8|10|8|7|8|8|7|3|16|4|7|2|2|3|12|7|4|11|6|5|7|51	0
TPCN2_734E	P41252	IARS	8|0|0	2|0|0|0|0	2|3|4|1|8|1|1|2|0|2|0|0|1|0|0|2|0|3|5|1|1|3|10|3|4|8|5|5|3|4	0
TPCN2_734E	Q9UHB6	LIMA1	4|0|0	0|0|0|0|0	53|51|27|15|15|16|22|8|6|6|3|4|2|67|66|38|20|42|67|63|80|8|12|6|10|12|60|88|0|0	0
TPCN2_734E	P41743	PRKCI	0|0|0	0|0|0|0|0	0|0|0|0|0|0|0|0|0|0|0|0|0|0|0|0|0|0|0|0|0|0|0|0|0|0|0|0|0|0|0	0
TPCN2_734E	Q12931	TRAP1	10|0|0	6|0|0|0|6	1|1|6|7|7|23|19|8|9|8|9|9|11|1|2|10|5|2|3|1|1|8|13|6|6|5|2|2|11|24	0
TPCN2_734E	P02545	LMNA	50|0|18	51|6|11|0|45	6|6|0|2|4|0|0|18|16|15|12|15|18|7|3|13|11|4|4|1|3|0|5|0|0|1|10|7|0|1	0
TPCN2_734E	P49006	MARCKSL1	0|0|0	0|0|0|0|0	0|0|3|0|1|0|0|0|0|0|0|0|0|0|0|0|0|0|0|0|0|0|0|0|0|0|0|0|0|0|0	0
TPCN2_734E	P40429	RPL13A	3|15|15	11|14|12|25|15	2|2|3|6|4|5|5|0|1|0|0|0|0|1|1|6|3|1|1|0|1|2|5|0|0|5|0|0|2|0	0
TPCN2_734E	Q9HB71	CACYBP	0|0|0	0|0|0|0|0	1|3|3|0|0|10|8|1|1|1|2|0|1|0|2|0|0|0|0|1|0|1|3|0|0|1|0|0|0|4	0
TPCN2_734E	P37837	TALDO1	0|0|0	6|0|0|0|3	0|0|0|0|0|1|0|0|0|0|0|0|0|0|0|0|0|0|0|0|0|0|0|0|0|0|0|0|0|0|0	0
TPCN2_734E	Q8N163	CCAR2	8|0|0	4|0|0|0|0	5|8|13|13|11|6|11|1|0|0|0|0|1|1|7|5|2|3|6|6|5|14|2|4|8|5|5|12|14	0

TPCN2_734E	Q9H2I8	LRMDA	0|0|0	0|0|0|0|0	0|0|0|0|0|0|0|0|0|0|0|0|0|0|0|0|0|0|0|0|0|0|0|0|0|0|0|0	0
TPCN2_734E	Q93009	USP7	2|0|0	0|0|0|0|0	5|2|16|11|7|7|12|0|0|0|0|0|0|3|2|3|1|5|3|5|5|9|19|5|7|8|3|3|4|8	0
TPCN2_734E	P62879	GNB2	2|0|0	6|0|0|0|5	1|0|1|0|1|4|1|2|2|2|0|2|2|1|1|1|0|0|3|0|1|0|1|1|1|1|0|0|0|1	0
TPCN2_734E	P78347	GTF2I	24|0|5	15|2|0|0|7	20|17|15|11|5|5|7|5|5|4|1|2|2|14|5|22|3|22|24|24|27|7|13|3|4|8|23|21|8|43	0
TPCN2_734E	P05388	RPLP0	5|0|4	7|0|2|2|7	2|1|6|8|10|3|2|9|7|8|8|7|9|2|1|4|1|3|3|4|3|3|4|5|6|7|5|4|7|4	0
TPCN2_734E	P62979	RPS27A	15|7|16	16|12|18|5|13	0|0|1|0|0|0|1|0|0|0|0|0|1|2|1|0|0|1|3|1|2|0|2|0|0|2|2|2|1|2	0
TPCN2_734E	P07355	ANXA2	7|11|13	10|5|14|5|13	25|35|4|2|5|7|10|12|11|11|10|11|12|25|35|46|8|15|19|20|22|7|9|1|6|5|19|15|0|0	0
TPCN2_734E	O76021	RSL1D1	3|21|0	8|0|2|27|6	8|4|6|3|7|0|0|3|5|4|3|5|3|9|12|4|9|4|5|2|4|1|5|0|1|4|6|4|7|0	0
TPCN2_734E	P52272	HNRNPM	25|0|0	29|2|0|0|18	14|9|21|10|24|31|15|14|13|18|12|13|13|15|7|19|11|17|20|22|18|8|29|4|7|12|13|15|32|17	0
TPCN2_734E	P29966	MARCKS	5|0|0	4|0|0|0|0	5|3|2|1|0|0|0|3|5|4|3|3|3|5|3|0|0|1|1|2|0|0|5|0|0|0|1|2|0|1	0
TPCN2_734E	P67809	YBX1	14|36|20	26|13|15|27|18	0|0|14|8|6|7|11|0|0|0|0|0|0|0|0|3|1|0|0|0|0|5|7|1|2|7|0|0|3|15	0

TPCN2_734E	P39656	DDOST	2|0|0	6|0|0|0|6	5|6|1|0|0|2|2|9|9|9|8|6|8|0|3|0|1|1|0|1|1|0|2|0|0|0|2|2|2|0	0
TPCN2_734E	Q15366	PCBP2	0|0|0	9|0|0|0|0	10|12|17|16|13|30|27|4|4|4|2|2|5|6|8|8|9|4|5|8|10|19|14|13|15|16|4|5|7|8	0
TPCN2_734E	P25789	PSMA4	0|0|0	0|0|0|0|0	0|0|1|0|0|0|0|0|0|0|0|0|0|0|0|0|0|0|0|0|0|0|0|0|0|0|0|0|0|0|5	0
TPCN2_734E	Q15365	PCBP1	3|0|0	7|0|0|0|6	8|13|10|8|15|18|15|3|4|4|3|2|7|6|7|7|7|5|6|7|10|11|16|9|10|10|7|6|3|9	0
TPCN2_734E	B5ME19	EIF3CL	11|0|0	7|0|0|0|0	4|4|9|6|13|8|6|0|0|0|0|0|0|1|1|2|1|0|0|3|1|8|6|6|4|9|0|0|0|4	0
TPCN2_734E	Q96RP9	GFM1	0|0|0	2|0|0|0|0	0|0|0|0|0|0|0|0|7|11|8|10|11|14|0|0|0|0|0|0|0|0|0|0|0|0|0|0|0|0|0|0|0	0
TPCN2_734E	Q9UMS4	PRPF19	2|0|0	3|0|0|0|2	0|0|21|13|19|7|10|1|1|3|3|1|2|0|0|25|9|1|2|2|0|9|20|5|4|5|0|2|5|4	0
TPCN2_734E	Q14669	TRIP12	3|0|0	0|0|0|0|0	2|0|1|0|0|0|0|1|0|0|0|0|0|1|2|4|2|9|9|5|6|0|0|0|0|0|6|5|0|0	0
TPCN2_734E	P39023	RPL3	16|43|19	23|22|23|41|38	4|3|20|20|18|17|18|3|2|3|3|3|4|8|5|8|6|3|5|3|3|9|5|6|7|16|3|3|12|1	0
TPCN2_734E	O75436	VPS26A	0|0|0	0|0|0|0|0	0|0|0|0|0|0|0|1|0|1|1|0|2|0|0|0|0|0|0|0|0|0|0|0|0|0|0|0|0|0|1	0
TPCN2_734E	O75533	SF3B1	23|0|0	15|0|0|0|7	63|52|42|44|40|29|38|2|2|3|1|2|1|55|60|34|35|38|54|46|68|28|39|17|25|27|49|47|20|18	0

TPCN2_734E	P61158	ACTR3	0|0|0	0|0|0|0|0	0|0|0|0|0|0|0|0|0|0|0|0|0|0|0|0|0|0|0|0|0|1|0|0|0|0|0|0|0|0	0
TPCN2_734E	O75439	PMPCB	0|0|0	2|0|0|0|3	0|0|0|0|0|0|0|9|4|8|9|10|8|0|0|1|0|2|3|0|0|0|1|0|0|0|2|1|0|1	0
TPCN2_734E	P43034	PAFAH1B1	0|0|0	0|0|0|0|0	0|0|0|0|0|0|0|0|0|0|0|0|0|0|0|0|0|0|0|0|0|0|0|0|0|0|0|0	0
TPCN2_734E	P08621	SNRNP70	3|0|0	2|0|0|0|0	0|0|5|7|7|6|8|0|0|0|0|0|0|0|0|5|2|0|0|0|1|2|6|2|0|3|2|1|4|11	0
TPCN2_734E	P09651	HNRNPA1	2|0|3	11|2|0|0|8	10|15|18|22|7|21|14|11|11|15|12|9|12|13|16|8|5|10|21|13|16|1|16|3|4|8|13|14|6|47	0
TPCN2_734E	Q9UQE7	SMC3	6|0|0	3|0|0|0|0	0|0|9|14|12|1|2|0|1|0|0|0|0|0|0|10|6|0|0|0|0|4|21|5|7|15|0|0|10|11	0
TPCN2_734E	P62805	HIST1H4	4|5|8	6|11|8|6|6	10|8|6|19|13|14|13|10|7|9|4|7|7|13|14|16|8|9|12|7|7|12|18|7|7|12|10|9|8|29	0
TPCN2_734E	Q14103	HNRNPD	3|0|0	3|0|0|0|3	7|5|10|5|5|4|5|10|10|8|10|9|11|6|5|3|0|4|4|4|8|2|8|2|1|5|7|5|3|13	0
TPCN2_734E	O94776	MTA2	0|10|0	2|0|0|8|3	4|5|10|11|12|0|4|1|0|3|1|0|0|2|1|18|15|3|4|3|4|8|16|8|9|13|2|0|18|7	0
TPCN2_734E	P17931	LGALS3	0|0|2	3|2|3|0|4	0|0|0|0|0|0|0|0|0|0|0|0|0|0|0|0|0|0|0|0|0|0|0|0|0|0|0|2	0
TPCN2_734E	Q641Q2	WASHC2A	2|0|0	0|0|0|0|0	7|11|7|6|1|2|4|0|0|0|0|0|0|0|7|2|0|5|4|9|8|10|4|3|3|1|2|2|0|0	0

TPCN2_734E	P68104	EEF1A1	11|0|12	14|14|11|0|17	50|62|75|71|54|239|109|24|21|25|21|20|15|31|48|40|40|21|32|30|41|128|48|158|189|79|37|38	0
TPCN2_734E	P27635	RPL10	0|3|0	3|0|0|4|2	2|2|7|9|8|7|6|1|2|2|2|1|2|1|1|3|6|0|1|0|0|9|7|13|9|5|0|0|4|1	0
TPCN2_734E	P62191	PSMC1	3|0|0	5|0|0|0|3	0|0|3|0|2|0|0|0|1|0|0|0|0|0|0|2|1|0|0|0|0|2|6|2|2|1|0|0|1|11	0
TPCN2_734E	P36542	ATP5C1	0|0|2	2|0|0|0|0	0|0|9|2|5|4|3|4|3|3|3|4|3|0|1|10|8|0|0|0|0|0|5|0|1|6|0|0|6|1	0
TPCN2_734E	Q5BKZ1	ZNF326	5|0|0	4|0|0|0|0	0|1|1|5|5|0|1|2|1|3|1|2|0|0|0|3|6|0|1|0|0|2|13|2|1|9|1|2|3|0	0
TPCN2_734E	P11142	HSPA8	55|12|38	52|39|41|15|47	56|57|96|123|78|73|95|40|40|45|36|39|42|56|64|81|74|58|86|61|83|64|76|62|58|83|69|68|50|	0
TPCN2_734E	O43837	IDH3B	0|0|0	4|0|0|0|0	0|0|0|0|0|1|1|4|2|2|5|5|5|0|0|0|0|0|0|0|0|0|0|0|0|0|0|0|2|0	0
TPCN2_734E	P10155	TROVE2	0|0|0	0|0|0|0|0	0|0|0|0|0|0|0|0|0|0|0|0|0|0|0|0|0|0|0|0|0|0|0|0|0|0|0|0|1	0
TPCN2_734E	P33992	MCM5	6|0|0	12|0|0|0|6	0|0|1|1|0|0|1|0|0|0|0|0|0|0|0|0|0|0|0|0|0|1|3|0|0|1|0|0|5|23	0
TPCN2_734E	P48643	CCT5	3|0|0	13|3|0|0|10	2|1|67|53|57|26|12|5|4|5|4|3|6|0|0|8|18|2|3|0|5|58|38|120|97|64|3|2|18|95	0
TPCN2_734E	Q9HD33	MRPL47	0|0|0	0|0|0|0|0	0|0|0|0|0|0|0|0|0|0|0|0|0|0|0|0|0|0|0|0|0|0|0|0|0|0|0|0|1	0

TPCN2_734E	Q9NR30	DDX21	8|3|0	9|0|0|0|2	20|18|21|28|22|36|35|18|14|11|9|13|9|24|20|35|26|15|16|11|13|18|34|11|18|23|21|19|17|0	0
TPCN2_734E	P50502	ST13	0|0|0	3|0|0|0|0	0|0|0|0|0|0|0|0|1|0|0|0|0|0|0|0|0|0|0|0|0|0|0|0|0|0|0|0|0|0|16	0
TPCN2_734E	P34897	SHMT2	23|0|3	17|3|0|0|16	0|0|0|0|0|0|0|3|1|4|6|4|7|0|0|0|0|0|0|0|0|0|7|0|2|0|0|1|0|27	0
TPCN2_734E	Q9UHD8	SEPT9	4|0|0	4|0|0|0|0	7|8|12|19|13|10|26|0|0|0|0|0|0|9|8|7|1|4|5|6|8|11|12|7|5|16|5|7|0|1	0
TPCN2_734E	Q96DV4	MRPL38	0|0|0	0|0|0|0|0	0|0|0|0|0|0|0|0|0|0|0|0|0|0|0|0|0|0|0|0|0|0|0|0|0|0|0|0|0|0	0
TPCN2_734E	Q13601	KRR1	0|0|0	0|0|0|0|0	0|0|0|1|0|0|0|0|0|0|0|0|0|0|0|0|0|0|0|0|0|0|0|0|0|0|0|0|0|0	0
TPCN2_734E	P13798	APEH	0|0|0	2|0|0|0|0	0|0|0|0|0|0|0|0|0|0|0|0|0|0|0|0|0|0|0|0|0|0|0|0|0|0|0|0|0|0	0
TPCN2_734E	Q92616	GCN1	7|0|0	0|0|0|0|0	4|2|70|38|49|25|28|0|0|0|0|0|0|0|13|5|6|13|2|2|57|65|42|46|52|5|4|6|12	0
TPCN2_734E	Q14203	DCTN1	3|0|0	2|0|0|0|0	4|1|18|10|10|4|9|0|0|0|0|0|0|5|2|1|0|3|3|5|7|10|16|4|6|14|2|3|2|4	0
TPCN2_734E	Q53H12	AGK	0|0|0	0|2|3|0|3	0|0|0|0|0|0|1|0|0|0|0|0|0|0|0|0|0|0|0|0|0|0|0|0|0|0|0|0|0|0	0
TPCN2_734E	O14776	TCERG1	3|0|0	0|0|0|0|0	16|17|5|8|3|4|3|0|0|1|0|0|0|9|10|0|0|3|4|5|9|1|6|2|3|3|7|5|4|0	0

TPCN2_734E	A0FGR8	ESYT2	4|0|0	3|0|0|0|0	4|2|5|1|1|1|0|0|0|0|0|0|0|0|0|0|0|2|1|3|2|0|5|0|0|0|2|0|0|0	0
TPCN2_734E	O60763	USO1	2|0|0	2|0|0|0|0	2|0|3|1|1|1|1|0|0|0|0|0|0|1|1|1|2|0|0|1|2|0|2|0|1|3|1|1|0|4	0
TPCN2_734E	Q14566	MCM6	10|0|3	11|2|0|0|4	3|1|4|2|3|4|5|0|1|1|1|1|0|0|0|0|4|0|0|0|0|0|7|1|2|3|0|0|7|26	0
TPCN2_734E	P00338	LDHA	4|0|7	11|6|6|0|9	4|6|0|0|0|0|0|4|6|4|5|3|5|3|5|0|0|3|3|2|1|0|1|0|0|0|2|2|0|2	0
TPCN2_734E	P62263	RPS14	0|0|0	0|2|2|0|0	3|2|9|11|12|8|6|5|4|4|4|4|4|2|1|4|6|1|1|0|0|5|7|5|2|10|0|0|7|5	0
TPCN2_734E	P09960	LTA4H	0|0|0	3|0|0|0|2	0|0|0|0|0|0|0|0|0|0|0|0|0|0|0|0|0|0|0|0|0|0|0|0|0|0|0|0	0
TPCN2_734E	P17844	DDX5	10|0|4	13|5|2|0|12	13|12|13|7|7|10|11|11|8|7|6|5|6|14|13|12|7|9|16|13|13|5|11|5|5|7|13|10|11|18	0
TPCN2_734E	P50570	DNM2	0|0|0	3|0|0|0|0	0|0|0|1|0|0|1|0|0|0|0|0|0|0|0|0|0|0|0|0|0|1|0|0|0|0|0|0|3	0
TPCN2_734E	P68032	ACTC1	0|0|0	0|0|0|0|0	18|16|25|35|38|33|26|32|28|26|27|35|29|19|22|41|52|17|35|18|24|16|30|14|11|30|24|22|93|3	0
TPCN2_734E	Q9NVI7	ATAD3A	8|0|0	10|0|0|0|6	0|0|2|1|6|1|0|11|8|10|10|9|10|0|0|0|4|0|0|0|0|0|1|0|1|2|0|0|2|1	0
TPCN2_734E	Q00796	SORD	0|0|0	2|0|0|0|0	0|0|0|0|0|0|0|0|0|0|0|0|0|0|0|0|0|0|0|0|0|0|0|0|0|0|0|0	0

TPCN2_734E	P06744	GPI	10|0|7	18|11|13|0|10	0|0|0|0|0|0|0|0|0|0|0|0|0|0|0|0|0|0|0|0|0|0|0|0|0|0|0|0|0|0|0	0
TPCN2_734E	O75643	SNRNP200	25|0|0	0|0|0|0|0	15|16|29|13|27|14|18|8|4|10|2|2|4|4|6|40|26|10|12|20|19|23|27|14|14|24|17|19|17|23	0
TPCN2_734E	Q92522	H1FX	0|0|2	0|0|0|0|0	0|0|2|2|6|2|0|0|0|0|0|0|0|0|0|1|0|0|0|0|1|0|4|0|1|3|0|0|4|0	0
TPCN2_734E	O43242	PSMD3	0|4|3	6|0|0|3|0	0|0|7|5|5|11|5|0|0|0|0|0|0|0|1|0|0|0|0|0|0|3|7|1|6|5|0|0|9|18	0
TPCN2_734E	P06748	NPM1	29|0|5	21|7|8|0|13	146|149|101|112|50|46|123|8|6|6|3|7|8|106|94|157|72|70|124|99|175|85|107|46|43|54|100|10	0
TPCN2_734E	Q658Y4	FAM91A1	0|0|0	0|0|0|0|0	3|3|3|4|1|4|2|0|0|0|0|0|0|1|3|0|0|1|2|2|3|5|1|3|4|2|1|1|0|0	0
TPCN2_734E	Q29RF7	PDS5A	2|0|0	0|0|0|0|0	3|3|7|4|3|2|1|0|0|0|0|1|0|3|3|2|1|4|3|4|5|2|3|1|1|3|2|1|2|0	0
TPCN2_734E	Q08945	SSRP1	4|0|0	3|0|0|0|3	1|4|0|0|0|0|2|0|0|1|0|0|0|1|1|0|0|4|7|4|5|0|1|0|0|0|3|3|5|0	0
TPCN2_734E	Q7Z4V5	HDGFL2	2|0|0	0|0|0|0|0	4|3|6|6|8|6|10|0|0|0|0|0|0|4|4|0|0|2|2|1|2|6|2|2|7|6|3|1|1|2	0
TPCN2_734E	Q02978	SLC25A11	0|0|0	0|0|0|0|0	0|0|13|6|4|13|5|0|0|0|0|0|0|0|0|2|2|0|0|0|0|2|3|2|2|2|0|0|2|0	0
TPCN2_734E	Q02878	RPL6	15|20|12	18|11|13|23|16	20|13|18|9|17|19|15|11|5|8|6|4|11|13|14|15|5|4|11|5|7|6|14|8|6|15|8|10|4|1	0

TPCN2_734E	P07195	LDHB	11|0|14	17|13|12|0|17	3|3|1|2|0|3|0|1|3|2|1|2|2|1|2|0|0|3|0|2|0|0|3|0|0|0|0|1|0|6	0
TPCN2_734E	Q9BTT0	ANP32E	0|0|0	3|0|0|0|0	0|0|2|2|0|0|0|0|0|0|0|0|0|0|0|0|0|0|0|0|0|0|0|0|2|1|1|0|0|0|9	0
TPCN2_734E	P49756	RBM25	3|0|0	2|0|0|0|0	8|6|6|5|2|3|0|0|0|0|0|0|0|3|0|7|4|2|2|2|2|3|7|3|0|7|0|3|3|0	0
TPCN2_734E	P31689	DNAJA1	0|0|0	5|0|0|0|0	0|0|5|0|0|2|1|0|1|0|0|0|0|0|0|0|0|1|0|0|0|0|1|1|0|0|0|0|0|30	0
TPCN2_734E	Q15046	KARS	6|0|2	7|0|0|0|2	0|0|1|1|2|0|0|0|0|0|0|0|0|0|0|2|3|0|0|0|0|4|1|0|3|3|0|0|0|2	0
TPCN2_734E	A5YKK6	CNOT1	4|0|0	0|0|0|0|0	0|0|6|1|2|2|2|0|0|0|0|0|0|1|0|1|0|0|0|1|1|6|1|3|4|5|0|0|0|0	0
TPCN2_734E	P26640	VARS	12|0|3	8|0|0|0|0	3|1|8|4|4|8|4|0|0|0|0|0|1|0|1|4|2|0|0|0|0|11|3|7|6|9|0|0|1|20	0
TPCN2_734E	P26641	EEF1G	14|0|8	15|8|9|0|16	3|0|18|11|10|13|3|5|5|3|4|7|5|1|1|19|11|4|3|2|2|12|13|12|7|10|3|5|1|27	0
TPCN2_734E	Q8TEH3	DENND1A	0|0|0	0|0|0|0|0	0|0|0|0|0|0|0|0|0|0|0|0|0|0|0|0|0|0|0|0|0|0|0|0|0|0|0|0	0
TPCN2_734E	Q99460	PSMD1	9|0|0	9|0|2|0|5	0|1|5|0|2|4|1|0|0|0|0|0|0|0|0|0|0|1|1|2|2|0|1|2|3|1|0|0|0|18	0
TPCN2_734E	Q9NTJ3	SMC4	3|0|0	0|0|0|0|0	3|3|7|1|3|2|3|0|0|0|0|0|0|1|0|2|6|0|0|2|4|1|5|2|1|9|1|1|3|8	0

TPCN2_734E	O43491	EPB41L2	5|0|0	0|0|0|0|0	41|33|40|42|25|31|33|0|0|0|0|0|0|58|43|11|7|26|38|33|59|16|22|12|13|18|43|42|1|3	0
TPCN2_734E	P62910	RPL32	0|3|3	0|3|5|3|4	0|0|2|0|1|1|0|0|0|0|0|0|0|0|0|1|0|0|0|0|0|0|1|2|1|0|0|0|0	0
TPCN2_734E	P49915	GMPS	0|0|0	3|0|0|0|0	3|6|2|1|0|5|4|1|0|1|1|0|2|1|2|2|1|1|1|2|3|2|6|0|2|8|0|1|0|1	0
TPCN2_734E	P13639	EEF2	50|0|27	51|37|28|0|25	17|26|19|3|5|32|19|15|13|17|15|11|14|17|19|16|5|7|11|5|11|16|26|8|7|8|9|10|1|49	0
TPCN2_734E	O60264	SMARCA5	22|0|0	12|0|0|0|4	30|32|34|41|42|13|17|2|4|3|0|2|1|33|26|84|70|22|30|24|25|28|59|23|25|42|36|43|20|0	0
TPCN2_734E	P11586	MTHFD1	8|0|2	9|2|3|0|3	0|0|3|5|2|11|7|0|0|0|1|0|0|0|0|0|0|0|0|0|0|6|15|4|5|7|0|0|5|21	0
TPCN2_734E	P61353	RPL27	0|0|0	2|2|2|0|0	0|0|6|2|5|1|0|1|0|0|0|1|2|0|0|1|3|0|0|0|0|1|4|1|0|3|0|0|2|0	0
TPCN2_734E	P62847	RPS24	0|2|0	0|0|0|3|0	3|2|9|11|8|6|5|2|2|2|0|0|1|0|2|7|4|0|1|0|0|5|8|10|4|10|1|0|8|4	0
TPCN2_734E	P04264	KRT1	17|79|64	34|64|75|86|39	14|20|26|20|7|4|13|110|74|98|28|34|29|15|26|56|18|11|26|20|15|5|18|9|6|18|37|64|4|35	0
TPCN2_734E	P14324	FDPS	0|0|0	0|0|0|0|0	0|0|0|0|0|0|0|0|0|0|0|0|0|0|0|0|0|0|0|0|0|0|0|0|0|0|0|0|0|1	0
TPCN2_734E	Q9BY44	EIF2A	0|0|0	0|0|0|0|0	4|6|7|0|0|11|4|0|0|0|0|0|0|4|2|1|0|1|2|5|1|1|1|0|0|3|1|2|0|0	0

TPCN2_734E	P38919	EIF4A3	2|0|0	8|0|0|0|4	1|2|7|7|6|11|7|3|2|5|3|2|5|0|0|4|7|0|2|1|1|4|13|3|3|16|1|1|5|9	0
TPCN2_734E	P15880	RPS2	3|4|3	8|5|5|3|8	3|3|15|14|10|20|10|2|3|2|1|2|2|1|2|12|8|1|3|1|1|11|7|11|15|12|1|2|6|9	0
TPCN2_734E	P46459	NSF	0|0|0	0|0|0|0|0	0|0|1|0|0|1|1|0|0|0|0|0|0|0|0|0|0|0|0|0|0|1|1|1|1|2|0|0|0|0	0
TPCN2_734E	Q14678	KANK1	17|6|16	0|14|33|5|14	1|0|1|0|0|0|0|0|0|0|0|0|0|0|0|0|0|0|0|3|0|0|0|0|0|0|0|0	0
TPCN2_734E	O60506	SYNCRIP	4|0|0	6|0|0|0|6	4|6|4|4|2|3|9|4|2|4|2|1|2|6|8|1|3|6|8|12|9|1|9|2|1|8|7|7|1|20	0
TPCN2_734E	P49411	TUFM	8|0|2	13|0|0|0|12	4|5|12|23|27|17|14|25|22|27|30|27|34|3|3|13|21|4|5|0|1|10|32|10|5|21|5|5|10|32	0
TPCN2_734E	P62314	SNRPD1	2|0|0	0|0|0|0|2	6|6|1|2|3|4|2|0|0|0|0|0|0|3|4|1|2|0|0|0|0|3|2|1|2|2|0|0|2|3	0
TPCN2_734E	P07437	TUBB	20|9|19	39|14|20|7|17	21|23|86|120|87|90|68|30|22|27|23|19|21|20|29|40|52|11|21|11|10|80|80|116|117|93|12|22|9	0
TPCN2_734E	P63261	ACTG1	37|0|32	46|28|25|0|48	30|29|41|60|55|42|40|56|53|53|51|54|57|32|34|65|73|38|61|34|45|26|66|21|17|42|44|47|258|	0
TPCN2_734E	P43246	MSH2	8|0|2	7|0|0|0|4	0|0|8|6|1|1|3|0|0|0|0|0|0|0|0|0|0|0|1|0|0|1|1|0|0|4|0|0|2|6	0
TPCN2_734E	P01876	IGHA1	0|0|0	0|5|0|3|0	0|0|0|0|0|0|0|0|0|0|0|0|0|0|0|0|0|0|0|0|0|0|0|0|0|0|0|0|0	0

TPCN2_734E	P43243	MATR3	40|0|5	24|0|0|0|13	13|11|24|16|21|16|10|7|5|8|3|3|3|14|5|16|11|9|17|8|16|10|30|11|13|15|14|17|7|24	0
TPCN2_734E	P05165	PCCA	0|0|0	0|0|0|0|0	85|92|181|341|228|92|100|256|162|203|198|172|257|89|93|104|131|65|87|49|57|55|174|154|15	0
TPCN2_734E	P22314	UBA1	19|0|5	19|6|3|0|11	0|1|0|0|0|5|2|0|0|1|0|0|0|0|0|0|0|0|0|0|2|10|0|1|1|0|0|0|27	0
TPCN2_734E	Q53GQ0	HSD17B12	0|0|0	2|0|0|0|2	0|0|2|2|0|1|2|0|0|0|0|0|0|0|0|0|0|0|0|0|1|6|0|2|1|0|0|2|0	0
TPCN2_734E	P55145	MANF	0|0|0	0|0|0|0|0	0|0|0|0|0|0|0|0|0|0|0|0|0|0|0|0|0|0|0|0|0|0|0|0|0|0|0|0|0|0|0	0
TPCN2_734E	P50395	GDI2	5|0|6	11|4|3|0|5	3|2|0|0|0|0|0|0|0|0|0|0|0|0|0|0|0|1|0|0|0|1|0|0|0|0|1|0|4	0
TPCN2_734E	Q8NI27	THOC2	2|0|0	0|0|0|0|0	20|20|5|7|7|4|3|1|0|0|0|0|0|18|19|9|7|11|14|17|17|4|10|4|0|7|15|12|2|0	0
TPCN2_734E	P30101	PDIA3	26|0|4	24|5|2|0|18	0|0|0|0|0|0|0|9|8|9|7|7|6|0|0|0|0|0|0|0|0|0|7|0|0|0|1|0|0|10	0
TPCN2_734E	P27797	CALR	18|0|7	15|12|9|0|19	0|0|0|0|0|0|0|1|0|0|1|0|0|0|0|0|0|0|0|0|0|0|3|0|0|0|0|0|0|23	0
TPCN2_734E	P10323	ACR	0|0|0	2|0|0|0|0	0|0|0|0|0|0|0|0|0|0|0|0|0|0|0|0|0|0|0|0|0|0|0|0|0|0|0|0|0|0|0	0
TPCN2_734E	P35606	COPB2	2|2|3	6|2|0|0|2	2|2|0|0|0|2|0|1|0|0|0|0|1|0|0|1|1|0|0|0|1|0|1|0|0|0|0|1|0|9	0

TPCN2_734E	P41250	GARS	0|0|0	2|0|0|0|0	0|0|0|0|0|0|0|1|0|2|2|1|1|0|0|0|0|0|0|1|0|0|0|0|0|0|0|0|1	0
TPCN2_734E	Q13547	HDAC1	4|4|0	4|0|0|6|4	1|2|24|23|26|10|9|0|1|2|2|2|2|1|1|15|14|0|0|1|1|8|16|10|5|15|0|0|10|7	0
TPCN2_734E	P78527	PRKDC	4|0|0	0|3|4|0|0	0|0|68|65|71|21|11|10|8|11|5|2|7|0|0|5|7|0|4|0|0|28|70|23|38|56|1|1|38|95	0
TPCN2_734E	Q9H2P0	ADNP	4|0|0	0|0|0|0|0	50|41|34|38|48|12|20|0|0|0|0|0|0|50|52|43|56|29|41|43|54|16|31|11|16|32|47|67|14|0	0
TPCN2_734E	P25205	MCM3	15|0|2	16|2|0|0|6	1|2|2|0|0|1|0|0|0|1|0|0|1|1|1|1|0|0|0|1|0|1|2|1|1|1|0|0|3|25	0
TPCN2_734E	Q16186	ADRM1	0|0|0	2|0|0|0|0	1|1|2|2|1|3|0|0|1|1|0|1|0|1|0|1|1|0|0|0|0|0|1|0|0|2|1|1|0|2	0
TPCN2_734E	P48735	IDH2	4|0|0	8|0|0|0|10	0|0|0|0|0|0|0|2|4|4|5|5|6|0|0|0|0|0|0|0|0|0|0|0|0|0|0|0|0|0|0	0
TPCN2_734E	Q16181	SEPT7	0|0|0	2|0|0|0|0	2|0|14|15|7|15|17|0|0|0|0|0|1|0|12|6|0|0|1|1|6|8|4|4|12|1|2|0|4	0
TPCN2_734E	P62241	RPS8	0|8|3	0|0|3|5|0	5|4|12|13|13|14|12|6|8|6|4|3|4|5|4|17|13|0|3|0|2|9|11|4|8|13|2|3|13|6	0
TPCN2_734E	P27708	CAD	0|0|2	0|0|0|0|0	0|0|9|4|6|1|0|3|1|3|3|2|2|0|0|0|0|0|0|0|0|2|4|6|3|6|0|0|7|21	0
TPCN2_734E	Q9Y3F4	STRAP	0|0|0	0|0|0|0|0	0|1|21|20|11|24|28|0|1|0|2|1|1|1|0|4|0|1|1|1|0|14|13|8|9|8|0|1|0|4	0

TPCN2_734E	Q96AG4	LRRC59	0|0|2	2|7|10|0|0	1|0|1|0|0|0|0|0|0|0|0|0|0|0|0|0|0|0|0|1|1|0|1|0|0|0|0|0|0|4	0
TPCN2_734E	P17987	TCP1	12|6|8	21|8|7|3|15	0|0|104|91|59|28|24|6|2|5|4|2|3|0|0|13|24|2|2|2|0|75|46|147|117|67|1|0|20|63	0
TPCN2_734E	Q13162	PRDX4	10|0|0	8|0|4|0|7	0|2|3|8|4|2|2|2|3|1|2|2|2|2|6|0|1|2|1|2|4|2|6|4|6|3|2|0|3	0
TPCN2_734E	Q9NR45	NANS	0|0|0	4|0|0|0|0	0|0|0|0|0|0|0|0|0|0|0|0|0|0|0|0|0|0|0|0|0|0|0|0|0|0|0|0|0	0
TPCN2_734E	Q13283	G3BP1	9|0|0	6|0|0|0|0	8|7|20|15|10|12|13|0|0|0|0|0|8|8|7|6|3|6|2|10|13|8|10|10|13|5|3|1|4	0
TPCN2_734E	P61160	ACTR2	0|0|0	0|0|0|0|0	0|0|0|0|0|0|1|0|0|0|0|0|0|0|0|0|0|0|0|1|0|0|0|0|0|1|1	0
TPCN2_734E	P84098	RPL19	8|25|16	27|14|17|28|24	2|2|6|3|3|4|2|1|2|1|1|2|0|0|1|2|3|2|2|2|2|2|4|3|2|5|1|2|1|2	0
TPCN2_734E	Q709C8	VPS13C	0|5|19	0|52|76|0|4	0|0|0|0|0|0|0|0|0|0|0|0|0|0|0|0|0|0|0|0|0|0|0|0|0|0|0|0|0	0
TPCN2_734E	Q9H6R4	NOL6	4|0|0	3|0|0|0|0	0|0|3|1|2|0|2|0|0|0|0|0|0|2|1|5|2|1|0|1|0|0|8|0|0|5|1|0|0|0	0
TPCN2_734E	Q9Y678	COPG1	2|0|0	0|0|0|0|0	2|3|10|9|4|9|7|0|0|0|0|0|0|3|4|2|1|2|4|3|5|4|6|4|5|5|2|4|4|8	0
TPCN2_734E	O15067	PFAS	2|0|0	0|0|0|0|0	3|4|0|0|0|0|0|0|0|0|0|0|0|2|2|0|0|2|1|6|6|2|0|1|1|0|1|0|0|1	0

TPCN2_734E	P61221	ABCE1	0|0|0	0|0|0|0|0	1|0|0|0|0|7|7|0|0|0|0|0|0|0|0|0|1|0|0|0|0|0|1|0|0|0|0|0|0|2	0
TPCN2_734E	Q8WYA6	CTNNBL1	0|0|0	2|0|0|0|0	0|0|0|0|0|0|0|0|0|0|0|0|0|0|0|0|0|0|0|0|0|0|0|0|0|0|0|0	0
TPCN2_734E	Q14498	RBM39	2|0|0	2|0|0|0|0	3|2|3|1|0|3|1|1|0|0|0|0|0|0|3|1|1|3|2|2|2|1|4|1|0|1|1|2|4|28	0
TPCN2_734E	P0DME0	SETSIP	0|0|0	0|0|0|0|0	4|2|4|5|3|3|4|0|0|0|0|0|0|3|4|1|0|0|2|1|2|2|5|2|2|3|2|2|1|13	0
TPCN2_734E	Q96KP4	CNDP2	0|0|0	2|0|0|0|0	0|0|0|0|0|0|0|0|0|0|0|0|0|0|0|0|0|0|0|0|0|0|0|0|0|0|0|0	0
TPCN2_734E	P07099	EPHX1	0|0|0	3|0|0|0|8	0|0|0|0|0|0|0|0|0|0|0|0|0|0|0|0|0|0|0|0|0|0|0|0|0|0|0|0	0
TPCN2_734E	P61981	YWHAG	0|0|5	8|0|0|0|4	0|0|2|3|1|2|0|2|2|4|2|3|2|1|1|0|1|0|1|0|0|1|3|0|1|3|0|0|0|13	0
TPCN2_734E	Q8WX92	NELFB	0|0|0	0|0|0|0|3	0|0|0|0|0|0|0|0|0|0|0|0|0|0|0|0|0|0|0|0|0|0|0|0|0|0|0|1	0
TPCN2_734E	P55060	CSE1L	15|0|12	23|11|9|0|12	0|2|7|1|1|11|1|0|1|2|0|0|0|0|0|0|1|2|1|0|0|5|3|6|5|3|0|0|3|15	0
TPCN2_734E	Q13148	TARDBP	0|0|0	0|0|0|0|0	3|3|4|2|4|3|6|4|3|4|3|2|3|2|3|5|3|3|5|3|6|0|6|0|0|5|3|4|2|4	0
TPCN2_734E	Q14258	TRIM25	0|0|0	0|0|0|0|0	1|1|5|0|1|1|2|0|0|0|0|0|0|0|1|0|0|0|1|1|1|0|3|3|0|0|0|0|0|0	0

TPCN2_734E	Q14257	RCN2	0|0|0	0|0|0|0|2	0|0|0|0|0|0|0|0|0|0|0|0|0|0|0|0|0|0|0|0|0|0|0|0|0|0|0|0|0|0|0|15	0
TPCN2_734E	Q86U42	PABPN1	0|0|0	0|0|0|0|0	0|0|0|0|0|0|0|0|0|0|0|0|0|0|0|0|0|0|0|0|0|0|0|0|0|0|0|0|0|0|0|3	0
TPCN2_734E	P12236	SLC25A6	0|0|0	0|0|0|0|13	9|10|23|24|16|117|39|9|9|10|9|7|10|9|10|25|21|4|4|4|5|8|15|11|9|11|6|5|8|4	0
TPCN2_734E	P18669	PGAM1	0|0|0	4|0|0|0|0	0|1|3|3|0|11|5|0|0|0|0|0|0|0|0|0|0|0|0|0|0|0|0|0|0|0|0|2|11|0|1|1|0|0|0|7	0
TPCN2_734E	P05141	SLC25A5	10|13|12	13|11|8|13|14	8|9|27|30|21|28|14|9|7|9|8|9|8|9|8|27|32|4|3|3|5|14|20|16|15|16|6|4|13|5	0
TPCN2_734E	Q9UQ80	PA2G4	2|0|4	3|5|2|0|3	7|5|1|3|0|13|8|2|5|6|4|2|5|1|3|0|0|0|2|0|3|3|6|4|5|4|2|2|0|6	0
TPCN2_734E	P62280	RPS11	0|0|2	2|3|0|0|2	2|0|4|8|6|3|3|0|0|0|1|1|0|1|0|5|7|0|1|0|0|6|4|4|7|4|0|1|3|1	0
TPCN2_734E	P55209	NAP1L1	4|0|2	6|0|0|0|5	5|6|20|12|8|18|15|1|0|0|0|0|5|5|7|4|4|4|4|5|16|8|13|11|14|5|4|1|15	0
TPCN2_734E	Q8IWS0	PHF6	0|0|0	0|0|0|0|0	1|0|1|0|0|1|1|0|0|0|0|0|0|0|1|0|0|0|0|0|0|0|0|0|0|0|0|0|0|0|2	0
TPCN2_734E	P25705	ATP5A1	29|11|10	24|9|10|11|27	0|0|41|52|43|34|54|17|11|18|13|10|15|0|1|31|32|4|1|0|0|19|52|17|26|44|1|1|25|19	0
TPCN2_734E	Q13823	GNL2	0|12|0	4|0|0|6|0	33|32|10|15|9|0|8|0|0|0|0|0|0|27|27|25|11|16|20|22|24|11|14|7|4|9|30|54|5|0	0

TPCN2_734E	P12814	ACTN1	11|0|0	0|0|0|0|0	10|5|2|0|0|0|1|3|3|1|1|1|1|4|5|0|0|3|4|9|8|0|3|0|0|0|3|2|10|7	0
TPCN2_734E	Q9H3U1	UNC45A	0|0|0	0|0|0|0|0	4|10|5|1|0|5|4|0|0|0|0|0|0|5|3|1|0|0|2|4|5|11|4|4|6|1|1|0|0|2	0
TPCN2_734E	Q6P2E9	EDC4	3|0|0	2|0|0|0|0	8|7|13|6|3|6|7|0|0|0|0|0|0|1|3|1|1|3|7|11|14|14|10|7|9|8|4|3|0|1	0
TPCN2_734E	Q01813	PFKP	6|0|4	14|0|3|0|5	1|1|0|0|0|8|6|0|0|0|0|0|0|0|1|0|0|2|1|2|0|0|1|0|0|0|0|0|0|7	0
TPCN2_734E	Q92878	RAD50	5|0|0	0|0|0|0|2	0|0|5|8|10|0|1|0|0|0|0|0|0|0|0|0|0|1|1|0|0|1|16|0|1|10|0|0|3|1	0
TPCN2_734E	P51114	FXR1	2|0|2	4|0|0|0|3	0|1|1|1|0|4|2|0|0|0|0|0|0|2|2|1|0|0|0|0|0|0|1|0|0|1|0|0|0|0	0
TPCN2_734E	Q00341	HDLBP	9|0|0	0|0|0|0|0	25|22|28|22|7|23|26|0|0|1|0|0|0|18|18|11|5|12|10|18|24|21|11|8|15|9|13|15|2|3	0
TPCN2_734E	O76031	CLPX	0|0|0	0|0|0|0|2	0|0|0|0|0|0|0|4|3|3|6|8|9|0|0|0|0|0|0|0|0|0|0|0|0|0|0|0|0|0	0
TPCN2_734E	P61313	RPL15	5|8|7	10|12|8|8|15	7|10|20|20|17|9|16|3|2|2|3|1|2|3|6|17|8|1|1|1|2|10|30|14|11|19|4|4|5|2	0
TPCN2_734E	Q9HDC9	APMAP	0|0|0	0|0|0|0|0	0|0|0|0|0|0|0|1|0|0|0|0|0|0|0|0|0|0|0|0|0|0|0|0|0|0|1|0|0	0
TPCN2_734E	P33176	KIF5B	5|0|0	4|0|0|0|0	16|15|48|32|20|16|18|0|0|0|0|0|0|9|9|7|6|5|9|9|12|17|30|12|14|26|10|9|1|9	0

TPCN2_734E	O60814	HIST1H2BK	6|13|13	14|11|11|10|12	15|15|14|30|21|21|33|10|9|7|5|7|7|21|20|39|57|14|11|7|13|22|48|52|35|64|13|9|36|20	0
TPCN2_734E	P14866	HNRNPL	8|16|0	19|2|0|13|10	21|18|10|18|16|13|17|13|16|14|15|15|16|31|16|19|21|6|13|11|6|18|23|25|18|20|14|18|10|21	0
TPCN2_734E	P24941	CDK2	0|0|4	5|2|3|0|0	0|0|3|2|3|3|5|0|0|0|0|0|0|0|0|0|0|0|0|2|1|3|3|2|4|2|1|0|4|1	0
TPCN2_734E	P14868	DARS	2|0|2	7|0|0|0|2	1|1|4|9|4|2|1|0|0|0|0|0|0|0|1|1|0|0|0|0|0|2|5|2|1|4|0|0|2|8	0
TPCN2_734E	P63104	YWHAZ	4|0|7	13|9|7|0|9	0|3|5|4|3|2|1|8|5|6|5|6|6|1|2|1|1|3|3|0|1|2|8|2|2|3|3|2|1|28	0
TPCN2_734E	P11498	PC	6|17|56	10|34|66|24|14	691|770|428|416|295|106|88|1307|810|1086|1058|849|1284|383|418|702|699|289|459|206|325|1	0
TPCN2_734E	REV_P042	REV_P04280	0|0|0	0|0|0|0|0	0|0|0|0|0|0|0|0|0|0|0|0|0|0|0|0|0|0|0|0|0|0|0|0|0|0|0|0|0|0|0	0
TPCN2_734E	Q13263	TRIM28	29|0|2	21|0|0|0|7	32|39|52|61|50|26|37|10|11|11|7|4|9|36|40|19|9|25|32|31|39|29|37|43|28|29|28|26|16|41	0
TPCN2_734E	P11021	HSPA5	80|8|26	71|23|23|8|57	16|18|53|58|38|42|21|19|18|19|18|14|16|12|13|28|36|11|17|13|17|26|46|28|30|39|11|14|19|9	0
TPCN2_734E	Q9P0L0	VAPA	0|0|0	3|0|0|0|4	1|2|6|2|6|8|4|0|2|0|0|0|2|3|2|8|3|2|0|0|0|2|5|0|0|2|2|1|0|0	0
TPCN2_734E	Q9P0L1	ZKSCAN7	0|0|0	0|0|0|0|0	0|0|0|0|0|0|0|0|0|0|0|0|0|0|0|0|0|0|0|0|0|0|0|0|0|0|0|0|0|0|0	0

TPCN2_734E	Q02790	FKBP4	4|0|3	7|2|0|0|3	0|0|0|0|0|0|1|0|0|0|0|0|0|0|0|0|0|0|0|0|0|0|2|0|0|0|0|0|0|18	0
TPCN2_734E	Q96RQ3	MCCC1	3|11|17	4|14|19|12|12	65|57|184|276|188|44|42|169|104|125|116|93|161|56|53|55|43|31|54|26|40|62|149|125|220|21	0
TPCN2_734E	Q9Y617	PSAT1	0|0|0	0|0|0|0|0	0|0|0|0|0|0|0|0|0|0|0|0|0|0|0|0|0|0|0|0|0|0|0|0|0	0
TPCN2_734E	P31939	ATIC	0|0|0	4|0|0|0|0	0|0|0|0|0|0|0|0|0|0|0|0|0|0|0|0|0|0|0|0|0|0|0|0|0	0
TPCN2_734E	P09543	CNP	5|0|0	12|0|0|0|8	0|0|0|0|0|0|0|2|0|2|1|1|1|0|0|0|0|0|0|0|0|0|0|0|0|0|0|0|0|0	0
TPCN2_734E	Q9ULV4	CORO1C	8|0|0	6|0|0|0|4	11|10|7|3|3|16|8|0|0|0|0|0|0|7|7|2|2|6|6|8|9|0|3|1|0|3|7|7|4|0	0
TPCN2_734E	Q01105	SET	3|0|0	6|0|0|0|3	10|7|10|7|8|10|5|0|0|0|0|0|0|5|7|3|2|0|2|1|2|8|5|8|7|9|3|2|3|25	0
TPCN2_734E	Q08170	SRSF4	0|0|3	0|0|0|0|0	4|1|5|3|8|2|0|1|1|0|1|1|1|2|2|0|1|1|1|1|1|0|7|0|0|2|1|1|1|3	0
TPCN2_734E	P22626	HNRNPA2B1	0|0|0	9|0|0|0|0	15|10|14|28|23|11|17|18|12|16|10|12|16|10|12|15|21|14|13|13|14|4|29|11|8|27|18|12|9|58	0
TPCN2_734E	Q9UNF1	MAGED2	2|21|16	7|15|17|26|4	5|2|0|1|0|3|3|0|0|0|0|0|0|1|3|0|0|0|0|0|1|0|1|0|0|2|0|0|0|2	0
TPCN2_734E	Q92499	DDX1	7|0|0	4|0|0|0|3	1|1|2|4|3|7|6|0|0|0|0|0|0|0|0|4|3|0|0|0|0|8|5|4|3|5|0|0|1|8	0

TPCN2_734E	Q08J23	NSUN2	7|0|0	6|0|0|0|0	3|1|1|2|2|3|4|1|0|1|3|0|1|1|2|0|0|1|0|2|0|3|3|2|2|9|0|0|7|2	0
TPCN2_734E	P22061	PCMT1	0|0|0	0|0|0|0|0	1|0|0|0|0|0|1|1|1|2|0|0|1|1|0|0|0|1|0|1|0|0|0|0|0|0|0|0	0
TPCN2_734E	Q9UKM9	RALY	0|0|0	5|0|0|0|0	1|0|0|0|0|0|0|0|1|0|0|0|1|0|0|0|0|0|0|0|0|0|0|0|0|0|0|0|9	0
TPCN2_734E	Q7Z2W4	ZC3HAV1	0|0|0	0|0|0|0|0	17|17|5|12|4|11|14|3|4|1|1|2|2|14|11|4|6|13|21|19|28|4|5|0|2|7|11|11|0|0	0
TPCN2_734E	P04406	GAPDH	22|3|23	39|27|21|4|28	0|0|0|0|0|1|1|9|6|4|4|6|4|2|1|0|0|1|3|1|1|2|19|0|7|2|0|3|4|41	0
TPCN2_734E	Q7Z2W9	MRPL21	0|0|0	0|0|0|0|0	0|0|0|0|0|0|0|0|0|0|0|1|0|0|0|0|0|0|0|0|0|0|0|0|0|0|0|0	0
TPCN2_734E	Q8WVC0	LEO1	2|0|0	0|0|0|0|0	0|1|1|0|1|0|0|0|0|0|0|0|0|3|2|1|0|2|3|2|3|0|2|0|1|1|2|2|0|0	0
TPCN2_734E	P07339	CTSD	7|0|6	12|4|5|2|11	0|0|0|0|0|0|0|0|0|0|0|0|0|0|0|0|0|0|0|0|0|0|0|0|0|0|0|0	0
TPCN2_734E	Q9Y5L0	TNPO3	0|0|0	3|0|0|0|0	0|0|1|0|2|0|1|0|0|0|0|0|0|0|0|0|1|0|0|0|0|1|1|0|1|1|0|0|3|0	0
TPCN2_734E	P61764	STXBP1	0|0|0	2|2|0|0|0	0|0|0|0|0|0|0|0|0|0|0|0|0|0|0|0|0|0|0|0|0|0|0|0|0|0|0|0	0
TPCN2_734E	P11177	PDHB	0|0|0	3|0|0|0|4	0|0|0|0|0|0|0|11|8|8|13|16|16|0|0|0|0|0|1|0|1|0|0|0|0|0|1|0|0|1	0

TPCN2_734E	O00571	DDX3X	5|0|0	2|0|0|0|2	17|16|27|32|15|27|39|8|12|6|4|6|5|11|13|21|23|13|20|17|24|29|20|21|25|19|13|15|8|17	0
TPCN2_734E	O00299	CLIC1	0|0|0	2|2|0|0|2	1|2|0|0|0|1|1|1|2|1|1|2|1|0|1|0|0|0|5|0|2|0|0|0|1|0|1|1|0|1	0
TPCN2_734E	P29692	EEF1D	0|0|0	5|0|0|0|4	11|12|7|7|6|4|4|0|0|0|0|0|0|11|13|18|23|6|11|7|14|5|5|5|3|5|9|11|0|19	0
TPCN2_734E	Q06830	PRDX1	6|0|8	8|8|5|2|6	11|11|6|18|14|9|10|13|14|14|17|16|17|11|10|27|4|6|10|5|11|9|24|16|10|21|10|7|2|20	0
TPCN2_734E	Q9UIG0	BAZ1B	9|0|0	0|0|0|0|0	101|76|33|51|42|9|28|0|0|0|0|0|0|95|94|110|72|68|95|56|76|39|62|32|32|31|114|91|27|0	0
TPCN2_734E	P30153	PPP2R1A	3|0|0	10|0|0|0|3	0|0|11|3|7|3|0|4|0|0|0|0|0|0|0|0|0|0|1|0|0|10|10|10|5|11|0|0|0|21	0
TPCN2_734E	O75390	CS	11|0|4	16|6|2|0|13	2|2|1|0|0|0|0|9|5|7|9|6|12|0|0|0|0|2|4|3|3|0|5|0|2|0|2|3|1|11	0
TPCN2_734E	Q6ZR52	ZNF493	0|0|0	0|0|0|0|0	0|1|0|0|0|0|0|0|0|0|0|0|0|0|0|0|0|0|0|0|0|0|0|0|0|1|0|0|0|0	0
TPCN2_734E	O14646	CHD1	3|0|0	0|0|0|0|0	4|4|0|0|1|0|0|0|0|0|0|0|0|4|1|0|0|9|5|6|7|0|0|0|0|0|2|3|0|0	0
TPCN2_734E	Q9NX63	CHCHD3	0|0|0	0|0|0|0|4	0|0|0|0|0|0|0|0|0|0|0|0|0|0|0|0|0|0|0|0|0|0|0|0|0|1|0|0|0|0	0
TPCN2_734E	P49748	ACADVL	7|0|0	7|0|0|0|11	0|0|0|0|0|0|0|3|5|3|7|10|7|0|0|0|0|0|0|0|0|0|0|0|0|0|0|0|0|0	0

TPCN2_734E	P38646	HSPA9	54|12|27	52|16|34|14|42	7|10|47|45|38|12|18|90|73|125|128|112|155|6|5|25|20|12|19|10|11|27|81|13|23|21|25|23|23|	0
TPCN2_734E	Q9BSJ8	ESYT1	4|0|0	0|0|2|0|0	15|11|8|4|2|7|12|0|0|0|0|0|0|14|14|7|0|14|12|15|21|5|3|3|2|4|11|10|0|0	0
TPCN2_734E	P62701	RPS4X	0|2|2	2|2|3|0|3	0|0|6|7|2|14|12|5|2|4|2|1|4|0|1|4|3|0|2|0|0|8|8|4|2|8|1|0|1|10	0
TPCN2_734E	Q15424	SAFB	7|0|0	3|0|0|0|0	17|10|1|3|1|6|6|3|2|3|2|4|2|10|10|7|4|10|17|10|13|2|3|1|4|3|18|22|0|0	0
TPCN2_734E	P22531	SPRR2E	0|0|0	0|0|0|0|0	0|0|0|0|0|0|0|0|0|0|0|0|0|0|0|0|0|0|0|0|0|0|0|0|0|0|0|0|0|0	0
TPCN2_734E	P68431	HIST1H3	2|3|7	7|6|5|3|5	9|7|15|23|16|15|23|3|4|5|2|3|4|9|10|14|27|7|12|9|10|22|31|35|22|21|8|7|14|16	0
TPCN2_734E	P27695	APEX1	0|0|0	0|0|0|0|0	0|0|0|0|0|0|0|0|0|0|0|0|0|0|0|0|0|0|0|0|0|1|0|0|0|0|0|1|4	0
TPCN2_734E	P62277	RPS13	0|0|0	2|0|0|0|2	0|0|7|2|2|0|0|0|0|0|0|0|0|0|0|0|0|0|0|0|0|0|4|0|2|0|0|0|1|1	0
TPCN2_734E	Q9HCC0	MCCC2	0|10|15	0|16|19|15|13	0|0|257|271|200|71|59|0|0|0|0|0|0|1|0|74|70|0|0|0|0|94|273|204|384|255|0|0|83|0	0
TPCN2_734E	Q08379	GOLGA2	5|0|0	2|0|0|0|0	8|7|0|0|0|0|0|0|1|2|0|1|1|8|5|3|1|16|16|14|18|0|0|0|0|0|0|5|10|0|0	0
TPCN2_734E	P60842	EIF4A1	4|0|6	12|7|7|0|5	5|6|21|22|16|34|27|8|6|11|9|7|6|2|3|12|9|3|7|3|5|21|18|17|19|20|7|5|13|24	0

TPCN2_734E	O00232	PSMD12	0|0|0	3|0|0|0|2	1|1|1|1|0|1|1|0|0|0|0|0|0|1|0|0|0|1|0|1|3|1|1|0|1|0|0|0|0|15	0
TPCN2_734E	Q96PK6	RBM14	3|0|0	0|0|0|0|0	0|0|5|6|8|4|1|3|2|5|5|4|2|0|0|1|5|1|1|1|1|0|5|0|0|9|2|2|6|0	0
TPCN2_734E	Q9NYF8	BCLAF1	5|0|0	0|0|0|0|0	33|34|40|44|32|29|40|0|0|1|0|0|1|33|26|34|22|22|26|35|49|18|31|19|13|35|66|56|11|4	0
TPCN2_734E	P37108	SRP14	0|0|0	0|0|0|0|0	2|1|4|2|3|0|0|0|1|1|1|1|1|1|2|3|1|1|1|2|1|5|2|2|3|1|2|1|1	0
TPCN2_734E	P06733	ENO1	10|0|15	22|18|13|2|18	3|4|18|26|12|34|67|9|5|7|5|4|3|3|5|4|2|3|5|5|4|27|38|4|15|11|4|3|21|51	0
TPCN2_734E	Q9BQG0	MYBBP1A	11|0|2	3|0|5|2|4	8|3|39|21|29|9|12|2|0|3|0|0|0|2|2|9|6|7|5|5|2|7|49|6|6|24|8|4|14|2	0
TPCN2_734E	P54886	ALDH18A1	2|0|0	5|0|0|0|0	0|0|16|15|16|23|13|13|19|19|27|24|25|1|0|19|21|0|0|0|0|12|16|6|14|11|0|1|16|14	0
TPCN2_734E	P50991	CCT4	10|3|3	16|6|6|0|16	2|2|48|50|63|13|15|3|2|4|3|3|3|1|0|4|24|0|2|0|1|54|29|85|94|49|1|2|20|57	0
TPCN2_734E	P50990	CCT8	12|0|7	22|9|5|0|19	38|50|132|202|100|208|201|1|0|0|0|1|3|52|67|29|38|18|21|25|41|117|85|125|113|107|24|21|2	0
TPCN2_734E	O43399	TPD52L2	0|0|0	0|0|2|0|0	0|1|3|0|0|4|1|0|0|0|0|0|0|0|1|1|0|1|1|2|1|0|1|1|0|1|1|0|0|0	0
TPCN2_734E	P46782	RPS5	0|2|7	6|3|2|4|10	0|0|0|0|0|0|0|1|1|1|0|0|0|0|0|0|0|1|0|1|2|2|3|1|0|0|0|0|2	0

TPCN2_734E	P46781	RPS9	0|5|7	4|4|6|6|5	1|3|17|13|10|12|9|2|2|1|1|0|1|0|0|7|5|1|1|0|1|3|8|5|6|7|1|1|3|3	0
TPCN2_734E	P42704	LRPPRC	91|0|14	59|11|12|0|47	2|0|0|0|0|0|0|85|68|78|99|89|106|0|0|1|2|6|7|0|0|0|2|0|0|1|6|5|0|39	0
TPCN2_734E	Q96TA1	FAM129B	0|0|0	0|0|0|0|0	3|2|0|0|0|1|1|0|0|0|0|0|0|2|1|0|0|1|2|3|4|0|0|0|0|0|2|1|0|0	0
TPCN2_734E	P02787	TF	0|0|0	0|0|0|0|0	0|0|0|0|0|0|0|0|0|0|0|0|0|0|0|0|0|0|0|0|0|0|0|0|0|0|0|0	0
TPCN2_734E	O43719	HTATSF1	2|0|0	0|0|0|0|0	8|4|1|1|0|0|0|0|0|0|0|0|0|4|6|0|1|1|3|4|3|1|0|0|1|2|0|1|0|16	0
TPCN2_734E	P31040	SDHA	13|0|0	10|0|0|0|5	1|1|0|0|0|0|0|11|9|14|15|12|17|1|0|0|1|1|0|0|0|0|1|0|0|0|1|0|0|1	0
TPCN2_734E	P62888	RPL30	0|0|0	0|0|0|0|2	0|0|5|2|3|0|0|0|0|0|0|0|0|0|0|1|2|0|0|0|0|4|4|5|3|5|0|0|3|0	0
TPCN2_734E	P09104	ENO2	0|0|0	0|3|0|0|0	1|1|1|7|2|2|7|2|1|2|1|1|1|1|1|0|1|1|1|0|9|8|0|3|3|1|1|2|7	0
TPCN2_734E	Q9BTU6	PI4K2A	0|0|0	0|0|0|0|0	0|0|0|0|0|0|0|0|0|0|0|0|0|0|0|0|0|0|0|0|0|0|0|0|0|0|0|0	0
TPCN2_734E	P56192	MARS	2|0|0	2|0|2|0|0	0|1|9|12|10|14|9|1|0|0|0|0|0|0|0|0|0|0|1|0|1|4|10|12|9|10|0|0|9|5	0
TPCN2_734E	O60841	EIF5B	2|0|3	2|0|3|0|0	8|9|5|5|3|0|5|0|0|0|0|0|0|6|7|4|0|5|5|4|4|9|5|4|3|5|3|3|0|1	0

TPCN2_734E	Q02218	OGDH	9|0|0	0|0|0|0|3	0|0|0|0|0|0|0|4|5|5|11|9|8|0|0|0|0|0|0|0|0|0|0|0|0|0|0|0|0	0
TPCN2_734E	O95373	IPO7	10|0|2	7|0|0|0|0	4|11|5|0|0|2|2|0|1|0|0|0|0|4|7|0|0|5|5|5|4|1|1|0|0|0|3|4|0|2	0
TPCN2_734E	P20700	LMNB1	2|0|0	7|0|0|0|4	8|6|1|2|3|0|0|8|8|7|5|8|4|4|2|3|1|4|3|2|2|1|12|0|2|5|3|2|4|27	0
TPCN2_734E	P55884	EIF3B	5|0|0	4|0|0|0|0	0|0|16|6|4|6|4|0|0|0|0|0|0|0|2|2|5|0|0|0|0|7|7|3|5|2|1|1|1|4	0
TPCN2_734E	P21796	VDAC1	9|0|0	13|4|0|0|12	4|3|3|2|4|1|3|9|7|7|7|5|7|3|5|2|2|1|3|2|1|3|4|1|0|2|4|4|1|0	0
TPCN2_734E	O00763	ACACB	0|0|0	0|2|8|0|0	27|25|86|73|36|6|4|99|70|87|103|93|100|29|28|18|29|23|29|17|17|20|39|39|52|54|28|26|11|1	0
TPCN2_734E	Q01650	SLC7A5	0|0|0	2|0|0|0|0	6|11|2|1|0|0|1|4|4|5|4|4|5|11|8|5|4|5|5|4|4|0|1|0|0|1|3|5|0|0	0
TPCN2_734E	P12956	XRCC6	14|0|4	20|0|2|0|15	13|15|6|3|1|1|1|2|0|3|1|2|0|4|9|2|0|2|2|3|7|8|9|0|3|4|2|1|3|52	0
TPCN2_734E	O15143	ARPC1B	0|0|0	0|0|0|0|0	0|0|0|0|0|0|0|0|1|0|1|0|0|0|0|0|0|0|0|0|0|0|0|0|0|0|0|0|0	0
TPCN2_734E	Q9BVP2	GNL3	4|16|4	9|2|0|18|12	2|4|2|8|5|3|6|0|2|1|0|1|1|4|3|3|3|5|8|5|7|3|11|3|3|2|4|4|5|0	0
TPCN2_734E	P23246	SFPQ	10|0|2	5|3|0|0|0	15|15|49|39|30|29|18|5|2|4|2|2|3|14|11|25|26|8|13|13|17|21|25|24|19|29|13|12|15|24	0

TPCN2_734E	Q14008	CKAP5	4|0|0	0|0|0|0|0	32|19|36|21|24|20|14|0|0|0|0|0|0|17|14|8|9|22|28|25|32|42|25|23|28|33|29|23|1|10	0
TPCN2_734E	P62851	RPS25	0|3|4	2|4|5|4|2	0|0|0|0|0|0|0|1|0|0|0|0|1|0|0|0|0|0|0|0|0|0|2|1|0|0|0|0|0|8	0
TPCN2_734E	P0DMV8	HSPA1A	23|0|13	24|13|14|0|16	26|28|173|180|124|109|162|12|17|22|16|17|11|30|29|41|39|31|42|31|36|137|151|122|107|148|	0
TPCN2_734E	P40939	HADHA	44|0|8	37|9|9|0|34	0|0|0|0|0|0|0|21|14|18|24|22|23|0|0|0|0|2|1|0|0|0|1|0|0|0|0|0|0|2	0
TPCN2_734E	Q96CV9	OPTN	0|0|0	2|0|0|0|0	0|0|1|0|0|0|0|0|0|0|0|0|0|0|0|0|0|0|0|0|0|0|0|0|0|0|0|0	0
TPCN2_734E	Q9BVK6	TMED9	0|0|0	0|0|0|0|0	0|0|0|0|0|0|0|0|0|1|1|0|2|0|0|0|0|0|0|0|0|0|0|0|0|0|0|0|0	0
TPCN2_734E	P52597	HNRNPF	7|0|0	9|0|0|0|10	8|5|12|10|11|10|8|17|12|14|17|12|19|7|6|9|3|11|10|7|11|7|20|7|8|10|14|12|11|27	0
TPCN2_734E	P60709	ACTB	0|12|0	0|0|0|16|0	30|29|41|60|55|42|40|56|53|53|51|54|57|32|34|65|74|38|60|34|45|26|65|21|17|42|44|47|258|	0
TPCN2_734E	Q9NQC3	RTN4	7|0|0	9|0|0|0|7	10|10|7|8|2|8|11|1|0|1|1|1|1|6|8|12|2|11|12|12|16|0|4|2|0|3|11|7|1|2	0
TPCN2_734E	P52292	KPNA2	0|0|0	0|0|0|0|0	0|0|2|1|2|1|1|2|1|1|1|1|2|0|0|2|1|0|1|1|0|4|6|2|0|5|0|0|2|13	0
TPCN2_734E	P09211	GSTP1	2|0|2	6|3|0|0|2	0|1|0|0|0|0|0|6|7|6|7|7|5|0|0|0|0|4|5|1|0|0|0|0|0|3|2|0|0	0

TPCN2_734E	P62913	RPL11	0|0|0	0|0|0|0|4	4|4|8|9|10|13|7|3|5|3|3|3|3|4|5|6|8|2|4|0|1|6|7|3|4|9|4|3|8|6	0
TPCN2_734E	P06899	HIST1H2BJ	0|0|0	0|0|0|0|0	14|14|15|27|20|23|33|10|8|8|5|6|7|21|19|35|55|14|10|7|12|21|47|47|30|63|10|8|36|20	0
TPCN2_734E	P62917	RPL8	4|17|10	14|8|9|15|16	0|1|10|7|4|8|5|0|0|0|0|0|0|0|1|8|3|0|1|0|0|5|5|7|5|5|0|0|1|1	0
TPCN2_734E	P31943	HNRNPH1	20|0|6	19|5|0|0|21	4|3|8|7|13|9|7|9|7|11|9|10|11|5|4|6|4|9|8|6|7|7|13|9|7|11|7|5|12|24	0
TPCN2_734E	O15371	EIF3D	0|0|0	2|0|0|0|0	1|1|2|1|7|2|3|1|1|0|0|0|0|1|1|0|2|1|0|1|1|6|6|10|9|7|0|0|0|4	0
TPCN2_734E	Q15029	EFTUD2	15|0|4	11|0|3|0|5	1|2|16|16|10|7|14|1|1|3|1|1|2|1|2|21|7|4|3|2|2|26|16|13|15|19|0|2|16|28	0
TPCN2_734E	P31946	YWHAB	0|0|7	12|9|0|0|8	0|2|6|7|3|2|2|1|1|2|1|1|1|2|1|0|2|0|1|0|0|1|5|2|2|4|0|0|0|20	0
TPCN2_734E	Q8N1F7	NUP93	7|0|0	4|0|0|0|0	0|0|8|4|5|0|3|0|0|0|0|0|0|0|0|1|3|0|0|0|0|4|7|5|7|4|0|0|13|1	0
TPCN2_734E	P31948	STIP1	5|0|2	12|0|0|0|7	1|0|0|0|0|1|3|1|1|2|1|0|1|1|0|0|0|1|2|1|2|0|2|0|0|0|1|1|0|46	0
TPCN2_734E	Q15020	SART3	3|0|0	3|0|0|0|3	18|13|34|30|21|24|14|0|0|0|0|0|0|22|26|13|10|9|15|12|17|10|33|6|5|19|15|14|9|3	0
TPCN2_734E	P55072	VCP	45|0|15	35|16|15|0|24	0|0|3|1|1|3|4|0|0|0|0|0|0|0|0|0|1|6|1|2|4|5|2|3|1|0|0|0|84	0

TPCN2_734E	P63092	GNAS	0|0|2	0|2|3|0|3	0|0|0|0|0|1|1|2|2|1|1|0|1|0|0|1|0|0|0|0|0|0|1|0|0|0|0|0|0|2	0
TPCN2_734E	P23396	RPS3	11|7|8	14|8|9|8|14	6|5|39|39|32|33|39|7|9|6|6|5|6|3|5|23|23|2|3|2|2|27|26|32|35|34|4|3|29|17	0
TPCN2_734E	P30447	HLA-A	8|0|0	8|0|0|0|8	0|0|0|0|0|0|0|4|3|5|2|2|5|0|0|0|0|1|1|0|0|0|1|0|0|0|2|1|0|2	0
TPCN2_734E	P35268	RPL22	0|2|0	0|4|4|0|0	4|4|2|6|3|7|1|4|4|4|4|4|4|3|4|3|5|0|2|0|2|2|4|3|3|4|3|3|3|1	0
TPCN2_734E	Q12874	SF3A3	2|0|0	3|0|0|0|2	0|0|13|6|7|3|1|0|0|0|0|0|0|0|0|3|5|0|0|0|0|2|4|4|1|7|0|0|3|5	0
TPCN2_734E	Q9Y5B9	SUPT16H	8|0|0	7|0|0|0|0	4|5|0|1|0|5|6|1|1|1|1|1|1|2|2|1|2|4|4|1|1|0|0|1|0|1|0|1|7|0	0
TPCN2_734E	Q01130	SRSF2	0|0|0	2|0|0|0|0	0|0|2|1|0|0|0|0|0|0|0|0|0|0|0|0|0|0|0|0|0|0|2|0|0|0|0|0|2|18	0
TPCN2_734E	P48047	ATP5O	0|0|0	0|0|0|0|2	0|0|0|0|0|0|0|2|2|3|2|2|3|0|0|0|0|2|2|2|0|0|0|0|0|0|0|1|3	0
TPCN2_734E	P17812	CTPS1	0|0|0	3|0|0|0|2	22|23|22|21|14|25|21|0|0|1|2|0|0|21|27|9|2|3|10|7|15|17|13|17|14|18|9|8|3|6	0
TPCN2_734E	Q14318	FKBP8	0|0|0	2|0|0|0|0	0|0|0|0|0|0|0|0|1|2|1|0|0|0|0|0|0|4|1|0|1|0|2|0|0|0|1|0|0|1	0
TPCN2_734E	Q9UJZ1	STOML2	0|0|0	4|0|0|0|2	0|0|0|0|0|0|0|0|0|0|0|0|0|0|0|0|0|0|0|0|0|0|5|0|1|0|0|0|0|0	0

TPCN2_734E	Q16643	DBN1	25|0|0	9|0|0|0|7	19|15|5|3|5|4|13|5|1|3|2|0|4|21|19|8|6|16|12|16|20|2|7|0|0|2|12|13|27|0	0
TPCN2_734E	P82675	MRPS5	0|3|0	0|0|0|6|3	0|0|0|0|0|0|1|1|1|1|2|2|4|0|0|0|0|0|0|0|0|0|0|0|0|0|0|0|0|0	0
TPCN2_734E	Q9Y490	TLN1	13|0|4	0|5|7|0|0	22|21|43|21|10|42|42|1|0|0|0|0|0|10|10|9|1|16|25|19|32|40|32|19|33|16|18|25|0|1	0
TPCN2_734E	P00367	GLUD1	4|0|0	4|0|0|0|4	0|0|7|1|0|2|0|2|3|2|2|3|3|0|0|0|0|0|0|0|0|0|2|3|1|2|0|0|2|3	0
TPCN2_734E	P38606	ATP6V1A	8|0|2	10|0|0|0|6	1|0|5|5|2|7|6|1|0|0|0|0|0|0|0|2|1|0|1|2|0|4|4|1|2|3|0|0|0|1	0
TPCN2_734E	P08670	VIM	91|35|49	87|37|38|44|96	93|113|66|90|91|56|111|50|44|52|36|33|43|131|117|209|180|92|106|115|242|87|90|44|38|91|1	0
TPCN2_734E	P42285	SKIV2L2	6|0|0	0|0|0|0|0	1|1|30|35|43|2|2|0|0|0|0|0|0|0|0|12|3|1|2|0|0|12|38|21|27|39|0|0|8|1	0
TPCN2_734E	P32969	RPL9	0|3|3	3|4|4|4|5	8|6|13|9|6|7|5|6|5|5|5|4|8|3|2|9|4|3|2|2|1|4|8|5|6|5|4|3|8|1	0
TPCN2_734E	P31930	UQCRC1	5|0|0	6|0|0|0|7	0|0|0|0|0|0|1|3|3|3|5|3|2|0|0|3|0|1|2|0|0|0|1|0|0|0|0|1|0|0	0
TPCN2_734E	P04844	RPN2	7|0|0	4|0|0|0|3	2|1|3|0|1|4|9|6|6|8|3|2|3|0|0|4|2|1|2|0|1|0|6|0|1|3|0|1|5|0	0
TPCN2_734E	P04843	RPN1	14|0|3	12|0|3|0|11	3|0|2|0|3|3|4|2|3|2|2|1|2|0|0|1|1|1|0|1|0|0|2|0|0|0|0|0|7|8	0

TPCN2_734E	P49321	NASP	5|0|0	7|0|0|0|4	33|35|45|51|39|40|57|0|0|0|0|0|0|26|34|8|9|9|9|6|16|36|40|31|32|36|11|17|8|23	0
TPCN2_734E	Q99623	PHB2	10|3|3	13|5|7|2|15	0|0|14|23|15|13|21|1|0|0|1|0|0|0|0|18|19|0|0|0|0|11|18|7|9|13|0|0|15|1	0
TPCN2_734E	A6NHR9	SMCHD1	2|0|0	0|0|0|0|0	3|3|7|4|7|0|1|0|0|0|0|0|0|0|0|1|1|3|1|2|2|4|9|1|0|3|0|1|6|0	0
TPCN2_734E	P42224	STAT1	0|0|0	0|0|0|0|0	8|5|7|1|0|7|10|0|0|0|0|0|0|3|4|0|0|1|3|6|11|6|0|5|3|0|0|0|3|0	0
TPCN2_734E	P18085	ARF4	0|2|0	0|0|0|2|0	5|3|5|6|1|4|1|2|4|4|4|3|2|3|1|2|0|2|1|2|1|0|2|1|0|0|1|0|5|1	0
TPCN2_734E	Q9UBT2	UBA2	2|0|0	0|0|0|0|0	0|0|2|0|0|2|0|0|0|0|0|0|0|0|0|0|0|0|0|0|2|1|2|2|0|0|0|0|8	0
TPCN2_734E	Q9NWT1	PAK1IP1	0|0|0	0|0|2|0|0	0|0|0|0|0|0|0|0|0|0|0|1|1|0|0|0|0|0|0|0|0|0|0|0|0|0|0|0|0|0|0	0
TPCN2_734E	P08559	PDHA1	0|0|0	0|0|0|0|2	0|0|0|0|0|0|0|13|14|16|17|17|17|0|0|0|0|0|0|0|0|0|0|0|0|0|0|1|0|1	0
TPCN2_734E	P04792	HSPB1	0|0|2	3|0|0|0|0	1|1|0|0|0|0|0|0|0|0|0|0|0|0|0|9|21|0|1|0|0|0|0|0|0|0|0|1|0|0	0
TPCN2_734E	P30050	RPL12	0|0|0	4|2|2|0|6	4|3|5|6|7|2|1|4|4|4|5|5|5|4|1|1|3|2|2|1|2|4|6|2|5|5|5|3|4|0	0
TPCN2_734E	P61254	RPL26	0|0|3	0|5|4|0|0	0|0|10|4|6|7|5|0|0|0|0|0|0|0|0|0|2|0|0|0|0|2|4|1|2|2|0|0|1|2	0

TPCN2_734E	P21333	FLNA	76|0|29	0|31|37|0|10	1875|1821|839|866|394|425|442|22|18|18|15|15|16|914|1136|564|459|490|984|625|1175|445|57	0
TPCN2_734E	Q15459	SF3A1	9|0|0	10|0|0|0|3	23|20|15|12|4|6|13|3|1|1|1|1|2|17|17|9|13|11|15|14|22|7|15|7|2|9|15|12|7|15	0
TPCN2_734E	P49711	CTCF	0|0|0	0|0|0|0|0	4|1|2|0|1|0|2|0|0|0|0|0|0|1|1|2|1|1|5|2|5|1|3|0|0|2|3|1|1|0	0
TPCN2_734E	Q9UJV9	DDX41	0|0|0	0|0|2|0|0	0|0|1|1|1|2|0|0|0|0|0|0|0|0|0|0|0|0|1|0|0|2|1|0|0|2|0|0|0|0	0
TPCN2_734E	P30837	ALDH1B1	0|0|0	3|0|0|0|2	0|0|0|0|0|0|0|4|3|3|4|5|3|0|0|0|0|0|0|0|0|0|1|0|0|0|0|0|0|0	0
TPCN2_734E	O75683	SURF6	2|18|24	13|14|28|24|10	6|5|2|4|3|0|1|0|0|0|0|0|0|2|3|0|0|5|7|5|4|2|4|0|1|2|5|7|1|0	0
TPCN2_734E	Q7KZF4	SND1	38|0|20	38|19|17|0|33	5|4|4|4|2|9|10|5|10|10|5|7|4|5|7|0|0|5|8|5|8|3|11|6|8|2|5|6|1|13	0
TPCN2_734E	P51572	BCAP31	2|0|0	8|0|0|0|6	0|1|0|0|0|0|0|0|0|0|0|0|0|1|0|0|0|0|0|0|0|0|0|1|0|0|0|0|0|0|0	0
TPCN2_734E	Q14444	CAPRIN1	7|0|0	4|0|0|0|0	6|7|6|2|0|1|0|2|1|1|1|1|1|4|4|6|1|4|3|3|3|2|2|0|0|4|3|5|0|4	0
TPCN2_734E	P42566	EPS15	0|0|0	0|0|0|0|0	1|2|6|3|2|2|9|0|0|0|0|0|0|0|1|1|1|4|1|7|8|6|10|3|0|7|3|2|0|0	0
TPCN2_734E	P51610	HCFC1	19|0|0	5|0|0|0|0	48|40|43|43|40|36|46|2|0|0|0|0|0|53|51|36|16|45|64|58|84|28|59|17|15|39|52|50|17|1	0

TPCN2_734E	Q92688	ANP32B	0|0|0	0|0|0|0|0	0|0|0|0|0|0|0|0|0|0|0|0|0|0|0|0|0|0|0|0|0|0|0|0|0|0|0|0|0|16	0
TPCN2_734E	P14625	HSP90B1	70|0|21	59|17|18|0|50	2|2|3|1|2|1|3|12|13|12|10|10|10|2|2|1|0|4|4|1|1|1|9|1|2|2|2|2|0|58	0
TPCN2_734E	Q9Y285	FARSA	2|0|0	4|0|0|0|4	0|0|4|0|4|4|12|0|0|0|0|0|0|0|0|2|0|0|0|0|0|2|5|0|2|2|0|0|0|2	0
TPCN2_734E	Q96AY3	FKBP10	0|0|0	0|0|0|0|0	0|0|0|0|0|0|0|0|0|0|0|0|0|0|0|0|0|0|0|0|0|0|0|0|0|0|0|0|0|0	0
TPCN2_734E	P08865	RPSA	9|0|4	8|4|3|0|7	1|0|2|1|3|2|1|2|1|1|1|1|2|0|0|7|0|0|1|0|0|2|6|2|2|1|0|0|0|11	0
TPCN2_734E	P17174	GOT1	0|0|0	2|0|0|0|0	0|0|0|0|0|0|0|0|0|0|0|0|0|0|0|0|0|0|0|0|0|0|0|0|0|0|0|0|0|0	0
TPCN2_734E	P52701	MSH6	3|0|0	0|0|0|0|0	3|2|4|7|1|6|1|0|0|0|0|0|0|3|7|1|2|1|3|0|4|4|5|1|3|6|0|1|2|4	0
TPCN2_734E	P11310	ACADM	3|0|0	3|0|0|0|3	0|0|0|0|0|0|0|5|2|2|7|5|9|0|0|0|0|0|0|0|0|0|0|0|0|0|0|0|0|0|0	0
TPCN2_734E	Q07020	RPL18	13|20|11	21|11|15|20|18	1|1|10|4|8|5|6|0|2|1|1|2|1|2|1|3|3|0|1|1|0|2|6|4|3|5|1|0|11|0	0
TPCN2_734E	P22492	HIST1H1T	0|2|0	0|0|0|0|0	4|2|8|16|11|6|6|1|2|1|1|2|1|4|2|6|5|9|4|3|2|3|8|5|6|11|5|1|7|1	0
TPCN2_734E	O95573	ACSL3	20|4|8	22|8|8|4|19	1|1|1|0|0|5|3|1|2|2|2|1|1|0|0|0|1|1|2|1|1|2|1|1|0|1|1|1|1|0	0

TPCN2_734E	P13010	XRCC5	25|0|2	22|7|0|0|20	9|7|4|0|1|1|2|16|7|4|3|10|5|2|4|2|0|2|5|5|3|9|11|2|4|6|4|3|5|54	0
TPCN2_734E	P10809	HSPD1	74|2|21	63|14|18|3|65	9|5|3|2|5|2|2|67|53|64|71|66|82|5|4|32|16|14|27|11|19|2|32|2|9|9|22|15|5|40	0
TPCN2_734E	Q9Y2W1	THRAP3	18|0|0	0|0|0|0|0	35|37|44|41|23|25|45|0|0|0|0|0|0|43|37|40|21|27|38|35|61|6|41|13|16|31|38|40|11|7	0
TPCN2_734E	Q09028	RBBP4	5|0|4	4|5|0|0|2	0|1|21|17|22|10|6|2|0|1|1|1|1|1|0|3|5|0|0|1|0|5|13|6|7|8|0|0|6|13	0
TPCN2_734E	O95347	SMC2	3|0|0	4|0|0|0|0	0|0|2|0|4|1|1|0|0|0|0|0|0|0|0|0|1|0|0|0|0|3|4|2|4|7|0|0|5|12	0
TPCN2_734E	P49368	CCT3	13|2|7	20|4|5|0|14	0|0|54|55|64|22|10|1|0|1|0|0|0|0|0|4|23|0|1|0|0|69|43|116|108|72|0|0|21|41	0
TPCN2_734E	Q13310	PABPC4	13|5|2	14|4|0|3|7	3|4|14|10|4|10|6|1|0|1|1|0|1|1|2|3|0|1|2|1|3|7|10|3|7|6|2|2|6|7	0
TPCN2_734E	P10515	DLAT	0|0|0	2|0|0|0|2	0|0|0|0|0|0|0|0|0|0|0|1|1|0|0|0|0|0|0|0|0|0|0|0|0|0|0|0|0|0|0	0
TPCN2_734E	Q9HCU4	CELSR2	0|0|0	0|0|0|0|0	0|0|0|0|0|0|0|0|0|0|0|0|0|0|0|0|0|0|0|0|0|0|0|0|0|0|0|0	0
TPCN2_734E	P05023	ATP1A1	40|0|11	33|6|10|0|32	0|0|2|3|4|1|0|8|8|9|2|3|7|0|0|0|2|0|1|0|0|1|9|2|2|3|1|2|8|6	0
TPCN2_734E	P11387	TOP1	0|0|12	5|11|22|0|0	4|3|1|0|0|4|2|0|0|0|0|0|0|0|1|2|1|2|2|0|1|2|1|0|0|0|0|1|1|16	0

TPCN2_734E	P45880	VDAC2	8|2|3	11|5|2|0|9	10|9|7|7|10|9|9|17|20|14|10|11|15|11|11|14|6|9|8|8|7|5|8|0|1|6|8|9|2|0	0
TPCN2_734E	Q14152	EIF3A	17|0|0	2|0|2|0|3	2|1|17|16|20|9|5|0|0|0|0|0|0|1|0|5|4|0|2|2|4|9|23|13|6|25|0|1|6|5	0
TPCN2_734E	P11388	TOP2A	10|0|0	0|0|0|0|0	49|39|0|0|0|2|8|12|5|6|4|5|5|42|44|12|13|47|67|32|45|1|2|3|2|0|76|63|4|0	0
TPCN2_734E	Q14683	SMC1A	11|0|0	2|0|0|0|0	0|0|7|14|7|4|3|0|0|0|0|0|0|0|9|4|0|0|0|1|6|20|4|8|15|0|0|6|10	0
TPCN2_734E	P08237	PFKM	3|0|6	9|5|3|0|5	0|0|0|0|0|3|1|0|0|0|0|0|0|0|0|0|0|0|2|0|1|1|0|0|0|0|0|0|0|1	0
TPCN2_734E	P08238	HSP90AB1	69|5|50	80|40|39|2|56	29|26|14|18|11|30|28|25|23|25|23|22|24|28|30|13|8|12|17|12|18|14|24|10|16|16|14|16|16|14	0
TPCN2_734E	P28331	NDUFS1	2|0|0	3|0|0|2|2	0|0|0|0|0|0|0|0|1|2|2|2|4|0|0|0|0|0|0|0|0|0|0|0|0|0|0|0|0|0|0	0
TPCN2_734E	Q7L014	DDX46	6|0|0	0|0|0|0|0	46|50|68|85|44|31|59|0|0|0|0|0|62|58|37|27|25|42|43|50|36|51|33|40|50|45|39|42|32	0
TPCN2_734E	REV_Q9BX	REV_Q9BX63	0|0|0	0|0|0|0|0	0|0|0|0|0|0|0|0|0|0|0|0|0|0|0|0|0|0|0|0|0|0|0|0|0|0|0|0|0	0
TPCN2_734E	P62820	RAB1A	2|0|2	5|2|0|0|6	6|2|0|0|0|3|6|6|6|5|5|6|6|15|12|9|2|8|6|11|4|0|2|0|0|0|5|4|1|3	0
TPCN2_734E	P62826	RAN	3|0|5	3|4|4|0|0	9|12|41|37|30|27|29|10|11|11|8|8|8|8|9|12|17|4|6|2|9|15|23|14|15|25|11|9|13|11	0

TPCN2_734E	P50213	IDH3A	3|0|0	7|0|0|0|9	0|0|0|0|0|0|0|4|3|4|6|4|4|0|0|0|0|0|0|0|0|0|0|0|0|0|1|0|0|1	0
TPCN2_734E	Q9Y4W6	AFG3L2	10|0|0	6|0|0|0|6	0|0|0|0|0|0|0|4|3|7|10|6|7|0|0|0|0|0|0|0|0|0|0|0|0|0|0|0|0	0
TPCN2_734E	P63167	DYNLL1	0|0|0	0|0|4|0|2	2|2|6|4|5|5|0|1|1|0|1|1|1|1|2|1|1|0|1|3|1|6|3|4|4|4|0|1|0|0	0
TPCN2_734E	O15226	NKRF	3|0|0	0|0|0|0|0	1|1|1|3|0|0|0|0|0|0|0|0|0|1|1|0|1|1|1|0|2|0|4|0|0|3|1|1|0|0	0
TPCN2_734E	Q9P2J5	LARS	0|0|3	3|0|0|0|0	4|2|5|7|9|3|3|2|3|1|1|1|1|0|0|1|1|2|3|2|4|9|11|12|14|9|1|2|7|7	0
TPCN2_734E	Q92598	HSPH1	23|0|8	11|8|6|0|5	4|3|9|6|3|7|8|0|0|1|2|0|1|5|3|4|3|2|2|5|3|13|4|7|6|7|1|2|0|26	0
TPCN2_734E	P33993	MCM7	4|0|2	6|0|2|0|3	0|0|12|15|8|9|12|1|1|0|1|1|1|0|0|2|3|0|0|0|0|7|10|6|9|7|0|0|11|27	0
TPCN2_734E	P33991	MCM4	8|0|0	8|0|3|0|2	4|2|6|5|2|9|7|0|0|0|0|0|0|0|1|2|3|0|1|3|4|9|4|5|3|6|4|3|8|19	0
TPCN2_734E	P12081	HARS	0|0|0	0|0|0|0|0	0|0|0|0|0|0|0|0|0|0|0|0|0|0|0|0|0|0|0|0|0|0|0|0|0|0|0|0|4	0
TPCN2_734E	P50914	RPL14	5|6|3	6|7|6|6|9	1|3|3|3|6|8|2|0|0|0|0|0|0|0|4|4|1|2|1|1|1|5|5|1|6|1|1|3|1	0
TPCN2_734E	P62906	RPL10A	0|0|0	5|2|0|4|5	0|0|7|6|9|1|1|0|0|0|0|0|0|0|0|5|5|0|0|0|0|2|10|4|2|8|0|0|1|0	0

TPCN2_734E	P47914	RPL29	2|0|4	2|2|4|0|2	2|3|3|4|3|4|3|1|0|1|0|0|1|0|2|1|2|0|1|0|2|1|2|1|1|3|1|1|2|1	0
TPCN2_734E	Q86VP6	CAND1	23|0|6	22|3|3|0|9	0|0|9|4|1|10|5|0|0|0|0|0|0|0|0|0|0|0|0|0|0|6|13|5|9|4|0|0|10|10	0
TPCN2_734E	P57721	PCBP3	0|0|2	0|0|0|0|0	2|4|4|4|4|11|3|2|2|2|1|1|2|2|2|3|2|3|2|3|6|4|5|4|4|2|2|2|3	0
TPCN2_734E	P43490	NAMPT	0|0|4	3|4|5|0|0	0|0|4|5|4|4|8|0|0|0|0|0|0|0|0|0|2|0|0|0|0|7|5|3|7|3|0|0|1|0	0
TPCN2_734E	P35232	PHB	4|2|0	8|0|4|2|7	0|0|3|0|3|3|5|1|1|2|1|1|0|0|0|2|3|0|0|0|0|5|14|2|5|7|0|0|7|0	0
TPCN2_734E	P83731	RPL24	0|0|0	0|0|0|0|0	5|4|6|7|6|4|6|1|1|1|0|0|0|10|5|6|6|2|3|2|3|5|8|8|13|13|2|2|4|2	0
TPCN2_734E	P61513	RPL37A	0|0|0	0|3|0|0|0	1|0|0|0|0|2|0|1|1|1|1|1|1|1|0|0|0|0|0|0|0|0|0|0|0|0|0|0|1|0	0
TPCN2_734E	P15924	DSP	0|19|5	0|2|23|26|0	1|0|5|1|1|2|0|3|4|5|0|0|0|0|3|2|2|4|5|3|13|2|3|3|4|0|3|8|4	0
TPCN2_734E	Q12789	GTF3C1	2|0|0	0|0|0|0|0	1|0|7|4|4|0|0|0|0|0|0|0|0|0|0|7|3|3|4|2|2|4|9|0|3|5|4|2|1|0	0
TPCN2_734E	P06753	TPM3	0|0|0	0|0|0|0|0	3|2|1|0|0|1|0|3|3|2|4|5|3|2|1|1|0|2|2|2|1|0|4|0|0|0|0|3|5|12	0
TPCN2_734E	P11413	G6PD	0|0|0	0|0|0|0|0	0|2|0|0|0|0|0|0|0|1|0|0|0|0|0|0|0|0|1|1|1|0|0|0|1|0|0|0|0|0	0

TPCN2_734E	P49591	SARS	0|0|0	0|0|0|0|0	0|0|0|0|0|0|0|0|0|0|0|0|0|0|0|0|0|0|0|0|0|0|0|0|0|0|0|0|0|0|0	0
TPCN2_734E	Q9UH92	MLX	0|0|0	0|0|0|0|0	0|0|0|0|0|4|0|0|0|0|0|0|0|0|0|0|0|0|0|0|0|0|0|0|0|0|0|0|0|0|0|0	0
TPCN2_734E	P51532	SMARCA4	3|0|0	0|0|0|0|0	12|9|7|6|5|0|0|0|0|0|0|0|0|7|5|20|8|16|10|20|14|0|7|0|1|6|20|14|2|0	0
TPCN2_734E	P62081	RPS7	0|0|0	5|0|0|0|0	6|4|19|11|13|11|12|3|2|2|4|0|2|2|3|6|5|1|2|2|2|21|8|17|23|18|1|2|14|7	0
TPCN2_734E	P30405	PPIF	2|0|0	5|0|0|0|2	0|0|0|0|0|0|0|0|1|1|1|1|1|1|0|0|0|0|0|0|0|0|0|0|1|0|0|0|0|0|0|0	0
TPCN2_734E	Q9BXJ9	NAA15	0|0|0	2|0|0|0|0	0|0|0|1|0|3|0|0|0|0|0|0|0|0|0|0|0|0|0|0|0|0|0|0|0|0|0|0|0|0	0
TPCN2_734E	P62249	RPS16	0|0|0	0|2|0|0|0	3|2|6|7|7|8|4|3|3|2|2|2|4|3|1|6|2|1|3|0|0|1|6|2|3|9|0|1|0|7	0
TPCN2_734E	Q96A35	MRPL24	0|0|0	0|0|0|0|0	0|0|0|0|0|0|0|1|1|0|1|1|1|0|0|0|0|0|0|0|0|0|0|0|0|0|0|0|0|0|0	0
TPCN2_734E	Q8N0X7	SPG20	0|0|6	0|0|5|0|0	0|3|7|0|0|4|3|0|0|0|0|0|0|1|1|0|0|1|0|1|1|4|1|3|2|1|0|0|0|0	0
TPCN2_734E	P42765	ACAA2	0|0|0	3|0|0|0|3	0|0|0|0|0|0|0|2|2|3|5|4|7|0|0|0|0|0|0|0|0|0|0|0|0|0|0|0|0|0|1	0
TPCN2_734E	O75746	SLC25A12	0|0|0	0|0|0|0|0	0|0|0|0|0|0|0|0|0|0|0|0|0|0|0|0|0|0|0|0|0|0|0|0|0|0|0|0|1|0	0

TPCN2_734E	Q9H0D6	XRN2	8|0|0	5|0|0|0|2	0|1|7|1|2|1|4|0|0|0|0|0|0|0|0|5|0|3|1|3|3|4|1|2|0|0|1|1|4|2	0
TPCN2_734E	P68371	TUBB4B	18|8|19	33|13|20|5|14	19|22|74|96|78|68|46|23|17|23|20|16|18|14|23|35|45|8|15|7|9|66|66|85|82|81|11|17|92|137	0
TPCN2_734E	O43143	DHX15	8|0|0	6|0|0|0|0	9|8|18|15|11|7|14|9|7|6|5|4|5|7|9|26|16|4|4|6|8|7|16|10|10|13|9|4|5|12	0
TPCN2_734E	Q6NUQ4	TMEM214	0|0|0	2|0|0|0|2	0|0|0|0|0|0|0|0|0|0|0|0|0|0|0|0|0|0|0|0|0|0|0|0|0|0|0|0|0|0|0	0
TPCN2_734E	Q9Y3T9	NOC2L	2|0|0	3|0|0|2|2	0|0|1|0|4|0|0|0|0|0|0|0|0|0|0|0|0|0|0|0|0|0|0|0|0|0|1|1|0|0|2|0	0
TPCN2_734E	P61204	ARF3	0|0|2	0|0|0|0|0	7|3|15|7|4|20|6|2|5|5|4|4|1|6|3|8|2|4|0|2|2|6|7|1|1|4|4|3|8|5	0
TPCN2_734E	O15042	U2SURP	5|0|0	0|0|0|0|0	26|29|42|35|27|13|22|0|0|0|0|0|0|15|22|30|14|15|22|26|32|19|39|17|12|32|31|26|16|2	0
TPCN2_734E	P53618	COPB1	8|0|0	8|0|0|0|0	4|3|12|2|3|3|3|1|0|2|1|1|1|2|4|0|0|1|1|4|1|1|6|2|3|4|2|1|1|12	0
TPCN2_734E	P18124	RPL7	11|28|28	24|31|28|37|28	0|1|10|8|6|10|10|1|0|0|1|0|0|0|0|2|3|2|1|0|1|5|13|6|5|6|0|2|8|1	0
TPCN2_734E	P08195	SLC3A2	23|0|3	13|3|5|0|14	21|17|1|1|0|0|0|8|8|8|6|8|7|20|19|3|4|10|18|7|14|0|1|0|1|0|9|13|0|0	0
TPCN2_734E	P16403	HIST1H1C	9|0|16	21|11|13|0|9	10|6|40|51|33|22|25|11|13|9|6|6|5|7|6|21|30|19|16|12|7|10|31|29|22|39|15|7|20|10	0

TPCN2_734E	Q9Y2A7	NCKAP1	2|0|0	3|0|0|0|0	0|0|7|6|1|6|0|0|0|0|0|0|0|0|0|0|0|0|0|0|0|0|1|1|2|1|0|0|0|102	0
TPCN2_734E	Q96P11	NSUN5	0|0|0	0|0|0|0|0	0|0|0|0|0|0|0|0|0|0|0|0|0|0|0|0|0|0|0|0|0|0|0|0|0|0|0	0
TPCN2_734E	Q14980	NUMA1	8|12|0	0|0|0|13|0	108|84|31|54|89|3|17|10|6|10|1|1|1|92|103|174|173|176|277|124|150|24|111|27|20|66|250|26	0
TPCN2_734E	O43707	ACTN4	16|0|0	11|2|0|0|4	20|11|5|0|0|3|1|9|9|7|1|2|2|9|8|0|0|8|8|14|16|0|6|0|0|0|6|4|66|21	0
TPCN2_734E	Q5D862	FLG2	0|2|0	0|0|2|3|0	0|0|0|0|0|0|0|3|1|3|0|0|0|0|0|0|0|1|0|0|0|0|0|0|0|0|1|0|0	0
TPCN2_734E	P34932	HSPA4	36|0|15	27|11|12|0|12	2|1|18|5|4|2|2|0|2|1|1|3|2|2|1|2|2|2|0|1|0|10|13|8|8|7|0|1|6|37	0
TPCN2_734E	P51149	RAB7A	0|0|0	6|2|0|0|3	4|2|0|0|0|0|2|5|7|5|3|3|2|3|2|7|4|2|2|0|1|0|0|0|0|1|3|0|1	0
TPCN2_734E	P51148	RAB5C	0|0|0	2|0|0|0|4	0|0|1|0|1|2|2|2|1|1|1|0|2|0|0|6|1|0|0|0|0|1|0|0|0|0|0|0|2|0	0
TPCN2_734E	P09110	ACAA1	0|0|0	3|0|0|0|3	0|0|0|0|0|0|0|0|0|0|0|0|0|0|0|0|0|0|0|0|0|0|0|0|0|0|0	0
TPCN2_734E	P49327	FASN	48|0|37	0|28|37|0|4	63|59|554|261|157|600|327|0|0|0|0|0|0|42|43|135|72|44|57|39|53|497|160|242|234|208|84|69	0
TPCN2_734E	O43684	BUB3	0|0|0	3|0|0|0|0	3|2|8|8|6|6|4|5|4|6|7|3|4|3|2|2|1|1|4|1|3|2|3|2|3|4|2|2|1|6	0

TPCN2_734E	P55265	ADAR	22|0|0	17|0|0|0|11	13|9|18|11|12|12|4|3|4|2|1|1|1|14|11|13|7|7|10|12|10|2|25|5|3|11|7|5|6|0	0
TPCN2_734E	P10412	HIST1H1E	11|0|0	15|0|0|0|0	9|6|31|47|33|21|23|8|10|9|3|4|2|7|7|25|22|14|13|10|10|13|25|25|16|31|10|3|22|10	0
TPCN2_734E	P62424	RPL7A	5|8|6	11|6|8|9|10	1|1|17|15|10|14|10|3|3|1|1|1|1|2|2|6|9|1|2|1|2|7|10|8|10|10|2|1|12|0	0
TPCN2_734E	P07900	HSP90AA1	57|0|49	66|44|45|0|46	10|14|11|8|10|12|17|20|17|16|15|17|12|11|14|8|1|5|7|4|7|6|27|4|10|13|6|8|9|166	0
TPCN2_734E	P26373	RPL13	8|12|8	12|7|12|9|10	3|3|7|10|10|7|6|3|3|4|3|2|3|1|3|4|5|2|4|2|3|2|10|3|1|8|3|3|2|1	0
TPCN2_734E	P11940	PABPC1	8|7|3	15|4|0|4|7	6|8|17|14|9|11|7|1|1|1|1|0|1|2|5|6|0|1|3|4|6|11|13|9|9|12|2|3|6|12	0
TPCN2_734E	Q86YZ3	HRNR	0|0|9	3|5|9|2|9	0|0|1|0|0|0|0|11|12|10|1|0|1|0|0|9|1|0|0|0|0|0|0|0|0|4|3|14|0|0	0
TPCN2_734E	Q99729	HNRNPAB	6|0|0	10|0|0|0|6	2|1|8|8|9|3|2|4|8|5|7|3|3|3|3|3|2|2|3|2|3|0|4|1|2|3|4|3|2|11	0
TPCN2_734E	P55795	HNRNPH2	0|0|0	16|0|0|0|16	2|2|5|4|5|6|3|6|4|6|5|6|6|2|1|4|4|4|3|2|4|3|8|4|4|8|3|2|6|10	0
TPCN2_734E	P14618	PKM	46|18|32	63|27|24|14|31	23|24|18|5|3|29|31|12|11|9|12|8|11|16|19|24|2|7|7|10|7|28|24|12|15|9|8|6|3|48	0
TPCN2_734E	P27824	CANX	40|0|15	31|16|10|0|24	1|1|0|0|0|1|2|4|4|4|3|3|3|0|0|0|0|1|1|0|0|0|4|0|0|0|0|0|2|33	0

TPCN2_734E	P25685	DNAJB1	0|0|0	0|0|0|0|0	4|2|2|0|1|5|2|0|0|0|0|0|0|0|2|0|0|3|4|1|5|1|1|0|0|0|3|2|1|0	0
TPCN2_734E	Q14157	UBAP2L	2|0|0	2|0|0|0|0	27|30|43|26|19|43|33|0|0|0|0|0|0|24|27|20|11|19|21|24|29|27|21|26|19|30|14|18|0|1	0
TPCN2_734E	P42167	TMPO	4|0|0	4|0|0|0|0	47|52|54|79|46|49|66|6|3|5|3|5|4|55|61|45|40|32|48|33|48|26|40|25|28|41|46|38|31|8	0
TPCN2_734E	Q6PKG0	LARP1	3|0|0	0|0|0|0|0	49|49|36|33|29|47|52|0|0|0|0|0|0|46|56|26|16|17|26|38|53|40|29|18|23|23|33|29|2|3	0
TPCN2_734E	Q8N3U4	STAG2	2|0|0	0|0|0|0|0	2|2|0|0|1|0|0|0|0|0|0|0|0|1|1|0|0|0|0|0|1|1|2|2|1|1|1|0|2|2	0
TPCN2_734E	P21281	ATP6V1B2	0|0|0	0|0|0|0|3	0|0|2|0|0|4|8|0|0|0|0|0|0|0|0|0|0|0|0|0|0|2|6|1|1|0|0|0|0|1	0
TPCN2_734E	Q15393	SF3B3	18|0|0	17|5|5|0|12	1|1|24|12|15|13|13|2|1|3|2|1|3|0|0|14|10|3|3|4|4|20|25|11|16|14|2|0|13|21	0
TPCN2_734E	P26038	MSN	16|0|4	22|7|9|0|12	11|6|6|0|0|9|4|6|1|2|3|3|1|4|5|0|0|0|1|2|2|2|0|1|1|0|2|1|0|2	0
TPCN2_734E	P62861	FAU	0|0|0	0|0|2|0|0	0|0|1|0|0|0|0|0|0|0|0|0|0|0|0|0|0|0|0|0|0|0|1|1|1|0|0|0|0|3	0
TPCN2_734E	P19338	NCL	54|0|19	48|9|11|0|38	42|43|51|58|69|14|19|3|2|3|2|1|2|34|52|48|29|41|70|30|48|29|58|34|34|66|50|47|34|35	0
TPCN2_734E	Q00325	SLC25A3	6|3|4	8|2|5|3|6	2|1|7|6|6|5|4|2|2|2|3|1|3|2|2|5|4|1|2|1|1|1|8|4|2|4|2|1|3|2	0

TPCN2_734E	P63244	RACK1	0|0|2	8|2|2|0|6	10|10|7|3|5|10|8|16|16|14|12|15|16|13|14|8|3|8|16|8|8|5|6|1|4|2|15|14|2|4	0
TPCN2_734E	Q10567	AP1B1	0|0|0	0|0|0|0|0	0|1|2|0|0|2|0|0|0|0|0|0|0|0|0|0|0|0|0|0|0|1|0|2|2|0|0|0|0|1	0
TPCN2_734E	P02788	LTF	0|0|0	0|22|0|3|0	0|0|0|0|0|0|0|0|0|0|0|0|0|0|0|0|0|0|0|0|0|0|0|0|0|0|0|0|0	0
TPCN2_734E	P41091	EIF2S3	0|0|0	5|0|2|0|0	7|7|3|2|1|4|6|7|6|5|4|4|3|4|6|7|2|1|3|1|7|2|2|0|3|1|3|5|3|7	0
TPCN2_734E	O15260	SURF4	2|0|0	0|0|0|0|2	2|3|3|1|1|2|3|2|2|4|2|2|4|0|0|4|3|0|0|0|2|3|3|4|2|4|2|2|2|0	0
TPCN2_734E	P26639	TARS	3|0|3	4|2|0|0|2	0|0|2|1|0|0|3|0|0|0|0|0|0|0|0|0|0|0|0|1|0|1|5|0|1|0|0|0|0|1	0
TPCN2_734E	P61619	SEC61A1	0|0|0	0|0|0|0|3	0|0|3|3|2|3|1|0|0|0|0|0|0|0|0|0|3|0|0|0|0|1|2|3|2|0|0|0|1|0	0
TPCN2_734E	Q08211	DHX9	59|0|14	35|15|12|0|26	36|32|18|26|16|35|37|21|15|17|12|17|12|19|23|31|13|17|21|25|32|18|24|12|22|27|26|20|15|5	0
TPCN2_734E	Q9Y2J2	EPB41L3	4|0|0	0|0|0|0|0	2|0|67|52|36|55|84|0|0|0|0|0|0|3|3|0|0|1|2|2|3|25|54|24|24|44|2|2|1|5	0
TPCN2_734E	Q01518	CAP1	19|0|7	20|4|4|0|8	2|3|5|0|1|4|1|0|0|0|0|0|0|0|0|0|0|0|0|0|1|8|5|0|7|0|1|0|0|10	0
TPCN2_734E	Q8TDN6	BRIX1	0|2|0	0|0|0|0|2	2|2|3|5|3|4|2|2|2|3|3|1|4|1|1|9|1|0|2|0|1|1|2|0|2|5|1|1|0|0	0

TPCN2_734E	Q86UP2	KTN1	18|0|0	6|0|0|0|0	15|6|2|0|1|0|0|0|0|0|0|0|0|13|6|6|1|26|22|15|21|0|5|0|0|1|18|26|0|0	0
TPCN2_734E	Q13509	TUBB3	0|0|0	0|0|0|0|0	9|12|39|70|48|47|27|14|13|14|14|13|12|8|12|20|27|6|10|4|5|33|42|47|47|47|7|10|63|109	0
TPCN2_734E	Q8TAT6	NPLOC4	2|0|0	4|0|0|0|4	0|0|2|1|0|3|3|0|0|0|0|0|0|0|0|0|0|0|0|1|0|0|0|0|0|2|0|0|0|0	0
TPCN2_734E	Q13501	SQSTM1	2|0|0	6|0|0|0|0	15|14|6|2|0|8|7|1|0|2|1|1|1|11|10|27|14|6|11|11|14|8|3|4|2|7|13|9|0|0	0
TPCN2_734E	Q9UHX1	PUF60	0|0|0	2|0|3|0|0	15|17|11|12|10|13|21|0|0|2|0|0|0|16|19|10|3|16|22|20|24|11|17|6|9|8|14|11|14|22	0
TPCN2_734E	Q86XP3	DDX42	4|0|0	0|0|0|0|0	21|19|19|15|10|24|14|0|0|0|0|0|0|12|15|7|7|15|12|14|18|9|12|4|7|10|8|14|8|2	0
TPCN2_734E	P20042	EIF2S2	0|0|0	0|0|0|0|0	3|0|1|0|0|1|1|0|0|0|0|0|0|0|0|0|0|0|0|0|0|0|0|1|0|0|0|0|4	0
TPCN2_734E	P00558	PGK1	17|0|16	36|11|10|0|20	0|0|0|0|0|0|0|1|0|1|1|0|1|0|0|0|0|0|0|0|0|0|2|0|0|0|0|0|0|8	0
TPCN2_734E	Q9BZF1	OSBPL8	4|0|0	0|0|0|0|0	1|2|5|1|0|5|1|0|0|0|0|0|0|2|0|1|0|2|1|2|2|0|0|1|0|0|0|0|0|0	0
TPCN2_734E	Q92945	KHSRP	25|0|2	20|3|0|0|11	10|7|19|26|20|13|19|11|9|7|7|8|8|10|9|4|3|9|5|10|8|10|27|10|9|16|6|7|4|15	0
TPCN2_734E	Q15084	PDIA6	12|0|0	12|0|0|0|11	0|0|1|1|3|1|0|2|2|2|0|2|3|0|0|1|0|0|0|0|0|0|10|0|1|1|0|0|0|33	0

TPCN2_734E	Q8NB50	ZFP62	0|0|0	0|0|0|0|0	0|0|0|0|0|0|0|0|0|0|0|0|0|0|0|0|0|0|0|0|0|0|0|0|0|0|0|0|0|0|0	0
TPCN2_734E	Q99798	ACO2	17|0|0	16|0|0|0|11	0|0|0|0|0|0|0|12|8|9|14|11|13|0|0|0|0|1|2|0|0|0|1|0|0|0|0|0|0|0	0
TPCN2_734E	Q14CX7	NAA25	0|0|0	0|0|0|0|0	0|0|0|0|0|0|0|0|0|0|0|0|0|0|0|0|0|0|0|0|0|0|0|0|0|0|0|0|0|0|0	0
TPCN2_734E	Q7L576	CYFIP1	4|0|0	0|0|0|0|0	0|0|7|3|3|5|4|0|0|0|0|0|0|0|0|0|0|0|0|0|0|0|2|4|3|5|7|0|0|1|43	0
TPCN2_734E	P12273	PIP	0|0|0	0|0|0|2|0	0|0|0|0|0|0|0|0|0|0|0|0|0|0|0|0|0|0|0|0|0|0|0|0|0|0|0|0|0|0|0	0
TPCN2_734E	P12270	TPR	2|0|0	0|0|0|0|0	72|39|59|94|105|19|42|0|0|0|0|0|0|58|34|148|258|149|250|114|153|46|104|45|38|110|184|140	0
TPCN2_734E	Q05682	CALD1	7|0|0	10|0|0|0|2	73|52|29|8|7|20|21|0|0|0|0|0|0|90|97|20|21|26|31|37|57|1|5|1|3|11|43|87|0|0	0
TPCN2_734E	Q02413	DSG1	0|4|3	0|0|6|8|0	0|0|0|0|0|0|0|3|4|2|0|0|0|0|0|0|0|0|0|0|0|0|0|0|0|0|0|0|0|0	0
TPCN2_734E	Q14839	CHD4	4|0|0	0|0|0|0|0	106|94|103|101|100|31|41|3|3|3|1|1|3|105|95|121|88|61|79|73|83|69|89|63|53|84|102|101|39	0
TPCN2_734E	Q96KR1	ZFR	6|0|0	0|0|0|0|0	21|23|2|2|3|2|7|1|4|4|3|3|4|14|16|5|2|19|16|21|22|1|11|1|0|1|17|19|7|1	0
TPCN2_734E	P46087	NOP2	9|10|0	6|0|0|9|0	5|4|2|2|2|0|0|3|1|2|1|2|2|6|7|4|3|7|10|7|5|1|10|2|3|5|8|9|6|0	0

TPCN2_734E	Q9Y265	RUVBL1	0|0|0	0|0|0|0|3	33|34|57|75|50|50|65|2|1|1|1|1|0|33|38|51|45|24|32|29|32|72|61|65|56|56|30|25|9|15	0
TPCN2_734E	P61247	RPS3A	2|2|4	10|3|0|0|8	5|3|14|7|5|12|6|1|2|1|0|0|0|5|5|8|5|3|3|3|2|4|5|6|8|5|3|4|1|2	0
TPCN2_734E	Q13619	CUL4A	2|0|0	0|0|0|0|0	3|3|2|0|1|2|0|0|0|0|0|0|0|5|4|4|3|0|0|1|1|1|0|1|0|0|0|0|1|1	0
TPCN2_734E	P35579	MYH9	50|0|59	0|24|9|0|3	24|15|119|86|124|0|1|9|9|7|5|7|6|12|13|6|45|37|63|22|22|117|85|130|116|143|62|55|137|60	0
TPCN2_734E	Q14204	DYNC1H1	0|0|0	0|2|0|0|0	0|0|4|3|13|2|3|0|0|0|0|0|0|1|0|1|2|0|2|0|0|9|10|12|13|16|0|0|13|22	0
TPCN2_734E	P13804	ETFA	0|0|0	2|0|2|0|3	1|0|0|0|0|1|0|10|12|12|14|14|13|0|0|1|0|2|3|2|2|1|4|0|1|1|1|2|1|2	0
TPCN2_734E	Q13616	CUL1	0|0|0	2|0|0|0|0	0|0|0|0|0|0|0|0|0|0|0|0|0|0|0|0|0|0|0|0|0|0|0|0|0|0|0|0|0|0|1	0
TPCN2_734E	P23786	CPT2	2|0|0	0|0|0|0|4	0|0|0|0|0|0|0|0|1|2|3|3|5|0|0|0|0|0|0|0|0|0|0|0|0|0|0|0|0|0|0	0
TPCN2_734E	P15311	EZR	10|0|0	0|0|5|0|0	13|11|10|1|1|24|14|0|0|0|0|1|0|2|3|1|0|1|2|5|9|9|3|1|1|1|2|2|0|4	0
TPCN2_734E	P53396	ACLY	14|0|8	17|7|5|0|7	0|0|6|2|0|2|3|2|2|3|1|2|1|0|0|0|0|0|0|0|0|3|5|2|3|2|0|1|0|14	0
TPCN2_734E	Q99805	TM9SF2	0|0|0	2|0|0|0|2	0|0|0|0|0|0|0|0|0|0|0|0|0|0|0|0|0|0|0|0|0|0|0|0|0|0|0|0|0|0|0	0

TPCN2_734E	Q14562	DHX8	2|0|0	0|0|0|0|0	2|2|0|0|0|2|0|0|0|0|0|0|0|1|0|1|0|1|6|3|4|0|0|1|0|0|4|3|1|0	0
TPCN2_734E	P43686	PSMC4	0|0|0	4|0|0|0|6	0|0|4|0|1|2|1|0|0|0|0|0|0|0|0|1|1|0|1|0|0|1|2|1|2|2|0|1|0|22	0
TPCN2_734E	A1L0T0	ILVBL	0|0|0	0|0|0|0|0	0|0|2|0|0|1|2|0|0|0|0|0|0|0|0|0|0|0|0|0|0|0|2|0|0|2|0|0|0|0	0
TPCN2_734E	Q16629	SRSF7	2|0|0	2|0|0|0|2	2|2|1|5|4|0|2|1|2|0|1|1|1|2|2|1|3|0|1|0|0|1|6|3|2|3|1|0|3|14	0
TPCN2_734E	O43175	PHGDH	2|0|3	6|6|3|0|2	0|0|9|8|7|6|9|1|2|1|1|1|1|0|0|0|0|0|3|0|0|8|9|4|11|15|0|0|2|7	0
TPCN2_734E	Q96I59	NARS2	4|0|0	6|0|0|0|8	0|0|0|0|0|0|0|1|1|1|4|0|1|0|0|0|0|0|0|0|0|0|0|0|0|0|0|0|0|0|0	0
TPCN2_734E	O75306	NDUFS2	0|0|0	0|0|0|0|2	0|0|0|0|0|0|0|0|0|2|2|3|1|0|0|0|0|0|0|0|0|0|0|0|0|0|0|0|0|0|2	0
TPCN2_734E	P48444	ARCN1	0|0|0	2|0|0|0|0	1|1|6|3|4|7|6|0|0|0|0|0|0|1|4|0|0|2|2|3|2|4|5|2|1|1|1|1|4|10	0
TPCN2_734E	O95104	SCAF4	2|0|0	0|0|0|0|0	0|0|4|6|2|1|2|0|0|0|0|0|0|0|0|0|0|0|0|0|0|4|4|0|0|2|0|0|1|0	0
TPCN2_734E	O14974	PPP1R12A	4|0|0	0|0|0|0|0	6|4|9|6|3|8|7|0|0|0|0|0|0|0|1|7|1|2|2|2|2|3|2|4|1|7|1|4|0|0	0
TPCN2_734E	Q15233	NONO	5|0|0	11|0|0|0|4	28|31|45|63|37|64|51|10|5|8|5|5|9|56|45|38|42|26|26|30|38|36|39|33|24|38|26|22|28|16	0

TPCN2_734E	Q12906	ILF3	23|0|0	18|2|2|0|8	8|8|6|5|3|3|3|12|8|11|6|6|11|10|7|3|2|8|5|7|8|1|10|3|3|7|3|3|7|28	0
TPCN2_734E	Q12905	ILF2	3|0|0	8|0|0|0|5	0|0|7|2|1|4|3|0|2|0|2|1|1|0|0|2|0|1|1|1|0|2|14|0|1|3|0|0|9|18	0
TPCN2_734E	Q99459	CDC5L	2|0|0	0|0|0|0|0	17|12|6|9|10|4|12|0|0|0|0|0|0|19|14|15|16|17|21|21|22|13|14|8|3|10|19|15|8|0	0
TPCN2_734E	P11216	PYGB	0|0|0	2|0|0|0|0	0|0|0|0|0|0|0|0|0|0|0|0|0|0|0|0|0|0|0|0|0|0|0|0|0|0|0|0|0|0|0	0
TPCN2_734E	P26599	PTBP1	9|0|3	11|2|0|0|10	12|9|11|4|2|6|5|12|11|14|10|12|12|4|4|4|1|4|10|5|7|1|26|0|2|3|6|8|6|13	0
TPCN2_734E	P14923	JUP	0|11|8	0|6|13|10|0	4|5|2|1|0|4|3|5|5|4|0|0|0|6|4|6|3|1|6|7|10|0|4|1|0|0|5|6|0|0	0
TPCN2_734E	P36776	LONP1	31|0|4	21|0|2|0|14	0|0|0|2|0|2|5|13|14|12|20|16|17|0|0|0|2|0|0|0|0|2|6|0|2|1|0|0|1|8	0
TPCN2_734E	O43390	HNRNPR	4|0|2	5|0|0|0|6	6|7|5|3|7|1|5|1|3|2|2|3|0|9|10|8|7|8|9|10|12|1|14|5|3|4|6|9|6|31	0
TPCN2_734E	P23526	AHCY	4|0|5	11|6|8|0|4	0|0|0|0|0|0|1|2|0|2|0|0|2|0|0|0|0|0|0|0|0|0|3|0|0|0|0|1|0|7	0
TPCN2_734E	Q96HE7	ERO1A	0|0|0	0|0|0|0|3	0|0|0|0|0|0|0|1|1|1|1|1|1|0|0|0|0|0|0|0|0|0|0|0|0|0|0|0|0|0|0	0
TPCN2_734E	Q99575	POP1	2|0|0	0|0|0|0|0	0|0|3|3|0|1|3|0|0|0|0|0|0|0|0|2|0|0|0|0|0|2|1|0|0|1|0|0|1|0	0

TPCN2_734E	Q9UG63	ABCF2	0|0|0	0|0|0|2|0	7|9|1|0|0|3|0|0|0|0|0|0|0|4|4|1|0|3|2|5|6|0|4|1|0|0|3|3|2|0	0
TPCN2_734E	P09874	PARP1	40|0|6	27|0|0|0|16	8|12|5|8|3|27|31|5|3|4|2|2|5|14|10|2|0|5|4|5|7|10|20|18|25|15|3|9|18|54	0
TPCN2_734E	P23528	CFL1	0|0|2	7|3|2|0|6	4|4|1|2|2|2|5|2|4|4|6|5|5|1|0|5|5|3|2|3|2|6|8|5|6|5|2|5|11|12	0
TPCN2_734E	Q92997	DVL3	0|0|4	0|0|5|0|0	12|16|23|23|12|8|7|0|0|0|0|0|0|54|53|4|2|4|6|3|7|8|20|7|6|17|5|5|0|0	0
TPCN2_734E	Q9NZ01	TECR	0|0|0	2|0|0|0|2	1|4|3|2|2|2|2|2|0|1|0|0|1|4|1|2|1|0|0|0|0|0|4|1|2|1|0|0|1|0	0
TPCN2_734E	P27816	MAP4	11|0|2	0|0|0|0|0	80|86|65|68|36|34|46|1|1|1|1|2|1|67|88|31|21|28|51|46|78|56|39|36|42|57|81|63|0|2	0
TPCN2_734E	Q00839	HNRNPU	52|3|16	39|9|15|3|17	20|20|31|52|46|30|34|10|9|9|9|8|9|19|23|40|29|15|24|14|19|23|29|23|25|37|21|21|21|45	0
TPCN2_734E	Q16531	DDB1	10|0|3	14|3|2|0|5	0|0|1|0|0|0|0|0|0|0|0|0|0|0|0|0|0|0|0|0|0|0|0|0|0|0|0|0|0|18	0
TPCN2_734E	P06576	ATP5B	32|0|10	33|6|5|2|28	3|1|4|7|3|32|31|11|13|11|19|16|17|2|1|6|2|2|2|3|6|7|24|8|13|7|5|2|13|22	0
TPCN2_734E	Q13247	SRSF6	9|0|0	7|0|0|0|10	4|1|2|1|5|2|0|1|1|0|1|1|1|2|2|2|3|1|1|1|1|0|5|0|0|3|1|1|1|5	0
TPCN2_734E	O75152	ZC3H11A	3|0|0	3|0|0|0|0	15|16|8|18|14|2|5|0|0|0|0|0|0|21|13|8|4|17|15|18|17|4|15|5|3|8|13|15|5|0	0

TPCN2_734E	P16615	ATP2A2	30|0|3	27|0|0|0|24	2|1|8|3|7|4|3|4|4|5|5|3|4|1|1|0|1|1|1|2|2|2|10|4|6|6|1|0|8|5	0
TPCN2_734E	P57729	RAB38	0|0|0	2|0|0|0|4	0|0|0|0|0|0|0|0|0|0|0|0|0|0|0|0|0|0|0|0|0|0|0|0|0|0|0|0|0|0|0	0
TPCN2_734E	Q00688	FKBP3	0|0|0	0|0|2|0|0	0|0|1|0|0|0|0|0|0|0|0|0|0|0|0|0|0|0|0|0|0|0|0|0|0|0|0|0|0|0|1	0
TPCN2_734E	Q14699	RFTN1	0|0|0	0|0|0|0|0	0|0|0|0|0|0|0|0|0|0|0|0|0|0|0|0|0|0|0|0|0|0|0|0|0|0|0|0|0|0|0	0
TPCN2_734E	O60271	SPAG9	5|0|0	0|0|0|0|0	2|2|26|11|12|12|10|0|0|0|0|0|0|1|1|0|0|0|0|0|1|13|11|7|12|16|0|0|0|3	0
TPCN2_734E	P07814	EPRS	8|0|0	0|0|2|0|0	19|12|12|22|21|7|13|3|4|2|0|4|1|18|16|12|9|13|18|22|31|13|22|6|10|20|23|15|2|8	0
TPCN2_734E	Q02880	TOP2B	8|0|0	0|0|0|0|0	14|9|0|0|0|0|0|2|1|1|1|1|1|12|7|3|4|21|21|11|14|0|0|0|0|0|18|20|0|0	0
TPCN2_734E	P23284	PPIB	0|15|20	13|22|31|15|15	0|0|0|0|0|0|0|2|4|2|0|1|1|0|0|0|0|2|0|1|1|0|1|0|0|0|0|0|0|26	0
TPCN2_734E	Q8WXX5	DNAJC9	0|0|0	0|2|0|0|0	0|0|0|0|0|0|0|0|0|0|0|0|0|0|0|0|0|0|0|0|0|0|0|0|0|0|0|0|0|0|0	0
TPCN2_734E	P62937	PPIA	0|0|0	6|4|3|0|3	1|1|1|0|0|3|0|9|6|8|8|4|7|0|0|0|0|0|1|0|2|0|18|0|3|0|4|2|2|19	0
TPCN2_734E	P09622	DLD	10|0|0	13|0|0|0|10	0|0|1|6|0|4|4|1|0|1|1|2|4|0|0|0|0|0|0|0|0|0|4|0|0|2|0|0|1|0	0

TPCN2_734E	P36871	PGM1	0|0|0	2|0|0|0|0	0|0|0|0|0|0|0|0|0|0|0|0|0|0|0|0|0|0|0|0|0|0|0|0|0|0|0|0|0|0|0	0
TPCN2_734E	O43865	AHCYL1	0|0|0	3|0|0|0|0	0|1|2|0|0|4|5|0|0|0|0|0|0|0|0|0|0|0|0|0|0|1|1|2|1|1|0|0|0|1	0
TPCN2_734E	Q9BZZ5	API5	0|0|0	2|0|0|0|2	0|1|1|0|1|0|1|0|0|0|0|0|0|0|0|0|0|0|0|0|0|1|1|0|1|0|0|0|0|3	0
TPCN2_734E	Q13435	SF3B2	9|0|0	3|0|0|0|0	39|31|18|28|19|10|19|0|0|0|0|0|0|50|45|21|26|35|31|40|42|17|23|11|14|18|32|33|14|17	0
TPCN2_734E	Q8IY81	FTSJ3	11|27|4	15|2|0|22|9	25|25|13|11|5|4|3|3|1|0|0|0|0|17|24|14|10|20|23|12|23|5|9|7|5|8|24|23|13|0	0
TPCN2_734E	Q8NC51	SERBP1	0|0|0	2|0|0|0|0	35|41|54|73|30|58|73|1|2|1|1|2|1|33|43|31|19|16|28|15|27|19|40|13|12|44|104|26|5|2	0
TPCN2_734E	P53990	IST1	0|0|0	4|0|0|0|0	0|0|0|0|0|0|0|0|0|0|0|0|0|0|0|0|0|1|0|0|0|0|0|0|0|0|0|0|0|0|0	0
TPCN2_734E	P09429	HMGB1	0|0|0	0|0|0|0|0	1|1|1|0|0|0|1|0|0|0|0|0|0|1|0|0|0|1|0|1|0|3|6|0|1|3|0|0|0|4	0
TPCN2_734E	Q02543	RPL18A	4|5|3	4|3|3|4|9	3|3|8|10|11|6|4|13|4|3|2|2|3|4|4|5|8|0|0|0|0|3|7|1|0|8|1|1|0|0	0
TPCN2_734E	P36578	RPL4	36|74|39	55|44|38|81|59	3|3|14|12|16|7|8|1|1|1|2|2|1|3|2|12|8|1|2|0|0|12|6|13|11|14|2|2|6|2	0
TPCN2_734E	P78371	CCT2	9|0|4	19|2|3|0|11	1|1|96|69|87|29|7|6|5|7|6|6|4|0|0|4|32|2|3|3|0|95|52|245|214|87|2|1|19|62	0

TPCN2_734E	O15355	PPM1G	0|0|0	2|0|0|0|2	1|1|4|0|0|4|2|0|0|0|0|0|0|0|0|0|0|0|0|0|0|1|2|1|0|5|0|0|0|7	0
TPCN2_734E	Q9UJS0	SLC25A13	13|6|2	12|0|0|5|12	0|0|3|0|0|2|3|1|0|0|0|0|1|0|0|4|1|0|1|0|0|1|4|2|0|2|0|0|6|0	0
TPCN2_734E	Q05639	EEF1A2	0|2|0	0|0|0|2|0	28|37|42|27|22|178|56|12|10|13|13|10|10|21|28|19|16|12|18|10|20|79|16|113|144|43|17|11|1	0
TPCN2_734E	P30086	PEBP1	0|0|0	2|0|0|0|0	0|0|0|0|0|0|0|0|0|0|0|0|0|0|0|0|0|0|0|0|0|0|0|0|0|0|0|0|0|0|0	0
TPCN2_734E	P46777	RPL5	7|6|0	11|0|0|6|8	8|4|8|8|13|9|12|2|3|3|2|2|1|6|8|2|6|3|4|2|5|3|4|7|5|10|2|4|5|6	0
TPCN2_734E	Q8IX01	SUGP2	0|0|0	2|0|0|0|0	26|16|19|30|30|9|5|0|0|0|0|0|0|16|15|36|17|24|21|23|28|10|23|15|7|22|25|31|12|0	0
TPCN2_734E	Q99832	CCT7	6|0|3	18|4|2|0|10	0|2|51|34|50|14|5|3|2|1|1|1|1|0|1|2|14|1|1|0|1|69|32|115|101|51|0|1|7|43	0
TPCN2_734E	P46778	RPL21	0|0|0	2|0|0|0|0	1|1|9|8|7|12|10|1|0|1|0|0|1|0|0|6|8|0|1|0|1|3|4|3|2|7|1|1|1|0	0
TPCN2_734E	P46779	RPL28	3|9|8	7|3|6|10|10	5|5|11|12|6|26|10|3|0|1|0|2|1|1|2|8|4|0|0|0|0|4|6|4|2|12|0|1|8|0	0
TPCN2_734E	P35580	MYH10	35|0|66	0|9|0|0|0	0|1|12|8|11|0|0|0|1|1|0|1|0|0|0|0|1|4|9|1|2|11|19|11|9|15|4|3|131|41	0
TPCN2_734E	Q14978	NOLC1	3|0|0	3|0|0|0|0	15|16|21|11|9|11|5|0|0|0|0|0|0|12|10|22|17|7|8|7|12|6|12|9|6|14|13|11|4|0	0

TPCN2_734E	Q9H3P7	ACBD3	0|0|0	0|0|0|0|0	1|0|1|0|0|2|2|0|0|0|0|0|0|0|0|0|0|0|0|0|0|0|2|0|0|0|0|0|0|0	0
TPCN2_734E	Q8TAQ2	SMARCC2	5|0|0	2|0|0|0|0	2|2|4|4|9|0|1|0|0|0|0|0|0|1|0|7|1|1|2|5|2|0|13|1|2|4|2|2|1|0	0
TPCN2_734E	Q9BZH6	WDR11	3|0|0	0|0|0|0|0	0|0|11|3|1|1|3|0|0|0|0|0|0|0|0|1|1|0|0|0|0|7|1|2|5|6|0|0|0|0	0
TPCN2_734E	O60716	CTNND1	3|0|0	2|0|0|0|0	10|9|0|0|0|3|2|0|0|0|0|0|0|4|6|3|3|3|8|10|14|1|1|0|1|0|3|4|0|0	0
TPCN2_734E	Q01546	KRT76	0|0|0	0|0|0|0|0	1|2|0|1|1|0|0|9|5|5|0|0|0|1|0|2|2|0|1|1|1|0|0|0|0|1|1|2|0|2	0
TPCN2_734E	Q14974	KPNB1	18|0|9	22|8|9|0|14	0|1|40|11|19|16|9|9|7|8|4|2|2|0|0|7|4|1|5|1|1|15|36|8|17|25|2|3|3|31	0
TPCN2_734E	Q07866	KLC1	0|0|0	0|0|0|0|0	4|5|11|9|4|10|10|0|0|0|0|0|0|3|3|0|1|0|0|2|1|11|8|10|10|10|0|0|0|3	0
TPCN2_734E	Q9C0H2	TTYH3	0|0|0	0|0|0|0|0	0|0|0|0|0|0|0|0|0|0|0|0|0|0|0|0|0|0|0|0|0|0|0|0|0|0|0|0	0
TPCN2_734E	P22695	UQCRC2	5|0|0	5|0|0|0|5	0|1|1|1|0|8|4|3|2|2|3|2|3|0|0|1|4|1|0|0|0|0|0|0|0|0|0|0|1|0	0
TPCN2_734E	Q6P2Q9	PRPF8	25|0|0	0|0|2|0|0	11|8|34|23|26|15|14|2|5|3|1|1|4|7|6|20|15|21|18|24|21|45|32|16|18|18|20|12|22|29	0
TPCN2_734E	P35637	FUS	3|0|2	0|0|0|0|0	3|2|3|0|0|3|5|0|1|1|0|1|0|3|4|0|0|1|2|3|3|1|6|0|1|2|0|3|0|42	0

TPCN2_734E	P05455	SSB	3|0|0	3|0|0|0|5	0|2|3|2|0|4|0|0|0|0|0|0|0|0|2|0|0|1|0|1|1|0|1|0|0|0|0|0|1|3	0
TPCN2_734E	O75874	IDH1	13|0|11	29|14|9|0|15	0|1|0|0|0|4|0|0|0|0|0|0|0|0|0|0|0|0|0|2|1|0|0|0|0|0|0|0|0	0
TPCN2_734E	P62258	YWHAE	5|0|8	14|4|6|0|11	0|0|12|13|5|7|8|1|1|2|1|1|1|1|1|1|0|0|1|0|0|4|15|4|4|6|0|0|1|49	0
TPCN2_734E	P12004	PCNA	0|0|0	0|0|0|0|0	0|0|2|1|1|1|0|0|0|0|0|0|0|0|0|0|0|0|0|0|1|2|1|2|0|0|0|1|15	0
TPCN2_734E	Q7Z739	YTHDF3	2|0|0	0|0|0|0|0	0|1|4|3|1|3|1|0|0|0|0|0|0|1|1|0|0|0|0|0|1|0|0|0|0|1|1|0|1	0
TPCN2_734G	Q6PD62	CTR9	2|0|0	2|0|0|0|0	1|0|2|0|0|0|0|0|0|0|0|0|0|0|0|1|1|1|0|2|0|1|0|0|0|0|0|1|0	0
TPCN2_734G	P68363	TUBA1B	23|6|11	30|18|19|7|16	50|62|131|117|90|134|224|24|23|22|21|17|21|43|49|45|51|27|53|35|46|135|116|152|136|132|3	0
TPCN2_734G	Q9Y3U8	RPL36	0|2|0	2|4|4|4|2	0|0|1|0|1|0|0|0|0|0|0|0|0|0|0|0|0|0|0|0|0|0|0|0|0|1|0	0
TPCN2_734G	Q96N67	DOCK7	2|0|0	0|0|0|0|0	0|0|7|4|3|0|2|0|0|0|0|0|0|0|0|0|0|0|0|0|0|7|5|1|2|3|0|0|0|1	0
TPCN2_734G	P40227	CCT6A	15|0|6	21|5|5|2|14	3|3|91|55|52|32|12|2|0|2|1|0|0|2|0|11|29|1|3|3|2|77|42|145|126|78|0|1|12|56	0
TPCN2_734G	P05534	HLA-A	0|0|0	0|0|0|0|0	0|0|0|0|0|0|0|4|3|5|2|2|5|0|0|0|0|1|1|0|0|0|1|0|0|0|2|1|0|2	0

TPCN2_734G	O00148	DDX39A	0|0|0	4|0|0|0|3	11|7|10|17|13|7|9|5|6|5|4|1|3|7|6|14|5|3|4|5|2|6|20|8|13|7|4|5|9|7	0
TPCN2_734G	Q92572	AP3S1	0|0|2	0|0|0|0|0	0|1|1|1|1|2|3|0|0|0|0|0|0|0|1|0|0|0|1|0|1|2|0|0|1|2|0|1|3	0
TPCN2_734G	Q08AN1	ZNF616	4|10|6	5|3|16|9|9	0|0|0|0|0|0|0|0|0|0|0|0|0|0|0|0|0|0|0|0|0|0|0|1|0|0|0|0|0|0	0
TPCN2_734G	P35527	KRT9	16|54|46	37|44|47|57|42	9|11|15|19|4|1|9|109|96|123|40|36|51|6|8|35|10|8|7|18|6|1|11|2|2|18|32|52|1|15	0
TPCN2_734G	P51798	CLCN7	0|0|0	0|0|0|0|2	0|0|1|0|0|0|0|0|0|0|0|0|0|2|0|0|0|0|0|0|0|0|0|0|0|0|0|0|0|0	0
TPCN2_734G	P62753	RPS6	3|14|8	10|8|5|14|4	4|4|15|13|14|9|14|5|3|4|3|3|3|4|3|10|9|0|1|1|0|10|10|9|10|9|7|2|7|6	0
TPCN2_734G	P62750	RPL23A	0|0|0	0|0|0|0|0	0|1|8|4|4|9|9|0|0|0|0|0|0|0|0|3|7|0|0|0|0|3|7|3|1|5|1|0|3|2	0
TPCN2_734G	P22392	NME2	7|0|0	5|3|3|0|3	0|0|7|0|0|11|3|1|0|0|1|2|1|0|0|0|0|0|0|0|0|0|0|0|0|0|0|0|0|11	0
TPCN2_734G	P04075	ALDOA	22|0|8	30|13|12|2|20	0|2|0|0|0|0|0|1|1|2|1|1|2|1|2|0|0|1|1|1|1|0|7|0|0|0|1|0|0|16	0
TPCN2_734G	P61978	HNRNPK	12|0|0	11|3|2|0|10	29|32|22|39|26|34|30|16|13|15|14|12|12|33|32|26|16|19|25|26|30|29|38|25|23|27|25|24|27|8	0
TPCN2_734G	Q13724	MOGS	0|0|0	0|0|0|0|0	0|0|0|0|0|0|0|0|0|0|0|0|0|0|0|0|0|0|0|0|0|0|0|0|0|0|0|0|0	0

TPCN2_734G	P28370	SMARCA1	9|0|0	0|0|0|0|0	9|7|10|11|13|4|2|0|0|0|0|0|0|9|7|45|26|3|8|6|9|3|16|6|5|9|8|10|5|0	0
TPCN2_734G	P15559	NQO1	6|0|0	10|6|3|0|7	0|0|0|0|0|0|0|0|0|0|0|0|0|0|0|0|0|0|0|0|0|0|0|0|0|0|0|0|0|0|0	0
TPCN2_734G	P46977	STT3A	0|0|0	0|0|0|0|0	2|1|0|0|0|0|2|0|1|1|1|1|1|2|1|0|0|0|0|0|0|0|0|0|0|0|0|0|0|1|0	0
TPCN2_734G	Q14247	CTTN	22|27|22	17|0|6|2|3	45|42|44|50|41|81|84|2|1|0|0|0|0|61|67|59|38|31|39|40|60|22|29|21|27|40|47|41|0|7	0
TPCN2_734G	P49790	NUP153	0|0|0	0|0|0|0|0	39|40|25|37|30|21|28|5|5|3|2|6|3|51|43|53|38|38|56|57|68|18|23|14|8|31|45|46|13|0	0
TPCN2_734G	O96005	CLPTM1	0|0|0	0|0|0|0|3	0|0|0|0|0|0|0|0|0|0|0|0|0|1|0|0|0|0|0|0|0|0|0|0|0|0|0|0|0|0|0	0
TPCN2_734G	A8MPP1	DDX11L8	0|0|0	0|0|0|0|0	0|0|0|0|0|0|0|0|0|0|0|0|0|0|0|0|0|0|0|0|0|0|0|0|0|0|0|0|0|0|0	0
TPCN2_734G	Q3YEC7	RABL6	0|0|2	0|0|0|0|0	0|0|1|4|1|2|3|0|0|0|0|0|0|0|0|0|0|0|0|0|0|0|3|1|1|2|5|0|0|0|0	0
TPCN2_734G	Q04637	EIF4G1	3|0|0	0|0|0|0|0	46|43|78|71|36|47|49|0|0|0|0|0|0|57|52|25|24|26|44|43|52|38|57|27|25|49|31|31|1|13	0
TPCN2_734G	Q3B726	TWISTNB	0|0|0	0|0|0|0|0	0|0|0|0|0|0|0|0|0|0|0|0|0|0|0|0|0|0|0|0|0|0|0|0|0|0|0|0|0|0|0	0
TPCN2_734G	P30048	PRDX3	0|0|0	2|0|0|0|0	1|2|0|1|0|1|0|3|6|4|2|3|3|1|1|2|0|1|2|1|1|0|9|0|1|1|2|1|0|4	0

TPCN2_734G	Q13200	PSMD2	8|0|0	11|2|3|0|6	1|0|13|5|3|7|4|1|0|0|0|0|0|0|0|1|2|0|0|0|0|6|9|3|3|0|0|0|3|30	0
TPCN2_734G	P18077	RPL35A	5|4|5	3|3|3|4|3	1|0|6|3|22|1|3|2|1|1|1|1|1|0|0|6|5|0|0|0|0|0|3|0|1|6|0|0|1|0	0
TPCN2_734G	P0C0S8	HIST1H2A	2|0|3	4|4|3|0|2	10|7|16|23|16|15|23|2|3|3|2|2|1|9|11|17|28|7|12|9|10|21|33|36|23|24|8|7|14|16	0
TPCN2_734G	P30041	PRDX6	0|0|0	3|5|3|0|0	5|9|2|3|2|9|7|3|2|2|1|2|1|4|3|2|1|1|0|3|4|4|6|2|5|1|2|1|4|12	0
TPCN2_734G	P07910	HNRNPC	5|2|0	10|0|0|3|6	6|8|2|11|16|2|4|12|8|10|8|7|8|8|7|3|16|4|7|2|2|3|12|7|4|11|6|5|7|51	0
TPCN2_734G	P41252	IARS	8|0|0	2|0|0|0|0	2|3|4|1|8|1|1|2|0|2|0|0|1|0|0|2|0|3|5|1|1|3|10|3|4|8|5|5|3|4	0
TPCN2_734G	Q9UHB6	LIMA1	0|0|0	0|0|0|0|0	53|51|27|15|15|16|22|8|6|6|3|4|2|67|66|38|20|42|67|63|80|8|12|6|10|12|60|88|0|0	0
TPCN2_734G	Q12931	TRAP1	6|0|0	6|0|0|0|6	1|1|6|7|7|23|19|8|9|8|9|9|11|1|2|10|5|2|3|1|1|8|13|6|6|5|2|2|11|24	0
TPCN2_734G	P02545	LMNA	54|0|4	51|6|11|0|45	6|6|0|2|4|0|0|18|16|15|12|15|18|7|3|13|11|4|4|1|3|0|5|0|0|1|10|7|0|1	0
TPCN2_734G	P49006	MARCKSL1	0|0|0	0|0|0|0|0	0|0|3|0|1|0|0|0|0|0|0|0|0|0|0|0|0|0|0|0|0|0|1|0|0|0|0|0|0|0	0
TPCN2_734G	P40429	RPL13A	13|16|13	11|14|12|25|15	2|2|3|6|4|5|5|0|1|0|0|0|0|1|1|6|3|1|1|0|1|2|5|0|0|5|0|0|2|0	0

TPCN2_734G	Q9HB71	CACYBP	0|0|0	0|0|0|0|0	1|3|3|0|0|10|8|1|1|1|2|0|1|0|2|0|0|0|0|1|0|1|3|0|0|1|0|0|0|4	0
TPCN2_734G	Q8N163	CCAR2	2|0|0	4|0|0|0|0	5|8|13|13|11|6|11|1|0|0|0|0|1|1|7|5|2|3|6|6|5|14|2|4|8|5|5|12|14	0
TPCN2_734G	P13667	PDIA4	15|0|0	19|0|0|0|12	0|0|0|0|0|0|0|1|0|3|2|0|1|0|0|0|0|0|0|0|0|0|2|0|0|0|0|0|0|23	0
TPCN2_734G	Q93009	USP7	0|0|0	0|0|0|0|0	5|2|16|11|7|7|12|0|0|0|0|0|3|2|3|1|5|3|5|5|9|19|5|7|8|3|3|4|8	0
TPCN2_734G	P62879	GNB2	4|0|0	6|0|0|0|5	1|0|1|0|1|4|1|2|2|2|0|2|2|1|1|1|0|0|3|0|1|0|1|1|1|1|0|0|0|1	0
TPCN2_734G	P78347	GTF2I	19|0|0	15|2|0|0|7	20|17|15|11|5|5|7|5|5|4|1|2|2|14|5|22|3|22|24|24|27|7|13|3|4|8|23|21|8|43	0
TPCN2_734G	P05388	RPLP0	6|0|0	7|0|2|2|7	2|1|6|8|10|3|2|9|7|8|8|7|9|2|1|4|1|3|3|4|3|3|4|5|6|7|5|4|7|4	0
TPCN2_734G	P62979	RPS27A	20|7|14	16|12|18|5|13	0|0|1|0|0|0|1|0|0|0|0|0|1|2|1|0|0|1|3|1|2|0|2|0|0|2|2|2|1|2	0
TPCN2_734G	Q9C0C4	SEMA4C	0|0|0	0|0|0|0|0	0|0|0|0|0|0|0|0|0|0|0|0|0|0|0|0|0|0|0|0|0|0|0|0|0|0|0|0	0
TPCN2_734G	P07355	ANXA2	13|14|15	10|5|14|5|13	25|35|4|2|5|7|10|12|11|11|10|11|12|25|35|46|8|15|19|20|22|7|9|1|6|5|19|15|0|0	0
TPCN2_734G	O76021	RSL1D1	4|21|2	8|0|2|27|6	8|4|6|3|7|0|0|3|5|4|3|5|3|9|12|4|9|4|5|2|4|1|5|0|1|4|6|4|7|0	0

TPCN2_734G	P52272	HNRNPM	25|0|0	29|2|0|0|18	14|9|21|10|24|31|15|14|13|18|12|13|13|15|7|19|11|17|20|22|18|8|29|4|7|12|13|15|32|17	0
TPCN2_734G	P29966	MARCKS	0|0|0	4|0|0|0|0	5|3|2|1|0|0|0|3|5|4|3|3|3|5|3|0|0|1|1|2|0|0|5|0|0|0|1|2|0|1	0
TPCN2_734G	P67809	YBX1	18|30|19	26|13|15|27|18	0|0|14|8|6|7|11|0|0|0|0|0|0|0|0|3|1|0|0|0|0|5|7|1|2|7|0|0|3|15	0
TPCN2_734G	P39656	DDOST	5|0|0	6|0|0|0|6	5|6|1|0|0|2|2|9|9|9|8|6|8|0|3|0|1|1|0|1|1|0|2|0|0|0|2|2|2|0	0
TPCN2_734G	Q15366	PCBP2	0|0|0	9|0|0|0|0	10|12|17|16|13|30|27|4|4|4|2|2|5|6|8|8|9|4|5|8|10|19|14|13|15|16|4|5|7|8	0
TPCN2_734G	P25789	PSMA4	0|0|0	0|0|0|0|0	0|0|1|0|0|0|0|0|0|0|0|0|0|0|0|0|0|0|0|0|0|0|0|0|0|0|0|0|0|0|0|5	0
TPCN2_734G	Q15365	PCBP1	5|0|0	7|0|0|0|6	8|13|10|8|15|18|15|3|4|4|3|2|7|6|7|7|7|5|6|7|10|11|16|9|10|10|7|6|3|9	0
TPCN2_734G	Q8IXT5	RBM12B	0|0|0	0|0|0|0|0	0|0|0|0|0|0|0|0|0|0|0|0|0|0|0|0|0|0|0|0|0|0|0|0|0|0|0|0|0|0|0|1|0	0
TPCN2_734G	B5ME19	EIF3CL	8|0|0	7|0|0|0|0	4|4|9|6|13|8|6|0|0|0|0|0|0|1|1|2|1|0|0|3|1|8|6|6|4|9|0|0|0|4	0
TPCN2_734G	Q96RP9	GFM1	0|0|0	2|0|0|0|0	0|0|0|0|0|0|0|7|11|8|10|11|14|0|0|0|0|0|0|0|0|0|0|0|0|0|0|0|0|0	0
TPCN2_734G	Q9UMS4	PRPF19	0|0|0	3|0|0|0|2	0|0|21|13|19|7|10|1|1|3|3|1|2|0|0|25|9|1|2|2|0|9|20|5|4|5|0|2|5|4	0

TPCN2_734G	Q92575	UBXN4	0|0|0	2|0|0|0|2	0|0|1|1|0|3|1|0|0|0|0|0|0|0|0|0|0|0|0|0|1|0|0|1|0|1|1|0|0|0|0	0
TPCN2_734G	Q14669	TRIP12	0|0|0	0|0|0|0|0	2|0|1|0|0|0|0|1|0|0|0|0|0|1|2|4|2|9|9|5|6|0|0|0|0|0|6|5|0|0	0
TPCN2_734G	P39023	RPL3	30|35|22	23|22|23|41|38	4|3|20|20|18|17|18|3|2|3|3|3|4|8|5|8|6|3|5|3|3|9|5|6|7|16|3|3|12|1	0
TPCN2_734G	O75436	VPS26A	0|0|0	0|0|0|0|0	0|0|0|0|0|0|0|1|0|1|1|0|2|0|0|0|0|0|0|0|0|0|0|0|0|0|0|0|1	0
TPCN2_734G	O75533	SF3B1	12|0|0	15|0|0|0|7	63|52|42|44|40|29|38|2|2|3|1|2|1|55|60|34|35|38|54|46|68|28|39|17|25|27|49|47|20|18	0
TPCN2_734G	O75439	PMPCB	0|0|0	2|0|0|0|3	0|0|0|0|0|0|0|9|4|8|9|10|8|0|0|1|0|2|3|0|0|0|1|0|0|0|2|1|0|1	0
TPCN2_734G	Q9HAU0	PLEKHA5	2|0|0	0|0|0|0|0	4|4|1|0|0|1|2|0|0|0|0|0|0|0|2|0|0|0|0|2|1|0|1|0|0|0|0|0|0|0	0
TPCN2_734G	P08621	SNRNP70	3|0|0	2|0|0|0|0	0|0|5|7|7|6|8|0|0|0|0|0|0|0|0|5|2|0|0|0|1|2|6|2|0|3|2|1|4|11	0
TPCN2_734G	P09651	HNRNPA1	6|0|0	11|2|0|0|8	10|15|18|22|7|21|14|11|11|15|12|9|12|13|16|8|5|10|21|13|16|1|16|3|4|8|13|14|6|47	0
TPCN2_734G	Q9UQE7	SMC3	3|0|0	3|0|0|0|0	0|0|9|14|12|1|2|0|1|0|0|0|0|0|0|10|6|0|0|0|0|4|21|5|7|15|0|0|10|11	0
TPCN2_734G	Q5JRX3	PITRM1	0|0|0	0|0|0|0|0	0|0|0|0|0|0|0|2|1|1|0|2|3|0|0|0|0|0|0|0|0|0|1|0|0|0|0|0|0|0	0

TPCN2_734G	P62805	HIST1H4	6|6|8	6|11|8|6|6	10|8|6|19|13|14|13|10|7|9|4|7|7|13|14|16|8|9|12|7|7|12|18|7|7|12|10|9|8|29	0
TPCN2_734G	Q14103	HNRNPD	3|0|0	3|0|0|0|3	7|5|10|5|5|4|5|10|10|8|10|9|11|6|5|3|0|4|4|4|8|2|8|2|1|5|7|5|3|13	0
TPCN2_734G	O94776	MTA2	2|10|0	2|0|0|8|3	4|5|10|11|12|0|4|1|0|3|1|0|0|2|1|18|15|3|4|3|4|8|16|8|9|13|2|0|18|7	0
TPCN2_734G	P16435	POR	2|0|0	3|0|0|0|0	0|0|0|0|0|0|0|1|2|2|1|1|1|0|0|0|0|0|2|1|0|0|0|0|0|0|0|0|0	0
TPCN2_734G	P17931	LGALS3	0|0|0	3|2|3|0|4	0|0|0|0|0|0|0|0|0|0|0|0|0|0|0|0|0|0|0|0|0|0|0|0|0|0|0|0|0|2	0
TPCN2_734G	Q641Q2	WASHC2A	0|0|0	0|0|0|0|0	7|11|7|6|1|2|4|0|0|0|0|0|0|0|7|2|0|5|4|9|8|10|4|3|3|1|2|2|0|0	0
TPCN2_734G	P68104	EEF1A1	17|0|12	14|14|11|0|17	50|62|75|71|54|239|109|24|21|25|21|20|15|31|48|40|40|21|32|30|41|128|48|158|189|79|37|38	0
TPCN2_734G	P27635	RPL10	0|0|0	3|0|0|4|2	2|2|7|9|8|7|6|1|2|2|2|1|2|1|1|3|6|0|1|0|0|9|7|13|9|5|0|0|4|1	0
TPCN2_734G	P62191	PSMC1	3|0|0	5|0|0|0|3	0|0|3|0|2|0|0|0|1|0|0|0|0|0|2|1|0|0|0|0|2|6|2|2|1|0|0|1|11	0
TPCN2_734G	O14980	XPO1	7|0|0	9|2|3|0|5	0|0|1|0|0|4|3|3|1|3|1|1|1|0|0|1|1|0|0|0|0|2|1|4|2|1|0|0|4|2	0
TPCN2_734G	P36542	ATP5C1	0|0|0	2|0|0|0|0	0|0|9|2|5|4|3|4|3|3|3|4|3|0|1|10|8|0|0|0|0|0|5|0|1|6|0|0|6|1	0

TPCN2_734G	Q5BKZ1	ZNF326	2|0|0	4|0|0|0|0	0|1|1|5|5|0|1|2|1|3|1|2|0|0|0|3|6|0|1|0|0|2|13|2|1|9|1|2|3|0	0
TPCN2_734G	P11142	HSPA8	53|14|28	52|39|41|15|47	56|57|96|123|78|73|95|40|40|45|36|39|42|56|64|81|74|58|86|61|83|64|76|62|58|83|69|68|50|	0
TPCN2_734G	O43837	IDH3B	3|0|0	4|0|0|0|0	0|0|0|0|0|1|1|4|2|2|5|5|5|0|0|0|0|0|0|0|0|0|0|0|0|0|0|0|2|0	0
TPCN2_734G	P10155	TROVE2	0|0|0	0|0|0|0|0	0|0|0|0|0|0|0|0|0|0|0|0|0|0|0|0|0|0|0|0|0|0|0|0|0|0|0|0|1	0
TPCN2_734G	P33992	MCM5	5|0|0	12|0|0|0|6	0|0|1|1|0|0|1|0|0|0|0|0|0|0|0|0|0|0|0|0|0|1|3|0|0|1|0|0|5|23	0
TPCN2_734G	P48643	CCT5	7|0|0	13|3|0|0|10	2|1|67|53|57|26|12|5|4|5|4|3|6|0|0|8|18|2|3|0|5|58|38|120|97|64|3|2|18|95	0
TPCN2_734G	Q92614	MYO18A	0|0|0	0|0|0|0|0	0|0|0|0|0|0|0|0|0|0|0|0|0|0|0|0|0|0|0|0|0|0|0|0|0|0|0|0	0
TPCN2_734G	Q9HD33	MRPL47	0|0|0	0|0|0|0|0	0|0|0|0|0|0|0|0|0|0|0|0|0|0|0|0|0|0|0|0|0|0|0|0|0|0|0|1	0
TPCN2_734G	Q9NR30	DDX21	3|2|0	9|0|0|0|2	20|18|21|28|22|36|35|18|14|11|9|13|9|24|20|35|26|15|16|11|13|18|34|11|18|23|21|19|17|0	0
TPCN2_734G	P50502	ST13	0|0|0	3|0|0|0|0	0|0|0|0|0|0|0|0|1|0|0|0|0|0|0|0|0|0|0|0|0|0|0|0|0|0|0|0|16	0
TPCN2_734G	P34897	SHMT2	23|0|0	17|3|0|0|16	0|0|0|0|0|0|0|3|1|4|6|4|7|0|0|0|0|0|0|0|0|0|7|0|2|0|0|1|0|27	0

TPCN2_734G	Q9UHD8	SEPT9	4|0|0	4|0|0|0|0	7|8|12|19|13|10|26|0|0|0|0|0|0|9|8|7|1|4|5|6|8|11|12|7|5|16|5|7|0|1	0
TPCN2_734G	Q96DV4	MRPL38	0|0|0	0|0|0|0|0	0|0|0|0|0|0|0|0|0|0|0|0|0|0|0|0|0|0|0|0|0|0|0|0|0|0|0|0	0
TPCN2_734G	Q13601	KRR1	0|0|0	0|0|0|0|0	0|0|0|1|0|0|0|0|0|0|0|0|0|0|0|0|0|0|0|0|0|0|0|0|0|1|0	0
TPCN2_734G	P13798	APEH	0|0|0	2|0|0|0|0	0|0|0|0|0|0|0|0|0|0|0|0|0|0|0|0|0|0|0|0|0|0|0|0|0|0|0	0
TPCN2_734G	Q9Y2L1	DIS3	0|0|0	0|0|0|0|0	0|0|0|1|0|2|1|0|0|0|0|0|0|0|0|0|0|0|0|0|0|0|0|0|0|1|0	0
TPCN2_734G	Q92616	GCN1	2|0|0	0|0|0|0|0	4|2|70|38|49|25|28|0|0|0|0|0|0|0|13|5|6|13|2|2|57|65|42|46|52|5|4|6|12	0
TPCN2_734G	Q14203	DCTN1	4|0|0	2|0|0|0|0	4|1|18|10|10|4|9|0|0|0|0|0|0|5|2|1|0|3|3|5|7|10|16|4|6|14|2|3|2|4	0
TPCN2_734G	O14776	TCERG1	0|0|0	0|0|0|0|0	16|17|5|8|3|4|3|0|0|1|0|0|0|9|10|0|0|3|4|5|9|1|6|2|3|3|7|5|4|0	0
TPCN2_734G	A0FGR8	ESYT2	3|0|0	3|0|0|0|0	4|2|5|1|1|1|0|0|0|0|0|0|0|0|0|0|0|2|1|3|2|0|5|0|0|0|2|0|0|0	0
TPCN2_734G	O60763	USO1	2|0|0	2|0|0|0|0	2|0|3|1|1|1|1|0|0|0|0|0|0|1|1|1|2|0|0|1|2|0|2|0|1|3|1|1|0|4	0
TPCN2_734G	Q14566	MCM6	7|0|0	11|2|0|0|4	3|1|4|2|3|4|5|0|1|1|1|1|0|0|0|0|4|0|0|0|0|0|7|1|2|3|0|0|7|26	0

TPCN2_734G	P00338	LDHA	8|0|4	11|6|6|0|9	4|6|0|0|0|0|0|4|6|4|5|3|5|3|5|0|0|3|3|2|1|0|1|0|0|0|2|2|0|2	0
TPCN2_734G	P85037	FOXK1	0|0|0	0|0|0|0|0	0|0|0|0|0|0|0|0|0|0|0|0|0|0|0|0|0|1|0|0|0|0|0|0|0|0|0|0|0|0	0
TPCN2_734G	P62263	RPS14	0|0|0	0|2|2|0|0	3|2|9|11|12|8|6|5|4|4|4|4|4|2|1|4|6|1|1|0|0|5|7|5|2|10|0|0|7|5	0
TPCN2_734G	P17844	DDX5	14|0|0	13|5|2|0|12	13|12|13|7|7|10|11|11|8|7|6|5|6|14|13|12|7|9|16|13|13|5|11|5|5|7|13|10|11|18	0
TPCN2_734G	P50570	DNM2	0|0|0	3|0|0|0|0	0|0|0|1|0|0|1|0|0|0|0|0|0|0|0|0|0|0|0|0|0|0|1|0|0|0|0|0|0|3	0
TPCN2_734G	P68032	ACTC1	29|0|0	0|0|0|0|0	18|16|25|35|38|33|26|32|28|26|27|35|29|19|22|41|52|17|35|18|24|16|30|14|11|30|24|22|93|3	0
TPCN2_734G	Q9NVI7	ATAD3A	8|0|0	10|0|0|0|6	0|0|2|1|6|1|0|11|8|10|10|9|10|0|0|0|4|0|0|0|0|0|1|0|1|2|0|0|2|1	0
TPCN2_734G	O60488	ACSL4	0|0|0	4|0|0|0|0	1|1|0|0|0|1|2|1|1|2|1|0|0|0|0|0|1|1|2|1|1|1|1|0|0|1|1|1|1|0	0
TPCN2_734G	Q00796	SORD	0|0|0	2|0|0|0|0	0|0|0|0|0|0|0|0|0|0|0|0|0|0|0|0|0|0|0|0|0|0|0|0|0|0|0|0|0|0	0
TPCN2_734G	O75643	SNRNP200	4|0|0	0|0|0|0|0	15|16|29|13|27|14|18|8|4|10|2|2|4|4|6|40|26|10|12|20|19|23|27|14|14|24|17|19|17|23	0
TPCN2_734G	Q92522	H1FX	0|0|2	0|0|0|0|0	0|0|2|2|6|2|0|0|0|0|0|0|0|0|0|1|0|0|0|0|1|0|4|0|1|3|0|0|4|0	0

TPCN2_734G	O43242	PSMD3	2|4|0	6|0|0|3|0	0|0|7|5|5|11|5|0|0|0|0|0|0|0|1|0|0|0|0|0|0|3|7|1|6|5|0|0|9|18	0
TPCN2_734G	P06748	NPM1	21|0|4	21|7|8|0|13	146|149|101|112|50|46|123|8|6|6|3|7|8|106|94|157|72|70|124|99|175|85|107|46|43|54|100|10	0
TPCN2_734G	Q658Y4	FAM91A1	0|0|0	0|0|0|0|0	3|3|3|4|1|4|2|0|0|0|0|0|0|1|3|0|0|1|2|2|3|5|1|3|4|2|1|1|0|0	0
TPCN2_734G	Q29RF7	PDS5A	0|0|0	0|0|0|0|0	3|3|7|4|3|2|1|0|0|0|0|1|0|3|3|2|1|4|3|4|5|2|3|1|1|3|2|1|2|0	0
TPCN2_734G	Q8TCS8	PNPT1	4|0|0	3|0|0|0|2	0|0|0|0|0|0|0|1|1|0|6|1|4|0|0|0|0|0|0|0|0|0|0|0|0|0|0|0|0|0	0
TPCN2_734G	Q08945	SSRP1	3|0|0	3|0|0|0|3	1|4|0|0|0|0|2|0|0|1|0|0|0|1|1|0|0|4|7|4|5|0|1|0|0|0|3|3|5|0	0
TPCN2_734G	Q7Z4V5	HDGFL2	0|0|0	0|0|0|0|0	4|3|6|6|8|6|10|0|0|0|0|0|0|4|4|0|0|2|2|1|2|6|2|2|7|6|3|1|1|2	0
TPCN2_734G	Q02978	SLC25A11	0|0|0	0|0|0|0|0	0|0|13|6|4|13|5|0|0|0|0|0|0|0|0|2|2|0|0|0|0|2|3|2|2|2|0|0|2|0	0
TPCN2_734G	Q02878	RPL6	19|15|8	18|11|13|23|16	20|13|18|9|17|19|15|11|5|8|6|4|11|13|14|15|5|4|11|5|7|6|14|8|6|15|8|10|4|1	0
TPCN2_734G	P07195	LDHB	14|0|6	17|13|12|0|17	3|3|1|2|0|3|0|1|3|2|1|2|2|1|2|0|0|3|0|2|0|0|3|0|0|0|0|1|0|6	0
TPCN2_734G	Q9BTT0	ANP32E	0|0|0	3|0|0|0|0	0|0|2|2|0|0|0|0|0|0|0|0|0|0|0|0|0|0|0|0|0|0|0|0|0|2|1|1|0|0|0|9	0

TPCN2_734G	P49756	RBM25	3|0|0	2|0|0|0|0	8|6|6|5|2|3|0|0|0|0|0|0|0|3|0|7|4|2|2|2|2|3|7|3|0|7|0|3|3|0	0
TPCN2_734G	P99999	CYCS	0|0|0	0|0|0|0|0	1|2|0|0|0|0|0|0|0|0|0|1|0|1|0|0|0|1|0|3|1|0|0|0|0|0|0|0|0|0	0
TPCN2_734G	P31689	DNAJA1	5|0|0	5|0|0|0|0	0|0|5|0|0|2|1|0|1|0|0|0|0|0|0|0|0|1|0|0|0|0|1|1|0|0|0|0|0|30	0
TPCN2_734G	A5YKK6	CNOT1	0|0|0	0|0|0|0|0	0|0|6|1|2|2|2|0|0|0|0|0|0|1|0|1|0|0|0|1|1|6|1|3|4|5|0|0|0|0	0
TPCN2_734G	P26640	VARS	7|0|0	8|0|0|0|0	3|1|8|4|4|8|4|0|0|0|0|0|1|0|1|4|2|0|0|0|0|11|3|7|6|9|0|0|1|20	0
TPCN2_734G	P26641	EEF1G	15|0|0	15|8|9|0|16	3|0|18|11|10|13|3|5|5|3|4|7|5|1|1|19|11|4|3|2|2|12|13|12|7|10|3|5|1|27	0
TPCN2_734G	Q99460	PSMD1	12|0|0	9|0|2|0|5	0|1|5|0|2|4|1|0|0|0|0|0|0|0|0|0|1|1|2|2|0|1|2|3|1|0|0|0|18	0
TPCN2_734G	Q9NTJ3	SMC4	2|0|0	0|0|0|0|0	3|3|7|1|3|2|3|0|0|0|0|0|0|1|0|2|6|0|0|2|4|1|5|2|1|9|1|1|3|8	0
TPCN2_734G	O43491	EPB41L2	0|0|0	0|0|0|0|0	41|33|40|42|25|31|33|0|0|0|0|0|0|58|43|11|7|26|38|33|59|16|22|12|13|18|43|42|1|3	0
TPCN2_734G	O43493	TGOLN2	0|0|0	0|0|0|0|0	0|0|0|0|0|0|0|0|0|0|0|0|0|0|0|0|0|0|0|0|0|0|0|0|0|0|0|0|0	0
TPCN2_734G	P62910	RPL32	0|4|2	0|3|5|3|4	0|0|2|0|1|1|0|0|0|0|0|0|0|0|0|0|1|0|0|0|0|0|0|1|2|1|0|0|0|0	0

TPCN2_734G	P49915	GMPS	0|0|0	3|0|0|0|0	3|6|2|1|0|5|4|1|0|1|1|0|2|1|2|2|1|1|1|2|3|2|6|0|2|8|0|1|0|1	0
TPCN2_734G	P13639	EEF2	45|0|13	51|37|28|0|25	17|26|19|3|5|32|19|15|13|17|15|11|14|17|19|16|5|7|11|5|11|16|26|8|7|8|9|10|1|49	0
TPCN2_734G	O60264	SMARCA5	16|0|0	12|0|0|0|4	30|32|34|41|42|13|17|2|4|3|0|2|1|33|26|84|70|22|30|24|25|28|59|23|25|42|36|43|20|0	0
TPCN2_734G	P11586	MTHFD1	9|0|0	9|2|3|0|3	0|0|3|5|2|11|7|0|0|0|1|0|0|0|0|0|0|0|0|0|0|6|15|4|5|7|0|0|5|21	0
TPCN2_734G	P61353	RPL27	0|0|0	2|2|2|0|0	0|0|6|2|5|1|0|1|0|0|0|1|2|0|0|1|3|0|0|0|0|1|4|1|0|3|0|0|2|0	0
TPCN2_734G	P62847	RPS24	0|0|0	0|0|0|3|0	3|2|9|11|8|6|5|2|2|2|0|0|1|0|2|7|4|0|1|0|0|5|8|10|4|10|1|0|8|4	0
TPCN2_734G	P04264	KRT1	23|79|75	34|64|75|86|39	14|20|26|20|7|4|13|110|74|98|28|34|29|15|26|56|18|11|26|20|15|5|18|9|6|18|37|64|4|35	0
TPCN2_734G	P04181	OAT	15|0|0	18|2|2|0|14	0|0|0|0|0|0|0|3|2|4|4|6|6|0|0|0|0|0|0|0|0|0|1|0|0|0|0|0|0|6	0
TPCN2_734G	Q7KZ85	SUPT6H	0|0|0	0|0|0|0|0	1|0|0|1|0|0|1|0|0|0|0|0|0|0|0|0|0|0|1|0|1|0|0|1|0|1|0|0|1|6	0
TPCN2_734G	P14324	FDPS	0|0|0	0|0|0|0|0	0|0|0|0|0|0|0|0|0|0|0|0|0|0|0|0|0|0|0|0|0|0|0|0|0|0|0|0|0|0|0|0|0|0|0|0|0|0|1	0
TPCN2_734G	Q9BY44	EIF2A	0|0|0	0|0|0|0|0	4|6|7|0|0|11|4|0|0|0|0|0|0|4|2|1|0|1|2|5|1|1|1|0|0|3|1|2|0|0	0

TPCN2_734G	O14828	SCAMP3	0|0|0	0|0|0|0|0	1|1|0|0|0|3|1|1|0|1|2|0|0|0|0|0|0|1|0|0|0|0|0|0|0|0|0|1|0|0	0
TPCN2_734G	P38919	EIF4A3	2|0|0	8|0|0|0|4	1|2|7|7|6|11|7|3|2|5|3|2|5|0|0|4|7|0|2|1|1|4|13|3|3|16|1|1|5|9	0
TPCN2_734G	P15880	RPS2	6|3|0	8|5|5|3|8	3|3|15|14|10|20|10|2|3|2|1|2|2|1|2|12|8|1|3|1|1|11|7|11|15|12|1|2|6|9	0
TPCN2_734G	O60506	SYNCRIP	7|0|0	6|0|0|0|6	4|6|4|4|2|3|9|4|2|4|2|1|2|6|8|1|3|6|8|12|9|1|9|2|1|8|7|7|1|20	0
TPCN2_734G	P49411	TUFM	9|0|0	13|0|0|0|12	4|5|12|23|27|17|14|25|22|27|30|27|34|3|3|13|21|4|5|0|1|10|32|10|5|21|5|5|10|32	0
TPCN2_734G	P62314	SNRPD1	2|0|0	0|0|0|0|2	6|6|1|2|3|4|2|0|0|0|0|0|0|3|4|1|2|0|0|0|0|3|2|1|2|2|0|0|2|3	0
TPCN2_734G	Q13423	NNT	11|0|0	9|0|3|0|11	0|0|0|0|0|0|0|8|7|8|5|8|4|0|0|0|0|0|0|0|0|0|0|0|0|0|0|0|0|0|0	0
TPCN2_734G	P07437	TUBB	24|8|19	39|14|20|7|17	21|23|86|120|87|90|68|30|22|27|23|19|21|20|29|40|52|11|21|11|10|80|80|116|117|93|12|22|9	0
TPCN2_734G	P63261	ACTG1	44|0|32	46|28|25|0|48	30|29|41|60|55|42|40|56|53|53|51|54|57|32|34|65|73|38|61|34|45|26|66|21|17|42|44|47|258|	0
TPCN2_734G	P43246	MSH2	5|0|0	7|0|0|0|4	0|0|8|6|1|1|3|0|0|0|0|0|0|0|0|0|0|0|0|1|0|0|1|1|0|0|4|0|0|2|6	0
TPCN2_734G	P43243	MATR3	24|0|0	24|0|0|0|13	13|11|24|16|21|16|10|7|5|8|3|3|3|14|5|16|11|9|17|8|16|10|30|11|13|15|14|17|7|24	0

TPCN2_734G	O15118	NPC1	0|0|0	0|0|0|0|0	0|0|0|0|0|0|0|0|0|0|0|0|0|0|0|0|0|0|0|0|0|0|0|0|0|0|0|0	0
TPCN2_734G	P05165	PCCA	0|0|0	0|0|0|0|0	85|92|181|341|228|92|100|256|162|203|198|172|257|89|93|104|131|65|87|49|57|55|174|154|15	0
TPCN2_734G	P22314	UBA1	15|0|0	19|6|3|0|11	0|1|0|0|0|5|2|0|0|1|0|0|0|0|0|0|0|0|0|0|2|10|0|1|1|0|0|0|27	0
TPCN2_734G	Q53GQ0	HSD17B12	0|0|0	2|0|0|0|2	0|0|2|2|0|1|2|0|0|0|0|0|0|0|0|0|0|0|0|0|0|1|6|0|2|1|0|0|2|0	0
TPCN2_734G	P55145	MANF	0|0|0	0|0|0|0|0	0|0|0|0|0|0|0|0|0|0|0|0|0|0|0|0|0|0|0|0|0|0|0|0|0|0|0|0	0
TPCN2_734G	P50395	GDI2	6|0|4	11|4|3|0|5	3|2|0|0|0|0|0|0|0|0|0|0|0|0|0|0|0|1|0|0|0|1|0|0|0|1|0|4	0
TPCN2_734G	Q8NI27	THOC2	0|0|0	0|0|0|0|0	20|20|5|7|7|4|3|1|0|0|0|0|0|18|19|9|7|11|14|17|17|4|10|4|0|7|15|12|2|0	0
TPCN2_734G	P30101	PDIA3	23|0|0	24|5|2|0|18	0|0|0|0|0|0|0|9|8|9|7|7|6|0|0|0|0|0|0|0|0|0|7|0|0|0|1|0|0|10	0
TPCN2_734G	P27797	CALR	15|0|3	15|12|9|0|19	0|0|0|0|0|0|0|1|0|0|1|0|0|0|0|0|0|0|0|0|0|0|3|0|0|0|0|0|0|23	0
TPCN2_734G	P35606	COPB2	3|0|0	6|2|0|0|2	2|2|0|0|0|2|0|1|0|0|0|0|1|0|0|1|1|0|0|0|1|0|1|0|0|0|0|1|0|9	0
TPCN2_734G	P41250	GARS	0|0|0	2|0|0|0|0	0|0|0|0|0|0|0|1|0|2|2|1|1|0|0|0|0|0|0|1|0|0|0|0|0|0|0|0|1	0

TPCN2_734G	Q13547	HDAC1	2|3|0	4|0|0|6|4	1|2|24|23|26|10|9|0|1|2|2|2|2|1|1|15|14|0|0|1|1|8|16|10|5|15|0|0|10|7	0
TPCN2_734G	P78527	PRKDC	0|0|0	0|3|4|0|0	0|0|68|65|71|21|11|10|8|11|5|2|7|0|0|5|7|0|4|0|0|28|70|23|38|56|1|1|38|95	0
TPCN2_734G	Q9H2P0	ADNP	0|0|0	0|0|0|0|0	50|41|34|38|48|12|20|0|0|0|0|0|0|50|52|43|56|29|41|43|54|16|31|11|16|32|47|67|14|0	0
TPCN2_734G	P25205	MCM3	11|0|0	16|2|0|0|6	1|2|2|0|0|1|0|0|0|1|0|0|1|1|1|1|0|0|0|1|0|1|2|1|1|1|0|0|3|25	0
TPCN2_734G	Q16186	ADRM1	2|0|0	2|0|0|0|0	1|1|2|2|1|3|0|0|1|1|0|1|0|1|0|1|1|0|0|0|0|0|1|0|0|2|1|1|0|2	0
TPCN2_734G	P48735	IDH2	3|0|0	8|0|0|0|10	0|0|0|0|0|0|0|2|4|4|5|5|6|0|0|0|0|0|0|0|0|0|0|0|0|0|0|0|0|0|0	0
TPCN2_734G	Q16181	SEPT7	2|0|0	2|0|0|0|0	2|0|14|15|7|15|17|0|0|0|0|0|1|0|12|6|0|0|1|1|6|8|4|4|12|1|2|0|4	0
TPCN2_734G	P62241	RPS8	0|5|0	0|0|3|5|0	5|4|12|13|13|14|12|6|8|6|4|3|4|5|4|17|13|0|3|0|2|9|11|4|8|13|2|3|13|6	0
TPCN2_734G	P27708	CAD	0|0|0	0|0|0|0|0	0|0|9|4|6|1|0|3|1|3|3|2|2|0|0|0|0|0|0|0|0|2|4|6|3|6|0|0|7|21	0
TPCN2_734G	Q9Y3F4	STRAP	0|0|0	0|0|0|0|0	0|1|21|20|11|24|28|0|1|0|2|1|1|1|0|4|0|1|1|1|0|14|13|8|9|8|0|1|0|4	0
TPCN2_734G	Q96AG4	LRRC59	0|0|6	2|7|10|0|0	1|0|1|0|0|0|0|0|0|0|0|0|0|0|0|0|0|0|0|1|1|0|1|0|0|0|0|0|0|4	0

TPCN2_734G	P17987	TCP1	13|3|8	21|8|7|3|15	0|0|104|91|59|28|24|6|2|5|4|2|3|0|0|13|24|2|2|2|0|75|46|147|117|67|1|0|20|63	0
TPCN2_734G	Q13162	PRDX4	8|0|0	8|0|4|0|7	0|2|3|8|4|2|2|2|3|1|2|2|2|2|6|0|1|2|1|2|4|2|6|4|6|3|2|0|3	0
TPCN2_734G	P00390	GSR	0|0|0	2|0|0|0|0	0|0|0|0|0|0|0|0|0|0|0|0|0|0|0|0|0|0|0|0|0|0|0|0|0|0|0|0|0|0|0	0
TPCN2_734G	Q13283	G3BP1	0|0|0	6|0|0|0|0	8|7|20|15|10|12|13|0|0|0|0|0|8|8|7|6|3|6|2|10|13|8|10|10|13|5|3|1|4	0
TPCN2_734G	P61160	ACTR2	0|0|0	0|0|0|0|0	0|0|0|0|0|0|1|0|0|0|0|0|0|0|0|0|0|0|0|0|0|1|0|0|0|0|0|0|1|1	0
TPCN2_734G	Q7L2E3	DHX30	7|0|0	5|0|0|0|4	0|0|2|0|0|0|0|2|3|6|7|4|4|0|0|0|0|0|0|0|0|0|1|0|0|1|0|0|3|0	0
TPCN2_734G	P84098	RPL19	24|22|19	27|14|17|28|24	2|2|6|3|3|4|2|1|2|1|1|2|0|0|1|2|3|2|2|2|2|2|4|3|2|5|1|2|1|2	0
TPCN2_734G	O00159	MYO1C	7|0|3	8|2|0|0|5	1|0|0|0|0|0|0|0|0|0|0|0|0|0|0|1|1|0|0|0|0|0|1|0|0|0|0|0|10|0	0
TPCN2_734G	Q9H6R4	NOL6	0|0|0	3|0|0|0|0	0|0|3|1|2|0|2|0|0|0|0|0|0|2|1|5|2|1|0|1|0|0|8|0|0|5|1|0|0|0	0
TPCN2_734G	Q9Y678	COPG1	0|0|0	0|0|0|0|0	2|3|10|9|4|9|7|0|0|0|0|0|0|3|4|2|1|2|4|3|5|4|6|4|5|5|2|4|4|8	0
TPCN2_734G	O15067	PFAS	0|0|0	0|0|0|0|0	3|4|0|0|0|0|0|0|0|0|0|0|0|2|2|0|0|2|1|6|6|2|0|1|1|0|1|0|0|1	0

TPCN2_734G	P61221	ABCE1	2|0|0	0|0|0|0|0	1|0|0|0|0|7|7|0|0|0|0|0|0|0|0|0|1|0|0|0|0|0|1|0|0|0|0|0|0|2	0
TPCN2_734G	Q8WYA6	CTNNBL1	0|0|0	2|0|0|0|0	0|0|0|0|0|0|0|0|0|0|0|0|0|0|0|0|0|0|0|0|0|0|0|0|0|0|0|0	0
TPCN2_734G	Q14498	RBM39	0|0|0	2|0|0|0|0	3|2|3|1|0|3|1|1|0|0|0|0|0|0|3|1|1|3|2|2|2|1|4|1|0|1|1|2|4|28	0
TPCN2_734G	P0DME0	SETSIP	0|0|0	0|0|0|0|0	4|2|4|5|3|3|4|0|0|0|0|0|0|3|4|1|0|0|2|1|2|2|5|2|2|3|2|2|1|13	0
TPCN2_734G	Q9NZM5	NOP53	6|14|0	10|0|0|13|6	3|1|2|2|3|0|2|0|0|0|0|0|0|3|1|2|1|3|5|1|3|3|2|0|0|1|3|2|2|0	0
TPCN2_734G	P61981	YWHAG	5|0|0	8|0|0|0|4	0|0|2|3|1|2|0|2|2|4|2|3|2|1|1|0|1|0|1|0|0|1|3|0|1|3|0|0|0|13	0
TPCN2_734G	P55060	CSE1L	21|0|0	23|11|9|0|12	0|2|7|1|1|11|1|0|1|2|0|0|0|0|0|0|1|2|1|0|0|5|3|6|5|3|0|0|3|15	0
TPCN2_734G	O75691	UTP20	0|0|0	0|0|0|0|0	0|0|0|0|0|0|0|0|0|0|0|0|0|0|0|0|0|1|2|0|0|0|0|0|0|0|0|1|0	0
TPCN2_734G	Q13148	TARDBP	0|0|0	0|0|0|0|0	3|3|4|2|4|3|6|4|3|4|3|2|3|2|3|5|3|3|5|3|6|0|6|0|0|5|3|4|2|4	0
TPCN2_734G	Q14258	TRIM25	0|0|0	0|0|0|0|0	1|1|5|0|1|1|2|0|0|0|0|0|0|0|1|0|0|0|1|1|1|0|3|3|0|0|0|0|0|0	0
TPCN2_734G	O75694	NUP155	2|0|0	0|0|0|0|0	0|1|0|0|0|3|3|4|2|4|4|0|3|0|0|4|2|2|1|3|4|0|4|0|0|0|0|1|1|2	0

TPCN2_734G	Q14257	RCN2	0|0|0	0|0|0|0|2	0|0|0|0|0|0|0|0|0|0|0|0|0|0|0|0|0|0|0|0|0|0|0|0|0|0|0|0|0|15	0
TPCN2_734G	Q86U42	PABPN1	0|0|0	0|0|0|0|0	0|0|0|0|0|0|0|0|0|0|0|0|0|0|0|0|0|0|0|0|0|0|0|0|2|3	0
TPCN2_734G	P12236	SLC25A6	0|0|12	0|0|0|0|13	9|10|23|24|16|117|39|9|9|10|9|7|10|9|10|25|21|4|4|4|5|8|15|11|9|11|6|5|8|4	0
TPCN2_734G	P18669	PGAM1	0|0|0	4|0|0|0|0	0|1|3|3|0|11|5|0|0|0|0|0|0|0|0|0|0|0|0|0|0|0|0|2|11|0|1|1|0|0|0|7	0
TPCN2_734G	P05141	SLC25A5	11|13|15	13|11|8|13|14	8|9|27|30|21|28|14|9|7|9|8|9|8|9|8|27|32|4|3|3|5|14|20|16|15|16|6|4|13|5	0
TPCN2_734G	Q9UQ80	PA2G4	2|0|0	3|5|2|0|3	7|5|1|3|0|13|8|2|5|6|4|2|5|1|3|0|0|0|2|0|3|3|6|4|5|4|2|2|0|6	0
TPCN2_734G	P62280	RPS11	0|0|2	2|3|0|0|2	2|0|4|8|6|3|3|0|0|0|1|1|0|1|0|5|7|0|1|0|0|6|4|4|7|4|0|1|3|1	0
TPCN2_734G	P55209	NAP1L1	6|0|0	6|0|0|0|5	5|6|20|12|8|18|15|1|0|0|0|0|0|5|5|7|4|4|4|4|5|16|8|13|11|14|5|4|1|15	0
TPCN2_734G	Q8IWS0	PHF6	0|0|0	0|0|0|0|0	1|0|1|0|0|1|1|0|0|0|0|0|0|0|1|0|0|0|0|0|0|0|0|0|0|0|0|0|0|2	0
TPCN2_734G	Q5JWF2	GNAS	0|0|0	0|0|0|2|0	0|0|0|0|0|1|1|2|2|1|1|0|1|0|0|1|0|0|0|0|0|0|1|0|0|0|0|0|0|2	0
TPCN2_734G	P25705	ATP5A1	26|9|10	24|9|10|11|27	0|0|41|52|43|34|54|17|11|18|13|10|15|0|1|31|32|4|1|0|0|19|52|17|26|44|1|1|25|19	0

TPCN2_734G	Q13823	GNL2	0|11|0	4|0|0|6|0	33|32|10|15|9|0|8|0|0|0|0|0|0|27|27|25|11|16|20|22|24|11|14|7|4|9|30|54|5|0	0
TPCN2_734G	P12814	ACTN1	8|0|0	0|0|0|0|0	10|5|2|0|0|0|1|3|3|1|1|1|1|4|5|0|0|3|4|9|8|0|3|0|0|0|3|2|10|7	0
TPCN2_734G	Q9H3U1	UNC45A	0|0|0	0|0|0|0|0	4|10|5|1|0|5|4|0|0|0|0|0|0|5|3|1|0|0|2|4|5|11|4|4|6|1|1|0|0|2	0
TPCN2_734G	Q6P2E9	EDC4	2|0|0	2|0|0|0|0	8|7|13|6|3|6|7|0|0|0|0|0|0|1|3|1|1|3|7|11|14|14|10|7|9|8|4|3|0|1	0
TPCN2_734G	Q01813	PFKP	6|0|0	14|0|3|0|5	1|1|0|0|0|8|6|0|0|0|0|0|0|0|1|0|0|2|1|2|0|0|1|0|0|0|0|0|0|7	0
TPCN2_734G	Q92878	RAD50	4|0|0	0|0|0|0|2	0|0|5|8|10|0|1|0|0|0|0|0|0|0|0|0|0|1|1|0|0|1|16|0|1|10|0|0|3|1	0
TPCN2_734G	Q99490	AGAP2	0|0|0	0|0|0|0|0	0|0|0|0|0|0|0|0|0|0|0|0|0|0|0|0|0|0|0|0|0|0|0|0|0|0|0	0
TPCN2_734G	P51114	FXR1	3|0|0	4|0|0|0|3	0|1|1|1|0|4|2|0|0|0|0|0|0|2|2|1|0|0|0|0|0|0|1|0|0|1|0|0|0|0	0
TPCN2_734G	Q00341	HDLBP	3|0|0	0|0|0|0|0	25|22|28|22|7|23|26|0|0|1|0|0|0|18|18|11|5|12|10|18|24|21|11|8|15|9|13|15|2|3	0
TPCN2_734G	O76031	CLPX	0|0|0	0|0|0|0|2	0|0|0|0|0|0|0|4|3|3|6|8|9|0|0|0|0|0|0|0|0|0|0|0|0|0|0|0|0|0	0
TPCN2_734G	P61313	RPL15	11|7|6	10|12|8|8|15	7|10|20|20|17|9|16|3|2|2|3|1|2|3|6|17|8|1|1|1|2|10|30|14|11|19|4|4|5|2	0

TPCN2_734G	Q9HDC9	APMAP	0|0|0	0|0|0|0|0	0|0|0|0|0|0|0|1|0|0|0|0|0|0|0|0|0|0|0|0|0|0|0|0|0|0|0|1|0|0	0
TPCN2_734G	P33176	KIF5B	4|0|0	4|0|0|0|0	16|15|48|32|20|16|18|0|0|0|0|0|0|9|9|7|6|5|9|9|12|17|30|12|14|26|10|9|1|9	0
TPCN2_734G	O60814	HIST1H2BK	10|9|12	14|11|11|10|12	15|15|14|30|21|21|33|10|9|7|5|7|7|21|20|39|57|14|11|7|13|22|48|52|35|64|13|9|36|20	0
TPCN2_734G	P14866	HNRNPL	11|19|0	19|2|0|13|10	21|18|10|18|16|13|17|13|16|14|15|15|16|31|16|19|21|6|13|11|6|18|23|25|18|20|14|18|10|21	0
TPCN2_734G	P24941	CDK2	3|0|2	5|2|3|0|0	0|0|3|2|3|3|5|0|0|0|0|0|0|0|0|0|0|0|0|2|1|3|3|2|4|2|1|0|4|1	0
TPCN2_734G	P14868	DARS	7|0|0	7|0|0|0|2	1|1|4|9|4|2|1|0|0|0|0|0|0|0|1|1|0|0|0|0|0|2|5|2|1|4|0|0|2|8	0
TPCN2_734G	P63104	YWHAZ	11|0|0	13|9|7|0|9	0|3|5|4|3|2|1|8|5|6|5|6|6|1|2|1|1|3|3|0|1|2|8|2|2|3|3|2|1|28	0
TPCN2_734G	P11498	PC	10|24|54	10|34|66|24|14	691|770|428|416|295|106|88|1307|810|1086|1058|849|1284|383|418|702|699|289|459|206|325|1	0
TPCN2_734G	REV_P042	REV_P04280	0|0|0	0|0|0|0|0	0|0|0|0|0|0|0|0|0|0|0|0|0|0|0|0|0|0|0|0|0|0|0|0|0|0|0|0|0|0|0	0
TPCN2_734G	Q13263	TRIM28	17|0|0	21|0|0|0|7	32|39|52|61|50|26|37|10|11|11|7|4|9|36|40|19|9|25|32|31|39|29|37|43|28|29|28|26|16|41	0
TPCN2_734G	P11021	HSPA5	73|7|13	71|23|23|8|57	16|18|53|58|38|42|21|19|18|19|18|14|16|12|13|28|36|11|17|13|17|26|46|28|30|39|11|14|19|9	0

TPCN2_734G	Q9P0L0	VAPA	0|0|0	3|0|0|0|4	1|2|6|2|6|8|4|0|2|0|0|0|2|3|2|8|3|2|0|0|0|2|5|0|0|2|2|1|0|0	0
TPCN2_734G	Q9P0L1	ZKSCAN7	0|0|0	0|0|0|0|0	0|0|0|0|0|0|0|0|0|0|0|0|0|0|0|0|0|0|0|0|0|0|0|0|0|0|0|0|0|0|0	0
TPCN2_734G	P11717	IGF2R	0|0|0	0|0|0|0|0	0|1|0|0|0|0|0|0|0|0|0|0|0|0|1|1|0|0|0|1|1|0|0|0|0|1|0|0|0	0
TPCN2_734G	Q02790	FKBP4	5|0|0	7|2|0|0|3	0|0|0|0|0|0|1|0|0|0|0|0|0|0|0|0|0|0|0|0|0|0|2|0|0|0|0|0|0|18	0
TPCN2_734G	Q96RQ3	MCCC1	6|15|16	4|14|19|12|12	65|57|184|276|188|44|42|169|104|125|116|93|161|56|53|55|43|31|54|26|40|62|149|125|220|21	0
TPCN2_734G	Q9Y617	PSAT1	0|0|0	0|0|0|0|0	0|0|0|0|0|0|0|0|0|0|0|0|0|0|0|0|0|0|0|0|0|0|0|0|0|0|0|0|0|0	0
TPCN2_734G	P09543	CNP	4|0|0	12|0|0|0|8	0|0|0|0|0|0|0|2|0|2|1|1|1|0|0|0|0|0|0|0|0|0|0|0|0|0|0|0|0|0	0
TPCN2_734G	Q9ULV4	CORO1C	9|0|0	6|0|0|0|4	11|10|7|3|3|16|8|0|0|0|0|0|0|7|7|2|2|6|6|8|9|0|3|1|0|3|7|7|4|0	0
TPCN2_734G	Q01105	SET	5|0|0	6|0|0|0|3	10|7|10|7|8|10|5|0|0|0|0|0|0|5|7|3|2|0|2|1|2|8|5|8|7|9|3|2|3|25	0
TPCN2_734G	Q5JTH9	RRP12	3|2|0	0|0|0|2|5	0|0|3|0|1|0|0|0|0|0|0|0|0|0|0|0|2|2|5|2|2|0|0|4|0|1|4|1|2|0|0	0
TPCN2_734G	Q08170	SRSF4	0|0|0	0|0|0|0|0	4|1|5|3|8|2|0|1|1|0|1|1|1|2|2|0|1|1|1|1|1|0|7|0|0|2|1|1|1|3	0

TPCN2_734G	P22626	HNRNPA2B1	2|0|0	9|0|0|0|0	15|10|14|28|23|11|17|18|12|16|10|12|15|21|14|13|13|14|4|29|11|8|27|18|12|9|58	0
TPCN2_734G	P29590	PML	0|0|0	0|0|0|0|0	0|0|1|0|0|1|0|0|0|0|0|0|0|0|0|0|0|0|0|0|1|0|0|1|0|0|0|0|0	0
TPCN2_734G	Q9UNF1	MAGED2	5|19|15	7|15|17|26|4	5|2|0|1|0|3|3|0|0|0|0|0|0|1|3|0|0|0|0|0|1|0|1|0|0|2|0|0|0|2	0
TPCN2_734G	Q92499	DDX1	3|0|0	4|0|0|0|3	1|1|2|4|3|7|6|0|0|0|0|0|0|0|4|3|0|0|0|0|8|5|4|3|5|0|0|1|8	0
TPCN2_734G	Q08J23	NSUN2	6|0|0	6|0|0|0|0	3|1|1|2|2|3|4|1|0|1|3|0|1|1|2|0|0|1|0|2|0|3|3|2|2|9|0|0|7|2	0
TPCN2_734G	P22061	PCMT1	0|0|2	0|0|0|0|0	1|0|0|0|0|0|1|1|1|2|0|0|1|1|1|0|0|0|1|0|1|0|0|0|0|0|0|0|0|0	0
TPCN2_734G	Q9UKM9	RALY	0|0|0	5|0|0|0|0	1|0|0|0|0|0|0|0|1|0|0|0|1|0|0|0|0|0|0|0|0|0|0|0|0|0|0|0|9	0
TPCN2_734G	Q7Z2W4	ZC3HAV1	2|4|0	0|0|0|0|0	17|17|5|12|4|11|14|3|4|1|1|2|2|14|11|4|6|13|21|19|28|4|5|0|2|7|11|11|0|0	0
TPCN2_734G	P04406	GAPDH	33|3|10	39|27|21|4|28	0|0|0|0|0|1|1|9|6|4|4|6|4|2|1|0|0|1|3|1|1|2|19|0|7|2|0|3|4|41	0
TPCN2_734G	Q7Z2W9	MRPL21	0|0|0	0|0|0|0|0	0|0|0|0|0|0|0|0|0|0|0|1|0|0|0|0|0|0|0|0|0|0|0|0|0|0|0|0	0
TPCN2_734G	Q8WVC0	LEO1	0|0|0	0|0|0|0|0	0|1|1|0|1|0|0|0|0|0|0|0|0|3|2|1|0|2|3|2|3|0|2|0|1|1|2|2|0|0	0

TPCN2_734G	P07339	CTSD	7|3|4	12|4|5|2|11	0|0|0|0|0|0|0|0|0|0|0|0|0|0|0|0|0|0|0|0|0|0|0|0|0|0|0|0|0|0|0	0
TPCN2_734G	Q9Y5L0	TNPO3	0|0|0	3|0|0|0|0	0|0|1|0|2|0|1|0|0|0|0|0|0|0|0|0|1|0|0|0|0|1|1|0|1|1|0|0|3|0	0
TPCN2_734G	Q9Y6D5	ARFGEF2	0|0|0	0|0|0|0|0	0|0|0|0|0|0|0|0|0|0|0|0|0|0|0|0|0|0|0|0|0|0|0|0|0|0|0|0|0|0|0	0
TPCN2_734G	P11177	PDHB	2|0|0	3|0|0|0|4	0|0|0|0|0|0|0|11|8|8|13|16|16|0|0|0|0|0|1|0|1|0|0|0|0|0|1|0|0|1	0
TPCN2_734G	O00571	DDX3X	3|0|0	2|0|0|0|2	17|16|27|32|15|27|39|8|12|6|4|6|5|11|13|21|23|13|20|17|24|29|20|21|25|19|13|15|8|17	0
TPCN2_734G	O00299	CLIC1	0|0|0	2|2|0|0|2	1|2|0|0|0|1|1|1|2|1|1|2|1|0|1|0|0|0|5|0|2|0|0|0|1|0|1|1|0|1	0
TPCN2_734G	P29692	EEF1D	4|0|0	5|0|0|0|4	11|12|7|7|6|4|4|0|0|0|0|0|0|11|13|18|23|6|11|7|14|5|5|5|3|5|9|11|0|19	0
TPCN2_734G	Q06830	PRDX1	5|0|6	8|8|5|2|6	11|11|6|18|14|9|10|13|14|14|17|16|17|11|10|27|4|6|10|5|11|9|24|16|10|21|10|7|2|20	0
TPCN2_734G	Q9UIG0	BAZ1B	3|0|0	0|0|0|0|0	101|76|33|51|42|9|28|0|0|0|0|0|0|95|94|110|72|68|95|56|76|39|62|32|32|31|114|91|27|0	0
TPCN2_734G	P30153	PPP2R1A	4|0|0	10|0|0|0|3	0|0|11|3|7|3|0|4|0|0|0|0|0|0|0|0|0|0|0|1|0|0|10|10|10|5|11|0|0|0|21	0
TPCN2_734G	O75390	CS	12|0|0	16|6|2|0|13	2|2|1|0|0|0|0|9|5|7|9|6|12|0|0|0|0|2|4|3|3|0|5|0|2|0|2|3|1|11	0

TPCN2_734G	Q6ZR52	ZNF493	0|0|0	0|0|0|0|0	0|1|0|0|0|0|0|0|0|0|0|0|0|0|0|0|0|0|0|0|0|0|0|0|0|0|1|0|0|0|0	0
TPCN2_734G	O14646	CHD1	0|0|0	0|0|0|0|0	4|4|0|0|1|0|0|0|0|0|0|0|0|4|1|0|0|9|5|6|7|0|0|0|0|0|2|3|0|0	0
TPCN2_734G	P35221	CTNNA1	4|0|0	7|0|0|0|2	2|2|0|0|0|0|1|0|0|1|0|0|0|0|0|0|2|2|2|2|0|1|0|0|0|0|0|0|3	0
TPCN2_734G	P49748	ACADVL	5|0|0	7|0|0|0|11	0|0|0|0|0|0|0|3|5|3|7|10|7|0|0|0|0|0|0|0|0|0|0|0|0|0|0|0|0|0|0	0
TPCN2_734G	P38646	HSPA9	52|10|21	52|16|34|14|42	7|10|47|45|38|12|18|90|73|125|128|112|155|6|5|25|20|12|19|10|11|27|81|13|23|21|25|23|23|	0
TPCN2_734G	Q9BSJ8	ESYT1	0|0|0	0|0|2|0|0	15|11|8|4|2|7|12|0|0|0|0|0|0|14|14|7|0|14|12|15|21|5|3|3|2|4|11|10|0|0	0
TPCN2_734G	Q92797	SYMPK	0|0|0	0|0|0|0|0	1|2|1|1|0|0|1|0|0|0|0|0|0|0|1|0|0|2|1|3|2|1|3|1|1|2|0|1|1|0	0
TPCN2_734G	P62701	RPS4X	2|0|0	2|2|3|0|3	0|0|6|7|2|14|12|5|2|4|2|1|4|0|1|4|3|0|2|0|0|8|8|4|2|8|1|0|1|10	0
TPCN2_734G	Q15424	SAFB	5|0|0	3|0|0|0|0	17|10|1|3|1|6|6|3|2|3|2|4|2|10|10|7|4|10|17|10|13|2|3|1|4|3|18|22|0|0	0
TPCN2_734G	P22531	SPRR2E	0|0|0	0|0|0|0|0	0|0|0|0|0|0|0|0|0|0|0|0|0|0|0|0|0|0|0|0|0|0|0|0|0|0|0|0|0|0|0	0
TPCN2_734G	P68431	HIST1H3	3|0|5	7|6|5|3|5	9|7|15|23|16|15|23|3|4|5|2|3|4|9|10|14|27|7|12|9|10|22|31|35|22|21|8|7|14|16	0

TPCN2_734G	P27695	APEX1	0|0|0	0|0|0|0|0	0|0|0|0|0|0|0|0|0|0|0|0|0|0|0|0|0|0|0|0|0|0|1|0|0|0|0|0|1|4	0
TPCN2_734G	P62277	RPS13	0|0|0	2|0|0|0|2	0|0|7|2|2|0|0|0|0|0|0|0|0|0|0|0|0|0|0|0|0|0|4|0|2|0|0|0|1|1	0
TPCN2_734G	Q9HCC0	MCCC2	4|15|14	0|16|19|15|13	0|0|257|271|200|71|59|0|0|0|0|0|0|1|0|74|70|0|0|0|0|94|273|204|384|255|0|0|83|0	0
TPCN2_734G	Q08379	GOLGA2	0|0|0	2|0|0|0|0	8|7|0|0|0|0|0|0|1|2|0|1|1|8|5|3|1|16|16|14|18|0|0|0|0|0|5|10|0|0	0
TPCN2_734G	P60842	EIF4A1	9|0|3	12|7|7|0|5	5|6|21|22|16|34|27|8|6|11|9|7|6|2|3|12|9|3|7|3|5|21|18|17|19|20|7|5|13|24	0
TPCN2_734G	Q8NBS9	TXNDC5	0|0|0	4|0|0|0|3	0|0|0|0|0|0|0|2|0|1|1|2|2|0|0|0|0|0|0|0|0|0|0|0|0|0|0|0|0|0|1	0
TPCN2_734G	O00232	PSMD12	3|0|0	3|0|0|0|2	1|1|1|1|0|1|1|0|0|0|0|0|0|1|0|0|0|1|0|1|3|1|1|0|1|0|0|0|0|15	0
TPCN2_734G	Q96PK6	RBM14	0|0|0	0|0|0|0|0	0|0|5|6|8|4|1|3|2|5|5|4|2|0|0|1|5|1|1|1|1|0|5|0|0|9|2|2|6|0	0
TPCN2_734G	Q8TDD1	DDX54	15|32|3	18|2|0|28|13	0|0|7|1|5|1|2|0|0|0|0|0|0|0|0|4|4|0|0|0|0|2|12|3|6|9|1|0|6|0	0
TPCN2_734G	Q9NYF8	BCLAF1	3|0|0	0|0|0|0|0	33|34|40|44|32|29|40|0|0|1|0|0|1|33|26|34|22|22|26|35|49|18|31|19|13|35|66|56|11|4	0
TPCN2_734G	P37108	SRP14	0|0|0	0|0|0|0|0	2|1|4|2|3|0|0|0|1|1|1|1|1|1|2|3|1|1|1|2|1|5|2|2|3|1|2|1|1	0

TPCN2_734G	P06733	ENO1	19|0|6	22|18|13|2|18	3|4|18|26|12|34|67|9|5|7|5|4|3|3|5|4|2|3|5|5|4|27|38|4|15|11|4|3|21|51	0
TPCN2_734G	P55084	HADHB	14|0|0	21|0|0|0|15	0|0|0|0|0|0|0|1|3|4|5|5|4|0|0|0|0|0|0|0|0|0|0|0|0|0|0|0|0|0|0	0
TPCN2_734G	Q9BQG0	MYBBP1A	7|2|0	3|0|5|2|4	8|3|39|21|29|9|12|2|0|3|0|0|0|2|2|9|6|7|5|5|2|7|49|6|6|24|8|4|14|2	0
TPCN2_734G	P54886	ALDH18A1	3|0|0	5|0|0|0|0	0|0|16|15|16|23|13|13|19|19|27|24|25|1|0|19|21|0|0|0|0|12|16|6|14|11|0|1|16|14	0
TPCN2_734G	P05556	ITGB1	2|0|0	0|0|0|0|2	0|0|0|0|0|0|0|0|0|0|0|0|0|0|0|0|0|1|1|1|2|0|0|0|0|0|2|1|0|0	0
TPCN2_734G	P28838	LAP3	0|0|0	0|0|0|0|0	0|0|0|0|0|0|0|0|0|0|1|1|0|0|0|1|0|0|0|0|0|0|0|0|0|0|0|0|0|0	0
TPCN2_734G	Q01082	SPTBN1	3|0|0	0|0|0|0|0	2|0|0|0|0|0|0|1|0|1|0|0|0|0|1|0|8|9|8|5|0|3|0|0|0|2|1|26|0	0
TPCN2_734G	P50991	CCT4	11|3|4	16|6|6|0|16	2|2|48|50|63|13|15|3|2|4|3|3|3|1|0|4|24|0|2|0|1|54|29|85|94|49|1|2|20|57	0
TPCN2_734G	P50990	CCT8	15|0|0	22|9|5|0|19	38|50|132|202|100|208|201|1|0|0|0|1|3|52|67|29|38|18|21|25|41|117|85|125|113|107|24|21|2	0
TPCN2_734G	O43399	TPD52L2	0|0|2	0|0|2|0|0	0|1|3|0|0|4|1|0|0|0|0|0|0|0|1|1|0|1|1|2|1|0|1|1|0|1|1|0|0|0	0
TPCN2_734G	P46782	RPS5	5|0|4	6|3|2|4|10	0|0|0|0|0|0|0|1|1|1|0|0|0|0|0|0|0|1|0|1|2|2|3|1|0|0|0|0|2	0

TPCN2_734G	P46781	RPS9	2|5|2	4|4|6|6|5	1|3|17|13|10|12|9|2|2|1|1|0|1|0|0|7|5|1|1|0|1|3|8|5|6|7|1|1|3|3	0
TPCN2_734G	P42704	LRPPRC	66|0|0	59|11|12|0|47	2|0|0|0|0|0|0|85|68|78|99|89|106|0|0|1|2|6|7|0|0|0|2|0|0|1|6|5|0|39	0
TPCN2_734G	Q96TA1	FAM129B	0|0|0	0|0|0|0|0	3|2|0|0|0|1|1|0|0|0|0|0|0|2|1|0|0|1|2|3|4|0|0|0|0|0|2|1|0|0	0
TPCN2_734G	P02787	TF	0|0|0	0|0|0|0|0	0|0|0|0|0|0|0|0|0|0|0|0|0|0|0|0|0|0|0|0|0|0|0|0|0|0|0|0	0
TPCN2_734G	O43719	HTATSF1	0|0|0	0|0|0|0|0	8|4|1|1|0|0|0|0|0|0|0|0|0|4|6|0|1|1|3|4|3|1|0|0|1|2|0|1|0|16	0
TPCN2_734G	Q9HD20	ATP13A1	0|0|0	0|0|0|0|0	0|1|0|0|0|0|0|0|0|0|0|0|0|0|0|0|0|0|0|0|0|1|0|0|0|0|0|0|0	0
TPCN2_734G	O94806	PRKD3	19|21|53	31|46|46|14|26	0|0|0|0|0|0|0|0|0|0|0|0|0|0|0|0|0|0|0|0|0|0|0|0|0|0|0|0	0
TPCN2_734G	P31040	SDHA	5|0|0	10|0|0|0|5	1|1|0|0|0|0|0|11|9|14|15|12|17|1|0|0|1|1|0|0|0|0|1|0|0|0|1|0|0|1	0
TPCN2_734G	P62888	RPL30	2|0|0	0|0|0|0|2	0|0|5|2|3|0|0|0|0|0|0|0|0|0|0|0|1|2|0|0|0|0|4|4|5|3|5|0|0|3|0	0
TPCN2_734G	P09104	ENO2	0|0|0	0|3|0|0|0	1|1|1|7|2|2|7|2|1|2|1|1|1|1|1|1|0|1|1|1|0|9|8|0|3|3|1|1|2|7	0
TPCN2_734G	P56192	MARS	3|0|0	2|0|2|0|0	0|1|9|12|10|14|9|1|0|0|0|0|0|0|0|0|0|1|0|1|4|10|12|9|10|0|0|9|5	0

TPCN2_734G	O60841	EIF5B	0|0|0	2|0|3|0|0	8|9|5|5|3|0|5|0|0|0|0|0|0|6|7|4|0|5|5|4|4|9|5|4|3|5|3|3|0|1	0
TPCN2_734G	Q02218	OGDH	5|0|0	0|0|0|0|3	0|0|0|0|0|0|0|4|5|5|11|9|8|0|0|0|0|0|0|0|0|0|0|0|0|0|0|0|0	0
TPCN2_734G	O95373	IPO7	9|0|0	7|0|0|0|0	4|11|5|0|0|2|2|0|1|0|0|0|0|4|7|0|0|5|5|5|4|1|1|0|0|0|3|4|0|2	0
TPCN2_734G	P20700	LMNB1	6|0|0	7|0|0|0|4	8|6|1|2|3|0|0|8|8|7|5|8|4|4|2|3|1|4|3|2|2|1|12|0|2|5|3|2|4|27	0
TPCN2_734G	P55884	EIF3B	2|0|0	4|0|0|0|0	0|0|16|6|4|6|4|0|0|0|0|0|0|0|2|2|5|0|0|0|0|7|7|3|5|2|1|1|1|4	0
TPCN2_734G	P21796	VDAC1	9|0|0	13|4|0|0|12	4|3|3|2|4|1|3|9|7|7|7|5|7|3|5|2|2|1|3|2|1|3|4|1|0|2|4|4|1|0	0
TPCN2_734G	O00763	ACACB	0|0|0	0|2|8|0|0	27|25|86|73|36|6|4|99|70|87|103|93|100|29|28|18|29|23|29|17|17|20|39|39|52|54|28|26|11|1	0
TPCN2_734G	Q01650	SLC7A5	3|0|0	2|0|0|0|0	6|11|2|1|0|0|1|4|4|5|4|4|5|11|8|5|4|5|5|4|4|0|1|0|0|1|3|5|0|0	0
TPCN2_734G	P12956	XRCC6	19|0|0	20|0|2|0|15	13|15|6|3|1|1|1|2|0|3|1|2|0|4|9|2|0|2|2|3|7|8|9|0|3|4|2|1|3|52	0
TPCN2_734G	Q5ZPR3	CD276	0|0|0	0|0|0|0|0	0|0|0|0|0|0|0|0|0|0|0|0|0|0|0|0|0|0|0|0|0|0|0|0|0|0|0|0|0	0
TPCN2_734G	Q6P158	DHX57	0|0|0	0|0|0|0|0	0|0|0|0|0|0|0|0|0|0|0|1|1|0|0|0|0|0|0|0|0|0|0|0|0|0|0|0|0|0	0

TPCN2_734G	Q13797	ITGA9	0|0|0	0|0|0|0|0	0|0|0|0|0|0|0|0|0|0|0|0|0|0|0|0|0|0|0|0|0|0|0|0|0|0|0|0	0
TPCN2_734G	O15143	ARPC1B	0|0|0	0|0|0|0|0	0|0|0|0|0|0|0|0|1|0|1|0|0|0|0|0|0|0|0|0|0|0|0|0|0|0|0|0|0|0	0
TPCN2_734G	Q9BVP2	GNL3	11|13|3	9|2|0|18|12	2|4|2|8|5|3|6|0|2|1|0|1|1|4|3|3|3|5|8|5|7|3|11|3|3|2|4|4|5|0	0
TPCN2_734G	P23246	SFPQ	8|0|0	5|3|0|0|0	15|15|49|39|30|29|18|5|2|4|2|2|3|14|11|25|26|8|13|13|17|21|25|24|19|29|13|12|15|24	0
TPCN2_734G	Q14008	CKAP5	0|0|0	0|0|0|0|0	32|19|36|21|24|20|14|0|0|0|0|0|0|17|14|8|9|22|28|25|32|42|25|23|28|33|29|23|1|10	0
TPCN2_734G	Q13813	SPTAN1	3|0|0	0|0|0|0|0	7|5|1|0|2|0|1|3|1|3|0|0|0|4|2|1|2|11|14|10|17|0|4|0|1|2|4|5|16|0	0
TPCN2_734G	P62851	RPS25	2|2|3	2|4|5|4|2	0|0|0|0|0|0|0|1|0|0|0|0|1|0|0|0|0|0|0|0|0|0|0|2|1|0|0|0|0|0|8	0
TPCN2_734G	P0DMV8	HSPA1A	24|8|11	24|13|14|0|16	26|28|173|180|124|109|162|12|17|22|16|17|11|30|29|41|39|31|42|31|36|137|151|122|107|148|	0
TPCN2_734G	P40939	HADHA	29|0|0	37|9|9|0|34	0|0|0|0|0|0|0|21|14|18|24|22|23|0|0|0|0|2|1|0|0|0|1|0|0|0|0|0|0|2	0
TPCN2_734G	Q96CV9	OPTN	0|0|0	2|0|0|0|0	0|0|1|0|0|0|0|0|0|0|0|0|0|0|0|0|0|0|0|0|0|0|0|0|0|0|0|0	0
TPCN2_734G	Q9BVK6	TMED9	0|0|0	0|0|0|0|0	0|0|0|0|0|0|0|0|0|1|1|0|2|0|0|0|0|0|0|0|0|0|0|0|0|0|0|0|0|0	0

TPCN2_734G	P52597	HNRNPF	7|0|0	9|0|0|0|10	8|5|12|10|11|10|8|17|12|14|17|12|19|7|6|9|3|11|10|7|11|7|20|7|8|10|14|12|11|27	0
TPCN2_734G	P60709	ACTB	0|11|0	0|0|0|16|0	30|29|41|60|55|42|40|56|53|53|51|54|57|32|34|65|74|38|60|34|45|26|65|21|17|42|44|47|258|	0
TPCN2_734G	Q9NQC3	RTN4	7|0|0	9|0|0|0|7	10|10|7|8|2|8|11|1|0|1|1|1|1|6|8|12|2|11|12|12|16|0|4|2|0|3|11|7|1|2	0
TPCN2_734G	P52292	KPNA2	0|0|0	0|0|0|0|0	0|0|2|1|2|1|1|2|1|1|1|1|2|0|0|2|1|0|1|1|0|4|6|2|0|5|0|0|2|13	0
TPCN2_734G	P05204	HMGN2	0|0|3	0|0|0|0|0	0|0|0|1|3|0|0|0|0|0|0|0|0|0|0|0|0|0|0|0|0|0|4|0|0|6|0|0|0|1	0
TPCN2_734G	P09211	GSTP1	3|0|0	6|3|0|0|2	0|1|0|0|0|0|0|6|7|6|7|7|5|0|0|0|0|4|5|1|0|0|0|0|0|3|2|0|0	0
TPCN2_734G	P62913	RPL11	0|0|0	0|0|0|0|4	4|4|8|9|10|13|7|3|5|3|3|3|3|4|5|6|8|2|4|0|1|6|7|3|4|9|4|3|8|6	0
TPCN2_734G	P06899	HIST1H2BJ	0|0|0	0|0|0|0|0	14|14|15|27|20|23|33|10|8|8|5|6|7|21|19|35|55|14|10|7|12|21|47|47|30|63|10|8|36|20	0
TPCN2_734G	P62917	RPL8	11|17|3	14|8|9|15|16	0|1|10|7|4|8|5|0|0|0|0|0|0|0|1|8|3|0|1|0|0|5|5|7|5|5|0|0|1|1	0
TPCN2_734G	P31943	HNRNPH1	15|0|0	19|5|0|0|21	4|3|8|7|13|9|7|9|7|11|9|10|11|5|4|6|4|9|8|6|7|7|13|9|7|11|7|5|12|24	0
TPCN2_734G	O15371	EIF3D	0|0|0	2|0|0|0|0	1|1|2|1|7|2|3|1|1|0|0|0|0|1|1|0|2|1|0|1|1|6|6|10|9|7|0|0|0|4	0

TPCN2 _734G	Q15029	EFTUD2	12|0|0	11|0|3|0|5	1|2|16|16|10|7|14|1|1|3|1|1|2|1|2|21|7|4|3|2|2|26|16|13|15|19|0|2|16|28	0
TPCN2 _734G	P31946	YWHAB	9|0|0	12|9|0|0|8	0|2|6|7|3|2|2|1|1|2|1|1|1|2|1|0|2|0|1|0|0|1|5|2|2|4|0|0|0|20	0
TPCN2 _734G	Q8N1F7	NUP93	6|0|0	4|0|0|0|0	0|0|8|4|5|0|3|0|0|0|0|0|0|0|0|1|3|0|0|0|0|4|7|5|7|4|0|0|13|1	0
TPCN2 _734G	P31948	STIP1	9|0|0	12|0|0|0|7	1|0|0|0|0|1|3|1|1|2|1|0|1|1|0|0|0|1|2|1|2|0|2|0|0|0|1|1|0|46	0
TPCN2 _734G	Q15020	SART3	3|0|0	3|0|0|0|3	18|13|34|30|21|24|14|0|0|0|0|0|0|22|26|13|10|9|15|12|17|10|33|6|5|19|15|14|9|3	0
TPCN2 _734G	P55072	VCP	30|0|0	35|16|15|0|24	0|0|3|1|1|3|4|0|0|0|0|0|0|0|0|0|0|1|6|1|2|4|5|2|3|1|0|0|0|84	0
TPCN2 _734G	P63092	GNAS	0|0|0	0|2|3|0|3	0|0|0|0|0|1|1|2|2|1|1|0|1|0|0|1|0|0|0|0|0|0|1|0|0|0|0|0|0|2	0
TPCN2 _734G	P23396	RPS3	10|3|12	14|8|9|8|14	6|5|39|39|32|33|39|7|9|6|6|5|6|3|5|23|23|2|3|2|2|27|26|32|35|34|4|3|29|17	0
TPCN2 _734G	P30447	HLA-A	7|0|0	8|0|0|0|8	0|0|0|0|0|0|0|4|3|5|2|2|5|0|0|0|0|1|1|0|0|0|1|0|0|0|2|1|0|2	0
TPCN2 _734G	P50416	CPT1A	2|0|0	2|0|0|0|5	1|0|0|0|0|0|0|0|0|0|0|0|0|1|1|0|0|1|1|0|0|0|0|0|0|0|1|0|0|0	0
TPCN2 _734G	P35613	BSG	0|0|0	0|0|0|0|2	0|0|0|0|0|0|0|0|0|0|0|0|0|0|0|0|0|0|0|0|0|0|1|0|0|0|0|0|0|3	0

TPCN2_734G	P35268	RPL22	0|0|0	0|4|4|0|0	4|4|2|6|3|7|1|4|4|4|4|4|4|3|4|3|5|0|2|0|2|2|4|3|3|4|3|3|3|1	0
TPCN2_734G	Q12874	SF3A3	0|0|0	3|0|0|0|2	0|0|13|6|7|3|1|0|0|0|0|0|0|0|0|3|5|0|0|0|0|2|4|4|1|7|0|0|3|5	0
TPCN2_734G	Q9P1Z3	HCN3	0|0|0	0|0|0|0|0	0|0|0|0|0|0|0|0|0|0|0|0|0|0|0|0|0|0|0|0|0|0|0|0|0|0|0|0|0|0|0	0
TPCN2_734G	Q9Y5B9	SUPT16H	8|0|0	7|0|0|0|0	4|5|0|1|0|5|6|1|1|1|1|1|1|2|2|1|2|4|4|1|1|0|0|1|0|1|0|1|7|0	0
TPCN2_734G	Q01130	SRSF2	0|0|0	2|0|0|0|0	0|0|2|1|0|0|0|0|0|0|0|0|0|0|0|0|0|0|0|0|0|0|0|2|0|0|0|0|0|2|18	0
TPCN2_734G	P48047	ATP5O	0|0|0	0|0|0|0|2	0|0|0|0|0|0|0|2|2|3|2|2|3|0|0|0|0|2|2|2|0|0|0|0|0|0|0|1|3	0
TPCN2_734G	P17812	CTPS1	3|0|0	3|0|0|0|2	22|23|22|21|14|25|21|0|0|1|2|0|0|21|27|9|2|3|10|7|15|17|13|17|14|18|9|8|3|6	0
TPCN2_734G	Q14318	FKBP8	2|0|0	2|0|0|0|0	0|0|0|0|0|0|0|0|1|2|1|0|0|0|0|0|0|4|1|0|1|0|2|0|0|0|1|0|0|1	0
TPCN2_734G	Q9UJZ1	STOML2	2|0|0	4|0|0|0|2	0|0|0|0|0|0|0|0|0|0|0|0|0|0|0|0|0|0|0|0|0|0|5|0|1|0|0|0|0|0	0
TPCN2_734G	Q16643	DBN1	14|0|0	9|0|0|0|7	19|15|5|3|5|4|13|5|1|3|2|0|4|21|19|8|6|16|12|16|20|2|7|0|0|2|12|13|27|0	0
TPCN2_734G	P82675	MRPS5	0|0|0	0|0|0|6|3	0|0|0|0|0|0|1|1|1|1|2|2|4|0|0|0|0|0|0|0|0|0|0|0|0|0|0|0|0|0	0

TPCN2_734G	Q9Y490	TLN1	5|0|0	0|5|7|0|0	22|21|43|21|10|42|42|1|0|0|0|0|0|10|10|9|1|16|25|19|32|40|32|19|33|16|18|25|0|1	0
TPCN2_734G	P14314	PRKCSH	20|0|0	22|11|6|0|15	0|0|0|0|0|0|0|0|1|1|0|1|0|0|0|0|0|0|0|0|0|0|2|0|0|0|0|0|0|10	0
TPCN2_734G	P00367	GLUD1	3|0|0	4|0|0|0|4	0|0|7|1|0|2|0|2|3|2|2|3|3|0|0|0|0|0|0|0|0|0|2|3|1|2|0|0|2|3	0
TPCN2_734G	P38606	ATP6V1A	11|0|0	10|0|0|0|6	1|0|5|5|2|7|6|1|0|0|0|0|0|0|0|2|1|0|1|2|0|4|4|1|2|3|0|0|0|1	0
TPCN2_734G	P23634	ATP2B4	0|0|0	0|0|0|0|0	0|0|0|1|0|0|0|0|0|0|0|0|0|1|0|0|0|0|0|0|0|0|0|0|0|1|0|0|2|0	0
TPCN2_734G	P08670	VIM	90|29|25	87|37|38|44|96	93|113|66|90|91|56|111|50|44|52|36|33|43|131|117|209|180|92|106|115|242|87|90|44|38|91|1	0
TPCN2_734G	P42285	SKIV2L2	4|0|0	0|0|0|0|0	1|1|30|35|43|2|2|0|0|0|0|0|0|0|0|12|3|1|2|0|0|12|38|21|27|39|0|0|8|1	0
TPCN2_734G	P32969	RPL9	3|0|0	3|4|4|4|5	8|6|13|9|6|7|5|6|5|5|5|4|8|3|2|9|4|3|2|2|1|4|8|5|6|5|4|3|8|1	0
TPCN2_734G	P31930	UQCRC1	5|0|0	6|0|0|0|7	0|0|0|0|0|0|1|3|3|3|5|3|2|0|0|3|0|1|2|0|0|0|1|0|0|0|0|1|0|0	0
TPCN2_734G	P04844	RPN2	2|0|0	4|0|0|0|3	2|1|3|0|1|4|9|6|6|8|3|2|3|0|0|4|2|1|2|0|1|0|6|0|1|3|0|1|5|0	0
TPCN2_734G	P04843	RPN1	12|0|0	12|0|3|0|11	3|0|2|0|3|3|4|2|3|2|2|1|2|0|0|1|1|1|0|1|0|0|2|0|0|0|0|0|7|8	0

TPCN2_734G	P49321	NASP	6|0|0	7|0|0|0|4	33|35|45|51|39|40|57|0|0|0|0|0|0|26|34|8|9|9|9|6|16|36|40|31|32|36|11|17|8|23	0
TPCN2_734G	Q99623	PHB2	13|2|3	13|5|7|2|15	0|0|14|23|15|13|21|1|0|0|1|0|0|0|0|18|19|0|0|0|0|11|18|7|9|13|0|0|15|1	0
TPCN2_734G	A6NHR9	SMCHD1	0|0|0	0|0|0|0|0	3|3|7|4|7|0|1|0|0|0|0|0|0|0|0|1|1|3|1|2|2|4|9|1|0|3|0|1|6|0	0
TPCN2_734G	P42224	STAT1	2|0|0	0|0|0|0|0	8|5|7|1|0|7|10|0|0|0|0|0|0|3|4|0|0|1|3|6|11|6|0|5|3|0|0|0|3|0	0
TPCN2_734G	P18085	ARF4	0|3|0	0|0|0|2|0	5|3|5|6|1|4|1|2|4|4|4|3|2|3|1|2|0|2|1|2|1|0|2|1|0|0|1|0|5|1	0
TPCN2_734G	Q9P2E9	RRBP1	28|0|0	5|0|0|5|4	1|1|0|1|1|0|0|1|1|0|1|1|1|2|3|2|4|22|26|13|12|0|1|0|0|0|14|10|0|0	0
TPCN2_734G	Q9UBT2	UBA2	0|0|0	0|0|0|0|0	0|0|2|0|0|2|0|0|0|0|0|0|0|0|0|0|0|0|0|0|0|2|1|2|2|0|0|0|0|8	0
TPCN2_734G	Q9NWT1	PAK1IP1	0|0|0	0|0|2|0|0	0|0|0|0|0|0|0|0|0|0|0|1|1|0|0|0|0|0|0|0|0|0|0|0|0|0|0|0|0|0|0	0
TPCN2_734G	Q8WTT2	NOC3L	9|24|5	10|4|8|26|14	0|1|6|3|3|0|1|0|0|0|0|0|0|0|0|1|0|2|2|2|1|4|5|2|1|4|0|1|3|0	0
TPCN2_734G	P08559	PDHA1	0|0|0	0|0|0|0|2	0|0|0|0|0|0|0|13|14|16|17|17|17|0|0|0|0|0|0|0|0|0|0|0|0|0|0|1|0|1	0
TPCN2_734G	Q9UHN6	TMEM2	0|0|0	0|0|0|0|0	0|0|0|0|0|0|0|0|0|0|0|0|0|0|0|0|0|0|0|0|0|0|0|0|0|0|0|0|0|0	0

TPCN2_734G	P04792	HSPB1	0|0|2	3|0|0|0|0	1|1|0|0|0|0|0|0|0|0|0|0|0|0|0|9|21|0|1|0|0|0|0|0|0|0|0|1|0|0	0
TPCN2_734G	P30050	RPL12	4|0|0	4|2|2|0|6	4|3|5|6|7|2|1|4|4|4|5|5|5|4|1|1|3|2|2|1|2|4|6|2|5|5|5|3|4|0	0
TPCN2_734G	P61254	RPL26	0|0|0	0|5|4|0|0	0|0|10|4|6|7|5|0|0|0|0|0|0|0|0|0|2|0|0|0|0|2|4|1|2|2|0|0|1|2	0
TPCN2_734G	P21333	FLNA	32|0|13	0|31|37|0|10	1875|1821|839|866|394|425|442|22|18|18|15|15|16|914|1136|564|459|490|984|625|1175|445|57	0
TPCN2_734G	Q15459	SF3A1	7|0|0	10|0|0|0|3	23|20|15|12|4|6|13|3|1|1|1|1|2|17|17|9|13|11|15|14|22|7|15|7|2|9|15|12|7|15	0
TPCN2_734G	P49711	CTCF	2|0|0	0|0|0|0|0	4|1|2|0|1|0|2|0|0|0|0|0|0|1|1|2|1|1|5|2|5|1|3|0|0|2|3|1|1|0	0
TPCN2_734G	Q9UJV9	DDX41	0|0|0	0|0|2|0|0	0|0|1|1|1|2|0|0|0|0|0|0|0|0|0|0|0|0|1|0|0|2|1|0|0|2|0|0|0|0	0
TPCN2_734G	P30837	ALDH1B1	0|0|0	3|0|0|0|2	0|0|0|0|0|0|0|4|3|3|4|5|3|0|0|0|0|0|0|0|0|0|1|0|0|0|0|0|0|0	0
TPCN2_734G	O75683	SURF6	9|19|21	13|14|28|24|10	6|5|2|4|3|0|1|0|0|0|0|0|0|2|3|0|0|5|7|5|4|2|4|0|1|2|5|7|1|0	0
TPCN2_734G	Q7KZF4	SND1	40|0|2	38|19|17|0|33	5|4|4|4|2|9|10|5|10|10|5|7|4|5|7|0|0|5|8|5|8|3|11|6|8|2|5|6|1|13	0
TPCN2_734G	Q14444	CAPRIN1	3|0|0	4|0|0|0|0	6|7|6|2|0|1|0|2|1|1|1|1|1|4|4|6|1|4|3|3|3|2|2|0|0|4|3|5|0|4	0

TPCN2_734G	P42566	EPS15	0|0|0	0|0|0|0|0	1|2|6|3|2|2|9|0|0|0|0|0|0|0|1|1|1|4|1|7|8|6|10|3|0|7|3|2|0|0	0
TPCN2_734G	P51610	HCFC1	10|0|0	5|0|0|0|0	48|40|43|43|40|36|46|2|0|0|0|0|0|53|51|36|16|45|64|58|84|28|59|17|15|39|52|50|17|1	0
TPCN2_734G	Q92688	ANP32B	0|0|0	0|0|0|0|0	0|0|0|0|0|0|0|0|0|0|0|0|0|0|0|0|0|0|0|0|0|0|0|0|0|0|0|0|0|0|16	0
TPCN2_734G	P14625	HSP90B1	67|0|6	59|17|18|0|50	2|2|3|1|2|1|3|12|13|12|10|10|10|2|2|1|0|4|4|1|1|1|9|1|2|2|2|2|0|58	0
TPCN2_734G	Q9Y285	FARSA	4|0|0	4|0|0|0|4	0|0|4|0|4|4|12|0|0|0|0|0|0|0|0|2|0|0|0|0|0|2|5|0|2|2|0|0|0|2	0
TPCN2_734G	O00267	SUPT5H	4|0|0	0|0|0|0|0	1|0|0|1|0|1|0|1|0|0|0|0|0|2|1|1|0|0|0|0|0|0|0|0|0|1|1|0|0|12	0
TPCN2_734G	Q96AY3	FKBP10	0|0|0	0|0|0|0|0	0|0|0|0|0|0|0|0|0|0|0|0|0|0|0|0|0|0|0|0|0|0|0|0|0|0|0|0|0|0|0	0
TPCN2_734G	P08865	RPSA	7|0|2	8|4|3|0|7	1|0|2|1|3|2|1|2|1|1|1|1|2|0|0|7|0|0|1|0|0|2|6|2|2|1|0|0|0|11	0
TPCN2_734G	P52701	MSH6	0|0|0	0|0|0|0|0	3|2|4|7|1|6|1|0|0|0|0|0|0|3|7|1|2|1|3|0|4|4|5|1|3|6|0|1|2|4	0
TPCN2_734G	P11310	ACADM	5|0|0	3|0|0|0|3	0|0|0|0|0|0|0|5|2|2|7|5|9|0|0|0|0|0|0|0|0|0|0|0|0|0|0|0|0|0|0|0|0	0
TPCN2_734G	Q07020	RPL18	17|17|10	21|11|15|20|18	1|1|10|4|8|5|6|0|2|1|1|2|1|2|1|3|3|0|1|1|0|2|6|4|3|5|1|0|11|0	0

TPCN2_734G	P46019	PHKA2	0|0|0	0|0|0|0|2	0|0|0|0|0|0|0|0|0|0|0|0|0|0|0|0|0|0|0|0|0|0|0|0|0|0|0|0|0|0|0	0
TPCN2_734G	Q9NSE4	IARS2	8|0|0	8|0|0|0|6	0|0|0|0|0|0|0|2|4|1|4|4|3|0|0|0|0|0|0|0|0|0|0|0|0|0|0|0|0|0|1	0
TPCN2_734G	P22492	HIST1H1T	0|2|0	0|0|0|0|0	4|2|8|16|11|6|6|1|2|1|1|2|1|4|2|6|5|9|4|3|2|3|8|5|6|11|5|1|7|1	0
TPCN2_734G	O95573	ACSL3	20|3|2	22|8|8|4|19	1|1|1|0|0|5|3|1|2|2|2|1|1|0|0|0|1|1|2|1|1|2|1|1|0|1|1|1|1|0	0
TPCN2_734G	P13010	XRCC5	25|0|0	22|7|0|0|20	9|7|4|0|1|1|2|16|7|4|3|10|5|2|4|2|0|2|5|5|3|9|11|2|4|6|4|3|5|54	0
TPCN2_734G	P10809	HSPD1	65|3|9	63|14|18|3|65	9|5|3|2|5|2|2|67|53|64|71|66|82|5|4|32|16|14|27|11|19|2|32|2|9|9|22|15|5|40	0
TPCN2_734G	Q8WUM4	PDCD6IP	4|0|0	6|0|7|0|0	0|0|1|1|1|3|5|1|0|1|0|0|0|0|0|0|0|0|0|0|0|2|3|2|2|2|0|1|4|0	0
TPCN2_734G	Q9Y2W1	THRAP3	6|0|0	0|0|0|0|0	35|37|44|41|23|25|45|0|0|0|0|0|0|43|37|40|21|27|38|35|61|6|41|13|16|31|38|40|11|7	0
TPCN2_734G	Q09028	RBBP4	3|0|2	4|5|0|0|2	0|1|21|17|22|10|6|2|0|1|1|1|1|1|0|3|5|0|0|1|0|5|13|6|7|8|0|0|6|13	0
TPCN2_734G	P07237	P4HB	30|0|2	35|17|14|0|30	0|0|0|0|0|0|0|5|1|3|0|1|1|0|0|0|0|0|0|0|0|0|2|0|0|0|0|1|0|13	0
TPCN2_734G	O95347	SMC2	3|0|0	4|0|0|0|0	0|0|2|0|4|1|1|0|0|0|0|0|0|0|0|0|1|0|0|0|0|3|4|2|4|7|0|0|5|12	0

TPCN2_734G	P55854	SUMO3	2|0|0	0|0|0|0|2	1|1|0|1|0|0|1|0|0|0|0|0|0|1|1|0|0|0|1|0|1|0|1|0|0|1|1|1|1|0	0
TPCN2_734G	P54709	ATP1B3	0|0|0	0|0|0|0|0	0|0|1|2|0|0|0|0|0|0|0|0|0|0|0|0|0|0|0|0|0|0|0|0|0|0|0|0|0|0	0
TPCN2_734G	Q13510	ASAH1	0|0|0	0|0|0|0|0	0|0|1|0|2|0|1|0|0|0|0|0|0|0|0|0|0|0|0|0|0|0|0|0|0|0|0|0|0|0	0
TPCN2_734G	Q93050	ATP6V0A1	0|0|0	0|0|0|0|2	0|0|0|0|0|0|0|0|0|0|0|0|0|0|0|0|0|0|0|0|0|0|0|0|0|0|0|0|0	0
TPCN2_734G	P49368	CCT3	18|0|4	20|4|5|0|14	0|0|54|55|64|22|10|1|0|1|0|0|0|0|0|4|23|0|1|0|0|69|43|116|108|72|0|0|21|41	0
TPCN2_734G	Q13310	PABPC4	12|7|0	14|4|0|3|7	3|4|14|10|4|10|6|1|0|1|1|0|1|1|2|3|0|1|2|1|3|7|10|3|7|6|2|2|6|7	0
TPCN2_734G	P05023	ATP1A1	35|0|0	33|6|10|0|32	0|0|2|3|4|1|0|8|8|9|2|3|7|0|0|0|2|0|1|0|0|1|9|2|2|3|1|2|8|6	0
TPCN2_734G	P11387	TOP1	2|0|7	5|11|22|0|0	4|3|1|0|0|4|2|0|0|0|0|0|0|0|1|2|1|2|2|0|1|2|1|0|0|0|0|1|1|16	0
TPCN2_734G	P45880	VDAC2	6|0|0	11|5|2|0|9	10|9|7|7|10|9|9|17|20|14|10|11|15|11|11|14|6|9|8|8|7|5|8|0|1|6|8|9|2|0	0
TPCN2_734G	Q14152	EIF3A	9|0|0	2|0|2|0|3	2|1|17|16|20|9|5|0|0|0|0|0|0|1|0|5|4|0|2|2|4|9|23|13|6|25|0|1|6|5	0
TPCN2_734G	P11388	TOP2A	7|0|0	0|0|0|0|0	49|39|0|0|0|2|8|12|5|6|4|5|5|42|44|12|13|47|67|32|45|1|2|3|2|0|76|63|4|0	0

TPCN2_734G	Q14683	SMC1A	3|0|0	2|0|0|0|0	0|0|7|14|7|4|3|0|0|0|0|0|0|0|0|9|4|0|0|0|1|6|20|4|8|15|0|0|6|10	0
TPCN2_734G	O95782	AP2A1	0|0|0	0|0|0|0|0	0|0|3|0|0|2|0|0|0|0|0|0|0|0|0|0|0|0|0|0|0|0|1|2|0|1|1|0|1|0|0	0
TPCN2_734G	P08237	PFKM	3|0|0	9|5|3|0|5	0|0|0|0|0|3|1|0|0|0|0|0|0|0|0|0|0|0|2|0|1|1|0|0|0|0|0|0|0|1	0
TPCN2_734G	P15586	GNS	0|0|0	2|0|0|0|3	0|0|0|0|0|0|0|0|0|0|0|0|0|0|0|0|0|0|0|0|0|0|0|0|0|0|0|0|0|0|0	0
TPCN2_734G	P08238	HSP90AB1	76|6|22	80|40|39|2|56	29|26|14|18|11|30|28|25|23|25|23|22|24|28|30|13|8|12|17|12|18|14|24|10|16|16|14|16|16|14	0
TPCN2_734G	P28331	NDUFS1	0|0|0	3|0|0|2|2	0|0|0|0|0|0|0|0|1|2|2|2|4|0|0|0|0|0|0|0|0|0|0|0|0|0|0|0|0|0|0	0
TPCN2_734G	Q7L014	DDX46	3|0|0	0|0|0|0|0	46|50|68|85|44|31|59|0|0|0|0|0|62|58|37|27|25|42|43|50|36|51|33|40|50|45|39|42|32	0
TPCN2_734G	Q2TB10	ZNF800	0|0|0	0|0|0|0|0	0|0|0|0|0|0|0|0|0|0|0|0|0|0|0|0|0|0|0|0|0|0|0|0|0|0|0|0|0|0|0	0
TPCN2_734G	REV_Q9BX	REV_Q9BX63	0|0|0	0|0|0|0|0	0|0|0|0|0|0|0|0|0|0|0|0|0|0|0|0|0|0|0|0|0|0|0|0|0|0|0|0|0|0|0	0
TPCN2_734G	P62820	RAB1A	2|0|0	5|2|0|0|6	6|2|0|0|0|3|6|6|6|5|5|6|6|15|12|9|2|8|6|11|4|0|2|0|0|0|5|4|1|3	0
TPCN2_734G	Q1KMD3	HNRNPUL2	2|0|0	7|0|0|0|0	1|1|0|0|0|0|1|1|2|0|1|1|1|2|2|0|0|0|0|0|1|0|0|0|0|0|2|1|0|4	0

TPCN2_734G	P62826	RAN	4|0|5	3|4|4|0|0	9|12|41|37|30|27|29|10|11|11|8|8|8|8|9|12|17|4|6|2|9|15|23|14|15|25|11|9|13|11	0
TPCN2_734G	P50213	IDH3A	7|0|0	7|0|0|0|9	0|0|0|0|0|0|0|0|4|3|4|6|4|4|0|0|0|0|0|0|0|0|0|0|0|0|0|0|1|0|0|1	0
TPCN2_734G	Q9Y4W6	AFG3L2	10|0|0	6|0|0|0|6	0|0|0|0|0|0|0|0|4|3|7|10|6|7|0|0|0|0|0|0|0|0|0|0|0|0|0|0|0|0	0
TPCN2_734G	P63167	DYNLL1	0|0|2	0|0|4|0|2	2|2|6|4|5|5|0|1|1|0|1|1|1|1|2|1|1|0|1|3|1|6|3|4|4|4|0|1|0|0	0
TPCN2_734G	O15226	NKRF	0|0|0	0|0|0|0|0	1|1|1|3|0|0|0|0|0|0|0|0|0|1|1|0|1|1|1|0|2|0|4|0|0|3|1|1|0|0	0
TPCN2_734G	Q9P2J5	LARS	4|0|0	3|0|0|0|0	4|2|5|7|9|3|3|2|3|1|1|1|1|0|0|1|1|2|3|2|4|9|11|12|14|9|1|2|7|7	0
TPCN2_734G	O43852	CALU	11|0|0	9|4|2|0|11	0|0|0|0|0|0|0|0|0|0|0|0|0|0|0|0|0|0|0|0|0|0|0|0|0|0|0|18	0
TPCN2_734G	Q9BZE4	GTPBP4	4|6|0	9|0|0|7|6	3|1|2|3|2|0|0|0|0|0|0|0|0|1|1|1|1|1|2|2|1|0|3|1|0|1|0|1|1|0	0
TPCN2_734G	Q92598	HSPH1	21|0|0	11|8|6|0|5	4|3|9|6|3|7|8|0|0|1|2|0|1|5|3|4|3|2|2|5|3|13|4|7|6|7|1|2|0|26	0
TPCN2_734G	P33993	MCM7	5|0|2	6|0|2|0|3	0|0|12|15|8|9|12|1|1|0|1|1|1|0|0|2|3|0|0|0|0|7|10|6|9|7|0|0|11|27	0
TPCN2_734G	P33991	MCM4	5|0|0	8|0|3|0|2	4|2|6|5|2|9|7|0|0|0|0|0|0|0|1|2|3|0|1|3|4|9|4|5|3|6|4|3|8|19	0

TPCN2_734G	P12081	HARS	0|0|0	0|0|0|0|0	0|0|0|0|0|0|0|0|0|0|0|0|0|0|0|0|0|0|0|0|0|0|0|0|0|0|0|0|4	0
TPCN2_734G	P50914	RPL14	6|3|3	6|7|6|6|9	1|3|3|3|6|8|2|0|0|0|0|0|0|0|4|4|1|2|1|1|1|5|5|1|6|1|1|3|1	0
TPCN2_734G	P62906	RPL10A	3|0|0	5|2|0|4|5	0|0|7|6|9|1|1|0|0|0|0|0|0|0|0|5|5|0|0|0|0|2|10|4|2|8|0|0|1|0	0
TPCN2_734G	P47914	RPL29	3|0|3	2|2|4|0|2	2|3|3|4|3|4|3|1|0|1|0|0|1|0|2|1|2|0|1|0|2|1|2|1|1|3|1|1|2|1	0
TPCN2_734G	Q86VP6	CAND1	20|0|0	22|3|3|0|9	0|0|9|4|1|10|5|0|0|0|0|0|0|0|0|0|0|0|0|0|0|6|13|5|9|4|0|0|10|10	0
TPCN2_734G	P57721	PCBP3	0|0|0	0|0|0|0|0	2|4|4|4|4|11|3|2|2|2|1|1|2|2|2|2|3|2|3|2|3|6|4|5|4|4|2|2|2|3	0
TPCN2_734G	P43490	NAMPT	3|0|4	3|4|5|0|0	0|0|4|5|4|4|8|0|0|0|0|0|0|0|0|0|2|0|0|0|0|7|5|3|7|3|0|0|1|0	0
TPCN2_734G	P35232	PHB	8|2|0	8|0|4|2|7	0|0|3|0|3|3|5|1|1|2|1|1|0|0|0|2|3|0|0|0|0|5|14|2|5|7|0|0|7|0	0
TPCN2_734G	P83731	RPL24	0|0|0	0|0|0|0|0	5|4|6|7|6|4|6|1|1|1|0|0|0|10|5|6|6|2|3|2|3|5|8|8|13|13|2|2|4|2	0
TPCN2_734G	P61513	RPL37A	0|0|0	0|3|0|0|0	1|0|0|0|0|2|0|1|1|1|1|1|1|1|0|0|0|0|0|0|0|0|0|0|0|0|0|0|0|1|0	0
TPCN2_734G	P15924	DSP	0|26|20	0|2|23|26|0	1|0|5|1|1|2|0|3|4|5|0|0|0|0|3|2|2|4|5|3|13|2|3|3|4|0|3|8|4	0

TPCN2_734G	Q12789	GTF3C1	0|0|0	0|0|0|0|0	1|0|7|4|4|0|0|0|0|0|0|0|0|0|7|3|3|4|2|2|4|9|0|3|5|4|2|1|0	0
TPCN2_734G	P06753	TPM3	0|0|0	0|0|0|0|0	3|2|1|0|0|1|0|3|3|2|4|5|3|2|1|1|0|2|2|2|1|0|4|0|0|0|0|3|5|12	0
TPCN2_734G	P11413	G6PD	0|0|0	0|0|0|0|0	0|2|0|0|0|0|0|0|0|1|0|0|0|0|0|0|0|1|1|1|0|0|0|1|0|0|0|0|0	0
TPCN2_734G	Q9H8Y8	GORASP2	0|0|0	2|0|0|0|2	1|0|0|0|0|2|0|0|0|0|0|0|0|2|0|0|0|0|1|0|1|0|0|0|0|0|0|0|0	0
TPCN2_734G	P51532	SMARCA4	0|0|0	0|0|0|0|0	12|9|7|6|5|0|0|0|0|0|0|0|0|7|5|20|8|16|10|20|14|0|7|0|1|6|20|14|2|0	0
TPCN2_734G	P62081	RPS7	0|0|0	5|0|0|0|0	6|4|19|11|13|11|12|3|2|2|4|0|2|2|3|6|5|1|2|2|2|21|8|17|23|18|1|2|14|7	0
TPCN2_734G	Q9BXJ9	NAA15	0|0|0	2|0|0|0|0	0|0|0|1|0|3|0|0|0|0|0|0|0|0|0|0|0|0|0|0|0|0|0|0|0|0|0|0|0	0
TPCN2_734G	P62249	RPS16	0|0|0	0|2|0|0|0	3|2|6|7|7|8|4|3|3|2|2|2|4|3|1|6|2|1|3|0|0|1|6|2|3|9|0|1|0|7	0
TPCN2_734G	Q96A35	MRPL24	0|0|0	0|0|0|0|0	0|0|0|0|0|0|0|1|1|0|1|1|1|0|0|0|0|0|0|0|0|0|0|0|0|0|0|0|0	0
TPCN2_734G	Q8N0X7	SPG20	0|0|3	0|0|5|0|0	0|3|7|0|0|4|3|0|0|0|0|0|0|1|1|0|0|1|0|1|1|4|1|3|2|1|0|0|0|0	0
TPCN2_734G	P42765	ACAA2	0|0|0	3|0|0|0|3	0|0|0|0|0|0|0|2|2|3|5|4|7|0|0|0|0|0|0|0|0|0|0|0|0|0|0|0|0|1	0

TPCN2_734G	O75746	SLC25A12	0|0|0	0|0|0|0|0	0|0|0|0|0|0|0|0|0|0|0|0|0|0|0|0|0|0|0|0|0|0|0|0|0|0|0|0|1|0	0
TPCN2_734G	P42766	RPL35	2|0|6	7|6|7|0|0	0|0|1|0|0|0|0|0|0|0|0|0|0|0|0|0|0|0|0|0|0|0|0|1|3|0|1|0|0|0|0	0
TPCN2_734G	Q9H0D6	XRN2	2|0|0	5|0|0|0|2	0|1|7|1|2|1|4|0|0|0|0|0|0|0|0|5|0|3|1|3|3|4|1|2|0|0|1|1|4|2	0
TPCN2_734G	P68371	TUBB4B	19|5|17	33|13|20|5|14	19|22|74|96|78|68|46|23|17|23|20|16|18|14|23|35|45|8|15|7|9|66|66|85|82|81|11|17|92|137	0
TPCN2_734G	O43143	DHX15	5|0|0	6|0|0|0|0	9|8|18|15|11|7|14|9|7|6|5|4|5|7|9|26|16|4|4|6|8|7|16|10|10|13|9|4|5|12	0
TPCN2_734G	Q9NZT1	CALML5	0|0|0	0|0|0|0|0	0|0|0|0|0|0|0|0|0|0|0|0|0|0|0|0|0|0|0|0|0|0|0|0|0|0|0|0|0	0
TPCN2_734G	P61204	ARF3	0|0|0	0|0|0|0|0	7|3|15|7|4|20|6|2|5|5|4|4|1|6|3|8|2|4|0|2|2|6|7|1|1|4|4|3|8|5	0
TPCN2_734G	O15042	U2SURP	0|0|0	0|0|0|0|0	26|29|42|35|27|13|22|0|0|0|0|0|0|15|22|30|14|15|22|26|32|19|39|17|12|32|31|26|16|2	0
TPCN2_734G	P53618	COPB1	7|0|0	8|0|0|0|0	4|3|12|2|3|3|3|1|0|2|1|1|1|2|4|0|0|1|1|4|1|1|6|2|3|4|2|1|1|12	0
TPCN2_734G	Q5T1M5	FKBP15	0|0|0	0|0|0|0|0	1|1|0|1|0|0|0|0|0|0|0|0|0|0|1|0|0|0|0|1|2|0|0|0|0|0|1|0|0	0
TPCN2_734G	P04062	GBA	0|0|0	0|0|0|0|0	0|0|0|0|0|0|0|0|0|0|0|0|0|0|0|0|0|0|0|0|0|0|0|0|0|0|0|0|0	0

TPCN2_734G	P18124	RPL7	23|27|39	24|31|28|37|28	0|1|10|8|6|10|10|1|0|0|1|0|0|0|0|2|3|2|1|0|1|5|13|6|5|6|0|2|8|1	0
TPCN2_734G	P08195	SLC3A2	14|0|0	13|3|5|0|14	21|17|1|1|0|0|0|8|8|8|6|8|7|20|19|3|4|10|18|7|14|0|1|0|1|0|9|13|0|0	0
TPCN2_734G	P16403	HIST1H1C	8|0|11	21|11|13|0|9	10|6|40|51|33|22|25|11|13|9|6|6|5|7|6|21|30|19|16|12|7|10|31|29|22|39|15|7|20|10	0
TPCN2_734G	Q9Y2A7	NCKAP1	0|0|0	3|0|0|0|0	0|0|7|6|1|6|0|0|0|0|0|0|0|0|0|0|0|0|0|0|0|0|1|1|2|1|0|0|0|102	0
TPCN2_734G	Q96P11	NSUN5	0|0|0	0|0|0|0|0	0|0|0|0|0|0|0|0|0|0|0|0|0|0|0|0|0|0|0|0|0|0|0|0|0|0|0|0	0
TPCN2_734G	Q14980	NUMA1	8|6|0	0|0|0|13|0	108|84|31|54|89|3|17|10|6|10|1|1|1|92|103|174|173|176|277|124|150|24|111|27|20|66|250|26	0
TPCN2_734G	O43707	ACTN4	8|0|0	11|2|0|0|4	20|11|5|0|0|3|1|9|9|7|1|2|2|9|8|0|0|8|8|14|16|0|6|0|0|0|6|4|66|21	0
TPCN2_734G	Q5D862	FLG2	0|2|0	0|0|2|3|0	0|0|0|0|0|0|0|3|1|3|0|0|0|0|0|0|0|0|1|0|0|0|0|0|0|0|0|1|0|0	0
TPCN2_734G	P34932	HSPA4	32|0|0	27|11|12|0|12	2|1|18|5|4|2|2|0|2|1|1|3|2|2|1|2|2|2|0|1|0|10|13|8|8|7|0|1|6|37	0
TPCN2_734G	P51149	RAB7A	0|0|0	6|2|0|0|3	4|2|0|0|0|0|2|5|7|5|3|3|2|3|2|7|4|2|2|0|1|0|0|0|0|0|1|3|0|1	0
TPCN2_734G	P51148	RAB5C	2|0|0	2|0|0|0|4	0|0|1|0|1|2|2|2|1|1|1|0|2|0|0|6|1|0|0|0|0|1|0|0|0|0|0|0|2|0	0

TPCN2_734G	P09110	ACAA1	0|0|0	3|0|0|0|3	0|0|0|0|0|0|0|0|0|0|0|0|0|0|0|0|0|0|0|0|0|0|0|0|0|0|0|0	0
TPCN2_734G	P49327	FASN	23|0|11	0|28|37|0|4	63|59|554|261|157|600|327|0|0|0|0|0|0|42|43|135|72|44|57|39|53|497|160|242|234|208|84|69	0
TPCN2_734G	O43684	BUB3	0|0|0	3|0|0|0|0	3|2|8|8|6|6|4|5|4|6|7|3|4|3|2|2|1|1|4|1|3|2|3|2|3|4|2|2|1|6	0
TPCN2_734G	P55265	ADAR	23|0|0	17|0|0|0|11	13|9|18|11|12|12|4|3|4|2|1|1|1|14|11|13|7|7|10|12|10|2|25|5|3|11|7|5|6|0	0
TPCN2_734G	P10412	HIST1H1E	0|0|0	15|0|0|0|0	9|6|31|47|33|21|23|8|10|9|3|4|2|7|7|25|22|14|13|10|10|13|25|25|16|31|10|3|22|10	0
TPCN2_734G	P04920	SLC4A2	0|0|0	0|0|0|0|0	0|0|0|0|0|0|0|0|0|0|0|0|0|0|0|0|0|0|0|0|0|0|0|0|0|0|0|0|0	0
TPCN2_734G	P62424	RPL7A	6|6|4	11|6|8|9|10	1|1|17|15|10|14|10|3|3|1|1|1|1|2|2|6|9|1|2|1|2|7|10|8|10|10|2|1|12|0	0
TPCN2_734G	O95602	POLR1A	0|0|0	0|0|0|0|0	0|0|0|0|0|0|0|0|0|0|0|0|0|0|0|0|0|0|0|0|0|0|0|0|0|0|0|0|0	0
TPCN2_734G	P07900	HSP90AA1	63|0|19	66|44|45|0|46	10|14|11|8|10|12|17|20|17|16|15|17|12|11|14|8|1|5|7|4|7|6|27|4|10|13|6|8|9|166	0
TPCN2_734G	P26373	RPL13	9|7|6	12|7|12|9|10	3|3|7|10|10|7|6|3|3|4|3|2|3|1|3|4|5|2|4|2|3|2|10|3|1|8|3|3|2|1	0
TPCN2_734G	P11940	PABPC1	9|9|0	15|4|0|4|7	6|8|17|14|9|11|7|1|1|1|1|0|1|2|5|6|0|1|3|4|6|11|13|9|9|12|2|3|6|12	0

TPCN2_734G	Q86YZ3	HRNR	0|0|8	3|5|9|2|9	0|0|1|0|0|0|0|11|12|10|1|0|1|0|0|9|1|0|0|0|0|0|0|0|4|3|14|0|0	0
TPCN2_734G	Q99729	HNRNPAB	6|0|0	10|0|0|0|6	2|1|8|8|9|3|2|4|8|5|7|3|3|3|3|3|2|2|3|2|3|0|4|1|2|3|4|3|2|11	0
TPCN2_734G	P55795	HNRNPH2	13|0|0	16|0|0|0|16	2|2|5|4|5|6|3|6|4|6|5|6|6|2|1|4|4|4|3|2|4|3|8|4|4|8|3|2|6|10	0
TPCN2_734G	P14618	PKM	56|12|17	63|27|24|14|31	23|24|18|5|3|29|31|12|11|9|12|8|11|16|19|24|2|7|7|10|7|28|24|12|15|9|8|6|3|48	0
TPCN2_734G	O95140	MFN2	0|0|0	0|0|0|0|0	0|0|0|0|0|0|0|0|0|0|0|0|0|0|0|0|0|0|0|0|0|0|0|0|0|0|0|0|0|0|0	0
TPCN2_734G	P27824	CANX	32|0|4	31|16|10|0|24	1|1|0|0|0|1|2|4|4|4|3|3|3|0|0|0|0|1|1|0|0|0|4|0|0|0|0|0|2|33	0
TPCN2_734G	P25685	DNAJB1	2|0|0	0|0|0|0|0	4|2|2|0|1|5|2|0|0|0|0|0|0|0|2|0|0|3|4|1|5|1|1|0|0|0|3|2|1|0	0
TPCN2_734G	Q14157	UBAP2L	2|0|0	2|0|0|0|0	27|30|43|26|19|43|33|0|0|0|0|0|0|24|27|20|11|19|21|24|29|27|21|26|19|30|14|18|0|1	0
TPCN2_734G	P42167	TMPO	3|0|0	4|0|0|0|0	47|52|54|79|46|49|66|6|3|5|3|5|4|55|61|45|40|32|48|33|48|26|40|25|28|41|46|38|31|8	0
TPCN2_734G	Q6PKG0	LARP1	0|0|0	0|0|0|0|0	49|49|36|33|29|47|52|0|0|0|0|0|0|46|56|26|16|17|26|38|53|40|29|18|23|23|33|29|2|3	0
TPCN2_734G	Q8N3U4	STAG2	0|0|0	0|0|0|0|0	2|2|0|0|1|0|0|0|0|0|0|0|0|1|1|0|0|0|0|0|1|1|2|2|1|1|1|0|2|2	0

TPCN2_734G	P21281	ATP6V1B2	0|0|0	0|0|0|0|3	0|0|2|0|0|4|8|0|0|0|0|0|0|0|0|0|0|0|0|0|0|2|6|1|1|0|0|0|0|1	0
TPCN2_734G	Q15393	SF3B3	18|0|0	17|5|5|0|12	1|1|24|12|15|13|13|2|1|3|2|1|3|0|0|14|10|3|3|4|4|20|25|11|16|14|2|0|13|21	0
TPCN2_734G	Q9UDR5	AASS	2|0|0	3|0|0|0|0	0|0|0|0|0|1|0|0|0|0|0|0|0|0|0|0|0|1|0|1|0|1|0|1|1|0|0|1|0	0
TPCN2_734G	P26038	MSN	16|0|0	22|7|9|0|12	11|6|6|0|0|9|4|6|1|2|3|3|1|4|5|0|0|0|1|2|2|2|0|1|1|0|2|1|0|2	0
TPCN2_734G	P62861	FAU	0|0|0	0|0|2|0|0	0|0|1|0|0|0|0|0|0|0|0|0|0|0|0|0|0|0|0|0|0|1|1|1|0|0|0|0|3	0
TPCN2_734G	P40926	MDH2	14|0|0	18|6|5|0|13	0|0|0|0|0|0|0|0|0|0|0|0|0|0|0|0|0|0|0|0|0|5|0|0|0|0|0|0|5	0
TPCN2_734G	P19338	NCL	52|0|6	48|9|11|0|38	42|43|51|58|69|14|19|3|2|3|2|1|2|34|52|48|29|41|70|30|48|29|58|34|34|66|50|47|34|35	0
TPCN2_734G	P51810	GPR143	0|0|0	0|0|0|0|0	0|0|0|0|0|0|0|0|0|0|0|0|0|0|0|0|0|0|0|0|0|0|0|0|0|0|0|0	0
TPCN2_734G	Q00325	SLC25A3	4|3|4	8|2|5|3|6	2|1|7|6|6|5|4|2|2|2|3|1|3|2|2|5|4|1|2|1|1|1|8|4|2|4|2|1|3|2	0
TPCN2_734G	O00410	IPO5	4|0|0	8|0|0|0|0	0|0|0|0|0|2|0|3|0|3|2|1|1|0|0|0|0|1|4|0|1|2|4|1|1|0|1|2|0|4	0
TPCN2_734G	P02786	TFRC	17|0|0	19|9|11|0|17	2|1|0|0|0|0|0|8|4|4|3|4|3|0|1|3|0|1|2|2|1|0|0|0|0|0|0|0|0	0

TPCN2_734G	P63244	RACK1	4|0|0	8|2|2|0|6	10|10|7|3|5|10|8|16|16|14|12|15|16|13|14|8|3|8|16|8|8|5|6|1|4|2|15|14|2|4	0
TPCN2_734G	Q10567	AP1B1	0|0|0	0|0|0|0|0	0|1|2|0|0|2|0|0|0|0|0|0|0|0|0|0|0|0|0|0|0|1|0|2|2|0|0|0|0|1	0
TPCN2_734G	P02788	LTF	0|3|0	0|22|0|3|0	0|0|0|0|0|0|0|0|0|0|0|0|0|0|0|0|0|0|0|0|0|0|0|0|0|0|0|0|0	0
TPCN2_734G	P41091	EIF2S3	0|0|0	5|0|2|0|0	7|7|3|2|1|4|6|7|6|5|4|4|3|4|6|7|2|1|3|1|7|2|2|0|3|1|3|5|3|7	0
TPCN2_734G	O15260	SURF4	0|0|0	0|0|0|0|2	2|3|3|1|1|2|3|2|2|4|2|2|4|0|0|4|3|0|0|0|2|3|3|4|2|4|2|2|2|0	0
TPCN2_734G	P26639	TARS	4|0|0	4|2|0|0|2	0|0|2|1|0|0|3|0|0|0|0|0|0|0|0|0|0|0|0|1|0|1|5|0|1|0|0|0|0|1	0
TPCN2_734G	P61619	SEC61A1	0|0|0	0|0|0|0|3	0|0|3|3|2|3|1|0|0|0|0|0|0|0|0|0|3|0|0|0|0|1|2|3|2|0|0|0|1|0	0
TPCN2_734G	Q9NZB2	FAM120A	0|0|0	0|0|0|0|0	1|0|1|1|0|0|0|0|0|0|0|1|0|1|2|0|0|1|1|1|1|0|1|0|0|1|1|2|0|0	0
TPCN2_734G	Q08211	DHX9	36|0|5	35|15|12|0|26	36|32|18|26|16|35|37|21|15|17|12|17|12|19|23|31|13|17|21|25|32|18|24|12|22|27|26|20|15|5	0
TPCN2_734G	Q9Y2J2	EPB41L3	0|0|0	0|0|0|0|0	2|0|67|52|36|55|84|0|0|0|0|0|0|3|3|0|0|1|2|2|3|25|54|24|24|44|2|2|1|5	0
TPCN2_734G	Q8TDN6	BRIX1	0|2|0	0|0|0|0|2	2|2|3|5|3|4|2|2|2|3|3|1|4|1|1|9|1|0|2|0|1|1|2|0|2|5|1|1|0|0	0

TPCN2_734G	Q86UP2	KTN1	4|0|0	6|0|0|0|0	15|6|2|0|1|0|0|0|0|0|0|0|0|13|6|6|1|26|22|15|21|0|5|0|0|1|18|26|0|0	0
TPCN2_734G	Q13509	TUBB3	0|0|0	0|0|0|0|0	9|12|39|70|48|47|27|14|13|14|14|13|12|8|12|20|27|6|10|4|5|33|42|47|47|47|7|10|63|109	0
TPCN2_734G	P52569	SLC7A2	0|0|0	0|0|0|0|0	0|0|0|0|0|0|0|0|0|0|0|0|0|0|0|0|0|0|0|0|0|0|0|0|0|0|0|0|0|0|0	0
TPCN2_734G	Q13501	SQSTM1	5|0|0	6|0|0|0|0	15|14|6|2|0|8|7|1|0|2|1|1|1|11|10|27|14|6|11|11|14|8|3|4|2|7|13|9|0|0	0
TPCN2_734G	Q9UHX1	PUF60	0|0|0	2|0|3|0|0	15|17|11|12|10|13|21|0|0|2|0|0|0|16|19|10|3|16|22|20|24|11|17|6|9|8|14|11|14|22	0
TPCN2_734G	Q86XP3	DDX42	3|0|0	0|0|0|0|0	21|19|19|15|10|24|14|0|0|0|0|0|0|12|15|7|7|15|12|14|18|9|12|4|7|10|8|14|8|2	0
TPCN2_734G	P20042	EIF2S2	0|0|0	0|0|0|0|0	3|0|1|0|0|1|1|0|0|0|0|0|0|0|0|0|0|0|0|0|0|0|0|0|0|1|0|0|0|0|4	0
TPCN2_734G	P00558	PGK1	26|0|0	36|11|10|0|20	0|0|0|0|0|0|0|1|0|1|1|0|1|0|0|0|0|0|0|0|0|0|2|0|0|0|0|0|0|8	0
TPCN2_734G	Q9BZF1	OSBPL8	2|0|0	0|0|0|0|0	1|2|5|1|0|5|1|0|0|0|0|0|0|2|0|1|0|2|1|2|2|0|0|1|0|0|0|0|0|0	0
TPCN2_734G	Q96AE4	FUBP1	7|0|0	7|0|0|0|7	3|0|2|1|1|2|1|0|0|0|0|0|0|2|2|0|0|0|0|0|1|0|3|0|0|1|1|2|0|2	0
TPCN2_734G	Q92945	KHSRP	16|0|0	20|3|0|0|11	10|7|19|26|20|13|19|11|9|7|7|8|8|10|9|4|3|9|5|10|8|10|27|10|9|16|6|7|4|15	0

TPCN2_734G	Q15084	PDIA6	11|0|0	12|0|0|0|11	0|0|1|1|3|1|0|2|2|2|0|2|3|0|0|1|0|0|0|0|0|0|10|0|1|1|0|0|0|33	0
TPCN2_734G	Q8NB50	ZFP62	0|0|0	0|0|0|0|0	0|0|0|0|0|0|0|0|0|0|0|0|0|0|0|0|0|0|0|0|0|0|0|0|0|0|0|0	0
TPCN2_734G	Q99798	ACO2	14|0|0	16|0|0|0|11	0|0|0|0|0|0|0|12|8|9|14|11|13|0|0|0|0|1|2|0|0|0|1|0|0|0|0|0|0|0	0
TPCN2_734G	Q14CX7	NAA25	0|0|0	0|0|0|0|0	0|0|0|0|0|0|0|0|0|0|0|0|0|0|0|0|0|0|0|0|0|0|0|0|0|0|0|0	0
TPCN2_734G	Q7L576	CYFIP1	3|0|0	0|0|0|0|0	0|0|7|3|3|5|4|0|0|0|0|0|0|0|0|0|0|0|0|0|0|0|2|4|3|5|7|0|0|1|43	0
TPCN2_734G	P12270	TPR	0|0|0	0|0|0|0|0	72|39|59|94|105|19|42|0|0|0|0|0|0|58|34|148|258|149|250|114|153|46|104|45|38|110|184|140	0
TPCN2_734G	Q9UIQ6	LNPEP	0|0|0	0|0|0|0|0	0|0|0|0|0|0|0|0|0|0|0|0|0|0|0|0|0|0|0|0|0|0|0|0|0|0|0|0	0
TPCN2_734G	Q05682	CALD1	11|0|0	10|0|0|0|2	73|52|29|8|7|20|21|0|0|0|0|0|0|90|97|20|21|26|31|37|57|1|5|1|3|11|43|87|0|0	0
TPCN2_734G	Q14839	CHD4	0|0|0	0|0|0|0|0	106|94|103|101|100|31|41|3|3|3|1|1|3|105|95|121|88|61|79|73|83|69|89|63|53|84|102|101|39	0
TPCN2_734G	Q96KR1	ZFR	3|0|0	0|0|0|0|0	21|23|2|2|3|2|7|1|4|4|3|3|4|14|16|5|2|19|16|21|22|1|11|1|0|1|17|19|7|1	0
TPCN2_734G	P46087	NOP2	6|3|0	6|0|0|9|0	5|4|2|2|2|0|0|3|1|2|1|2|2|6|7|4|3|7|10|7|5|1|10|2|3|5|8|9|6|0	0

TPCN2_734G	Q92621	NUP205	0|0|0	0|0|0|0|0	0|0|8|2|3|1|0|0|1|1|1|1|0|0|0|2|3|1|1|1|1|1|5|3|1|0|1|0|3|0	0
TPCN2_734G	Q9Y265	RUVBL1	2|0|0	0|0|0|0|3	33|34|57|75|50|50|65|2|1|1|1|1|0|33|38|51|45|24|32|29|32|72|61|65|56|56|30|25|9|15	0
TPCN2_734G	P61247	RPS3A	5|0|0	10|3|0|0|8	5|3|14|7|5|12|6|1|2|1|0|0|0|5|5|8|5|3|3|3|2|4|5|6|8|5|3|4|1|2	0
TPCN2_734G	Q13619	CUL4A	0|0|0	0|0|0|0|0	3|3|2|0|1|2|0|0|0|0|0|0|0|5|4|4|3|0|0|1|1|1|0|1|0|0|0|0|1|1	0
TPCN2_734G	P35579	MYH9	29|0|135	0|24|9|0|3	24|15|119|86|124|0|1|9|9|7|5|7|6|12|13|6|45|37|63|22|22|117|85|130|116|143|62|55|137|60	0
TPCN2_734G	Q14204	DYNC1H1	0|0|0	0|2|0|0|0	0|0|4|3|13|2|3|0|0|0|0|0|0|1|0|1|2|0|2|0|0|9|10|12|13|16|0|0|13|22	0
TPCN2_734G	P13804	ETFA	0|0|0	2|0|2|0|3	1|0|0|0|0|1|0|10|12|12|14|14|13|0|0|1|0|2|3|2|2|1|4|0|1|1|1|2|1|2	0
TPCN2_734G	Q6AZW8	ZNF660	0|0|0	0|3|0|0|0	0|0|0|0|0|0|0|0|0|0|0|0|0|0|0|0|0|0|0|0|0|0|0|0|0|0|0|0|1|0|0|0|0|0|0	0
TPCN2_734G	P23786	CPT2	2|0|0	0|0|0|0|4	0|0|0|0|0|0|0|0|1|2|3|3|5|0|0|0|0|0|0|0|0|0|0|0|0|0|0|0|0|0|0	0
TPCN2_734G	P15311	EZR	10|0|0	0|0|5|0|0	13|11|10|1|1|24|14|0|0|0|0|1|0|2|3|1|0|1|2|5|9|9|3|1|1|1|2|2|0|4	0
TPCN2_734G	P53396	ACLY	19|0|0	17|7|5|0|7	0|0|6|2|0|2|3|2|2|3|1|2|1|0|0|0|0|0|0|0|0|3|5|2|3|2|0|1|0|14	0

TPCN2_734G	Q99805	TM9SF2	0|0|0	2|0|0|0|2	0|0|0|0|0|0|0|0|0|0|0|0|0|0|0|0|0|0|0|0|0|0|0|0|0|0|0|0|0|0|0	0
TPCN2_734G	Q14562	DHX8	0|0|0	0|0|0|0|0	2|2|0|0|0|2|0|0|0|0|0|0|0|1|0|1|0|1|6|3|4|0|0|1|0|0|4|3|1|0	0
TPCN2_734G	P43686	PSMC4	4|0|0	4|0|0|0|6	0|0|4|0|1|2|1|0|0|0|0|0|0|0|0|1|1|0|1|0|0|1|2|1|2|2|0|1|0|22	0
TPCN2_734G	A1L0T0	ILVBL	0|0|0	0|0|0|0|0	0|0|2|0|0|1|2|0|0|0|0|0|0|0|0|0|0|0|0|0|0|0|2|0|0|2|0|0|0|0	0
TPCN2_734G	Q16629	SRSF7	3|0|0	2|0|0|0|2	2|2|1|5|4|0|2|1|2|0|1|1|1|2|2|1|3|0|1|0|0|1|6|3|2|3|1|0|3|14	0
TPCN2_734G	Q14590	ZNF235	0|0|0	0|4|0|0|0	0|0|0|0|0|0|0|0|0|0|0|0|0|0|0|0|0|0|0|0|0|0|0|1|0|0|0|0|0|0	0
TPCN2_734G	O43175	PHGDH	4|0|0	6|6|3|0|2	0|0|9|8|7|6|9|1|2|1|1|1|1|0|0|0|0|3|0|0|8|9|4|11|15|0|0|2|7	0
TPCN2_734G	P22059	OSBP	0|0|0	0|0|0|0|0	0|0|0|0|0|0|0|0|0|0|0|0|0|0|0|0|0|0|0|0|0|0|0|0|0|0|0|0|0|0	0
TPCN2_734G	Q96I59	NARS2	4|0|0	6|0|0|0|8	0|0|0|0|0|0|0|1|1|1|4|0|1|0|0|0|0|0|0|0|0|0|0|0|0|0|0|0|0|0	0
TPCN2_734G	Q15437	SEC23B	0|0|0	4|0|0|0|0	0|0|0|0|0|1|2|1|0|0|0|0|0|0|0|0|0|0|0|0|0|0|1|1|0|1|0|0|0|0|1	0
TPCN2_734G	O75306	NDUFS2	2|0|0	0|0|0|0|2	0|0|0|0|0|0|0|0|0|2|2|3|1|0|0|0|0|0|0|0|0|0|0|0|0|0|0|0|0|2	0

TPCN2_734G	P49207	RPL34	0|0|0	0|0|0|2|3	0|1|2|0|1|0|0|0|0|0|0|0|0|1|0|1|1|0|0|0|0|1|1|1|1|1|0|0|0|0	0
TPCN2_734G	P48444	ARCN1	0|0|0	2|0|0|0|0	1|1|6|3|4|7|6|0|0|0|0|0|0|1|4|0|0|2|2|3|2|4|5|2|1|1|1|1|4|10	0
TPCN2_734G	O95104	SCAF4	0|0|0	0|0|0|0|0	0|0|4|6|2|1|2|0|0|0|0|0|0|0|0|0|0|0|0|0|0|4|4|0|0|2|0|0|1|0	0
TPCN2_734G	Q8N983	MRPL43	0|0|0	0|0|0|0|0	0|0|0|0|0|0|0|0|0|0|0|0|0|0|0|0|0|0|0|0|0|0|0|0|0	0
TPCN2_734G	O14974	PPP1R12A	0|0|0	0|0|0|0|0	6|4|9|6|3|8|7|0|0|0|0|0|0|0|1|7|1|2|2|2|2|3|2|4|1|7|1|4|0|0	0
TPCN2_734G	Q15233	NONO	8|0|0	11|0|0|0|4	28|31|45|63|37|64|51|10|5|8|5|5|9|56|45|38|42|26|26|30|38|36|39|33|24|38|26|22|28|16	0
TPCN2_734G	P53621	COPA	9|0|0	9|0|3|4|5	1|0|0|0|0|0|1|0|0|0|0|0|0|0|1|0|0|0|1|1|0|0|1|0|0|0|0|0|0|18	0
TPCN2_734G	Q12906	ILF3	16|0|0	18|2|2|0|8	8|8|6|5|3|3|3|12|8|11|6|6|11|10|7|3|2|8|5|7|8|1|10|3|3|7|3|3|7|28	0
TPCN2_734G	Q12905	ILF2	5|0|0	8|0|0|0|5	0|0|7|2|1|4|3|0|2|0|2|1|1|0|0|2|0|1|1|1|0|2|14|0|1|3|0|0|9|18	0
TPCN2_734G	Q99459	CDC5L	2|0|0	0|0|0|0|0	17|12|6|9|10|4|12|0|0|0|0|0|0|19|14|15|16|17|21|21|22|13|14|8|3|10|19|15|8|0	0
TPCN2_734G	Q9NSD9	FARSB	4|0|0	9|3|2|0|5	0|0|0|1|0|2|1|0|0|0|0|0|0|0|0|0|0|0|0|0|0|0|0|0|0|0|0|0|0|1	0

TPCN2_734G	P26599	PTBP1	14|0|0	11|2|0|0|10	12|9|11|4|2|6|5|12|11|14|10|12|12|4|4|4|1|4|10|5|7|1|26|0|2|3|6|8|6|13	0
TPCN2_734G	Q8IZL8	PELP1	0|0|0	0|0|0|0|0	0|0|0|0|0|0|0|0|0|0|0|0|0|0|0|0|0|0|0|0|0|0|0|0|0|0|0|0|0|0|0	0
TPCN2_734G	P14923	JUP	0|11|11	0|6|13|10|0	4|5|2|1|0|4|3|5|5|4|0|0|0|6|4|6|3|1|6|7|10|0|4|1|0|0|5|6|0|0	0
TPCN2_734G	P36776	LONP1	26|0|0	21|0|2|0|14	0|0|0|2|0|2|5|13|14|12|20|16|17|0|0|0|2|0|0|0|0|2|6|0|2|1|0|0|1|8	0
TPCN2_734G	O43390	HNRNPR	5|0|0	5|0|0|0|6	6|7|5|3|7|1|5|1|3|2|2|3|0|9|10|8|7|8|9|10|12|1|14|5|3|4|6|9|6|31	0
TPCN2_734G	P23526	AHCY	4|0|0	11|6|8|0|4	0|0|0|0|0|0|1|2|0|2|0|0|2|0|0|0|0|0|0|0|0|0|3|0|0|0|0|1|0|7	0
TPCN2_734G	Q99575	POP1	2|0|0	0|0|0|0|0	0|0|3|3|0|1|3|0|0|0|0|0|0|0|0|2|0|0|0|0|0|2|1|0|0|1|0|0|1|0	0
TPCN2_734G	Q9UG63	ABCF2	2|0|0	0|0|0|2|0	7|9|1|0|0|3|0|0|0|0|0|0|0|4|4|1|0|3|2|5|6|0|4|1|0|0|3|3|2|0	0
TPCN2_734G	P09874	PARP1	22|0|0	27|0|0|0|16	8|12|5|8|3|27|31|5|3|4|2|2|5|14|10|2|0|5|4|5|7|10|20|18|25|15|3|9|18|54	0
TPCN2_734G	P23528	CFL1	4|0|0	7|3|2|0|6	4|4|1|2|2|2|5|2|4|4|6|5|5|1|0|5|5|3|2|3|2|6|8|5|6|5|2|5|11|12	0
TPCN2_734G	Q92997	DVL3	0|2|7	0|0|5|0|0	12|16|23|23|12|8|7|0|0|0|0|0|0|54|53|4|2|4|6|3|7|8|20|7|6|17|5|5|0|0	0

TPCN2_734G	Q9NZ01	TECR	2|0|0	2|0|0|0|2	1|4|3|2|2|2|2|2|0|1|0|0|1|4|1|2|1|0|0|0|0|0|4|1|2|1|0|0|1|0	0
TPCN2_734G	P27816	MAP4	2|0|0	0|0|0|0|0	80|86|65|68|36|34|46|1|1|1|1|2|1|67|88|31|21|28|51|46|78|56|39|36|42|57|81|63|0|2	0
TPCN2_734G	Q00839	HNRNPU	38|3|8	39|9|15|3|17	20|20|31|52|46|30|34|10|9|9|9|8|9|19|23|40|29|15|24|14|19|23|29|23|25|37|21|21|21|45	0
TPCN2_734G	Q16531	DDB1	9|0|0	14|3|2|0|5	0|0|1|0|0|0|0|0|0|0|0|0|0|0|0|0|0|0|0|0|0|0|0|0|0|0|0|0|18	0
TPCN2_734G	P06576	ATP5B	26|2|0	33|6|5|2|28	3|1|4|7|3|32|31|11|13|11|19|16|17|2|1|6|2|2|2|3|6|7|24|8|13|7|5|2|13|22	0
TPCN2_734G	Q13247	SRSF6	10|0|0	7|0|0|0|10	4|1|2|1|5|2|0|1|1|0|1|1|1|2|2|2|3|1|1|1|1|0|5|0|0|3|1|1|1|5	0
TPCN2_734G	O75150	RNF40	0|0|0	0|0|0|0|0	0|0|0|1|2|0|0|0|0|0|0|0|0|0|0|0|0|0|0|0|0|0|1|1|0|0|0|0|0|0	0
TPCN2_734G	O75152	ZC3H11A	3|0|0	3|0|0|0|0	15|16|8|18|14|2|5|0|0|0|0|0|21|13|8|4|17|15|18|17|4|15|5|3|8|13|15|5|0	0
TPCN2_734G	P16615	ATP2A2	27|0|0	27|0|0|0|24	2|1|8|3|7|4|3|4|4|5|5|3|4|1|1|0|1|1|1|2|2|2|10|4|6|6|1|0|8|5	0
TPCN2_734G	P57729	RAB38	0|0|0	2|0|0|0|4	0|0|0|0|0|0|0|0|0|0|0|0|0|0|0|0|0|0|0|0|0|0|0|0|0|0|0|0|0	0
TPCN2_734G	Q00688	FKBP3	0|0|0	0|0|2|0|0	0|0|1|0|0|0|0|0|0|0|0|0|0|0|0|0|0|0|0|0|0|0|0|0|0|0|0|0|2|0|0|0|0|0|0|1	0

TPCN2_734G	Q14699	RFTN1	0|0|0	0|0|0|0|0	0|0|0|0|0|0|0|0|0|0|0|0|0|0|0|0|0|0|0|0|0|0|1|0|0|0|0|0|0|0	0
TPCN2_734G	Q14697	GANAB	19|0|0	19|4|2|0|5	0|0|0|0|0|0|0|7|5|5|3|5|1|0|0|0|0|0|0|1|0|0|3|0|0|0|0|0|0|23	0
TPCN2_734G	O60271	SPAG9	4|0|0	0|0|0|0|0	2|2|26|11|12|12|10|0|0|0|0|0|0|1|1|0|0|0|0|0|1|13|11|7|12|16|0|0|0|3	0
TPCN2_734G	Q14690	PDCD11	0|0|0	0|0|0|0|0	0|0|0|0|0|0|0|0|0|0|0|0|0|0|0|0|1|1|0|0|0|2|0|0|0|0|0|1|0	0
TPCN2_734G	P07814	EPRS	3|0|0	0|0|2|0|0	19|12|12|22|21|7|13|3|4|2|0|4|1|18|16|12|9|13|18|22|31|13|22|6|10|20|23|15|2|8	0
TPCN2_734G	O75400	PRPF40A	4|0|0	0|0|0|0|0	1|2|3|5|5|2|3|0|0|0|0|0|0|1|0|1|1|1|3|3|2|2|6|2|3|5|2|2|4|0	0
TPCN2_734G	Q02880	TOP2B	7|0|0	0|0|0|0|0	14|9|0|0|0|0|0|2|1|1|1|1|1|12|7|3|4|21|21|11|14|0|0|0|0|0|18|20|0|0	0
TPCN2_734G	P23284	PPIB	7|10|26	13|22|31|15|15	0|0|0|0|0|0|0|2|4|2|0|1|1|0|0|0|0|2|0|1|1|0|1|0|0|0|0|0|0|26	0
TPCN2_734G	P62937	PPIA	0|0|0	6|4|3|0|3	1|1|1|0|0|3|0|9|6|8|8|4|7|0|0|0|0|0|1|0|2|0|18|0|3|0|4|2|2|19	0
TPCN2_734G	P09622	DLD	12|0|0	13|0|0|0|10	0|0|1|6|0|4|4|1|0|1|1|2|4|0|0|0|0|0|0|0|0|0|4|0|0|2|0|0|1|0	0
TPCN2_734G	Q32P28	P3H1	0|0|0	0|0|0|0|2	0|0|0|0|0|0|0|0|0|0|0|0|0|0|0|0|0|0|0|0|0|0|0|0|0|0|0|0|0	0

TPCN2_734G	O43865	AHCYL1	3|0|0	3|0|0|0|0	0|1|2|0|0|4|5|0|0|0|0|0|0|0|0|0|0|0|0|0|0|1|1|2|1|1|0|0|0|1	0
TPCN2_734G	Q9BZZ5	API5	0|0|0	2|0|0|0|2	0|1|1|0|1|0|1|0|0|0|0|0|0|0|0|0|0|0|0|0|1|1|0|1|0|0|0|3	0
TPCN2_734G	Q13435	SF3B2	2|0|0	3|0|0|0|0	39|31|18|28|19|10|19|0|0|0|0|0|0|50|45|21|26|35|31|40|42|17|23|11|14|18|32|33|14|17	0
TPCN2_734G	Q8IY81	FTSJ3	22|23|2	15|2|0|22|9	25|25|13|11|5|4|3|3|1|0|0|0|0|17|24|14|10|20|23|12|23|5|9|7|5|8|24|23|13|0	0
TPCN2_734G	Q8NC51	SERBP1	0|0|0	2|0|0|0|0	35|41|54|73|30|58|73|1|2|1|1|2|1|33|43|31|19|16|28|15|27|19|40|13|12|44|104|26|5|2	0
TPCN2_734G	P09429	HMGB1	0|0|0	0|0|0|0|0	1|1|1|0|0|0|1|0|0|0|0|0|0|1|0|0|0|1|0|1|0|3|6|0|1|3|0|0|0|4	0
TPCN2_734G	Q02543	RPL18A	3|3|3	4|3|3|4|9	3|3|8|10|11|6|4|13|4|3|2|2|3|4|4|5|8|0|0|0|0|3|7|1|0|8|1|1|0|0	0
TPCN2_734G	P36578	RPL4	54|62|35	55|44|38|81|59	3|3|14|12|16|7|8|1|1|1|2|2|1|3|2|12|8|1|2|0|0|12|6|13|11|14|2|2|6|2	0
TPCN2_734G	P78371	CCT2	9|0|0	19|2|3|0|11	1|1|96|69|87|29|7|6|5|7|6|6|4|0|0|4|32|2|3|3|0|95|52|245|214|87|2|1|19|62	0
TPCN2_734G	O94906	PRPF6	5|0|0	2|0|0|0|0	0|0|6|2|2|2|0|1|0|2|1|1|1|0|2|3|2|0|2|1|5|2|5|0|1|2|1|0|1|3	0
TPCN2_734G	O15355	PPM1G	4|0|0	2|0|0|0|2	1|1|4|0|0|4|2|0|0|0|0|0|0|0|0|0|0|0|0|0|0|1|2|1|0|5|0|0|0|7	0

TPCN2_734G	Q9UJS0	SLC25A13	10|6|0	12|0|0|5|12	0|0|3|0|0|2|3|1|0|0|0|0|1|0|0|4|1|0|1|0|0|1|4|2|0|2|0|0|6|0	0
TPCN2_734G	Q05639	EEF1A2	0|4|0	0|0|0|2|0	28|37|42|27|22|178|56|12|10|13|13|10|10|21|28|19|16|12|18|10|20|79|16|113|144|43|17|11|1	0
TPCN2_734G	P30086	PEBP1	0|0|0	2|0|0|0|0	0|0|0|0|0|0|0|0|0|0|0|0|0|0|0|0|0|0|0|0|0|0|0|0|0|0|0|0|0|0|0	0
TPCN2_734G	P46777	RPL5	6|4|0	11|0|0|6|8	8|4|8|8|13|9|12|2|3|3|2|2|1|6|8|2|6|3|4|2|5|3|4|7|5|10|2|4|5|6	0
TPCN2_734G	Q8IX01	SUGP2	2|0|0	2|0|0|0|0	26|16|19|30|30|9|5|0|0|0|0|0|16|15|36|17|24|21|23|28|10|23|15|7|22|25|31|12|0	0
TPCN2_734G	Q99832	CCT7	8|0|0	18|4|2|0|10	0|2|51|34|50|14|5|3|2|1|1|1|1|0|1|2|14|1|1|0|1|69|32|115|101|51|0|1|7|43	0
TPCN2_734G	P46778	RPL21	0|0|0	2|0|0|0|0	1|1|9|8|7|12|10|1|0|1|0|0|1|0|0|6|8|0|1|0|1|3|4|3|2|7|1|1|1|0	0
TPCN2_734G	P46779	RPL28	7|7|5	7|3|6|10|10	5|5|11|12|6|26|10|3|0|1|0|2|1|1|2|8|4|0|0|0|0|4|6|4|2|12|0|1|8|0	0
TPCN2_734G	Q14978	NOLC1	3|0|0	3|0|0|0|0	15|16|21|11|9|11|5|0|0|0|0|0|0|12|10|22|17|7|8|7|12|6|12|9|6|14|13|11|4|0	0
TPCN2_734G	Q9H3P7	ACBD3	0|0|0	0|0|0|0|0	1|0|1|0|0|2|2|0|0|0|0|0|0|0|0|0|0|0|0|0|0|0|0|0|0|0|0|0|0|0|0|2|0|0|0|0|0|0|0	0
TPCN2_734G	Q8TAQ2	SMARCC2	2|0|0	2|0|0|0|0	2|2|4|4|9|0|1|0|0|0|0|0|0|1|0|7|1|1|2|5|2|0|13|1|2|4|2|2|1|0	0

TPCN2_734G	Q9BZH6	WDR11	2|0|0	0|0|0|0|0	0|0|11|3|1|1|3|0|0|0|0|0|0|0|0|1|1|0|0|0|0|7|1|2|5|6|0|0|0|0	0
TPCN2_734G	O60716	CTNND1	2|0|0	2|0|0|0|0	10|9|0|0|0|3|2|0|0|0|0|0|0|4|6|3|3|3|8|10|14|1|1|0|1|0|3|4|0|0	0
TPCN2_734G	Q01546	KRT76	0|0|0	0|0|0|0|0	1|2|0|1|1|0|0|9|5|5|0|0|0|1|0|2|2|0|1|1|1|0|0|0|0|1|1|2|0|2	0
TPCN2_734G	Q14974	KPNB1	17|0|0	22|8|9|0|14	0|1|40|11|19|16|9|9|7|8|4|2|2|0|0|7|4|1|5|1|1|15|36|8|17|25|2|3|3|31	0
TPCN2_734G	Q07866	KLC1	0|0|0	0|0|0|0|0	4|5|11|9|4|10|10|0|0|0|0|0|0|3|3|0|1|0|0|2|1|11|8|10|10|10|0|0|0|3	0
TPCN2_734G	P22695	UQCRC2	5|0|0	5|0|0|0|5	0|1|1|1|0|8|4|3|2|2|3|2|3|0|0|1|4|1|0|0|0|0|0|0|0|0|0|0|1|0	0
TPCN2_734G	Q6P2Q9	PRPF8	9|0|0	0|0|2|0|0	11|8|34|23|26|15|14|2|5|3|1|1|4|7|6|20|15|21|18|24|21|45|32|16|18|18|20|12|22|29	0
TPCN2_734G	P35637	FUS	0|0|0	0|0|0|0|0	3|2|3|0|0|3|5|0|1|1|0|1|0|3|4|0|0|1|2|3|3|1|6|0|1|2|0|3|0|42	0
TPCN2_734G	P05455	SSB	5|0|0	3|0|0|0|5	0|2|3|2|0|4|0|0|0|0|0|0|0|0|2|0|0|1|0|1|1|0|1|0|0|0|0|0|1|3	0
TPCN2_734G	O75874	IDH1	14|0|6	29|14|9|0|15	0|1|0|0|0|4|0|0|0|0|0|0|0|0|0|0|0|0|0|2|1|0|0|0|0|0|0|0|0	0
TPCN2_734G	P62258	YWHAE	9|0|0	14|4|6|0|11	0|0|12|13|5|7|8|1|1|2|1|1|1|1|1|1|0|0|1|0|0|4|15|4|4|6|0|0|1|49	0

TPCN2_734G	P12004	PCNA	0|0|0	0|0|0|0|0	0|0|2|1|1|1|0|0|0|0|0|0|0|0|0|0|0|0|0|0|0|1|2|1|2|0|0|0|1|15	0
TPCN2_734G	Q7Z739	YTHDF3	0|0|0	0|0|0|0|0	0|1|4|3|1|3|1|0|0|0|0|0|0|1|1|0|0|0|0|0|1|0|0|0|0|0|1|1|0|1	0
TPCN2_DeltaCT	Q6PD62	CTR9	0|0|0	2|0|0|0|0	1|0|2|0|0|0|0|0|0|0|0|0|0|0|1|1|1|0|2|0|1|0|0|0|0|0|1|0	0
TPCN2_DeltaCT	P68363	TUBA1B	30|8|20	30|18|19|7|16	50|62|131|117|90|134|224|24|23|22|21|17|21|43|49|45|51|27|53|35|46|135|116|152|136|132|3	0
TPCN2_DeltaCT	Q96N67	DOCK7	0|0|0	0|0|0|0|0	0|0|7|4|3|0|2|0|0|0|0|0|0|0|0|0|0|0|0|0|0|7|5|1|2|3|0|0|0|1	0
TPCN2_DeltaCT	P40227	CCT6A	18|0|9	21|5|5|2|14	3|3|91|55|52|32|12|2|0|2|1|0|0|2|0|11|29|1|3|3|2|77|42|145|126|78|0|1|12|56	0
TPCN2_DeltaCT	P40222	TXLNA	0|0|0	2|0|0|0|0	0|0|0|1|1|0|0|0|0|0|0|0|0|0|0|0|0|0|0|0|0|0|1|0|0|1|0|0|0|0	0
TPCN2_DeltaCT	P05534	HLA-A	0|0|2	0|0|0|0|0	0|0|0|0|0|0|0|0|4|3|5|2|2|5|0|0|0|0|1|1|0|0|0|1|0|0|0|2|1|0|2	0
TPCN2_DeltaCT	O00148	DDX39A	0|0|3	4|0|0|0|3	11|7|10|17|13|7|9|5|6|5|4|1|3|7|6|14|5|3|4|5|2|6|20|8|13|7|4|5|9|7	0
TPCN2_DeltaCT	Q92572	AP3S1	0|0|0	0|0|0|0|0	0|1|1|1|1|2|3|0|0|0|0|0|0|0|0|1|0|0|0|1|0|1|2|0|0|1|2|0|1|3	0
TPCN2_DeltaCT	P35527	KRT9	19|40|42	37|44|47|57|42	9|11|15|19|4|1|9|109|96|123|40|36|51|6|8|35|10|8|7|18|6|1|11|2|2|18|32|52|1|15	0

TPCN2_DeltaCT	P51798	CLCN7	0|0|0	0|0|0|0|2	0|0|1|0|0|0|0|0|0|0|0|0|0|2|0|0|0|0|0|0|0|0|0|0|0|0|0|0|0|0	0
TPCN2_DeltaCT	P62753	RPS6	5|6|11	10|8|5|14|4	4|4|15|13|14|9|14|5|3|4|3|3|3|4|3|10|9|0|1|1|0|10|10|9|10|9|7|2|7|6	0
TPCN2_DeltaCT	P62750	RPL23A	0|0|6	0|0|0|0|0	0|1|8|4|4|9|9|0|0|0|0|0|0|0|0|3|7|0|0|0|0|3|7|3|1|5|1|0|3|2	0
TPCN2_DeltaCT	P22392	NME2	6|0|5	5|3|3|0|3	0|0|7|0|0|11|3|1|0|0|1|2|1|0|0|0|0|0|0|0|0|0|0|0|0|0|0|0|0|11	0
TPCN2_DeltaCT	P04075	ALDOA	24|2|15	30|13|12|2|20	0|2|0|0|0|0|0|1|1|2|1|1|2|1|2|0|0|1|1|1|1|0|7|0|0|0|1|0|0|16	0
TPCN2_DeltaCT	P61978	HNRNPK	13|0|4	11|3|2|0|10	29|32|22|39|26|34|30|16|13|15|14|12|12|33|32|26|16|19|25|26|30|29|38|25|23|27|25|24|27|8	0
TPCN2_DeltaCT	P28370	SMARCA1	0|0|0	0|0|0|0|0	9|7|10|11|13|4|2|0|0|0|0|0|0|9|7|45|26|3|8|6|9|3|16|6|5|9|8|10|5|0	0
TPCN2_DeltaCT	P46977	STT3A	2|0|0	0|0|0|0|0	2|1|0|0|0|0|2|0|1|1|1|1|1|2|1|0|0|0|0|0|0|0|0|0|0|0|0|0|1|0	0
TPCN2_DeltaCT	Q14247	CTTN	21|10|17	17|0|6|2|3	45|42|44|50|41|81|84|2|1|0|0|0|0|61|67|59|38|31|39|40|60|22|29|21|27|40|47|41|0|7	0
TPCN2_DeltaCT	P49790	NUP153	0|0|0	0|0|0|0|0	39|40|25|37|30|21|28|5|5|3|2|6|3|51|43|53|38|38|56|57|68|18|23|14|8|31|45|46|13|0	0
TPCN2_DeltaCT	O96005	CLPTM1	0|0|0	0|0|0|0|3	0|0|0|0|0|0|0|0|0|0|0|0|0|1|0|0|0|0|0|0|0|0|0|0|0|0|0|0|0|0	0

TPCN2_DeltaCT	Q3YEC7	RABL6	0|0|0	0|0|0|0|0	0|0|1|4|1|2|3|0|0|0|0|0|0|0|0|0|0|0|0|0|0|0|3|1|1|2|5|0|0|0|0	0
TPCN2_DeltaCT	Q04637	EIF4G1	11|0|0	0|0|0|0|0	46|43|78|71|36|47|49|0|0|0|0|0|0|57|52|25|24|26|44|43|52|38|57|27|25|49|31|31|1|13	0
TPCN2_DeltaCT	P30048	PRDX3	3|0|0	2|0|0|0|0	1|2|0|1|0|1|0|3|6|4|2|3|3|1|1|2|0|1|2|1|1|0|9|0|1|1|2|1|0|4	0
TPCN2_DeltaCT	Q13200	PSMD2	12|0|3	11|2|3|0|6	1|0|13|5|3|7|4|1|0|0|0|0|0|0|0|1|2|0|0|0|0|6|9|3|3|0|0|0|3|30	0
TPCN2_DeltaCT	P18077	RPL35A	4|0|4	3|3|3|4|3	1|0|6|3|22|1|3|2|1|1|1|1|1|0|0|6|5|0|0|0|0|0|3|0|1|6|0|0|1|0	0
TPCN2_DeltaCT	P0C0S8	HIST1H2A	3|0|4	4|4|3|0|2	10|7|16|23|16|15|23|2|3|3|2|2|1|9|11|17|28|7|12|9|10|21|33|36|23|24|8|7|14|16	0
TPCN2_DeltaCT	P30041	PRDX6	2|0|3	3|5|3|0|0	5|9|2|3|2|9|7|3|2|2|1|2|1|4|3|2|1|1|0|3|4|4|6|2|5|1|2|1|4|12	0
TPCN2_DeltaCT	P07910	HNRNPC	8|3|0	10|0|0|3|6	6|8|2|11|16|2|4|12|8|10|8|7|8|8|7|3|16|4|7|2|2|3|12|7|4|11|6|5|7|51	0
TPCN2_DeltaCT	P41252	IARS	10|0|0	2|0|0|0|0	2|3|4|1|8|1|1|2|0|2|0|0|1|0|0|2|0|3|5|1|1|3|10|3|4|8|5|5|3|4	0
TPCN2_DeltaCT	Q9UHB6	LIMA1	2|0|0	0|0|0|0|0	53|51|27|15|15|16|22|8|6|6|3|4|2|67|66|38|20|42|67|63|80|8|12|6|10|12|60|88|0|0	0
TPCN2_DeltaCT	P41743	PRKCI	0|0|0	0|0|0|0|0	0|0|0|0|0|0|0|0|0|0|0|0|0|0|0|0|0|0|0|0|0|0|0|0|0|0|0|0|0|0|0	0

TPCN2_DeltaCT	Q12931	TRAP1	7|0|0	6|0|0|0|6	1|1|6|7|7|23|19|8|9|8|9|9|11|1|2|10|5|2|3|1|1|8|13|6|6|5|2|2|11|24	0
TPCN2_DeltaCT	P02545	LMNA	50|2|13	51|6|11|0|45	6|6|0|2|4|0|0|18|16|15|12|15|18|7|3|13|11|4|4|1|3|0|5|0|0|1|10|7|0|1	0
TPCN2_DeltaCT	P40429	RPL13A	15|13|15	11|14|12|25|15	2|2|3|6|4|5|5|0|1|0|0|0|0|1|1|6|3|1|1|0|1|2|5|0|0|5|0|0|2|0	0
TPCN2_DeltaCT	Q9HB71	CACYBP	0|0|3	0|0|0|0|0	1|3|3|0|0|10|8|1|1|1|2|0|1|0|2|0|0|0|0|1|0|1|3|0|0|1|0|0|0|4	0
TPCN2_DeltaCT	Q8N163	CCAR2	4|0|0	4|0|0|0|0	5|8|13|13|11|6|11|1|0|0|0|0|1|1|7|5|2|3|6|6|5|14|2|4|8|5|5|12|14	0
TPCN2_DeltaCT	P13667	PDIA4	17|0|0	19|0|0|0|12	0|0|0|0|0|0|0|1|0|3|2|0|1|0|0|0|0|0|0|0|0|0|2|0|0|0|0|0|0|23	0
TPCN2_DeltaCT	Q93009	USP7	0|0|0	0|0|0|0|0	5|2|16|11|7|7|12|0|0|0|0|0|0|3|2|3|1|5|3|5|5|9|19|5|7|8|3|3|4|8	0
TPCN2_DeltaCT	P62879	GNB2	6|0|0	6|0|0|0|5	1|0|1|0|1|4|1|2|2|2|0|2|2|1|1|1|0|0|3|0|1|0|1|1|1|1|0|0|0|1	0
TPCN2_DeltaCT	P78347	GTF2I	17|0|2	15|2|0|0|7	20|17|15|11|5|5|7|5|5|4|1|2|2|14|5|22|3|22|24|24|27|7|13|3|4|8|23|21|8|43	0
TPCN2_DeltaCT	P05388	RPLP0	7|0|2	7|0|2|2|7	2|1|6|8|10|3|2|9|7|8|8|7|9|2|1|4|1|3|3|4|3|3|4|5|6|7|5|4|7|4	0
TPCN2_DeltaCT	P62979	RPS27A	15|6|18	16|12|18|5|13	0|0|1|0|0|0|1|0|0|0|0|0|1|2|1|0|0|1|3|1|2|0|2|0|0|2|2|2|1|2	0

TPCN2_DeltaCT	Q9C0C4	SEMA4C	0|0|0	0|0|0|0|0	0|0|0|0|0|0|0|0|0|0|0|0|0|0|0|0|0|0|0|0|0|0|0|0|0|0|0|0|0|0|0	0
TPCN2_DeltaCT	P07355	ANXA2	12|4|17	10|5|14|5|13	25|35|4|2|5|7|10|12|11|11|10|11|12|25|35|46|8|15|19|20|22|7|9|1|6|5|19|15|0|0	0
TPCN2_DeltaCT	Q16795	NDUFA9	0|0|0	0|0|0|2|2	0|0|0|0|0|0|0|0|0|0|0|0|0|0|0|0|2|1|0|0|0|0|0|0|0|0|0|0|0|0|0	0
TPCN2_DeltaCT	O76021	RSL1D1	0|13|7	8|0|2|27|6	8|4|6|3|7|0|0|3|5|4|3|5|3|9|12|4|9|4|5|2|4|1|5|0|1|4|6|4|7|0	0
TPCN2_DeltaCT	P52272	HNRNPM	26|0|2	29|2|0|0|18	14|9|21|10|24|31|15|14|13|18|12|13|13|15|7|19|11|17|20|22|18|8|29|4|7|12|13|15|32|17	0
TPCN2_DeltaCT	P29966	MARCKS	4|0|0	4|0|0|0|0	5|3|2|1|0|0|0|3|5|4|3|3|3|5|3|0|0|1|1|2|0|0|5|0|0|0|1|2|0|1	0
TPCN2_DeltaCT	P67809	YBX1	15|28|24	26|13|15|27|18	0|0|14|8|6|7|11|0|0|0|0|0|0|0|0|3|1|0|0|0|0|5|7|1|2|7|0|0|3|15	0
TPCN2_DeltaCT	Q08188	TGM3	0|0|0	0|0|0|3|0	0|0|0|0|0|0|0|0|0|0|0|0|0|0|0|0|0|0|0|0|0|0|0|0|0|0|0|0|0|0|0	0
TPCN2_DeltaCT	P39656	DDOST	3|0|0	6|0|0|0|6	5|6|1|0|0|2|2|9|9|9|8|6|8|0|3|0|1|1|0|1|1|0|2|0|0|0|2|2|2|0	0
TPCN2_DeltaCT	O75127	PTCD1	0|0|0	0|0|0|0|0	0|0|0|0|0|0|0|0|0|0|1|2|2|0|0|0|0|0|0|0|0|0|0|0|0|0|0|0|0|0|0	0
TPCN2_DeltaCT	Q15366	PCBP2	6|0|0	9|0|0|0|0	10|12|17|16|13|30|27|4|4|4|2|2|5|6|8|8|9|4|5|8|10|19|14|13|15|16|4|5|7|8	0

TPCN2_DeltaCT	Q15365	PCBP1	4|0|0	7|0|0|0|6	8|13|10|8|15|18|15|3|4|4|3|2|7|6|7|7|7|5|6|7|10|11|16|9|10|10|7|6|3|9	0
TPCN2_DeltaCT	Q8IXT5	RBM12B	0|0|0	0|0|0|0|0	0|0|0|0|0|0|0|0|0|0|0|0|0|0|0|0|0|0|0|0|0|0|0|0|0|0|0|0|0|0|1|0	0
TPCN2_DeltaCT	B5ME19	EIF3CL	10|0|0	7|0|0|0|0	4|4|9|6|13|8|6|0|0|0|0|0|0|1|1|2|1|0|0|3|1|8|6|6|4|9|0|0|0|4	0
TPCN2_DeltaCT	Q96RP9	GFM1	3|0|0	2|0|0|0|0	0|0|0|0|0|0|0|7|11|8|10|11|14|0|0|0|0|0|0|0|0|0|0|0|0|0|0|0|0|0	0
TPCN2_DeltaCT	Q9UMS4	PRPF19	0|0|0	3|0|0|0|2	0|0|21|13|19|7|10|1|1|3|3|1|2|0|0|25|9|1|2|2|0|9|20|5|4|5|0|2|5|4	0
TPCN2_DeltaCT	Q92575	UBXN4	0|0|0	2|0|0|0|2	0|0|1|1|0|3|1|0|0|0|0|0|0|0|0|0|0|0|0|1|0|0|1|0|1|1|0|0|0|0	0
TPCN2_DeltaCT	Q14669	TRIP12	0|0|0	0|0|0|0|0	2|0|1|0|0|0|0|1|0|0|0|0|0|1|2|4|2|9|9|5|6|0|0|0|0|6|5|0|0	0
TPCN2_DeltaCT	P39023	RPL3	27|20|31	23|22|23|41|38	4|3|20|20|18|17|18|3|2|3|3|3|4|8|5|8|6|3|5|3|3|9|5|6|7|16|3|3|12|1	0
TPCN2_DeltaCT	O75533	SF3B1	12|0|0	15|0|0|0|7	63|52|42|44|40|29|38|2|2|3|1|2|1|55|60|34|35|38|54|46|68|28|39|17|25|27|49|47|20|18	0
TPCN2_DeltaCT	O75439	PMPCB	3|0|0	2|0|0|0|3	0|0|0|0|0|0|0|9|4|8|9|10|8|0|0|1|0|2|3|0|0|0|1|0|0|0|2|1|0|1	0
TPCN2_DeltaCT	Q9HAU0	PLEKHA5	2|0|0	0|0|0|0|0	4|4|1|0|0|1|2|0|0|0|0|0|0|0|2|0|0|0|0|2|1|0|1|0|0|0|0|0|0|0	0

TPCN2_DeltaCT	P43034	PAFAH1B1	0|0|0	0|0|0|0|0	0|0|0|0|0|0|0|0|0|0|0|0|0|0|0|0|0|0|0|0|0|0|0|0|0|0|0|0	0
TPCN2_DeltaCT	P08621	SNRNP70	4|0|0	2|0|0|0|0	0|0|5|7|7|6|8|0|0|0|0|0|0|0|0|5|2|0|0|0|1|2|6|2|0|3|2|1|4|11	0
TPCN2_DeltaCT	P09651	HNRNPA1	7|0|3	11|2|0|0|8	10|15|18|22|7|21|14|11|11|15|12|9|12|13|16|8|5|10|21|13|16|1|16|3|4|8|13|14|6|47	0
TPCN2_DeltaCT	Q9UQE7	SMC3	3|0|0	3|0|0|0|0	0|0|9|14|12|1|2|0|1|0|0|0|0|0|0|10|6|0|0|0|0|4|21|5|7|15|0|0|10|11	0
TPCN2_DeltaCT	Q5JRX3	PITRM1	0|0|0	0|0|0|0|0	0|0|0|0|0|0|0|2|1|1|0|2|3|0|0|0|0|0|0|0|0|0|1|0|0|0|0|0|0|0	0
TPCN2_DeltaCT	P62805	HIST1H4	7|5|10	6|11|8|6|6	10|8|6|19|13|14|13|10|7|9|4|7|7|13|14|16|8|9|12|7|7|12|18|7|7|12|10|9|8|29	0
TPCN2_DeltaCT	Q14103	HNRNPD	3|0|2	3|0|0|0|3	7|5|10|5|5|4|5|10|10|8|10|9|11|6|5|3|0|4|4|4|8|2|8|2|1|5|7|5|3|13	0
TPCN2_DeltaCT	O94776	MTA2	4|14|2	2|0|0|8|3	4|5|10|11|12|0|4|1|0|3|1|0|0|2|1|18|15|3|4|3|4|8|16|8|9|13|2|0|18|7	0
TPCN2_DeltaCT	Q641Q2	WASHC2A	0|0|0	0|0|0|0|0	7|11|7|6|1|2|4|0|0|0|0|0|0|0|7|2|0|5|4|9|8|10|4|3|3|1|2|2|0|0	0
TPCN2_DeltaCT	P68104	EEF1A1	21|0|16	14|14|11|0|17	50|62|75|71|54|239|109|24|21|25|21|20|15|31|48|40|40|21|32|30|41|128|48|158|189|79|37|38	0
TPCN2_DeltaCT	P27635	RPL10	0|0|0	3|0|0|4|2	2|2|7|9|8|7|6|1|2|2|2|1|2|1|1|3|6|0|1|0|0|9|7|13|9|5|0|0|4|1	0

TPCN2_DeltaCT	P62191	PSMC1	3|0|0	5|0|0|0|3	0|0|3|0|2|0|0|0|1|0|0|0|0|0|0|2|1|0|0|0|0|2|6|2|2|1|0|0|1|11	0
TPCN2_DeltaCT	P36542	ATP5C1	2|0|2	2|0|0|0|0	0|0|9|2|5|4|3|4|3|3|3|4|3|0|1|10|8|0|0|0|0|0|5|0|1|6|0|0|6|1	0
TPCN2_DeltaCT	Q5BKZ1	ZNF326	3|0|0	4|0|0|0|0	0|1|1|5|5|0|1|2|1|3|1|2|0|0|0|3|6|0|1|0|0|2|13|2|1|9|1|2|3|0	0
TPCN2_DeltaCT	P11142	HSPA8	54|9|41	52|39|41|15|47	56|57|96|123|78|73|95|40|40|45|36|39|42|56|64|81|74|58|86|61|83|64|76|62|58|83|69|68|50|	0
TPCN2_DeltaCT	O43837	IDH3B	2|0|0	4|0|0|0|0	0|0|0|0|0|1|1|4|2|2|5|5|5|0|0|0|0|0|0|0|0|0|0|0|0|0|0|0|2|0	0
TPCN2_DeltaCT	P33992	MCM5	7|0|0	12|0|0|0|6	0|0|1|1|0|0|1|0|0|0|0|0|0|0|0|0|0|0|0|0|1|3|0|0|1|0|0|5|23	0
TPCN2_DeltaCT	P48643	CCT5	16|0|7	13|3|0|0|10	2|1|67|53|57|26|12|5|4|5|4|3|6|0|0|8|18|2|3|0|5|58|38|120|97|64|3|2|18|95	0
TPCN2_DeltaCT	Q92614	MYO18A	0|0|0	0|0|0|0|0	0|0|0|0|0|0|0|0|0|0|0|0|0|0|0|0|0|0|0|0|0|0|0|0|0|0|0|0|0|0|0	0
TPCN2_DeltaCT	Q9NR30	DDX21	0|0|0	9|0|0|0|2	20|18|21|28|22|36|35|18|14|11|9|13|9|24|20|35|26|15|16|11|13|18|34|11|18|23|21|19|17|0	0
TPCN2_DeltaCT	P50502	ST13	2|0|0	3|0|0|0|0	0|0|0|0|0|0|0|0|1|0|0|0|0|0|0|0|0|0|0|0|0|0|0|0|0|0|0|0|0|16	0
TPCN2_DeltaCT	P34897	SHMT2	19|0|2	17|3|0|0|16	0|0|0|0|0|0|0|3|1|4|6|4|7|0|0|0|0|0|0|0|0|0|7|0|2|0|0|1|0|27	0

TPCN2_DeltaCT	Q9UHD8	SEPT9	4|0|0	4|0|0|0|0	7|8|12|19|13|10|26|0|0|0|0|0|9|8|7|1|4|5|6|8|11|12|7|5|16|5|7|0|1	0
TPCN2_DeltaCT	Q9Y2L1	DIS3	0|0|0	0|0|0|0|0	0|0|0|1|0|2|1|0|0|0|0|0|0|0|0|0|0|0|0|0|0|0|0|0|1|0|0|1|0	0
TPCN2_DeltaCT	Q92616	GCN1	2|0|0	0|0|0|0|0	4|2|70|38|49|25|28|0|0|0|0|0|0|0|13|5|6|13|2|2|57|65|42|46|52|5|4|6|12	0
TPCN2_DeltaCT	Q14203	DCTN1	4|0|0	2|0|0|0|0	4|1|18|10|10|4|9|0|0|0|0|0|5|2|1|0|3|3|5|7|10|16|4|6|14|2|3|2|4	0
TPCN2_DeltaCT	O14776	TCERG1	0|0|0	0|0|0|0|0	16|17|5|8|3|4|3|0|0|1|0|0|0|9|10|0|0|3|4|5|9|1|6|2|3|3|7|5|4|0	0
TPCN2_DeltaCT	A0FGR8	ESYT2	3|0|0	3|0|0|0|0	4|2|5|1|1|1|0|0|0|0|0|0|0|0|0|0|0|2|1|3|2|0|5|0|0|0|2|0|0|0	0
TPCN2_DeltaCT	O60763	USO1	0|0|0	2|0|0|0|0	2|0|3|1|1|1|1|0|0|0|0|0|0|1|1|1|2|0|0|1|2|0|2|0|1|3|1|1|0|4	0
TPCN2_DeltaCT	Q14566	MCM6	9|0|0	11|2|0|0|4	3|1|4|2|3|4|5|0|1|1|1|1|0|0|0|0|4|0|0|0|0|0|7|1|2|3|0|0|7|26	0
TPCN2_DeltaCT	P00338	LDHA	9|2|9	11|6|6|0|9	4|6|0|0|0|0|0|4|6|4|5|3|5|3|5|0|0|3|3|2|1|0|1|0|0|0|2|2|0|2	0
TPCN2_DeltaCT	P62263	RPS14	0|0|2	0|2|2|0|0	3|2|9|11|12|8|6|5|4|4|4|4|4|2|1|4|6|1|1|0|0|5|7|5|2|10|0|0|7|5	0
TPCN2_DeltaCT	P17844	DDX5	14|0|9	13|5|2|0|12	13|12|13|7|7|10|11|11|8|7|6|5|6|14|13|12|7|9|16|13|13|5|11|5|5|7|13|10|11|18	0

TPCN2_DeltaCT	P68032	ACTC1	28|0|0	0|0|0|0|0	18|16|25|35|38|33|26|32|28|26|27|35|29|19|22|41|52|17|35|18|24|16|30|14|11|30|24|22|93|3	0
TPCN2_DeltaCT	Q9NVI7	ATAD3A	8|0|0	10|0|0|0|6	0|0|2|1|6|1|0|11|8|10|10|9|10|0|0|0|4|0|0|0|0|0|1|0|1|2|0|0|2|1	0
TPCN2_DeltaCT	O60488	ACSL4	0|0|0	4|0|0|0|0	1|1|0|0|0|1|2|1|1|2|1|0|0|0|0|0|1|1|2|1|1|1|1|0|0|1|1|1|1|0	0
TPCN2_DeltaCT	O75643	SNRNP200	7|0|0	0|0|0|0|0	15|16|29|13|27|14|18|8|4|10|2|2|4|4|6|40|26|10|12|20|19|23|27|14|14|24|17|19|17|23	0
TPCN2_DeltaCT	Q92522	H1FX	0|0|3	0|0|0|0|0	0|0|2|2|6|2|0|0|0|0|0|0|0|0|1|0|0|0|0|1|0|4|0|1|3|0|0|4|0	0
TPCN2_DeltaCT	O43242	PSMD3	6|3|0	6|0|0|3|0	0|0|7|5|5|11|5|0|0|0|0|0|0|0|1|0|0|0|0|0|0|3|7|1|6|5|0|0|9|18	0
TPCN2_DeltaCT	P06748	NPM1	24|0|7	21|7|8|0|13	146|149|101|112|50|46|123|8|6|6|3|7|8|106|94|157|72|70|124|99|175|85|107|46|43|54|100|10	0
TPCN2_DeltaCT	Q658Y4	FAM91A1	2|0|0	0|0|0|0|0	3|3|3|4|1|4|2|0|0|0|0|0|0|1|3|0|0|1|2|2|3|5|1|3|4|2|1|1|0|0	0
TPCN2_DeltaCT	Q29RF7	PDS5A	0|0|0	0|0|0|0|0	3|3|7|4|3|2|1|0|0|0|0|1|0|3|3|2|1|4|3|4|5|2|3|1|1|3|2|1|2|0	0
TPCN2_DeltaCT	Q08945	SSRP1	4|0|0	3|0|0|0|3	1|4|0|0|0|0|2|0|0|1|0|0|0|1|1|0|0|4|7|4|5|0|1|0|0|0|3|3|5|0	0
TPCN2_DeltaCT	Q7Z4V5	HDGFL2	2|0|0	0|0|0|0|0	4|3|6|6|8|6|10|0|0|0|0|0|0|4|4|0|0|2|2|1|2|6|2|2|7|6|3|1|1|2	0

TPCN2_DeltaCT	Q02978	SLC25A11	2|0|0	0|0|0|0|0	0|0|13|6|4|13|5|0|0|0|0|0|0|0|0|2|2|0|0|0|0|2|3|2|2|2|0|0|2|0	0
TPCN2_DeltaCT	Q02878	RPL6	14|12|14	18|11|13|23|16	20|13|18|9|17|19|15|11|5|8|6|4|11|13|14|15|5|4|11|5|7|6|14|8|6|15|8|10|4|1	0
TPCN2_DeltaCT	P07195	LDHB	19|0|19	17|13|12|0|17	3|3|1|2|0|3|0|1|3|2|1|2|2|1|2|0|0|3|0|2|0|0|3|0|0|0|0|1|0|6	0
TPCN2_DeltaCT	Q9BTT0	ANP32E	3|0|0	3|0|0|0|0	0|0|2|2|0|0|0|0|0|0|0|0|0|0|0|0|0|0|0|0|0|0|0|2|1|1|0|0|0|9	0
TPCN2_DeltaCT	P49756	RBM25	0|0|0	2|0|0|0|0	8|6|6|5|2|3|0|0|0|0|0|0|0|3|0|7|4|2|2|2|2|3|7|3|0|7|0|3|3|0	0
TPCN2_DeltaCT	O75165	DNAJC13	5|0|0	0|0|0|15|3	0|0|0|0|1|0|0|0|0|0|0|0|0|0|0|0|3|5|2|2|0|0|1|1|0|2|3|0|0	0
TPCN2_DeltaCT	P99999	CYCS	0|0|0	0|0|0|0|0	1|2|0|0|0|0|0|0|0|0|0|1|0|1|0|0|0|1|0|3|1|0|0|0|0|0|0|0|0|0	0
TPCN2_DeltaCT	P31689	DNAJA1	8|0|0	5|0|0|0|0	0|0|5|0|0|2|1|0|1|0|0|0|0|0|0|0|0|1|0|0|0|0|1|1|0|0|0|0|0|30	0
TPCN2_DeltaCT	A5YKK6	CNOT1	0|0|0	0|0|0|0|0	0|0|6|1|2|2|2|0|0|0|0|0|0|1|0|1|0|0|0|1|1|6|1|3|4|5|0|0|0|0	0
TPCN2_DeltaCT	P26640	VARS	8|0|0	8|0|0|0|0	3|1|8|4|4|8|4|0|0|0|0|0|1|0|1|4|2|0|0|0|0|11|3|7|6|9|0|0|1|20	0
TPCN2_DeltaCT	P26641	EEF1G	19|2|9	15|8|9|0|16	3|0|18|11|10|13|3|5|5|3|4|7|5|1|1|19|11|4|3|2|2|12|13|12|7|10|3|5|1|27	0

TPCN2_DeltaCT	Q8TEH3	DENND1A	0|0|0	0|0|0|0|0	0|0|0|0|0|0|0|0|0|0|0|0|0|0|0|0|0|0|0|0|0|0|0|0|0|0|0|0|0|0|0	0
TPCN2_DeltaCT	Q99460	PSMD1	10|0|2	9|0|2|0|5	0|1|5|0|2|4|1|0|0|0|0|0|0|0|0|0|0|1|1|2|2|0|1|2|3|1|0|0|0|18	0
TPCN2_DeltaCT	Q9NTJ3	SMC4	2|0|0	0|0|0|0|0	3|3|7|1|3|2|3|0|0|0|0|0|0|1|0|2|6|0|0|2|4|1|5|2|1|9|1|1|3|8	0
TPCN2_DeltaCT	O43491	EPB41L2	2|0|0	0|0|0|0|0	41|33|40|42|25|31|33|0|0|0|0|0|0|58|43|11|7|26|38|33|59|16|22|12|13|18|43|42|1|3	0
TPCN2_DeltaCT	O43493	TGOLN2	0|0|0	0|0|0|0|0	0|0|0|0|0|0|0|0|0|0|0|0|0|0|0|0|0|0|0|0|0|0|0|0|0|0|0|0|0|0|0	0
TPCN2_DeltaCT	P49915	GMPS	3|0|0	3|0|0|0|0	3|6|2|1|0|5|4|1|0|1|1|0|2|1|2|2|1|1|1|2|3|2|6|0|2|8|0|1|0|1	0
TPCN2_DeltaCT	P13639	EEF2	60|0|32	51|37|28|0|25	17|26|19|3|5|32|19|15|13|17|15|11|14|17|19|16|5|7|11|5|11|16|26|8|7|8|9|10|1|49	0
TPCN2_DeltaCT	O60264	SMARCA5	10|0|0	12|0|0|0|4	30|32|34|41|42|13|17|2|4|3|0|2|1|33|26|84|70|22|30|24|25|28|59|23|25|42|36|43|20|0	0
TPCN2_DeltaCT	P11586	MTHFD1	10|0|3	9|2|3|0|3	0|0|3|5|2|11|7|0|0|0|1|0|0|0|0|0|0|0|0|0|0|6|15|4|5|7|0|0|5|21	0
TPCN2_DeltaCT	P61353	RPL27	2|0|2	2|2|2|0|0	0|0|6|2|5|1|0|1|0|0|0|1|2|0|0|1|3|0|0|0|0|1|4|1|0|3|0|0|2|0	0
TPCN2_DeltaCT	P62847	RPS24	0|0|2	0|0|0|3|0	3|2|9|11|8|6|5|2|2|2|0|0|1|0|2|7|4|0|1|0|0|5|8|10|4|10|1|0|8|4	0

TPCN2_DeltaCT	P04264	KRT1	28|59|68	34|64|75|86|39	14|20|26|20|7|4|13|110|74|98|28|34|29|15|26|56|18|11|26|20|15|5|18|9|6|18|37|64|4|35	0
TPCN2_DeltaCT	P04181	OAT	16|0|3	18|2|2|0|14	0|0|0|0|0|0|0|3|2|4|4|6|6|0|0|0|0|0|0|0|0|0|1|0|0|0|0|0|0|6	0
TPCN2_DeltaCT	Q7KZ85	SUPT6H	2|0|0	0|0|0|0|0	1|0|0|1|0|0|1|0|0|0|0|0|0|0|0|0|0|0|1|0|1|0|0|1|0|1|0|0|1|6	0
TPCN2_DeltaCT	Q9BY44	EIF2A	0|0|2	0|0|0|0|0	4|6|7|0|0|11|4|0|0|0|0|0|0|4|2|1|0|1|2|5|1|1|1|0|0|3|1|2|0|0	0
TPCN2_DeltaCT	O14828	SCAMP3	0|0|0	0|0|0|0|0	1|1|0|0|0|3|1|1|0|1|2|0|0|0|0|0|0|1|0|0|0|0|0|0|0|0|0|1|0|0	0
TPCN2_DeltaCT	P38919	EIF4A3	3|0|3	8|0|0|0|4	1|2|7|7|6|11|7|3|2|5|3|2|5|0|0|4|7|0|2|1|1|4|13|3|3|16|1|1|5|9	0
TPCN2_DeltaCT	P15880	RPS2	8|4|4	8|5|5|3|8	3|3|15|14|10|20|10|2|3|2|1|2|2|1|2|12|8|1|3|1|1|11|7|11|15|12|1|2|6|9	0
TPCN2_DeltaCT	Q14678	KANK1	10|0|12	0|14|33|5|14	1|0|1|0|0|0|0|0|0|0|0|0|0|0|0|0|0|0|0|0|3|0|0|0|0|0|0|0|0	0
TPCN2_DeltaCT	O60506	SYNCRIP	8|0|0	6|0|0|0|6	4|6|4|4|2|3|9|4|2|4|2|1|2|6|8|1|3|6|8|12|9|1|9|2|1|8|7|7|1|20	0
TPCN2_DeltaCT	P49411	TUFM	14|0|2	13|0|0|0|12	4|5|12|23|27|17|14|25|22|27|30|27|34|3|3|13|21|4|5|0|1|10|32|10|5|21|5|5|10|32	0
TPCN2_DeltaCT	P62314	SNRPD1	0|0|0	0|0|0|0|2	6|6|1|2|3|4|2|0|0|0|0|0|0|3|4|1|2|0|0|0|0|3|2|1|2|2|0|0|2|3	0

TPCN2_DeltaCT	Q13423	NNT	12|0|2	9|0|3|0|11	0|0|0|0|0|0|0|8|7|8|5|8|4|0|0|0|0|0|0|0|0|0|0|0|0|0|0|0|0|0	0
TPCN2_DeltaCT	P07437	TUBB	32|7|19	39|14|20|7|17	21|23|86|120|87|90|68|30|22|27|23|19|21|20|29|40|52|11|21|11|10|80|80|116|117|93|12|22|9	0
TPCN2_DeltaCT	P63261	ACTG1	44|0|36	46|28|25|0|48	30|29|41|60|55|42|40|56|53|53|51|54|57|32|34|65|73|38|61|34|45|26|66|21|17|42|44|47|258|	0
TPCN2_DeltaCT	P43246	MSH2	5|0|0	7|0|0|0|4	0|0|8|6|1|1|3|0|0|0|0|0|0|0|0|0|0|1|0|0|1|1|0|0|4|0|0|2|6	0
TPCN2_DeltaCT	P43243	MATR3	18|0|3	24|0|0|0|13	13|11|24|16|21|16|10|7|5|8|3|3|3|14|5|16|11|9|17|8|16|10|30|11|13|15|14|17|7|24	0
TPCN2_DeltaCT	O15118	NPC1	0|0|0	0|0|0|0|0	0|0|0|0|0|0|0|0|0|0|0|0|0|0|0|0|0|0|0|0|0|0|0|0|0|0|0|0	0
TPCN2_DeltaCT	P05165	PCCA	0|0|3	0|0|0|0|0	85|92|181|341|228|92|100|256|162|203|198|172|257|89|93|104|131|65|87|49|57|55|174|154|15	0
TPCN2_DeltaCT	P22314	UBA1	21|0|0	19|6|3|0|11	0|1|0|0|0|5|2|0|0|1|0|0|0|0|0|0|0|0|0|0|2|10|0|1|1|0|0|0|27	0
TPCN2_DeltaCT	Q53GQ0	HSD17B12	0|2|0	2|0|0|0|2	0|0|2|2|0|1|2|0|0|0|0|0|0|0|0|0|0|0|0|0|0|1|6|0|2|1|0|0|2|0	0
TPCN2_DeltaCT	Q8NI27	THOC2	2|0|0	0|0|0|0|0	20|20|5|7|7|4|3|1|0|0|0|0|0|18|19|9|7|11|14|17|17|4|10|4|0|7|15|12|2|0	0
TPCN2_DeltaCT	P30101	PDIA3	28|0|3	24|5|2|0|18	0|0|0|0|0|0|0|9|8|9|7|7|6|0|0|0|0|0|0|0|0|0|7|0|0|0|1|0|0|10	0

TPCN2_DeltaCT	P27797	CALR	20|0|9	15|12|9|0|19	0|0|0|0|0|0|0|1|0|0|1|0|0|0|0|0|0|0|0|0|0|0|3|0|0|0|0|0|0|23	0
TPCN2_DeltaCT	P35606	COPB2	4|0|0	6|2|0|0|2	2|2|0|0|0|2|0|1|0|0|0|0|1|0|0|1|1|0|0|0|1|0|1|0|0|0|0|1|0|9	0
TPCN2_DeltaCT	Q13547	HDAC1	5|6|0	4|0|0|6|4	1|2|24|23|26|10|9|0|1|2|2|2|2|1|1|15|14|0|0|1|1|8|16|10|5|15|0|0|10|7	0
TPCN2_DeltaCT	P78527	PRKDC	21|0|0	0|3|4|0|0	0|0|68|65|71|21|11|10|8|11|5|2|7|0|0|5|7|0|4|0|0|28|70|23|38|56|1|1|38|95	0
TPCN2_DeltaCT	Q9H2P0	ADNP	0|0|0	0|0|0|0|0	50|41|34|38|48|12|20|0|0|0|0|0|0|50|52|43|56|29|41|43|54|16|31|11|16|32|47|67|14|0	0
TPCN2_DeltaCT	P25205	MCM3	7|0|3	16|2|0|0|6	1|2|2|0|0|1|0|0|0|1|0|0|1|1|1|1|0|0|0|1|0|1|2|1|1|1|0|0|3|25	0
TPCN2_DeltaCT	Q16186	ADRM1	2|0|0	2|0|0|0|0	1|1|2|2|1|3|0|0|1|1|0|1|0|1|0|1|1|0|0|0|0|0|1|0|0|2|1|1|0|2	0
TPCN2_DeltaCT	P48735	IDH2	8|0|0	8|0|0|0|10	0|0|0|0|0|0|0|2|4|4|5|5|6|0|0|0|0|0|0|0|0|0|0|0|0|0|0|0|0|0	0
TPCN2_DeltaCT	Q16181	SEPT7	2|0|0	2|0|0|0|0	2|0|14|15|7|15|17|0|0|0|0|0|1|0|12|6|0|0|1|1|6|8|4|4|12|1|2|0|4	0
TPCN2_DeltaCT	P62241	RPS8	0|0|4	0|0|3|5|0	5|4|12|13|13|14|12|6|8|6|4|3|4|5|4|17|13|0|3|0|2|9|11|4|8|13|2|3|13|6	0
TPCN2_DeltaCT	P27708	CAD	0|0|0	0|0|0|0|0	0|0|9|4|6|1|0|3|1|3|3|2|2|0|0|0|0|0|0|0|0|2|4|6|3|6|0|0|7|21	0

TPCN2_DeltaCT	Q9Y3F4	STRAP	2|0|0	0|0|0|0|0	0|1|21|20|11|24|28|0|1|0|2|1|1|1|0|4|0|1|1|1|0|14|13|8|9|8|0|1|0|4	0
TPCN2_DeltaCT	P17987	TCP1	17|3|11	21|8|7|3|15	0|0|104|91|59|28|24|6|2|5|4|2|3|0|0|13|24|2|2|2|0|75|46|147|117|67|1|0|20|63	0
TPCN2_DeltaCT	Q13162	PRDX4	9|0|2	8|0|4|0|7	0|2|3|8|4|2|2|2|3|1|2|2|2|2|6|0|1|2|1|2|4|2|6|4|6|3|2|0|3	0
TPCN2_DeltaCT	Q13283	G3BP1	7|0|0	6|0|0|0|0	8|7|20|15|10|12|13|0|0|0|0|0|8|8|7|6|3|6|2|10|13|8|10|10|13|5|3|1|4	0
TPCN2_DeltaCT	Q7L2E3	DHX30	7|0|0	5|0|0|0|4	0|0|2|0|0|0|0|2|3|6|7|4|4|0|0|0|0|0|0|0|0|0|1|0|0|1|0|0|3|0	0
TPCN2_DeltaCT	P84098	RPL19	20|22|25	27|14|17|28|24	2|2|6|3|3|4|2|1|2|1|1|2|0|0|1|2|3|2|2|2|2|2|4|3|2|5|1|2|1|2	0
TPCN2_DeltaCT	Q709C8	VPS13C	0|0|11	0|52|76|0|4	0|0|0|0|0|0|0|0|0|0|0|0|0|0|0|0|0|0|0|0|0|0|0|0|0|0|0|0	0
TPCN2_DeltaCT	Q9H6R4	NOL6	0|0|0	3|0|0|0|0	0|0|3|1|2|0|2|0|0|0|0|0|0|2|1|5|2|1|0|1|0|0|8|0|0|5|1|0|0|0	0
TPCN2_DeltaCT	Q9Y678	COPG1	3|0|0	0|0|0|0|0	2|3|10|9|4|9|7|0|0|0|0|0|0|3|4|2|1|2|4|3|5|4|6|4|5|5|2|4|4|8	0
TPCN2_DeltaCT	O15067	PFAS	0|0|0	0|0|0|0|0	3|4|0|0|0|0|0|0|0|0|0|0|0|2|2|0|0|2|1|6|6|2|0|1|1|0|1|0|0|1	0
TPCN2_DeltaCT	P61221	ABCE1	2|0|0	0|0|0|0|0	1|0|0|0|0|7|7|0|0|0|0|0|0|0|0|0|1|0|0|0|0|0|1|0|0|0|0|0|0|2	0

TPCN2_DeltaCT	Q14498	RBM39	2|0|0	2|0|0|0|0	3|2|3|1|0|3|1|1|0|0|0|0|0|0|3|1|1|3|2|2|2|1|4|1|0|1|1|2|4|28	0
TPCN2_DeltaCT	P0DME0	SETSIP	0|0|3	0|0|0|0|0	4|2|4|5|3|3|4|0|0|0|0|0|0|3|4|1|0|0|2|1|2|2|5|2|2|3|2|2|1|13	0
TPCN2_DeltaCT	Q96KP4	CNDP2	0|0|0	2|0|0|0|0	0|0|0|0|0|0|0|0|0|0|0|0|0|0|0|0|0|0|0|0|0|0|0|0|0|0|0|0|0|0|0	0
TPCN2_DeltaCT	P61981	YWHAG	7|0|0	8|0|0|0|4	0|0|2|3|1|2|0|2|2|4|2|3|2|1|1|0|1|0|1|0|0|1|3|0|1|3|0|0|0|13	0
TPCN2_DeltaCT	Q8WX92	NELFB	0|0|0	0|0|0|0|3	0|0|0|0|0|0|0|0|0|0|0|0|0|0|0|0|0|0|0|0|0|0|0|0|0|0|0|0|0|0|1	0
TPCN2_DeltaCT	P55060	CSE1L	23|0|8	23|11|9|0|12	0|2|7|1|1|11|1|0|1|2|0|0|0|0|0|1|2|1|0|0|5|3|6|5|3|0|0|3|15	0
TPCN2_DeltaCT	Q13148	TARDBP	2|0|0	0|0|0|0|0	3|3|4|2|4|3|6|4|3|4|3|2|3|2|3|5|3|3|5|3|6|0|6|0|0|5|3|4|2|4	0
TPCN2_DeltaCT	Q14258	TRIM25	3|0|0	0|0|0|0|0	1|1|5|0|1|1|2|0|0|0|0|0|0|0|1|0|0|0|1|1|1|0|3|3|0|0|0|0|0|0	0
TPCN2_DeltaCT	O75694	NUP155	2|0|0	0|0|0|0|0	0|1|0|0|0|3|3|4|2|4|4|0|3|0|0|4|2|2|1|3|4|0|4|0|0|0|0|1|1|2	0
TPCN2_DeltaCT	P12236	SLC25A6	0|0|8	0|0|0|0|13	9|10|23|24|16|117|39|9|9|10|9|7|10|9|10|25|21|4|4|4|5|8|15|11|9|11|6|5|8|4	0
TPCN2_DeltaCT	P18669	PGAM1	2|0|0	4|0|0|0|0	0|1|3|3|0|11|5|0|0|0|0|0|0|0|0|0|0|0|0|0|0|0|2|11|0|1|1|0|0|0|7	0

TPCN2_DeltaCT	O95625	ZBTB11	4|0|4	0|0|4|10|11	2|0|0|0|0|0|0|0|0|0|0|0|0|0|0|0|0|0|0|0|0|0|1|0|0|0|0|0|0|0	0
TPCN2_DeltaCT	P05141	SLC25A5	13|14|9	13|11|8|13|14	8|9|27|30|21|28|14|9|7|9|8|9|8|9|8|27|32|4|3|3|5|14|20|16|15|16|6|4|13|5	0
TPCN2_DeltaCT	Q9UQ80	PA2G4	5|0|3	3|5|2|0|3	7|5|1|3|0|13|8|2|5|6|4|2|5|1|3|0|0|0|2|0|3|3|6|4|5|4|2|2|0|6	0
TPCN2_DeltaCT	P62280	RPS11	0|0|4	2|3|0|0|2	2|0|4|8|6|3|3|0|0|0|1|1|0|1|0|5|7|0|1|0|0|6|4|4|7|4|0|1|3|1	0
TPCN2_DeltaCT	P55209	NAP1L1	7|0|0	6|0|0|0|5	5|6|20|12|8|18|15|1|0|0|0|0|5|5|7|4|4|4|4|5|16|8|13|11|14|5|4|1|15	0
TPCN2_DeltaCT	O94874	UFL1	0|0|0	0|0|0|0|2	2|0|0|0|0|0|0|0|0|0|0|0|0|0|0|0|0|0|1|2|0|1|0|1|0|0|0|0|0	0
TPCN2_DeltaCT	Q5JWF2	GNAS	0|0|0	0|0|0|2|0	0|0|0|0|0|1|1|2|2|1|1|0|1|0|0|1|0|0|0|0|0|0|1|0|0|0|0|0|0|2	0
TPCN2_DeltaCT	P25705	ATP5A1	28|12|16	24|9|10|11|27	0|0|41|52|43|34|54|17|11|18|13|10|15|0|1|31|32|4|1|0|0|19|52|17|26|44|1|1|25|19	0
TPCN2_DeltaCT	Q13823	GNL2	0|0|0	4|0|0|6|0	33|32|10|15|9|0|8|0|0|0|0|0|0|27|27|25|11|16|20|22|24|11|14|7|4|9|30|54|5|0	0
TPCN2_DeltaCT	P12814	ACTN1	9|0|0	0|0|0|0|0	10|5|2|0|0|0|1|3|3|1|1|1|1|4|5|0|0|3|4|9|8|0|3|0|0|0|3|2|10|7	0
TPCN2_DeltaCT	Q9H3U1	UNC45A	2|0|0	0|0|0|0|0	4|10|5|1|0|5|4|0|0|0|0|0|0|5|3|1|0|0|2|4|5|11|4|4|6|1|1|0|0|2	0

TPCN2_DeltaCT	Q6P2E9	EDC4	2|0|0	2|0|0|0|0	8|7|13|6|3|6|7|0|0|0|0|0|0|1|3|1|1|3|7|11|14|14|10|7|9|8|4|3|0|1	0
TPCN2_DeltaCT	Q96GQ7	DDX27	0|0|0	3|0|0|0|0	1|0|0|0|0|0|0|1|2|1|0|2|0|0|1|0|1|0|0|0|0|0|2|0|0|0|0|0|4|0	0
TPCN2_DeltaCT	Q01813	PFKP	10|0|5	14|0|3|0|5	1|1|0|0|0|8|6|0|0|0|0|0|0|0|1|0|0|2|1|2|0|0|1|0|0|0|0|0|0|7	0
TPCN2_DeltaCT	Q92878	RAD50	3|0|0	0|0|0|0|2	0|0|5|8|10|0|1|0|0|0|0|0|0|0|0|0|0|1|1|0|0|1|16|0|1|10|0|0|3|1	0
TPCN2_DeltaCT	Q99490	AGAP2	0|0|0	0|0|0|0|0	0|0|0|0|0|0|0|0|0|0|0|0|0|0|0|0|0|0|0|0|0|0|0|0|0|0|0|0|0	0
TPCN2_DeltaCT	P51114	FXR1	3|0|0	4|0|0|0|3	0|1|1|1|0|4|2|0|0|0|0|0|0|2|2|1|0|0|0|0|0|0|1|0|0|1|0|0|0|0	0
TPCN2_DeltaCT	Q00341	HDLBP	0|0|0	0|0|0|0|0	25|22|28|22|7|23|26|0|0|1|0|0|0|18|18|11|5|12|10|18|24|21|11|8|15|9|13|15|2|3	0
TPCN2_DeltaCT	O76031	CLPX	3|0|0	0|0|0|0|2	0|0|0|0|0|0|0|4|3|3|6|8|9|0|0|0|0|0|0|0|0|0|0|0|0|0|0|0|0|0	0
TPCN2_DeltaCT	P61313	RPL15	13|4|8	10|12|8|8|15	7|10|20|20|17|9|16|3|2|2|3|1|2|3|6|17|8|1|1|1|2|10|30|14|11|19|4|4|5|2	0
TPCN2_DeltaCT	P33176	KIF5B	8|0|0	4|0|0|0|0	16|15|48|32|20|16|18|0|0|0|0|0|9|9|7|6|5|9|9|12|17|30|12|14|26|10|9|1|9	0
TPCN2_DeltaCT	O60814	HIST1H2BK	8|11|14	14|11|11|10|12	15|15|14|30|21|21|33|10|9|7|5|7|7|21|20|39|57|14|11|7|13|22|48|52|35|64|13|9|36|20	0

TPCN2_DeltaCT	P14866	HNRNPL	13|18|0	19|2|0|13|10	21|18|10|18|16|13|17|13|16|14|15|15|16|31|16|19|21|6|13|11|6|18|23|25|18|20|14|18|10|21	0
TPCN2_DeltaCT	P24941	CDK2	5|0|5	5|2|3|0|0	0|0|3|2|3|3|5|0|0|0|0|0|0|0|0|0|0|0|0|2|1|3|3|2|4|2|1|0|4|1	0
TPCN2_DeltaCT	P14868	DARS	8|0|2	7|0|0|0|2	1|1|4|9|4|2|1|0|0|0|0|0|0|0|1|1|0|0|0|0|0|2|5|2|1|4|0|0|2|8	0
TPCN2_DeltaCT	P63104	YWHAZ	11|0|8	13|9|7|0|9	0|3|5|4|3|2|1|8|5|6|5|6|6|1|2|1|1|3|3|0|1|2|8|2|2|3|3|2|1|28	0
TPCN2_DeltaCT	P11498	PC	2|7|55	10|34|66|24|14	691|770|428|416|295|106|88|1307|810|1086|1058|849|1284|383|418|702|699|289|459|206|325|1	0
TPCN2_DeltaCT	Q13263	TRIM28	16|0|0	21|0|0|0|7	32|39|52|61|50|26|37|10|11|11|7|4|9|36|40|19|9|25|32|31|39|29|37|43|28|29|28|26|16|41	0
TPCN2_DeltaCT	P11021	HSPA5	69|0|27	71|23|23|8|57	16|18|53|58|38|42|21|19|18|19|18|14|16|12|13|28|36|11|17|13|17|26|46|28|30|39|11|14|19|9	0
TPCN2_DeltaCT	Q9P0L0	VAPA	4|0|0	3|0|0|0|4	1|2|6|2|6|8|4|0|2|0|0|0|2|3|2|8|3|2|0|0|0|2|5|0|0|2|2|1|0|0	0
TPCN2_DeltaCT	Q02790	FKBP4	5|0|4	7|2|0|0|3	0|0|0|0|0|0|1|0|0|0|0|0|0|0|0|0|0|0|0|0|0|2|0|0|0|0|0|0|18	0
TPCN2_DeltaCT	Q96RQ3	MCCC1	2|13|21	4|14|19|12|12	65|57|184|276|188|44|42|169|104|125|116|93|161|56|53|55|43|31|54|26|40|62|149|125|220|21	0
TPCN2_DeltaCT	Q9ULV4	CORO1C	5|0|2	6|0|0|0|4	11|10|7|3|3|16|8|0|0|0|0|0|0|7|7|2|2|6|6|8|9|0|3|1|0|3|7|7|4|0	0

TPCN2_DeltaCT	Q01105	SET	5|0|0	6|0|0|0|3	10|7|10|7|8|10|5|0|0|0|0|0|0|5|7|3|2|0|2|1|2|8|5|8|7|9|3|2|3|25	0
TPCN2_DeltaCT	Q5JTH9	RRP12	4|0|0	0|0|0|2|5	0|0|3|0|1|0|0|0|0|0|0|0|0|0|0|2|2|5|2|2|0|0|4|0|1|4|1|2|0|0	0
TPCN2_DeltaCT	Q08170	SRSF4	0|0|0	0|0|0|0|0	4|1|5|3|8|2|0|1|1|0|1|1|1|2|2|0|1|1|1|1|1|0|7|0|0|2|1|1|1|3	0
TPCN2_DeltaCT	P22626	HNRNPA2B1	5|0|0	9|0|0|0|0	15|10|14|28|23|11|17|18|12|16|10|12|16|10|12|15|21|14|13|13|14|4|29|11|8|27|18|12|9|58	0
TPCN2_DeltaCT	P29590	PML	0|0|0	0|0|0|0|0	0|0|1|0|0|1|0|0|0|0|0|0|0|0|0|0|0|0|0|0|1|0|0|1|0|0|0|0|0	0
TPCN2_DeltaCT	Q9UNF1	MAGED2	4|7|18	7|15|17|26|4	5|2|0|1|0|3|3|0|0|0|0|0|0|1|3|0|0|0|0|0|1|0|1|0|0|2|0|0|0|2	0
TPCN2_DeltaCT	Q92499	DDX1	6|0|0	4|0|0|0|3	1|1|2|4|3|7|6|0|0|0|0|0|0|0|4|3|0|0|0|0|8|5|4|3|5|0|0|1|8	0
TPCN2_DeltaCT	Q08J23	NSUN2	5|0|0	6|0|0|0|0	3|1|1|2|2|3|4|1|0|1|3|0|1|1|2|0|0|1|0|2|0|3|3|2|2|9|0|0|7|2	0
TPCN2_DeltaCT	Q7Z2W4	ZC3HAV1	0|0|0	0|0|0|0|0	17|17|5|12|4|11|14|3|4|1|1|2|2|14|11|4|6|13|21|19|28|4|5|0|2|7|11|11|0|0	0
TPCN2_DeltaCT	P04406	GAPDH	37|3|27	39|27|21|4|28	0|0|0|0|0|1|1|9|6|4|4|6|4|2|1|0|0|1|3|1|1|2|19|0|7|2|0|3|4|41	0
TPCN2_DeltaCT	Q8WVC0	LEO1	0|0|0	0|0|0|0|0	0|1|1|0|1|0|0|0|0|0|0|0|0|3|2|1|0|2|3|2|3|0|2|0|1|1|2|2|0|0	0

TPCN2_DeltaCT	Q9Y5L0	TNPO3	2|0|0	3|0|0|0|0	0|0|1|0|2|0|1|0|0|0|0|0|0|0|0|0|1|0|0|0|0|1|1|0|1|1|0|0|3|0	0
TPCN2_DeltaCT	Q9Y6D5	ARFGEF2	0|0|0	0|0|0|0|0	0|0|0|0|0|0|0|0|0|0|0|0|0|0|0|0|0|0|0|0|0|0|0|0|0|0|0	0
TPCN2_DeltaCT	P11177	PDHB	0|0|0	3|0|0|0|4	0|0|0|0|0|0|0|11|8|8|13|16|16|0|0|0|0|0|1|0|1|0|0|0|0|0|1|0|0|1	0
TPCN2_DeltaCT	O00571	DDX3X	5|0|0	2|0|0|0|2	17|16|27|32|15|27|39|8|12|6|4|6|5|11|13|21|23|13|20|17|24|29|20|21|25|19|13|15|8|17	0
TPCN2_DeltaCT	O00299	CLIC1	3|0|4	2|2|0|0|2	1|2|0|0|0|1|1|1|2|1|1|2|1|0|1|0|0|0|5|0|2|0|0|0|1|0|1|1|0|1	0
TPCN2_DeltaCT	P29692	EEF1D	4|0|0	5|0|0|0|4	11|12|7|7|6|4|4|0|0|0|0|0|0|11|13|18|23|6|11|7|14|5|5|5|3|5|9|11|0|19	0
TPCN2_DeltaCT	Q06830	PRDX1	9|0|6	8|8|5|2|6	11|11|6|18|14|9|10|13|14|14|17|16|17|11|10|27|4|6|10|5|11|9|24|16|10|21|10|7|2|20	0
TPCN2_DeltaCT	Q9UIG0	BAZ1B	3|0|0	0|0|0|0|0	101|76|33|51|42|9|28|0|0|0|0|0|0|95|94|110|72|68|95|56|76|39|62|32|32|31|114|91|27|0	0
TPCN2_DeltaCT	P30153	PPP2R1A	7|0|2	10|0|0|0|3	0|0|11|3|7|3|0|4|0|0|0|0|0|0|0|0|0|0|1|0|0|10|10|5|11|0|0|0|21	0
TPCN2_DeltaCT	O75390	CS	13|0|7	16|6|2|0|13	2|2|1|0|0|0|0|9|5|7|9|6|12|0|0|0|0|2|4|3|3|0|5|0|2|0|2|3|1|11	0
TPCN2_DeltaCT	O14646	CHD1	0|0|0	0|0|0|0|0	4|4|0|0|1|0|0|0|0|0|0|0|0|4|1|0|0|9|5|6|7|0|0|0|0|0|2|3|0|0	0

TPCN2_DeltaCT	Q9NX63	CHCHD3	0|0|0	0|0|0|0|4	0|0|0|0|0|0|0|0|0|0|0|0|0|0|0|0|0|0|0|0|0|0|0|0|0|1|0|0|0|0	0
TPCN2_DeltaCT	P49748	ACADVL	6|0|0	7|0|0|0|11	0|0|0|0|0|0|0|3|5|3|7|10|7|0|0|0|0|0|0|0|0|0|0|0|0|0|0|0|0|0|0	0
TPCN2_DeltaCT	P38646	HSPA9	50|8|29	52|16|34|14|42	7|10|47|45|38|12|18|90|73|125|128|112|155|6|5|25|20|12|19|10|11|27|81|13|23|21|25|23|23|	0
TPCN2_DeltaCT	Q9BSJ8	ESYT1	0|0|0	0|0|2|0|0	15|11|8|4|2|7|12|0|0|0|0|0|0|14|14|7|0|14|12|15|21|5|3|3|2|4|11|10|0|0	0
TPCN2_DeltaCT	P62701	RPS4X	0|3|0	2|2|3|0|3	0|0|6|7|2|14|12|5|2|4|2|1|4|0|1|4|3|0|2|0|0|8|8|4|2|8|1|0|1|10	0
TPCN2_DeltaCT	Q15424	SAFB	0|0|0	3|0|0|0|0	17|10|1|3|1|6|6|3|2|3|2|4|2|10|10|7|4|10|17|10|13|2|3|1|4|3|18|22|0|0	0
TPCN2_DeltaCT	P68431	HIST1H3	5|3|9	7|6|5|3|5	9|7|15|23|16|15|23|3|4|5|2|3|4|9|10|14|27|7|12|9|10|22|31|35|22|21|8|7|14|16	0
TPCN2_DeltaCT	P62277	RPS13	2|0|0	2|0|0|0|2	0|0|7|2|2|0|0|0|0|0|0|0|0|0|0|0|0|0|0|0|0|0|0|0|0|4|0|2|0|0|0|1|1	0
TPCN2_DeltaCT	O75955	FLOT1	4|0|3	0|2|11|5|9	0|0|0|0|0|0|0|0|0|0|0|0|0|0|0|0|0|0|0|0|0|0|0|0|0|0|0|0|0|0|0	0
TPCN2_DeltaCT	Q9HCC0	MCCC2	2|9|16	0|16|19|15|13	0|0|257|271|200|71|59|0|0|0|0|0|0|1|0|74|70|0|0|0|0|94|273|204|384|255|0|0|83|0	0
TPCN2_DeltaCT	Q08379	GOLGA2	3|0|0	2|0|0|0|0	8|7|0|0|0|0|0|0|1|2|0|1|1|8|5|3|1|16|16|14|18|0|0|0|0|0|5|10|0|0	0

TPCN2_DeltaCT	P60842	EIF4A1	10|0|9	12|7|7|0|5	5|6|21|22|16|34|27|8|6|11|9|7|6|2|3|12|9|3|7|3|5|21|18|17|19|20|7|5|13|24	0
TPCN2_DeltaCT	Q8NBS9	TXNDC5	0|0|0	4|0|0|0|3	0|0|0|0|0|0|0|2|0|1|1|2|2|0|0|0|0|0|0|0|0|0|0|0|0|0|0|0|0|1	0
TPCN2_DeltaCT	O00232	PSMD12	3|0|0	3|0|0|0|2	1|1|1|1|0|1|1|0|0|0|0|0|0|1|0|0|0|1|0|1|3|1|1|0|1|0|0|0|0|15	0
TPCN2_DeltaCT	Q96PK6	RBM14	2|0|0	0|0|0|0|0	0|0|5|6|8|4|1|3|2|5|5|4|2|0|0|1|5|1|1|1|1|0|5|0|0|9|2|2|6|0	0
TPCN2_DeltaCT	Q8TDD1	DDX54	13|17|7	18|2|0|28|13	0|0|7|1|5|1|2|0|0|0|0|0|0|0|0|4|4|0|0|0|0|2|12|3|6|9|1|0|6|0	0
TPCN2_DeltaCT	Q9NYF8	BCLAF1	0|0|0	0|0|0|0|0	33|34|40|44|32|29|40|0|0|1|0|0|1|33|26|34|22|22|26|35|49|18|31|19|13|35|66|56|11|4	0
TPCN2_DeltaCT	P37108	SRP14	0|0|2	0|0|0|0|0	2|1|4|2|3|0|0|0|1|1|1|1|1|1|2|3|1|1|1|2|1|5|2|2|3|1|2|1|1	0
TPCN2_DeltaCT	P06733	ENO1	26|0|15	22|18|13|2|18	3|4|18|26|12|34|67|9|5|7|5|4|3|3|5|4|2|3|5|5|4|27|38|4|15|11|4|3|21|51	0
TPCN2_DeltaCT	Q9BQG0	MYBBP1A	7|2|0	3|0|5|2|4	8|3|39|21|29|9|12|2|0|3|0|0|0|2|2|9|6|7|5|5|2|7|49|6|6|24|8|4|14|2	0
TPCN2_DeltaCT	P54886	ALDH18A1	6|0|0	5|0|0|0|0	0|0|16|15|16|23|13|13|19|19|27|24|25|1|0|19|21|0|0|0|0|12|16|6|14|11|0|1|16|14	0
TPCN2_DeltaCT	Q9UN73	PCDHA6	0|0|0	0|0|0|0|0	0|0|0|0|0|0|0|0|0|0|0|0|0|0|0|0|0|0|0|0|0|0|0|0|0|0|0|0|0	0

TPCN2_DeltaCT	P50991	CCT4	14|3|6	16|6|6|0|16	2|2|48|50|63|13|15|3|2|4|3|3|3|1|0|4|24|0|2|0|1|54|29|85|94|49|1|2|20|57	0
TPCN2_DeltaCT	P50990	CCT8	19|0|9	22|9|5|0|19	38|50|132|202|100|208|201|1|0|0|0|1|3|52|67|29|38|18|21|25|41|117|85|125|113|107|24|21|2	0
TPCN2_DeltaCT	O43399	TPD52L2	0|0|0	0|0|2|0|0	0|1|3|0|0|4|1|0|0|0|0|0|0|0|1|1|0|1|1|2|1|0|1|1|0|1|1|0|0|0	0
TPCN2_DeltaCT	P46782	RPS5	6|3|3	6|3|2|4|10	0|0|0|0|0|0|0|1|1|1|0|0|0|0|0|0|0|1|0|1|2|2|3|1|0|0|0|0|2	0
TPCN2_DeltaCT	P46781	RPS9	2|3|8	4|4|6|6|5	1|3|17|13|10|12|9|2|2|1|1|0|1|0|0|7|5|1|1|0|1|3|8|5|6|7|1|1|3|3	0
TPCN2_DeltaCT	P42704	LRPPRC	58|0|10	59|11|12|0|47	2|0|0|0|0|0|0|85|68|78|99|89|106|0|0|1|2|6|7|0|0|0|2|0|0|1|6|5|0|39	0
TPCN2_DeltaCT	Q96TA1	FAM129B	2|0|0	0|0|0|0|0	3|2|0|0|0|1|1|0|0|0|0|0|0|2|1|0|0|1|2|3|4|0|0|0|0|0|2|1|0|0	0
TPCN2_DeltaCT	O43719	HTATSF1	0|0|0	0|0|0|0|0	8|4|1|1|0|0|0|0|0|0|0|0|0|4|6|0|1|1|3|4|3|1|0|0|1|2|0|1|0|16	0
TPCN2_DeltaCT	Q9HD20	ATP13A1	0|0|0	0|0|0|0|0	0|1|0|0|0|0|0|0|0|0|0|0|0|0|0|0|0|0|0|0|0|1|0|0|0|0|0|0|0	0
TPCN2_DeltaCT	O94806	PRKD3	22|7|49	31|46|46|14|26	0|0|0|0|0|0|0|0|0|0|0|0|0|0|0|0|0|0|0|0|0|0|0|0|0|0|0	0
TPCN2_DeltaCT	P31040	SDHA	13|0|0	10|0|0|0|5	1|1|0|0|0|0|0|11|9|14|15|12|17|1|0|0|1|1|0|0|0|0|1|0|0|0|1|0|0|1	0

TPCN2_DeltaCT	P62888	RPL30	0|0|0	0|0|0|0|2	0|0|5|2|3|0|0|0|0|0|0|0|0|0|0|1|2|0|0|0|0|4|4|5|3|5|0|0|3|0	0
TPCN2_DeltaCT	P09104	ENO2	0|0|2	0|3|0|0|0	1|1|1|7|2|2|7|2|1|2|1|1|1|1|1|0|1|1|1|0|9|8|0|3|3|1|1|2|7	0
TPCN2_DeltaCT	P56192	MARS	0|0|0	2|0|2|0|0	0|1|9|12|10|14|9|1|0|0|0|0|0|0|0|0|0|1|0|1|4|10|12|9|10|0|0|9|5	0
TPCN2_DeltaCT	O60841	EIF5B	0|0|0	2|0|3|0|0	8|9|5|5|3|0|5|0|0|0|0|0|0|6|7|4|0|5|5|4|4|9|5|4|3|5|3|3|0|1	0
TPCN2_DeltaCT	Q02218	OGDH	6|0|0	0|0|0|0|3	0|0|0|0|0|0|0|4|5|5|11|9|8|0|0|0|0|0|0|0|0|0|0|0|0|0|0|0|0|0|0	0
TPCN2_DeltaCT	O95373	IPO7	7|0|0	7|0|0|0|0	4|11|5|0|0|2|2|0|1|0|0|0|0|4|7|0|0|5|5|5|4|1|1|0|0|0|3|4|0|2	0
TPCN2_DeltaCT	P20700	LMNB1	5|0|0	7|0|0|0|4	8|6|1|2|3|0|0|8|8|7|5|8|4|4|2|3|1|4|3|2|2|1|12|0|2|5|3|2|4|27	0
TPCN2_DeltaCT	P55884	EIF3B	9|0|0	4|0|0|0|0	0|0|16|6|4|6|4|0|0|0|0|0|0|0|2|2|5|0|0|0|0|7|7|3|5|2|1|1|1|4	0
TPCN2_DeltaCT	P21796	VDAC1	13|0|4	13|4|0|0|12	4|3|3|2|4|1|3|9|7|7|7|5|7|3|5|2|2|1|3|2|1|3|4|1|0|2|4|4|1|0	0
TPCN2_DeltaCT	O00763	ACACB	0|0|3	0|2|8|0|0	27|25|86|73|36|6|4|99|70|87|103|93|100|29|28|18|29|23|29|17|17|20|39|39|52|54|28|26|11|1	0
TPCN2_DeltaCT	Q01650	SLC7A5	3|0|0	2|0|0|0|0	6|11|2|1|0|0|1|4|4|5|4|4|5|11|8|5|4|5|5|4|4|0|1|0|0|1|3|5|0|0	0

TPCN2_DeltaCT	P12956	XRCC6	15|0|2	20|0|2|0|15	13|15|6|3|1|1|1|2|0|3|1|2|0|4|9|2|0|2|2|3|7|8|9|0|3|4|2|1|3|52	0
TPCN2_DeltaCT	Q5ZPR3	CD276	0|0|0	0|0|0|0|0	0|0|0|0|0|0|0|0|0|0|0|0|0|0|0|0|0|0|0|0|0|0|0|0|0|0|0|0	0
TPCN2_DeltaCT	Q6P158	DHX57	0|0|0	0|0|0|0|0	0|0|0|0|0|0|0|0|0|0|1|1|0|0|0|0|0|0|0|0|0|0|0|0|0|0|0|0|0	0
TPCN2_DeltaCT	Q13797	ITGA9	0|0|0	0|0|0|0|0	0|0|0|0|0|0|0|0|0|0|0|0|0|0|0|0|0|0|0|0|0|0|0|0|0|0|0|0	0
TPCN2_DeltaCT	Q9BVP2	GNL3	6|7|4	9|2|0|18|12	2|4|2|8|5|3|6|0|2|1|0|1|1|4|3|3|3|5|8|5|7|3|11|3|3|2|4|4|5|0	0
TPCN2_DeltaCT	P23246	SFPQ	4|0|0	5|3|0|0|0	15|15|49|39|30|29|18|5|2|4|2|2|3|14|11|25|26|8|13|13|17|21|25|24|19|29|13|12|15|24	0
TPCN2_DeltaCT	Q14008	CKAP5	3|0|0	0|0|0|0|0	32|19|36|21|24|20|14|0|0|0|0|0|0|17|14|8|9|22|28|25|32|42|25|23|28|33|29|23|1|10	0
TPCN2_DeltaCT	P0DMV8	HSPA1A	25|5|19	24|13|14|0|16	26|28|173|180|124|109|162|12|17|22|16|17|11|30|29|41|39|31|42|31|36|137|151|122|107|148|	0
TPCN2_DeltaCT	P40939	HADHA	41|0|8	37|9|9|0|34	0|0|0|0|0|0|0|21|14|18|24|22|23|0|0|0|0|2|1|0|0|0|1|0|0|0|0|0|0|2	0
TPCN2_DeltaCT	P52597	HNRNPF	11|0|0	9|0|0|0|10	8|5|12|10|11|10|8|17|12|14|17|12|19|7|6|9|3|11|10|7|11|7|20|7|8|10|14|12|11|27	0
TPCN2_DeltaCT	P60709	ACTB	0|18|0	0|0|0|16|0	30|29|41|60|55|42|40|56|53|53|51|54|57|32|34|65|74|38|60|34|45|26|65|21|17|42|44|47|258|	0

TPCN2_DeltaCT	Q9NQC3	RTN4	8|0|0	9|0|0|0|7	10|10|7|8|2|8|11|1|0|1|1|1|1|6|8|12|2|11|12|12|16|0|4|2|0|3|11|7|1|2	0
TPCN2_DeltaCT	P52292	KPNA2	2|0|0	0|0|0|0|0	0|0|2|1|2|1|1|2|1|1|1|1|2|0|0|2|1|0|1|1|0|4|6|2|0|5|0|0|2|13	0
TPCN2_DeltaCT	P09211	GSTP1	5|0|0	6|3|0|0|2	0|1|0|0|0|0|0|6|7|6|7|7|5|0|0|0|0|4|5|1|0|0|0|0|0|3|2|0|0	0
TPCN2_DeltaCT	P62913	RPL11	0|0|2	0|0|0|0|4	4|4|8|9|10|13|7|3|5|3|3|3|3|4|5|6|8|2|4|0|1|6|7|3|4|9|4|3|8|6	0
TPCN2_DeltaCT	P06899	HIST1H2BJ	0|0|14	0|0|0|0|0	14|14|15|27|20|23|33|10|8|8|5|6|7|21|19|35|55|14|10|7|12|21|47|47|30|63|10|8|36|20	0
TPCN2_DeltaCT	P62917	RPL8	10|17|11	14|8|9|15|16	0|1|10|7|4|8|5|0|0|0|0|0|0|0|1|8|3|0|1|0|0|5|5|7|5|5|0|0|1|1	0
TPCN2_DeltaCT	P31943	HNRNPH1	24|0|5	19|5|0|0|21	4|3|8|7|13|9|7|9|7|11|9|10|11|5|4|6|4|9|8|6|7|7|13|9|7|11|7|5|12|24	0
TPCN2_DeltaCT	O15371	EIF3D	2|0|0	2|0|0|0|0	1|1|2|1|7|2|3|1|1|0|0|0|0|1|1|0|2|1|0|1|1|6|6|10|9|7|0|0|0|4	0
TPCN2_DeltaCT	Q15029	EFTUD2	11|0|0	11|0|3|0|5	1|2|16|16|10|7|14|1|1|3|1|1|2|1|2|21|7|4|3|2|2|26|16|13|15|19|0|2|16|28	0
TPCN2_DeltaCT	P31946	YWHAB	9|0|7	12|9|0|0|8	0|2|6|7|3|2|2|1|1|2|1|1|1|2|1|0|2|0|1|0|0|1|5|2|2|4|0|0|0|20	0
TPCN2_DeltaCT	Q8N1F7	NUP93	7|0|0	4|0|0|0|0	0|0|8|4|5|0|3|0|0|0|0|0|0|0|0|1|3|0|0|0|0|4|7|5|7|4|0|0|13|1	0

TPCN2_DeltaCT	P31948	STIP1	12|0|0	12|0|0|0|7	1|0|0|0|0|1|3|1|1|2|1|0|1|1|0|0|0|1|2|1|2|0|2|0|0|0|1|1|0|46	0
TPCN2_DeltaCT	Q15020	SART3	0|0|0	3|0|0|0|3	18|13|34|30|21|24|14|0|0|0|0|0|0|22|26|13|10|9|15|12|17|10|33|6|5|19|15|14|9|3	0
TPCN2_DeltaCT	P55072	VCP	37|0|12	35|16|15|0|24	0|0|3|1|1|3|4|0|0|0|0|0|0|0|0|0|0|1|6|1|2|4|5|2|3|1|0|0|0|84	0
TPCN2_DeltaCT	Q3SXM5	HSDL1	0|0|0	0|0|0|0|5	0|0|0|0|0|0|0|0|0|0|0|0|0|0|0|0|0|0|0|0|0|0|0|0|0|0|0|0|0|0|0	0
TPCN2_DeltaCT	P23396	RPS3	14|0|14	14|8|9|8|14	6|5|39|39|32|33|39|7|9|6|6|5|6|3|5|23|23|2|3|2|2|27|26|32|35|34|4|3|29|17	0
TPCN2_DeltaCT	P35613	BSG	0|0|0	0|0|0|0|2	0|0|0|0|0|0|0|0|0|0|0|0|0|0|0|0|0|0|0|0|0|0|0|0|0|0|0|0|0|0|3	0
TPCN2_DeltaCT	P35268	RPL22	0|0|4	0|4|4|0|0	4|4|2|6|3|7|1|4|4|4|4|4|4|3|4|3|5|0|2|0|2|2|4|3|3|4|3|3|3|1	0
TPCN2_DeltaCT	Q12874	SF3A3	2|0|0	3|0|0|0|2	0|0|13|6|7|3|1|0|0|0|0|0|0|0|0|3|5|0|0|0|0|2|4|4|1|7|0|0|3|5	0
TPCN2_DeltaCT	Q9P1Z3	HCN3	0|0|0	0|0|0|0|0	0|0|0|0|0|0|0|0|0|0|0|0|0|0|0|0|0|0|0|0|0|0|0|0|0|0|0|0|0|0|0	0
TPCN2_DeltaCT	Q9Y5B9	SUPT16H	2|0|0	7|0|0|0|0	4|5|0|1|0|5|6|1|1|1|1|1|1|2|2|1|2|4|4|1|1|0|0|1|0|1|0|1|7|0	0
TPCN2_DeltaCT	Q01130	SRSF2	3|0|0	2|0|0|0|0	0|0|2|1|0|0|0|0|0|0|0|0|0|0|0|0|0|0|0|0|0|0|0|0|0|0|0|0|0|0|0|2|0|0|0|0|0|2|18	0

TPCN2_DeltaCT	P48047	ATP5O	2|0|0	0|0|0|0|2	0|0|0|0|0|0|0|2|2|3|2|2|3|0|0|0|0|2|2|2|0|0|0|0|0|0|0|1|3	0
TPCN2_DeltaCT	P17812	CTPS1	5|0|2	3|0|0|0|2	22|23|22|21|14|25|21|0|0|1|2|0|0|21|27|9|2|3|10|7|15|17|13|17|14|18|9|8|3|6	0
TPCN2_DeltaCT	Q14318	FKBP8	0|0|0	2|0|0|0|0	0|0|0|0|0|0|0|0|1|2|1|0|0|0|0|0|0|4|1|0|1|0|2|0|0|0|1|0|0|1	0
TPCN2_DeltaCT	Q9UJZ1	STOML2	0|0|0	4|0|0|0|2	0|0|0|0|0|0|0|0|0|0|0|0|0|0|0|0|0|0|0|0|0|0|5|0|1|0|0|0|0|0	0
TPCN2_DeltaCT	Q16643	DBN1	10|0|0	9|0|0|0|7	19|15|5|3|5|4|13|5|1|3|2|0|4|21|19|8|6|16|12|16|20|2|7|0|0|2|12|13|27|0	0
TPCN2_DeltaCT	P82675	MRPS5	0|2|0	0|0|0|6|3	0|0|0|0|0|0|1|1|1|1|2|2|4|0|0|0|0|0|0|0|0|0|0|0|0|0|0|0|0|0|0	0
TPCN2_DeltaCT	Q9Y490	TLN1	16|0|0	0|5|7|0|0	22|21|43|21|10|42|42|1|0|0|0|0|0|10|10|9|1|16|25|19|32|40|32|19|33|16|18|25|0|1	0
TPCN2_DeltaCT	P14314	PRKCSH	18|0|8	22|11|6|0|15	0|0|0|0|0|0|0|0|1|1|0|1|0|0|0|0|0|0|0|0|0|0|2|0|0|0|0|0|0|10	0
TPCN2_DeltaCT	P00367	GLUD1	4|0|0	4|0|0|0|4	0|0|7|1|0|2|0|2|3|2|2|3|3|0|0|0|0|0|0|0|0|0|2|3|1|2|0|0|2|3	0
TPCN2_DeltaCT	P38606	ATP6V1A	9|0|0	10|0|0|0|6	1|0|5|5|2|7|6|1|0|0|0|0|0|0|0|2|1|0|1|2|0|4|4|1|2|3|0|0|0|1	0
TPCN2_DeltaCT	P08670	VIM	101|33|50	87|37|38|44|96	93|113|66|90|91|56|111|50|44|52|36|33|43|131|117|209|180|92|106|115|242|87|90|44|38|91|1	0

TPCN2_DeltaCT	P42285	SKIV2L2	6|0|0	0|0|0|0|0	1|1|30|35|43|2|2|0|0|0|0|0|0|0|0|12|3|1|2|0|0|12|38|21|27|39|0|0|8|1	0
TPCN2_DeltaCT	P32969	RPL9	3|0|5	3|4|4|4|5	8|6|13|9|6|7|5|6|5|5|5|4|8|3|2|9|4|3|2|2|1|4|8|5|6|5|4|3|8|1	0
TPCN2_DeltaCT	P31930	UQCRC1	5|0|0	6|0|0|0|7	0|0|0|0|0|0|1|3|3|3|5|3|2|0|0|3|0|1|2|0|0|0|1|0|0|0|0|1|0|0	0
TPCN2_DeltaCT	P04844	RPN2	5|0|2	4|0|0|0|3	2|1|3|0|1|4|9|6|6|8|3|2|3|0|0|4|2|1|2|0|1|0|6|0|1|3|0|1|5|0	0
TPCN2_DeltaCT	P04843	RPN1	10|0|0	12|0|3|0|11	3|0|2|0|3|3|4|2|3|2|2|1|2|0|0|1|1|1|0|1|0|0|2|0|0|0|0|0|7|8	0
TPCN2_DeltaCT	Q5C9Z4	NOM1	7|9|12	11|6|6|22|11	0|0|0|0|0|0|0|0|0|0|0|0|0|0|0|0|0|0|0|0|0|0|0|0|0|0|0|0|0|0|0	0
TPCN2_DeltaCT	P49321	NASP	7|0|2	7|0|0|0|4	33|35|45|51|39|40|57|0|0|0|0|0|0|26|34|8|9|9|9|6|16|36|40|31|32|36|11|17|8|23	0
TPCN2_DeltaCT	Q99623	PHB2	15|2|4	13|5|7|2|15	0|0|14|23|15|13|21|1|0|0|1|0|0|0|0|18|19|0|0|0|0|11|18|7|9|13|0|0|15|1	0
TPCN2_DeltaCT	A6NHR9	SMCHD1	0|0|0	0|0|0|0|0	3|3|7|4|7|0|1|0|0|0|0|0|0|0|0|1|1|3|1|2|2|4|9|1|0|3|0|1|6|0	0
TPCN2_DeltaCT	P42224	STAT1	0|0|0	0|0|0|0|0	8|5|7|1|0|7|10|0|0|0|0|0|0|3|4|0|0|1|3|6|11|6|0|5|3|0|0|0|3|0	0
TPCN2_DeltaCT	P18085	ARF4	0|2|0	0|0|0|2|0	5|3|5|6|1|4|1|2|4|4|4|3|2|3|1|2|0|2|1|2|1|0|2|1|0|0|1|0|5|1	0

TPCN2_DeltaCT	Q9P2E9	RRBP1	21|0|0	5|0|0|5|4	1|1|0|1|1|0|0|1|1|0|1|1|1|2|3|2|4|22|26|13|12|0|1|0|0|0|14|10|0|0	0
TPCN2_DeltaCT	Q9UBT2	UBA2	3|0|0	0|0|0|0|0	0|0|2|0|0|2|0|0|0|0|0|0|0|0|0|0|0|0|0|0|0|0|2|1|2|2|0|0|0|0|8	0
TPCN2_DeltaCT	Q8WTT2	NOC3L	6|9|7	10|4|8|26|14	0|1|6|3|3|0|1|0|0|0|0|0|0|0|0|1|0|2|2|2|1|4|5|2|1|4|0|1|3|0	0
TPCN2_DeltaCT	P08559	PDHA1	6|0|0	0|0|0|0|2	0|0|0|0|0|0|0|13|14|16|17|17|17|0|0|0|0|0|0|0|0|0|0|0|0|0|0|1|0|1	0
TPCN2_DeltaCT	P04792	HSPB1	0|0|2	3|0|0|0|0	1|1|0|0|0|0|0|0|0|0|0|0|0|0|0|9|21|0|1|0|0|0|0|0|0|0|0|1|0|0	0
TPCN2_DeltaCT	P30050	RPL12	3|0|2	4|2|2|0|6	4|3|5|6|7|2|1|4|4|4|5|5|5|4|1|1|3|2|2|1|2|4|6|2|5|5|5|3|4|0	0
TPCN2_DeltaCT	P61254	RPL26	0|0|6	0|5|4|0|0	0|0|10|4|6|7|5|0|0|0|0|0|0|0|0|0|2|0|0|0|0|2|4|1|2|2|0|0|1|2	0
TPCN2_DeltaCT	P21333	FLNA	90|0|0	0|31|37|0|10	1875|1821|839|866|394|425|442|22|18|18|15|15|16|914|1136|564|459|490|984|625|1175|445|57	0
TPCN2_DeltaCT	Q15459	SF3A1	6|0|0	10|0|0|0|3	23|20|15|12|4|6|13|3|1|1|1|1|2|17|17|9|13|11|15|14|22|7|15|7|2|9|15|12|7|15	0
TPCN2_DeltaCT	P49711	CTCF	0|0|0	0|0|0|0|0	4|1|2|0|1|0|2|0|0|0|0|0|0|1|1|2|1|1|5|2|5|1|3|0|0|2|3|1|1|0	0
TPCN2_DeltaCT	Q9UJV9	DDX41	0|0|2	0|0|2|0|0	0|0|1|1|1|2|0|0|0|0|0|0|0|0|0|0|0|0|1|0|0|2|1|0|0|2|0|0|0|0	0

TPCN2_DeltaCT	P30837	ALDH1B1	3|0|0	3|0|0|0|2	0|0|0|0|0|0|0|4|3|3|4|5|3|0|0|0|0|0|0|0|0|0|1|0|0|0|0|0|0|0	0
TPCN2_DeltaCT	O75683	SURF6	3|12|29	13|14|28|24|10	6|5|2|4|3|0|1|0|0|0|0|0|0|2|3|0|0|5|7|5|4|2|4|0|1|2|5|7|1|0	0
TPCN2_DeltaCT	Q7KZF4	SND1	32|0|12	38|19|17|0|33	5|4|4|4|2|9|10|5|10|10|5|7|4|5|7|0|0|5|8|5|8|3|11|6|8|2|5|6|1|13	0
TPCN2_DeltaCT	Q14444	CAPRIN1	5|0|0	4|0|0|0|0	6|7|6|2|0|1|0|2|1|1|1|1|1|4|4|6|1|4|3|3|3|2|2|0|0|4|3|5|0|4	0
TPCN2_DeltaCT	P42566	EPS15	2|2|2	0|0|0|0|0	1|2|6|3|2|2|9|0|0|0|0|0|0|0|1|1|1|4|1|7|8|6|10|3|0|7|3|2|0|0	0
TPCN2_DeltaCT	P51610	HCFC1	10|0|0	5|0|0|0|0	48|40|43|43|40|36|46|2|0|0|0|0|0|53|51|36|16|45|64|58|84|28|59|17|15|39|52|50|17|1	0
TPCN2_DeltaCT	Q92688	ANP32B	2|0|0	0|0|0|0|0	0|0|0|0|0|0|0|0|0|0|0|0|0|0|0|0|0|0|0|0|0|0|0|0|0|0|0|0|0|16	0
TPCN2_DeltaCT	P14625	HSP90B1	65|4|23	59|17|18|0|50	2|2|3|1|2|1|3|12|13|12|10|10|10|2|2|1|0|4|4|1|1|1|9|1|2|2|2|2|0|58	0
TPCN2_DeltaCT	Q9Y285	FARSA	5|0|0	4|0|0|0|4	0|0|4|0|4|4|12|0|0|0|0|0|0|0|0|2|0|0|0|0|0|2|5|0|2|2|0|0|0|2	0
TPCN2_DeltaCT	O00267	SUPT5H	0|0|0	0|0|0|0|0	1|0|0|1|0|1|0|1|0|0|0|0|0|2|1|1|0|0|0|0|0|0|0|0|0|0|1|1|0|0|12	0
TPCN2_DeltaCT	P08865	RPSA	9|0|4	8|4|3|0|7	1|0|2|1|3|2|1|2|1|1|1|1|2|0|0|7|0|0|1|0|0|2|6|2|2|1|0|0|0|11	0

TPCN2_DeltaCT	P17174	GOT1	0|0|0	2|0|0|0|0	0|0|0|0|0|0|0|0|0|0|0|0|0|0|0|0|0|0|0|0|0|0|0|0|0|0|0|0|0|0|0	0
TPCN2_DeltaCT	P52701	MSH6	0|0|0	0|0|0|0|0	3|2|4|7|1|6|1|0|0|0|0|0|0|3|7|1|2|1|3|0|4|4|5|1|3|6|0|1|2|4	0
TPCN2_DeltaCT	P11310	ACADM	0|0|0	3|0|0|0|3	0|0|0|0|0|0|0|5|2|2|7|5|9|0|0|0|0|0|0|0|0|0|0|0|0|0|0|0|0|0|0	0
TPCN2_DeltaCT	Q07020	RPL18	15|15|16	21|11|15|20|18	1|1|10|4|8|5|6|0|2|1|1|2|1|2|1|3|3|0|1|1|0|2|6|4|3|5|1|0|11|0	0
TPCN2_DeltaCT	P46019	PHKA2	0|0|0	0|0|0|0|2	0|0|0|0|0|0|0|0|0|0|0|0|0|0|0|0|0|0|0|0|0|0|0|0|0|0|0|0|0|0|0	0
TPCN2_DeltaCT	P22492	HIST1H1T	0|2|0	0|0|0|0|0	4|2|8|16|11|6|6|1|2|1|1|2|1|4|2|6|5|9|4|3|2|3|8|5|6|11|5|1|7|1	0
TPCN2_DeltaCT	O95573	ACSL3	21|5|7	22|8|8|4|19	1|1|1|0|0|5|3|1|2|2|2|1|1|0|0|0|1|1|2|1|1|2|1|1|0|1|1|1|1|0	0
TPCN2_DeltaCT	P13010	XRCC5	29|0|4	22|7|0|0|20	9|7|4|0|1|1|2|16|7|4|3|10|5|2|4|2|0|2|5|5|3|9|11|2|4|6|4|3|5|54	0
TPCN2_DeltaCT	P10809	HSPD1	71|7|23	63|14|18|3|65	9|5|3|2|5|2|2|67|53|64|71|66|82|5|4|32|16|14|27|11|19|2|32|2|9|9|22|15|5|40	0
TPCN2_DeltaCT	Q8WUM4	PDCD6IP	4|0|4	6|0|7|0|0	0|0|1|1|1|3|5|1|0|1|0|0|0|0|0|0|0|0|0|0|0|2|3|2|2|2|0|1|4|0	0
TPCN2_DeltaCT	Q9Y2W1	THRAP3	2|0|0	0|0|0|0|0	35|37|44|41|23|25|45|0|0|0|0|0|0|43|37|40|21|27|38|35|61|6|41|13|16|31|38|40|11|7	0

TPCN2_DeltaCT	Q09028	RBBP4	3|0|6	4|5|0|0|2	0|1|21|17|22|10|6|2|0|1|1|1|1|1|0|3|5|0|0|1|0|5|13|6|7|8|0|0|6|13	0
TPCN2_DeltaCT	P07237	P4HB	38|0|15	35|17|14|0|30	0|0|0|0|0|0|0|5|1|3|0|1|1|0|0|0|0|0|0|0|0|0|2|0|0|0|0|1|0|13	0
TPCN2_DeltaCT	O95347	SMC2	0|0|0	4|0|0|0|0	0|0|2|0|4|1|1|0|0|0|0|0|0|0|0|0|1|0|0|0|0|3|4|2|4|7|0|0|5|12	0
TPCN2_DeltaCT	P55854	SUMO3	2|0|0	0|0|0|0|2	1|1|0|1|0|0|1|0|0|0|0|0|0|1|1|0|0|0|1|0|1|0|1|0|0|1|1|1|1|0	0
TPCN2_DeltaCT	P49368	CCT3	17|0|11	20|4|5|0|14	0|0|54|55|64|22|10|1|0|1|0|0|0|0|0|4|23|0|1|0|0|69|43|116|108|72|0|0|21|41	0
TPCN2_DeltaCT	Q13310	PABPC4	13|0|3	14|4|0|3|7	3|4|14|10|4|10|6|1|0|1|1|0|1|1|2|3|0|1|2|1|3|7|10|3|7|6|2|2|6|7	0
TPCN2_DeltaCT	P10515	DLAT	0|0|0	2|0|0|0|2	0|0|0|0|0|0|0|0|0|0|1|1|0|0|0|0|0|0|0|0|0|0|0|0|0|0|0|0|0	0
TPCN2_DeltaCT	Q9HCU4	CELSR2	0|0|0	0|0|0|0|0	0|0|0|0|0|0|0|0|0|0|0|0|0|0|0|0|0|0|0|0|0|0|0|0|0|0|0|0	0
TPCN2_DeltaCT	P05023	ATP1A1	31|0|8	33|6|10|0|32	0|0|2|3|4|1|0|8|8|9|2|3|7|0|0|0|2|0|1|0|0|1|9|2|2|3|1|2|8|6	0
TPCN2_DeltaCT	P45880	VDAC2	9|0|4	11|5|2|0|9	10|9|7|7|10|9|9|17|20|14|10|11|15|11|11|14|6|9|8|8|7|5|8|0|1|6|8|9|2|0	0
TPCN2_DeltaCT	Q14152	EIF3A	11|0|0	2|0|2|0|3	2|1|17|16|20|9|5|0|0|0|0|0|0|1|0|5|4|0|2|2|4|9|23|13|6|25|0|1|6|5	0

TPCN2_DeltaCT	P11388	TOP2A	0|0|0	0|0|0|0|0	49|39|0|0|0|2|8|12|5|6|4|5|5|42|44|12|13|47|67|32|45|1|2|3|2|0|76|63|4|0	0
TPCN2_DeltaCT	Q14683	SMC1A	3|0|0	2|0|0|0|0	0|0|7|14|7|4|3|0|0|0|0|0|0|0|0|9|4|0|0|0|1|6|20|4|8|15|0|0|6|10	0
TPCN2_DeltaCT	P08237	PFKM	4|0|5	9|5|3|0|5	0|0|0|0|0|3|1|0|0|0|0|0|0|0|0|0|0|0|2|0|1|1|0|0|0|0|0|0|0|1	0
TPCN2_DeltaCT	P15586	GNS	0|0|0	2|0|0|0|3	0|0|0|0|0|0|0|0|0|0|0|0|0|0|0|0|0|0|0|0|0|0|0|0|0|0|0|0|0|0|0	0
TPCN2_DeltaCT	P08238	HSP90AB1	80|10|43	80|40|39|2|56	29|26|14|18|11|30|28|25|23|25|23|22|24|28|30|13|8|12|17|12|18|14|24|10|16|16|14|16|16|14	0
TPCN2_DeltaCT	P28331	NDUFS1	0|0|0	3|0|0|2|2	0|0|0|0|0|0|0|0|1|2|2|2|4|0|0|0|0|0|0|0|0|0|0|0|0|0|0|0|0|0|0	0
TPCN2_DeltaCT	Q7L014	DDX46	0|0|0	0|0|0|0|0	46|50|68|85|44|31|59|0|0|0|0|0|62|58|37|27|25|42|43|50|36|51|33|40|50|45|39|42|32	0
TPCN2_DeltaCT	Q2TB10	ZNF800	0|0|0	0|0|0|0|0	0|0|0|0|0|0|0|0|0|0|0|0|0|0|0|0|0|0|0|0|0|0|0|0|0|0|0|0|0|0	0
TPCN2_DeltaCT	P62820	RAB1A	4|0|3	5|2|0|0|6	6|2|0|0|0|3|6|6|6|5|5|6|6|15|12|9|2|8|6|11|4|0|2|0|0|0|5|4|1|3	0
TPCN2_DeltaCT	Q1KMD3	HNRNPUL2	0|0|0	7|0|0|0|0	1|1|0|0|0|0|1|1|2|0|1|1|1|2|2|0|0|0|0|0|1|0|0|0|0|2|1|0|4	0
TPCN2_DeltaCT	P62826	RAN	4|0|5	3|4|4|0|0	9|12|41|37|30|27|29|10|11|11|8|8|8|8|9|12|17|4|6|2|9|15|23|14|15|25|11|9|13|11	0

TPCN2_DeltaCT	P50213	IDH3A	8|0|0	7|0|0|0|9	0|0|0|0|0|0|0|4|3|4|6|4|4|0|0|0|0|0|0|0|0|0|0|0|0|0|1|0|0|1	0
TPCN2_DeltaCT	Q9Y4W6	AFG3L2	8|0|0	6|0|0|0|6	0|0|0|0|0|0|0|4|3|7|10|6|7|0|0|0|0|0|0|0|0|0|0|0|0|0|0|0|0	0
TPCN2_DeltaCT	P63167	DYNLL1	0|0|3	0|0|4|0|2	2|2|6|4|5|5|0|1|1|0|1|1|1|1|2|1|1|0|1|3|1|6|3|4|4|4|0|1|0|0	0
TPCN2_DeltaCT	O15226	NKRF	0|0|0	0|0|0|0|0	1|1|1|3|0|0|0|0|0|0|0|0|0|1|1|0|1|1|1|0|2|0|4|0|0|3|1|1|0|0	0
TPCN2_DeltaCT	Q9P2J5	LARS	7|0|0	3|0|0|0|0	4|2|5|7|9|3|3|2|3|1|1|1|1|0|0|1|1|2|3|2|4|9|11|12|14|9|1|2|7|7	0
TPCN2_DeltaCT	Q9BZE4	GTPBP4	2|2|2	9|0|0|7|6	3|1|2|3|2|0|0|0|0|0|0|0|0|1|1|1|1|2|2|1|0|3|1|0|1|0|1|1|0	0
TPCN2_DeltaCT	Q92598	HSPH1	15|0|5	11|8|6|0|5	4|3|9|6|3|7|8|0|0|1|2|0|1|5|3|4|3|2|2|5|3|13|4|7|6|7|1|2|0|26	0
TPCN2_DeltaCT	P33993	MCM7	6|0|3	6|0|2|0|3	0|0|12|15|8|9|12|1|1|0|1|1|1|0|0|2|3|0|0|0|0|7|10|6|9|7|0|0|11|27	0
TPCN2_DeltaCT	P33991	MCM4	5|0|0	8|0|3|0|2	4|2|6|5|2|9|7|0|0|0|0|0|0|0|1|2|3|0|1|3|4|9|4|5|3|6|4|3|8|19	0
TPCN2_DeltaCT	P50914	RPL14	5|5|11	6|7|6|6|9	1|3|3|3|6|8|2|0|0|0|0|0|0|0|0|4|4|1|2|1|1|1|5|5|1|6|1|1|3|1	0
TPCN2_DeltaCT	P62906	RPL10A	4|0|0	5|2|0|4|5	0|0|7|6|9|1|1|0|0|0|0|0|0|0|0|5|5|0|0|0|0|2|10|4|2|8|0|0|1|0	0

TPCN2_DeltaCT	P47914	RPL29	2|0|5	2|2|4|0|2	2|3|3|4|3|4|3|1|0|1|0|0|1|0|2|1|2|0|1|0|2|1|2|1|1|3|1|1|2|1	0
TPCN2_DeltaCT	Q86VP6	CAND1	18|0|6	22|3|3|0|9	0|0|9|4|1|10|5|0|0|0|0|0|0|0|0|0|0|0|0|0|0|6|13|5|9|4|0|0|10|10	0
TPCN2_DeltaCT	P57721	PCBP3	0|0|3	0|0|0|0|0	2|4|4|4|4|11|3|2|2|2|1|1|2|2|2|3|2|3|2|3|6|4|5|4|4|2|2|2|3	0
TPCN2_DeltaCT	P43490	NAMPT	5|0|6	3|4|5|0|0	0|0|4|5|4|4|8|0|0|0|0|0|0|0|0|2|0|0|0|0|7|5|3|7|3|0|0|1|0	0
TPCN2_DeltaCT	P35232	PHB	7|2|3	8|0|4|2|7	0|0|3|0|3|3|5|1|1|2|1|1|0|0|0|2|3|0|0|0|0|5|14|2|5|7|0|0|7|0	0
TPCN2_DeltaCT	P83731	RPL24	0|0|3	0|0|0|0|0	5|4|6|7|6|4|6|1|1|1|0|0|0|10|5|6|6|2|3|2|3|5|8|8|13|13|2|2|4|2	0
TPCN2_DeltaCT	P15924	DSP	0|2|16	0|2|23|26|0	1|0|5|1|1|2|0|3|4|5|0|0|0|0|0|3|2|2|4|5|3|13|2|3|3|4|0|3|8|4	0
TPCN2_DeltaCT	Q12789	GTF3C1	0|0|0	0|0|0|0|0	1|0|7|4|4|0|0|0|0|0|0|0|0|0|0|7|3|3|4|2|2|4|9|0|3|5|4|2|1|0	0
TPCN2_DeltaCT	P06753	TPM3	2|0|0	0|0|0|0|0	3|2|1|0|0|1|0|3|3|2|4|5|3|2|1|1|0|2|2|2|1|0|4|0|0|0|0|3|5|12	0
TPCN2_DeltaCT	P49591	SARS	0|0|0	0|0|0|0|0	0|0|0|0|0|0|0|0|0|0|0|0|0|0|0|0|0|0|0|0|0|0|0|0|0|0|0|0|0	0
TPCN2_DeltaCT	Q9H8Y8	GORASP2	2|0|0	2|0|0|0|2	1|0|0|0|0|2|0|0|0|0|0|0|0|2|0|0|0|0|1|0|1|0|0|0|0|0|0|0|0|0	0

TPCN2_DeltaCT	Q9UH92	MLX	0|0|0	0|0|0|0|0	0|0|0|0|0|4|0|0|0|0|0|0|0|0|0|0|0|0|0|0|0|0|0|0|0|0|0|0|0|0|0	0
TPCN2_DeltaCT	P51532	SMARCA4	0|0|0	0|0|0|0|0	12|9|7|6|5|0|0|0|0|0|0|0|0|7|5|20|8|16|10|20|14|0|7|0|1|6|20|14|2|0	0
TPCN2_DeltaCT	P62081	RPS7	3|0|3	5|0|0|0|0	6|4|19|11|13|11|12|3|2|2|4|0|2|2|3|6|5|1|2|2|2|21|8|17|23|18|1|2|14|7	0
TPCN2_DeltaCT	P30405	PPIF	0|0|0	5|0|0|0|2	0|0|0|0|0|0|0|1|1|1|1|1|1|0|0|0|0|0|0|0|0|0|1|0|0|0|0|0|0|0	0
TPCN2_DeltaCT	P62249	RPS16	0|0|2	0|2|0|0|0	3|2|6|7|7|8|4|3|3|2|2|2|4|3|1|6|2|1|3|0|0|1|6|2|3|9|0|1|0|7	0
TPCN2_DeltaCT	Q8N0X7	SPG20	0|0|2	0|0|5|0|0	0|3|7|0|0|4|3|0|0|0|0|0|0|1|1|0|0|1|0|1|1|4|1|3|2|1|0|0|0|0	0
TPCN2_DeltaCT	Q16610	ECM1	0|0|0	0|0|0|0|2	0|0|0|0|0|0|0|0|0|0|0|0|0|0|0|0|0|0|0|0|0|0|0|0|0|0|0|0|0|0	0
TPCN2_DeltaCT	P42765	ACAA2	2|0|0	3|0|0|0|3	0|0|0|0|0|0|0|2|2|3|5|4|7|0|0|0|0|0|0|0|0|0|0|0|0|0|0|0|0|0|1	0
TPCN2_DeltaCT	Q9H0D6	XRN2	3|0|0	5|0|0|0|2	0|1|7|1|2|1|4|0|0|0|0|0|0|0|0|5|0|3|1|3|3|4|1|2|0|0|1|1|4|2	0
TPCN2_DeltaCT	P68371	TUBB4B	29|0|19	33|13|20|5|14	19|22|74|96|78|68|46|23|17|23|20|16|18|14|23|35|45|8|15|7|9|66|66|85|82|81|11|17|92|137	0
TPCN2_DeltaCT	O43143	DHX15	4|0|0	6|0|0|0|0	9|8|18|15|11|7|14|9|7|6|5|4|5|7|9|26|16|4|4|6|8|7|16|10|10|13|9|4|5|12	0

TPCN2_DeltaCT	Q9NZT1	CALML5	0|0|0	0|0|0|0|0	0|0|0|0|0|0|0|0|0|0|0|0|0|0|0|0|0|0|0|0|0|0|0|0|0|0|0|0|0|0|0	0
TPCN2_DeltaCT	Q6NUQ4	TMEM214	0|0|0	2|0|0|0|2	0|0|0|0|0|0|0|0|0|0|0|0|0|0|0|0|0|0|0|0|0|0|0|0|0|0|0|0|0|0|0	0
TPCN2_DeltaCT	P61204	ARF3	0|0|0	0|0|0|0|0	7|3|15|7|4|20|6|2|5|5|4|4|1|6|3|8|2|4|0|2|2|6|7|1|1|4|4|3|8|5	0
TPCN2_DeltaCT	O15042	U2SURP	0|0|0	0|0|0|0|0	26|29|42|35|27|13|22|0|0|0|0|0|0|15|22|30|14|15|22|26|32|19|39|17|12|32|31|26|16|2	0
TPCN2_DeltaCT	P53618	COPB1	7|0|0	8|0|0|0|0	4|3|12|2|3|3|3|1|0|2|1|1|1|2|4|0|0|1|1|4|1|1|6|2|3|4|2|1|1|12	0
TPCN2_DeltaCT	Q5T1M5	FKBP15	0|0|0	0|0|0|0|0	1|1|0|1|0|0|0|0|0|0|0|0|0|1|0|0|0|0|1|2|0|0|0|0|0|1|0|0	0
TPCN2_DeltaCT	P04062	GBA	0|0|0	0|0|0|0|0	0|0|0|0|0|0|0|0|0|0|0|0|0|0|0|0|0|0|0|0|0|0|0|0|0|0|0|0|0|0|0	0
TPCN2_DeltaCT	P18124	RPL7	21|27|31	24|31|28|37|28	0|1|10|8|6|10|10|1|0|0|1|0|0|0|0|2|3|2|1|0|1|5|13|6|5|6|0|2|8|1	0
TPCN2_DeltaCT	P08195	SLC3A2	17|0|5	13|3|5|0|14	21|17|1|1|0|0|0|8|8|8|6|8|7|20|19|3|4|10|18|7|14|0|1|0|1|0|9|13|0|0	0
TPCN2_DeltaCT	P16403	HIST1H1C	7|0|21	21|11|13|0|9	10|6|40|51|33|22|25|11|13|9|6|6|5|7|6|21|30|19|16|12|7|10|31|29|22|39|15|7|20|10	0
TPCN2_DeltaCT	Q9Y2A7	NCKAP1	3|0|0	3|0|0|0|0	0|0|7|6|1|6|0|0|0|0|0|0|0|0|0|0|0|0|0|0|0|0|0|0|0|0|0|0|0|1|1|2|1|0|0|0|102	0

TPCN2_DeltaCT	Q14980	NUMA1	4|0|0	0|0|0|13|0	108|84|31|54|89|3|17|10|6|10|1|1|1|92|103|174|173|176|277|124|150|24|111|27|20|66|250|26	0
TPCN2_DeltaCT	O43707	ACTN4	12|0|0	11|2|0|0|4	20|11|5|0|0|3|1|9|9|7|1|2|2|9|8|0|0|8|8|14|16|0|6|0|0|0|6|4|66|21	0
TPCN2_DeltaCT	Q5D862	FLG2	0|2|0	0|0|2|3|0	0|0|0|0|0|0|0|3|1|3|0|0|0|0|0|0|0|1|0|0|0|0|0|0|0|0|1|0|0	0
TPCN2_DeltaCT	P34932	HSPA4	27|0|12	27|11|12|0|12	2|1|18|5|4|2|2|0|2|1|1|3|2|2|1|2|2|2|0|1|0|10|13|8|8|7|0|1|6|37	0
TPCN2_DeltaCT	P51149	RAB7A	0|0|2	6|2|0|0|3	4|2|0|0|0|0|2|5|7|5|3|3|2|3|2|7|4|2|2|0|1|0|0|0|0|0|1|3|0|1	0
TPCN2_DeltaCT	P51148	RAB5C	3|0|0	2|0|0|0|4	0|0|1|0|1|2|2|2|1|1|1|0|2|0|0|6|1|0|0|0|0|1|0|0|0|0|0|0|2|0	0
TPCN2_DeltaCT	Q13045	FLII	0|0|0	0|0|0|0|0	0|0|1|0|0|0|0|0|0|0|0|0|0|0|0|0|0|0|0|0|0|0|0|1|0|0|0|0|1	0
TPCN2_DeltaCT	P49327	FASN	44|0|5	0|28|37|0|4	63|59|554|261|157|600|327|0|0|0|0|0|0|42|43|135|72|44|57|39|53|497|160|242|234|208|84|69	0
TPCN2_DeltaCT	O43684	BUB3	0|0|2	3|0|0|0|0	3|2|8|8|6|6|4|5|4|6|7|3|4|3|2|2|1|1|4|1|3|2|3|2|3|4|2|2|1|6	0
TPCN2_DeltaCT	P55265	ADAR	17|0|0	17|0|0|0|11	13|9|18|11|12|12|4|3|4|2|1|1|1|14|11|13|7|7|10|12|10|2|25|5|3|11|7|5|6|0	0
TPCN2_DeltaCT	P10412	HIST1H1E	0|0|0	15|0|0|0|0	9|6|31|47|33|21|23|8|10|9|3|4|2|7|7|25|22|14|13|10|10|13|25|25|16|31|10|3|22|10	0

TPCN2_DeltaCT	P04920	SLC4A2	0|0|0	0|0|0|0|0	0|0|0|0|0|0|0|0|0|0|0|0|0|0|0|0|0|0|0|0|0|0|0|0|0|0|0|0|0|0|0	0
TPCN2_DeltaCT	P62424	RPL7A	7|7|10	11|6|8|9|10	1|1|17|15|10|14|10|3|3|1|1|1|1|2|2|6|9|1|2|1|2|7|10|8|10|10|2|1|12|0	0
TPCN2_DeltaCT	O95602	POLR1A	0|0|0	0|0|0|0|0	0|0|0|0|0|0|0|0|0|0|0|0|0|0|0|0|0|0|0|0|0|0|0|0|0|0|0|0|0|0|0	0
TPCN2_DeltaCT	P07900	HSP90AA1	63|0|44	66|44|45|0|46	10|14|11|8|10|12|17|20|17|16|15|17|12|11|14|8|1|5|7|4|7|6|27|4|10|13|6|8|9|166	0
TPCN2_DeltaCT	P26373	RPL13	9|7|13	12|7|12|9|10	3|3|7|10|10|7|6|3|3|4|3|2|3|1|3|4|5|2|4|2|3|2|10|3|1|8|3|3|2|1	0
TPCN2_DeltaCT	P11940	PABPC1	14|4|0	15|4|0|4|7	6|8|17|14|9|11|7|1|1|1|1|0|1|2|5|6|0|1|3|4|6|11|13|9|9|12|2|3|6|12	0
TPCN2_DeltaCT	Q86YZ3	HRNR	0|0|11	3|5|9|2|9	0|0|1|0|0|0|0|11|12|10|1|0|1|0|0|9|1|0|0|0|0|0|0|0|0|4|3|14|0|0	0
TPCN2_DeltaCT	Q99729	HNRNPAB	6|0|0	10|0|0|0|6	2|1|8|8|9|3|2|4|8|5|7|3|3|3|3|3|2|2|3|2|3|0|4|1|2|3|4|3|2|11	0
TPCN2_DeltaCT	P55795	HNRNPH2	20|0|0	16|0|0|0|16	2|2|5|4|5|6|3|6|4|6|5|6|6|2|1|4|4|4|3|2|4|3|8|4|4|8|3|2|6|10	0
TPCN2_DeltaCT	P14618	PKM	58|12|25	63|27|24|14|31	23|24|18|5|3|29|31|12|11|9|12|8|11|16|19|24|2|7|7|10|7|28|24|12|15|9|8|6|3|48	0
TPCN2_DeltaCT	O95140	MFN2	0|0|0	0|0|0|0|0	0|0|0|0|0|0|0|0|0|0|0|0|0|0|0|0|0|0|0|0|0|0|0|0|0|0|0|0|0|0|0	0

TPCN2_DeltaCT	P27824	CANX	32|0|8	31|16|10|0|24	1|1|0|0|0|1|2|4|4|4|3|3|3|0|0|0|0|1|1|0|0|0|4|0|0|0|0|0|2|33	0
TPCN2_DeltaCT	P25685	DNAJB1	0|0|2	0|0|0|0|0	4|2|2|0|1|5|2|0|0|0|0|0|0|0|2|0|0|3|4|1|5|1|1|0|0|0|3|2|1|0	0
TPCN2_DeltaCT	Q14157	UBAP2L	3|0|0	2|0|0|0|0	27|30|43|26|19|43|33|0|0|0|0|0|0|24|27|20|11|19|21|24|29|27|21|26|19|30|14|18|0|1	0
TPCN2_DeltaCT	P42167	TMPO	4|0|0	4|0|0|0|0	47|52|54|79|46|49|66|6|3|5|3|5|4|55|61|45|40|32|48|33|48|26|40|25|28|41|46|38|31|8	0
TPCN2_DeltaCT	Q6PKG0	LARP1	0|0|0	0|0|0|0|0	49|49|36|33|29|47|52|0|0|0|0|0|0|46|56|26|16|17|26|38|53|40|29|18|23|23|33|29|2|3	0
TPCN2_DeltaCT	Q8N3U4	STAG2	0|0|0	0|0|0|0|0	2|2|0|0|1|0|0|0|0|0|0|0|0|1|1|0|0|0|0|0|1|1|2|2|1|1|1|0|2|2	0
TPCN2_DeltaCT	P21281	ATP6V1B2	2|0|0	0|0|0|0|3	0|0|2|0|0|4|8|0|0|0|0|0|0|0|0|0|0|0|0|0|0|2|6|1|1|0|0|0|0|1	0
TPCN2_DeltaCT	Q15393	SF3B3	15|0|0	17|5|5|0|12	1|1|24|12|15|13|13|2|1|3|2|1|3|0|0|14|10|3|3|4|4|20|25|11|16|14|2|0|13|21	0
TPCN2_DeltaCT	Q9UDR5	AASS	0|0|0	3|0|0|0|0	0|0|0|0|0|1|0|0|0|0|0|0|0|0|0|0|0|0|1|0|1|0|1|0|1|1|0|0|1|0	0
TPCN2_DeltaCT	P19338	NCL	48|0|14	48|9|11|0|38	42|43|51|58|69|14|19|3|2|3|2|1|2|34|52|48|29|41|70|30|48|29|58|34|34|66|50|47|34|35	0
TPCN2_DeltaCT	Q00325	SLC25A3	5|4|6	8|2|5|3|6	2|1|7|6|6|5|4|2|2|2|3|1|3|2|2|5|4|1|2|1|1|1|8|4|2|4|2|1|3|2	0

TPCN2_DeltaCT	P02786	TFRC	19|0|8	19|9|11|0|17	2|1|0|0|0|0|0|8|4|4|3|4|3|0|1|3|0|1|2|2|1|0|0|0|0|0|0|0|0|0	0
TPCN2_DeltaCT	P63244	RACK1	6|0|2	8|2|2|0|6	10|10|7|3|5|10|8|16|16|14|12|15|16|13|14|8|3|8|16|8|8|5|6|1|4|2|15|14|2|4	0
TPCN2_DeltaCT	P02788	LTF	0|0|0	0|22|0|3|0	0|0|0|0|0|0|0|0|0|0|0|0|0|0|0|0|0|0|0|0|0|0|0|0|0|0|0|0|0|0|0	0
TPCN2_DeltaCT	P41091	EIF2S3	3|0|3	5|0|2|0|0	7|7|3|2|1|4|6|7|6|5|4|4|3|4|6|7|2|1|3|1|7|2|2|0|3|1|3|5|3|7	0
TPCN2_DeltaCT	O15260	SURF4	0|0|0	0|0|0|0|2	2|3|3|1|1|2|3|2|2|4|2|2|4|0|0|4|3|0|0|0|2|3|3|4|2|4|2|2|2|0	0
TPCN2_DeltaCT	P61619	SEC61A1	3|0|0	0|0|0|0|3	0|0|3|3|2|3|1|0|0|0|0|0|0|0|0|0|3|0|0|0|0|1|2|3|2|0|0|0|1|0	0
TPCN2_DeltaCT	Q9NZB2	FAM120A	0|0|0	0|0|0|0|0	1|0|1|1|0|0|0|0|0|0|0|1|0|1|2|0|0|1|1|1|1|0|1|0|0|1|1|2|0|0	0
TPCN2_DeltaCT	Q08211	DHX9	46|0|11	35|15|12|0|26	36|32|18|26|16|35|37|21|15|17|12|17|12|19|23|31|13|17|21|25|32|18|24|12|22|27|26|20|15|5	0
TPCN2_DeltaCT	Q9Y4I1	MYO5A	0|0|0	0|0|0|0|0	0|0|0|0|0|0|0|0|0|0|0|0|0|0|0|0|0|0|0|0|0|0|0|0|0|0|0|0|0|2|0	0
TPCN2_DeltaCT	Q9Y2J2	EPB41L3	0|0|0	0|0|0|0|0	2|0|67|52|36|55|84|0|0|0|0|0|0|3|3|0|0|1|2|2|3|25|54|24|24|44|2|2|1|5	0
TPCN2_DeltaCT	Q8TDN6	BRIX1	0|0|0	0|0|0|0|2	2|2|3|5|3|4|2|2|2|3|3|1|4|1|1|9|1|0|2|0|1|1|2|0|2|5|1|1|0|0	0

TPCN2_DeltaCT	Q86UP2	KTN1	6|0|0	6|0|0|0|0	15|6|2|0|1|0|0|0|0|0|0|0|0|13|6|6|1|26|22|15|21|0|5|0|0|1|18|26|0|0	0
TPCN2_DeltaCT	Q13509	TUBB3	22|0|13	0|0|0|0|0	9|12|39|70|48|47|27|14|13|14|14|13|12|8|12|20|27|6|10|4|5|33|42|47|47|47|7|10|63|109	0
TPCN2_DeltaCT	P52569	SLC7A2	0|0|0	0|0|0|0|0	0|0|0|0|0|0|0|0|0|0|0|0|0|0|0|0|0|0|0|0|0|0|0|0|0|0|0|0|0|0|0	0
TPCN2_DeltaCT	Q13501	SQSTM1	6|0|0	6|0|0|0|0	15|14|6|2|0|8|7|1|0|2|1|1|1|11|10|27|14|6|11|11|14|8|3|4|2|7|13|9|0|0	0
TPCN2_DeltaCT	Q9UHX1	PUF60	0|0|3	2|0|3|0|0	15|17|11|12|10|13|21|0|0|2|0|0|0|16|19|10|3|16|22|20|24|11|17|6|9|8|14|11|14|22	0
TPCN2_DeltaCT	Q86XP3	DDX42	2|0|0	0|0|0|0|0	21|19|19|15|10|24|14|0|0|0|0|0|0|12|15|7|7|15|12|14|18|9|12|4|7|10|8|14|8|2	0
TPCN2_DeltaCT	Q9BZF1	OSBPL8	3|0|0	0|0|0|0|0	1|2|5|1|0|5|1|0|0|0|0|0|0|2|0|1|0|2|1|2|2|0|0|1|0|0|0|0|0|0	0
TPCN2_DeltaCT	Q92945	KHSRP	19|0|2	20|3|0|0|11	10|7|19|26|20|13|19|11|9|7|7|8|8|10|9|4|3|9|5|10|8|10|27|10|9|16|6|7|4|15	0
TPCN2_DeltaCT	Q15084	PDIA6	11|0|0	12|0|0|0|11	0|0|1|1|3|1|0|2|2|2|0|2|3|0|0|1|0|0|0|0|0|0|10|0|1|1|0|0|0|33	0
TPCN2_DeltaCT	Q99798	ACO2	11|0|0	16|0|0|0|11	0|0|0|0|0|0|0|12|8|9|14|11|13|0|0|0|0|1|2|0|0|0|1|0|0|0|0|0|0|0	0
TPCN2_DeltaCT	Q7L576	CYFIP1	3|0|0	0|0|0|0|0	0|0|7|3|3|5|4|0|0|0|0|0|0|0|0|0|0|0|0|0|0|2|4|3|5|7|0|0|1|43	0

TPCN2_DeltaCT	P12270	TPR	2|0|0	0|0|0|0|0	72|39|59|94|105|19|42|0|0|0|0|0|0|58|34|148|258|149|250|114|153|46|104|45|38|110|184|140	0
TPCN2_DeltaCT	Q9UIQ6	LNPEP	0|0|0	0|0|0|0|0	0|0|0|0|0|0|0|0|0|0|0|0|0|0|0|0|0|0|0|0|0|0|0|0|0|0|0|0|0|0|0	0
TPCN2_DeltaCT	Q05682	CALD1	10|0|0	10|0|0|0|2	73|52|29|8|7|20|21|0|0|0|0|0|90|97|20|21|26|31|37|57|1|5|1|3|11|43|87|0|0	0
TPCN2_DeltaCT	Q02413	DSG1	0|2|0	0|0|6|8|0	0|0|0|0|0|0|0|3|4|2|0|0|0|0|0|0|0|0|0|0|0|0|0|0|0|0|0|0|0|0	0
TPCN2_DeltaCT	Q6ZVF9	GPRIN3	0|0|0	0|0|2|0|0	0|0|0|0|0|0|0|0|0|0|0|0|0|0|0|0|0|0|0|0|0|0|0|0|0|0|0|0|0|0|0	0
TPCN2_DeltaCT	Q14839	CHD4	0|0|0	0|0|0|0|0	106|94|103|101|100|31|41|3|3|3|1|1|3|105|95|121|88|61|79|73|83|69|89|63|53|84|102|101|39	0
TPCN2_DeltaCT	Q96KR1	ZFR	2|0|0	0|0|0|0|0	21|23|2|2|3|2|7|1|4|4|3|3|4|14|16|5|2|19|16|21|22|1|11|1|0|1|17|19|7|1	0
TPCN2_DeltaCT	P46087	NOP2	2|11|0	6|0|0|9|0	5|4|2|2|2|0|0|3|1|2|1|2|2|6|7|4|3|7|10|7|5|1|10|2|3|5|8|9|6|0	0
TPCN2_DeltaCT	Q92621	NUP205	0|0|0	0|0|0|0|0	0|0|8|2|3|1|0|0|1|1|1|1|0|0|0|2|3|1|1|1|1|1|5|3|1|0|1|0|3|0	0
TPCN2_DeltaCT	Q9Y265	RUVBL1	3|0|0	0|0|0|0|3	33|34|57|75|50|50|65|2|1|1|1|1|0|33|38|51|45|24|32|29|32|72|61|65|56|56|30|25|9|15	0
TPCN2_DeltaCT	P61247	RPS3A	6|0|9	10|3|0|0|8	5|3|14|7|5|12|6|1|2|1|0|0|0|5|5|8|5|3|3|3|2|4|5|6|8|5|3|4|1|2	0

TPCN2_DeltaCT	Q13619	CUL4A	2|0|0	0|0|0|0|0	3|3|2|0|1|2|0|0|0|0|0|0|0|5|4|4|3|0|0|1|1|1|0|1|0|0|0|0|1|1	0
TPCN2_DeltaCT	P35579	MYH9	32|0|12	0|24|9|0|3	24|15|119|86|124|0|1|9|9|7|5|7|6|12|13|6|45|37|63|22|22|117|85|130|116|143|62|55|137|60	0
TPCN2_DeltaCT	Q14204	DYNC1H1	2|0|0	0|2|0|0|0	0|0|4|3|13|2|3|0|0|0|0|0|0|1|0|1|2|0|2|0|0|9|10|12|13|16|0|0|13|22	0
TPCN2_DeltaCT	P13804	ETFA	4|0|0	2|0|2|0|3	1|0|0|0|0|1|0|10|12|12|14|14|13|0|0|1|0|2|3|2|2|1|4|0|1|1|1|2|1|2	0
TPCN2_DeltaCT	Q13616	CUL1	0|0|0	2|0|0|0|0	0|0|0|0|0|0|0|0|0|0|0|0|0|0|0|0|0|0|0|0|0|0|0|0|0|0|0|0|0|1	0
TPCN2_DeltaCT	P23786	CPT2	2|0|0	0|0|0|0|4	0|0|0|0|0|0|0|0|1|2|3|3|5|0|0|0|0|0|0|0|0|0|0|0|0|0|0|0|0|0|0|0	0
TPCN2_DeltaCT	P15311	EZR	13|0|9	0|0|5|0|0	13|11|10|1|1|24|14|0|0|0|0|1|0|2|3|1|0|1|2|5|9|9|3|1|1|1|2|2|0|4	0
TPCN2_DeltaCT	P53396	ACLY	14|0|8	17|7|5|0|7	0|0|6|2|0|2|3|2|2|3|1|2|1|0|0|0|0|0|0|0|0|3|5|2|3|2|0|1|0|14	0
TPCN2_DeltaCT	Q14562	DHX8	0|0|0	0|0|0|0|0	2|2|0|0|0|2|0|0|0|0|0|0|0|1|0|1|0|1|6|3|4|0|0|1|0|0|4|3|1|0	0
TPCN2_DeltaCT	P43686	PSMC4	0|0|0	4|0|0|0|6	0|0|4|0|1|2|1|0|0|0|0|0|0|0|0|1|1|0|1|0|0|1|2|1|2|2|0|1|0|22	0
TPCN2_DeltaCT	Q16629	SRSF7	2|0|0	2|0|0|0|2	2|2|1|5|4|0|2|1|2|0|1|1|1|2|2|1|3|0|1|0|0|1|6|3|2|3|1|0|3|14	0

TPCN2_DeltaCT	O43175	PHGDH	7|0|6	6|6|3|0|2	0|0|9|8|7|6|9|1|2|1|1|1|1|0|0|0|0|0|3|0|0|8|9|4|11|15|0|0|2|7	0
TPCN2_DeltaCT	P22059	OSBP	0|0|0	0|0|0|0|0	0|0|0|0|0|0|0|0|0|0|0|0|0|0|0|0|0|0|0|0|0|0|0|0|0|0|0|0	0
TPCN2_DeltaCT	P83881	RPL36A	0|0|3	0|0|2|0|0	1|0|1|1|1|4|2|0|0|0|0|0|0|0|0|2|0|0|0|0|0|0|1|0|0|1|0|0|0|0	0
TPCN2_DeltaCT	P49207	RPL34	0|0|0	0|0|0|2|3	0|1|2|0|1|0|0|0|0|0|0|0|0|1|0|1|1|0|0|0|0|1|1|1|1|0|0|0|0	0
TPCN2_DeltaCT	P48444	ARCN1	2|0|0	2|0|0|0|0	1|1|6|3|4|7|6|0|0|0|0|0|0|1|4|0|0|2|2|3|2|4|5|2|1|1|1|1|4|10	0
TPCN2_DeltaCT	O95104	SCAF4	0|0|0	0|0|0|0|0	0|0|4|6|2|1|2|0|0|0|0|0|0|0|0|0|0|0|0|0|0|4|4|0|0|2|0|0|1|0	0
TPCN2_DeltaCT	O14974	PPP1R12A	2|0|0	0|0|0|0|0	6|4|9|6|3|8|7|0|0|0|0|0|0|0|1|7|1|2|2|2|2|3|2|4|1|7|1|4|0|0	0
TPCN2_DeltaCT	Q15233	NONO	7|0|0	11|0|0|0|4	28|31|45|63|37|64|51|10|5|8|5|5|9|56|45|38|42|26|26|30|38|36|39|33|24|38|26|22|28|16	0
TPCN2_DeltaCT	P53621	COPA	7|0|0	9|0|3|4|5	1|0|0|0|0|0|1|0|0|0|0|0|0|0|1|0|0|0|1|1|0|0|1|0|0|0|0|0|0|18	0
TPCN2_DeltaCT	Q12906	ILF3	19|0|2	18|2|2|0|8	8|8|6|5|3|3|3|12|8|11|6|6|11|10|7|3|2|8|5|7|8|1|10|3|3|7|3|3|7|28	0
TPCN2_DeltaCT	Q12905	ILF2	5|0|0	8|0|0|0|5	0|0|7|2|1|4|3|0|2|0|2|1|1|0|0|2|0|1|1|1|0|2|14|0|1|3|0|0|9|18	0

TPCN2_DeltaCT	Q99459	CDC5L	0|0|0	0|0|0|0|0	17|12|6|9|10|4|12|0|0|0|0|0|19|14|15|16|17|21|21|22|13|14|8|3|10|19|15|8|0	0
TPCN2_DeltaCT	P26599	PTBP1	16|0|4	11|2|0|0|10	12|9|11|4|2|6|5|12|11|14|10|12|12|4|4|4|1|4|10|5|7|1|26|0|2|3|6|8|6|13	0
TPCN2_DeltaCT	Q8IZL8	PELP1	0|0|0	0|0|0|0|0	0|0|0|0|0|0|0|0|0|0|0|0|0|0|0|0|0|0|0|0|0|0|0|0|0|0|0|0|0|0|0	0
TPCN2_DeltaCT	P14923	JUP	0|3|12	0|6|13|10|0	4|5|2|1|0|4|3|5|5|4|0|0|0|6|4|6|3|1|6|7|10|0|4|1|0|0|5|6|0|0	0
TPCN2_DeltaCT	P36776	LONP1	25|0|4	21|0|2|0|14	0|0|0|2|0|2|5|13|14|12|20|16|17|0|0|0|2|0|0|0|0|2|6|0|2|1|0|0|1|8	0
TPCN2_DeltaCT	O43390	HNRNPR	0|0|0	5|0|0|0|6	6|7|5|3|7|1|5|1|3|2|2|3|0|9|10|8|7|8|9|10|12|1|14|5|3|4|6|9|6|31	0
TPCN2_DeltaCT	Q96HE7	ERO1A	0|0|0	0|0|0|0|3	0|0|0|0|0|0|0|1|1|1|1|1|1|0|0|0|0|0|0|0|0|0|0|0|0|0|0|0|0|0|0	0
TPCN2_DeltaCT	Q99575	POP1	0|0|0	0|0|0|0|0	0|0|3|3|0|1|3|0|0|0|0|0|0|0|0|2|0|0|0|0|0|2|1|0|0|1|0|0|1|0	0
TPCN2_DeltaCT	Q9UG63	ABCF2	2|0|0	0|0|0|2|0	7|9|1|0|0|3|0|0|0|0|0|0|0|4|4|1|0|3|2|5|6|0|4|1|0|0|3|3|2|0	0
TPCN2_DeltaCT	P09874	PARP1	24|0|3	27|0|0|0|16	8|12|5|8|3|27|31|5|3|4|2|2|5|14|10|2|0|5|4|5|7|10|20|18|25|15|3|9|18|54	0
TPCN2_DeltaCT	P23528	CFL1	6|0|4	7|3|2|0|6	4|4|1|2|2|2|5|2|4|4|6|5|5|1|0|5|5|3|2|3|2|6|8|5|6|5|2|5|11|12	0

TPCN2_Delta CT	Q92997	DVL3	0|0|6	0|0|5|0|0	12|16|23|23|12|8|7|0|0|0|0|0|0|54|53|4|2|4|6|3|7|8|20|7|6|17|5|5|0|0	0
TPCN2_Delta CT	Q9NZ01	TECR	0|0|0	2|0|0|0|2	1|4|3|2|2|2|2|2|0|1|0|0|1|4|1|2|1|0|0|0|0|0|4|1|2|1|0|0|1|0	0
TPCN2_Delta CT	P27816	MAP4	10|0|0	0|0|0|0|0	80|86|65|68|36|34|46|1|1|1|1|2|1|67|88|31|21|28|51|46|78|56|39|36|42|57|81|63|0|2	0
TPCN2_Delta CT	Q00839	HNRNPU	39|2|15	39|9|15|3|17	20|20|31|52|46|30|34|10|9|9|9|8|9|19|23|40|29|15|24|14|19|23|29|23|25|37|21|21|21|45	0
TPCN2_Delta CT	Q16531	DDB1	7|0|0	14|3|2|0|5	0|0|1|0|0|0|0|0|0|0|0|0|0|0|0|0|0|0|0|0|0|0|0|0|0|0|0|0|0|18	0
TPCN2_Delta CT	P06576	ATP5B	40|0|6	33|6|5|2|28	3|1|4|7|3|32|31|11|13|11|19|16|17|2|1|6|2|2|2|3|6|7|24|8|13|7|5|2|13|22	0
TPCN2_Delta CT	O75150	RNF40	0|0|0	0|0|0|0|0	0|0|0|1|2|0|0|0|0|0|0|0|0|0|0|0|0|0|0|0|0|0|1|1|0|0|0|0|0|0	0
TPCN2_Delta CT	O75152	ZC3H11A	0|0|0	3|0|0|0|0	15|16|8|18|14|2|5|0|0|0|0|0|0|21|13|8|4|17|15|18|17|4|15|5|3|8|13|15|5|0	0
TPCN2_Delta CT	P16615	ATP2A2	21|0|2	27|0|0|0|24	2|1|8|3|7|4|3|4|4|5|5|3|4|1|1|0|1|1|1|2|2|2|10|4|6|6|1|0|8|5	0
TPCN2_Delta CT	Q14697	GANAB	17|0|3	19|4|2|0|5	0|0|0|0|0|0|0|7|5|5|3|5|1|0|0|0|0|0|0|1|0|0|3|0|0|0|0|0|0|23	0
TPCN2_Delta CT	O60271	SPAG9	2|0|0	0|0|0|0|0	2|2|26|11|12|12|10|0|0|0|0|0|0|1|1|0|0|0|0|0|1|13|11|7|12|16|0|0|0|3	0

TPCN2_DeltaCT	Q14690	PDCD11	0|0|0	0|0|0|0|0	0|0|0|0|0|0|0|0|0|0|0|0|0|0|0|0|0|1|1|0|0|0|2|0|0|0|0|0|1|0	0
TPCN2_DeltaCT	P07814	EPRS	4|0|0	0|0|2|0|0	19|12|12|22|21|7|13|3|4|2|0|4|1|18|16|12|9|13|18|22|31|13|22|6|10|20|23|15|2|8	0
TPCN2_DeltaCT	O75400	PRPF40A	0|0|0	0|0|0|0|0	1|2|3|5|5|2|3|0|0|0|0|0|0|1|0|1|1|1|3|3|2|2|6|2|3|5|2|2|4|0	0
TPCN2_DeltaCT	Q02880	TOP2B	2|0|0	0|0|0|0|0	14|9|0|0|0|0|0|2|1|1|1|1|1|12|7|3|4|21|21|11|14|0|0|0|0|0|18|20|0|0	0
TPCN2_DeltaCT	P23284	PPIB	4|14|30	13|22|31|15|15	0|0|0|0|0|0|0|2|4|2|0|1|1|0|0|0|0|2|0|1|1|0|1|0|0|0|0|0|0|26	0
TPCN2_DeltaCT	P62937	PPIA	4|0|4	6|4|3|0|3	1|1|1|0|0|3|0|9|6|8|8|4|7|0|0|0|0|0|1|0|2|0|18|0|3|0|4|2|2|19	0
TPCN2_DeltaCT	P09622	DLD	9|0|3	13|0|0|0|10	0|0|1|6|0|4|4|1|0|1|1|2|4|0|0|0|0|0|0|0|0|0|4|0|0|2|0|0|1|0	0
TPCN2_DeltaCT	Q32P28	P3H1	0|0|0	0|0|0|0|2	0|0|0|0|0|0|0|0|0|0|0|0|0|0|0|0|0|0|0|0|0|0|0|0|0|0|0|0	0
TPCN2_DeltaCT	P36871	PGM1	0|0|0	2|0|0|0|0	0|0|0|0|0|0|0|0|0|0|0|0|0|0|0|0|0|0|0|0|0|0|0|0|0|0|0|0	0
TPCN2_DeltaCT	O43865	AHCYL1	4|0|0	3|0|0|0|0	0|1|2|0|0|4|5|0|0|0|0|0|0|0|0|0|0|0|0|0|0|0|1|1|2|1|1|0|0|0|1	0
TPCN2_DeltaCT	Q13435	SF3B2	0|0|0	3|0|0|0|0	39|31|18|28|19|10|19|0|0|0|0|0|0|50|45|21|26|35|31|40|42|17|23|11|14|18|32|33|14|17	0

TPCN2_DeltaCT	Q8IY81	FTSJ3	11|9|0	15|2|0|22|9	25|25|13|11|5|4|3|3|1|0|0|0|0|17|24|14|10|20|23|12|23|5|9|7|5|8|24|23|13|0	0
TPCN2_DeltaCT	Q8NC51	SERBP1	2|0|0	2|0|0|0|0	35|41|54|73|30|58|73|1|2|1|1|2|1|33|43|31|19|16|28|15|27|19|40|13|12|44|104|26|5|2	0
TPCN2_DeltaCT	P53990	IST1	0|0|0	4|0|0|0|0	0|0|0|0|0|0|0|0|0|0|0|0|0|0|0|0|0|1|0|0|0|0|0|0|0|0|0|0|0|0|0|0|0|0	0
TPCN2_DeltaCT	P09429	HMGB1	4|0|0	0|0|0|0|0	1|1|1|0|0|0|1|0|0|0|0|0|0|1|0|0|0|1|0|1|0|3|6|0|1|3|0|0|0|4	0
TPCN2_DeltaCT	Q02543	RPL18A	3|3|4	4|3|3|4|9	3|3|8|10|11|6|4|13|4|3|2|2|3|4|4|5|8|0|0|0|0|3|7|1|0|8|1|1|0|0	0
TPCN2_DeltaCT	P36578	RPL4	49|55|46	55|44|38|81|59	3|3|14|12|16|7|8|1|1|1|2|2|1|3|2|12|8|1|2|0|0|12|6|13|11|14|2|2|6|2	0
TPCN2_DeltaCT	P78371	CCT2	14|0|5	19|2|3|0|11	1|1|96|69|87|29|7|6|5|7|6|6|4|0|0|4|32|2|3|3|0|95|52|245|214|87|2|1|19|62	0
TPCN2_DeltaCT	O94906	PRPF6	6|0|0	2|0|0|0|0	0|0|6|2|2|2|0|1|0|2|1|1|1|0|2|3|2|0|2|1|5|2|5|0|1|2|1|0|1|3	0
TPCN2_DeltaCT	O15355	PPM1G	3|0|0	2|0|0|0|2	1|1|4|0|0|4|2|0|0|0|0|0|0|0|0|0|0|0|0|0|0|0|1|2|1|0|5|0|0|0|7	0
TPCN2_DeltaCT	Q9UJS0	SLC25A13	13|4|3	12|0|0|5|12	0|0|3|0|0|2|3|1|0|0|0|0|1|0|0|4|1|0|1|0|0|1|4|2|0|2|0|0|6|0	0
TPCN2_DeltaCT	Q05639	EEF1A2	0|3|0	0|0|0|2|0	28|37|42|27|22|178|56|12|10|13|13|10|10|21|28|19|16|12|18|10|20|79|16|113|144|43|17|11|1	0

TPCN2_DeltaCT	P46777	RPL5	10|6|0	11|0|0|6|8	8|4|8|8|13|9|12|2|3|3|2|2|1|6|8|2|6|3|4|2|5|3|4|7|5|10|2|4|5|6	0
TPCN2_DeltaCT	Q8IX01	SUGP2	0|0|0	2|0|0|0|0	26|16|19|30|30|9|5|0|0|0|0|0|0|16|15|36|17|24|21|23|28|10|23|15|7|22|25|31|12|0	0
TPCN2_DeltaCT	Q99832	CCT7	9|0|6	18|4|2|0|10	0|2|51|34|50|14|5|3|2|1|1|1|1|0|1|2|14|1|1|0|1|69|32|115|101|51|0|1|7|43	0
TPCN2_DeltaCT	P46778	RPL21	3|0|0	2|0|0|0|0	1|1|9|8|7|12|10|1|0|1|0|0|1|0|0|6|8|0|1|0|1|3|4|3|2|7|1|1|1|0	0
TPCN2_DeltaCT	P46779	RPL28	5|5|9	7|3|6|10|10	5|5|11|12|6|26|10|3|0|1|0|2|1|1|2|8|4|0|0|0|0|4|6|4|2|12|0|1|8|0	0
TPCN2_DeltaCT	P35580	MYH10	13|0|8	0|9|0|0|0	0|1|12|8|11|0|0|0|1|1|0|1|0|0|0|0|1|4|9|1|2|11|19|11|9|15|4|3|131|41	0
TPCN2_DeltaCT	Q14978	NOLC1	0|0|0	3|0|0|0|0	15|16|21|11|9|11|5|0|0|0|0|0|0|12|10|22|17|7|8|7|12|6|12|9|6|14|13|11|4|0	0
TPCN2_DeltaCT	Q8TAQ2	SMARCC2	3|0|0	2|0|0|0|0	2|2|4|4|9|0|1|0|0|0|0|0|0|1|0|7|1|1|2|5|2|0|13|1|2|4|2|2|1|0	0
TPCN2_DeltaCT	Q9BZH6	WDR11	0|0|0	0|0|0|0|0	0|0|11|3|1|1|3|0|0|0|0|0|0|0|0|1|1|0|0|0|0|7|1|2|5|6|0|0|0|0	0
TPCN2_DeltaCT	O60716	CTNND1	0|0|0	2|0|0|0|0	10|9|0|0|0|3|2|0|0|0|0|0|0|4|6|3|3|3|8|10|14|1|1|0|1|0|3|4|0|0	0
TPCN2_DeltaCT	Q14974	KPNB1	19|0|7	22|8|9|0|14	0|1|40|11|19|16|9|9|7|8|4|2|2|0|0|7|4|1|5|1|1|15|36|8|17|25|2|3|3|31	0

TPCN2_DeltaCT	Q07866	KLC1	2|0|0	0|0|0|0|0	4|5|11|9|4|10|10|0|0|0|0|0|0|3|3|0|1|0|0|2|1|11|8|10|10|10|0|0|0|3	0
TPCN2_DeltaCT	P22695	UQCRC2	6|0|0	5|0|0|0|5	0|1|1|1|0|8|4|3|2|2|3|2|3|0|0|1|4|1|0|0|0|0|0|0|0|0|0|0|1|0	0
TPCN2_DeltaCT	Q6P2Q9	PRPF8	14|0|0	0|0|2|0|0	11|8|34|23|26|15|14|2|5|3|1|1|4|7|6|20|15|21|18|24|21|45|32|16|18|18|20|12|22|29	0
TPCN2_DeltaCT	P35637	FUS	0|0|0	0|0|0|0|0	3|2|3|0|0|3|5|0|1|1|0|1|0|3|4|0|0|1|2|3|3|1|6|0|1|2|0|3|0|42	0
TPCN2_DeltaCT	P62258	YWHAE	12|0|10	14|4|6|0|11	0|0|12|13|5|7|8|1|1|2|1|1|1|1|1|1|0|0|1|0|0|4|15|4|4|6|0|0|1|49	0
TPCN2_DeltaCT	P12004	PCNA	2|0|0	0|0|0|0|0	0|0|2|1|1|1|0|0|0|0|0|0|0|0|0|0|0|0|0|0|0|1|2|1|2|0|0|0|1|15	0
TPCN2_DeltaCT	Q7Z739	YTHDF3	0|0|0	0|0|0|0|0	0|1|4|3|1|3|1|0|0|0|0|0|0|1|1|0|0|0|0|0|1|0|0|0|0|0|1|1|0|1	0

APPENDIX 5

LIST OF POOLED TPC2 PROXIMITY INTERACTOME

The table shows a list of all positively enriched proteins in the pooled analysis of all TPC2-BioID2-HA interactomes. Only TPC2 positively enriched proteins are shown. TPC2-BioID2-HA mass spectrometry datasets were pooled from n=9 independent cultures (combining n=3 TPC2-734E-BioID2-HA experiments, n=3 TPC2-734G-BioID2-HA experiments, and n=3 TPC2-ΔCT-BioID2-HA experiments) ignoring TPC2 variant used, and compared with n=35 negative control datasets (combining untransfected MNT1 cells (n=2), MNT1 cells expressing soluble BioID2-HA (n=2), MNT1 cells expressing TPC1-BioID2-HA (n=1) and n=30 CRAPome BirA negative controls). GraphPad Prism was used to perform Multiple T tests with Two-stage step-up method of Benjamini, Krieger, and Yekutieli with a 1% False Discovery Rate (FDR) to test for significance. SE is standard error determined in the T test. df is degrees of freedom. q value is a p-value that has been adjusted for the FDR. $p<0.05$ is considered statistically significant without accounting for FDR, whereas $q<0.01$ is considered statistically significant when accounting for FDR.

Protein Name	Mean Spectral Counts of 9 Pooled TPC2 Reps	Mean Spectral Counts of 35 Negative Controls	Difference of Means	SE of difference	t ratio	df	P value	q value
TPCN2	10.78	0	10.78	0.7375	14.61	42	<0.000001	<0.000001
TSPAN10	1.667	0	1.667	0.2158	7.724	42	<0.000001	<0.000001
PLD1	4.667	0	4.667	0.6317	7.387	42	<0.000001	0.000001
YBX1	22.67	5.4	17.27	2.812	6.139	42	<0.000001	0.00005
RPS27A	13.11	2.514	10.6	1.781	5.95	42	<0.000001	0.000075
RPL19	20.11	5	15.11	2.658	5.684	42	0.000001	0.000151
RPL4	50	12.69	37.31	6.778	5.505	42	0.000002	0.000205
RAB27A	3.556	0.3429	3.213	0.5827	5.513	42	0.000002	0.000205
NOM1	11.33	1.6	9.733	1.84	5.289	42	0.000004	0.000371
RPL7	26.11	7.143	18.97	3.617	5.245	42	0.000005	0.000386
EPB41L5	15	2.057	12.94	2.578	5.021	42	0.00001	0.000727
RPL18	14.89	4.857	10.03	2.043	4.91	42	0.000014	0.000955
RPL13A	13.11	3.8	9.311	1.963	4.744	42	0.000024	0.001224
MYO1D	6.556	0.6286	5.927	1.235	4.8	42	0.00002	0.001224
SV2A	4.111	0	4.111	0.8648	4.754	42	0.000024	0.001224
UPF1	1.556	0.1429	1.413	0.2969	4.758	42	0.000023	0.001224
PRKD3	28.11	4.657	23.45	5.174	4.533	42	0.000048	0.002236
KANK1	13.56	2.029	11.53	2.551	4.518	42	0.00005	0.002236
RPL3	27	10.51	16.49	3.679	4.48	42	0.000056	0.002386
AP3B1	4.667	1.114	3.552	0.8064	4.405	42	0.000072	0.002739
CD63	6.222	0.9143	5.308	1.24	4.281	42	0.000106	0.003862
CLUH	3.111	0.1429	2.968	0.7091	4.186	42	0.000142	0.004958
MAGED2	11.89	2.657	9.232	2.237	4.127	42	0.00017	0.005711
SURF6	15.22	4.514	10.71	2.659	4.027	42	0.000232	0.006477
ZBTB11	4.667	0.8	3.867	0.9609	4.024	42	0.000234	0.006477
RPL8	11.11	3.971	7.14	1.8	3.967	42	0.000278	0.006774
SPRR1B	0.7778	0	0.7778	0.196	3.967	42	0.000278	0.006774
ZNF616	6.333	1.229	5.105	1.308	3.904	42	0.000337	0.007767
DDX54	14.44	3.543	10.9	2.83	3.852	42	0.000395	0.00835
CAPG	8.111	1.343	6.768	1.791	3.778	42	0.000491	0.009407
TKT	14.78	2.4	12.38	3.286	3.767	42	0.000508	0.009501
CYB5R3	0.6667	0.02857	0.6381	0.1727	3.694	42	0.000632	0.010581
IQGAP1	9.333	1.4	7.933	2.199	3.607	42	0.000816	0.012154
ANXA6	7	0.9714	6.029	1.67	3.609	42	0.000812	0.012154
SLC25A13	6.333	1.714	4.619	1.278	3.614	42	0.0008	0.012154
LAMP2	1.444	0.05714	1.387	0.383	3.622	42	0.000781	0.012154
EEA1	5.111	0.2857	4.825	1.345	3.587	42	0.000865	0.012421
NOC3L	10.78	2.971	7.806	2.208	3.535	42	0.001009	0.013983

CLTC	36	7.029	28.97	8.387	3.454	42	0.001273	0.015315
TYRP1	12.22	1.8	10.42	2.995	3.48	42	0.001183	0.015315
ACSL3	10	2.714	7.286	2.087	3.492	42	0.001143	0.015315
GSN	6.222	0.9143	5.308	1.537	3.453	42	0.001276	0.015315
CTSD	5	0.9714	4.029	1.161	3.471	42	0.001212	0.015315
VPS35	4.111	0.5714	3.54	1.031	3.434	42	0.00135	0.015726
MDH1	4.111	0.5143	3.597	1.05	3.425	42	0.001386	0.015916
DCD	2.111	0.4	1.711	0.507	3.375	42	0.001598	0.017133
PRKD1	16.56	3.114	13.44	4.016	3.347	42	0.001732	0.01726
CTNNB1	14.33	2.229	12.1	3.6	3.363	42	0.001655	0.01726
VCL	7.778	1.771	6.006	1.787	3.362	42	0.001659	0.01726
AARS	3.778	0.6	3.178	0.951	3.341	42	0.001759	0.01726
ANXA11	2.889	0.4	2.489	0.7459	3.337	42	0.001782	0.01726
NOMO1	2	0.08571	1.914	0.5731	3.34	42	0.001763	0.01726
STXBP1	1.556	0.1143	1.441	0.4307	3.347	42	0.001732	0.01726
RPL13	8.778	4.886	3.892	1.181	3.297	42	0.001996	0.01783
GLG1	1.333	0.02857	1.305	0.3952	3.301	42	0.001971	0.01783
AKR1B1	1.444	0.1714	1.273	0.3877	3.284	42	0.002071	0.018037
MYO1C	4	0.8286	3.171	0.9701	3.269	42	0.002157	0.018251
P4HB	16.44	3.514	12.93	4.006	3.228	42	0.002421	0.019464
GDI2	4	1	3	0.9335	3.214	42	0.002518	0.019464
VAT1	8.444	1.486	6.959	2.175	3.199	42	0.002626	0.020104
PPIB	14	3.914	10.09	3.177	3.175	42	0.002807	0.020747
FMNL2	1.556	0	1.556	0.4901	3.174	42	0.002813	0.020747
TTN	2.111	0.2286	1.883	0.5967	3.155	42	0.002966	0.021479
LDHB	9.222	2.857	6.365	2.022	3.147	42	0.003029	0.021684
FLOT2	5.778	1.057	4.721	1.501	3.145	42	0.003048	0.021684
GPI	7.333	1.486	5.848	1.866	3.134	42	0.003141	0.021956
RPL32	2.889	0.6857	2.203	0.7026	3.136	42	0.003126	0.021956
UGGT1	3.889	0.1714	3.717	1.196	3.109	42	0.003364	0.023009
PRKCE	3.222	0.2571	2.965	0.955	3.105	42	0.003405	0.023009
PYGB	1	0.05714	0.9429	0.3045	3.096	42	0.003486	0.023009
DDX11L8	0.4444	0	0.4444	0.1439	3.09	42	0.003549	0.023009
PCDHA6	0.4444	0	0.4444	0.1439	3.09	42	0.003549	0.023009
PI4K2A	0.4444	0	0.4444	0.1439	3.09	42	0.003549	0.023009
TTYH3	0.4444	0	0.4444	0.1439	3.09	42	0.003549	0.023009
WDR1	3.667	0.6571	3.01	0.9819	3.065	42	0.003795	0.023722
PSAP	2.889	0.4	2.489	0.8141	3.057	42	0.003877	0.023739
PMEL	2.667	0.4	2.267	0.7439	3.047	42	0.003986	0.023739
LRMDA	1.556	0	1.556	0.51	3.05	42	0.003955	0.023739
DSC1	1.333	0.2	1.133	0.372	3.047	42	0.003986	0.023739
GPR143	0.7778	0	0.7778	0.255	3.05	42	0.003955	0.023739
RPL35	3.444	0.7429	2.702	0.8876	3.044	42	0.004023	0.023782

DPP4	1.556	0.1143	1.441	0.4747	3.036	42	0.004107	0.0241
LAMP1	1.444	0.2286	1.216	0.4012	3.031	42	0.004165	0.024267
MYO5A	4.444	0.05714	4.387	1.45	3.026	42	0.00422	0.02441
ALDOA	11.67	3.371	8.295	2.75	3.016	42	0.004332	0.024707
SEC24C	2.222	0.3143	1.908	0.6346	3.006	42	0.004449	0.024707
ATIC	1.333	0.1143	1.219	0.4059	3.003	42	0.004487	0.02471
TMEM2	0.5556	0	0.5556	0.1844	3.013	42	0.004369	0.024707
MRPL43	0.5556	0	0.5556	0.1844	3.013	42	0.004369	0.024707
PLCD3	1.111	0.08571	1.025	0.3442	2.979	42	0.004793	0.025691
FLOT1	3.556	0.7714	2.784	0.9518	2.925	42	0.005532	0.028692
HK2	2	0.2286	1.771	0.6053	2.926	42	0.005512	0.028692
MOGS	0.6667	0	0.6667	0.2307	2.89	42	0.006072	0.030508
PGK1	11.44	2.6	8.844	3.084	2.867	42	0.006445	0.031983
CAP1	8.556	2.4	6.156	2.151	2.862	42	0.006532	0.032023
SCARB1	0.8889	0.08571	0.8032	0.2803	2.865	42	0.006487	0.031997
IMMT	9.333	1.571	7.762	2.724	2.85	42	0.006751	0.032651
XPO1	4.444	1.571	2.873	1.013	2.835	42	0.007017	0.032651
SOD2	1.778	0.2	1.578	0.5566	2.835	42	0.007025	0.032651
NR4A3	0.8889	0.1143	0.7746	0.2731	2.836	42	0.007	0.032651
AHSG	0.8889	0.1143	0.7746	0.2731	2.836	42	0.007	0.032651
NPEPPS	3.111	0.7143	2.397	0.8476	2.828	42	0.007154	0.033053
PRKCSH	8.333	1.971	6.362	2.258	2.818	42	0.007345	0.033186
AIFM1	6.444	1.429	5.016	1.78	2.818	42	0.007342	0.033186
DHTKD1	0.8889	0.1429	0.746	0.2654	2.811	42	0.007467	0.033351
TARS	2.222	0.6571	1.565	0.5575	2.808	42	0.007541	0.033494
IDH1	8.778	2.143	6.635	2.382	2.786	42	0.007983	0.034343
OPA1	6.111	0.8	5.311	1.908	2.784	42	0.008021	0.034343
TPI1	4.667	0.9714	3.695	1.324	2.791	42	0.007866	0.034343
HSD17B4	3.333	0.4857	2.848	1.023	2.783	42	0.008031	0.034343
PRKD2	7.778	1.143	6.635	2.389	2.777	42	0.008153	0.034497
LETM1	2.889	0.4	2.489	0.8958	2.778	42	0.008134	0.034497
M6PR	1.444	0.2	1.244	0.4534	2.744	42	0.008879	0.037372
KPRP	2.556	0.4	2.156	0.7878	2.736	42	0.009072	0.037986
RPS5	3.333	1.143	2.19	0.8038	2.725	42	0.009333	0.038879
TNPO1	2	0.3143	1.686	0.6199	2.719	42	0.00947	0.039245
HSP90B1	28.44	9.057	19.39	7.15	2.711	42	0.009663	0.03968
TFRC	8.889	2.714	6.175	2.279	2.709	42	0.009723	0.03968
CAPN5	2	0.2	1.8	0.6666	2.7	42	0.009941	0.040186
TRPV2	1.333	0.08571	1.248	0.464	2.689	42	0.010242	0.040563
ACTR3	0.4444	0.02857	0.4159	0.1547	2.689	42	0.010242	0.040563
FOXK1	0.4444	0.02857	0.4159	0.1547	2.689	42	0.010242	0.040563
ANXA5	4.111	0.9143	3.197	1.193	2.681	42	0.010454	0.040799
RECQL	1.444	0.2571	1.187	0.4426	2.682	42	0.010407	0.040799

CANX	14.56	4.229	10.33	3.871	2.668	42	0.010807	0.041375
RPS25	2.778	0.8571	1.921	0.7199	2.668	42	0.0108	0.041375
PCYOX1	0.7778	0.08571	0.6921	0.2598	2.664	42	0.010916	0.041593
DNAJC13	4.667	1.086	3.581	1.351	2.651	42	0.011277	0.042766
HK1	8.333	1.543	6.79	2.591	2.621	42	0.012164	0.044859
LTA4H	1	0.1429	0.8571	0.3277	2.616	42	0.012315	0.04521
ACSL1	10.22	1.829	8.394	3.227	2.601	42	0.01277	0.046626
DNAJC9	0.8889	0.05714	0.8317	0.3199	2.6	42	0.012817	0.046626
PTCD3	0.7778	0.1714	0.6063	0.2344	2.586	42	0.013258	0.047798
MSN	9.667	3.571	6.095	2.388	2.553	42	0.01442	0.050847
PKM	30.67	17.14	13.52	5.303	2.55	42	0.014494	0.050885
GAPDH	17.89	6.886	11	4.324	2.545	42	0.014707	0.051185
RAB32	1.333	0.2	1.133	0.4452	2.546	42	0.014669	0.051185
FH	4.111	1	3.111	1.225	2.541	42	0.014851	0.051244
LAP3	0.7778	0.08571	0.6921	0.2723	2.541	42	0.014824	0.051244
SACM1L	1.778	0.2857	1.492	0.5901	2.529	42	0.015299	0.05234
CD44	1.778	0.2857	1.492	0.5901	2.529	42	0.015299	0.05234
MRPL44	2.333	0.3714	1.962	0.7826	2.507	42	0.016139	0.054307
FARSB	2.556	0.6857	1.87	0.747	2.503	42	0.01628	0.054307
RAD23B	0.7778	0.1143	0.6635	0.2649	2.505	42	0.016221	0.054307
RBM12	0.7778	0.1143	0.6635	0.2649	2.505	42	0.016221	0.054307
ACLY	7	2.571	4.429	1.772	2.499	42	0.016466	0.054703
RPL14	5.222	2.771	2.451	0.9816	2.497	42	0.016544	0.054734
MCM2	6.111	1.2	4.911	1.97	2.493	42	0.016677	0.05495
TGM3	1	0.08571	0.9143	0.3681	2.484	42	0.017075	0.055647
S100A8	0.8889	0.1429	0.746	0.3006	2.482	42	0.017166	0.055647
RBM28	5.667	1.457	4.21	1.7	2.477	42	0.017376	0.056102
IARS2	4	0.9429	3.057	1.239	2.467	42	0.017803	0.057022
S100A9	0.6667	0.08571	0.581	0.236	2.462	42	0.018006	0.057295
ATP1A1	13.89	4.714	9.175	3.745	2.45	42	0.018529	0.058419
AP3D1	8	3.343	4.657	1.907	2.442	42	0.018912	0.059162
HYOU1	2.889	0.4	2.489	1.021	2.438	42	0.019067	0.059415
MDH2	5.667	1.486	4.181	1.717	2.435	42	0.019237	0.059715
HGS	1.778	0.4571	1.321	0.5478	2.411	42	0.020379	0.062559
CALR	8	2.371	5.629	2.354	2.391	42	0.021357	0.064309
AP1G1	1.333	0.2286	1.105	0.462	2.391	42	0.021341	0.064309
ATP6V0A1	0.6667	0.05714	0.6095	0.2572	2.37	42	0.022449	0.067095
POR	1.778	0.4	1.378	0.5823	2.366	42	0.022668	0.067496
LMNA	21.22	8.429	12.79	5.419	2.361	42	0.022937	0.068045
NOP53	5.667	2.114	3.552	1.519	2.339	42	0.024166	0.071427
GSTO1	1.667	0.4286	1.238	0.5303	2.335	42	0.024425	0.071928
HADHB	6.333	1.657	4.676	2.008	2.329	42	0.02473	0.07256
DSP	9.778	3.771	6.006	2.59	2.319	42	0.025354	0.074122

CALU	4.889	1.257	3.632	1.573	2.309	42	0.025907	0.074921
SRRT	3.556	0.8	2.756	1.193	2.31	42	0.025867	0.074921
GSR	0.5556	0.05714	0.4984	0.2166	2.301	42	0.026425	0.075875
ECM1	0.5556	0.05714	0.4984	0.2166	2.301	42	0.026425	0.075875
CAT	1.111	0.2571	0.854	0.3718	2.297	42	0.026698	0.076384
NCSTN	1	0.1429	0.8571	0.375	2.286	42	0.027387	0.077528
AP2B1	5.333	1.486	3.848	1.686	2.282	42	0.027616	0.077865
ABCB6	1.667	0.2857	1.381	0.608	2.271	42	0.02831	0.079028
GFPT1	1.556	0.3714	1.184	0.5235	2.262	42	0.028929	0.080198
KARS	2.667	0.8857	1.781	0.794	2.243	42	0.030223	0.082928
GOT2	3.889	0.7714	3.117	1.402	2.224	42	0.031616	0.0852
CSE1L	8.778	3.571	5.206	2.353	2.213	42	0.032381	0.086014
OAT	6.444	1.943	4.502	2.032	2.215	42	0.032251	0.086014
PDIA3	9.333	3.229	6.105	2.768	2.205	42	0.032962	0.086403
GNL3	7.556	4.257	3.298	1.496	2.205	42	0.032994	0.086403
LARS2	2.778	0.7143	2.063	0.9453	2.183	42	0.034688	0.089362
TOMM70	2.333	0.4571	1.876	0.8606	2.18	42	0.034902	0.089362
SPTBN1	9.333	1.914	7.419	3.406	2.178	42	0.035068	0.089502
UTP20	0.6667	0.1143	0.5524	0.2549	2.167	42	0.03598	0.091539
NQO1	2.889	0.7429	2.146	0.9948	2.157	42	0.036759	0.092351
NOC2L	1.444	0.4571	0.9873	0.4574	2.158	42	0.036652	0.092351
IGSF8	0.8889	0.1714	0.7175	0.3356	2.138	42	0.038381	0.094819
ZNF660	0.7778	0.1143	0.6635	0.3111	2.133	42	0.038828	0.095462
DSG1	2.222	0.6571	1.565	0.7373	2.123	42	0.039708	0.097032
IGF2R	0.7778	0.1714	0.6063	0.2856	2.123	42	0.039688	0.097032
HSPA4	13.56	5.857	7.698	3.633	2.119	42	0.040042	0.097551
SLC1A4	2.444	0.4857	1.959	0.928	2.111	42	0.040802	0.09757
ITGB1	1.111	0.2857	0.8254	0.3913	2.11	42	0.040899	0.09757
ACR	0.4444	0.05714	0.3873	0.1833	2.112	42	0.040641	0.09757
PIP	0.4444	0.05714	0.3873	0.1833	2.112	42	0.040641	0.09757
GPRIN3	0.4444	0.05714	0.3873	0.1833	2.112	42	0.040641	0.09757
KRT1	54.67	33.09	21.58	10.26	2.104	42	0.041426	0.098244
SND1	16	7.971	8.029	3.895	2.061	42	0.04549	0.098267
GANAB	7.222	2.371	4.851	2.314	2.096	42	0.042103	0.098267
FUBP1	3.111	1.086	2.025	0.9781	2.071	42	0.044556	0.098267
CPT1A	1.444	0.3714	1.073	0.5171	2.075	42	0.044135	0.098267
RPL36	1.556	0.5429	1.013	0.4924	2.057	42	0.045973	0.098267
HM13	1.444	0.4571	0.9873	0.4787	2.062	42	0.045392	0.098267
PELP1	0.5556	0	0.5556	0.2719	2.044	42	0.047303	0.098267
MANF	0.4444	0	0.4444	0.2175	2.044	42	0.047303	0.098267
FLII	0.4444	0.08571	0.3587	0.1727	2.078	42	0.043905	0.098267
TWISTNB	0.3333	0	0.3333	0.1631	2.044	42	0.047303	0.098267
ZKSCAN7	0.3333	0	0.3333	0.1631	2.044	42	0.047303	0.098267

ARFGEF2	0.3333	0	0.3333	0.1631	2.044	42	0.047303	0.098267
ITGA9	0.3333	0	0.3333	0.1631	2.044	42	0.047303	0.098267
HCN3	0.3333	0	0.3333	0.1631	2.044	42	0.047303	0.098267
GBA	0.3333	0	0.3333	0.1631	2.044	42	0.047303	0.098267
MFN2	0.3333	0	0.3333	0.1631	2.044	42	0.047303	0.098267
LNPEP	0.3333	0	0.3333	0.1631	2.044	42	0.047303	0.098267
PRKCI	0.2222	0	0.2222	0.1087	2.044	42	0.047303	0.098267
SEMA4C	0.2222	0	0.2222	0.1087	2.044	42	0.047303	0.098267
PAFAH1B1	0.2222	0	0.2222	0.1087	2.044	42	0.047303	0.098267
MYO18A	0.2222	0	0.2222	0.1087	2.044	42	0.047303	0.098267
MRPL38	0.2222	0	0.2222	0.1087	2.044	42	0.047303	0.098267
DENND1A	0.2222	0	0.2222	0.1087	2.044	42	0.047303	0.098267
TGOLN2	0.2222	0	0.2222	0.1087	2.044	42	0.047303	0.098267
NPC1	0.2222	0	0.2222	0.1087	2.044	42	0.047303	0.098267
AGAP2	0.2222	0	0.2222	0.1087	2.044	42	0.047303	0.098267
REV_P04280	0.2222	0	0.2222	0.1087	2.044	42	0.047303	0.098267
PSAT1	0.2222	0	0.2222	0.1087	2.044	42	0.047303	0.098267
SPRR2E	0.2222	0	0.2222	0.1087	2.044	42	0.047303	0.098267
TF	0.2222	0	0.2222	0.1087	2.044	42	0.047303	0.098267
CD276	0.2222	0	0.2222	0.1087	2.044	42	0.047303	0.098267
FKBP10	0.2222	0	0.2222	0.1087	2.044	42	0.047303	0.098267
CELSR2	0.2222	0	0.2222	0.1087	2.044	42	0.047303	0.098267
ZNF800	0.2222	0	0.2222	0.1087	2.044	42	0.047303	0.098267
REV_Q9BX63	0.2222	0	0.2222	0.1087	2.044	42	0.047303	0.098267
SARS	0.2222	0	0.2222	0.1087	2.044	42	0.047303	0.098267
CALML5	0.2222	0	0.2222	0.1087	2.044	42	0.047303	0.098267
NSUN5	0.2222	0	0.2222	0.1087	2.044	42	0.047303	0.098267
SLC4A2	0.2222	0	0.2222	0.1087	2.044	42	0.047303	0.098267
POLR1A	0.2222	0	0.2222	0.1087	2.044	42	0.047303	0.098267
SLC7A2	0.2222	0	0.2222	0.1087	2.044	42	0.047303	0.098267
ZFP62	0.2222	0	0.2222	0.1087	2.044	42	0.047303	0.098267
NAA25	0.2222	0	0.2222	0.1087	2.044	42	0.047303	0.098267
OSBP	0.2222	0	0.2222	0.1087	2.044	42	0.047303	0.098267
ATP2B4	0.7778	0.1429	0.6349	0.315	2.015	42	0.05029	0.104204
TMEM263	1.444	0.3714	1.073	0.536	2.002	42	0.051794	0.107044
TXNRD1	1.222	0.2571	0.9651	0.4833	1.997	42	0.052362	0.107941
RRBP1	11.11	3.771	7.34	3.69	1.989	42	0.053259	0.10923
CAND1	8.111	3.514	4.597	2.331	1.972	42	0.055204	0.112644
AHCY	3.556	1.343	2.213	1.127	1.963	42	0.056312	0.114036
CTNNA1	2.333	0.7714	1.562	0.7994	1.954	42	0.057415	0.115979
JUP	6.222	3.457	2.765	1.432	1.931	42	0.060193	0.12008
SLC25A12	0.6667	0.02857	0.6381	0.3311	1.927	42	0.060769	0.120202
ASAH1	0.5556	0.1143	0.4413	0.229	1.927	42	0.060747	0.120202

AGPS	1.111	0.2571	0.854	0.4451	1.919	42	0.06186	0.121578
MYH10	27.56	8.714	18.84	9.848	1.913	42	0.062556	0.122069
NARS2	2.111	0.6286	1.483	0.7803	1.9	42	0.064308	0.124886
PDCD6IP	2.667	1.2	1.467	0.7729	1.898	42	0.064621	0.124886
PNPT1	1.667	0.5143	1.152	0.6069	1.899	42	0.064467	0.124886
SHMT2	7.778	2.8	4.978	2.628	1.894	42	0.065141	0.125289
PFKM	2.333	0.8857	1.448	0.7641	1.895	42	0.065045	0.125289
SAMM50	1	0.2286	0.7714	0.4085	1.889	42	0.065876	0.1258
LDHA	4.778	2.657	2.121	1.126	1.883	42	0.066665	0.126705
ATP1B3	0.4444	0.08571	0.3587	0.191	1.879	42	0.067263	0.12754
IFI16	1.778	0.3714	1.406	0.7513	1.872	42	0.068202	0.129016
PDIA4	6	1.8	4.2	2.258	1.86	42	0.069939	0.131068
GTPBP4	3	1.429	1.571	0.8487	1.852	42	0.071122	0.132975
USP5	1.444	0.4286	1.016	0.5495	1.849	42	0.07155	0.133464
ZNF235	0.7778	0.1429	0.6349	0.3453	1.839	42	0.072992	0.134996
RPL36A	1.222	0.4571	0.7651	0.4247	1.801	42	0.078832	0.143713
DLST	1.444	0.5143	0.9302	0.5189	1.793	42	0.080256	0.145649
NNT	4.556	1.8	2.756	1.545	1.783	42	0.081745	0.147353
RPL6	14.33	10.94	3.39	1.921	1.765	42	0.084883	0.152667
HADHA	14.44	6.2	8.244	4.689	1.758	42	0.085963	0.153274
LONP1	10	4.571	5.429	3.108	1.747	42	0.088014	0.155858
DLD	3.778	1.543	2.235	1.295	1.726	42	0.09173	0.161021
RPSA	3.889	2.057	1.832	1.083	1.691	42	0.098226	0.171301
DHX30	2.889	1.2	1.689	1.003	1.684	42	0.099633	0.173116
UBA1	6.667	2.543	4.124	2.459	1.677	42	0.101016	0.175028
NPLOC4	1.556	0.5714	0.9841	0.5904	1.667	42	0.102954	0.178003
ATP2A2	9.222	4.429	4.794	2.878	1.666	42	0.103206	0.178055
COPA	3.667	1.286	2.381	1.433	1.662	42	0.103975	0.178997
PFKP	3.444	1.486	1.959	1.183	1.655	42	0.105296	0.180884
HMGN2	1.333	0.4286	0.9048	0.5488	1.649	42	0.106709	0.182921
TXLNA	0.5556	0.1714	0.3841	0.2391	1.606	42	0.115687	0.195806
EEF2	25.22	16.34	8.879	5.55	1.6	42	0.117114	0.197494
STT3B	1.333	0.4	0.9333	0.5836	1.599	42	0.117242	0.197494
HSDL1	0.6667	0.1429	0.5238	0.3277	1.599	42	0.117421	0.197494
LGALS3	1.222	0.4	0.8222	0.5157	1.594	42	0.118328	0.198189
VCP	15.44	6.029	9.416	5.97	1.577	42	0.12223	0.200876
RPN1	4.333	2.114	2.219	1.403	1.582	42	0.121135	0.200876
RBM12B	0.2222	0.02857	0.1937	0.1227	1.578	42	0.122017	0.200876
TROVE2	0.2222	0.02857	0.1937	0.1227	1.578	42	0.122017	0.200876
MRPL47	0.2222	0.02857	0.1937	0.1227	1.578	42	0.122017	0.200876
FDPS	0.2222	0.02857	0.1937	0.1227	1.578	42	0.122017	0.200876
MRPL21	0.2222	0.02857	0.1937	0.1227	1.578	42	0.122017	0.200876
RFTN1	0.2222	0.02857	0.1937	0.1227	1.578	42	0.122017	0.200876

IPO5	2.556	1.171	1.384	0.8993	1.539	42	0.131292	0.21324
SLC25A3	4.333	3.229	1.105	0.7207	1.533	42	0.132793	0.214812
SSB	1.889	0.8286	1.06	0.6917	1.533	42	0.132795	0.214812
KRR1	0.3333	0.05714	0.2762	0.1813	1.523	42	0.135202	0.217409
TMEM163	1	0.2857	0.7143	0.4725	1.512	42	0.138134	0.221091
NANS	0.5556	0.1143	0.4413	0.2927	1.507	42	0.139182	0.221577
AP2A1	0.8889	0.3143	0.5746	0.3844	1.495	42	0.14245	0.225023
AP1B1	1.333	0.3143	1.019	0.6909	1.475	42	0.147702	0.231926
HLA-A	2.778	1.286	1.492	1.013	1.473	42	0.148324	0.232449
VPS13C	14.22	3.771	10.45	7.141	1.463	42	0.150788	0.235851
PAK1IP1	0.5556	0.1143	0.4413	0.3039	1.452	42	0.153893	0.24024
LRRC59	2.222	0.8	1.422	0.984	1.445	42	0.155794	0.242267
HSPH1	8	4.771	3.229	2.254	1.432	42	0.159512	0.247092
HSP90AB1	40.11	26.34	13.77	9.717	1.417	42	0.163898	0.252865
AFG3L2	3.111	1.4	1.711	1.209	1.416	42	0.16425	0.252865
RSL1D1	7.889	4.886	3.003	2.127	1.412	42	0.165354	0.253215
AASS	0.7778	0.2857	0.4921	0.3494	1.408	42	0.166349	0.254254
P3H1	0.3333	0.05714	0.2762	0.1988	1.389	42	0.172109	0.262061
SRSF6	3.444	1.886	1.559	1.133	1.376	42	0.176072	0.267084
PTCD1	0.4444	0.1429	0.3016	0.2197	1.373	42	0.177045	0.268055
PSMD1	3.667	1.714	1.952	1.426	1.369	42	0.178136	0.268695
ACTR2	0.4444	0.1143	0.3302	0.2431	1.358	42	0.181623	0.272893
DDB1	3.222	1.229	1.994	1.472	1.354	42	0.182927	0.273357
AGK	0.7778	0.2857	0.4921	0.3679	1.337	42	0.188266	0.279258
TALDO1	1	0.3143	0.6857	0.5143	1.333	42	0.189652	0.280797
ATP6V1A	3.333	1.829	1.505	1.134	1.326	42	0.191868	0.283035
SPTAN1	6.778	3.314	3.463	2.617	1.324	42	0.192823	0.283924
BCAP31	1.333	0.4857	0.8476	0.6644	1.276	42	0.209072	0.303404
CNP	2	0.7714	1.229	0.9722	1.264	42	0.213287	0.308962
PABPC4	6.111	4.171	1.94	1.564	1.24	42	0.221895	0.318596
CTR9	0.7778	0.3429	0.4349	0.3529	1.233	42	0.224616	0.320738
APMAP	0.2222	0.05714	0.1651	0.1345	1.227	42	0.226602	0.320738
ZNF493	0.2222	0.05714	0.1651	0.1345	1.227	42	0.226602	0.320738
ATP13A1	0.2222	0.05714	0.1651	0.1345	1.227	42	0.226602	0.320738
DHX57	0.2222	0.05714	0.1651	0.1345	1.227	42	0.226602	0.320738
ARPC1B	0.2222	0.05714	0.1651	0.1345	1.227	42	0.226602	0.320738
NME2	2.778	1.457	1.321	1.079	1.224	42	0.22791	0.321909
PLEKHA5	1.111	0.5143	0.5968	0.4881	1.223	42	0.22823	0.321909
HSP90AA1	32.78	19.6	13.18	10.81	1.219	42	0.229577	0.323242
GNS	0.4444	0.1429	0.3016	0.2481	1.216	42	0.230929	0.32401
MRPL24	0.4444	0.1429	0.3016	0.2481	1.216	42	0.230929	0.32401
FKBP4	2.333	0.9429	1.39	1.156	1.203	42	0.23582	0.329721
FKBP3	0.5556	0.1714	0.3841	0.3221	1.193	42	0.23972	0.332859

MCM3	4.222	2	2.222	1.879	1.183	42	0.243585	0.337643
TOP1	4.667	2.343	2.324	2.001	1.161	42	0.252059	0.347591
RRP12	1.778	1.029	0.7492	0.6589	1.137	42	0.261936	0.359362
PHF6	0.5556	0.2	0.3556	0.3149	1.129	42	0.265308	0.363369
PML	0.3333	0.1143	0.219	0.1959	1.118	42	0.269928	0.369003
PITRM1	0.7778	0.2857	0.4921	0.4493	1.095	42	0.279678	0.381101
CDK2	2.111	1.4	0.7111	0.6557	1.084	42	0.28435	0.386159
UFL1	0.5556	0.2571	0.2984	0.276	1.081	42	0.285808	0.387262
APEX1	0.5556	0.1714	0.3841	0.361	1.064	42	0.293431	0.395154
APEH	0.2222	0.05714	0.1651	0.1573	1.049	42	0.300015	0.398678
SORD	0.2222	0.05714	0.1651	0.1573	1.049	42	0.300015	0.398678
CTNNBL1	0.2222	0.05714	0.1651	0.1573	1.049	42	0.300015	0.398678
CNDP2	0.2222	0.05714	0.1651	0.1573	1.049	42	0.300015	0.398678
GOT1	0.2222	0.05714	0.1651	0.1573	1.049	42	0.300015	0.398678
PHKA2	0.2222	0.05714	0.1651	0.1573	1.049	42	0.300015	0.398678
PGM1	0.2222	0.05714	0.1651	0.1573	1.049	42	0.300015	0.398678
PEBP1	0.2222	0.05714	0.1651	0.1573	1.049	42	0.300015	0.398678
DDX27	1	0.5143	0.4857	0.464	1.047	42	0.301207	0.399601
FXR1	1.111	0.6571	0.454	0.4421	1.027	42	0.310394	0.409761
MSH2	2.222	1.286	0.9365	0.9131	1.026	42	0.310939	0.409807
RPL29	2.111	1.6	0.5111	0.507	1.008	42	0.319172	0.417918
NDUFA9	0.4444	0.2	0.2444	0.2435	1.004	42	0.321107	0.418468
COPB2	1.556	0.9143	0.6413	0.67	0.9572	42	0.343965	0.444588
SUMO3	0.6667	0.4286	0.2381	0.2485	0.958	42	0.343527	0.444588
CS	5.222	3.6	1.622	1.722	0.9419	42	0.351644	0.453602
PCMT1	0.5556	0.3143	0.2413	0.2564	0.941	42	0.352066	0.453602
SEC23B	0.6667	0.3429	0.3238	0.3455	0.9373	42	0.353959	0.454583
PRPF6	2.111	1.429	0.6825	0.7418	0.9201	42	0.362776	0.462214
NAA15	0.4444	0.1714	0.273	0.3007	0.9078	42	0.369144	0.468103
KRT76	2.222	1.086	1.137	1.256	0.9049	42	0.37068	0.469311
ACO2	4.667	2.8	1.867	2.074	0.9	42	0.373276	0.471113
IPO7	3.111	2.086	1.025	1.156	0.8872	42	0.380013	0.478114
PDCD11	0.3333	0.1429	0.1905	0.218	0.8739	42	0.387162	0.48559
RPL28	6.444	4.857	1.587	1.833	0.8659	42	0.391491	0.489492
RPL37A	0.7778	0.4	0.3778	0.4465	0.846	42	0.402342	0.499177
NSF	0.4444	0.2571	0.1873	0.2227	0.8412	42	0.405014	0.500946
SYMPK	1.111	0.7143	0.3968	0.4757	0.8343	42	0.408859	0.503379
OGDH	2.222	1.286	0.9365	1.125	0.8323	42	0.409953	0.503954
OPTN	0.2222	0.08571	0.1365	0.1661	0.8217	42	0.415887	0.508141
CUL1	0.2222	0.08571	0.1365	0.1661	0.8217	42	0.415887	0.508141
IDH3A	2	1.229	0.7714	0.9549	0.8079	42	0.423721	0.516144
FLG2	0.6667	0.4	0.2667	0.3479	0.7664	42	0.447708	0.538831
HNRNPUL2	1.333	0.8	0.5333	0.7194	0.7414	42	0.462582	0.553875

DARS	2.333	1.629	0.7048	0.9584	0.7354	42	0.4662	0.556919
RPS6	7.889	6.657	1.232	1.74	0.7077	42	0.48302	0.574451
KRT9	35.33	28.06	7.276	10.63	0.6844	42	0.497496	0.589053
HSPA5	33.67	28.09	5.581	8.201	0.6806	42	0.499888	0.590146
PPIF	0.6667	0.4	0.2667	0.3928	0.6788	42	0.500967	0.590553
XRCC5	9.444	6.829	2.616	3.88	0.6741	42	0.503911	0.593154
PSMD2	4.667	3.229	1.438	2.147	0.6698	42	0.506663	0.595522
UQCRC1	1.667	1.171	0.4952	0.7496	0.6606	42	0.512454	0.601449
NDUFS2	0.5556	0.3429	0.2127	0.3268	0.6509	42	0.518659	0.605197
NAMPT	2.444	1.857	0.5873	0.9308	0.631	42	0.531483	0.617473
TMED9	0.2222	0.1143	0.1079	0.174	0.6205	42	0.538284	0.624471
HSPD1	30.56	24.51	6.041	9.832	0.6145	42	0.542223	0.628135
IGHA1	0.4444	0.2286	0.2159	0.3573	0.6041	42	0.549014	0.635087
ATP5B	12.89	10.49	2.403	4.122	0.5831	42	0.562957	0.646994
PDIA6	3.778	2.457	1.321	2.263	0.5835	42	0.562676	0.646994
G6PD	0.3333	0.2	0.1333	0.2278	0.5854	42	0.561432	0.646994
NOP2	4.556	3.829	0.727	1.286	0.5653	42	0.574845	0.653619
PHB	3.111	2.457	0.654	1.161	0.5631	42	0.57637	0.653619
DNM2	0.4444	0.2571	0.1873	0.3308	0.5662	42	0.574293	0.653619
ACAA1	0.3333	0.1714	0.1619	0.2882	0.5618	42	0.57723	0.653619
TMEM214	0.2222	0.1143	0.1079	0.1921	0.5618	42	0.57723	0.653619
TM9SF2	0.2222	0.1143	0.1079	0.1921	0.5618	42	0.57723	0.653619
UQCRC2	1.778	1.343	0.4349	0.7853	0.5538	42	0.582646	0.658078
EZR	4.667	3.6	1.067	2.025	0.5269	42	0.601053	0.674892
CLPTM1	0.2222	0.1143	0.1079	0.2087	0.5171	42	0.607768	0.679584
NELFB	0.2222	0.1143	0.1079	0.2087	0.5171	42	0.607768	0.679584
OSBPL8	1	0.7429	0.2571	0.505	0.5092	42	0.613291	0.682911
ACTN1	3.111	2.457	0.654	1.292	0.5063	42	0.615266	0.684162
YWHAB	3.556	2.8	0.7556	1.564	0.483	42	0.631615	0.700404
GORASP2	0.4444	0.3143	0.1302	0.269	0.4838	42	0.631056	0.700404
EPHX1	0.5556	0.3143	0.2413	0.5151	0.4684	42	0.641895	0.708241
LRPPRC	26.56	20.71	5.841	12.83	0.4554	42	0.651135	0.717104
FKBP15	0.3333	0.2286	0.1048	0.2319	0.4517	42	0.653785	0.719038
IARS	2.889	2.4	0.4889	1.114	0.4388	42	0.663074	0.72634
RNF40	0.2222	0.1429	0.07937	0.1809	0.4387	42	0.663135	0.72634
GNAS	0.7778	0.6	0.1778	0.4157	0.4277	42	0.671072	0.730061
GARS	0.4444	0.3143	0.1302	0.3039	0.4283	42	0.6706	0.730061
HARS	0.2222	0.1143	0.1079	0.252	0.4283	42	0.670639	0.730061
MLX	0.2222	0.1143	0.1079	0.252	0.4283	42	0.670639	0.730061
ACADVL	2	1.514	0.4857	1.16	0.4186	42	0.677609	0.735183
FTSJ3	12.11	10.71	1.397	3.374	0.4141	42	0.680944	0.737112
IDH2	1.667	1.257	0.4095	0.99	0.4137	42	0.681221	0.737112
PRDX4	3.222	2.8	0.4222	1.033	0.4085	42	0.684951	0.738168

CLCN7	0.2222	0.1429	0.07937	0.1984	0.3999	42	0.691235	0.741956
SUPT6H	0.5556	0.4	0.1556	0.4021	0.3868	42	0.700834	0.751257
RPL7A	6.556	5.914	0.6413	1.664	0.3853	42	0.701971	0.751474
MARCKSL1	0.2222	0.1429	0.07937	0.2146	0.3699	42	0.713309	0.760573
SUPT5H	0.8889	0.6286	0.2603	0.7454	0.3492	42	0.728656	0.774882
ESYT2	1.111	0.9143	0.1968	0.5698	0.3454	42	0.731508	0.776886
RPL35A	2.778	2.314	0.4635	1.364	0.3399	42	0.735626	0.780229
CPT2	0.6667	0.5143	0.1524	0.4568	0.3336	42	0.740355	0.781459
MCM6	3.222	2.657	0.5651	1.756	0.3218	42	0.749237	0.788425
AHCYL1	0.7778	0.6286	0.1492	0.4816	0.3098	42	0.758213	0.793647
CHCHD3	0.2222	0.1429	0.07937	0.2569	0.309	42	0.758882	0.793647
IST1	0.2222	0.1429	0.07937	0.2569	0.309	42	0.758882	0.793647
MCM5	2	1.543	0.4571	1.567	0.2917	42	0.771983	0.80083
SDHA	3.444	2.886	0.5587	1.959	0.2852	42	0.776869	0.801782
SUPT16H	2	1.743	0.2571	0.9058	0.2839	42	0.777887	0.801782
FAM120A	0.5556	0.4571	0.09841	0.3407	0.2888	42	0.774132	0.801782
FAU	0.3333	0.2571	0.07619	0.2747	0.2774	42	0.782848	0.803804
ILVBL	0.3333	0.2571	0.07619	0.2747	0.2774	42	0.782848	0.803804
VPS26A	0.2222	0.1714	0.05079	0.1871	0.2715	42	0.787365	0.806382
DIS3	0.2222	0.1714	0.05079	0.1871	0.2715	42	0.787365	0.806382
GNB2	1.333	1.171	0.1619	0.6075	0.2665	42	0.791153	0.809231
NSUN2	2	1.771	0.2286	0.8673	0.2635	42	0.793418	0.810517
MTHFD1	3.556	3.114	0.4413	1.762	0.2504	42	0.803497	0.81563
DLAT	0.2222	0.1714	0.05079	0.2041	0.2489	42	0.804689	0.815686
HRNR	3.111	2.714	0.3968	1.623	0.2445	42	0.808033	0.81714
STIP1	3.111	2.486	0.6254	2.763	0.2263	42	0.822036	0.830257
PABPN1	0.2222	0.1714	0.05079	0.2344	0.2167	42	0.829527	0.833633
BSG	0.2222	0.1714	0.05079	0.2344	0.2167	42	0.829527	0.833633
NUP93	2.222	1.971	0.2508	1.18	0.2126	42	0.832688	0.835765
VARS	3.333	3	0.3333	1.651	0.2018	42	0.84101	0.841409
SPG20	1.222	1.086	0.1365	0.6782	0.2013	42	0.84145	0.841409
EIF3CL	3.222	2.943	0.2794	1.438	0.1943	42	0.846859	0.845765
RAB38	0.2222	0.1714	0.05079	0.2737	0.1856	42	0.853674	0.850458
YWHAG	1.889	1.714	0.1746	0.9922	0.176	42	0.861164	0.856182
PSMA4	0.2222	0.1714	0.05079	0.308	0.1649	42	0.86981	0.861197
VDAC1	3.889	3.686	0.2032	1.353	0.1502	42	0.881353	0.870482
UBXN4	0.4444	0.4	0.04444	0.3294	0.1349	42	0.89331	0.879052
XRCC6	6	5.6	0.4	3.424	0.1168	42	0.907548	0.889796
YWHAZ	4.556	4.429	0.127	1.889	0.06723	42	0.94672	0.922424
H1FX	0.7778	0.7429	0.03492	0.5293	0.06597	42	0.947712	0.922424
NUP205	1.222	1.171	0.05079	0.8247	0.06159	42	0.951184	0.924684
DNAJA1	1.444	1.343	0.1016	1.793	0.05667	42	0.955074	0.927203
SLC3A2	6.889	6.829	0.06032	2.685	0.02246	42	0.982184	0.944542

UBA2	0.5556	0.5429	0.0127	0.5314	0.0239	42	0.981049	0.944542